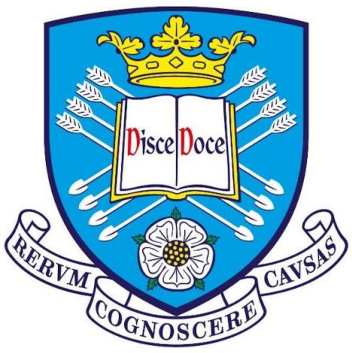

The University Of Sheffield.

An Investigation on the Impact of Feed Grain Anti-nutrients on Monogastric Animal Digestion with a Focus on Exogenous Feed Enzymes

Hayden Edward Hodges

A Dissertation Submitted for the Degree of Doctor of Philosophy

Department of Chemical and Biological Engineering

University of Sheffield

September 2021

Publications

Journal Articles

Kempapidis, T.*, Bradshaw, N.J.*, **Hodges, H.E.***, Cowieson, A.J., Cameron, D.D., Falconer, R.J., (2020). Phytase Catalysis of Dephosphorylation Studied using Isothermal Titration Calorimetry and Electrospray Ionization Time-of-Flight Mass Spectroscopy. *Analytical Biochemistry* [online]. **606**, 113859. Available from: doi: 10.1016/j.ab.2020.113859. (*denotes equal authorship)

All authors contributed to the conception and design of the study. TK, NB and HH collected the data. TK, NB, HH, RF and DC analysed the data. TK, NB, HH, DC and RF wrote the manuscript. All authors contributed to manuscript revision, reading, and approval of the submitted version. Elsevier retains copyright for this article, however, as stated in their copyright policy: authors may re-use their own material in new works without permission.

Hodges, H.E., Walker, H.J., Cowieson, A.J., Falconer, R.J., Cameron, D.D., (2021). Latent Anti-nutrients and Unintentional Breeding Consequences in Australian *Sorghum bicolor* Varieties. *Frontiers in Plant Science* [online]. **12**(625260), 1-12. Available from: doi:10.3389/fpls.2021.625260.

All authors contributed to the conception and design of the study. HH collected the data. HH, RF and DC analyzed the data. HH wrote the manuscript. All authors contributed to manuscript revision, reading, and approval of the submitted version. As stated by *Frontiers*, all authors retain copyright.

Conference Paper

Hodges, H., Cowieson, A., Falconer, R., Cameron, D., (2020). Chemical profile and effects of modern Australian sorghum polyphenolic-rich extracts on feed phytase and protease activity. *Proceedings of the Australian Poultry Science Symposium* [online]. 31, 76-79. Available from: doi: https://az659834.vo.msecnd.net/eventsairaueprod/production-usyd-public/8f563f4140d24984879bd01be567dfc2.

All authors contributed to the conception and design of the study. HH collected the data. HH, RF and DC analyzed the data. HH wrote the manuscript. All authors contributed to manuscript revision, reading, and approval of the submitted version. Authors are free to use their own work from this publication without permission.

Abstract

Supplementation of monogastric animal feed with exogenous enzymes has become standard practice with many positive impacts observed in animals and the environment. Recently there has arisen a need to investigate the effects that anti-nutrients, specifically those found in sorghum grain, might have on the activity of the exogenous feed enzymes. Consequently, we sought to better understand the role played by one anti-nutrient, polyphenols, and its role in muted exogenous phytase and protease performance in monogastric diets containing sorghum. Polyphenols from three commercially relevant sorghum grains, and two commercial tannin extracts, were first characterised to better understand the anti-nutrients of interest. Metabolomic analyses revealed a complex polyphenol-like environment which lacked the traditional, large polyphenol anti-nutrients of historic sorghum grains. A multi-method approach allowed for layers of complexity to be revealed and indicated that simpler spectral methods were better suited for fingerprinting than mass spectrometry. The polyphenol extracts were next tested as *in vitro* inhibitors of exogenous protease and phytase activity. The two commercial tannins, grape seed and quebracho wood, strongly inhibited both enzymes at low concentrations. Sorghum polyphenol extracts had a weaker effect on both enzymes, particularly the protease. Finally, the extracts were incorporated into a standard poultry diet in a simulated *in vitro* digestion model to measure their effects on nutrient digestibility. In this complex environment, all extracts had minimal effects on both protein and phosphorus digestibility. A rapid mass spectrometry method was trialled to fingerprint the supernatant of different diets with varying degrees of success. The results found in this work indicate that while modern sorghum grains may have minimal impact on exogenous enzyme activity, attention is needed at the metabolite level to determine which anti-nutrients may be implicated in sorghum's performance variability.

Acknowledgements

To my supervisors, Duncan Cameron and Robert Falconer: Thank you so much for this opportunity to study and learn at the University of Sheffield. You have always been so supportive and helpful through the highs and lows or even just around for a quick chat through an open door. I've been able to thrive as a researcher under your guidance and will no doubt continue to reflect on the skills you've left me in the future. And a big thank you to Denis Cumming for helping me in a transitional period of my studies and supporting me through the final stages of my thesis.

This thesis and the amazing experiences involved with it wouldn't have been possible without the financial support of our industry partner DSM Nutritional Products directed by Aaron Cowieson. While incredibly busy himself, Aaron was always free to respond to any questions I might have and provide crucial insights into the realms of animal nutrition. A huge thank you to Aaron for also helping coordinate my brief time learning at the facilities of Novozymes in Denmark. The experiences gained there were critical for certain parts of this work.

I wouldn't have been successful in the laboratory without the experience and help of some amazing researchers, Heather Walker and Irene Johnson. A huge thank you for all your patience, time and hard work in aiding my experiments, helping with orders and bookings and providing feedback on manuscripts. It was truly a pleasure to work alongside you both for so long.

I want to say a big thanks to Theo Kempapidis and Niall Bradshaw as PhD mentors and lab buddies. You both were welcoming and helpful to me as a bright-eyed first year student and remained steadfast throughout all our collective ups and downs. I'm so happy for you both in your careers and wish you the best. To my dear friend Hannah and those I've met along the way in both CBE and APS, thank you for your friendship and support. To my new friends in Denmark, Lærke, Katrine, Mia and Camilla, thank you so much for your hospitality, friendship and scientific expertise during my visit to Lyngby. I learned so much in those two weeks and couldn't have done it without your technical capability and subject knowledge. I look forward to visiting your wonderful country again!

I wouldn't be where I am today without my wonderful family both back home in the US and my new family here in the UK. To my UK family, thank you for always being there for support, laughter and love from the South West. To my family back home in the US, I miss you all every day and hope I'm making you proud. Although our times together are never as long as we would like them, we make so many lasting memories and I couldn't get through all of this without your love and support. To Nan, thank you for always being there for me throughout it all. Mom, you've been so supportive of me throughout really everything and I'm so proud to be your son. You're the hardest worker I've ever met and inspire me every day. Dad, you may not have always remembered or understood where I was or what I was doing but I love you so much, miss you always and hope you're staying free like a butterfly.

Finally to my incredible wife, Fran: Thank you for being you, for being my rock and biggest cheerleader every step of this long, long process while also working so hard on your own PhD. I genuinely couldn't have done it without you and am so excited to move to the next stage of our lives together. I love you so much!

Dedicated to my father, Edward Bonneau Hodges Jr.
You were the true engineer of the family, we miss you so much xxx

Table of Contents

Publications ..... *ii*

Abstract ..... *iii*

Acknowledgements ..... *iv*

Table of Contents ..... *vi*

List of Figures ..... *ix*

List of Tables ..... *xi*

Chapter 1 – A General Introduction to Monogastric Digestion for the Commercial Livestock: A Complex Interplay of Feed Ingredient, Endogenous Digestion and Exogenous Additives *1*

1.1 Literature review summary **2**

1.2 Overview of monogastric digestion **3**

1.3 Feed grain with a focus on sorghum **4**

1.4 Anti-nutritional components of feed ingredients **7**

1.4.1 Indigestible starches 7

1.4.2 Trypsin inhibitors 8

1.4.3 Phytate 8

1.4.4 Phenolic and polyphenolic compounds 10

1.5 Monogastric diet and feed formulation **15**

1.5.1 Feed form and formulation 15

1.5.2 Use of exogenous feed enzymes 17

1.6 Focus of work in this thesis **22**

1.6.1 General research hypotheses and methodology 23

Chapter 2 – Methodology for the Analysis of Polyphenolic Compounds *24*

2.1 Overview of analytical techniques **25**

2.2 Extraction and purification **25**

2.3 Basic spectroscopic analysis **27**

2.4 High-performance liquid chromatography (HPLC) **27**

2.5 Direct-injection electrospray ionisation (ESI) **30**

2.6 Matrix-assisted laser desorption/ionisation (MALDI) **31**

2.7 Supercritical fluid chromatography (SFC) **33**

2.8 Conclusions **35**

Chapter 3 – Profiling and Characterisation of Sorghum Polyphenol Extracts and Tannin Extracts Using Complementary Spectroscopic and Spectrometric Techniques *36*

3.1 Summary **38**

3.2 Introduction (adapted from Hodges et al., 2021) **39**

3.2.1 Sorghum grain polyphenols 39

3.2.2 Research aims, hypotheses and methodology 45

3.3 Materials and methods (adapted from Hodges et al., 2021) **46**

3.3.1 Chemicals and materials 46

3.3.2 Preparation of sorghum polyphenol extracts 46
3.3.5 Direct-injection electrospray ionisation (ESI) 47
3.3.6 Matrix-assisted laser desorption/ionisation (MALDI) 48
3.3.7 Tandem mass spectrometry (MS^2) 48
3.3.8 Data processing and statistical analysis 49

3.4 Results and discussion 51
3.4.1 Qualitative analysis of sorghum polyphenol extracts and tannin extract UV/Vis spectra 51
3.4.2 Qualitative analysis of sorghum polyphenol extract and tannin extract FT-IR spectra (adapted from Hodges et al., 2021) 53
3.4.3 Multivariate analysis of sorghum polyphenol extract and tannin extract metabolic profile from FT-IR spectra (PCA and OPLS-DA) (adapted from Hodges et al., 2021) 62
3.4.4 Unsupervised analysis of sorghum polyphenol and tannin extract metabolic profile from mass spectrometry (PCA) (adapted from Hodges et al., 2021) 65
3.4.5 Supervised analysis of sorghum polyphenol extract metabolite profiles from mass spectrometry (OPLS-DA) (adapted from Hodges et al., 2021) 69
3.4.6 Analysis of select compounds in sorghum polyphenol extracts using tandem mass spectrometry (MS^2) (adapted from Hodges et al., 2021) 87
3.4.7 Usefulness of multiple techniques to characterise polyphenol and tannin extracts (adapted from Hodges et al., 2021) 91

3.5 Conclusions and future work 94
3.5.1 Conclusions (adapted from Hodges et al., 2021) 94
3.5.1 Future work 95

Chapter 4 – A study of the impact of sorghum polyphenol extracts and tannin extracts on the activity of exogenous feed enzymes – phytase and protease 97

4.1 Summary 99

4.2 Introduction 100
4.2.1 Protein/enzyme-polyphenol interactions and their anti-nutritional impact 100
4.2.2 Isothermal Titration Calorimetry (ITC) Overview and Use in Polyphenol Interactions 102
4.2.3 Research aims, hypotheses and methodology 105

4.3 Materials and methods 106
4.3.1 Chemicals and materials 106
4.3.2 Preparation of sorghum polyphenol extracts 107
4.3.3 Total phenolic content assay (TPC) 107
4.3.4 Isothermal titration calorimetry (ITC) monitoring of exogenous feed phytase activity 107
4.3.5 Exogenous feed protease activity assay 108
4.3.6 Statistical analysis 109

4.4 Results and discussion 109
4.4.1 Sorghum polyphenol extract yield and extract phenolic content 110
4.4.2 Exogenous phytase activity and inhibition 113
4.4.3 Exogenous feed protease activity and inhibition 121
4.4.4 Relationship between sorghum polyphenol extract/tannin extract composition and exogenous feed enzyme inhibition 127

4.5 Conclusions and future work 133
4.5.1 Conclusions 133
4.5.2 Future work 133

Chapter 5 - A Study of the Interactions of Sorghum Polyphenol Extracts and Tannin Extracts with Exogenous Feed Enzymes in an In Vitro Simulated Digestion Model 135

5.1 Summary 136

5.2 Introduction 137
5.2.1 Sorghum's current role in animal feed 137

5.2.2 Use of simulated digestion models and *in vivo* feeding trials 141
5.2.3 Research aims, hypotheses and methodology 142

5.3 Materials and methods 144
5.3.1 Chemicals and materials 144
5.3.2 Preparation of sorghum polyphenol extracts 144
5.3.3 *In vitro* simulated poultry digestion model 144
5.3.4 Protein and nitrogen content determination 147
5.3.5 Degree of protein hydrolysis determination 147
5.3.6 Total phosphorous determination 148
5.3.7 MALDI analysis of soluble protein and data processing 149
5.3.8 Statistical analysis 149

5.4 Results and discussion 149
5.4.1 Effects of sorghum polyphenol extracts and tannin extracts on protein digestibility 150
5.4.2 Effects of sorghum polyphenol extracts and tannin extracts on phosphorous digestibility 157
5.4.3 MALDI-ToF-MS metabolite profile analysis of simulated digesta 162

5.5 Conclusions and future work 185
5.5.1 Conclusions 185
5.5.2 Future work 186

Chapter 6 – General Discussion 188

6.1 Paradigm shift in polyphenol and tannin chemistry methodology 189

6.2 Re-evaluation of plant and grain breeding practices 191

6.3 Modification of current animal feeding practices 193

6.4 Conclusions 197

References 199

Appendix 223

Appendix A 223

Appendix B 351

Appendix C 355

Appendix D 357

List of Figures

Figure 1.1 Pathway for swine and poultry upper digestive tract
Figure 1.2 Diagram of sorghum grain (adapted from Taylor and Emmambux, 2008)
Figure 1.3 Phytate structures
Figure 1.4 Pathways for polyphenol synthesis
Figure 1.5 Common phenolic acids
Figure 1.6 Common flavonoids
Figure 1.7 Condensed tannin synthesis
Figure 1.8 Procyanidin dimers
Figure 3.1 Sorghum 3-deoxyanthocyanins
Figure 3.2 Commerical sorghum grain from Australia
Figure 3.3 Metabolomic data processing workflow (adapted from Austen, 2016)
Figure 3.4 UV/Vis spectra of sorghum polyphenol extracts and tannin extracts
Figure 3.5 FT-IR spectrum of grape seed tannin extract
Figure 3.6 FT-IR spectrum of quebracho wood tannin extract
Figure 3.7 FT-IR spectra of MR-Buster sorghum polyphenol extracts
Figure 3.8 FT-IR spectra of Cracka sorghum polyphenol extracts
Figure 3.9 FT-IR spectra of Liberty sorghum polyphenol extracts
Figure 3.10 FT-IR spectrum of sorghum polyphenol extracts and tannin extracts
Figure 3.11 FT-IR fingerprint spectra of sorghum polyphenol extracts and tannin extracts
Figure 3.12 PCA plots for FT-IR spectra from sorghum polyphenol extracts and tannin extracts
Figure 3.13 PCA scores plots of mass spectrometry analysis of sorghum polyphenol extracts and tannin extracts
Figure 3.14 Heat map of percent total ion counts (TICs) for compounds identified from orthogonal partial least squares discriminant analysis (OPLS-DA) from ESI (-)
Figure 3.15 Pathway analysis of identified compounds from ESI (−)
Figure 3.16 Routes for the synthesis of phenolic compounds and other related secondary metabolites
Figure 4.1 Diagram of an ITC reaction chamber
Figure 4.2 Total phenolic content of sorghum polyphenol extracts and tannin extracts
Figure 4.3 Sample thermograms of enzyme and substrate blank measurements
Figure 4.4 Phytate-phytase reaction thermogram
Figure 4.5 Phytase-phytate thermogram with white sorghum polyphenol extract
Figure 4.6 Phytase-phytate thermogram with red sorghum polyphenol extract
Figure 4.7 Phytase-phytate thermogram with tannin extracts
Figure 4.8 Remaining phytase activity with sorghum polyphenol extracts and grape seed and quebracho tannin extracts
Figure 4.9 Activity of protease standards
Figure 4.10 Protease activity in presence of grape seed and quebracho tannin extracts
Figure 4.11 Protease activity in presence of red sorghum polyphenol extract
Figure 4.12 Protease activity in presence of white sorghum polyphenol extract
Figure 4.13 Protease activity with sorghum polyphenol extracts and tannin extracts
Figure 4.14 Effect of sorghum polyphenol extracts and tannin extracts on protease kinetics
Figure 4.15 Lineweaver-Burk plots of protease reaction kinetics and mode of inhibition
Figure 4.16 Conversion of *in vitro* inhibition results to commercial enzyme – sorghum polyphenol extract inclusions
Figure 5.1 Historical chicken yield and feed conversion ratio data
Figure 5.2 Stages of simulated digestion and sample analysis workflow

Figure 5.3 Measures of protein digestibility of digesta supernatant with grape seed tannin extract
Figure 5.4 Measures of protein digestibility of digesta supernatant with quebracho tannin extract
Figure 5.5 Measures of protein digestibility of digesta supernatant with MR-Buster sorghum polyphenol extract
Figure 5.6 Measures of protein digestibility of digesta supernatant with Cracka sorghum polyphenol extract
Figure 5.7 Measures of protein digestibility of digesta supernatant with Liberty sorghum polyphenol extract
Figure 5.8 Phosphorous digestibility of simulated digesta with grape seed tannin extract
Figure 5.9 Phosphorous digestibility of simulated digesta with quebracho tannin extract
Figure 5.10 Phosphorous digestibility of simulated digesta with MR-Buster sorghum polyphenol extract
Figure 5.11 Phosphorous digestibility of simulated digesta with Cracka sorghum polyphenol extract
Figure 5.12 Phosphorous digestibility of simulated digesta with Liberty sorghum polyphenol extract
Figure 5.13 Principal component analysis (PCA) scores plots for MALDI spectra from all digestion conditions
Figure 5.14 Principal component analysis (PCA) scores plots for MALDI spectra from all digestion conditions containing exogenous feed enzymes
Figure 5.15 Principal component analysis (PCA) scores plots for MALDI spectra from all digestion conditions containing only endogenous enzymes
Figure 5.16 Principal component analysis (PCA) scores plots for MALDI spectra from digestion conditions containing tannin extract or no extract
Figure 5.17 Principal component analysis (PCA) scores plots for MALDI spectra from digestion conditions containing tannin extract or no extract with exogenous feed enzymes
Figure 5.18 Principal component analysis (PCA) scores plots for MALDI spectra from digestion conditions containing tannin extract or no extract and only endogenous enzymes
Figure 5.19 Principal component analysis (PCA) scores plots for MALDI spectra from digestion conditions containing sorghum polyphenol extracts/no extract
Figure 5.20 Principal component analysis (PCA) scores plots for MALDI spectra from digestion conditions containing sorghum polyphenol extracts/no extract containing exogenous feed enzymes
Figure 5.21 Principal component analysis (PCA) scores plots for MALDI spectra from digestion conditions containing sorghum polyphenol extracts/no extract with only endogenous enzymes
Figure 5.22 Principal component analysis (PCA) scores plots for MALDI spectra without tannin/sorghum polyphenol extracts
Figure 5.23 Principal component analysis (PCA) scores plots for MALDI spectra from digestion conditions containing grape seed tannin extract
Figure 5.24 Principal component analysis (PCA) scores plots for MALDI spectra from digestion conditions containing grape seed tannin extract (extract dose)
Figure 5.25 Principal component analysis (PCA) scores plots for MALDI spectra from digestion conditions containing quebracho tannin extract
Figure 5.26 Principal component analysis (PCA) scores plots for MALDI spectra from digestion conditions containing quebracho tannin extract (extract dose)
Figure 5.27 Principal component analysis (PCA) scores plots for MALDI spectra from digestion conditions containing MR-Buster sorghum polyphenol extract

Figure 5.28 Principal component analysis (PCA) scores plots for MALDI spectra from digestion conditions containing MR-Buster sorghum polyphenol extract (extract dose)
Figure 5.29 Principal component analysis (PCA) scores plots for MALDI spectra from digestion conditions containing Cracka sorghum polyphenol extract
Figure 5.30 Principal component analysis (PCA) scores plots for MALDI spectra from digestion conditions containing Cracka sorghum polyphenol extract (extract dose)
Figure 5.31 Principal component analysis (PCA) scores plots for MALDI spectra from digestion conditions containing Liberty sorghum polyphenol extract
Figure 5.32 Principal component analysis (PCA) scores plots for MALDI spectra from digestion conditions containing Liberty sorghum polyphenol extract (extract dose)

List of Tables

Table 2.1 HPLC studies of polyphenol extracts
Table 2.2 MALDI studies of polyphenol extracts
Table 2.3 SFC studies of polyphenol extracts
Table 3.1 Parameters for ESI-ToF-MS analysis of sorghum polyphenol extracts
Table 3.2 Specific voltage ranges used in tandem MS
Table 3.3 FT-IR wavenumbers (cm^{-1}) identified from OPLS-DA loadings plots
Table 3.4 Binned peak masses identified from ESI (−) OPLS-DA loadings plots
Table 3.5 Binned peak masses identified from ESI (+) OPLS-DA loadings plots
Table 3.6 Binned peak masses identified from MALDI (+) OPLS-DA loadings plots
Table 3.7 Putative identification of discriminant mass bins responsible for separation of sorghum polyphenol extracts (ESI [-])
Table 3.8 Fragmentation of selected peaks from sorghum polyphenol extracts
Table 3.9 Putative identifications of unknown peaks in sorghum polyphenol extracts
Table 4.1 Yield of acetone polyphenol extracts from sorghum grain
Table 4.2 Time to 50% ($T_{50\%}$ - minutes) phytate-phytase reaction completion in the presence of sorghum polyphenol extracts and tannin extracts
Table 4.3 Kinetic constants of protease with sorghum polyphenol extracts and tannin extracts
Table 5.1 Dosage conversion from extract (mg) to feed formulation (%)
Table 6.1 Experimental conditions/outcomes to evaluate prior to natural product research

Chapter 1 – A General Introduction to Monogastric Digestion for the Commercial Livestock: A Complex Interplay of Feed Ingredient, Endogenous Digestion and Exogenous Additives

1.1 Literature review summary

The commercial livestock and meat production industries strive to provide high quality products at an affordable price to an ever-growing global population. Parallel to these goals, the many parties involved seek to optimise resources, reduce waste and limit negative environmental impacts. A comprehensive understanding of the complexities of animal production will invariably help to achieve these goals. Monogastric digestion is a key component of this process as the optimisation of digestion can result in improved animal nutrition and health, enhanced growth and performance parameters and reduced environmental emissions. Addressing these important environmental aspects can provide these industries ways of maintaining sustainable operations. This is a crucial goal for modern business as the world continues to adapt to a rapidly changing climate and environment. Understanding digestion and the inefficiencies that exist might to help provide new opportunities to increase production efficiency, maintain animal health and welfare and further reduce environmental concerns.

This introduction/literature review begins with a brief overview of monogastric animal upper digestion from ingestion through to the small intestines with a view to understanding the complexities of digestion from a physical and chemical perspective. It then turns to the current state of animal feed, with a focus on common anti-nutrients found in feed grain, as well the routine addition of exogenous feed enzymes to diets. The anti-nutrients focussed on in this chapter and throughout this thesis are phenolic and polyphenolic compounds. While the focus of this thesis is on monogastric nutrition and digestion, poultry production for meat is the model industry emphasised with the broiler chicken as the primary animal.

1.2 Overview of monogastric digestion

Animal digestion is a complex process and will be reviewed briefly from intake of feed to the small intestinal tract (duodenum) and limited in discussion to non-ruminant animals, with a focus on poultry and swine. Ruminant animals, including cows, goats and sheep, are beyond the scope of this thesis as their diets are not directly compatible with the research questions asked within.

Swine and poultry upper digestive systems follow similar tracts, with poultry having slight variations (**Figure 1.1)**.

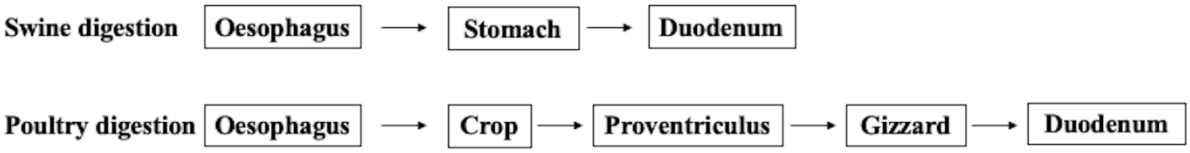

Figure 1.1 Upper digestive tract for swine and poultry
Swine and poultry upper digestive systems have several similarities with three basic phases: oesophageal, gastric and intestinal. Differences appear in the poultry gastric phase as the stomach is composed of two parts, proventriculus and gizzard.

Ingestion and initial digestion occur in the mouth with the intake of feed. Poultry differ here as food is not properly chewed or fully moisturised but is swallowed and directed to the crop via the oesophagus. Feed in the crop is moisturised but does not undergo significant chemical alterations or digestion as no endogenous enzymes are secreted; however, any exogenous feed enzymes formulated into diets may have significant effects during these early stages of digestion (Svihus, 2014). While relatively brief, the initial intake of feed can result in several physical and chemical changes. Physically, maceration by teeth in pigs or grit in the crop of poultry results in a reduction in the size of feed which increases the surface area for greater nutrient uptake and utilisation upon enzyme action and further digestion. Salivary enzymes, including amylase, begin the initial stages of digestion and nutrient uptake. Proteins in saliva can bind to specific components of the feed materials, particularly polyphenols, which often results in astringency, or a sense of drying out the mouth (Hagerman and Butler, 1981).

This mixture of food enters the stomach of pigs or the proventriculus and gizzard in poultry where the enzymatic degradation of proteins and other nutrients begins as hydrochloric acid and pepsinogen are secreted here. The gizzard is a specialized part of the poultry stomach that has strong muscles and a grinding surface known as the koilin layer which helps to further

break down feed ingredients and free nutrients for uptake (Svihus, 2014). Like maceration by teeth or grit, this process helps to increase nutrient uptake through an increase in surface area. This gastric phase may last between 20 – 45 minutes and two to four hours for poultry and swine, respectively (Bedford and Schulze, 1998). In swine, the pH of the stomach is between 2 – 2.5 and increases with the intake of feed (Dersjant-Li et al., 2015). The pH of the poultry gizzard has been found to vary from 1.9 – 4.5 with 3.5 as the average reading (Svihus, 2014).

The digesta and gastric juices then flow into the upper small intestines, also known as the duodenum, as a mixture called chyme which combines with three other secretions: pancreatic juice, intestinal juice and bile from the liver. The duodenum is where most nutrients from feed are absorbed for energy usage, storage or nutrient uptake (Svihus, 2014). Pancreatic juice, produced by the pancreas, contains proteases, amylases and lipases while the intestinal juice contributes further proteases. The contribution, volume wise, of pancreatic juices from swine is considerably larger than poultry (Bedford and Schulze, 1998).

1.3 Feed grain with a focus on sorghum

The majority of monogastric animal feed is composed of maize and often wheat and is commonly supplemented with soybean-meal (SBM) for additional protein requirements (Alhotan, 2021; Selle et al., 2021). While maize and wheat dominate most formulations, there is a need to find more reliably priced and sustainable alternatives. Both maize and wheat are widely used for human consumption and biofuel which makes the market more competitive and volatile (Alhotan, 2021). Alternatives for these ingredients include barley, cottonseed, millet, legumes and sorghum. Sorghum is of focus in this thesis for several reasons: 1) the use of sorghum grain in monogastric animal diets is often associated with suboptimal animal growth and performance, as well as reduced nutrient and energy digestibility; 2) sorghum is of interest as a replacement for maize and wheat due to its resilience in arid climates; and 3) the research in this thesis has come about from research and communications from farmers, feed formulators and researchers in Australia where sorghum is an important crop. The grain structure and nutrient content of sorghum grain will be focussed on here.

Sorghum (*Sorghum bicolour* [L]), family Poaceae and subfamily Panicoideae, is the fifth-most important cereal crop grown in the world today after wheat, rice, maize and barley and has many diverse applications and uses, including alcoholic beverages, animal feed, biofuel and

human consumption. In the most recent figures from the Food and Agriculture Organisation (FAO) of the United Nations, approximately 58 million tonnes of sorghum were produced in 2019 with half of the production coming from Africa and a third from the Americas. The top producing countries were the United States, Nigeria, Ethiopia, Mexico and Sudan (FAO, 2021). As can be appreciated from this list, sorghum often grows best in warm, sunny climates and is drought-tolerant due to its efficient C_4 carbon fixation (Davis and Hoseney, 1979; Gualtieri and Rapaccini, 1990). Beyond its ability to tolerate heat and high levels of ultraviolet (UV) light, the grain has many reported health benefits, including being gluten-free and high in antioxidants (Awika and Rooney, 2004; Stefoska-Needham et al., 2015). Sorghum grain is particularly important in developing countries with regard to human consumption and nutrition (Gualtieri and Rapaccini, 1990). Traditional foods made with sorghum in these countries include beer, porridge and unleavened bread. Foods with improved fibre and nutraceutical levels can be produced by removing the bran (decorticating) of polyphenol-rich grains, like sorghum, and incorporating them into traditional recipes (Dykes and Rooney, 2007).

As a feed ingredient, sorghum is nutritionally comparable to maize and wheat with similar fibre and protein levels. The three grains were compared by Hulan and Proudfoot (1982) and sorghum was found to have intermediate crude protein and lipid levels while fibre was found to be lower than both maize and wheat. Sorghum grain can be divided into three major areas and include the outer pericarp, endosperm and germ (**Figure 1.2**).

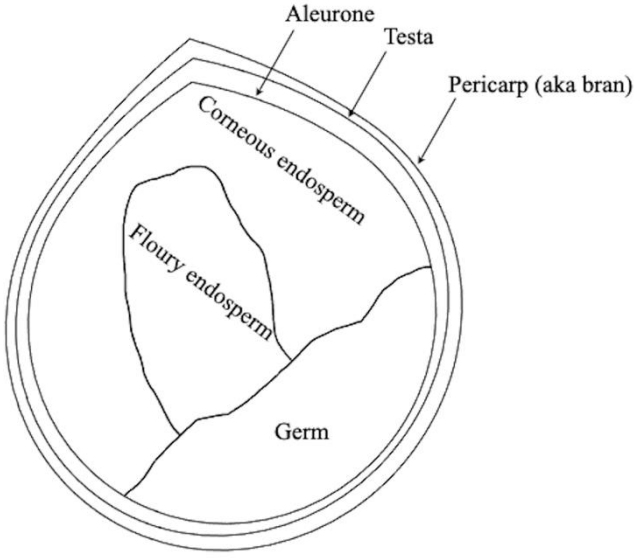

Figure 1.2 Diagram of sorghum grain (adapted from Taylor and Emmambux, 2008)

The outermost layer of the grain is the pericarp, or bran, which contains some starches, fibre, proteins and lipids and can be coloured white, red, brown or black. As reported by Liu et al. (2010), 95% of the sorghum produced in Australia was red in colour and the white sorghum grains produced were almost exclusively the Liberty variety. While there are numerous varieties of sorghum grain, only a handful are used extensively in commercial settings. Higher molecular weight compounds called polyphenols, including structures known as condensed tannins, are found in the testa layer just below the pericarp in certain varieties known as high-tannin and 'bird-resistant' which are no longer commonly utilised in animal feed (Bullard, 1988; Bean et al., 2018). The aleurone layer is where the majority of phytate, a common anti-nutrient, is found (discussed further in **Section 1.4.3**).

Beyond the aleurone layer is the endosperm, which makes up most the grain's structure. The endosperm is divided into two sections: a hard, outer layer (corneous) followed by the inner, soft (floury) component. The endosperm is where most of the protein and carbohydrates are found. Sorghum starch comprises approximately 45 – 71% of the grain's nutrients and is primarily located in the endosperm (Wall and Blessin, 1969; Bean et al., 2018). Within the endosperm, starch can be differentiated depending on its location. In the outer, hard section, starch is tightly packed and is mostly polygonal in shape. In contrast, starch in the inner, soft section is loosely packed with a more spherical shape. The two major starches found in sorghum are amylose and amylopectin, with amylopectin being the more common of the two (Bean et al., 2018).

Sorghum grain contains several protein families including albumins, globulins, prolamins (also known as kafirins) and glutelins. These proteins families can be distinguished chemically by their solubility: albumins are water-soluble, globulins are salt-soluble, kafirins are alcohol-soluble and glutelins are dilute-alkali soluble. Some of the proteins can be found in the outer layers of the grain as dehulling has been demonstrated to reduce protein content between 7.5-8.3% (Youssef, 1998). However, the endosperm is where most proteins are found, albeit, the higher quality proteins, containing essential amino acids for optimal animal health and performance, are found in the germ (Bean et al., 2018). Kafirins, composed of primarily proline and glutamine residues, like zein protein in maize, are the major storage proteins in sorghum and comprise between 48 – 70% of total protein (Bean et al., 2018; Selle, et al., 2020). Within this family, kafirins can be divided into four groups: α, β, γ and δ (Bean et al., 2018). Sorghum proteins, principally kafirins, are considered low quality as they lack several

essential amino acids, especially lysine, resulting in diets containing sorghum grain needing supplementation with high quality protein sources like SBM, crystalline amino acid supplements and exogenous proteases (Wall and Blessin, 1969; Youssef, 1998; Selle et al., 2020). Additionally, kafirins have high concentrations of disulphide bonds which decrease protein digestibility through the formation of starch-protein complexes, possibly formed during feed steam-pelleting (Selle et al., 2020). Red coloured kernels are believed to have a higher kafirin content than white sorghum, a fact that helps support the belief that white sorghum is superior in feed formulations (Liu et al., 2010). Mariscal-Landín et al. (2004) evaluated four sorghum varieties with different tannin contents and found that as the ratio of kafirin and glutelins increased the ratio of albumins and globulins subsequently decreased.

Finally, the germ makes up the final major section of the grain and is where most lipids, vitamins and minerals are found (Bean et al., 2018). Sorghum has a relatively low lipid content of about 3 – 4% most of which is found in the germ and primarily composed of triacylglycerols (Bean et al., 2018). Total phosphorous, on average, makes up 2.92 g/kg of the grain's mass with approximately 83% of that in the bound form of phytate (Liu et al., 2013). Sorghum is also reported to contain more than double the amount of calcium as maize (Gualtieri and Rapaccini, 1990). These two minerals play key roles in both maintaining normal metabolism and anti-nutrient balance with regards to phytate.

1.4 Anti-nutritional components of feed ingredients

1.4.1 Indigestible starches

While most carbohydrates are digested during the intestinal phase, small amounts of non-starch polysaccharides (NSPs) remain intact and act as anti-nutrients. Anti-nutritional effects are thought to occur via increased viscosity of the digesta as well as through negative interactions with proteins and enzymes (Williams, 1997). Viscous feed grains include wheat, rye, barley, oats, triticale. These grains contain high levels of soluble NSPs. β-glucan, of which barley is known to have high concentrations of, differs from normal, digestible starch in that it contains a mixture of linkages which result in a branched-chain polysaccharide as opposed to starch which is made up of straight-chain linkages (Choct, 2006). Like barley, wheat and rye both have high levels of NSPs, including arabinoxylan. Non-viscous grains include maize, sorghum, millet, and rice which contain lower concentrations of soluble NSP (Bedford, 1996; Choct, 2006). In non-viscous grains, higher levels of insoluble NSPs, including cellulose, act

in a different manner to produce similar anti-nutritional effects. The anti-nutritional effects are caused by inhibiting enzyme action indirectly by blocking substrates embedded in the cell wall matrix (Choct, 2006).

1.4.2 Trypsin inhibitors

Certain feed ingredients are rich in proteinaceous anti-nutrients, notably trypsin inhibitors. SBM is well-established as having high levels of these small proteins/polypeptides, which include Bowman-Birk and Kunitz inhibitors. These anti-nutrients have been previously reviewed (Losso et al., 2008). When tested as inhibitors of trypsin activity, Kunitz inhibitors were found to have a greater inhibitory effect compared to Bowman-Birk inhibitors. Both inhibitors had a greater negative impact on activity than another key grain anti-nutrient, polyphenols (Huang and Zhao, 2008). The effect of these inhibitors relies in large part on the processing of ingredients. Heat treatment plays an important role in this effect as high heat can denature these small peptides. Additionally, fat content has been found to increase levels of these anti-nutrients. Levels of trypsin inhibitor increased as the amount of raw (untreated) full-fat SBM was added to poultry diets (Erdaw et al., 2017). This group fed broiler chickens increasing amounts of full-fat SBM and observed reduced feed intake, lowered body weight and reduced protein digestibility. Sorghum grain is known to contain trypsin inhibitors. Sorghum from India was analysed for a variety of nutrient parameters, including anti-nutrients, after various grain flour treatments including cooking and fermentation. Raw, untreated sorghum flour was found to have trypsin inhibitor concentration of 52.26 mg/g and this value was subsequently reduced by up to 58% when fermented and steamed (Mohapatra et al., 2019).

1.4.3 Phytate

Phytate, usually bound to magnesium or calcium, is a common component of oilseeds and cereal grains found in the outer layers of the seeds and is the primary form of phosphate storage (Bedford and Schulze, 1998; Dersjant-Li et al., 2015). This comprises between 1 – 6% of the grain's weight as well as 60 – 90% of its phosphorous content (Cheryan and Rackis, 1980). Phytate, also known as inositol hexakisphosphate (IP6), is composed of a myo-inositol ring that can hold up to six phosphate ions and is typically represented either traditionally in a cyclic structure or more commonly in its 'turtle shape' (**Figure 1.3**). Phytate and the products of its degradation are commonly referred to by their inositol abbreviations. These include inositol

pentaphosphate (IP5), inositol tetraphosphate (IP4) and so on until there is only IP1 or theoretically IP0 with 100% of the phosphate groups removed.

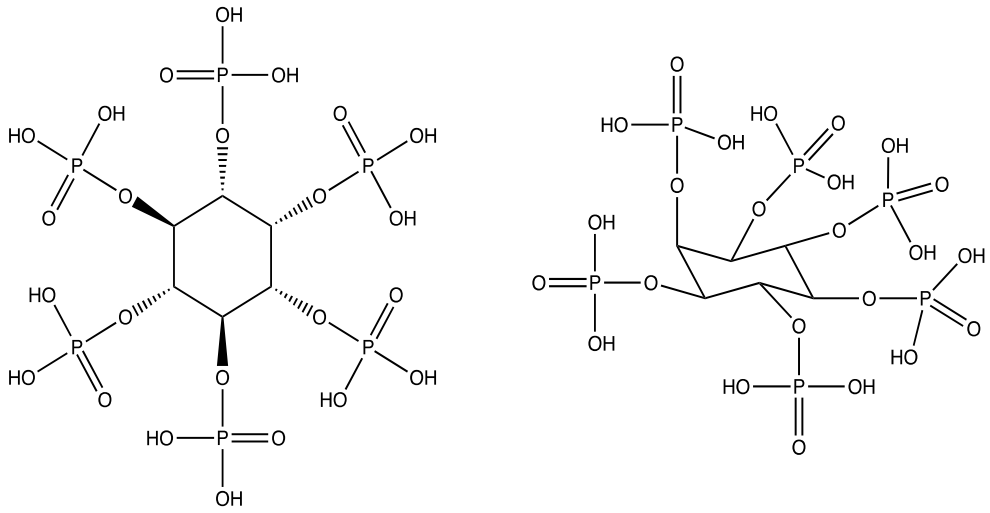

Figure 1.3 Phytate structures
Phytate, or phytic acid, is typically represented in either of these two forms: cyclic (left) or 'turtle' (right).

The trapped phosphorous is essential to animal growth and development especially regarding bones (Kebreab et al., 2012). Due to a lack of sufficient endogenous phytase, monogastrics are unable to effectively breakdown phytate to access phosphorous. Traditionally feed is supplemented with mineral phosphorous in the form of monocalcium phosphate (MCP). This approach, however, often leads to increased levels of phosphorus runoff pollution, increased cost to farmers and greater effect on global warming and greenhouse gas emission. Worldwide phosphorous reserves are dwindling and accessibility to mines is limited to a handful of countries with Morocco and areas of sub-Saharan Africa controlling most of the reserves (Childers et al., 2011).

Phytate acts anti-nutritionally by binding proteins, digestive enzymes, minerals and other components of feed ingredients which reduces nutrient utilisation and digestibility (Selle et al., 2000; Selle et al., 2012; Bye et al., 2013). The twelve hydroxyl groups on phytate carry strong negative charges when at physiological conditions during digestion which enables the molecule to bind to minerals, particularly calcium, and proteins. Protein-phytate interaction occurs primarily in the low pH environment of the stomach where the negatively charged phytate readily binds to positively charged amino acids within proteins and forms a mostly soluble complex between pH 2.5 – 4 (Cheryan and Rackis, 1980; Kies et al., 2006; Yu et al., 2012; Dersjant-Li et al., 2015). Interactions are less likely to occur in higher pH environments but

are known to happen at alkaline pH values and these interactions are most likely influences by ionic content (Cheryan and Rackis, 1980). In addition to reducing protein solubility and digestibility, phytate can interfere with endogenous protease activity. Phytate at feed-relevant levels has been found to inhibit pepsin activity approximately 87% (Yu et al., 2012). This inhibition was reduced as levels of phytate decreased and levels of the lower esters (IP5 – IP1) increased with phytate-degrading enzyme supplementation.

1.4.4 Phenolic and polyphenolic compounds

Phenolic and polyphenolic compounds, hereafter generally referred to as polyphenols, are ubiquitous plant secondary metabolites composed of several thousand compounds organised into families including phenolic acids, flavonoids, anthocyanins and tannins. These compounds are crucial for plant survival supporting morphology, growth, reproduction and defense (Quideau et al., 2011). High levels of polyphenols act as defense for plants against ingestion by animals. Animals combat this through a defense mechanism known as astringency, which binds polyphenols and tannins to salivary proteins rich in proline residues (Hagerman and Butler, 1981; Charlton et al., 1996; Baxter et al., 1997). This sensation remains a desired characteristic in certain styles of wine and is present in coffee and tea products. Polyphenols are reported to have beneficial properties to humans and some animals including antioxidant, antibacterial and antiviral effects (Dykes and Rooney, 2007; Lipiński et al., 2016; Alu'datt et al., 2017; Barrett et al., 2018). Conversely, undesirable effects have been reported in livestock fed grains with high polyphenol and tannin contents (Selle et al., 2010a; Bordenave et al., 2014). Certain grains, notably sorghum, are known to have high levels of polyphenols which can limit animal growth and development. The nature of these effects is thought to be due to polyphenols associating with proteins, starches and enzymes during digestion which reduces the bioavailability of nutrients (Alu'datt et al., 2017). However, both the exact mechanism through which polyphenols behave as anti-nutrients and the full effects of medium to small compounds are not fully understood.

The building blocks of polyphenols are erythrose 4-phosphate, phosphoenolpyruvate (PEP) and acetyl co-enzyme A (acetyl-CoA). Erythrose 4-phosphate and PEP lead into the shikimic acid pathway, while acetyl-CoA starts the polyketide, or acetate, pathway. The shikimic acid pathway is responsible for the synthesis of three amino acids, tryptophan, tyrosine and phenylalanine (**Figure 1.4**) (Waterman and Mole, 1994).

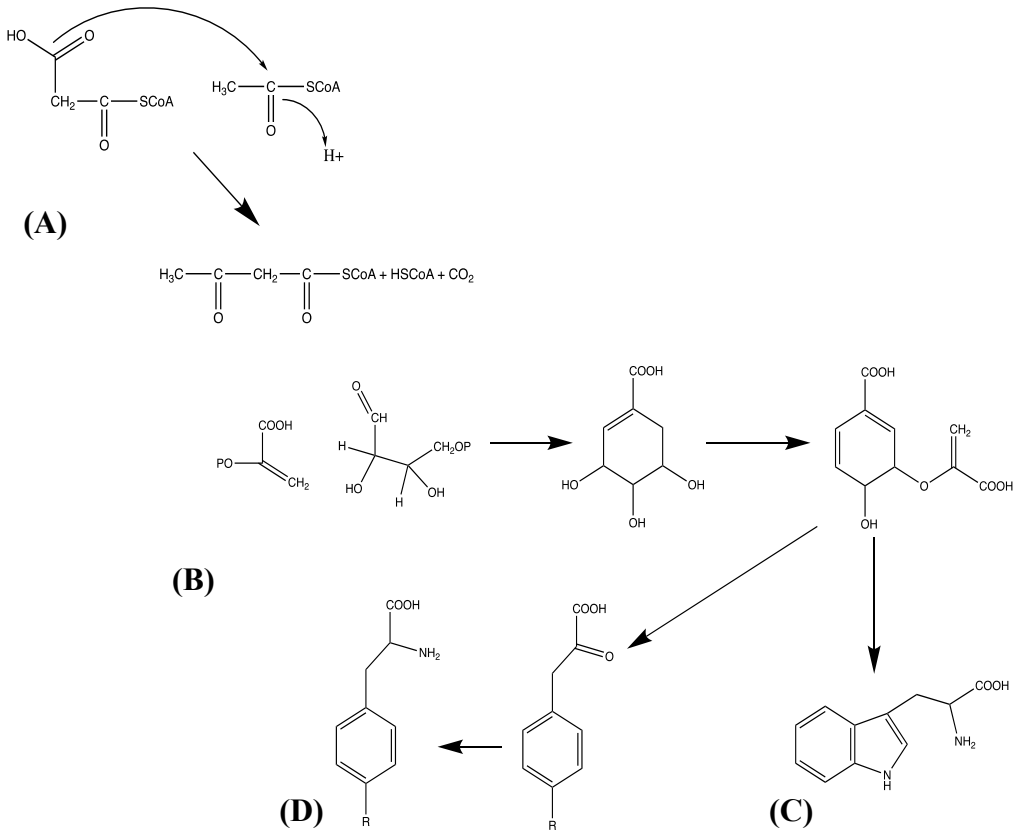

Figure 1.4 Pathways for polyphenol biosynthesis
Phenolic compounds are synthesized via either two primary pathways, **(A)** polyketide (acetate) or **(B**) shikimic acid, or a combination of the two. The shikimic acid pathways leads to the synthesis of **(C)** tryptophan, **(D)** phenylalanine or tyrosine (Waterman and Mole, 1994).

Phenolic compounds are defined by the presence of a phenolic group (hydroxyl attached to a benzene ring) and are acidic due to the propensity of the hydroxyl group to lose a hydrogen and form a phenoxide ion. An important property of polyphenols is their ability to form hydrogen bonds, a key feature of protein/enzyme interaction. Polyphenols differ from simple phenolic compounds as they contain two or more phenolic moieties. Polyphenols can be divided into families based on the number of carbon atoms in a sidechain attached to a phenolic group as well as the number of aromatic rings attached (Waterman and Mole, 1994). The smallest phenolic compounds, called phenolic acids, contain one aromatic ring and include such compounds as phloroglucinol, gallic acid, protocatechuic acid, caffeic acid and ferulic acid (**Figure 1.5**).

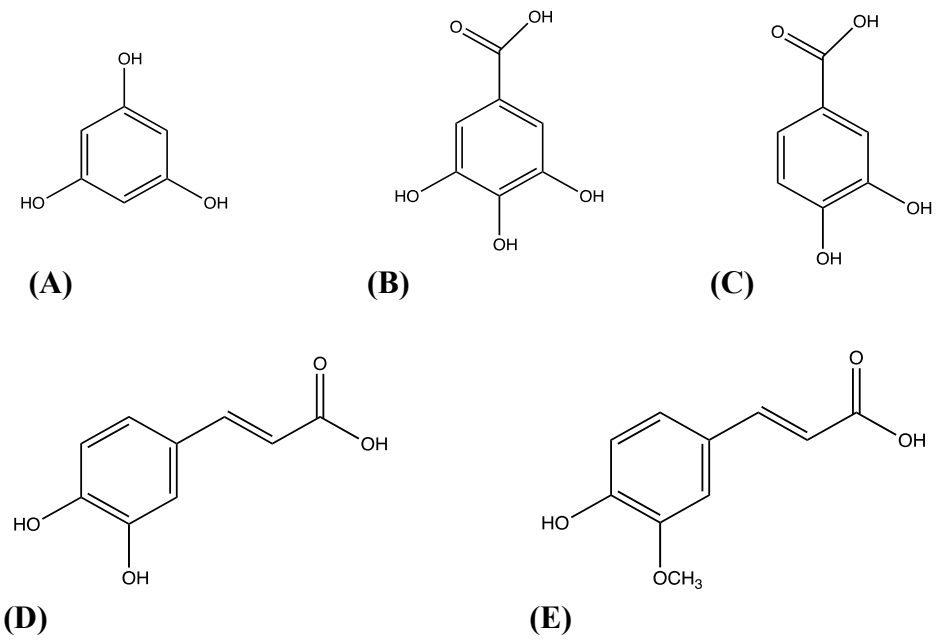

Figure 1.5 Common phenolic acids
Structures of common phenolic acids: **(A)** phloroglucinol, **(B)** gallic acid, **(C)** protocatechuic acid, **(D)** caffeic acid and **(E)** ferulic acid.

The most common polyphenol structures contain two phenolic rings, $C_6C_3C_6$, forming the basis for flavonoids and condensed tannins, some of the most well-known and studied polyphenols. Of the approximately 8,000 polyphenols so far discovered, the largest and most important class are the flavonoids with over 4,000 compounds discovered (Tsao, 2010). Flavonoids are themselves broken into several sub-categories including flavanones, flavanols, flavones, flavonols, flavan-3-ols and anthocyanidins. Common flavonoids include (epi)catechin, cyanidin, naringenin, taxifolin, luteolin and quercetin (**Figure 1.6**). Beyond basic structural differences, flavonoids can be further modified through methylation, prenylation, oxygenation and glycosylation. The true nature and chemical reactivity of a phenolic compound can be masked by these changes, especially glycosylation (Waterman and Mole, 1994).

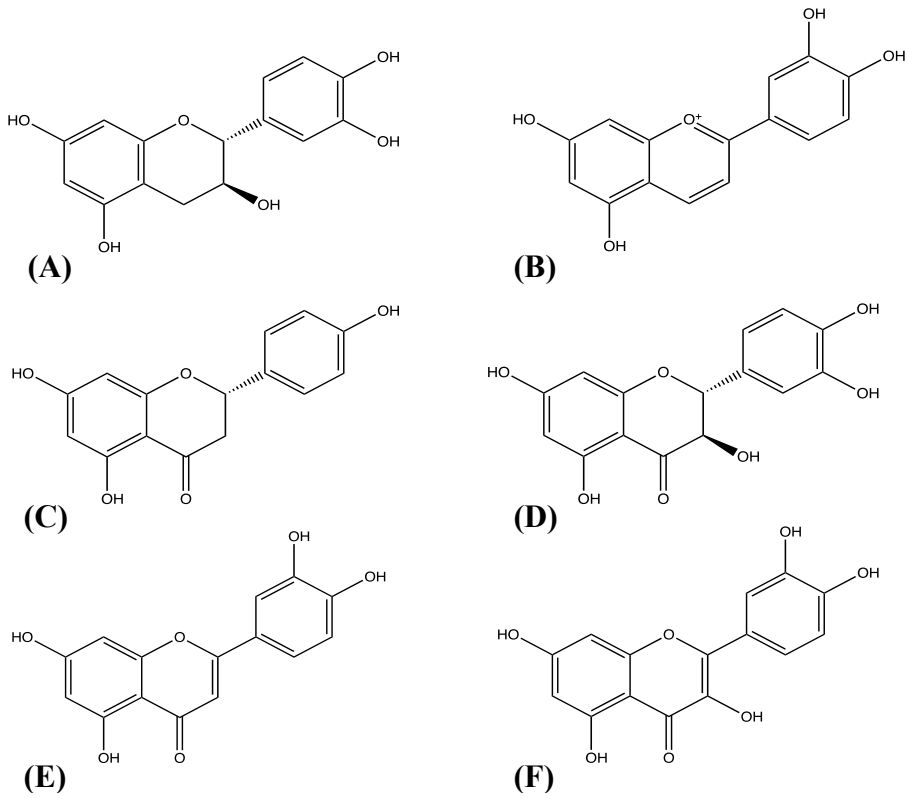

Figure 1.6 Common flavonoids
Structures of common flavonoids: **(A)** catechin, **(B)** cyanidin, **(C)** naringenin, **(D)** taxifolin, **(E)** luteolin and **(F)** quercetin.

Tannins are an important subclass of flavonoids, containing three groups including phlorotannins, hydrolysable tannins and condensed tannins, and are polymers constructed from flavonoid monomers like (epi)catechin and gallocatechin. Tannins take their name from their use in the historic tanning process of turning animal skins into leather. The compound's ability to bind collagen in animal skins highlights the main feature of this group (Velickovic and Stanic-Vucinic, 2018). Tannins can have a wide range of sizes from dimers of 300 Da up to highly polymerised structures of 30,000 Daltons (Da) and are highly hydroxylated which aides their potential interactions with proteins and carbohydrates (Bravo, 1998). Condensed tannins, of most relevance to this thesis, are composed of monomers of flavan-3-ols most often linked between the C-4 and C-8 of two aromatic rings and formed from the condensation of flavan-3,4-diol units (**Figure 1.7**).

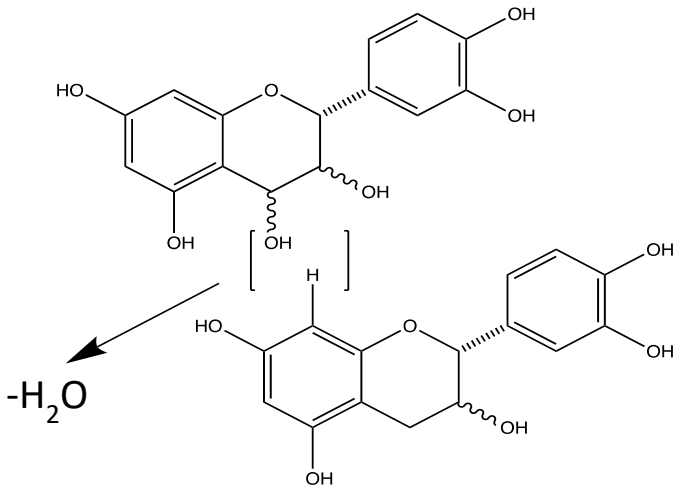

Figure 1.7 Condensed tannin synthesis
Two flavonoids join through a condensation reaction to form a procyanidin (condensed tannin) dimer.

Condensed tannins vary based on their hydroxylation patterns, stereochemistry of the two rings and the pattern of monomers used in building polymerised structures. For example, a condensed tannin dimer made of (-)-epicatechin and (+)-catechin four different structures can form (**Figure 1.8**) (Waterman and Mole, 1994). Due to the diversity of these metabolites, several methods exist for the extraction and analysis of them which are discussed in more detail in **Chapter 2**.

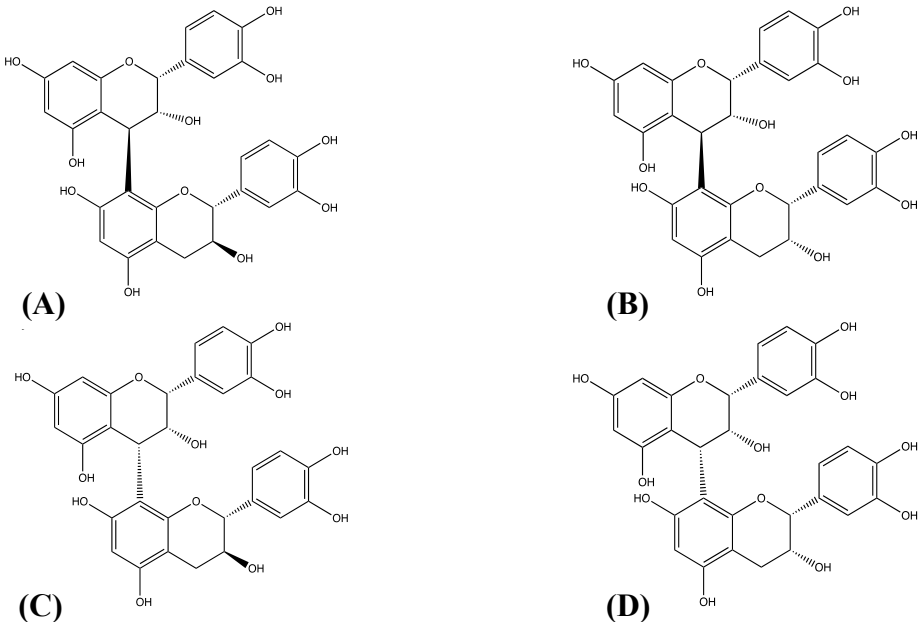

Figure 1.8 Procyanidin dimers
Two common flavonoids, (+)-catechin and (-)-epicatechin join to create four possible procyanidin dimers: **(A)** procyanidin B1 (epicatechin – catechin), **(B)** procyanidin B2 (epicatechin – epicatechin), **(C)** procyanidin B3 (catechin – catechin) and **(D)** procyanidin B4 (catechin – epicatechin).

1.5 Monogastric diet and feed formulation

1.5.1 Feed form and formulation

Animal feed can be divided into two forms: fodder and forage. Fodder is of focus in this thesis as this form of feed most relates to the rearing and raising of domesticated, monogastric animals as opposed to grazing ruminant animals. Most fodder today takes the form of a mash or pellet specifically designed and formulated to meet the nutritional requirements of the animals to be fed, e.g., the average male broiler chicken needs approximately 10% of its live weight in feed per day (Svihus, 2014). Pelleting is achieved through a process known as extrusion in which feed components are forced through a die to create uniform pellets. The resulting friction from this force heats the feed components up to 70 – 95°C. This effect has been found to be beneficial to certain feed grains, especially SBM. As previously discussed, SBM contains high levels of trypsin inhibitors, particularly the Kunitz variety. Extrusion at high temperatures has been found to effectively lower concentrations of these anti-nutrients thus increasing feed conversion efficiency and digestibility (Williams, 1997). There is evidence to suggest that pelleting feed, while increasing feed uptake, can reduce nutrient uptake and limit the digestive capacity of poultry. Poultry fed mash diets tend to consume less feed and gain more energy and nutrients due to a longer retention time in the gizzard. The digestive systems of poultry fed pelleted diets can become overloaded and unable to function appropriately thus becoming underdeveloped (Svihus, 2014).

Animal nutritionists and feed manufacturers must consider the key components necessary for a healthy diet of the animal, including carbohydrates, fats, protein, minerals, water and vitamins (National Research Council [NRC], 1994). The base grain of the fodder pellet or mash is the determining factor for these components. Grain for feed purposes includes, but is not limited to, maize, rice, barley, wheat, oats, sorghum, barley, triticale and millet. Typically, two to three grains are mixed to form approximately 70% of the total mixture and thus much of the nutritive content derives from this grain base (Bedford and Schulze, 1998). Certain requirements, notably protein, are difficult to meet from grains alone and require additional protein and amino acid supplementation (Dosković et al., 2013). High levels of protein are essential for growth, especially in the starting phases of development for swine and poultry. The need for increased protein levels through non-animal sources is partly being met with vegetable proteins, including SBM and lupin from legumes (Choct, 2006).

Feed composition is calculated and formulated using a variety of strategies, including least cost formulation, linear programming, multi-criteria models, phase feeding and precision feeding (Kebreab et al., 2012). Least cost formulation seeks to minimise cost while gaining the largest benefit in nutrition by using lowest cost grains. However, this method can disregard possible negative factors like high levels of anti-nutrients which could negate any financial gains (Bedford and Schulze, 1998). Rising demand for certain grains, such as maize, for use in biofuels and for human consumption, has shifted how feed manufacturers and farmers view non-traditional feed sources including sorghum. Diet formulations are also dictated by the geographic location they are made in. While some parts of the world may have easy access to high-quality, high-energy ingredients, others may only have low quality, lower energy ingredients. The balance of weighing up cost and ingredient quality allows for the appropriate energy levels to yield the lowest feed cost per weight gain (NRC, 1994).

The most important components of poultry feed are carbohydrates, protein and fat. Most of the energy used by the birds comes from carbohydrates and fats. The best source of carbohydrate is starch, although other types of polysaccharides can be utilised sufficiently for energy purposes. Fats help to provide a quick source of energy for poultry and are typically supplemented into diets with grease, animal by-products and vegetable oils. Linoleic and linolenic acids are essential to poultry health (NRC, 1994).

Amino acid/protein composition and quality are important factors in broiler chicken nutrition. Proteins, which are composed of the crucial nutrient amino acids, help contribute to important structural tissues like bones, skin and feathers, as well as normal metabolic function. A steady supply of proteins and amino acids is crucial to broiler chickens as this nutrient is dynamic, i.e. constantly being used to supply normal growth measures and maximise meat yield as meat-yielding poultry can grow 50 – 55 times over 6 weeks (NRC, 1994). Among the 20 amino acids available, there are two main groups: essential and non-essential. The essential amino acids in broiler feed are methionine, lysine and threonine, which in sorghum are typically quite low with values of approximately 1, 2 and 3 g/kg, respectively (Selle et al., 2020). Additionally, some sorghum varieties tend to display an inverse relationship as increased protein concentration results in decreased concentrations of lysine. This is thought to be due to increased levels of prolamins (aka kafirin protein) in sorghum grains which are deficient in lysine (NRC, 1994). These essential amino acids must be supplemented in diets as poultry are not able to synthesise them. Diets can be supplemented with more direct protein-rich sources

including SBM, animal-related products (feather, bone, meat, fish), crystallised amino acids, cottonseed mean and rapeseed meal.

Two of the most important minerals needed for normal poultry health and development are calcium and phosphorous which are crucial for health bone development. These minerals are also necessary for the development of eggshells in layer hens (NRC, 1994).

1.5.2 Use of exogenous feed enzymes

Exogenous feed enzymes have been included in animal feed for approximately 40 years. Their primary purposes are two-fold: 1) increase the bioavailability of nutrients for the animal resulting in healthier and more predictable growth and development, better utilisation of feed components and optimisation of costs; 2) reduce harmful environmental impacts from the raising of animals to create more sustainable farming practices (Walsh et al., 1994). Since the 1980s, exogenous feed enzymes have been industrially developed and utilised to enhance the nutritional properties of animal feed. While most diets have been optimised for optimum nutrient absorption, performance is still often limited to 85 – 90% nutrient digestibility even in highly digestible diets, such as maize – SBM (Ravindran, 2013). The basic principle of exogenous feed enzymes is to enable nutrients including proteins, starches and minerals to be freed from non- or low-available states. Factors accounted for in feed formulations with exogenous enzymes include whether action takes place upon ingestion and is complete by the small intestine, the enzyme is active and stable at a wide range of pH values and the enzyme is resistant to degradation by endogenous enzymes (Svihus, 2014). Beyond evaluating the use of single enzymes, the effects of different cocktails of exogenous feed enzymes on growth and performance has been investigated with positive results seen for phytase – amylase – xylanase (Stefanello et al., 2015), phytase – xylanase (dos Santos et al., 2017), phytase – tannase (Weihua et al., 2015) and xylanase – amylase – protease – phytase (Olukosi et al., 2007). The developments and use of exogenous feed enzymes have been extensively reviewed (Cowieson et al., 2006; Slominski, 2011; Dosković et al., 2013, Ravindran, 2013).

The first of three commonly added exogenous feed enzymes are NSP-degrading enzymes. To combat the anti-nutritional effects of these components (see **Section 1.4.1**), xylanases and β-glucanases are routinely included into diets, particularly those composed primarily of viscous grains including wheat, barley, oats, rye and triticale (Williams, 1997; Choct, 2006). These enzymes mainly work by degrading the polymeric chains of non-digestible starches into

manageable fragments and oligomers which are less likely to interfere with normal digestion and be more available up uptake by the animal (Choct, 2006). Another mode by which amylase and NSP-degrading enzymes may function is by enhancing the accessibility of nutrients in the cell wall matrix, usually bound and held by insoluble NSPs (Choct, 2006). NSP-degrading enzymes are beyond the scope of this thesis and will not be discussed in further detail.

Since the 1950s, exogenous proteases have been added to animal feed to increase protein and amino acid digestibility with the aim of reducing the amount of protein-rich material formulated into diets and thus the overall cost of feed (Smith, 2011). They provide a low-cost route of supplementation as opposed to the traditional method of adding animal/vegetable protein and/or amino acid mixtures as the prices associated with these ingredients can be volatile. Many of the early exogenous feed proteases were subtilisin proteases, non-specific alkaline proteases and those developed for use in detergents rather than feed. Important factors for a suitable exogenous feed protease include activity at low pH environments as found in the gastric phase of digestion, complementarity with endogenous enzymes, use for a variety of diets and thermo-stability. Exogenous feed protease addition to diets can lead to increases in protein digestibility between 3 – 8% resulting in a reduction of approximately €4 per ton of feed. Poultry in the early phases of growth can have underdeveloped digestive systems meaning they will produce less endogenous enzyme reducing the nutritive value of the feed. Aminopeptidase activity in 7-day old broilers was found to be 40% less than that of 21-and 42-day old broilers (Bedford, 1996; Torres et al., 2013). The addition of an exogenous feed protease can take the place of endogenous proteases until the animal has developed adequately (Dosković et al., 2013). Exogenous feed proteases have further added value in degrading proteins that are not completely digested by endogenous proteases, including trypsin and pepsin.

Some feed ingredients are low in easily digestible protein and/or low in energy density and require supplementation to provide optimal nutrient utilisation and cost-effectiveness. Proteins in these mixtures are for the most part readily digested, however, there remain opportunities to increase performance measures and nutrient digestibility with exogenous feed proteases. The digestibility and utilisation of individual amino acids for broilers is improved with exogenous feed protease supplementation (Cowieson et al., 2020). In addition to the proteins found in primary feed grains, supplemental plant protein meals, such as soybean and legumes, can reduce overall protein and nitrogen digestibility. The increased uptake of plant over animal

protein due to ethical concerns has been observed to lower digestibility and nutrient uptake in monogastrics (Brufau et al., 2006). The addition of exogenous feed proteases allows for the inclusion of grains and vegetable matter typically lower in both cost and nutrient digestibility. Additionally, the inclusion of exogenous feed proteases can alleviate environmental concerns surrounding the waste produced by animals through lowering nitrogen contents in manure (Oxenboll et al., 2011).

One solution to the phytate anti-nutrient problem in feed, discussed previously in **Section 1.4.3,** is through the addition of the most routinely added exogenous feed enzymes, phytase. Phytase is an enzyme that hydrolyses the phosphate groups attached to myo-inositol ring that makes up the core of the anti-nutrient phytate (see **Figure 1.3**). The enzyme is commonly found in nature both in plants and animals. Monogastrics possess some phytase/phosphorylase activity but typically at very low levels and depending on the age of the animal. In broiler jejunal mucosa, alkaline phosphatase activity was found to be significantly lower in 7-day old broilers than in older birds of 21- and 42-days (Torres et al, 2013).

DSM, a company based in the Netherlands, developed the first commercial exogenous feed phytase, Natuphos®, from *Aspergillus niger* (Kies et al., 2001). Unlike proteases, phytase is uniquely specific in its substrate preference with different enzyme varieties attacking different locations on phytate, e.g., a 6-phytase always cleaves the phosphate at carbon 6 first on the myo-inositol ring. An enzyme with broader actions, such as a protease, may produce unwanted negative or positive side effects in the animal (Acamovic, 2001). There are several classes of phytase and include histidine acid phosphatases (HAPs), β-propeller (or alkaline) phytases, purple acid phytases and protein tyrosine phosphatases (Dersjant-Li et al., 2015). Normal phytase activity, one FTU or FYT, is defined as the amount of enzymes that releases 1 mmol of phosphate per minute from 5 mM sodium phytate at 37°C and pH 5.5. pH is a very important factor for optimal enzyme activity, especially in the context of animal digestion. Almost all exogenous feed phytases are of the HAP class and have pH optima below 5.5 thus ensuring their activity in the acidic environment of the gastric phase. Added phytase is most active in the stomach for swine and crop for poultry while both animals maintain activity at the beginning of the intestinal phase (Dersjant-Li et al., 2015).

Exogenous feed phytase has been shown to be robust during simulated digestion, maintaining 76% of its activity through the gastric phase (Pontoppidan et al., 2007). Although the decrease in activity was significant, there was little effect on phytase's ability to degrade phytate. Similarly, another key factor for exogenous feed phytase effectiveness is its resilience to enzymatic degradation by endogenous and exogenous proteases (Smith, 2011; Glitsø et al., 2012). Most of the phytate degradation takes place in the initial phases of gastric digestion around a pH of 4 and 5 while no further degradation occurs once in the intestinal phase due to optimal enzyme pH levels (Pontoppidan et al., 2007). Interestingly, this research found a kind of steady-state reaction to occur with the degradation of phytate. As soluble phytate was degraded, levels of insoluble phytate decreased leading to a rise in levels of soluble phytate. The use of exogenous feed phytase was found to increase mineral solubility, a common finding, as phytase is degraded. Phytate is a well-known chelator and forms insoluble complexes with minerals and so as the anti-nutrient is broken down, metal ions are released. Cowieson et al. (2011) describes the phytate problem as not hinging on phytate-degrading enzyme activity but more to do with the solubility of phytate especially when complexed with calcium in the alkaline intestinal tract.

Generally, all phytase enzymes work in the same way: they catalyse the hydrolysis of phosphate groups from myo-inositol in a stepwise manner, removing phosphate groups until theoretically six free phosphates and a myo-inositol ring remain. However, the complete hydrolysis of phosphate from myo-inositol does not typically occur in practice and most enzymes leave one to two phosphate groups remaining. The addition of exogenous feed phytase increases the bioavailability of phosphorous to the animal which decreases its excretion into the environment (Kies et al., 2001). When added to feed, increasing amounts of exogenous phytase do not always lead to reciprocal, linear responses in liberated phosphorous (Bedford and Schulze, 1998). This result is echoed by Kies et al. (2001) in their review on early exogenous phytase supplementation. They state that supplementation of feed with one g/kg of MCP is equivalent to the addition of 500 FTU/kg thus providing a benchmark for the early transition from MCP supplementation to exogenous phytases. Positive results have also been gained through super-dosing exogenous phytase, the method of using unconventionally high levels of phytase in formulations. These improvements are thought to be due to increased phosphate levels and more persistent reductions in the anti-nutritive effect of phytate and its lower inositol phosphate (IP) esters as they interact with proteins and starches (Cowieson et al., 2011). IP6 has been found to be the most detrimental ester with regard to mineral, starch

and protein binding so the basic effectiveness of exogenous feed phytases can be measured by how quickly IP6 isomer levels reduce in relation to their lower mass downstream products (Dersjant-Li et al., 2015). While IP6 has been found to be most detrimental for nutrition, IP5 has demonstrated protein binding capacity, albeit at a diminished capacity as compared to IP6. The lower esters, IP4 to IP1, have been shown to have negligible impact on protein solubility as opposed to having a dose-dependent effect (Yu et al., 2012).

Beyond their targeted substrates and primary effects, exogenous feed enzymes have been found to have added beneficial effects not directly related to their target substrates, including extra-phosphoric effects for exogenous phytase and extra-proteinaceous effects for exogenous protease. Beyond increasing phosphorous availability, exogenous phytase has also been shown to positively influence amino acid/protein, starch and mineral digestibility (Cowieson et al., 2008; Cowieson et al., 2009; Liu et al., 2013; Troesch et al., 2013). *In vitro* protein precipitation studies have found phytate to complex with protein in acidic pH environments. The addition of both endogenous pepsin and an exogenous phytase were found to dissociate phytate from the protein as well as degrade the protein further thus acting in a complementary way (Kies et al., 2006). The addition of exogenous phytase is thought to increase nutrient utilisation and protein digestibility through the degradation of phytate and phytate-protein and phytate-starch complexes and has been found to increase the digestibility of phytate up to 70% in some poultry diets (Choct, 2006; Liu et al., 2013). Another of these 'extra-' effects is an indirect improvement of poultry gut health. Liu et al. (2017) studied the effects of a multienzyme supplement, including protease, phytase and xylanase, in broilers fed high- or low-protein diets. This supplementation was found to increase beneficial probiotic bacteria, including *Lactobacillus* and *Bifidobacteria*, while decreasing levels of *Clostridium perfringens*, a known causative agent in necrotic enteritis in poultry.

A major focus for development of phytase in the 1980 – 1990s was to reduce environmental stress brought about by excessive phosphate levels in soil and water associated with farming. As described in **Section 1.4.3**, traditionally, farmers supplemented feed with mineral MCP as the phosphorous in feedstuffs was bound and inaccessible to the animal as phytate. The use of phytases allows for this reliance on a non-renewable resource to be removed. Nielsen and Wenzel (2006) conducted a life cycle assessment (LCA) for a phytase in the setting of Danish pig farming and generally found that implementation of the phytase over MCP had a beneficial environmental impact. The gains observed through phytase supplementation included

reduction in harsh MCP processing methods (1900 vs. 32000 g CO_2 equivalents), energy to produce phytase (26 megajoules [MJ] per kg phytase vs. 400 MJ per kg MCP) and reduced acidification of waterways by run-off from phosphorous-rich manure (4.8 vs. 530 g SO_2 equivalents).

1.6 Focus of work in this thesis

Monogastric animal feed is routinely supplemented with a variety of additives, including exogenous feed enzymes, to increase the nutritional value of the feed and reduce environmental emissions from the animals. Two prominent and commonly used exogenous feed enzymes are phytases and proteases. Phytases act to hydrolyse and release phosphate otherwise bound to phytate in feed grain. Animals lack sufficient endogenous phytase to take fully release phosphorus bound to phytate. Additionally, unabsorbed phosphorous can enter the environment through animal waste resulting in water and soil pollution. Proteases similarly act on previously unavailable protein thus enabling greater nitrogen uptake for the animal. The use of proteases also allows for a reduction in nitrogen pollution.

While these enzymes are routinely incorporated into monogastric diets, their predicted and perceived effects can be muted, especially in diets containing sorghum grain. Sorghum grain has high energy density and is comparable to maize and wheat when incorporated into monogastric diets. Sorghum grain is also well-known to contain high concentrations anti-nutrients, especially polyphenols. These compounds are established anti-nutrients and with digestion by reducing of feed intake, binding proteins and interfering with normal digestive enzyme activity. While the interaction of polyphenols with proteins and endogenous digestive enzymes has been studied, the effects of polyphenols on exogenous feed enzymes is unknown. The purpose of this thesis was to determine the polyphenol composition of modern Australian sorghum feed grain, establish key metabolic differences between grain varieties and better understand the potential interactions these compounds might have with two exogenous feed enzymes, a protease and phytase in both simple and complex *in vitro* environments.

1.6.1 General research hypotheses and methodology

1. **Experimental Chapter 1 (Chapter 3)**
    a. Acetone polyphenol extracts from modern Australian sorghum varieties will be found to contain a variety of medium to small polyphenols, as opposed to large tannins found in historical, high-tannin varieties.
        i. Ultraviolet/visible spectroscopy (UV/Vis), Fourier-transform infrared spectroscopy (FT-IR), electrospray ionisation (ESI) and matrix-assisted laser desorption/ionisation (MALDI) were used to characterise the acetone extracts from modern Australian sorghum grains.
    b. There will be differences in the metabolic profiles between different sorghum polyphenol extracts, e.g., red grain colour vs. white grain colour.
        i. Multivariate analysis (MVA) methodologies including principal components analysis (PCA) and orthogonal partial least squares discriminant analysis (OPLS-DA) were used to analyse the spectra from FT-IR, ESI and MALDI, putatively identify compounds of interest and determine relationships between extract types.
    c. Broad analytical approaches to polyphenol extract characterisation will be suitable for generally identifying anti-nutrients and allow for rapid fingerprinting to be performed.
        i. Comparisons were made between the MVA results of FT-IR, ESI and MALDI to determine the suitability of each technique for different applications.

2. **Experimental Chapter 2 (Chapter 4)**
    a. If sorghum polyphenol extracts are introduced to exogenous phytase and protease in a simple *in vitro* environment, then they will interfere with normal enzyme activity.

3. **Experimental Chapter 3 (Chapter 5)**
    a. If interference is present in simple *in vitro* assays, do the effects persist in an *in vitro* simulated gastrointestinal model containing other feed components and endogenous digestive enzymes?
    b. If sorghum polyphenol extracts are incorporated into a simulated diet, they will interfere significantly less so than in a simple *in vitro* environment.

Chapter 2 – Methodology for the Analysis of Polyphenolic Compounds

2.1 Overview of analytical techniques

Polyphenols are an expansive group of secondary metabolites comprising several thousand compounds ranging from simple phenolic acids to highly polymerised proanthocyanidins (see **Section 1.4.4**). This unique diversity hinders the complete extraction, separation and analysis of all polyphenols using a single methodology. The study of polyphenols is of great interest to a wide variety of industries including pharmaceutical, food/beverage and agriculture as the compounds display beneficial traits including anti-viral (Park et al., 2017), anti-cancer (Dai and Mumper, 2010; Mojzer et al., 2016), astringency in wine (Sarni-Manchado et al., 1999) and defense against insects in plants (Quideau et al., 2011). However, polyphenols also have negative characteristics to be avoided like anti-nutrition in monogastric animals (Kumar and Singh, 1984; Gilani et al., 2012).

The analysis and characterisation of plant polyphenols is a key aspect of research surrounding these compounds. As new technologies emerge and methods improve, more and more compounds are being discovered bringing useful industrial applications, as well as improving knowledge of polyphenol chemistry and biosynthesis. This chapter aims to highlight the techniques used to characterise plant polyphenol extracts primarily through mass spectrometry (MS). Analysis by mass spectrometry may occur either after separation and purification of compounds using technologies including high-performance liquid chromatography (HPLC) and supercritical fluid chromatography (SFC) or by direct analysis through electrospray ionisation (ESI) and matrix-assisted laser desorption/ionisation (MALDI).

2.2 Extraction and purification

The analysis of polyphenols begins with the physical preparation of plant tissue or food samples, usually through manual grinding/shredding/macerating or mechanical processing, i.e., decortication which typically removes the outer layer of grains. Often, samples are lyophilised, or freeze-dried, prior to processing to both preserve tissue condition and ease the physical processing of the material. The most common extraction method is a liquid-liquid or solid-liquid extraction. In their basic forms, these methods use large volumes of pure or aqueous solvents (mostly aqueous), with some form of agitation or stirring, to extract metabolites from plant material over a period of a few minutes up to 24 hours. A variety of extraction techniques exist and include liquid-liquid, solid-liquid, microwave-assisted extraction, ultrasound-assisted extraction and supercritical fluid extraction (SFE). SFE is a

promising technology as it is environmentally friendly, if used with carbon dioxide (CO_2), inexpensive (after initial operating costs) and leaves the extract solvent-free and thus available for human consumption if necessary (Díaz-Reinoso et al., 2006; Aizpurua-Olaizola et al., 2015; Poontawee et al., 2015).

Unfortunately, due to the complex nature of plant extracts and the diversity of polyphenols, there is no universal solvent or method for total extraction. Solvent choice is primarily up to the researcher based on personal experience, experimental validation or through literature review but is typically a polar solvent base, primarily methanol, acetone or ethanol. The final extraction solvent preparation is usually an aqueous solution of approximately 70% (v/v) which may also be acidified. Acidification is thought to help release polyphenols, through acid hydrolysis, which are bound to certain plant tissues and may not be as readily extractable with traditional solvent preparations. Methanol appears to be the most popular extraction solvent and primarily targets small to medium sized polyphenols (up to around 500 MW) but has been used to target larger compounds. Typically, methanol and/or acetone are used for the extraction of larger proanthocyanidins, however, aqueous acetone is usually regarded as the superior choice (Foo and Porter, 1980; Cork and Krockenberger, 1991; Waterman and Mole, 1994; Barros et al., 2013). A final processing step to either the starting sample material or the liquid extract is the use of a defatting solvent, usually hexane, chloroform, dichloromethane, trichloromethane or petroleum ether, which helps clean up the sample by removing non-polar lipids and pigments, including chlorophylls, that might otherwise complicate further analyses. There is a need to be cognisant when dealing with plant extracts as the complex matrix within plant material could interfere and interact with the compound(s) of interest. Additionally, variables such as the length of extraction time and temperature need to be considered, as phenolic compounds are prone to degradation and oxidation (Naczk and Shahidi, 2006).

Finally, the extract is either lyophilised, resulting in a crude extract, or is further refined through size-exclusion fractionation typically on columns filled with Sephadex LH-20 resin or C18 cartridges, additional solvent extractions (usually with ethyl acetate) and/or preparative separation using HPLC (Monagas et al., 2010). Solid phase extraction, i.e., using column chromatography or HPLC, is most used prior to any further analysis and characterisation of polyphenol extracts. A wide range of resins are available and can be combined with variable solvent washes to isolate specific fractions from the original crude extracts based on size, charge or polarity. However, size exclusion practices can be flawed as tannins tend to bind to

columns unless very aprotic solvents are used (Gu et al., 2002). Faster and more accurate separations can be performed using liquid chromatography (LC), HPLC (Bianchi et al., 2016), ultra-performance liquid chromatography (UPLC) (Karonen et al., 2015) and SFC (Kamangerpour et al., 2002; Ashraf-Khorassani and Taylor, 2004; Fernández-Ponce et al., 2004; Ganzera, 2015; Eisath et al., 2017) techniques primarily using a reverse-phase (RP) C-18 column. These techniques, like a gravity column, can be optimised and adjusted in a variety of ways including solvent type, elution pattern, temperature and pressure.

2.3 Basic spectroscopic analysis

Once a crude or purified extract has been obtained, a common first step of analysis is the quantification of phenolic content, typically through colourimetric measurement. The most common assay used is the Folin – Ciocalteu (F – C) method for determining total phenolic content (TPC) of a plant extract. This method relies on the transfer of electrons from phenolic compounds to phosphomolybdic/phosphotungstic acid complexes. The complex formed produces a blue colour that is measured at 760 nm and can be used to determine concentration in gallic acid equivalents (GAE) (Ainsworth and Gillespie, 2007). Besides the F – C method, TPC can be measured using the Folin-Denis method, similar to F – C, and the Price-Butler method, which relies on Prussian blue. These assays use a range of standards to determine TPC including gallic acid, tannic acid and chlorogenic acid. For more detailed analysis, individual families of phenolic and polyphenolic can be quantified separately by a variety of assays, e.g., condensed tannins may be measured using the proanthocyanidin or vanillin-HCl method (Waterman and Mole, 1994). Spectroscopic analysis of polyphenols can lead to overestimation as other compounds in an extract can interfere with the reagents and give false-positive results (Naczk and Shahidi, 2006). There are several issues regarding the analysis of tannin content in plant tissues, including the inability to quantify the insoluble tannins (Bravo, 2009).

2.4 High-performance liquid chromatography (HPLC)

One of the most common methods for analysing and characterising polyphenols is by using HPLC combined with a variety of detectors, including a UV detector and/or a mass spectrometer (**Table 2.1**).

Table 2.1 HPLC studies of polyphenol extracts

Reference	Sample	Chromatography	Detection/analysis	Identification/compounds
Kilmister et al., 2016	*Theobroma cacao* (cacao)	HPLC (Agilent 1100), 250 x 4.6 mm, 5 um Develosil diol column	ESI - ion trap mass spectrometer (G2445D Bruker, negative mode	Procyanidins – 1-7+ DP
Harbertson et al., 2014	*Theobroma cacao* (cacao)	HPLC (Agilent 1100), 250 x 4.6 mm, 5 um Develosil diol column	ESI - ion trap mass spectrometer (G2445D Bruker (negative mode)	Procyanidins – 1-7+ DP
Poncet-Legrand et al., 2007	*Vitis vinifera* (grape seed, Shiraz)	Nucleosil C18 (125×4mm) (Macherey-Nagel)	DAD 280 nm	14% epicatechin gallate, aDP 3.8, procyanidins/prodelphinidins 3-28 DP
Svensson et al., 2010	Red sorghum	HPLC (Luna C18 RP-HPLC column (5 µm, 250 x 4.6 mm, Phenomenex) and C18 precolumn (Phenomenex) for separation of the polyphenols	DAD (190-400 nm) 4000 Q TRAP LC-MS/ MS System (MDS SCIEX)	Mostly phenolic acids, highest was procyanidin dimer (577), quantified with standards
Langer et al., 2011	Cocoa	Develosil Diol (250 mm x 4.6 mm, 5 µm)	DAD (280), FLC (excitation 230 nm, emission 321 nm)	Quantification using standards up to a group of compounds with DP greater than 11
Rao et al., 2018	Sorghum – red, white, brown, black	Agilent UHPLC (Agilent Technologies, CA, USA) system with a C18 Poroshell120 column (3.0 mm×100 mm, 2.7 µm)	DAD (280 nm) Agilent 6530 Accurate-Mass Q-TOF LC/MS	56 different polyphenols

The most common HPLC solvent/column format is reverse phase (RP). This method involves the use of predominately C18 (non-polar) columns with a gradient elution system of water, typically acidified, followed by a polar solvent, usually methanol or acetonitrile (Ignat et al., 2011; Oroian and Escriche, 2015). The detection of compounds is then made with a variety of analysers but most often involves UV diode array detection (DAD) and/or MS (Ignat et al., 2011). DAD appears to be most popular with detection at either 254 or 280 nm. This is due to the ease of detection of phenolic structures in the ultraviolet/visible spectra (UV/Vis) because of their plethora of conjugated double bonds and aromatics (Dai and Mumper, 2010). More frequently, HPLC conjugated to both DAD and MS analysis provides even more information and accuracy as the general groups of compounds can be first identified in a non-destructive manner prior to being more thoroughly scrutinised by destructive MS analysis (de Villiers et al., 2016).

RP-HPLC methods have been shown to be successful at separating and identifying both aglycone and glycone species, different oxidation variants, isomers and various acylated compounds (de Villiers et al., 2016). The use of RP-HPLC separates polyphenols based on their hydrophobicity, with most systems using a highly non-polar C18 column. This column, and others like it, have a predictable elution order of compounds that is determined by structural features including hydroxyl groups, methyl group, acylation and sugar moieties (de Villiers et al., 2016). RP-HPLC has been used countless times to successfully quantify and detect lower MW polyphenols based on comparison of retention times, mass spectra and chemical

standards. Using RP-HPLC-ESI-MS and RP-HPLC-ion trap MS, Kang et al. (2016) identified approximately 75 compounds in white and red sorghum grain hydromethanolic extracts. This was achieved by chromatographic separation in the mass range 150 – 550 *m/z* over 40 minutes. Another common technique involves a thiolysis or phloroglucinolysis reaction followed by RP-HPLC-MS, often incorporating ESI. These reactions are selective acid depolymerisations using a thiol, usually toluene-α-thiol, or phloroglucinol as a nucleophile. The depolymerising agent is added to the sample, heated for a short period and then usually directly injected onto a RP column (Vivas et al., 2004). This method allows for the characterisation of all proanthocyanidins in a sample by releasing the monomers and identifying them using MS. This technique also provides the average degree of polymerisation (aDP) of the sample analysed. The method has been used by Gu et al. (2002) to successfully calculate an aDP of over 100 for blueberry procyanidins. However, thiolysis cannot give the MW distribution of proanthocyanidins and is non-specific as the reagents used are indiscriminate with the cleavage of interflavan bonds (Mané et al., 2007; Mouls et al., 2011).

Normal phase (NP) HPLC is primarily used for larger proanthocyanidin analysis due to solvent compatibility and column type. A silica column is commonly used which allows the polymerised polyphenols to elute based on increasing molecular weight and degree of polymerisation (DP). Langer et al. (2011) were able to achieve chromatographic separation of cocoa proanthocyanidins up to DP 10 using NP-HPLC with fluorescence detection followed by quantification of the polymers using pure standards. Similar chromatographic separation was also achieved in cocoa by Hammerstone et al. (1999) using ESI-MS to detect proanthocyanidins with a DP up to 10. However, isomers at the same DP co-elute and their elucidation is not possible without further analysis and refinement (de Villiers et al., 2016). In addition to RP- and NP-HPLC, hydrophilic interaction liquid chromatography (HILIC) is an interesting and growing methodology in polyphenol research. It provides a middle ground between RP and NP in that smaller phenolics limited to RP can be analysed, often better than before, in NP conditions thus allowing a greater range of compounds to be included in a single analysis (de Villiers et al., 2016). Recently, several HPLC methods have been combined to increase separation and visualisation of a larger variety of compounds using a single methodology. Venter et al. (2018) combined ion mobility spectrometry with two LC columns: one a RP C18 and the other a HILIC amide column. They found this method to increase sensitivity, separate isomers and improve identification and characterisation.

A challenge to using these methods is the limitation of compound size when using certain columns, particularly in RP. Beyond a DP of approximately 4, RP-HPLC is not capable of sufficiently separating larger proanthocyanidins (Hayasaka et al., 2003; Monagas et al., 2010) While HPLC methods are frequently used for quantification of certain compounds in samples, there is the need to have purified standard chemicals in order to properly quantify unknowns (Tsao, 2010). This is an issue, especially when dealing with proanthocyanidins, as no true standard exists for these large molecules. Procyanidin dimers and some oligomers have been purified and standardised for use in quantifying large proanthocyanidins. The most successful quantifications have been made using standards extracted and prepared from individual research groups (Gu et al., 2002; Awika et al., 2003). For quantification of proanthocyanidins and polyphenols, HPLC methods provide the most reliable and reproducible results. They fall short, however, in the identification of large molecular weight compounds and are limited to DP 4 for RP and DP 10 for NP.

2.5 Direct-injection electrospray ionisation (ESI)

Direct-injection ESI allows for the rapid analysis of polyphenols using a small volume of diluted extract and provides a 'soft ionisation' technique. ESI-MS is a useful method for obtaining a fingerprint of the extract at hand (Ignat et al., 2011; Oroian and Escriche, 2015). Negative ion mode is the most popular and successful mode with ESI polyphenol analysis due to the propensity of the acidic hydroxyl groups to lose a proton (H+) (Vivas et al., 2004). Positive mode has been successful in smaller oligomers, especially in conjunction with HPLC methods that use acidified solvents (Rue et al., 2018). ESI is typically applied in conjunction with an HPLC system as the ionising system but can be successfully used as in a direct injection system. In grape seed extracts, direct injection ESI-MS was used to identify proanthocyanidins up to DP 28. Modifications and alterations to the core structures were also identified and characterised (Hayasaka et al., 2003). The analysis of thiolysis products using ESI-MS allows for the identification of monomers in a mixture of polymers, the degree of galloylation as well as the average DP (Vivas et al., 2004). The interpretation of ESI spectra can become complicated, especially with highly polymerised structures, due to the formation of multiply charged ions (Monagas et al., 2010). While the presence of multiply charged ions can complicate interpretation it also increases the total mass range of a spectrometer (Rue et al., 2018). While ESI alone cannot provide the same quantitative power as HPLC, it is an excellent

method for the characterisation and identification of compounds, especially highly polymerised proanthocyanidins.

2.6 Matrix-assisted laser desorption/ionisation (MALDI)

MALDI combined with time of flight (ToF) mass analysis of polyphenols and tannins has proved to be a successful way of ionising large, highly polymerised compounds without fragmenting them (**Table 2.2**).

Table 2.2 MALDI studies of polyphenol extracts

Reference	Sample	Sample solvent	Matrix	Cationization agent	Mode	DP	Proanthocyanidin
Bianchi et al., 2014	*Picea abies, Abies alba*	2.5 mg/mL in 50% acetone	DHB (10 mg/mL in pure acetone)	KCl (10 g/L in water)	Linear, positive	2-13	Procyanidin, prodelphinidin
Bianchi et al., 2015	Abies alba Larix decidua Picea abies Pseudotsuga menziesii Pinus sylvestris, commercial Quebracho and Mimosa extracts (Silvateam)	2.5 mg/mL in 50% acetone	DHB (10 mg/mL in pure acetone)	KCl (10 g/L in water)	Linear, positive	3-14	Procyanidin, prodelphinidin
Krueger et al., 2003	*Sorghum bicolor* (Ruby Red)	Not specified, methanol and acetone fractions mixed 1:2 with matrix, ethanol fraction mixed 1:1 with matrix	*t*-IAA (50 mg/mL in 80% acetone)	NaCl and KCl (0.1 M), silver trifluoroacetate (0.01 M), cesium trifluoroacetate (0.01 M)	Reflectron, positive	3-9	Procyanidin, prodelphinidin, heteropolyflavan
Pasch et al., 2001	Pecan nut, Mimosa, Quebracho	4 mg/mL in acetone	DHB (10 mg/mL in acetone)	NaCl	Linear, positive	2-10	Profisetinidin, prorobinetinidin/procyanidin
Ohnishi-Kameyama et al., 1997	Apple	500 mg/L in acetone	Tested a variety, *t*-IAA, DHB, CHCA, SA, 9-NA, 5CSA, HABA, dithranol (10 mg/mL, exact solvents not given but probably acetone)	Silver trifluoroacetic acid, lithium trimethanesulfonate (1 mM in acetone)	Linear and reflectron, positive	3-11	Procyanidin
Vivas et al., 2004	Grape, Quebracho	10 mg/mL in methanol	DHB (10 mg/mL in methanol)	NaCl?	Reflectron, positive	3-10	Procyanidin, prodelphinidin, profisetinidin

A similar ‘soft ionisation’ technique to ESI, MALDI provides several benefits including the generation of singly charged ions, as opposed to multiple, and the ability to analyse samples more than once (Monagas et al., 2010). In sorghum extracts, MALDI has been successfully

applied to characterise proanthocyanidins up to dodecamer (Qi et al., 2018). There are several variables and optimisations to be considered when using MALDI, including choice of matrix chemical, sample concentration and solvent, the presence of any cationisation agents, ratio of sample components and variations to the time-of-flight (ToF) analyser. A range of matrix chemicals are available but the most common ones for polyphenol and tannin analysis are 2,5-dihydroxybenzoic acid (DHB) or *trans*-3-indoleacrylic acid (*t*-IAA). The first major study to investigate the effect of matrix on proanthocyanidin detection was Ohnishi-Kameyama et al. (1997). They concluded that *t*-IAA and DHB ionised larger proanthocyanidins better than the other six matrix compounds tested. Several cationisation agents have been used including silver trifluoroacetate, sodium chloride, cesium trifluoroacetate, sodium iodide and cesium chloride, in varying concentrations and solvents. Almost all studies use a laser set to 337 nm but other variations have been used. The ToF analyser can be set to either reflectron or linear mode as well as positive or negative ion mode. Positive mode in MALDI is routinely used for polyphenol and proanthocyanidin analysis. High resolution is achieved with the reflectron mode and higher sensitivity in linear. Linear spectra typically give a better representation of the total mass range while reflectron is better suited to allowing identification of compounds (Monagas et al., 2010). MALDI can resolve slightly higher DP than ESI (Mouls et al., 2011).

Interpretation of MALDI spectra can be complicated by several factors. Due to the nature of the method, the use of a chemical matrix mixed with the sample provides room for interference in interpreting the final spectrum, especially below 500 *m/z*, where most of the ions from the matrix form (Monagas et al., 2010). A second feature to note in the spectra are the presence of different cation adducts, which may or may not be purposely formed. The analysis of a natural extract will invariably include the many cations present, like Na+ and K+, in the tissue when the polyphenols were extracted. These cations often appear in the final spectra and must be accounted for when elucidating chemical structures. Identifications may become more complex if several cations are present in the same spectra. MALDI is typically not very useful for quantitative measures as the observed ion intensities can vary greatly (Monagas et al., 2010). This puts MALDI at a significant disadvantage to HPLC methods which routinely use standards to accurately quantify phenolic compounds. While this is a useful approach often, it is not always a desired one and obtaining a general fingerprint and observing total mass range are better suited for MALDI.

2.7 Supercritical fluid chromatography (SFC)

SFC employs the use of a supercritical fluid, usually CO_2, as a liquid phase like traditional solvents in HPLC methods. Instead of a liquid solvent, such as methanol or acetonitrile as is common in polyphenol analysis, SFC uses solvents in supercritical states where they act as both a gas and a liquid. This kind of mobile phase exhibits several beneficial properties including high diffusivity, low viscosity and high solvating power (Liu et al., 1999; Ramirez et al., 2006). SFC allows for better separation of extract components, reduces the use of solvents, shortens analysis time and provides better analysis of thermolabile compounds due to lower running temperatures (Ramirez et al., 2006; Ajila et al., 2011). SFC can resolve both non-polar and polar analytes in the same separation by modifying the base CO_2 supercritical fluid with a variety of polar solvents and often acidic modifiers. SFC has been shown to be able to separate and resolve crude plant extracts at very low concentration in short periods of time (Ganzera, 2015). These attributes give it a distinct advantage over traditional HPLC methods.

Several solvents have been used in their supercritical states in SFC but the most commonly used is CO_2 due to its low toxicity, low flammability and low critical temperature (Liu et al., 1999). However, CO_2 on its own is not suitable as a mobile phase for polyphenol analysis as the solvent is highly non-polar and the analytes are mostly polar. To counter this, cosolvents, also known as modifiers, are added in a linear or gradient fashion to bring out the polar components of the sample. Further additives, mostly organic acids, can also be added to the mixture to optimise analysis, similar to HPLC. Liu et al. (1999) found CO_2 alone, as well as mixed with ethanol, to be unsuitable for the complete analysis of four common flavonoids: isorhamnetin, kampcetin, quercetin and fisetin. While an increase in phosphoric acid did not affect the retention time, peak shapes improved with addition of the weak acid. The reverse effect was observed as the concentration of ethanol was varied with a constant additive concentration. As the percentage of ethanol increased, from 8 to 10%, the retention times of the compounds decreased significantly. Methanol has been used successfully as a cosolvent to CO_2 in SFC with the addition of organic acids (Kamangerpour et al., 2002). This group tested citric, formic and trifluoroacetic acids and found citric acid to be the most successful additive and performed best when diluted to 0.25%. Xia et al. (2014) improved upon this and found methanol accompanied by both 0.1% TFA with 10 mM citric acid to be most successful in separating a mixture of polyphenols which included the non-polar compound scopoletin and

the more polar compounds quercetin and rutin. Similarly, Ganzera (2015) was able to separate and resolve a mixture of non-polar and polar polyphenols from both refined and crude plant extracts using methanol with 0.05% phosphoric acid as the modifier.

Beyond the mobile phase, other variables can be adjusted to optimise separation. Increasing the temperature has been found to slightly increase retention time (Liu et al., 1999; Kamangerpour et al., 2002; Ramirez et al., 2006). Additionally, lower temperature has been shown to produce higher resolution of later peaks while the earlier peaks benefited from higher temperatures (Kamangerpour et al., 2002). Care must be taken when adding higher concentrations of cosolvent as the critical temperature of CO_2 will increase, thus making the temperature subcritical (Ajila et al., 2011). Increasing the pressure increases the solubility of solutes into the mobile phase, reduces retention time and sharpens peaks (Liu et al., 1999; Ramirez et al., 2006).

SFC has been used sparingly in the analysis of polyphenolic compounds and primarily limited to the identification of smaller phenolic acids and monomeric flavonoids (**Table 2.3**).

Table 2.3 SFC studies of polyphenol extracts

Reference	Sample	Column	Solvent	Modifier	Elution	Pressure	Temperature	Compounds
Liu et al., 1999	Standards	Phenyl	CO_2	Ethanol Phosphoric acid	Isocratic - 90:9.98:0.02 v/v/v	25 MPa	50°C	Fisetin, quercetin, kampcetin, isorhamnetin
Kamangerpour et al., 2002	Standards Grape seed extract	Two Diol (250 x 4.6 mm OD) in series	CO_2	Methanol 0.25% citric acid	93/7% for 1 min, ramp 1.7%/min I to 83/17%, then ramp to 55/45% CO2/MeOH at 4%/min, hold for 10 min	125 atm	40°C	In extract: 2-phenylethanol, gallic acid, catechin, and epicatechin)
Ganzera, 2015	Standards Soy (*Glycine max*), red glover (*Trifolium pratense*) and kudzu (*Pueraria lobata*)	Acquity UPC2 BEH 1.7 um column (3.0 mm × 100 mm)	CO_2	Methanol 0.05% phosphoric acid	98A/2B, changed in 10 min to 75A/25B; column flushed for 5 min with 75A/25B, equilibrated for 5 min under the initial conditions	150 bar	50°C	In extracts: Biochanin A, formononetin, genistein, glycitein, daidzein, genistin, glycitin, daidzin, puerarin
Xia et al., 2014	Standards	Acquity UPC2 BEH 1.7 um column (3.0 mm × 100 mm)	CO_2	Methanol 0.1% TFA 10 mM citric acid	90/10% A/B, hold for 1 min, linear gradient from 10-30% A/B (1-3 min), hold for 3 min	1800 psi	70°C	Scopoletin, quercetin, rutin

The technology has not been, to this researcher's knowledge, applied to the separation of larger polymerised polyphenols. Proanthocyanidins, while polar due to their many hydroxyl groups, are still large molecules that exhibit non-polar properties. The combination of a non-polar mobile phase of supercritical CO_2 with polar alcohols and solvents may prove beneficial to the separation of large proanthocyanidins. SFC may outperform previous HPLC methods with respect to quantification and combined with MS analysis might prove useful in the separation and identification of new compounds.

2.8 Conclusions

Polyphenols are an incredibly diverse group of plant secondary metabolites ranging from small, polar phenolic acids to highly polymerised, bulky proanthocyanidins. Individual plants can contain this wide range of compounds in small sections of tissue which hampers their categorical extraction and characterisation using only one or even two methods. This roadblock towards universal extraction and characterisation means researchers must be cognisant of their sample types and compounds of interest before extraction and analysis.

Chapter 3 – Profiling and Characterisation of Sorghum Polyphenol Extracts and Tannin Extracts Using Complementary Spectroscopic and Spectrometric Techniques

A significant amount of this experimental chapter has been peer reviewed and accepted for publication in a conference paper and full original research article. Portions of the text have been copied from the citations below and/or modified/expanded on for the purposes of this thesis. Copies of both published works can be found in **Appendix D**.

Hodges, H., Cowieson, A., Falconer, R., Cameron, D., (2020). Chemical profile and effects of modern Australian sorghum polyphenolic-rich extracts on feed phytase and protease activity. *Proceedings of the Australian Poultry Science Symposium*. **31**, 76-79.

Hodges, H.E., Walker, H.J., Cowieson, A.J., Falconer, R.J., Cameron, D.D., (2021). Latent Anti-Nutrients and Unintentional Breeding Consequences in Australian *Sorghum bicolour* varieties. *Frontiers in Plant Science*, **12**, 626260.

3.1 Summary

The beneficial roles polyphenols play in human health are recognised and well-studied. However, these compounds have reported negative effects, especially regarding animal nutrition. Sorghum, an important feed grain for monogastric animals, has long been established as having high levels of polyphenols relative to similar cereal grains like maize and wheat. These compounds range from small phenolic acids to large, highly polymerised condensed tannins. Since the 1990s, sorghum varieties have been selected for desirable trains including increased digestible protein and starch content, increased mould resistance and most significantly, reduced levels of polyphenols, especially larger tannin structures. This has led to the belief that modern sorghum varieties used today are 'tannin-free' and thus free of the real and perceived anti-nutritional effects observed in diets containing high-tannin varieties. However, current diets using sorghum grain alongside exogenous feed enzymes do not show expected responses regarding certain nutrient digestibility and utilisation parameters. Several negative intrinsic factors of sorghum gain are thought to be at fault: kafirin protein, phytate and polyphenols. As large polyphenols, i.e., tannins, have been reduced or eliminated in modern sorghum grains, a more diverse group of non-tannin polyphenols and anti-nutrients may be a contributing factor to muted exogenous enzyme responses in feed containing sorghum grain.

To better understand the non-tannin polyphenols that might have negative effects on nutritional parameters, the chemical compositions of sorghum grain acetone polyphenol extracts from three modern Australian commercial varieties (MR-Buster, Cracka, Liberty) were determined through the use of an under-studied, alternative analytical approach utilising ultraviolet/visible (UV/Vis) spectroscopy, Fourier-transform infrared (FT-IR) spectroscopy and direct ionisation mass spectrometry (MS). Supervised analyses and interrogation of the data contributing to variation between sorghum polyphenol extracts resulted in the putative identification of a variety of metabolites, including established polyphenols, lignin-like anti-nutrients, sugars, as well as high levels of fatty acids which could contribute to nutritional variation and underperformance in monogastrics. FT-IR and MS could both discriminate among the different sorghum varieties indicating that FT-IR, rather than more sophisticated chromatographic and MS methods, could be incorporated into quality control applications.

3.2 Introduction (adapted from Hodges et al., 2021)

3.2.1 Sorghum grain polyphenols

While polyphenols are ubiquitous to grains and fruits, sorghum grain has long been known to have markedly high levels of these compounds. The high concentration of polyphenols, up to 10 – 20% of the grain's mass in certain varieties, is also partly why sorghum grain has been stigmatised as an inferior ingredient when used in animal feed (Bravo, 1998; Kaufman et al., 2013). The elevated polyphenol contents are particularly noticeable in certain high-tannin varieties, often referred to as 'bird-resistant.' Bullard et al. (1980) found, when studying bird preference for sorghum, that the least preferred 'bird-resistant' grains were the ones with the worst reputations regarding their nutrition. This has encouraged farmers to still plant some 'bird-resistant' sorghum grains among their fields as a deterrent to bird predation. Polyphenols are well-established anti-nutrients and antifeedants, particularly to monogastrics, and routinely lead to reduced feed intake and weight gain, increased FCR (reduced efficiency) and endogenous digestive enzyme inhibition (Bravo, 1998; Cadogan and Finn, 2010; Pasquali et al., 2016; Alu'datt et al., 2018).

The highest levels of polyphenols in sorghum are found in the leaves and outer portions of the plants as UV light is a necessary stimulus for the synthesis of certain metabolites (Stafford, 1965; Bravo, 1998; Wu et al., 2017). Light was not found, however, to be a necessary stimulus for the formation of some lower molecular weight polyphenols and anthocyanins (Stafford, 1965). Flavonoids have been found to accumulate after initial plant growth has ended. Glennie et al. (1981) developed a preparative HPLC method for separating acetone extracts from 'bird-resistant' sorghum and studied the patterns of appearance of condensed tannins. At the flowering stage, only the (epi)catechin monomer was detected. Upon fertilisation, tannin content increased as the testa was formed. Within sorghum grain, polyphenols are primarily located in the bran, testa and aleurone layer and can be effectively removed with an 88 – 96% reduction in tannin content with dehulling of the grain (Youssef, 1998; Dykes and Rooney, 2007) (see **Figure 1.2**). The biological roles of polyphenols in sorghum are varied and still being investigated but are thought to be important primarily for structure and defense. Phenylpropane glycerides, often found in sorghum extracts, have been linked to roles in cell wall stability and formation (de O. Buanafina, 2009; Kang et al., 2016). A higher concentration and greater variety of polyphenols has also been linked to fungal infection resistance (Hahn et al., 1983) and bacterial infection (Mareya et al., 2019).

The genetics of sorghum polyphenol biosynthesis have only recently been uncovered as the genome was fully sequenced in 2009 (Paterson et al., 2009). Following this discovery, Wu et al. (2012) identified the *Tannin1* gene that is responsible for late-stage flavonoid and anthocyanin biosynthesis and regulates the synthesis of condensed tannins. This gene is well-conserved, homologous to *TTG1* in *Arabidopsis thaliana* and encodes for a WD40 protein that forms a complex with two other factors to help regulate flavonoid biosynthesis, particularly during panicle and seed coat development in the grain. Sorghum breeding efforts have focussed on genetic controls of pericarp and other secondary plant colours to alter polyphenol content (Awika et al., 2004a). The resulting modern varieties from these breeding strategies are now thought of as 'tannin-free,' i.e., free of large condensed tannins that were traditionally detected in sorghum polyphenol extracts. While these primary anti-nutrients have been successfully removed, sorghum grains still present issues in feed formulations with certain nutrient targets not being met and responses to exogenous feed additives, like enzymes, being muted (Liu et al., 2014; Truong et al., 2014; Truong et al., 2016; Selle et al., 2017). This indicates that the issue of anti-nutrients in sorghum grain may not be entirely due to condensed tannins but to latent non-tannin anti-nutrients making up much larger and complex polyphenol metabolite profiles.

Most polyphenols routinely detected in sorghum grain can be split into two broad groups: phenolic acids and flavonoids. Within the flavonoid grouping a range of compounds are found, including flavanones, flavan-3-ols, anthocyanidins and condensed tannins.

The phenolic acids, the smallest of the phenolic compounds, can be divided into two families: hydroxycinnamic and hydroxybenzoic acids (see **Section 1.3.4**). These compounds originate from the shikimate and phenylpropanoid biosynthesis pathways and have a common precursor of *p*-coumaric acid. The primary phenolic acids routinely detected in sorghum include *p*-coumaric acid, ferulic acid, caffeic acid, chlorogenic acid and ellagic acid (Hahn et al., 1983; Svensson et al., 2010; Luthria and Liu, 2013; Wu et al., 2017; Irondi et al., 2019). These simple compounds provide the building blocks for a vast array of polyphenols including phenylpropanoids and flavonoids. Related to phenolic acids, more complex phenylpropane glycerides include a wide variety of phenolic acid-based structures including caffeoylglycerol, coumaroylglycerol, dicaffeoylglycerol, coumaroyl-caffeoylglycerol, and coumaroyl-feruloylglycerol (de O. Buanafina, 2009; Svensson et al., 2010; Kang et al., 2016). An

overlooked source of phenolic acids in sorghum grain is the unique waxy coating of the seed which contains approximately 30% *p*-hydroxybenzaldehyde, a simple phenolic acid, bound to dhurrin, a cyanogenic glycoside derivative of tyrosine (Woodhead et al., 1982; Haskins and Gorz, 1985). Sorghum has been previously found to be toxic to livestock due to its consumption as a forage crop, especially the growing green leaves containing high concentrations of cyanide within the compound dhurrin. While dhurrin may be present in contemporary animal feed, concentrations are minimal in fully formed grain (Wall and Blessin, 1969). This indicates that other compounds, including polyphenols, may be contributing to the overall anti-nutritional effects still seen today in feed containing sorghum grain.

Flavonoids make up the largest class of plant polyphenols and include subclasses such as anthocyanidins, flavones, flavonols, flavanones, flavans and flavanols. Flavanones commonly found in sorghum grains include eriodictyol and naringenin (Taleon et al., 2012; Taleon et al., 2014; Wu et al., 2017). Differences have been reported among varieties as Taleon et al. (2014) identified eriodictyol in four of seven varieties of red and white grains, while naringenin was found in all. Flavones are found in both red and white sorghum varieties and include luteolin and apigenin (Svensson et al., 2010; Taleon et al., 2012; Taleon et al., 2014; Wu et al., 2017). These compounds can be found in either two states: un-glycosylated or glycosylated, with glycosylated being the more natural and ubiquitous form.

Sorghum grains also contain unique polyphenols known as 3-deoxyanthocyanins (3-DAs) which help give the different grain varieties their colours. The primary 3-DAs found in sorghum are apigenindin, luteolinidin, 5-methoxy-luteolinidin and 7-methoxy-apigenidin (Khoddami et al., 2017) (**Figure 3.1**). The monomeric 3-DAs have also been found to polymerise with flavones to create unique dimers, e.g. apigenindin-apigenin (Geera et al., 2012).

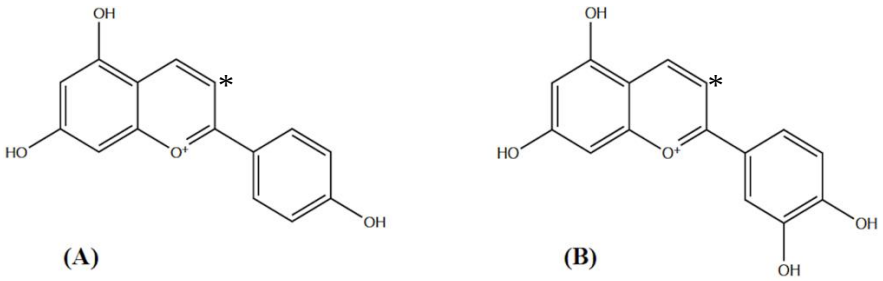

Figure 3.1 Sorghum 3-deoxyanthocyanins (3-DAs)

Sorghum is unique in its polyphenol content as it contains high levels of 3-DAs, compounds stable at acidic pH levels due to lack of hydroxyl group at C-3 (*). **(A)** apigeninidin, **(B)** luteolinidin (adapted from Awika et al., 2004b).

The presence of a pigmented testa has been found to correlate with higher levels of 3-DAs and condensed tannins. Black and red coloured sorghum grains contain more 3-DAs than brown or white coloured grains, while brown varieties have been found to have more condensed tannins than red, white or yellow coloured grains (Awika et al., 2005; Rhodes et al., 2014). While colour may be a generalised indicator of polyphenol type or content, this is not always true and should be confirmed through quantitative analysis using the TPC assay or similar methods (Bullard et al., 1980). Taleon et al. (2012) found that flavonoid content in eight different black sorghum varieties did not correlate with colour. 3-DAs are of important economic and health interest as they have been reported to have strong anti-proliferative properties towards specific cancer cells (Yang et al., 2009). These unique compounds can act as phytoalexins as concentrations of luteolinidin and apigeninidin were shown to increase with fungal infection (Boddu et al., 2004).

One of the most widely studied groups of sorghum flavonoids are condensed tannins. While primarily found in certain high-tannin and 'bird-resistant' varieties, condensed tannins composed of flavonol monomers, such as (epi)catechin, are an important group of compounds routinely associated with anti-nutritional effects observed in monogastrics. While this group of polyphenols is difficult to fully characterise (see **Chapter 2**), some studies have produced significant results. The primary condensed tannins found in sorghum are (epi)catechin based and can range from simple dimers, such as procyanidin B1 and B2 (see **Section 1.3.4**, **Figure 1.8**), to polymers with 10 or more subunits (Awika et al., 2003; Gu et al., 2003; Gu et al., 2004; Kaufman et al., 2009; Svensson et al., 2010). Within purified fractions of polyphenols, larger compounds have been identified in groupings of increasing degrees of polymerisation, e.g., 1-2, 3-9, 10-22 and >22 (Kaufman et al., 2013). Some heterogeneity of polymers within sorghum polyphenol extracts has been detected with other flavonoid monomers, delphinidin, (epi)afzelechin and (epi)gallocatechin, making up a small proportion of tannins found in sorghum grain (Brandon et al., 1982; Jiang et al., 2020).

Traditionally, sorghum varieties have been grouped into categories based on their tannin type and content and classed as Types I, II or III (Rooney and Miller, 1982). These groupings have been used to correlate tannin content with perceived anti-nutritional effect and thus nutritional

value. Type I sorghum is characterised as having an unpigmented testa and no condensed tannins present. Type II sorghum grains have a pigmented tested and condensed tannins present. However, these tannins are classed as being unextractable with traditional solvents, i.e., aqueous methanol and acetone, but need acidified solvents to hydrolyse phenolics bound to components of the grain matrix. du Plessis (2014) evaluated sorghum phenolic content with different extraction solvents and found acidified methanol to have the highest content. This study also found solvent extractability to increase significantly with the addition of 30% water. Type III varieties have both a pigmented testa and condensed tannins, however, tannins may also be found in the pericarp (Asquith et al., 1983). Asquith et al. (1983) compared tannins of Type II and III and found them to be effectively identical in quantity (total phenol, vanillin, protein precipitation, anthocyanin), chain length and structure. This classification system, while useful for the presence of condensed tannins, does exclude the presence of non-tannin polyphenols and related anti-nutritional compounds present in the grain (Awika et al., 2004a).

While certain varieties of sorghum grain are known to contain high concentrations of condensed tannins, there is some debate about whether modern feed-relevant grain varieties contain meaningful or even detectable levels of these compounds (Perez-Maldonado and Rodrigues, 2009; Liu et al., 2015; Bean et al., 2018). Research surrounding this notion seeks to move the debate and discussion from condensed tannins and similar large polyphenols to smaller and more variable non-tannin polyphenols which may contribute to muted and sub-standard results seen in animal nutrition, even with 'tannin-free' grains. However, considerable debate remains regarding this issue with most discourse arising about methodologies used to detect and quantify tannins. Several assays are available to detect and/or quantify polyphenols and include rapid, qualitative and more thorough, quantitative methods (Bean et al., 2018). There is a need for a unified, rapid and reliable method for the determination of tannin in sorghum grain and other plant materials.

While complex approaches to purification have most often been used when dealing with polyphenol extracts, including sorghum, the purposeful study and analysis of crude extracts, specifically, has been little evaluated. Most previous sorghum polyphenol analyses have used purification and fractionation followed by LC-MS with compound identification achieved through use of standards, retention time comparison, and MS^n fragmentation (Kang et al., 2016; Rao et al., 2018; Tugizimana et al., 2019; Jiang et al., 2020; Zhou et. al, 2020). These studies are incredibly useful when determining specific pathway regulations, isolating bioactive

compounds for medicinal studies or as standard benchmarks to compare to previous studies. However, the purposeful study of crude extracts is important as it helps to better understand the realities of interactions occurring within biologically relevant systems. Within the grain matrix, interactions occur and might result in sugar-, protein-, lipid- or mineral-polyphenol complexes. Purification processes remove these complexes and when purified compounds are tested as inhibitors or added to animal feed, the effects observed are most likely amplified from what they might have been in a more natural state. The testing of crude extracts, while still removed from reality, attempts to keep these important complexes together.

The use and comparison of less intensive methodologies, including direct ionisation and infrared spectroscopy, has been little studied in sorghum, especially regarding characterising metabolic variation between grain varieties important to the animal feed industry. Currently, there exists no comparative framework for the assessment of orthogonal methods of analysis for polyphenol extracts, particularly crude extracts, from feed-relevant sorghum grains. This chapter presents an alternative analytical framework for characterising polyphenol anti-nutrients in crude acetone polyphenol extracts from three Australian sorghum varieties (MR-Buster, Cracka, and Liberty). Using a series of analytical techniques from simple spectroscopy to more complicated mass spectrometric methods, untargeted and targeted metabolomics methodologies were applied to the data to determine both bulk and subtle differences in metabolite profiles.

3.2.2 Research aims, hypotheses and methodology

The aim of the present work was to evaluate an alternative analytical framework for characterising polyphenol anti-nutrients in three Australian sorghum grain varieties (MR-Buster, Cracka, Liberty). Alongside the sorghum polyphenol extracts, two commercially produced tannin extracts were evaluated as standards to provide reference and comparison. Through these approaches, it was sought to detect non-tannin polyphenol anti-nutrients which may contribute to variable performance in animal feed. From these aims, specific research hypotheses and methods have been devised:

1. Simple spectral analyses will provide basic information about the chemical environments of the extracts including functional groups and structural information. Simple spectral analyses will provide for the clear separation of different extracts and standards.
    a. UV/Vis and FT-IR spectroscopy were used to evaluate the potential of simpler spectroscopic methods in characterising and analysing sorghum polyphenol extracts and the two tannin extracts.

2. More complex analytical techniques will provide more detailed information about the chemical environments including putative compound identification. More complex techniques will provide for the clear separation of different extracts and standards.
    a. Direct ionisation ESI and MALDI methods were used to evaluate the potential of more complex spectrometric methods in characterising and analysing sorghum polyphenol extracts and the two tannin extracts.

3. Red sorghum polyphenol extracts will have a more diverse polyphenol metabolite profile than the white sorghum polyphenol extract. Red sorghum polyphenol extracts will contain more large compounds than the white sorghum polyphenol extract.
    a. Multivariate analysis using PCA, OPLS-DA and putative compound identification were used to demonstrate differences in the sorghum polyphenol extracts as well as identify compounds driving variability between grain varieties.

3.3 Materials and methods (adapted form Hodges et al., 2021)

3.3.1 Chemicals and materials

The sorghum grains, MR-Buster, Cracka, Liberty, (**Figure 3.2**) were provided by DSM Nutritional Products (Kaiseraugst, Switzerland) and harvested in February 2017 in Aubigny, Central Darling Downs, Queensland, Australia by Nuseed (Nufarm Ltd.) and Pacific Seeds (Advanta Seeds Pty Ltd.). Grape seed and quebracho tannin extracts were kindly provided by Silvateam (Italy). Grape seed extract is labelled as Tan'Activ GUT and was from the batch 010915. Quebracho extract is labelled as Tan'Activ QS-SOL and was from the batch 010618. Solvents used were of HPLC grade.

Figure 3.2 Commercial sorghum grain from Australia

3.3.2 Preparation of sorghum polyphenol extracts

Sorghum grain was extracted for polyphenols following Harbertson et al. (2014) with modifications. Approximately 20 g of each grain were soaked overnight in ultra-high purity (UHP) water. The soaked grain was ground in a mortar and pestle and rinsed with UHP water six times and allowed to dry overnight at room temperature. The dried bran was then defatted for four hours with 200 mL of *n*-hexane in a Soxhlet extractor. The defatted bran was allowed to dry overnight at room temperature prior to being extracted twice with 200 mL 70% (v/v) aqueous acetone for 30 minutes on an orbital mixer (170 rpm). The acetone extract was filtered through glass filter paper, solvent removed in a rotary evaporator, lyophilised and stored under nitrogen gas at -80°C. The resulting extracts were light to reddish brown fluffy solids. Three separate extracts were prepared per sorghum variety.

3.3.3 Ultraviolet-visible spectroscopy (UV/Vis)

UV/Vis spectroscopy was performed on a GENESYS 150 Vis/UV-Vis spectrophotometer (Thermo Fisher Scientific; Waltham, MA, USA). A full scan was performed on each sample from 210 to 1100 nm. Samples were prepared in 100% ethanol at a concentration of 1 mg/mL.

3.3.4 Fourier-transform infrared spectroscopy (FT-IR)

FT-IR spectroscopy was performed on an IRAffinity-1S spectrometer (Shimadzu; MD, USA) using a diamond attenuated total reflectance (ATR) crystal (Specac; Orpington, UK) in the wavenumber region between 4000 – 400 cm^{-1} with a resolution of 4 cm^{-1} using Happ-Genzel Apodisation. At each position 40 scans were averaged. Three repeat scans were performed for each extract and three different extracts were used per sorghum variety. The three technical repeats of each extract were averaged. The spectra were baseline corrected with IR Solutions software (Shimadzu). The spectra obtained from the sorghum polyphenol extracts and tannin extracts were then analyzed for polyphenol and tannin structural features based on published spectra (Laghi et al., 2010; Falcão and Araújo, 2013; Falcão and Araújo, 2014; Ricci et al., 2016).

3.3.5 Direct-injection electrospray ionisation (ESI)

ESI, negative (–) and positive (+) modes, was performed on a Waters Synapt G2-Si ESI-ToF mass spectrometer (Waters Corporation; Milford, MA, USA). MassLynx data (Waters Corporation) system provided instrument control, data acquisition and data processing. Extracts were prepared to a concentration of 0.1 and 0.01 mg/mL in 50% aqueous methanol (v/v). Extracts were prepared in triplicate and three different extracts were analysed. Solutions were injected at a flow rate of 5 µL min^{-1}. Detailed parameters for ESI analysis are found in Table 3.1.

Table 3.1 Parameters for ESI-ToF-MS analysis of polyphenol and tannin extracts

Instrument Parameter	**Value**
Capillary (kV)	2.2
Source Temperature (°C)	100
Desolvation Temperature (°C)	280
Mass Range (Da)	50 – 1500

3.3.6 Matrix-assisted laser desorption/ionisation (MALDI)

MALDI (+) was performed on a Waters Synapt G2-Si ToF mass spectrometer (Waters Corporation). The MassLynx data system (Water Corporation) provided instrument control, data acquisition and data processing. For sample preparation, the matrix chemical alpha-cyano-4-hydroxycinnamic acid (CHCA) (5 mg/mL in methanol with 0.1% formic acid) was mixed with the extract solution (0.1 mg/mL in 50% aqueous methanol) in a 1:1 ratio. From this mixture, 1 μL was spotted onto a steel MALDI plate for analysis.

3.3.7 Tandem mass spectrometry (MS^2)

ESI – tandem MS (MS^2) was performed on specific ions produced by ESI (-) following a similar protocol to standard ESI analysis as described above. The applied voltages varied for each target mass (**Table 3.2**).

Table 3.2 Specific Voltage Ranges used in MS^2

Extract Type	Target Ion	Voltage Range (kV)
Grape seed	289.1	14.0
	577.2	10.0
	865.2	6.0
MR-Buster	135.0	6.0
	247.0	28.0
	563.2	2.0
	601.2	2.0
	689.2	6.0
	739.2	4.0
	851.3	14.0
	1107.4	8.0
	1123.3	8.0
	1269.4	8.0
	1367.4	8.0
	1411.4	6.0
Cracka	279.2	23.0
	289.1	10.0
	293.2	14.0
	329.2	20.0
	399.1	14.0
	577.2	2.0
	689.2	6.0
	739.2	2.0
	865.2	8.0
	1107.3	8.0
	1269.4	3.0
Liberty	279.2	24.0
	289.0	14.0
	295.2	18.0
	329.2	20.0
	341.1	12.0
	577.2	2.0

3.3.8 Data processing and statistical analysis

Raw spectra from each from each type of spectroscopy and mass spectrometry were then processed following a stepwise method based on and Overy et al. (2005), Austen (2016) and Austen et al. (2019) (**Figure 3.3**).

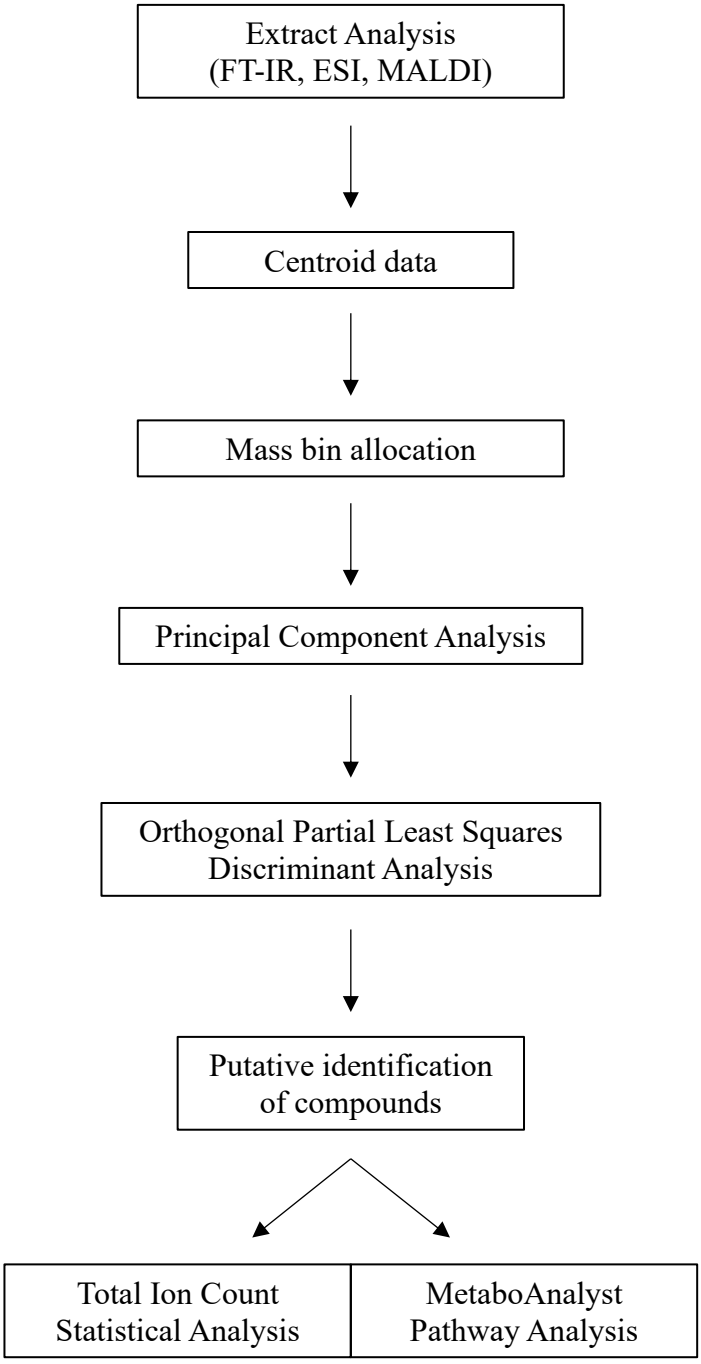

Figure 3.3 Metabolomic data processing workflow (adapted from Austen, 2016)

Briefly, the raw spectra obtained were centroided and converted into text files using an in-house Visual Basic macro. The triplicate runs of each sample were then combined to determine the average masses of each compound to make-up the metabolite profile for each sample. The

masses determined, along with their respective percent total ion count (TIC) were found using equations defined by Overy et al. (2005). For ease of analysis, masses were grouped together into ‘mass bins’ based on groupings of 0.2 Da.

Principal component analysis (PCA) and orthogonal partial least squares discriminant analysis (OPLS-DA) were performed on the spectra obtained from FT-IR and the mass bins identified from the MS spectra using SIMCA (Sartorius Stedim Biotech; Göttingen, Germany). PCA allows for the unsupervised, or untargeted, analysis of the metabolite profiles in the extracts which enables the separation of extracts based on metabolite variations among them. PCA provided the initial overview of the data to determine relationships between extract types and to highlight whether further investigation with more targeted analyses was needed. A covariance matrix was utilised over a correlation matrix as the data sets for each PCA were single-source and of the same data type (relative abundance units for FT-IR and percent TIC for mass spectrometry) and normalised using Pareto scaling prior to analysis. OPLS-DA is a supervised, or targeted, analysis which allows for pairwise comparisons to be made between two different extract types. This analysis maximises variation between samples and produces quantitative loadings plots which highlight components of the spectra responsible for causing variation, i.e., wavenumbers (cm^{-1}) from the FT-IR spectra and mass bins from the MS spectra. OPLS-DA was performed between MR-Buster and Cracka, MR-Buster and Liberty, and Cracka and Liberty sorghum polyphenol extracts.

For MS spectra, the top 10 mass bins causing variation for each extract in each pairing, as well as the 10 most abundant peaks, were interrogated further for putative identifications. Compound identification was conducted using online databases, including METLIN (Scripps Research Institute; La Jolla, CA, United States; https://metlin.scripps.edu) and Kyoto Encyclopedia of Genes and Genomes (KEGG; Kanehisa Laboratories; Kyoto, Japan; https://www.kegg.jp; Kaneshisa and Goto, 2000). In the negative mode, compounds were identified having an ion adduct of -H (−1.008 Da) while in positive mode ion adducts included +H (+1.008 Da), +Na (+22.99 Da), and +K (+39.10 Da). Following identifications, the KEGG IDs for all possible identifications in each mass bin were analysed using MetaboAnalyst through the pathway analysis function with *Arabidopsis thaliana* as the pathway library, hypergeometric test as the over representation analysis, and relative-betweenness centrality for the pathway topology analysis (Chong et al., 2019).

The guidelines for compound identification were made following the guidance set by the Chemical Analysis Working Group and the Metabolomics Standards Initiative (Sumner et al., 2007). These guidelines allow for four levels of identification of metabolites: (1) identified compound with two independent orthogonal data compared with an authentic sample; (2) putatively annotated compound relying on literature or database comparison; (3) putatively characterised compound classes; and (4) unknown compounds. The data obtained from FT-IR analysis are classified as a level 3 identification as established structural features of compound classes can be clearly identified. The identifications through mass spectrometry are classified as a level 2 identification and were accepted if below an *m/z* margin of error of 40 ppm or less.

3.4 Results and discussion

While efforts to reduce anti-nutrients in sorghum grain, most notably tannins, have been successful, gaps in efficiency and efficacy of feed additives remain, possibly due to unintended consequences in the breeding of feed quality sorghum. An understudied, alternative analytical approach was used to identify anti-nutrients that might be causing varied performance in sorghum feed and to determine the suitability of different analytical techniques for assessing metabolic variation among different sorghum grain polyphenol extracts. In the present study, the aim was not to fully characterise or quantify the polyphenols in the extracts but rather obtain a more holistic, qualitative metabolomic profile using multiple analytical techniques to highlight both bulk and subtle differences in different sorghum grains which might impact their nutritional values.

3.4.1 Qualitative analysis of sorghum polyphenol extracts and tannin extract UV/Vis spectra

UV/Vis spectroscopy was performed on the sorghum polyphenol extracts and tannin extracts. The two tannin extracts, grape seed and quebracho, are routinely found to contain flavonoid monomers, as well as highly polymerised tannin structures (Vivas et al., 2004). The extracts were dissolved in 100% ethanol and scanned from 200 – 1100 nm (**Figure 3.4**).

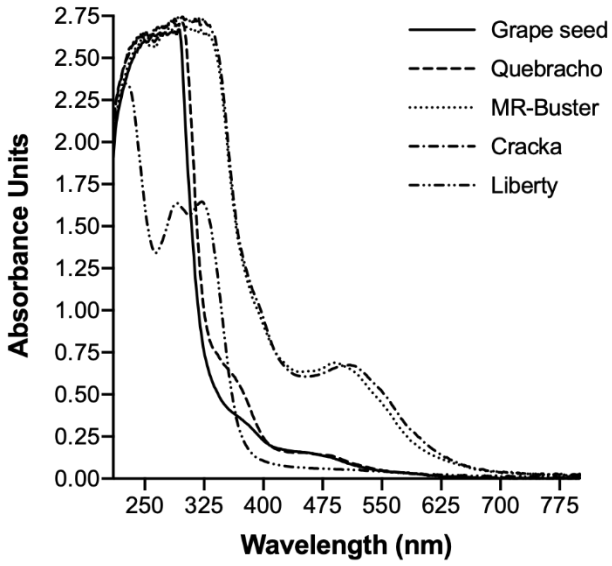

Figure 3.4 UV/Vis spectra of sorghum polyphenol extracts and tannin extracts
UV/Vis spectra were obtained from 210 – 1100 nm (210 – 800 nm shown here) for each extract dissolved in 100% ethanol.

Three patterns emerged among the five extracts analysed using UV/Vis spectroscopy. The first was observed for the two tannin extracts, grape seed and quebracho. A maximum was quickly reached between 280 – 300 nm followed by a steep drop-off. There was then a slight hump between 350 – 380 nm. This second pattern was also observed for the two red sorghum polyphenol extracts, MR-Buster and Cracka. Two maxima appeared for these extracts: the first at approximately 250 nm and the second at approximately 300 nm. These peaks were then followed by a broad hump at 500 nm. The third pattern observed was that of the white sorghum variety, Liberty. Here, a first maximum was found at 226 nm and followed by double peaks with maxima at 290 and 322 nm.

While these spectral patterns were all slightly different from each other, they did share the common feature of at least one maximum at approximately 280 nm. This peak is synonymous with phenolic compounds and is routinely used in conjunction with chromatographic separation methods to identify eluting polyphenol rich fractions. It arises from the presence of non-conjugated aromatic rings that are the hallmark of phenolics. Quebracho tannin extract has been previously found to show a maximum at 280 nm, as well as mimosa tannin extract which contains similar tannins to those found in grape seed tannin extracts (She et al., 2010; Grasel et al., 2016). As all five extracts here contain a peak of this nature, it can be concluded that they all contain at least the necessary aromatic ring(s) characteristic of phenolic and polyphenolic compounds. This, however, is not a full confirmation of polyphenolic

compounds as other metabolites contain similar structures. The Liberty sorghum polyphenol extract spectrum presented an interesting picture of the chemical environment as it contained a peak at 280 nm as well as one at 322 nm. This second peak around 320 nm has been previously detected in sweet sorghum stem extracts at 318 nm and is characteristic of lignin (She et al., 2010).

UV/Vis spectroscopy provided a very basic look at the chemical environment of the extracts and did not on its own allow for much to be discerned. However, it did confirm the presence of aromatics in all samples, as well as potential lignin structures in white Liberty sorghum polyphenol extract.

3.4.2 Qualitative analysis of sorghum polyphenol extract and tannin extract FT-IR spectra (adapted from Hodges et al., 2021)

FT-IR spectroscopy was performed on the sorghum polyphenol extracts and tannin extracts. Spectra were obtained from 4000 – 400 cm^{-1} and baseline corrected using a multi-point method. Three separate extracts from each sorghum variety were analysed in triplicate, averaged and baseline corrected. Overall, the spectra for the three sorghum polyphenol extracts matched very closely to one another and shared similar features to the tannin extracts (**Figures 3.5 – 3.10**). As reviewed by Ricci et al. (2015), the spectra obtained matched the general profile of samples containing polyphenols, particularly tannins.

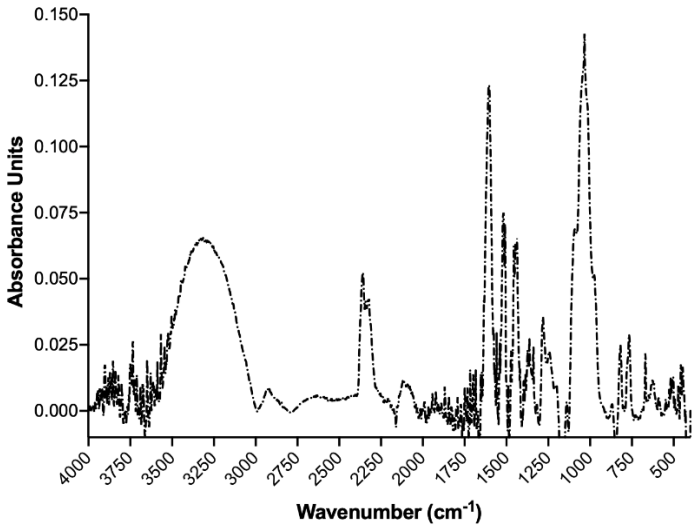

Figure 3.5 FT-IR spectrum of grape seed tannin extract
Spectra were obtained from 4000 – 400 cm^{-1} and baseline corrected using a multi-point method. The composite spectrum above is an average of three separate spectra from the same extract.

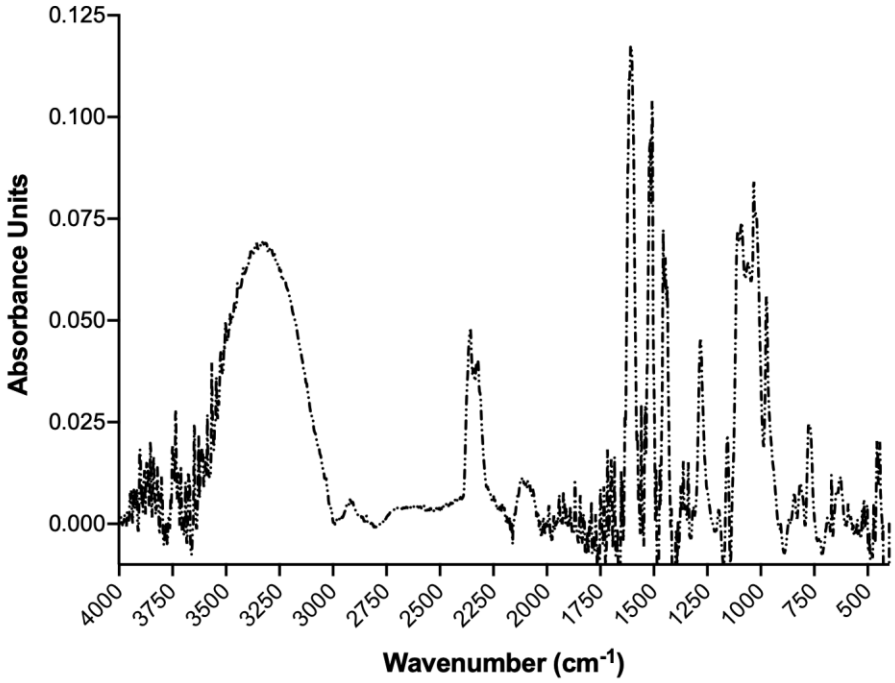

Figure 3.6 FT-IR spectrum of quebracho wood tannin extract

Spectra were obtained from 4000 – 400 cm^{-1} and baseline corrected using a multi-point method. The composite spectrum above is an average of three separate spectra from the same extract.

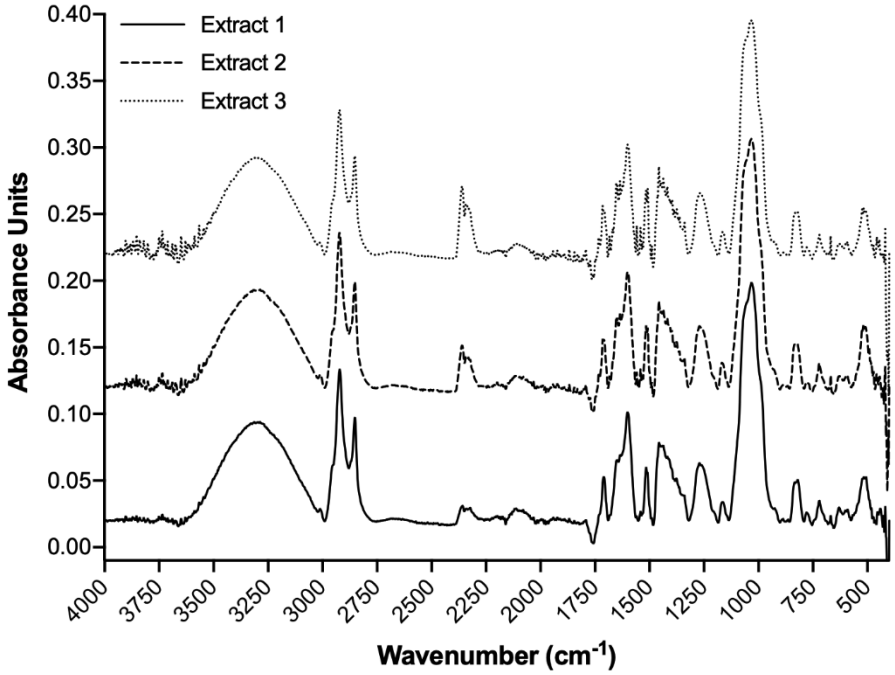

Figure 3.7 FT-IR spectra of MR-Buster sorghum polyphenol extracts

Spectra were obtained from 4000 – 400 cm^{-1} and baseline corrected using a multi-point method. Three replicate spectra were averaged for each extract.

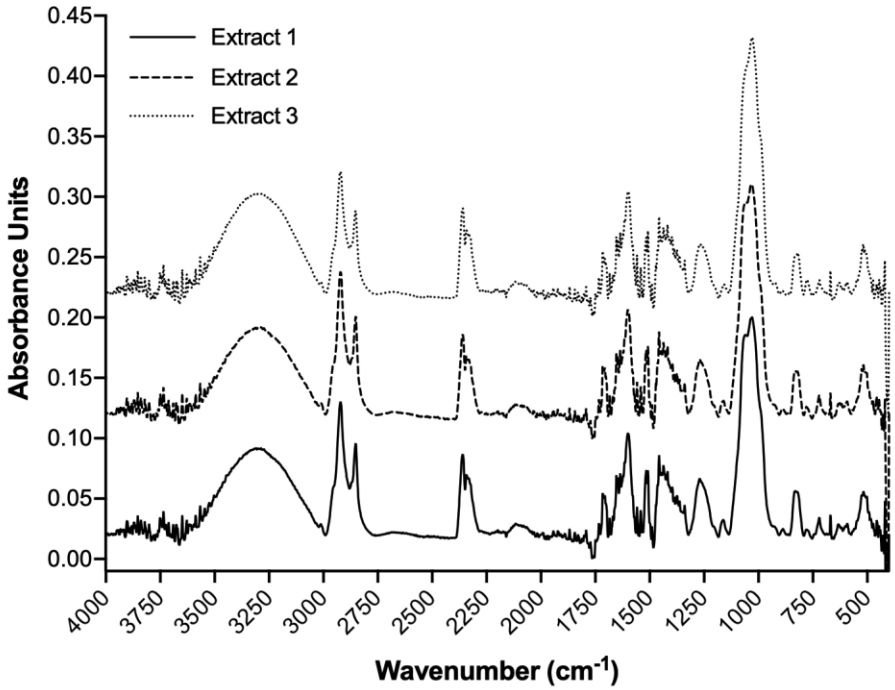

Figure 3.8 FT-IR spectra of Cracka sorghum polyphenol extracts

Spectra were obtained from 4000 – 400 cm^{-1} and baseline corrected using a multi-point method. Three replicate spectra were averaged for each extract.

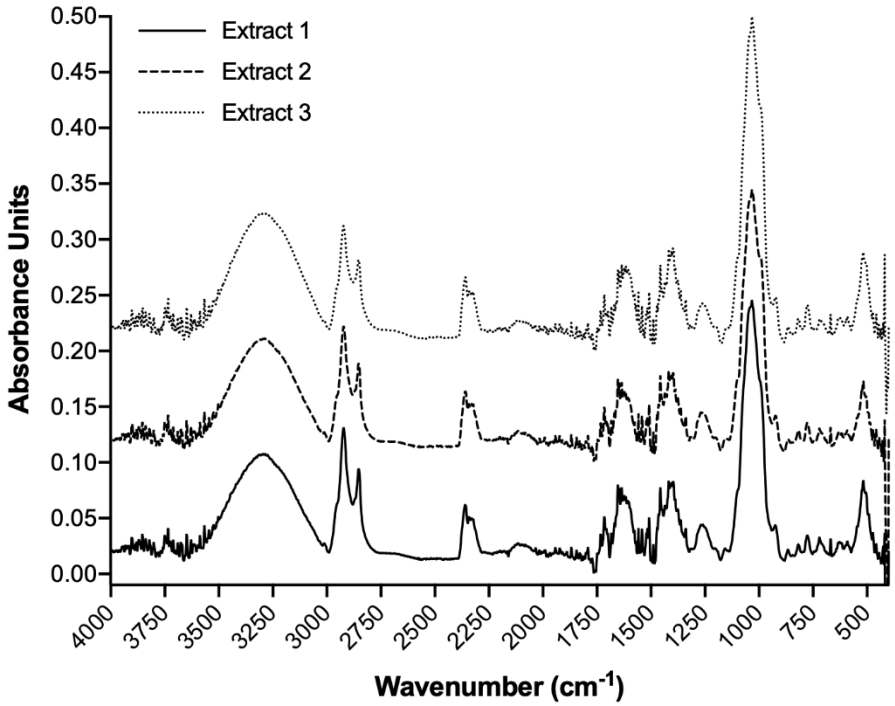

Figure 3.9 FT-IR spectra of Liberty sorghum polyphenol extracts

Spectra were obtained from 4000 – 400 cm^{-1} and baseline corrected using a multi-point method. Three replicate spectra were averaged for each extract.

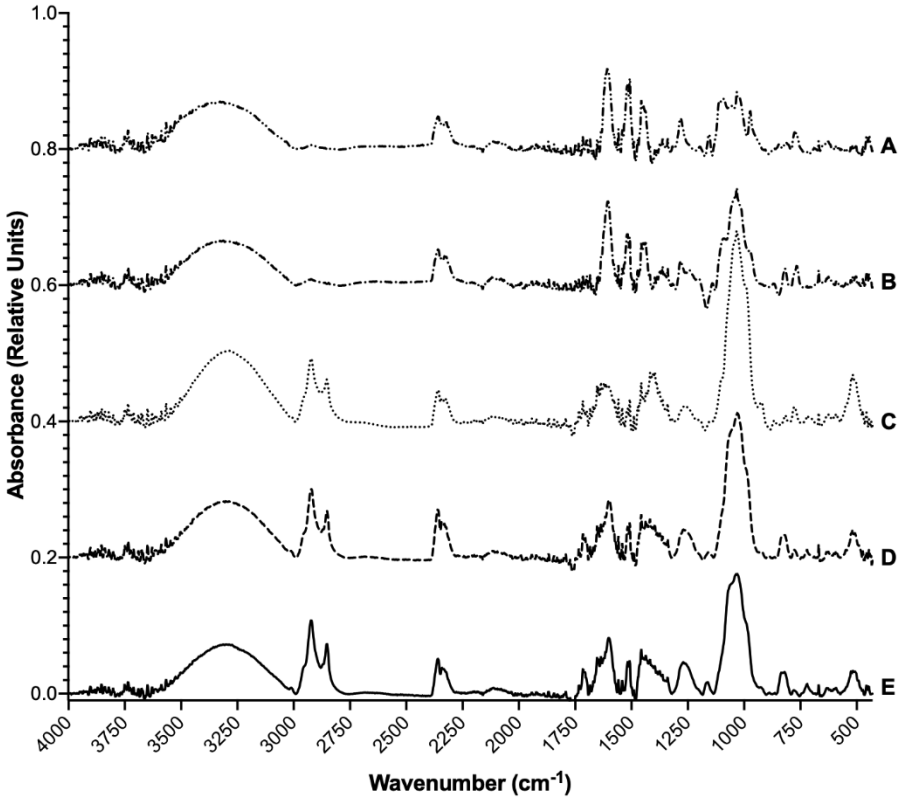

Figure 3.10 FT-IR spectra of sorghum polyphenol extracts and tannin extracts
Spectra were obtained from 4000 – 400 cm^{-1} and baseline corrected using a multi-point method. **A** – Quebracho, **B** – Grape seed, **C** – Liberty, **D** – Cracka, **E** – MR-Buster.

All three sorghum polyphenol extracts displayed similarities to each other with Cracka and MR-Buster extracts producing almost identical spectra while the Liberty extract deviated slightly. In comparison to the two tannin extracts, there were some similarities indicating a likeness to the sorghum polyphenol extracts. However, slight variations to peak structure and maximum values suggested the presence of competing compounds indicative of a crude, complex plant extract. The main structural features of polyphenol extracts were displayed in the sorghum polyphenol extracts and included characteristic hydroxyl groups O – H, aromatic C – H bonds and C – O bonding. The basic interpretation of the spectra was divided into six distinct wavenumber (cm^{-1}) regions: 3600 – 3100, O – H bonds; 3100 – 2800, C – H bonds; 1800 – 1630, C = O bonds; 1630 – 1400, C = C bonds; 1200 – 1000, C – O bonds; and 1000 – 500, C – H bonds.

Polyphenols have several key structural features that make FT-IR spectroscopy a particularly useful method for understanding the make-up of a complex sample, like the sorghum polyphenol extracts. All sorghum polyphenol extracts clearly showed the presence of a hydroxyl group (O – H) marked by the presence of a large, broad peak centered around 3300

– 3200 cm^{-1}. The two tannin extracts showed slightly lower values for the maximum at 3244 cm^{-1} for grape seed tannin extract and 3265 cm^{-1} for quebracho tannin extract. Polyphenols are well-known to contain at least one hydroxyl group, from one in the simplest phenol to dozens in large, polymerised tannins. Natural tannin extracts contain this peak and functional group; however, the location can often be found throughout the literature anywhere from 3700 – 3100 cm^{-1} often with the maximum appearing around 3400 cm^{-1}, especially for extracts with a high degree of polymerisation (Ricci et al., 2015). Sorghum flour exhibited a slightly higher peak of 3425 cm^{-1} (Manuhara et al., 2017). Similar maximum peaks have been reported in extracts from blueberry (Arancibia-Avila, et al., 2012), walnut (Oladoja et al., 2011), Aleppo pine (Saad et al., 2014) and a variety of different woods including quebracho, chestnut, black wattle, tara, valonea and myrobalan (Grasel et al., 2016). The lower peak values found here may be because of the complex nature of the extract in which other compounds, particularly sugars, may be lowering the value of the maximum.

The sorghum polyphenol extracts differed considerably from the tannin extracts with the appearance of several peaks/shoulders from 3016 – 2848 cm^{-1}. While very small, the sorghum polyphenol extracts showed a single peak/shoulder at approximately 3010 cm^{-1} representative of an aromatic C – H bond. The quebracho and grape seed tannin extracts did not show this peak. Small peaks and shoulders appearing between 3100 – 3000 cm^{-1} indicated the presence of aromatic compounds. The peaks are typically smaller due to overlap with the hydroxyl region observed previously in the spectrum (Ricci et al., 2015). The sorghum polyphenol extracts next displayed a series of sharp, strong peaks from 2957 – 2848 cm^{-1} representing aliphatic C – H bonds. This section took the form of two distinct peaks and was seen throughout all of the sorghum polyphenol extracts emphasising the consistent reproducibility of the extraction methodology. While matching peaks for the aliphatic C – H were found in both quebracho (2906 cm^{-1}) and grape seed (2923 cm^{-1}) tannin extracts, they were weaker and less defined than those detected in the sorghum polyphenol extracts. These peaks are associated with C – H bonds, most likely indicating the presence of fatty acids and/or possibly sugars (**Appendix Figures A.1, A.2)**. Similar peaks have been found in other extract types including sorghum (She et al., 2010; Manuhara et al., 2017). These peaks could be representative of fatty acids and/or triacylglycerols, as mushroom crude hexane extracts, found to contain mixtures of several compounds including palmitic, oleic, stearic and linoleic acids, exhibited similar peaks as the sorghum extracts did in this region (Sillapachaiyaporn et al., 2019). In their natural state, polyphenols are most likely to be conjugated to sugars rather than

not (Bravo, 1998). Quebracho tannin extract from the same manufacturer has been previously found by Bianchi et al. (2015) to have a carbohydrate content of 9%, which was lower than that of non-commercially prepared samples, like the sorghum polyphenol extracts in the present study. As previously described, the sorghum polyphenol extracts in this thesis are crude and almost certainly contain other components of the grain matrix other than polyphenols.

These first two diagnostic regions of the spectrum were useful in making basic structural determinations, such as the presence of a hydroxyl group. To help make more specific identifications and characterisations, the region from approximately 1800 – 450 cm^{-1}, often referred to as the fingerprint region, was used to distinguish between chemically similar groups of compounds in the five different extracts. A range of these regions for the analysis of polyphenol extracts can be found throughout the literature from 1750 – 900 cm^{-1} (Palma et al., 2017), 1485 – 1425 cm^{-1} (Jensen et al., 2008) and 1060 – 995 cm^{-1} (Ricci et al., 2015). For the extracts in question here, a broader fingerprint region was chosen to include a large number of function groups due to the complex nature of the extract. The baseline corrected fingerprint regions for the three sorghum polyphenol extracts and two tannin extracts were plotted for comparison (**Figure 3.11**).

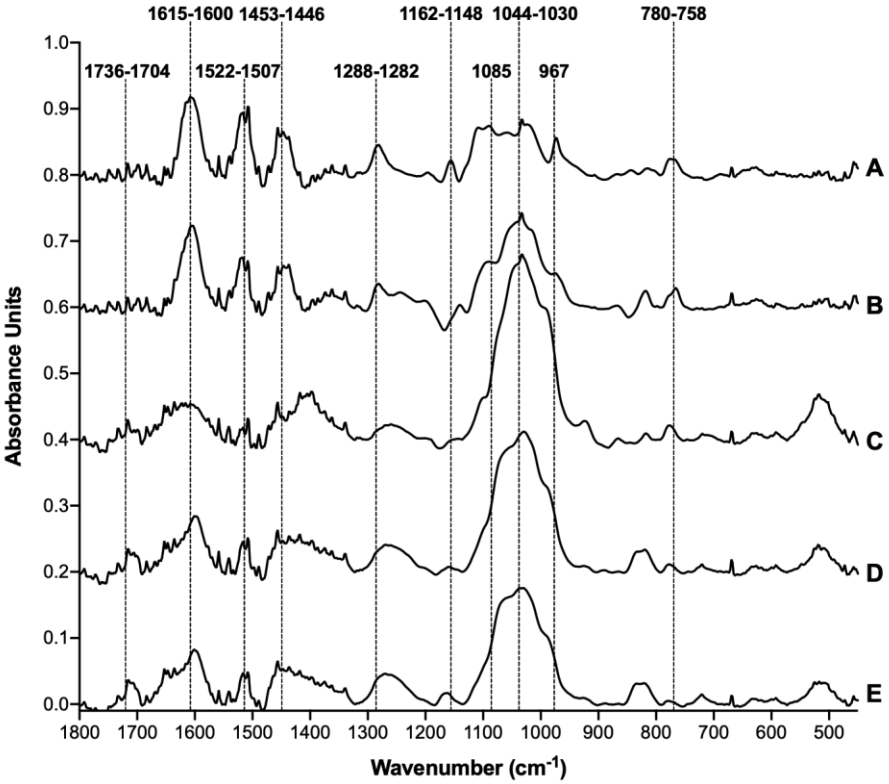

Figure 3.11 Fourier-transform infrared (FT-IR) fingerprint spectra of sorghum polyphenol extracts and tannin extracts

FT-IR spectra were obtained from the fingerprint region from 1800 – 450 cm^{-1}. Three replicate spectra were averaged for each extract type. **A** – Quebracho, **B** – Grape seed, **C** – Liberty, **D** – Cracka, **E** – MR-Buster. Wavenumbers specific to polyphenol and tannin extracts were determined from the literature (Laghi et al., 2010; Falcão and Araújo, 2013; Falcão and Araújo, 2014; Ricci et al., 2016) and used to show presence and absence of these functional groups and structural chemistry.

Within the fingerprint region (1800 – 450 cm^{-1}), 10 bands/peaks common to published tannin and polyphenol extract FT-IR spectra were highlighted in the spectra of the sorghum polyphenol extracts. All sorghum polyphenol extracts matched three of these highlighted wavenumber regions (1736 – 1704 cm^{-1}, 1044 – 1,030 cm^{-1} and 780 – 758 cm^{-1}). The two red sorghum polyphenols extracts, MR-Buster and Cracka, matched closely with another three regions (1615 – 1600 cm^{-1}, 1522 – 1507 cm^{-1} and 1162 – 1148 cm^{-1}). The four regions of the spectra not closely matched with any sorghum polyphenol extract were 1453 – 1446 cm^{-1}, 1288 – 1282 cm^{-1}, 1085 cm^{-1} and 967 cm^{-1}. Both tannin extracts matched all wavenumber regions, with the exception of 1162 – 1148 cm^{-1} for grape seed tannin extract.

The first major functional group in the fingerprint region lies between 1800 – 1630 cm^{-1}. The sorghum polyphenol extracts displayed a medium, broad peak from approximately 1760 – 1580 cm^{-1}. While the small peaks and shoulders seen between 1800 – 1630 cm^{-1} appeared

unresolved, they were most likely overlapping with several peaks correlating to other functional groups. Red sorghum, MR-Buster and Cracka, polyphenol extracts showed similar peak maxima and shapes here with a defined small peak at approximately at 1710 cm^{-1} followed by three small peaks at 1680, 1645 and 1630 cm^{-1}. White sorghum, Liberty, polyphenol extract had a less defined peak at 1710 cm^{-1} but only two small peaks around 1650 and 1630 cm^{-1}. This area of the spectrum is associated with the presence of a carbonyl (C = O) functional group. Most polyphenol extracts contain at least one or two peaks in this range, especially those containing hydrolysable tannins. This is due to the plethora of carbonyl groups of the gallic acid and ellagic acid moieties that makes up that specific group of tannins. Another common functional group associated with this range is an amide, typically found in proteins. Duodu et al. (2001) studied highly digestible sorghum and maize mutants for protein structure and identified the bands between 1670 – 1620 cm^{-1} as amide I and from 1550 – 1500 cm^{-1} as amide II. While the extraction process did not target proteins, it is possible that small peptides may have been extracted in the final freeze-dried product. The extraction solvent, acetone, was chosen as the literature indicates that it typically extracts larger polyphenols compared to methanol (see **Section 2.2**). A much more complex extraction method would be needed to properly extract proteins, involving a buffered solution, dialysis and purification. The lack of a similar broad peak in this region in the spectra of the two tannin extracts indicated a higher purity extract. The subtle differences between red and white sorghum grain extracts in these regions might indicate important differences in protein content and structure with possible nutritional implications. Selle et al. (2020) studied amino acids and kafirin protein in several sorghum varieties, including a Buster and Liberty variety. Regarding crude protein and kafirin content, Liberty had 80.9 and 41.4 g/kg, while Buster reported 99.2 and 44.6 g/kg, respectively. The higher proportion of kafirin protein found in Liberty may be causing the spectral differences observed in the current study.

Tailing off the end of this range, the next portion of the fingerprint (1630 – 1400 cm^{-1}) is one of best diagnostic regions for the presence of polyphenols as it indicates aromatic carbon-carbon double bonding (C = C) found in the aromatic rings of the phenolic compounds (Ricci et al., 2015). Polyphenols exhibit several peaks, usually three, in this range with some being particularly sharp around 1620 – 1600 cm^{-1}. Red sorghum, MR-Buster and Cracka, polyphenol extracts had strong, sharp peaks at approximately 1600 cm^{-1}, small peaks at 1557, 1537 and 1454 cm^{-1} and another strong, sharp peak at 1514 cm^{-1}. There was also a medium, broad band from approximately 1454 – 1335 cm^{-1} most likely due to overlapping of several compounds

and functional groups. The peak bleeding into the 1300s cm^{-1} might have been due to C – O bonds and/or C – C bonds, the latter of which is not very reliably used in FT-IR analysis. White sorghum, Liberty, polyphenol extract showed several similarities to the red coloured grains but differed most in having a weaker, less defined peak at 1600 cm^{-1} while having a medium, broad peak at 1400 cm^{-1} as opposed to just a broad, undefined band. These profiles for the sorghum polyphenol extracts loosely followed those of both grape seed and quebracho tannin extracts. A maximum peak was reached at 1600 cm^{-1}, like MR-Buster and Cracka sorghum polyphenol extracts, and the peak at 1515 cm^{-1} matched up with those in all three sorghum polyphenol extracts. The sorghum polyphenol extracts lacked the matching peak at 1440 cm^{-1} as well as the shape and definition that the tannin extracts had. This trio of sharp, strong peaks was much different from the broad, medium profile that the sorghum polyphenol extracts exhibited. The differences in the sorghum polyphenol extract spectra in these regions indicate that the white variety (Liberty) likely has reduced polyphenol content compared to the red varieties (MR-Buster, Cracka), a common finding in sorghum polyphenol studies, which can correlate with nutritional variations observed in feeding (Truong et al., 2016).

Following from approximately 1400 cm^{-1}, the range from 1400 – 1000 cm^{-1} provides information about C – O bonding. These types of bonds characterise both C – OH as well as C – O – C, both of which are present in high quantities in condensed tannins (Chen et al., 2010; Ricci et al., 2015). Peaks of note in the sorghum polyphenol extracts included a broad, medium peak at approximately 1260 cm^{-1}, a medium shoulder found at 1158 cm^{-1} and the largest peak of the spectrum found at 1030 cm^{-1} for Cracka and MR-Buster and at 1042 cm^{-1} for Liberty. Cracka and MR-Buster sorghum polyphenol extracts also appeared to have a second, slightly lower peak/shoulder at around 1060 cm^{-1}. Both tannin extracts had a broad, medium peak around 1280 cm^{-1} but with more defined peaks within it. The peak at approximately 1150 cm^{-1} resembled the matching one present in the sorghum polyphenol extract spectra. Most notably, the two tannin extracts differed in their large peak around 1000 cm^{-1}. Quebracho had a maximum at around 1107 cm^{-1} whereas the peak in the grape seed tannin extract spectra was at 1033 cm^{-1}, like the two red sorghum polyphenol extracts.

Finally, the end of the IR spectra from 1000 – 450 cm^{-1} correlates to aromatic C – H bonds similar to the earlier section around 3000 cm^{-1}. Of note for the sorghum polyphenol extracts, Liberty sorghum polyphenol extract did not have the same small peak that Cracka and MR-Buster polyphenol extracts did around 830 cm^{-1}. A similar peak appeared at 815 cm^{-1} in grape

seed tannin extract. All three sorghum varieties exhibited the same medium peak at 516 cm^{-1}. The two tannin extracts were noticeably void of peak beyond 814 cm^{-1}.

In the current study, FT-IR spectroscopy revealed there were structural similarities, regarding polyphenols and tannins, among the sorghum polyphenol extracts. The subtle differences in sorghum extract peak structures and maxima suggested the presence of competing compounds indicative of a complex plant extract. As reviewed by Ricci et al. (2015), the spectra matched the general profile of extracts containing phenolic, polyphenolic and tannin compounds, including characteristic O – H hydroxyl groups, aromatic C – H bonds, aromatic C = C bonds, and C – O groups. A similar approach in evaluating the presence/absence of specific metabolite structures was taken by Cameron et al. (2006) in their investigation into alterations to lignin and suberin content in grasses, legumes, and forbs subject to attack by a root hemiparasitic plant.

3.4.3 Multivariate analysis of sorghum polyphenol extract and tannin extract metabolic profile from FT-IR spectra (PCA and OPLS-DA) (adapted from Hodges et al., 2021)

Once visual and qualitative analyses had been performed on the five polyphenol and tannin extract spectra, more robust analytical methods were applied. PCA was first performed to determine relationships between extract types both on the full spectra as well as fingerprint regions (**Figures 3.12A – D**).

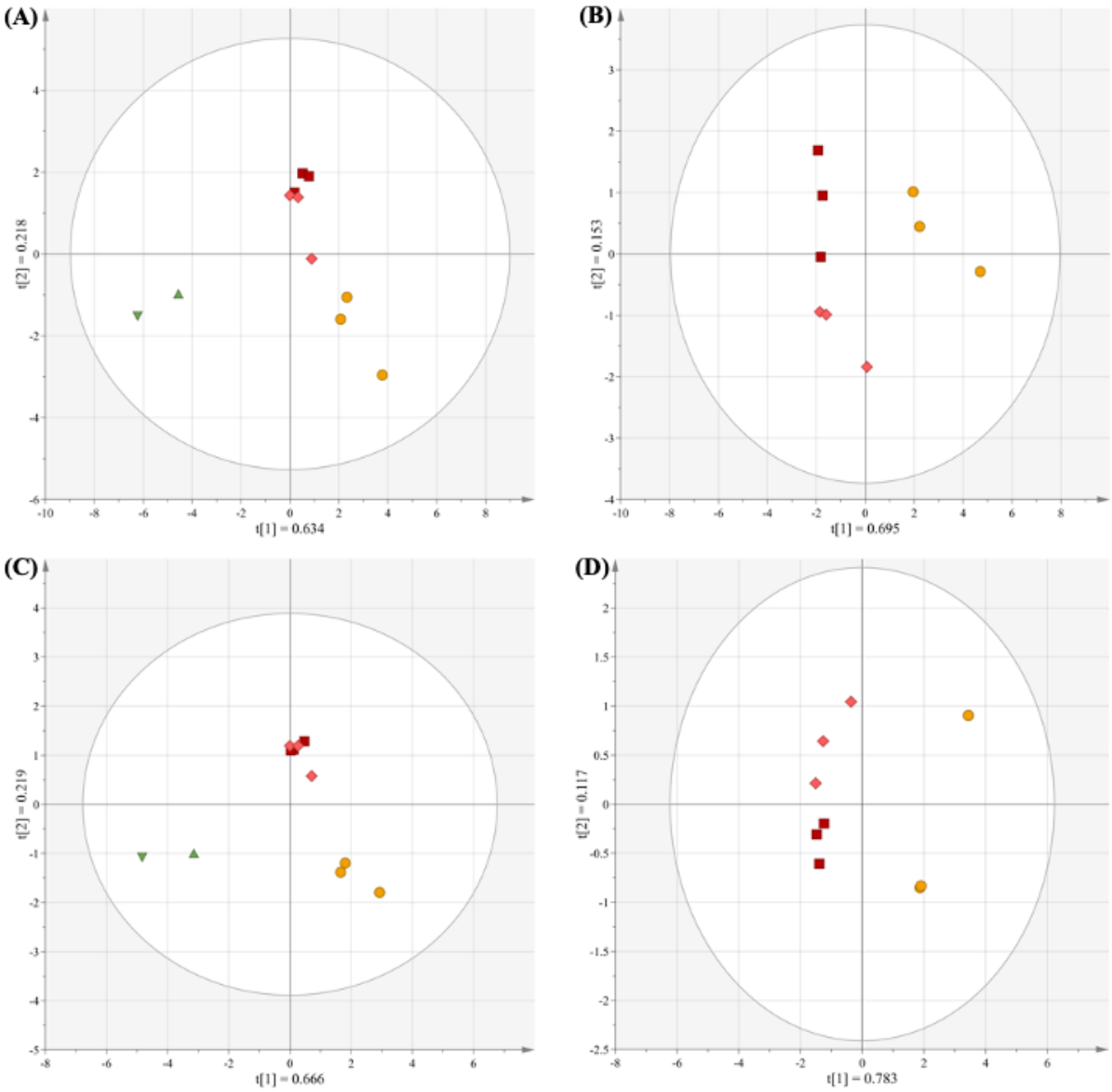

Figure 3.12 Principal component analysis (PCA) scores plots for FT-IR spectra from sorghum polyphenol extracts and tannin extracts
PCA was performed on the full spectra (4000 – 400 cm^{-1}) to determine relationships and variance between the two tannin extracts and the three red and white sorghum polyphenol extracts. **A, B** – Full spectra; **C, D** – Fingerprint region. The ellipse represents a 95% CI. t(1) and t(2) represent principal components 1 and 2, respectively. Grape seed (△) is green, Quebracho (▽) is green, MR-Buster (□) is dark red, Cracka (◇) is light red, and Liberty (○) is yellow.

The two tannin extracts were found to clearly differ from the three sorghum polyphenol extracts. Red sorghum, MR-Buster and Cracka, polyphenol extracts were also differentiated from the white sorghum, Liberty, polyphenol extract in each of the analyses. When analysing all five extract types, the first two principal components explained 85.2% of the variation for the full spectra (4000 – 400 cm^{-1}) and 84.8% for the fingerprint region (1800 – 450 cm^{-1}). When analysing the three sorghum polyphenol extracts, the first two principal components

explained 88.5% of the variation for the full spectra (4000 – 400 cm^{-1}) and 90.1% for the fingerprint region (1800 – 450 cm^{-1}).

With validation from the PCA that sufficient separation and grouping was present among the different extract types, supervised multivariate analysis was conducted using OPLS-DA on the fingerprint regions of the FT-IR spectra to determine the specific wavenumbers (cm^{-1}) and regions of the spectra responsible for variation between extract types (**Table 3.3**, **Appendix Figure A.3**).

Table 3.3 FT-IR wavenumbers (cm^{-1}) identified from OPLS-DA loadings plots

	MR-Buster (Red)	**Cracka (Red)**	**Liberty (White)**	**Grape seed**	**Quebracho**
MR-Buster (Red)	N/A	1167 – 1173 1462 1641 – 1643 1657 – 1161	831 – 837 1593 – 1603	1061 – 1078	1028 1036 – 1051
Cracka (Red)	1055 – 1074	N/A	829 – 837 1595 – 1601	1061 – 1078	1028 – 1030 1036 – 1049
Liberty (White)	988 – 997 1030 – 1034 1045	984 – 997 1034 1045	N/A	986 – 995 1024 – 1030	1028 – 1030 1036 – 1049
Grape seed	1522 – 1526 1605 – 1616	1524 – 1526 1603 – 1616	1506 – 1522 1607	N/A	1034 – 1051
Quebracho	1506 – 1508 1516 – 1526 1614 – 1616	1506 – 1508 1520 – 1526 1611 – 1616	1506 – 1522 1607	1153 – 1165 1504 – 1508	N/A

OPLS-DA highlighted regions of the spectra most responsible for variations between pairwise comparisons of the five different extracts. Red sorghum, MR-Buster and Cracka, polyphenol extracts were most varied in the regions corresponding to aromatic C – H (800s cm^{-1}) and aromatic C = C bonds (1600 cm^{-1}), while white grain (Liberty) extract was most different in the aromatic C – H region (1000 – 900 cm^{-1}) and C – O bonding (1030s cm^{-1}). These regions also applied to both commercial tannin extracts. When compared to the three sorghum polyphenol extracts, both tannin extracts exhibited similar differences in peaks associated most with C – O, O – H and C = C in aromatic compounds. These regions from 1600 to 1500 are routinely identified in other tannins extracts and are a key marker of polyphenolic compounds (see **Section 3.4.3**). Grape seed and quebracho tannin extracts differed from each other with variations in C – O stretching and C – O/O – H stretching, respectively.

While FT-IR spectroscopy was very useful in determining the general chemical environment of the sorghum polyphenol extracts, their use in assigning specific structures and identifying compounds is limited. The multivariate analysis performed here showed clear separation between white and red sorghum varieties indicating chemical differences in their polyphenol extracts. To better determine the specifics of these differences, more precise methods of analysis are needed, specifically those employing the use of mass spectrometry.

3.4.4 Unsupervised analysis of sorghum polyphenol and tannin extract metabolic profile from mass spectrometry (PCA) (adapted from Hodges et al., 2021)

FT-IR spectroscopy allowed for more detail about specific chemical structures and functional groups as compared to UV/Vis spectroscopy. However, FT-IR did not allow for the identification of compounds and/or specific groups of compounds within the different extracts. For more detail within each extract, mass spectrometry is a highly useful and precise analytical tool for compound identifications and has been widely employed in the study of phenolic and polyphenolic extracts, including sorghum grain extracts. Direct ESI (–, +) and MALDI (+) mass spectrometry were chosen as these techniques are ideal for soft ionisation, i.e., producing ions with little fragmentation, which can allow for analysis of complex mixtures without extensive clean-up and separation. Both the positive and negative modes were used for ESI while just positive mode was used for MALDI (sample spectra found in **Appendix Figure A.4**). The spectra for grape seed and quebracho tannin extracts closely matched those of previous studies (Hayasaka et al., 2003; Vivas et al., 2004; Venter et al., 2012). The ESI spectra

for all extract types were much different to that of those from MALDI with a greater diversity of clearly identifiable peaks. The spectra produced from MALDI for each extract were all dominated by the same peak at *m/z* 379 which is a by-product of the matrix compound CHCA. Another commonly used matrix chemical, 2,5-dihydroxybenzoic acid (DHB), was trialled but resulted in lower ion counts and less reliable patterns of matrix ionisation (**Appendix Figure A.5**). The dominating presence of this peak indicated that sufficient ionisation was achieved. While the spectra indicated some differences in ions produced, more robust analysis was needed to determine more specific nuances.

Unsupervised analysis of ESI (–) spectra allowed for the clear separation of both tannin extracts, red sorghum (MR-Buster, Cracka) polyphenol extracts and the white sorghum (Liberty) polyphenol extract (**Figure 3.13A**). The first two principal components explained 56.7% of the variation among the five different extract types. There was little variation in the metabolite profiles within each sorghum polyphenol extract as the clustering within extracts was tight and compact. This indicated strong reproductivity among separately prepared extract. There was no deviation from the 95% confidence range of normal T-squared distribution as noted by the ellipse.

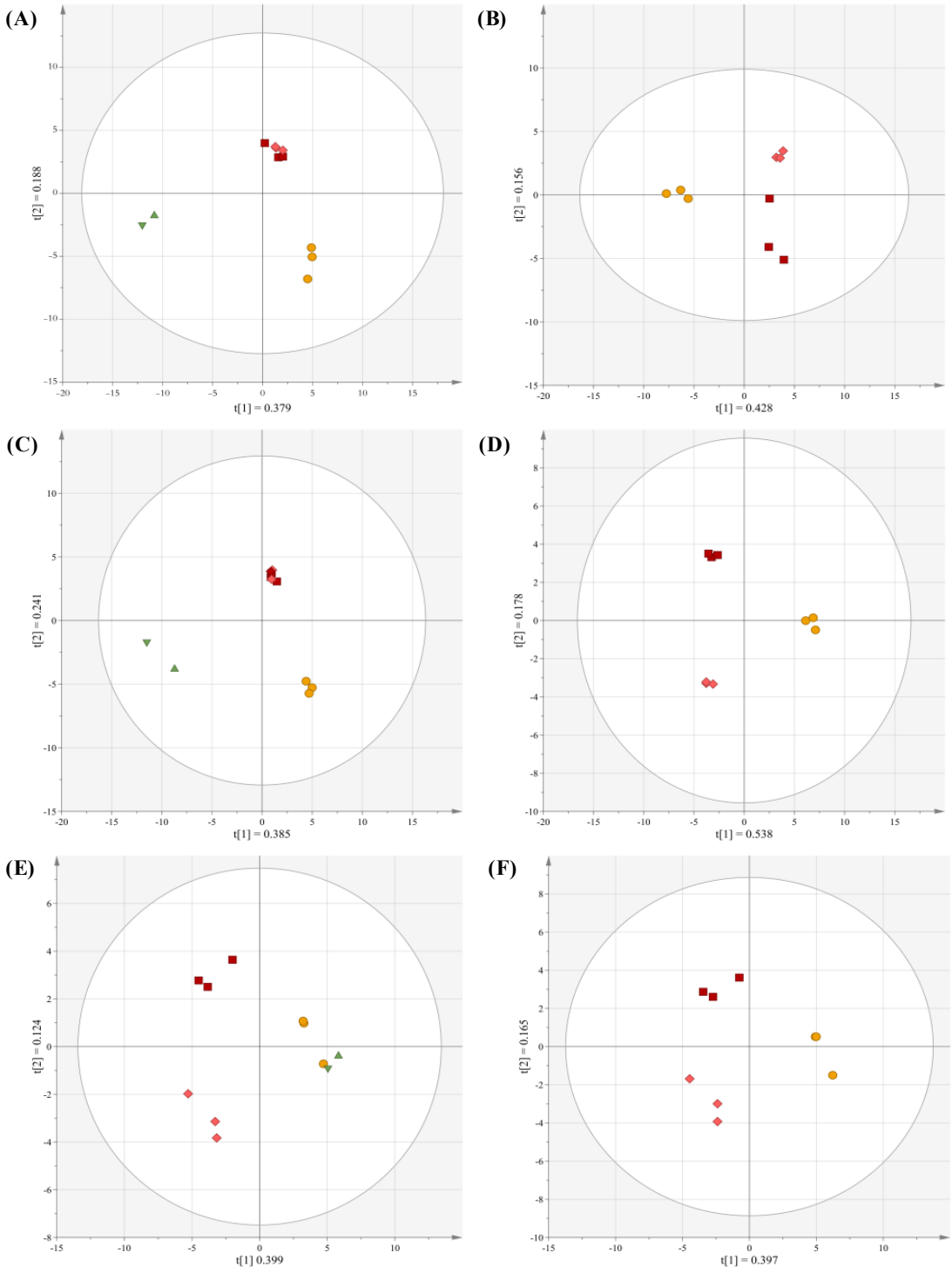

Figure 3.13. PCA scores plots of mass spectrometry analysis of sorghum polyphenol extracts and tannin extracts

Unsupervised analyses were performed on data collected using **A, B**: ESI (−), **C, D**: ESI (+) and **E, F**: MALDI (+) to determine relationships between tannin extracts and red and white sorghum polyphenol extracts. The ellipse represents a 95% CI. t(1) and t(2) represent principal components 1 and 2, respectively. Grape seed (△) is green, Quebracho (▽) is green, MR-Buster (□) is dark red, Cracka (◇) is light red, and Liberty (○) is yellow.

Unsupervised analyses of only the sorghum polyphenol extracts spectra allowed for the clear separation of red sorghum (MR-Buster, Cracka) and white sorghum (Liberty) polyphenol extracts (**Figure 3.13B**). The first two principal components explained 58.4% of variation among the three sorghum polyphenol extracts. These results indicated that there was enough separation and variation among the extract types to justify further supervised analyses to quantitatively determine specific mass bins, i.e., metabolites responsible for the variation in the extracts.

Analysis of metabolite profiles from ESI (+) resulted in similar plots to ESI (–) (**Figures 3.13C, D**). There were clear separations among all three extract types (tannin, red sorghum polyphenol, white sorghum polyphenol). The first two principal components explained 62.6% of the variation among the five different extract types. When only sorghum polyphenol extracts were compared, very clear separations appeared. The first two principal components explained 71.6% of variation among sorghum polyphenol extracts. This gave an indication that the different ionisation mode (+) was able to extract a more varied profile for each sorghum polyphenol extract.

The analysis of the spectra using MALDI (+) produced very different PCA scores plots compared to both ESI techniques (**Figures 3.13E, F**). When comparing among all extract types, MALDI mass spectrometry allowed for the clear separation between red and white sorghum polyphenol extracts. The first two principal components explained 54.7% of the variation among the five different extract types. However, the Liberty sorghum polyphenol extract showed overlap with the two tannin extracts. This result is surprising as the Liberty variety is thought to be the most 'tannin-free' sorghum grain in the current study. Among sorghum polyphenol extracts only, the first two principal components explained 57.0% of variation.

Sorghum polyphenol extracts have been sparingly analysed using MALDI (Krueger et al., 2003; Qi et al., 2018; Jiang et al., 2020; Reeves et al., 2020). Krueger et al. (2003) conducted a comprehensive study that putatively identified dozens of highly polymerised tannins and unique large structures in red sorghum grain extract. MALDI was used to analyse purified fractions using the matrix compound *trans*-3-indoleacrylic acid (*t*-IAA) along with cation solutions (K+, Na+, Ag+ and Cs+) to improve ionisation and compound identification. Traditional condensed tannins were identified from the tetramer to 20mers. A wide variety of

modified tannins within this range were also identified, differing by 16 Da (hydroxyl group). The spectra produced in this chapter did not show these high molecular weight compounds. This is most likely due to the matrix compound used, CHCA. As discussed in **Section 2.6,** Ohnishi-Kameyama et al. (1997) tested several different matrix compounds including CHCA and concluded that the best compounds for polyphenol ionisation were DHB and *t*-IAA. As previously mentioned, DHB was trialled in the current study and was found not to be suitable for the samples in their current state.

The unsupervised analysis of the sorghum polyphenol extracts and tannin extracts allowed for the clear separation of both extract types and in some cases between different sorghum varieties. The results found here justified the further investigation of the extracts and their relationships using supervised multivariate analysis through OPLS-DA to determine specific compounds or groups of compounds most responsible for separation between extract types.

3.4.5 Supervised analysis of sorghum polyphenol extract metabolite profiles from mass spectrometry (OPLS-DA) (adapted from Hodges et al., 2021)

Supervised analysis of the sorghum polyphenol extract metabolite profiles using OPLS-DA was performed and pairwise comparisons were made between extract type. The plots created from this analysis did not deviate much from those created by PCA. Corresponding loadings plots were then used to determine which specific mass bins (top 10 selected) correlated to the most difference between each variety extract (**Tables 3.4 – 3.6, Appendix Figures A.6 – A.8**).

Table 3.4 Binned peak masses identified from ESI (−) OPLS-DA loadings plots

	MR-Buster (Red)	**Cracka (Red)**	**Liberty (White)**
MR-Buster (Red)	N/A	271	851.2
		429.2	271
		285	852.2
		195	287
		383	269
		287	689.2
		267	303
		329.2	285
		447	867.2
		468.2	417

Cracka (Red)	399.2 416.2 303 851.2 383.2 689.2 283 852.2 414.2 269	N/A	851.2 303 852.2 689.2 269 283 417 271 383.2 416.2
Liberty (White)	399.2 341.2 377 400.2 379 329.2 387.2 439 191 342.2	341.2 399.2 377 329.2 379 439 400.2 191 297.2 387.2	N/A

Table 3.5 Binned peak masses identified from ESI (+) OPLS-DA loadings plots

	MR-Buster (Red)	**Cracka (Red)**	**Liberty (White)**
MR-Buster (Red)	N/A	255 269 523.2 509.2 537.2 353.2 524.2 470.2 287 270	269 255 271 285 523.2 509.2 257 273 537.2 287
Cracka (Red)	271 285 555.2 541.2 257 309 272 569.2 286 556.2	N/A	271 285 257 555.2 269 255 541.2 539.2 273 272

Liberty (White)	365.2 381 527.2 520.4 522.4 543.2 689.2 366.2 496.4 665.2	365.2 381 527.2 366.2 689.2 522.4 520.4 543.2 665.2 496.4	N/A

Table 3.6 Binned peak masses identified from MALDI (+) OPLS-DA loadings plots

	MR-Buster (Red)	**Cracka (Red)**	**Liberty (White)**
MR-Buster (Red)	N/A	523.2 509.2 269 255 470.2 524.2 510.2 287 377 289	523.2 269 509.2 255 537.2 271 285 539.2 525.2 553.2
Cracka (Red)	271 285 555.4 541.2 309 569.2 323 556.2 542.2 447.4	N/A	271 285 541.2 555.2 539.2 553.2 525.2 569.2 309 556.2
Liberty (White)	335.2 279.2 277.2 293.2 498.4 291.2 487.4 289.2 275.2 292.2	335.2 279.2 293.2 277.2 337.2 487.4 291.2 486.4 275.2 377	N/A

The identified mass bins from each analysis type were then interrogated through putative identification of detected masses using METLIN and KEGG online metabolite databases. The results for some of the top compounds putatively identified in the sorghum extracts using ESI

(–) are shown in **Table 3.7** (see **Appendix Tables A.1 – A.9** for full results). A heat map was created to illustrate differences in percent total ion count of the mass bins among the three sorghum polyphenol extracts (**Figure 3.14**).

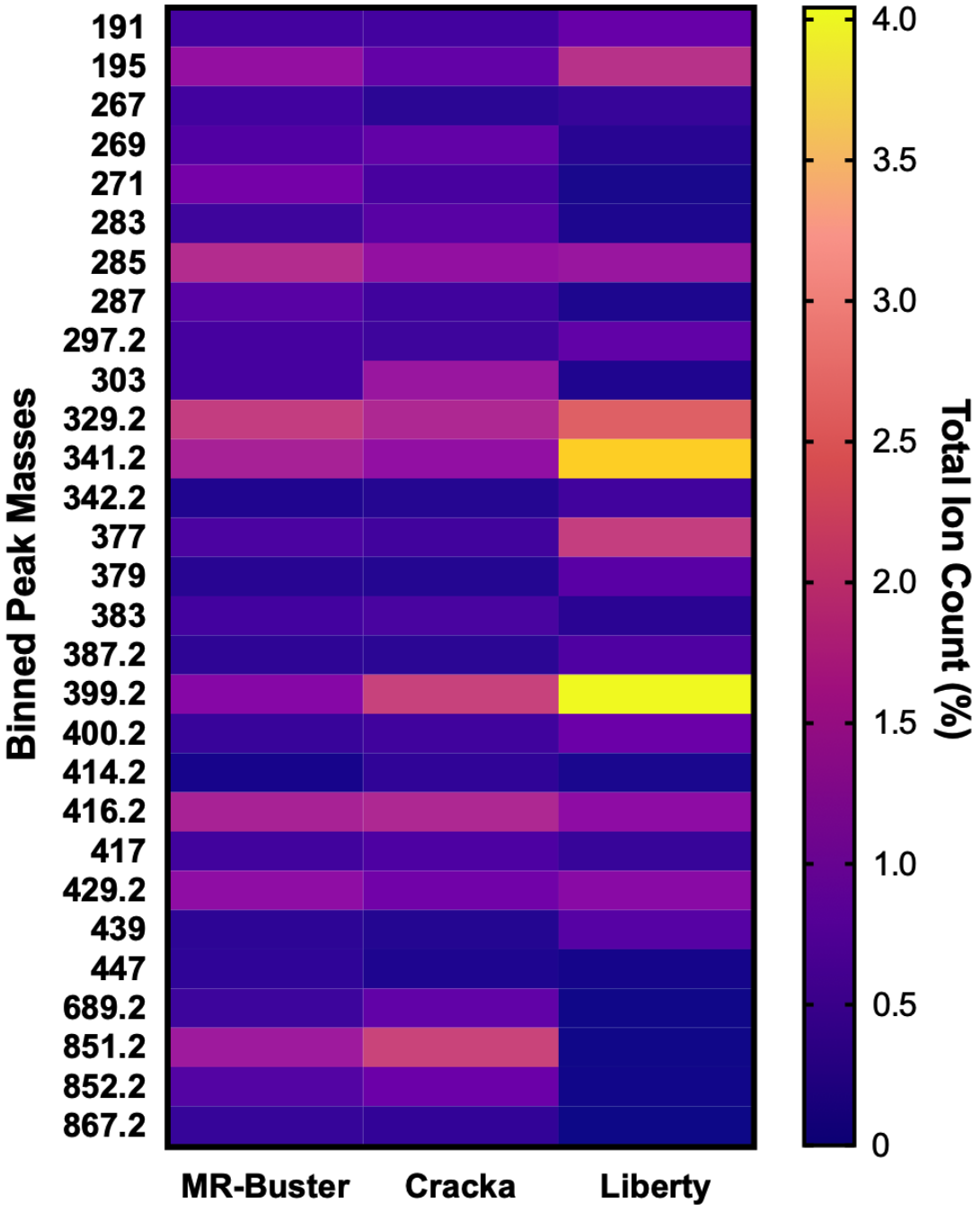

Figure 3.14 Heat map of percent total ion counts (TICs) for compounds identified from orthogonal partial least squares discriminant analysis (OPLS-DA) from ESI (–)
OPLS-DA (ESI [−]) indicated mass bins (*m/z*) most responsible for variation between pairwise comparisons of sorghum polyphenol extracts. The mean relative abundance (total % ion count) and SD were formatted into a heat map, n = 3 for each mass bin (*m/z*).

Table 3.7 Putative identification of discriminant mass bins responsible for separation of sorghum polyphenol extracts (ESI [–])

Bin	Detected Mass	Accurate Mass	Δppm	Name	Formula	Chemical Group	Pathway
269	268.9201	269.9281					
	269.042	270.05	13	Genistein	C15H10O5	Isoflavone	Isoflavonoid and phenylpropanoid biosynthesis
				6-Hydroxydaidzein		Isoflavone	Isoflavonoid biosynthesis
				3',4',7-Trihydroxyisoflavone		Isoflavone	
				2'-Hydroxydaidzein		Isoflavone	Isoflavonoid biosynthesis
				Islandicin		Anthraquinone	
				Purpurin 1-methyl ether		Anthraquinone	
				2-Hydroxychrysophanol		Anthraquinone	
				Morindone		Anthraquinone	
				Lucidin		Anthraquinone	
				Emodin		Anthraquinone	
				Aloe-emodin		Anthraquinone	
				Norwogonin		Flavone	
				Galangin		Flavone	Flavonoid biosynthesis
				5-Deoxykaempferol		Flavone	
				Baicalein		Flavone	
				3,6,4'-Trihydroxyflavone		Flavone	
				Apigenin		Flavone	Flavonoid, isoflavonoid, flavone, flavonol and
				Sulphuretin		Aurone	phenylpropanoid biosynthesis
	268.9195	269.9275					
	269.0423	270.0503	12	Genistein	C15H10O5	Isoflavone	Isoflavonoid and phenylpropanoid biosynthesis
				6-Hydroxydaidzein		Isoflavone	Isoflavonoid biosynthesis
				3',4',7-Trihydroxyisoflavone		Isoflavone	
				2'-Hydroxydaidzein		Isoflavone	Isoflavonoid biosynthesis
				Islandicin		Anthraquinone	
				Purpurin 1-methyl ether		Anthraquinone	
				2-Hydroxychrysophanol		Anthraquinone	
				Morindone		Anthraquinone	
				Lucidin		Anthraquinone	
				Emodin		Anthraquinone	
				Aloe-emodin		Anthraquinone	
				Norwogonin		Flavone	
				Galangin		Flavone	Flavonoid biosynthesis
				5-Deoxykaempferol		Flavone	
				Baicalein		Flavone	
				3,6,4'-Trihydroxyflavone		Flavone	
				Apigenin		Flavone	Flavonoid, isoflavonoid, flavone, flavonol and
				Sulphuretin		Aurone	phenylpropanoid biosynthesis
	268.927	269.935					

	269.0431333	270.0511333	8	Genistein	C15H10O5	Isoflavone	Isoflavonoid and phenylpropanoid biosynthesis
				6-Hydroxydaidzein		Isoflavone	Isoflavonoid biosynthesis
				3',4',7-Trihydroxyisoflavone		Isoflavone	
				2'-Hydroxydaidzein		Isoflavone	Isoflavonoid biosynthesis
				Islandicin		Anthraquinone	
				Purpurin 1-methyl ether		Anthraquinone	
				2-Hydroxychrysophanol		Anthraquinone	
				Morindone		Anthraquinone	
				Lucidin		Anthraquinone	
				Emodin		Anthraquinone	
				Aloe-emodin		Anthraquinone	
				Norwogonin		Flavone	
				Galangin		Flavone	Flavonoid biosynthesis
				5-Deoxykaempferol		Flavone	
				Baicalein		Flavone	
				3,6,4'-Trihydroxyflavone		Flavone	
				Apigenin		Flavone	Flavonoid, isoflavonoid, flavone, flavonol and
				Sulphuretin		Aurone	phenylpropanoid biosynthesis
271	271.0532333	272.0612333	29	Toralactone	C15H12O5	Naphthopyrone	
				Rubrofusarin		Naphthopyrone	
				6,7,4'-Trihydroxyflavanone		Flavanone	Isoflavonoid biosynthesis
				Naringenin		Flavanone	Flavonoid, isoflavonoid and phenylpropanoid
				Dihydrogenistein		Flavanone	biosynthesis
				Butin		Flavanone	Flavonoid biosynthesis
				2,7,4'-Trihydroxyisoflavanone		Isoflavanone	Isoflavonoid biosynthesis
				2'-Hydroxydihydrodaidzein		Isoflavanone	Isoflavonoid biosynthesis
				Pinobanksin		Dihydroflavonol	Flavonoid biosynthesis
				Garbanzol		Dihydroflavonol	Flavonoid biosynthesis
				p-Coumaroyltriacetic acid lactone		Chalcone	
				Butein		Chalcone	Flavonoid biosynthesis
				Naringenin chalcone		Chalcone	Flavonoid biosynthesis
				Licodione		Chalcone	
				(-)-Glycinol		Pterocarpan	Isoflavonoid biosynthesis
	271.0556333	272.0636333	20	Toralactone	C15H12O5	Naphthopyrone	
				Rubrofusarin		Naphthopyrone	
				6,7,4'-Trihydroxyflavanone		Flavanone	Isoflavonoid biosynthesis
				Naringenin		Flavanone	Flavonoid, isoflavonoid and phenylpropanoid
				Dihydrogenistein		Flavanone	biosynthesis
				Butin		Flavanone	Flavonoid biosynthesis
				2,7,4'-Trihydroxyisoflavanone		Isoflavanone	Isoflavonoid biosynthesis
				2'-Hydroxydihydrodaidzein		Isoflavanone	Isoflavonoid biosynthesis
				Pinobanksin		Dihydroflavonol	Flavonoid biosynthesis
				Garbanzol		Dihydroflavonol	Flavonoid biosynthesis
				p-Coumaroyltriacetic acid lactone		Chalcone	
				Butein		Chalcone	Flavonoid biosynthesis
				Naringenin chalcone		Chalcone	Flavonoid biosynthesis
				Licodione		Chalcone	
				(-)-Glycinol		Pterocarpan	Isoflavonoid biosynthesis

	270.9482	271.9562					
	271.0566	272.0646	16	Toralactone Rubrofusarin 6,7,4'-Trihydroxyflavanone Naringenin Dihydrogenistein Butin 2,7,4'-Trihydroxyisoflavanone 2'-Hydroxydihydrodaidzein Pinobanksin Garbanzol p-Coumaroyltriacetic acid lactone Butein Naringenin chalcone Licodione (-)-Glycinol	C15H12O5	Naphthopyrone Naphthopyrone Flavanone Flavanone Flavanone Flavanone Isoflavanone Isoflavanone Dihydroflavonol Dihydroflavonol Chalcone Chalcone Chalcone Chalcone Pterocarpan	 Isoflavonoid biosynthesis Flavonoid, isoflavonoid and phenylpropanoid biosynthesis Flavonoid biosynthesis Isoflavonoid biosynthesis Isoflavonoid biosynthesis Flavonoid biosynthesis Flavonoid biosynthesis Flavonoid biosynthesis Flavonoid biosynthesis Isoflavonoid biosynthesis
287	286.9263667	287.9343667					
	287.0408	288.0488					
	287.0836333	288.0916333	30	Shikonin 7,2'-Dihydroxy-4'-methoxy-isoflavanol Asebogenin	C16H16O5	Naphthoquinone Isoflavane Dihydrochalcone	Ubiquinone and terpenoid-quinone biosynthesis Isoflavonoid biosynthesis
	286.9290333	287.9370333					
	287.0444	288.0524					
	287.0867667	288.0947667	19	Shikonin 7,2'-Dihydroxy-4'-methoxy-isoflavanol Asebogenin	C16H16O5	Naphthoquinone Isoflavane Dihydrochalcone	Ubiquinone and terpenoid-quinone biosynthesis Isoflavonoid biosynthesis
	287.0476333	288.0556333	29	Carthamidin Eriodictyol 2,6,7,4'-Tetrahydroxyisoflavanone 2-Hydroxy-2,3-dihydrogenistein (+-)-Dalbergioidin Swerchirin 2-O-Methylswertianin Gentiacaulein 3,5-Dimethoxy-1,6-dihydroxyxanthone Micromelin Okanin Eriodictyol chalcone Fustin Dihydrokaempferol	C15H12O6	Flavanone Flavanone Isoflavanone Isoflavanone Isoflavanone Xanthene Xanthene Xanthene Xanthene Coumarin Chalcone Chalcone Dihydroflavonol Dihydroflavonol	 Flavonoid biosynthesis Isoflavonoid biosynthesis Isoflavonoid biosynthesis Flavonoid biosynthesis Flavonoid and phenylpropanoid biosynthesis
	287.0880667	288.0960667	15	Shikonin 7,2'-Dihydroxy-4'-methoxy-isoflavanol Asebogenin	C16H16O5	Naphthoquinone Isoflavane Dihydrochalcone	Ubiquinone and terpenoid-quinone biosynthesis Isoflavonoid biosynthesis
303	303.0751	304.0831	27	N-Acetylaspartylglutamate	C11H16N2O8	Amino acid	Alanine, aspartate and glutamate metabolism
	302.9024667	303.9104667					
	302.9668	303.9748					
	303.0785	304.0865	16	N-Acetylaspartylglutamate	C11H16N2O8	Amino acid	Alanine, aspartate and glutamate metabolism

			29	Griseophenone C beta-Cotonefuran 7-Hydroxy-6-methoxy-alpha-pyrufuran	C16H16O6 C16H16O6 C16H16O6	Benzophenone 2-arylbenzofuran flavonoid Hydrolyzable tannin	
	302.8983	303.9063					
	303.0792333	304.0872333	13	N-Acetylaspartylglutamate	C11H16N2O8	Amino acid	Alanine, aspartate and glutamate metabolism
			26	Griseophenone C 7-Hydroxy-6-methoxy-alpha-pyrufuran beta-Cotonefuran	C16H16O6	Benzophenone Hydrolyzable tannin 2-arylbenzofuran flavonoid	
	303.0149667	304.0229667					
	303.0828667	304.0908667	1	N-Acetylaspartylglutamate	C11H16N2O8	Amino acid	Alanine, aspartate and glutamate metabolism
			14	Griseophenone C 7-Hydroxy-6-methoxy-alpha-pyrufuran beta-Cotonefuran	C16H16O6	Benzophenone Hydrolyzable tannin 2-arylbenzofuran flavonoid	
	302.9649	303.9729					
	303.0304667	304.0384667					
	303.0832	304.0912	0	N-Acetylaspartylglutamate	C11H16N2O8	Amino acid	Alanine, aspartate and glutamate metabolism
			13	Griseophenone C 7-Hydroxy-6-methoxy-alpha-pyrufuran beta-Cotonefuran	C16H16O6	Benzophenone Hydrolyzable tannin 2-arylbenzofuran flavonoid	
			37	Vicine	C10H16N4O7	Alkaloid	
	303.0833	304.0913	0	N-Acetylaspartylglutamate	C11H16N2O8	Amino acid	Alanine, aspartate and glutamate metabolism
			13	Griseophenone C 7-Hydroxy-6-methoxy-alpha-pyrufuran beta-Cotonefuran	C16H16O6	Benzophenone Hydrolyzable tannin 2-arylbenzofuran flavonoid	
			37	Vicine	C10H16N4O7	Alkaloid	
329.2	329.2294667	330.2374667	11	9,10-Dihydroxy-12,13-epoxyoctadecanoic acid 9,10,13-Trihydroxyoctadec-11-enoic acid 9(S),12(S),13(S)-Trihydroxy-10(E)-octadecenoic acid	C18H34O5	Fatty acid	Linoleic acid metabolism
	329.2293	330.2373	12	9,10-Dihydroxy-12,13-epoxyoctadecanoic acid 9,10,13-Trihydroxyoctadec-11-enoic acid 9(S),12(S),13(S)-Trihydroxy-10(E)-octadecenoic acid	C18H34O5	Fatty acid	Linoleic acid metabolism
	329.2292	330.2372	12	9,10-Dihydroxy-12,13-epoxyoctadecanoic acid 9,10,13-Trihydroxyoctadec-11-enoic acid 9(S),12(S),13(S)-Trihydroxy-10(E)-octadecenoic acid	C18H34O5	Fatty acid	Linoleic acid metabolism

341.2	341.1040333	342.1120333	2	5,6,7,4'-Tetramethoxyisoflavone Tetra-O-methylscutellarein	C19H18O6	Isoflavone Flavone	
			14	3-O-alpha-D-Mannopyranosyl-alpha-D-mannopyranose Turanose Melibiulose Maltulose Kojibiose 2-alpha-D-Glucosyl-D-glucose Nigerose Galactinol Trehalose Isomaltose Lactose Maltose Sucrose Cellobiose Sophorose Gentiobiose Melibiose Epimelibiose alpha-D-Glucosyl-(1,3)-D-mannose Laminaribiose beta-Lactose Palatinose Levanbiose Inulobiose	C12H22O11	Disaccharide	 Galactose metabolism Starch and sucrose metabolism Starch and sucrose metabolism Galactose metabolism Starch and sucrose metabolism Galactose metabolism; Starch and sucrose metabolism Starch and sucrose metabolism Galactose metabolism Galactose metabolism Starch and sucrose metabolism
	341.2742333	342.2822333					
	341.1039333	342.1119333	2	5,6,7,4'-Tetramethoxyisoflavone Tetra-O-methylscutellarein	C19H18O6	Isoflavone Flavone	
			14	3-O-alpha-D-Mannopyranosyl-alpha-D-mannopyranose Turanose Melibiulose Maltulose Kojibiose 2-alpha-D-Glucosyl-D-glucose Nigerose Galactinol Trehalose Isomaltose Lactose Maltose Sucrose Cellobiose Sophorose Gentiobiose Melibiose	C12H22O11	Disaccharide	 Galactose metabolism Starch and sucrose metabolism Starch and sucrose metabolism Galactose metabolism Starch and sucrose metabolism Galactose metabolism; Starch and sucrose metabolism Starch and sucrose metabolism Galactose metabolism

				Epimelibiose alpha-D-Glucosyl-(1,3)-D-mannose Laminaribiose beta-Lactose Palatinose Levanbiose Inulobiose			Galactose metabolism Starch and sucrose metabolism
	341.1800333	342.1880333					
	341.2694333	342.2774333					
	341.1039667	342.1119667	2	5,6,7,4'-Tetramethoxyisoflavone Tetra-O-methylscutellarein	C19H18O6	Isoflavone Flavone	
			14	3-O-alpha-D-Mannopyranosyl-alpha-D-mannopyranose Turanose Melibiulose Maltulose Kojibiose 2-alpha-D-Glucosyl-D-glucose Nigerose Galactinol Trehalose Isomaltose Lactose Maltose Sucrose Cellobiose Sophorose Gentiobiose Melibiose Epimelibiose alpha-D-Glucosyl-(1,3)-D-mannose Laminaribiose beta-Lactose Palatinose Levanbiose Inulobiose	C12H22O11	Disaccharide	 Galactose metabolism Starch and sucrose metabolism Starch and sucrose metabolism Galactose metabolism Starch and sucrose metabolism Galactose metabolism; Starch and sucrose metabolism Starch and sucrose metabolism Galactose metabolism Galactose metabolism Starch and sucrose metabolism
	341.1797	342.1877					
	341.2701667	342.2781667					
	378.9617667	379.9697667					
	379.0789333	380.0869333	8	Diphyllin	C21H16O7	Lignan	
			36	S-(N-Hydroxy-N-methylcarbamoyl)glutathione	C12H20N4O8S	Amino acid	
	378.9690333	379.9770333					
379	379.0786667	380.0866667	9	Diphyllin	C21H16O7	Lignan	

			37	S-(N-Hydroxy-N-methylcarbamoyl)glutathione	C12H20N4O8S	Amino acid	
	378.9622333	379.9702333					
	379.0789667	380.0869667	8	Diphyllin	C21H16O7	Lignan	
			36	S-(N-Hydroxy-N-methylcarbamoyl)glutathione	C12H20N4O8S	Amino acid	
383	383.0993333	384.1073333	37	4'-Demethyldeoxypodophyllotoxin	C21H20O7	Lignan	
			39	S-Adenosylhomocysteine	C14H20N6O5S	Amino acid	Cysteine and methionine metabolism
	383.1009	384.1089	33	4'-Demethyldeoxypodophyllotoxin	C21H20O7	Lignan	
			35	S-Adenosylhomocysteine	C14H20N6O5S	Amino acid	Cysteine and methionine metabolism
383.2	383.1050667	384.1130667	22	4'-Demethyldeoxypodophyllotoxin	C21H20O7	Lignan	
			24	S-Adenosylhomocysteine	C14H20N6O5S	Amino acid	Cysteine and methionine metabolism
			37	Acetyl-maltose	C14H24O12	Disaccharide	
	383.1050333	384.1130333	22	4'-Demethyldeoxypodophyllotoxin	C21H20O7	Lignan	
			24	S-Adenosylhomocysteine	C14H20N6O5S	Amino acid	Cysteine and methionine metabolism
			37	Acetyl-maltose	C14H24O12	Disaccharide	
	383.2235333	384.2315333					
	383.1064	384.1144	18	4'-Demethyldeoxypodophyllotoxin	C21H20O7	Lignan	
			20	S-Adenosylhomocysteine	C14H20N6O5S	Amino acid	Cysteine and methionine metabolism
			34	Acetyl-maltose	C14H24O12	Disaccharide	
	383.1059	384.1139	20	4'-Demethyldeoxypodophyllotoxin	C21H20O7	Lignan	
			21	S-Adenosylhomocysteine	C14H20N6O5S	Amino acid	Cysteine and methionine metabolism
			35	Acetyl-maltose	C14H24O12	Disaccharide	
399.2	399.1028333	400.1108333	14	alpha-Peltatin 2-[4-(Acetyloxy)phenyl]-5,6,7,8-tetramethoxy-4H-1-benzopyran-4-one 4'-Demethylpodophyllotoxin Isoflavone 7-O-beta-D-glucoside Flavonol 3-O-D-glucoside Flavonol 3-O-D-galactoside Flavonol 3-O-D-glycoside	C21H20O8	Lignan Flavone Lignan Isoflavone Flavonol Flavonol Flavonol	Phenylpropanoid biosynthesis Phenylpropanoid biosynthesis
	399.2818667	400.2898667					
	399.104	400.112	11	alpha-Peltatin 2-[4-(Acetyloxy)phenyl]-5,6,7,8-tetramethoxy-4H-1-benzopyran-4-one 4'-Demethylpodophyllotoxin Isoflavone 7-O-beta-D-glucoside Flavonol 3-O-D-glucoside Flavonol 3-O-D-galactoside Flavonol 3-O-D-glycoside	C21H20O8	Lignan Flavone Lignan Isoflavone Flavonol Flavonol Flavonol	Phenylpropanoid biosynthesis Phenylpropanoid biosynthesis
	399.1046333	400.1126333	9	alpha-Peltatin 2-[4-(Acetyloxy)phenyl]-5,6,7,8-tetramethoxy-4H-1-benzopyran-4-one 4'-Demethylpodophyllotoxin Isoflavone 7-O-beta-D-glucoside Flavonol 3-O-D-glucoside Flavonol 3-O-D-galactoside Flavonol 3-O-D-glycoside	C21H20O8	Lignan Flavone Lignan Isoflavone Flavonol Flavonol Flavonol	Phenylpropanoid biosynthesis Phenylpropanoid biosynthesis

	399.1035667	400.1115667	12	alpha-Peltatin 2-[4-(Acetyloxy)phenyl]-5,6,7,8-tetramethoxy-4H-1-benzopyran-4-one 4'-Demethylpodophyllotoxin Isoflavone 7-O-beta-D-glucoside Flavonol 3-O-D-glucoside Flavonol 3-O-D-galactoside Flavonol 3-O-D-glycoside	C21H20O8	Lignan Flavone Lignan Isoflavone Flavonol Flavonol Flavonol	Phenylpropanoid biosynthesis Phenylpropanoid biosynthesis
	399.1808	400.1888	1	(+)-gamma-Schizandrin (-)-gamma-Schizandrin	C23H28O6	Lignan	
			29	11-O-Demethyl-17-O-deacetylvindoline	C22H28N2O5	Alkaloid	
	399.1033	400.1113	13	alpha-Peltatin 2-[4-(Acetyloxy)phenyl]-5,6,7,8-tetramethoxy-4H-1-benzopyran-4-one 4'-Demethylpodophyllotoxin Isoflavone 7-O-beta-D-glucoside Flavonol 3-O-D-glucoside Flavonol 3-O-D-galactoside Flavonol 3-O-D-glycoside	C21H20O8	Lignan Flavone Lignan Isoflavone Flavonol Flavonol Flavonol	Phenylpropanoid biosynthesis Phenylpropanoid biosynthesis
	399.1827333	400.1907333	3	(+)-gamma-Schizandrin (-)-gamma-Schizandrin	C23H28O6	Lignan	
			24	11-O-Demethyl-17-O-deacetylvindoline	C22H28N2O5	Alkaloid	
	399.28	400.288					
	399.1032	400.1112	13	alpha-Peltatin 2-[4-(Acetyloxy)phenyl]-5,6,7,8-tetramethoxy-4H-1-benzopyran-4-one 4'-Demethylpodophyllotoxin Isoflavone 7-O-beta-D-glucoside Flavonol 3-O-D-glucoside Flavonol 3-O-D-galactoside Flavonol 3-O-D-glycoside	C21H20O8	Lignan Flavone Lignan Isoflavone Flavonol Flavonol Flavonol	Phenylpropanoid biosynthesis Phenylpropanoid biosynthesis
	399.1834333	400.1914333	5	(+)-gamma-Schizandrin (-)-gamma-Schizandrin	C23H28O6	Lignan	
			22	11-O-Demethyl-17-O-deacetylvindoline	C22H28N2O5	Alkaloid	
	399.2784667	400.2864667					
429.2	429.1054	430.1134	7 31	N-Ethylmaleimide-S-glutathione Formononetin 7-O-glucoside	C16H22N4O8S C22H22O9	Peptide Isoflavone	 Isoflavonoid biosynthesis
	429.2057	430.2137	6 32	Cinegalline Athamantin	C23H30N2O6 C24H30O7	Alkaloid Furanocoumarin	
	429.1094	430.1174	1 22	N-Ethylmaleimide-S-glutathione Formononetin 7-O-glucoside	C16H22N4O8S C22H22O9	Peptide Isoflavone	 Isoflavonoid biosynthesis
	429.2095333	430.2175333	14	Cinegalline	C23H30N2O6	Alkaloid	
	429.1109	430.1189	5 19	N-Ethylmaleimide-S-glutathione Formononetin 7-O-glucoside	C16H22N4O8S C22H22O9	Peptide Isoflavone	 Isoflavonoid biosynthesis
	429.2119333	430.2199333	20	Cinegalline	C23H30N2O6	Alkaloid	

The mass bins responsible for variation of MR-Buster sorghum polyphenol extract from the other two sorghum polyphenol extracts included small sugars, flavones, flavanones, flavonols (including glycosylated counterparts), unsaturated fatty acids and several large un-resolved polyphenolic polymers. These putative identifications included commonly detected sorghum polyphenols, e.g., apigenin, naringenin, luteolin, and eriodictyol. Both MR-Buster and Cracka sorghum polyphenol extracts were found to have large peaks at the high mass end of the spectrum, most notably at *m/z* 689, 851, 1107 and 1269 (**Appendix Figures A.9**). Smaller peaks were observed to surround these and were separated by 16 Da (loss of hydroxyl group), 162 Da (loss of sugar) and 272/255 Da (possible loss of flavonoid). These peaks were notably absent from the Liberty sorghum polyphenol extract. Cracka sorghum polyphenol extract was found to have overlapping mass bins to those from the MR-Buster sorghum polyphenol extract but with less diversity of metabolites as most mass bin identifications were of routinely identified sorghum polyphenols, such as apigenin and naringenin. White sorghum (Liberty) polyphenol extract presented little similarity to both red coloured grain extracts as its mass bins contributing to variation included disaccharides, tricarboxylic acids, fatty acids and lignans. Interestingly, the most abundant mass bins across the three sorghum polyphenol extracts were essentially identical. The putative identifications for the most abundant mass bins indicated the presence of phenylpropanoid glycerides, flavone/flavanones, disaccharides, and most predominately fatty acids, including oleic acid, linoleic acid and oleic/linoleic acid-related compounds.

The putatively identified compounds from both OPLS-DA and the 10 most abundant from each sorghum polyphenol extract were then mapped to specific biosynthetic pathways using MetaboAnalyst Pathway Analysis (**Figure 3.15**).

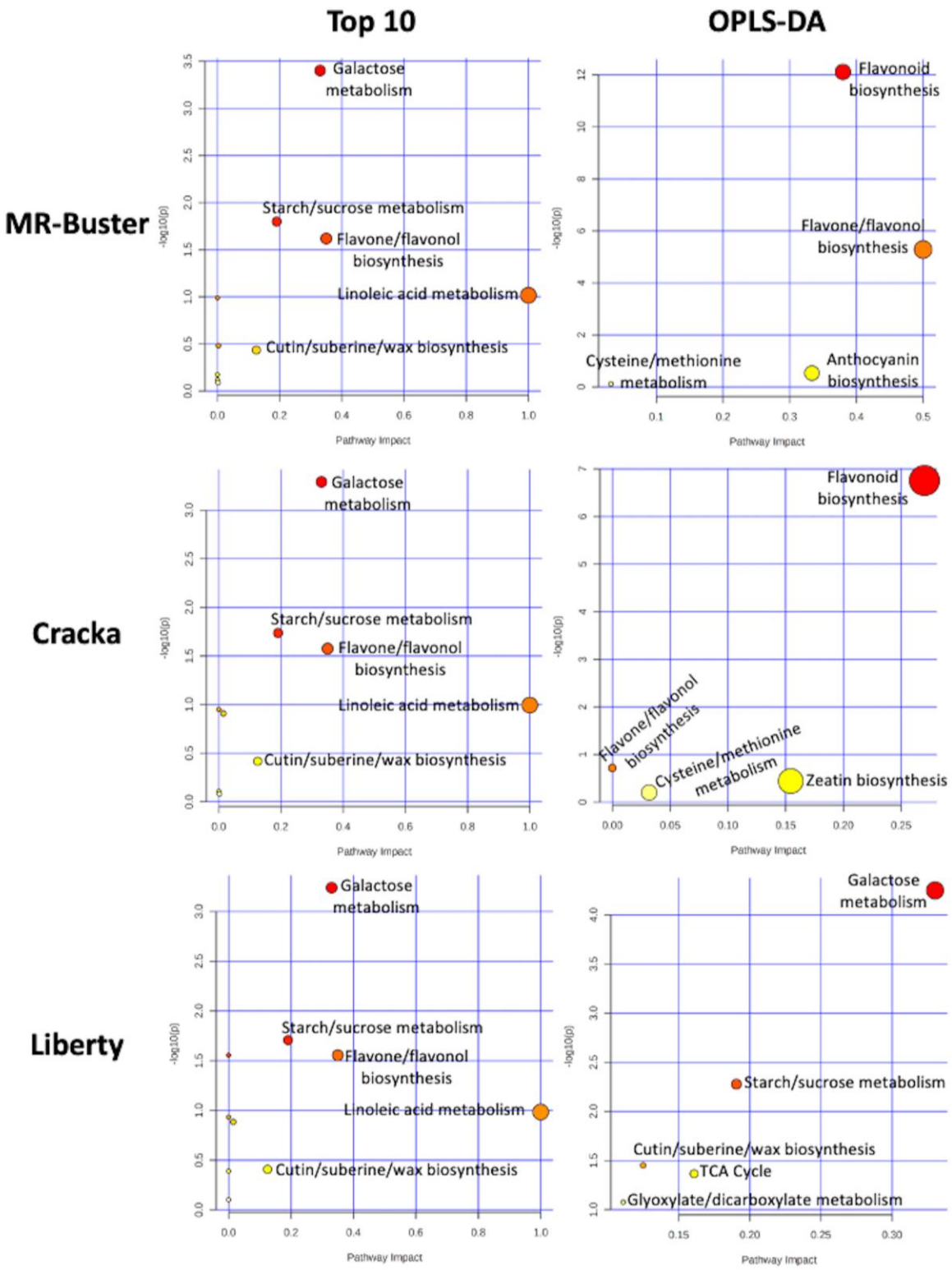

Figure 3.15 Pathway analysis of identified compounds from ESI (−)
Mass bins (*m/z*) representing the 10 most abundant ions and those highlighted as causing variance between sorghum polyphenol extracts were identified and mapped to biosynthetic pathways using MetaboAnalyst Pathway Analyst. This analysis identified the most relevant biosynthetic pathways associated with the compounds identified. The pathways were then ranked based on their impact with a value closer to one (red) as being more impactful than a value closer to zero (yellow). The *y*-axis, −log(10)p, is a measure of statistical significance.

The pathway mapping conducted using MetaboAnalyst was able to highlight potential pathways of interest based on the putative identifications made using mass spectrometry. This analysis highlight pathways of higher significance (further to the right on the x-axis) and how statistical significant pathways were based on how many putative identifications were labelled to them. Regarding the top 10 peaks identified from mass spectrometry, all three sorghum extracts have essentially identical pathway profiles. This indicates that any variations between grains are due to metabolites of lower abundance. When mass peaks causing variation between grains (OPLS-DA) were analysed clearer differences between the grains emerged. Both red grains strongly favor flavonoid biosynthesis, as compared to Liberty polyphenol extract, with Cracka showing a larger statistical significance indicating more flavonoid compounds could be attributed to this pathway. Liberty polyphenol extract was very different to the red grains instead favouring pathways for energy and fatty acid metabolism. These analyses support the notion that flavonoid and general polyphenol pathways have been downregulated in white sorghum grains but that all modern grains heavily favor energy and fatty acid metabolism.

While this work approached anti-nutrient characterisation from the perspective of metabolomics, several other '-omics' techniques can be valuable to understanding metabolic and biosynthetic pathways. Metabolomics is highly useful for understanding the broad chemical nature of a substance, in this case a polyphenol-rich extract from sorghum grain. This analysis provides insight into the chemical nature of the substance instead of detailed findings on often very specific groups of compounds. However, metabolomics can only give so much detail, as noted in this work. MetaboAnalyst pathway analysis indicated statistically significant pathways of interest but could not categorically identify them or link them in the broader scheme of biosynthetic pathways due to the fingerprinting approach used.

The use of gene expression/knockdown or combined proteomic/transcriptomic approaches would have been able to clearly identify pathways of interest. For example, Wu et al. (2012) used gene expression analysis in two sorghum varieties, a tannin and a non-tannin variety, to determine differential gene expression based on the production of tannins. They found that the non-tannin variety lacked certain gene products related to proanthocyanidin synthesis and that other late stage markers of anthocyanin production were downregulated compared to the high tannin grain.

Metabolomics was the preferred methodology in this work because the aim was to profile the metabolite fingerprint as opposed to focussing on a few specific pathways. Additionally, approaches like that used here can be most helpful in deciding where more targeted methods (gene expression, proteomics) can be most useful. Sorghum analyses of the past have typically focussed their metabolite searches in a more directed way – usually looking only at flavonoid biosynthesis. The current work sought to expand that point of view in an attempt to capture subtle patterns in global sorghum grain metabolites and detect unintentional consequences from directed sorghum breeding. Gene expression/knockdown approaches, while useful for specific pathway mechanistic understanding, ignore the fact that plant metabolite synthesis is not only controlled by genes. The formation and biosynthesis of metabolites is complex with both environmental and genetic inputs influencing how and when various compounds are synthesised. As previously discussed, polyphenol synthesis is influenced by environmental factors including UV light and animal predation. Recent genomic advances have revealed the more nuanced genomic influences that control general polyphenol synthesis (Wu et al., 2012).

A small number of studies have followed similar analytical approaches with metabolomics and sorghum grain extracts. Recently, Zhou et al. (2020), using LC-ESI-MS^2, compared three sorghum varieties of different colour (black, red, white) to study possible reasons for differences in colour. PCA revealed similar separation of grains based on colour, as seen here for ESI (+) and MALDI (+) and compound identification found that the darker grains contained more flavonoids than lighter grains. Flavonoids made up almost a quarter of the 651 compounds identified.

The compounds putatively identified in MR-Buster and Cracka sorghum polyphenol extracts overlapped considerably compared to those identified in Liberty sorghum polyphenol extract. This was expected as MR-Buster and Cracka are both red sorghum varieties while Liberty is a white coloured grain. Sorghum grain can have a variety of colours including black, brown, red, yellow and white. Typically, though not always, the colour of the grain gives some indication of the polyphenols present with darker and more coloured grains containing higher concentrations and often larger, more complex polyphenols (Awika et al., 2005; Rhodes et al., 2014). The two red varieties analysed here were expected to contain a greater variety and relative amount of polyphenols than the white grain, Liberty, which was found to be true. These results indicated that the Liberty variety has been successfully bred to reduce/limit the synthesis of polyphenols in favour of energy and fat metabolism. MR-Buster and Cracka,

while found to putatively contain many types of polyphenols, were not found, using this methodology, to contain the traditional condensed tannins routinely found in high-tannin 'bird-resistant' varieties most well-known to be anti-nutritional to monogastrics. This result matched those found by Dicko et al. (2002) in their study of 50 sorghum varieties from Burkina Faso. The results here support the notion that the breeding of modern red sorghum varieties has limited the synthesis/polymerisation of traditional condensed tannins but not small and medium sized polyphenols like those identified in this study. Another explanation for the low to zero concentration of traditional tannins may be due to the extraction method. In this study, the grain was soaked overnight to ease grain grinding and bran separation. However, tannin content, in high-tannin 'bird resistant' grains has been found to increase significantly with drying (Butler, 1982). This is thought to be due to an increase in flavan-3-ol, e.g. (epi)catechin, polymerisation into larger tannin structures.

The divergence of modern white and red sorghum grain varieties may be explained by pathway alteration of the fundamental routes to polyphenol biosynthesis as a result of breeding efforts. As described in **Section 1.3.4**, polyphenols are synthesised by a combination of two pathways, the shikimate and acetate-malonate pathway. For plant secondary metabolite biosynthesis, carbon dioxide is metabolised into four products, erythrose 4-phosphate, PEP, pyruvate and 3-phosphoglycerate (**Figure 3.17**).

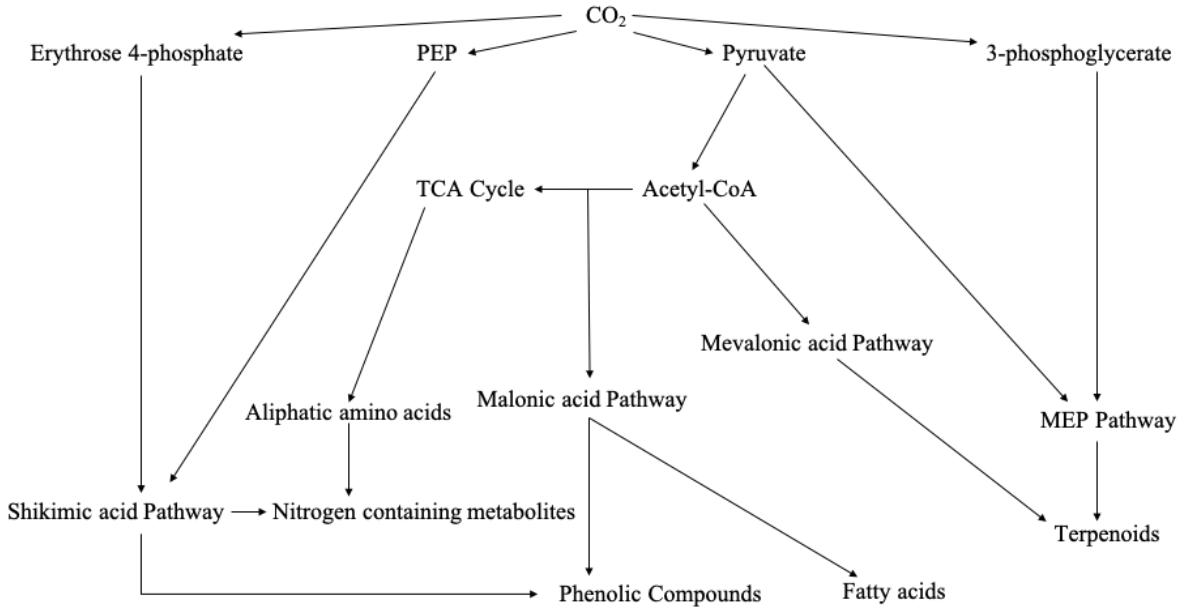

Figure 3.17 Routes for the synthesis of phenolic compounds and other related secondary metabolites (adapted from Ncube and Van Staden, 2015)

While a combination of both the shikimic and malonic acid pathways is used for the synthesis of phenolics, the sorghum varieties analysed here may be relying more on the malonic acid/malonyl-CoA and acetyl-CoA routes for synthesis. In this study, all three sorghum polyphenol extracts, especially from Liberty grain, were found to have high ion counts for mass bins putatively identified as fatty acids, including oleic acid, linoleic acid, vernolic acid, ricinoleic acid and trihydroxyoctadecenoic acid, which could result in nutritional variation in monogastric diets composed primarily of sorghum grain. With oleic acid as a starting point, vernolic acid is formed through an epoxidation reaction, ricinoleic acid through hydroxylation, linoleic acid through desaturation and trihydroxyoctadecenoic acid through the hydroxylation of linoleic acid (Mazur et al., 1999; Cao and Zhang, 2013). The identifications made through mass spectrometry echoed the strong, sharp FT-IR peaks between 3000 and 2900 cm^{-1} which correlate with C – H bonding found extensively in fatty acids (Shapaval et al., 2014).

Modern sorghum breeding, generally, may have shifted synthesis away from the shikimic acid pathway and more towards malonic acid. For white sorghum varieties, this shift may be even more profound as malonyl-CoA and constituents of the malonic acid pathway are re-directed to synthesising fatty acids over phenolics compounds. This hypothesis is supported by current work on sorghum grain and its management. As discussed in the introduction (see **Section 3.2**), older varieties of sorghum have often been referred to as 'bird-resistant.' Xie et al. (2019) studied sorghum varieties and preference by birds for feeding. They found that varieties avoided by birds had higher anthocyanin and tannin precursors (flavan-3-ols) than those that they preferred to eat. This behaviour correlated with the presence or absence of the *Tannin1* gene, previously found in sorghum to be involved in the regulation of polyphenols and tannins (Wu et al., 2012). In addition to determining the difference in polyphenols, the bird-preferred sorghum was found to have increased volatiles associated with fatty acids, as well as higher concentrations of fatty acids, including linolenic acid. Xie et al. (2019) concluded that the modulation of the *Tannin1* gene affects *SbGL2* which is involved in transcription of fatty acids. This change in fatty acid and tannin synthesis may play a role in the acetate/malonate pathway.

Juhaimi et al. (2019) analysed white and red sorghum grains and found white sorghum to contain 11.7% oil content versus 9.5% for red coloured grain. Additionally, the total phenolic content of the grains was found to negatively correlate with fatty acid content as red coloured sorghum had a significantly higher total phenolic content than white coloured sorghum. MR-Buster has been previously found to contain linoleic and oleic acids as the most dominant fatty

acids, making up 80% of unsaturated fatty acid content (Mehmood et al., 2008). White sorghum varieties are similarly dominated by oleic and linoleic acids but at slightly higher proportions (Afify et al., 2012). Wang et al. (2007) compared hexane and supercritical CO_2 extraction methodologies from sorghum dried distillers grain with solubles (DDGS) and found both methods to extract a range of compounds including triacylglycerols, free fatty acids, tocopherols, phytosterols and policosanols. Of the fatty acids extracted, 94% was palmitic, oleic and linoleic acid. Zhang et al. (2019) found that linoleic and oleic acids were the most dominant fatty acids, making up 80% of the fatty acid content in red sorghum oil.

Broiler chickens fed diets high in oleic acid have been found to have a higher FCR (reduced feed efficiency), as well as reduced muscle and carcass weights (Toomer et al., 2003). Similar long chain fatty acids have also been shown to inhibit enzyme activity which could result in muted responses of exogenous feed enzymes (Kido et al., 1984). The high levels of fatty acids detected in the current study indicate the potential of implementing an exogenous lipase or emulsifier, as high levels of these compounds could be detrimental to growth and performance parameters.

3.4.6 Analysis of select compounds in sorghum polyphenol extracts using tandem mass spectrometry (MS^2) (adapted from Hodges et al., 2021)

Several mass peaks were selected from the sorghum polyphenol extract spectra produced from ESI (–) and further analysed using MS^2. The fragmentation patterns of selected peaks are described in **Table 3.8**.

Table 3.8 Fragmentation of selected peaks from sorghum polyphenol extracts

m/z	Δppm	Fragments	Identified Compounds
191.0221	12.56	173, 129, 111, 87	(Iso)citric acid
329.2361	8.50	229, 211, 171	Trihydroxyoctadecenoic acid
341.1124	10.26	295, 179, 119, 113, 89	Disaccharide
399.1164	11.02	253, 235, 163, 145	Coumaroyl-caffeoylglycerol
415.0923	25.05	253, 179, 161, 135	Dicaffeoylglycerol or caffeoyl-glucosylglycerol
689.2124	N/A	563, 442, 417	Unknown glycosylated flavonoid dimer
851.2569	N/A	689, 563, 547, 279, 97	Unknown glycosylated flavonoid dimer

The compounds identified through MS^2 are routinely identified in sorghum polyphenol extracts (Kang et al., 2016; Wu et al., 2016). The categories of compounds identified here echoed the

putative identifications made previously (see **Table 3.7**, **Appendix Tables A.1 – A.9**). The lignin-like compounds of phenolic acids, similar to phenylpropanoid glycerides, are often associated with cross-linking polysaccharides, such as glucoarabinoxylans, in the cell wall matrix (Ayala-Soto et al., 2015; Hatfield et al., 2017).

Additionally, the two red sorghum (MR-Buster, Cracka) polyphenol extracts had large mass peaks at the higher end of the spectrum, most notably at *m/z* 689, 851, 1107 and 1269 (**Appendix Figure A.9**). Smaller peaks surrounded these major ones and were separated by 16 Da (loss of hydroxyl) while the larger separations included 162 Da (loss of sugar), 272 and 255 (possible loss of flavonoid). These peaks were notably absent from the Liberty sorghum polyphenol extract and both tannin extracts. However, the pattern and spacing of the peaks found in red sorghum was similar to those found in grape seed and quebracho tannin extracts associated with condensed tannins of increasing polymerisation. Interrogation of these masses resulted in some possible putatively identified compounds (**Table 3.9**).

Table 3.9 Putative identifications of unknown peaks in sorghum polyphenol extracts

m/z	**Identification**
1107	Malvidin 3-O-[6-O-(4-O-(4-O-(6-O-(trans-caffeoyl)-beta-D-glucopyranosyl)-trans-p-coumaroyl)-alpha-L-rhamnopyranosyl)-beta-D-glucopyranoside]
	Pelargonidin 3-O-[2-O-(2-(E)-feruloyl-beta-D-glucopyranosyl)-6-O-(E)-feruloyl-beta-D-glucopyranoside]-5-O-(beta-D-glucopyranoside)
	Pelargonidin 3-(6"-ferulyl-2'"-sinapylsambubioside)-5-glucoside
1123	Cyanidin 3-(6"-ferulyl-2'"-sinapylsambubioside)-5-glucoside
	Cyanidin 3-(6"-p-coumaryl-2"-sinapylsophoroside)-5-glucoside
1139	Delphinidin 3-(diferuloyl)sophoroside-5-glucoside
	Kaempferol 3-O-sinapoyl-caffeoyl-sophoroside 7-O-glucoside
	Kaempferol 3-(2'"-sinapoylsophoroside) 7-cellobioside
1269	Malvidin 3-O-[6-O-[4-O-[4-O-(6-O-caffeoyl-beta-D-glucopyranosyl)-p-coumaroyl]-alpha-L-rhamnosyl]-beta-D-glucopyranoside]-5-O-beta-D-glucopyranoside
	Cyanidin 3-O-[6-O-(malonyl)-beta-D-glucopyranoside]-7,3'-di-O-[6-O-(sinapyl)-beta-D-glucopyranoside]
1285	Malvidin 3-O-[6-O-[4-O-[4-O-(6-O-caffeoyl-beta-D-glucopyranosyl)caffeoyl]-alpha-L-rhamnosyl]-beta-D-glucopyranoside]-5-O-beta-D-glucopyranoside
	Delphinidin 3-(6-malonylglucoside)-7,3'-di-(6-sinapoylglucoside)
1421	Cyanidin 3-(6-malonylglucoside)-7,3'-bis[6-(4-glucosyl-p-hydroxybenzoyl)glucoside]

These putatively identified compounds are plausible to be found in sorghum polyphenol extracts. They are anthocyanidin (malvidin, pelargonidin, cyanidin, delphinidin) or flavanone (kaempferol) based and are all generally made up of complex mixtures of lignins, phenolics

acids and sugars. The compounds above mirror the lignin-like compounds identified using MS^2 (**Table 3.8**). Compounds with the same masses have previously been identified in sorghum polyphenols extracts and fall into two categories: pyrano-anthocyanin/flavanone or glucosylated heteropolyflavans.

Pyranoanthocyanins are formed from anthocyanins (including cyanidin, malvidin and delphinidin) and are commonly detected in red wines. There is uncertainty as to exactly how these compounds are formed but include oxidative reactions with small metabolites, including phenolics or vinyl molecules, and may be natural processes or derived from polyphenol extraction methods (de Freitas and Mateus, 2011). Sorghum grains are known to contain high levels of anthocyanins, in particular the unique class of compounds known as 3-deoxyanthocyanins. In sorghum leaf sheath, Khalil et al. (2010) describes the structural determination of a novel pyrano-3-deoxyanthocyanidin, pyrano-apigenindin. They hypothesised that the compounds could be synthesised within the plant through a combination of apigenindin and *p*-coumaric acid but also couldn't conclude that the compound was not a product of the extraction process.

Compounds with the same masses as detected in this study were found by Rao et al. (2018) as well as Yang (2013) in their studies of phenolic profiles and health benefits of white, red and black sorghum grains. Red and black sorghum grains were found to have unique flavanone structures including pyrano-naringenin-catechin (*m/z* 689), pyrano-naringenin-catechin-glucoside (*m/z* 851), pyrano-eriodictyol-catechin-glucoside (*m/z* 867) and pyrano-naringenin-pyrano-eriodictyol-catechin (*m/z* 1107). These identifications were based on MS^2 fragmentation interpretation and comparison to similar compounds previously identified in sorghum by Khalil et al. (2010) and in certain types of wood polyphenol extracts (Howell et al., 2007; Antal et al., 2010). The fragmentation patterns obtained in the current study do not closely match those from Yang (2013) but have some peaks that are similar. Purification of these compounds followed by MS^2 and even nuclear magnetic resonance (NMR) would allow for more definitive identifications.

Pyranoanthocyanins were identified in black currant extracts but later determined to be a product of the extraction process with acetone (Lu et al., 2000; Lu and Foo, 2001). Alcohol and acetone were compared as solvents and resulted in the pyranoanthocyanins being absent in the alcohol extracts. Furthermore, the formation of these compounds in acetone was

monitored at room temperature and 40°C with significant conversion of anthocyanins to pyranoanthocyanins detected over three days at the elevated temperature. However, Khalil et al. (2010) used a mixture of 1,3-butanediol and ethanol as the extraction solvent rather than acetone and found similar compounds. This indicates that extraction conditions may not be solely to blame for compound formation.

Another possibility for these large unknown compounds is that they are glucosylated heteropolyflavans. In one of the more comprehensive sorghum polyphenol extract MALDI studies, Krueger et al. (2003) characterised sorghum polyphenol extracts and detected large polymerised tannins in the traditional sense as well as unique polymerisations of eriodictyol/naringenin and luteolinidin/apigeninidin with varying degrees of glycosylation. These putative identifications were based on original findings by Gujer et al. (1986) who detected dimer and trimer flavonoids with eriodictyol as the base unit. From this early work, Krueger et al. (2003) predicted the molecular weights of these unique compounds with the equation 288 + 272*a* +256*b* +162*c* + cation with 288 representing the mass of an eriodictyol base unit, 272 referring to a proluteolinidin unit, 256 to a proapigeninidin unit, 162 to additional sugar units and the letters referring to possible degrees of polymerisations. Similar equations are routinely used in MALDI analysis to predict structures and masses. While the current work identified these compounds in the negative mode, the equation can be applied, albeit without the cation addition. Kruger et al. (2003) identified groups of masses at *m/z* 1435, 1419 and 1257, 1273, 1289 (with the addition of a cesium cation of 133). The first group represents a polyflavan trimer composed of eriodictyol plus two proapigeninidin units (1419) and one proluteolinidin and one proapigeninidin unit (1435) both with three sugar units. The subtraction of the cesium adduct gives the masses of 1302 (from 1435) and 1286 (from 1419) which correlate with the compounds detected at *m/z* 1301 and 1285 in this work. The second group represents a polyflavan dimer of similar structure but with one less sugar unit. The subtraction of cesium gives the masses 1156 (from 1289), 1140 (from 1273) and 1124 (from 1257) thus matching the compounds detected in this work at *m/z* 1155, 1139 and 1123. The MS^2 spectra support these identifications as the primary fragment masses detected correspond to losses of 256, 272 and 162. Again, further purification of these unknowns is needed along with additional structural evidence that could be gained using NMR.

While the origin of these classes of compounds is not fully understood, their presence poses interesting questions about sorghum polyphenols and polyphenol extractions generally. If the

compounds are true biosynthetic polymers synthesised within the grain, it reveals a possible unique pathway for polymerisation and a coordinated re-direction of resources and energy from traditional condensed tannin synthesis to something novel. As discussed earlier (see **Section 3.4.5**), a re-direction within pathways appears to be occurring as fatty acid synthesis seems to be up-regulated which could defer metabolites and precursors away from phenolics. The grains analysed here have been selected and bred to reduce tannin content as it is a known anti-nutrient. While condensed tannins may have been reduced and/or eliminated, another group of polymers may have been formed to take their place.

3.4.7 Usefulness of multiple techniques to characterise polyphenol and tannin extracts (adapted from Hodges et al., 2021)

Traditional analysis of polyphenol extracts follows the same methodology: extraction with aqueous methanol or acetone, purification and fractionation using column or liquid chromatography and finally chromatography-mass spectrometry. The identification of purified compounds is made based on retention times (if using chromatography) and fragmentation pattern comparison to commercially obtained standards if applying MS^2 techniques. This approach, while routine and well-tested, has limitations with respect to biologically relevant systems. The analysis of crude extracts can yield important information about potential interactions occurring upon consumption of a certain plant material, in this case sorghum grain. This study sought to analyse crude extracts from sorghum polyphenol extracts using an alternative analytical framework incorporating a variety of techniques including UV/Vis spectroscopy, FT-IR spectroscopy, MALDI and ESI-MS(/MS). Previous work has taken a similar approach in analysing sorghum tannins (Reeves et al., 2020) and tannins important to the wine industry (Laghi et al., 2010).

UV/Vis spectroscopy is an established technique that gives basic information about plant extracts, including those rich in polyphenols. The primary purpose of UV/Vis spectroscopy lies in HPLC detection of polyphenols at 280 nm. The use of UV/Vis is important for the rapid identification of polyphenols in a sample and can be used in online analysis with chromatographic systems or even incorporated into a simple and rapid extraction to confirm the presence/absence of polyphenols. The results in this study indicated a role for UV/Vis spectroscopy in the detection of high-tannin sorghum varieties as opposed to the three 'tannin-free' varieties analysed here. The two tannin extracts, grape seed and quebracho, are known

to contain condensed tannins that are detrimental to animal nutrition and have been previously detected in high-tannin sorghum grains. These two extracts had very different profiles to the three sorghum polyphenol extracts. While the three sorghum polyphenol extracts had different profiles among themselves, this was limited to differentiating between red and white sorghum grain, rather than each specific variety. This work could be improved by analysing more sorghum varieties and using multivariate analysis to further determine relationships based on their spectra. Profiles could then be built on these relationships based on evidential animal feeding studies, as well as farmer preference. UV/Vis spectrophotometers are widely used in scientific laboratories, quality control facilities and are affordable and small enough to be incorporated into grain processing sites and even large-scale, industrial farms. The comparison of a 'quick' extract of grain to a known tannin standard could be used to confirm the quality of the material as well as it's suitability for animal feed.

FT-IR spectroscopy is a widely used technique with primary applications in materials science. Most current FT-IR studies concerning tannins involve impregnating materials with the natural polymers to improve their surface characteristics. The use of FT-IR in this study allowed for a more detailed analysis of the chemical environment of the sorghum polyphenol extracts and tannin extracts as compared to UV/Vis spectroscopy. FT-IR has previously been shown to be successful in distinguishing bulk differences among general metabolite profiles (Johnson et al., 2003), identifying the presence/absence of certain chemical classes (Cameron et al., 2006) and nuancing subtle variations between sample types, e.g., tannin extracts separated based on tannin chemistry (Grasel et al., 2016). However, the use of FT-IR in characterising polyphenol extracts is, however, similar to UV/Vis. While providing detailed information about functional groups, FT-IR cannot make identifications of individual compounds but can give a strong indication of which groups of compounds are present. Use of known standards is still important here to provide spectra for comparison. Similar to UV/Vis, FT-IR is a simple, affordable method of analysis that could be done online versus only in a full scientific laboratory. A rapid testing method using near-infrared radiation (NIR) was analysed for use as a predictive measure of phenolic, tannin and 3-DA content in sorghum grains without being reliant on traditional wet chemistry techniques (Dykes et al., 2014). Only ground grain was used for testing and allowed for the successful prediction of total phenolic content, as well as tannin and 3-DA content to a lesser extent. While this study analysed freeze-dried extracts, FT-IR can easily be applied to liquid extracts taken on-site.

In the current study, spectra obtained from ESI (+, −) were clearer than those produced using MALDI (+) with a greater number of clearly identifiable peaks, most likely due to the lack of need for a matrix compound with ESI. ESI (+, −) analyses were also successful in detecting routinely identified polyphenol compounds in sorghum, including apigenin, naringenin, and phenylpropanoid glycerides (Kang et al., 2016). Sorghum polyphenol extracts have been sparingly analyzed using MALDI (Krueger et al., 2003; Qi et al., 2018; Jiang et al., 2020; Reeves et al., 2020). Unsupervised analysis of the ESI and MALDI spectra allowed for the clear separation between red and white coloured varieties and in some cases among all three extracts.

MALDI and ESI mass spectrometry provided the most information about phenolic profiles and individual compounds in the extracts analysed. Mass spectrometry is the most common analytical technique for characterising polyphenols as it gives detailed information about individual masses and fragmentation patterns thus allowing for clear identifications when compared to a standard. The approach taken here, that of metabolite profiling, cannot definitively identify compounds without tandem MS and is a limitation. Metabolite profiling, however, can be very useful in differentiating types of extracts, determining specific groups of compounds and making putative identifications. The putative identifications made here allowed for pathways of interest to be highlighted. Recently, Zhou et al. (2020) compared three sorghum varieties (black, red, and white) to study metabolic variation based on colour. PCA revealed a separation of the grains based on grain color and compound identification found that darker coloured grains contained more flavonoids than lighter coloured grains, similar to what was determined in this thesis. Typically, the colour of the grain gives some indication of the type and quantity of polyphenols present as darker and highly coloured grains often containing higher concentrations of polyphenols and have larger, more complex compounds (Rhodes et al., 2014). These methods are the least likely of the three used in this study to be directly applicable to industry settings and are most likely needed when first releasing a new variety of grain to the market.

FT-IR and the two MS techniques provided similar powers of separation among the sorghum polyphenol extracts and tannin extracts. Based on those results and the compatibility and pricing of equipment, FT-IR may be the most useful tool for determining the applicability of certain grains to feed formulations. However, extensive prior studies on major compounds

present in these grains should be used to guide the interpretation and analysis of FT-IR spectra in the field.

3.5 Conclusions and future work

3.5.1 Conclusions (adapted from Hodges et al., 2021)

While modern monogastric animal feed has been formulated for optimum nutrient utilisation and digestive efficiency, performance gains remain, especially in feed containing sorghum grain. Efforts to reduce anti-nutrient content in sorghum, most notably tannin and polyphenol concentrations, have been successful. However, gaps in the efficiency and efficacy of feed additives remain, possibly due to unintended breeding consequences of feed quality sorghum grain. An understudied alternative analytical approach was thus used to identify anti-nutrients that might be causing varied/suboptimal performance in feed containing sorghum and to determine the suitability of different analytical techniques for assessing metabolic variation among sorghum grain extracts.

Metabolite profiling allowed for specific pathways to be highlighted in each sorghum grain type. Clear differences were observed between red and white coloured varieties with white sorghum grain favouring energy and fatty acid metabolites over the more routinely identified flavonoids in the red sorghum varieties. High concentrations of fatty acids were also detected in the red coloured grains indicating that this may be a common pathway in modern sorghum varieties. The pathway involved may centre around malonate which provides a second route to phenolic synthesis to the more common shikimate pathway. Malonate also leads into fatty acid synthesis indicating that a re-direction of metabolites may be occurring as large polyphenols, like condensed tannins, have been bred out of feed relevant sorghum varieties. Additionally, high mass compounds were detected in the red sorghum polyphenol extracts which might be unique polymerisations of smaller flavonoid monomers in the extracts. The removal of traditional flavonol polymerised compounds may have led to the synthesis of something similar in size to maintain its original purpose.

This study of an alternate analytical framework for polyphenol characterisation highlighted the need for complementary methods to fully understand the complexity of the sorghum polyphenol extracts. UV/Vis and FT-IR spectroscopy provided information about the general chemical profiles of both sorghum polyphenol extracts and tannin extracts primarily

highlighting chemical functional groups and broad compound groups. FT-IR spectroscopy provided general chemical profiles which highlighted functional groups and classes of compounds specific to polyphenol and tannin structural chemistry. Multivariate analysis of the FT-IR spectra demonstrated that the technique was robust enough to separate different extract types and to explain greater variance in the data than any MS method. Both ESI analyses produced similar plots to that of FT-IR, albeit with slightly better grouping of the sorghum extracts. ESI also provided a clearer metabolite profile than MALDI. These results indicated that, with regard to untargeted analysis, FT-IR and ESI provide essentially the same end-product allowing for similar conclusions to be drawn on bulk differences in the spectra. Based on these results, compatibility, and pricing, FT-IR may be the most effective tool for determining the applicability of certain grains to feed formulations, particularly with regard to polyphenol content. This application could be especially important in varietal selection for grain breeding and feed applications. Markers for chosen nutritional parameters, such as protein structure and anti-nutrient content, could be selected for and used as a screening tool prior to more intensive analytical methodologies should they be needed. However, mass spectrometric studies of metabolites present in these grains should be used to guide the interpretation of FT-IR spectra in the field to further highlight subtle differences in the grains that may result in monogastric feed performance variation.

3.5.1 Future work

There are several options available to expand this work in future studies. These mostly revolve around the extraction and purification methods but also include alternative analytical tools. The current study evaluated one extraction solvent, aqueous acetone, as prior optimisation and literature review indicated that this mixture would target the compounds we believed to be of greatest importance to animal anti-nutrition – larger, polymerised polyphenols like condensed tannins. This is an area of contention in the literature as methanol and acetone are seemingly chosen by preference by different research groups. In future study, the evaluation of both methanol and acetone at varying aqueous concentrations could be evaluated. In addition to the extraction solvent, other methods of decortication and processing of the grain could be trialled. These could include but are not limited to preparing the grain in liquid nitrogen, using a mechanical decorticator and extracting the grain in an ultrasonic bath. Once extracted, the mixture of polyphenols could then go through a whole slew of purification and separation regimes, some of which were highlighted in **Section 2.2**. The various purified extracts and

separated fractions could then be individually analysed using the same methodology as used in this chapter. Although several common analytical techniques were employed in this thesis, the most utilised method, HPLC-MS, was not used. This is the clearest work to take into future research to identify specific compounds more clearly in the sorghum polyphenol extracts. This would be most important to grain breeding research as it could pinpoint very specific pathways and compounds of interest and potential measures to take in future work. Finally, NMR could be utilised to more clearly analyse and characterise specific compounds, particularly the large, unknown polymers detected in the red sorghum polyphenol extracts.

Chapter 4 – A study of the impact of sorghum polyphenol extracts and tannin extracts on the activity of exogenous feed enzymes – phytase and protease

A portion of this experimental chapter has been peer reviewed and accepted for publication in a conference paper. Full copies of these papers can be found in **Appendix D**.

Hodges, H., Cowieson, A., Falconer, R., Cameron, D., (2020). Chemical profile and effects of modern Australian sorghum polyphenolic-rich extracts on feed phytase and protease activity. *Proceedings of the Australian Poultry Science Symposium*. **31**, 76-79.

Kempapidis, T.*, Bradshaw, N.J.*, **Hodges, H.E.***, Cowieson, A.J., Cameron, D.D., Falconer, R.J., (2020). Phytase Catalysis of Dephosphorylation Studied using Isothermal Titration Calorimetry and Electrospray Ionization Time-of-Flight Mass Spectroscopy. *Analytical Biochemistry*, **606**, 113859. (*denotes equal authorship)

Some of the work in this chapter is an extension to that in the thesis of Theofilos Kempapidis, PhD. The ITC methodology used in this chapter was originally developed by Theofilos and was subsequently modified to improve the assay's precision.

4.1 Summary

Two *in vitro* methods were used to evaluate the activity of two exogenous feed enzymes, a *Citrobacter braakii* (*C. braakii*) 6-phytase and a *Nocardiopsis prasina* (*N. prasina*) serine protease (hereafter referred to as phytase and protease, respectively), in the presence of polyphenol extracts prepared from modern Australian sorghum grain varieties (MR-Buster, Cracka, Liberty), as well as two tannin extracts from grape seed and quebracho wood. Quantitative characterisation of the sorghum polyphenol extracts found both red sorghum (MR-Buster, Cracka) polyphenol extracts to have a significantly higher total phenolic content than the white sorghum (Liberty) polyphenol extract. Both tannin extracts (grape seed, quebracho) had significantly higher total phenolic contents than all three sorghum polyphenol extracts. An isothermal titration calorimetry (ITC) method was next used to monitor phytase activity in the presence of its substrate, phytate, as well as the sorghum polyphenol extracts and tannin extracts. The enzyme was found to be inhibited between 50 – 100%, by the highest concentration of sorghum polyphenol extract (0.125 mg/mL) and most by MR-Buster sorghum polyphenol extract. Both tannin extracts inhibited phytase activity 100% at much lower concentrations of 0.007 and 0.015 mg/mL. Using more traditional colourimetric techniques, ultraviolet absorbance was used to measure protease activity in the presence of a small, synthetic substrate as opposed to a more traditional proteinaceous substrate. Protease activity was significantly inhibited by all three sorghum polyphenol extracts at the highest concentration (1.6 mg/mL) up to ~20%. The two tannin extracts inhibited protease activity significantly to over 90% at the same concentration. Evaluation of the reaction kinetics found inhibition to be a mixture of non-competitive and uncompetitive inhibition. When converted to relevant agricultural feed and enzyme dosage values, the protease was found to be a robust feed additive enzyme while the phytase was inhibited below its normal commercial dosage. These results indicate that, when creating diets with large amounts of sorghum grain and exogenous feed enzymes, care should be taken to ensure full enzyme activity for optimal nutrient utilisation.

4.2 Introduction

4.2.1 Protein/enzyme-polyphenol interactions and their anti-nutritional impact

University of Sheffield organic chemist Edwin Haslam defines tannins as 'polydentate ligands with a multiplicity of potential binding sites provided by the numerous phenolic groups and aryl rings on the periphery of the molecule' (Haslam, 1989). These structural features give tannins and polyphenols their most well-known properties, including antioxidant, anti-nutrient, leather tanning and sensory in food/drink products. While polyphenols are routinely found to beneficial in human diets (see **Section 1.4.4**), they are known to be anti-nutritional, especially regarding monogastric animal nutrition (Jambunathan and Mertz, 1973; Armstrong et al., 1974; Bravo, 1998; Selle et al., 2017). This negative impact comes partly from the precipitation and binding of large macromolecules, most commonly proteins, and through enzyme inhibition which can limit nutrient uptake and digestibility. For example, animals fed high-tannin varieties of sorghum grain often have a higher nitrogen content in their faeces due to increased protein complexation and digestive enzyme inhibition (Haslam, 1989). High molecular weight compounds, including condensed and hydrolysable tannins, are thought to be the principal culprits of these negative effects and have been studied and reviewed extensively (Jansman, 1993; Nyamambi et al., 2000; Zhong et al., 2018). Polyphenols with the ability to interact and cause these effects are believed to have molecular weights between 500 – 3000 Da; beyond 3000 Da compounds are insoluble and below 500 Da compounds are thought to be too small to interact and interfere in any meaningful way (Haslam, 1989).

The exact mechanisms that cause polyphenol anti-nutritional behaviour in monogastric animals are not fully understood. Several explanations exist including the binding of salivary proteins, the binding of undigested proteins, starches and other nutrients and the inhibition of enzyme activity, both directly and indirectly (Goldstein and Swain, 1965; Horigome et al., 1988; Hagerman et al., 1998). Polyphenols may inhibit enzyme activity through several mechanisms including the precipitation of proteinaceous substrates, formation of an enzyme-polyphenol complex or by binding to the enzyme-substrate complex. Non-competitive inhibition, the most widely reported form of polyphenol-enzyme inhibition, primarily occurs as polyphenols cross-link on the surface of the enzyme which can prevent necessary conformational changes from occurring (Haslam, 1989). Within the monogastric digestive tract, numerous endogenous enzymes are encountered including pepsin, lipase, elastase, α-amylase, trypsin and α-chymotrypsin.

Early work on polyphenol-enzyme inhibition conducted by Tamir and Alumot (1969) investigated the inhibition of trypsin, α-amylase and lipase by carob condensed tannin extracts. The extracts, prepared from hot water/ethyl acetate, were found to strongly inhibit enzyme activity with 90% inhibition achieved by 0.6 mL of 0.2% extract solution. These authors determined that non-competitive inhibition was occurring and speculated this was through non-specific interactions. Notably, they found was that enzyme activity was restored by addition of polyvinylpyrrolidone (PVP), indicating that tannins were the cause of enzyme inhibition rather than a protein-based inhibitor, a result echoed by Griffiths (1979). This restoration of activity with PVP has also been observed in digestive enzymes of young chicks thus showing evidence of inhibition both *in vitro* and *in vivo* (Longstaff and McNab, 1991). However, the results of Tamir and Alumot (1969) were most likely caused by the tannin extracts binding to the proteinaceous substrate as no inhibition occurred when the extracts were incubated with the substrate casein. Griffiths (1979) measured the inhibitory properties of faba bean testa extracts on trypsin, α-amylase and lipase. They determined that enzyme inhibition was non-specific and most likely due to reversible binding of tannins. Trypsin lost approximately a third of activity with 0.2 mg/mL extract, α-amylase 95% activity with 20 mg/mL and lipase 70% with 2 mg/mL, indicating varying affinities of the tannin extracts towards different enzymes. Among the faba bean varieties tested, the plants with coloured flowers decreased enzyme activity whereas the white flowering varieties did not, suggesting a correlation between phenotype and anti-nutritional impact, a similar theory as for certain feed grains, including sorghum.

Sorghum is grouped into a family of grains called the pseudocereals along with amaranth, quinoa and buckwheat. These grains are characterised as being beneficial to human health as they are gluten free and high in phytochemical content (Awika and Rooney, 2004; Taylor et al., 2014; Stefoska-Needham et al., 2015). A detailed discussion on sorghum polyphenols can be found in **Section 3.2.1**. Polyphenols in sorghum are also known to be anti-nutritional, especially regarding animal nutrition (Nyamambi et al., 2000; Velickovic and Stanic-Vucinic, 2018). Sorghum polyphenols, including large tannins, have been shown to have specific anti-nutritional properties towards endogenous digestive enzymes *in vitro*. Methanolic extracts from bird-resistant sorghum grains were tested as amylase inhibitors with up to 30% inhibition at 0.0048 mg/mL and 75% at 0.024 mg/mL (Davis and Hoseney, 1979). However, the effects observed were most likely due to the interaction of extracts with proteinaceous substrates. The

authors do postulate that different groups and families of polyphenols may act differently regarding inhibition. Some may bind to the substrate while others are better suited for direct enzyme inhibition. Cai et al. (2015) extracted and isolated a procyanidin trimer from sorghum and determined its effects on porcine pancreatic α-amylase (PPA) through fluorescence quenching, circular dichroism and UV/Vis spectroscopy. Increasing concentrations of the trimer decreased the fluorescence of PPA, indicating that enzyme structural changes were occurring with a focus on aromatic amino acid residues on the enzymes.

As polyphenols, especially large tannins, are well-established as being detrimental to endogenous digestion processes, it is reasonable to conclude that these same anti-nutrients might have similar effects on exogenous feed additives, especially feed enzymes. While the inclusion of feed enzymes is routine in swine and poultry sorghum-based diets, the effects of certain exogenous feed enzymes are often muted or substandard, especially with phytase (Selle et al., 2017). The exact mechanisms for this complication are not known; however, it is most likely caused by one or all of three negative intrinsic components of sorghum: kafirin protein, phytate and polyphenols. Feed manufacturers must take these potential interactions into account when preparing grain and formulating feed mixtures to include additives such as exogenous enzymes.

4.2.2 Isothermal Titration Calorimetry (ITC) Overview and Use in Polyphenol Interactions

Polyphenol-protein interactions can be measured and evaluated in a variety of ways, including precipitation studies, enzyme assays, nuclear magnetic resonance (NMR) and isothermal titration calorimetry (ITC). Enzyme assays and ITC studies are particularly useful as they allow for the real-time monitoring of reactions, as opposed to the more static environments of precipitation studies and NMR. However, these more static methods can be very useful at gaining detailed information about binding events and creating full structures of enzyme and proteins complexed with polyphenols.

ITC is a valuable tool for studying molecular interactions and uses calorimetric principles to determine basic thermodynamic values of complicated reactions, mixtures and binding events. ITC methods can be applied across a wide variety of disciplines to accomplish many different experimental goals (Falconer et al., 2010; Falconer and Collins, 2011; Ghai et al., 2012; Falconer, 2016). The most common use of the technology is to obtain thermodynamic data for

the binding of two components with a single site of binding. However, other methods exist and allow for the study of multiple binding sites and the monitoring of enzyme activity and kinetics. An ITC method was previously described by Kempapidis et al. (2020) to monitor the enzymatic degradation of phytate by an exogenous feed phytase. ITC has been previously applied to the study of enzyme catalysis yielding kinetic constants and reaction rates (Todd and Gomez, 2001). These values are determined through either multiple injection or single injection studies of the substrate into the enzyme or vice versa. The single injection experiment of substrate into the enzyme used by Kempapidis et al. (2020) as it allowed for the continuous measurement of the rate of reaction. ITC, as opposed traditional colourimetric enzyme assays, allows for more detail to be determined about the reaction mechanism as opposed to just measuring activity (Kempapidis et al., 2020).

The basic ITC apparatus is built around a chamber containing two cells: the reaction and reference cell (**Figure 4.1**).

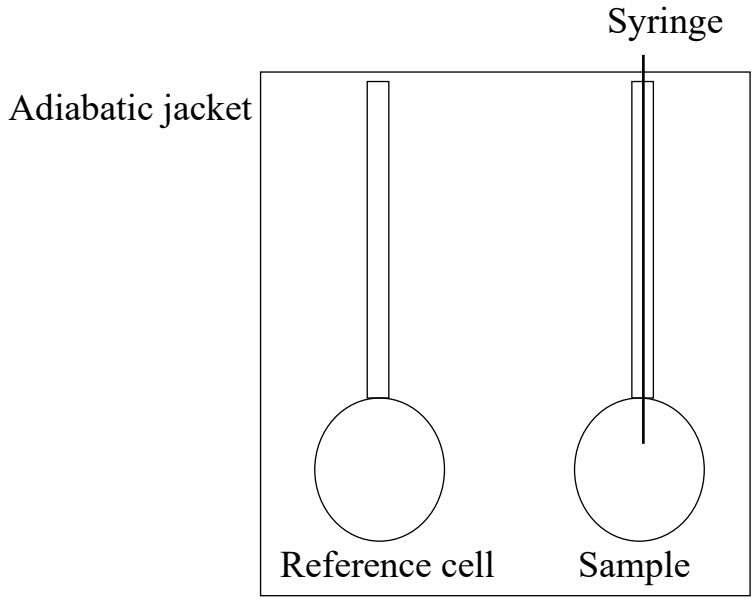

Figure 4.1 Diagram of an ITC reaction chamber

The reaction cell contains a solution of interest while the reference cell is typically filled with water. A titrant needle is filled with a second compound of interest and then the solution is slowly titrated into the reaction cell where any binding events may occur and changes in heat measured. As heat is released (exothermic) or absorbed (endothermic) power is applied to the reference cell to maintain its set temperature which is converted to a measurement of heat of

the reaction (Falconer and Collins, 2011). These measurements yield a thermogram, a plot of measured heat rate versus time, which is evaluated to determine thermodynamic values.

From these thermograms, a wealth of data can be obtained, including the stoichiometry of the reaction, dissociation constant (K_D), change in free energy (ΔG) and change in enthalpy (ΔH) (Falconer, 2016). Using Equation 1, the change in entropy (ΔS) can then be determined.

$$\Delta G = \Delta H - T\Delta S \qquad \text{(Eq. 1)}$$

ITC is an important technique used to study polyphenol-protein interactions and subsequent anti-nutritional effects. It is well suited to study these interactions as polyphenol-protein/enzyme interactions can often lead to the formation of insoluble complexes which can make traditional colourimetric methods for monitoring enzyme activity more difficult to use (Frazier et al., 2006). ITC has been routinely used to study interactions between polyphenols and different proteins and enzymes (Frazier et al., 2006; Poncet-Legrand et al., 2007; Darby, 2016; Kilmister et al., 2016; Kaspchak et al., 2018). As binding is known to occur in mixtures of proteins and polyphenols, the use of ITC elucidates the thermodynamic principles governing these interactions by determining whether interactions are exothermic or endothermic, driven by entropy and what types of binding are occurring, e.g., hydrophobic interactions, hydrogen bonding and van der Waals forces. In a simulated wine environment, Poncet-Legrand et al. (2007), characterised polyphenol-protein interactions between the model protein poly(L-proline) (PLP) and grape tannin extracts. PLP is often used in binding studies as it most closely reproduces the environment in the mouth where polyphenols bind to proline-rich salivary proteins causing the sensation of astringency. Significant interactions were observed with polymerised flavanols, especially modified ones, while smaller monomers, like (epi)catechin, showed no significant binding. These results indicated that anti-nutritional effects are often based on the size/molecular weight of polyphenols. Furthermore, this group found that interactions with modified flavonoids, like epicatechin gallate and epigallocatechin gallate, and PLP exhibited exothermic binding whereas flavonoids with a higher degree of polymerisation resulted in initial exothermic interactions followed by endothermicity near saturation. The interactions of polyphenols with various protein are highly complex and often not comprised of a single type of binding. A variety in binding interactions is most likely what would be encountered when testing the effects of crude extracts rather than purified extracts or chemical standards.

Along with PLP, bovine serum albumin (BSA) is another commonly used protein standard to investigate polyphenol-protein interactions. Using an (-)-epicatechin standard, Frazier et al. (2006) studied the binding of this flavonoid monomer to BSA in phosphate and citrate buffers. The binding was characterised as primarily exothermic and enthalpically driven as well as weak and non-specific and induced aggregation most likely through hydrogen bonding rather than electrostatic interaction. These findings are significant because they show the binding of a monomer, rather than polymer, to be able to influence the protein of interest. Kilmister et al. (2016) also observed interactions of BSA but with tannin polymers purified from cacao. They observed significant bindings occurring from the tetramer to the heptamer. Binding was characterised by a mixture of hydrogen bonding (exothermicity) and hydrophobic interactions (endothermicity) like Poncet-Legrand et al. (2007). Cooperativity is a mode of binding/interaction that describes how binding events may positively or negatively affect further ligand interactions in allosteric proteins and has been suggested as a potential explanation for the endothermicity seen here (Poncet-Legrand et al., 2007). Sorghum tannins have also been found to possibly exhibit cooperativity in an early precipitation study using a range of common binding partners such as PVP and BSA (Hagerman and Butler, 1981).

4.2.3 Research aims, hypotheses and methodology

Exogenous feed proteases and phytases are routinely incorporated into monogastric animal diets to increase nutrient bioavailability, to reduce the impact of anti-nutritional factors and to lower environmental phosphorous and nitrogen emissions in animal waste. However, these enzymes' possible interactions with polyphenols are under-studied. Polyphenol extracts were prepared from three modern Australian sorghum varieties (MR-Buster, Cracka, Liberty) routinely used in monogastric feed formulations. These extracts, along with two tannin extracts from grape seed and quebracho wood, were tested as inhibitors of exogenous feed enzyme, a phytase and a protease, activity. The effects were measured using ITC and a colourimetric, kinetic assay. The inhibition values were then quantified and put in context to relevant feed and enzyme formulations to determine their feed industry value.

1. Red coloured sorghum grains will have a higher total phenolic content than white coloured grains. Tannin extracts will have a higher total phenolic content than sorghum polyphenol extracts.

a. The total phenolic content (TPC) was used to quantitatively assess the polyphenol contents of the sorghum polyphenol extracts and the tannin extracts.

2. Sorghum polyphenol extracts and tannin extracts will inhibit exogenous feed protease activity and in a non-competitive manner. Tannin extracts will inhibit exogenous protease activity more than sorghum polyphenol extracts and at lower concentrations.
    a. A kinetics, colourimetric enzyme assay was used to determine exogenous feed protease activity in the presence of a small, synthetic substrate. Enzyme activity was monitored after incubation with the sorghum polyphenol extracts and the tannin extracts.

3. Sorghum polyphenol extracts and tannin extracts will inhibit exogenous feed phytase activity. Tannin extracts will inhibit exogenous phytase activity more than the sorghum polyphenol extracts.
    a. An ITC method was used to determine exogenous feed phytase activity in the presence of its natural substrate, phytate. Enzyme activity was monitored after incubation with the sorghum polyphenol extracts and the tannin extracts.

4.3 Materials and methods

4.3.1 Chemicals and materials

Sorghum grain and tannin extract information was previously described in **Section 3.3.1**. Exogenous feed enzymes, phytase and protease, were provided by DSM Nutritional Products (Kaiseraugst, Switzerland) under the commercial names Ronozyme® HiPhos (referred to as phytase) and Ronozyme® ProAct (referred to as protease), respectively. Phytase was used in its liquid product state containing sorbitol, water, sodium benzoate and potassium sorbate with a minimum enzyme activity of 2000 FYT g^{-1}. One unit of enzyme activity (FYT) is equal to the amount of enzyme that releases 1 µmol of inorganic phosphate from phytate per minute under conditions of phytate 5 mM, pH 5.5 and 37 °C. The protease was used in its liquid product state containing sorbitol and glycerol as stabilisers, and potassium sorbate and sodium benzoate as preservatives with an enzyme activity of 75,000 PROT g^{-1}. One unit of enzyme activity (PROT) is equal to the amount of enzyme that releases 1 µmol of *p*NA from 1 mM SAPNA per minute at pH 9.0 and 37°C. The protease substrate, N-Succinyl-Ala-Ala-Pro-Phe-

p-nitroanilide (SAPNA), and phytic acid sodium salt hydrate (extracted from rice bran) were purchased from Merck (formerly Sigma-Aldrich) (Gillingham, UK).

4.3.2 Preparation of sorghum polyphenol extracts

Sorghum grain was extracted for polyphenols following Harbertson et al. (2014) with modifications and previously described in **Section 3.3.2**.

4.3.3 Total phenolic content assay (TPC)

The Folin-Ciocalteu (F-C) method, following Ainsworth and Gillespie (2007), was used to determine the TPC of the sorghum polyphenol extracts and tannin extracts. Briefly, gallic acid standards and the extracts were prepared to 1 mg/mL in 95% (v/v) aq. methanol. F-C reagent (10% aq. [v/v]) was then added, followed by 700 mM sodium carbonate. Following a two-hour incubation at room temperature, absorbance was measured at 760 nm in an ultraviolet/visible (UV/Vis) spectrometer. Three separate extracts per sorghum grain variety were prepared.

4.3.4 Isothermal titration calorimetry (ITC) monitoring of exogenous feed phytase activity

The effect of sorghum polyphenol extracts and tannin extracts on a 6-phytase (EC 3.1.3.26), from *C. braakii* produced in *Aspergillus oryzae*, activity was determined through ITC, previously described by Kempapidis (2019) and Kempapidis et al. (2020), with modifications. ITC analysis was conducted using a TA Analysis NanoITC (TA Instruments; New Castle, DE). Sorghum polyphenol extracts and tannin extracts were prepared to a working concentration of 0.125 mg/mL in 5% ethanol and diluted accordingly. Phytate was prepared to a concentration of 20 mM in 5% ethanol. Phytase was prepared to 32.6 FYT/mL, in 5% ethanol with a pH of 5.0 ± 0.2. All solutions were degassed prior to the start of the experiment.

The injection syringe contained 20 mM phytate and was titrated into a mixture of tannin extract, sorghum polyphenol extract or 5% ethanol with phytase over one injection of 5 µL, at 30°C and 285 rpm stirring speed. The raw heat rate, measured in microjoules per second (µJ/s), was recorded over a total of 2600 seconds with 600 seconds of initial and final baseline measurements and 2000 seconds for the injection. Phytase was incubated with the sorghum polyphenol extracts, tannin extracts or 5% ethanol for 30 minutes prior to starting each experiment. A titration of 5% ethanol into phytase alone or with each concentration of tannin

extract or sorghum polyphenol extract was performed to determine the heat of dilution (blank run) for each experimental condition. Normal enzyme activity was determined by titrating phytate into phytase with 5% ethanol replacing the tannin extracts and sorghum polyphenol extracts.

The negative controls in the phytase ITC activity assay were reactions containing 5% ethanol into phytase alone or with each concentration of tannin extract or sorghum polyphenol extract. The positive controls were reactions containing phytate with phytase plus the addition of 5% ethanol (to simulate adding the tannins and polyphenols).

4.3.5 Exogenous feed protease activity assay

The effect of sorghum polyphenol extracts and tannin extracts on an exogenous feed protease (EC 3.4.21.-) from *N. prasina* produced by *Bacillus licheniformis*, activity was determined by colourimetric enzyme activity assay using the synthetic substrate SAPNA as per the protocol described by the Joint Food and Agriculture Organisation of the United Nation/World Health Organisation Expert Committee on Food Additives (JECFA) (2012). Enzyme activity was proportional to the hydrolysis of *p*-nitroanilide (*p*NA) from SAPNA which can be measured by absorbance at 405 – 410 nm.

SAPNA working solution was prepared by diluting 0.08 M SAPNA in dimethyl sulfoxide to 1.12 mM in 0.1 M Tris buffer (pH 9.0 ± 0.1). Protease working solution was prepared by dissolving 10 mg of stock enzyme (equivalent to 750.1 PROT according to product specifications) into 250 mL 10 mM citrate buffer (pH 3.40 ± 0.03). Seven enzyme standards were prepared with the middle standard chosen for inhibition assays. Sorghum polyphenol extracts and tannin extracts were prepared to 1.6 mg/mL in 5% ethanol and diluted accordingly.

To a polystyrene 96-well microplate, 30 µL of enzyme was added and incubated with 50 µL of sorghum polyphenol extract, tannin extract or 5% ethanol for 25 minutes. After incubation, 120 µL of 1.12 mM SAPNA or 120 µL Tris buffer was added and the plate was immediately placed in a FLUOstar OPTIMA plate reader (BMG Labtech, Aylesbury, United Kingdom) set to 37°C. Absorbance readings were taken every 60 seconds for approximately 20 minutes at 405 nm. Incubations were prepared in triplicate on each randomised plate for an experiment

and three experiments were conducted. For kinetic studies, the same procedure was followed but with five concentrations of SAPNA (2.24, 1.12, 0.56, 0.28, and 0.14 mM).

The negative controls in the protease activity assay were reactions containing the substrate (SAPNA), protease, and 5% ethanol (to simulate adding the tannins and polyphenols) as well as reactions containing the protease, tannin or polyphenol extracts and buffer (instead of the substrate. The positive controls were a set of seven enzyme standards that were run on every single microplate.

4.3.6 Statistical analysis

Statistical differences in the data were evaluated using one-way analysis of variance (ANOVA) and two-way ANOVA and the mean values were compared using a Tukey post-hoc test. All statistical analyses were performed using GraphPad Prism 8 (GraphPad Software, Inc.; San Diego, CA, USA).

4.4 Results and discussion

In monogastric diets containing sorghum grain, feed additive enzyme response is often muted, possibly due to the presence of anti-nutrients in the grain. Several negative intrinsic factors within sorghum grain are thought to cause this, including kafirin protein, phytate and polyphenols. To determine whether non-tannin polyphenols and related compounds in modern sorghum varieties were responsible for this effect, polyphenol extracts were prepared from three commercial sorghum grain varieties (MR-Buster, Cracka, Liberty) and tested as inhibitors of exogenous feed phytase and protease activity.

Two different methods of enzyme activity measurement were chosen as the protease and phytase are very different – both structurally and kinetically. The protease follows quite simple enzyme kinetics, i.e., Michaelis-Menten, and thus a standard colourimetric assay was used to match this. ITC was trialled, by Theofilos Kempapidis, for measuring protease activity but was unsuccessful. As highlighted, the protease assay was carefully selected so as to utilize a non-proteinaceous substrate to clearly highlight any interactions occurring between the enzyme and the polyphenol extracts. Phytase activity was measured using ITC and not a colourimetric assay because of the complexity of the enzyme's reaction. Phytase cleaves 5 phosphate molecules from phytate and does not follow simple Michaelis-Menten kinetics. ITC allowed

for the real-time tracking of the heat released or absorbed from the reaction and combined with prior mass spectrometry analyses, see Kempapidis et al., 2020, it allowed for the nuances of the reaction mechanism to be understood.

Tannin extracts from grape seed and quebracho wood were tested for comparison, similar to a standard. All extracts are classified as crude as opposed to the traditional method of using individual purified standard compounds. This was done to better characterise the possible interactions between the extracts and feed enzymes. The extracts used in this study were previously described and characterised (see **Chapter 3**; Hodges et al., 2021).

4.4.1 Sorghum polyphenol extract yield and extract phenolic content

Twenty grams of MR-Buster, Cracka and Liberty sorghum grain were extracted with 70% aq. acetone and lyophilised. **Table 4.1** shows the extracts quantified as grams of extract per kilogram of whole grain (g/kg), grams of extract per kilogram of bran (g/kg) and **Figure 4.2** illustrates the quantitative measurements as total phenolic content (TPC) in milligrams gallic acid equivalent per gram of dry material (DM) (mg GAE/g) as determined by the Folin-Ciocalteu method. Gallic acid standards were prepared from 0.006 to 0.2 mg/mL in 95% methanol.

Table 4.1 Yield of polyphenol extracts from sorghum grain varieties

	Liberty	**Cracka**	**MR-Buster**
Colour	White	Red	Red
Extract yield from bran (g/kg, ± 1 SD)	8.23 ± 4.70 (n = 11)	12.89 ± 1.98 (n = 8)	12.86 ± 2.17 (n = 4)
Extract yield from grain (g/kg, ± 1 SD)	3.66 ± 1.01 (n = 11)	5.31 ± 1.28 (n = 8)	4.41 ± 1.16 (n = 4)

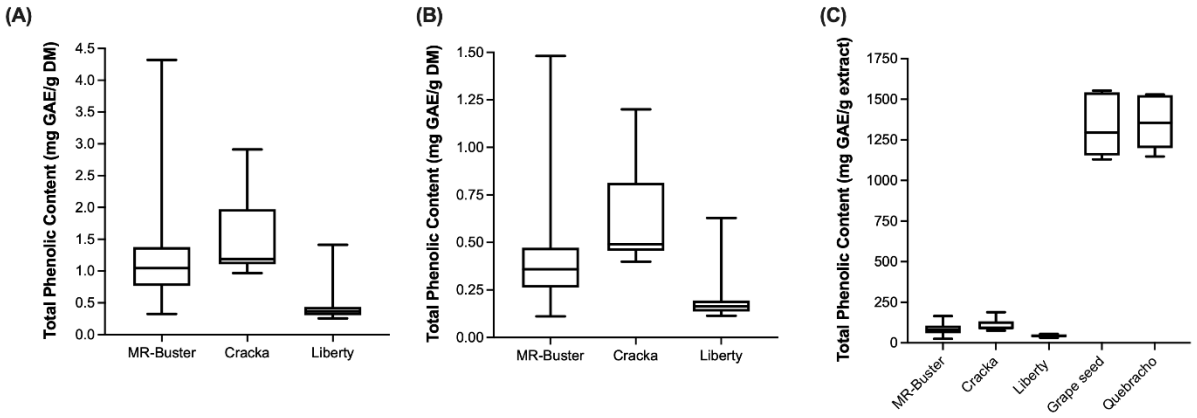

Figure 4.2 Total phenolic content of sorghum polyphenol extracts and tannin extracts
Total phenolic content was determined for sorghum polyphenol extracts and tannin extracts and expressed as both mg GAE/g dry material (DM) (**A** – bran; **B** – whole grain) and **C** - mg GAE/g extract. Error bars plotted as ± 1 SD; MR-Buster n = 30, Cracka n = 27, Liberty n = 24, Grape seed n = 6, Quebracho n = 6.

The yield of polyphenol extract from the three sorghum varieties was similar with only Cracka polyphenol extract having a significantly ($P < 0.05$) higher yield than MR-Buster and Liberty polyphenol extracts. Cracka polyphenol extract was also found to have a significantly ($P < 0.001$) higher TPC than both MR-Buster and Liberty polyphenol extracts. Both tannin extracts had significantly ($P < 0.001$) higher TPC values than all three of the sorghum polyphenol extracts.

The values for polyphenol yield from sorghum extracts compared well with common literature values. As reported by Bravo (1998) in her extensive review, cereals and grains have a wide range of polyphenol contents. Some cereals, including maize, wheat, rice and oats, have very low to negligible polyphenol contents, ranging from as low as 0.09 g/kg for rice and oats up to 0.4 g/kg in wheat. Barley and millet have intermediate values from 5.9 – 15 g/kg. Sorghum has the highest reported polyphenol content ranging from 1.7 g/kg all the way to 102.6 g/kg (Bravo, 1998). The sorghum grain varieties analysed here were modern, low-tannin and tannin-free grains that had been bred to reduce overall polyphenol content, among other desirable parameters, to improve nutritional value. While larger, historic tannins may not be present in these grains, their extract yields indicate that there might be a significant amount of small to medium polyphenols which place its polyphenol contents still above those of other feed grains like maize and wheat. This result matched with the qualitative analyses completed in **Chapter 3** and by Hodges et al. (2020) in which the sorghum polyphenol extracts were putatively found to contain a variety of medium-sized polyphenols.

The values determined for sorghum polyphenol extract TPC were lower than reported values in the literature. In high-tannin varieties, e.g., most brown coloured sorghum grains, TPC was found to range from 11.7 – 22.5 mg GAE/g of grain to 41 – 88.5 mg GAE/g of bran (Awika et al., 2004b; Barros et al., 2013; Ayala-Soto et al., 2015). Black coloured sorghum grain varieties are reported to have a wide range of TPC values from 5.3 – 19.8 mg GAE/g of grain upwards of 26.1 – 43 mg GAE/g from the bran (Barros et al., 2013; Dykes et al., 2013). After the darker coloured black sorghum grains, red and white coloured varieties, which make up the majority of animal diets, have the lowest reported TPC values. Red sorghum grains can have a TPC for the grain from 2.77 – 4.8 mg GAE/g and 7.13 – 19.5 mg GAE/g for the bran (Awika et al., 2004b; Ayala-Soto et al., 2015; Liu et al., 2016; Zhang et al., 2019). White coloured sorghum varieties tend to have the lowest TPC values with 1.09 – 1.17 mg GAE/g for the whole grain and 3.00 – 3.68 mg GAE/g of the bran (Afify et al., 2012; Ayala-Soto et al., 2015; Liu et al., 2016).

The differences between the TPC values of the sorghum polyphenol extracts and the literature may arise due to differences in extraction procedures, e.g., solvent type, extraction method, soaking and drying (see **Chapter 2**). The extraction process here included a soaking step which was done to ease the grinding of the grain but could have resulted in the lower TPC values found here. Steeping sorghum grains has previously been shown to leach polyphenols (Osuntogun et al., 1989; Acquisgrana et al., 2016). Differences in reported TPC values may also differ significantly between extraction methods due to the type of solvent used and the physical processing of the plant material itself. Barros et al. (2013) and Zhang et al. (2019) both found 60 – 70% acetone to be the superior extraction solvent with regard to total phenolic content when compared to other traditional solvents like aqueous methanol/acidified methanol. This is not to say that acetone is always the best polyphenol extraction solvent but is typically best for extracting the highest levels of phenolic compounds as well as larger polyphenol (see **Chapter 2**). These results and findings from the literature supported the use of 70% acetone as the polyphenol extraction solvent for the sorghum varieties studied here.

While the two tannin extracts could not be quantified with regard to their original dry material, it was important to determine their phenolic contents in relation to the sorghum polyphenol extracts. The two tannin extracts had significantly ($P < 0.0001$) higher phenolic contents than all three sorghum polyphenol extracts but were not different between themselves. The sizable

difference from the sorghum polyphenol extracts is most likely due to higher extract purity and the presence of large condensed and hydrolysable tannin structures. Sorghum grain extract extracts have historically been characterised as having high concentrations of polyphenols, especially large condensed tannins. These tannins are similar, and even identical to the large polymers previously detected in the grape seed and quebracho tannin extracts (see **Chapter 3**). Modern sorghum grains have been bred for many traits, including protein and starch content, colour and resistance to mould and insects (Berenji et al., 2011). In doing so, large tannins were also bred out of older varieties because of their known anti-nutritional effects. While 'tannins' in the traditional sense have been significantly reduced/eliminated from modern sorghum varieties, 'non-tannin' phenolics are very much still present and have the potential to produce anti-nutritional effects (Liu et al., 2015; Hodges et al., 2021). The effects of these compounds in newer varieties on exogenous feed enzymes is unknown and was determined in the present study.

4.4.2 Exogenous phytase activity and inhibition

The enzymatic degradation of phytate by an exogenous feed phytase was monitored in the presence and absence of sorghum polyphenol extracts and tannin extracts and was represented by a thermogram plotting time in minutes against the heat rate in microjoules/second (μJ/s). An enzyme blank thermogram was produced by titrating 5% ethanol into phytase only or phytase plus tannin extracts or sorghum polyphenol extracts (**Figure 4.3A** and **Appendix Figure B.1**). A substrate blank thermogram was produced by titrating phytate into tannin extracts or sorghum polyphenol extracts (**Figure 4.3B** and **Appendix Figure B.2**). This was done to demonstrate that phytate and the different extracts did not interact.

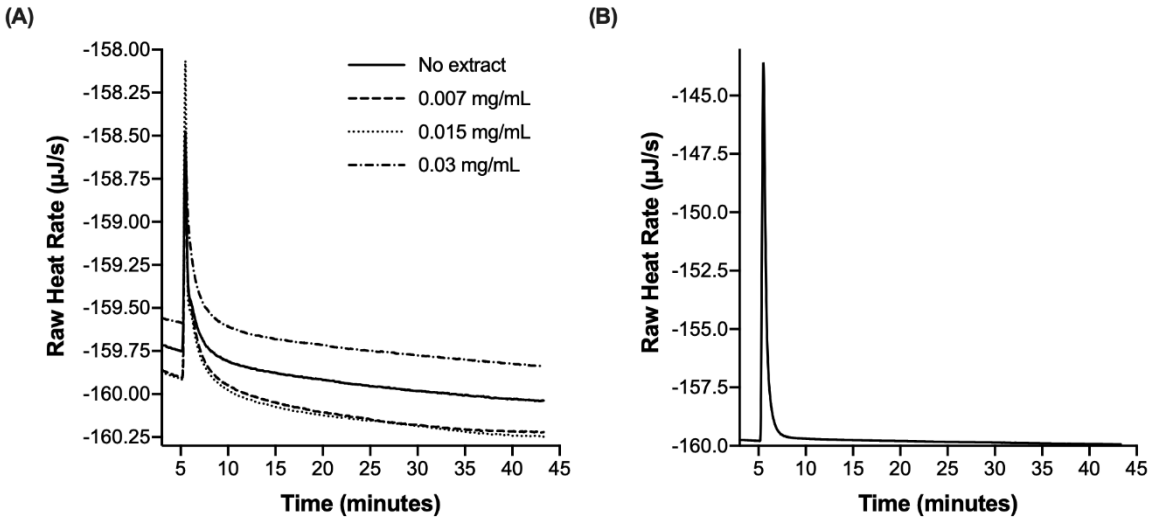

Figure 4.3 Sample thermograms of phytase and phytate blank measurements
(A) 5% ethanol was titrated into a solution of 32.6 FYT/mL phytase and 5% ethanol or grape seed tannin extract to represent an enzyme blank thermogram. (B) Phytate (20 mM) was titrated into a solution of grape seed tannin extract (0.125 mg/mL) and 5% ethanol to serve as a blank thermogram and to demonstrate the lack of interaction between phytate and the tannin extract. The sharp, upward spike in raw heat rate is called the heat of dilution and is caused by the mixing of the two solutions.

The two blank measurements provided important information moving forward with the phytase activity assay: 1) the value of the heat of dilution to subtract from enzyme activity thermograms; and 2) no evidence of interaction between phytate and the sorghum polyphenol extracts and tannin extracts. Phytate did not interact with the sorghum polyphenol extracts or the tannin extracts indicating that any changes to the activity of phytase would be caused by direct enzyme inhibition and not through indirect substrate inhibition. The heat of dilution, i.e. the initial large spike observed in the raw heat rate for each thermogram, was caused by mixing and dissolving of phytate in the sample cell below. These reactions were exothermic (indicated by upward peak structure) as phytate mixed with the other solution and the final mixture reaches its most stable thermodynamic state. Beyond the initial peak, the thermogram immediately flattened out indicating that the mixture is at equilibrium.

Normal phytase activity, as monitored by the heat released upon phytate degradation, was measured at the beginning of each set of extracts to ensure uniform preparation and provide a baseline for comparison (**Figure 4.4**).

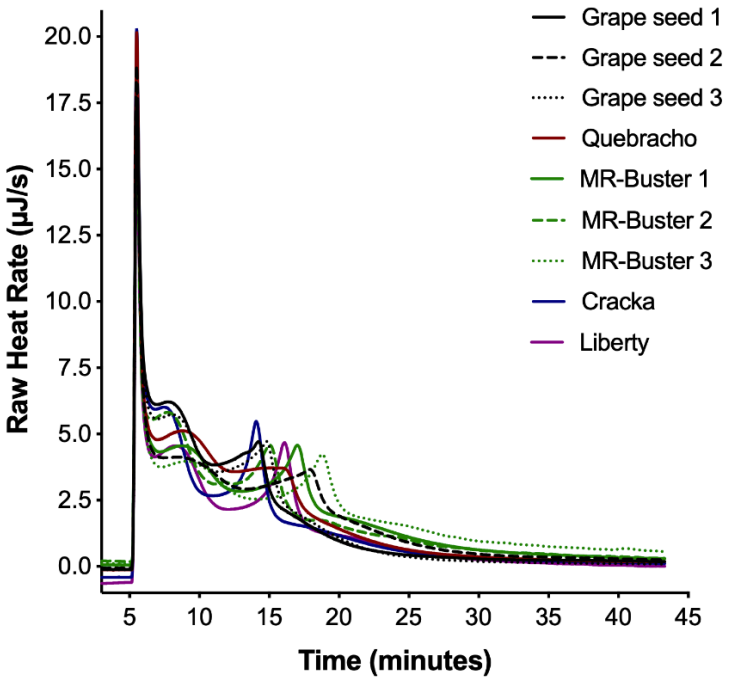

Figure 4.4 Phytate – phytase reaction control thermogram
Phytate (20 mM) was titrated into a solution of 32.6 FYT/mL phytase and 5% ethanol to serve as the enzyme control. Multiple thermograms were obtained at the beginning of experimentation as indicated by the three repeat measurements for grape seed tannin extract and MR-Buster sorghum polyphenol extract. Single measurements were required only to confirm phytase activity and thermogram shape were consistent among the different extract types.

Normal phytase activity presented with an initial heat of dilution, similar to the blank thermograms, upon the titration and mixing of phytate. This spike in heat rate was followed by a broad peak (first peak) appearing at ~7.5 minutes and a later sharper peak (second peak) appeared ~6.5 minutes later. The thermograms ended with a return to equilibrium as no further heat was released, indicating phytase-phytate reaction completion by ~35 minutes.

The incubation of increasing concentrations of sorghum polyphenol extracts and tannin extracts with phytase was observed to inhibit phytase activity in a dose-dependent manner (**Figures 4.5 – 4.7**). Inhibition could be ascertained by comparing the signals produced with the extracts to those from the controls.

The incubation of the white sorghum (Liberty) polyphenol extract with phytase altered the control thermograms indicating that the extracts were changing enzyme activity (**Figure 4.5**).

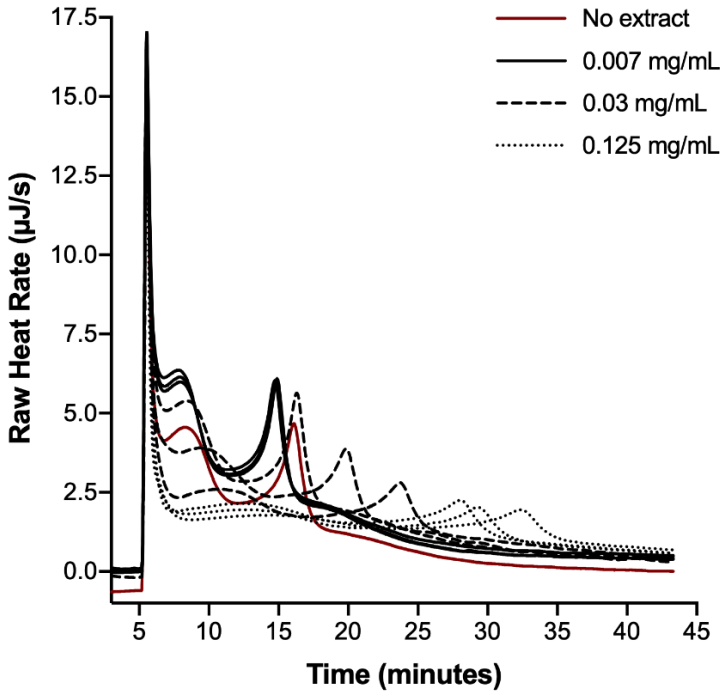

Figure 4.5 Phytase – phytate thermogram with white sorghum polyphenol extract
The raw heat rate (µJ/s) was measured for the titration of 20 mM phytic acid into a mixture of 32.6 FYT/mL phytase and Liberty sorghum polyphenol extract. Three technical replicates were performed for each concentration of the sorghum polyphenol extract.

Across the three Liberty sorghum extract concentrations tested, the general shape of the enzyme activity control thermogram (see **Figure 4.4**) was detected. However, at the highest concentration of Liberty extract (0.125 mg/mL) the maximum heat rate of the first peak had roughly halved. Additionally, the shape of the second peak had become broader and less defined and the time to reach this peak had doubled (15 minutes to 30 minutes). The intermediate concentration, 0.03 mg/mL, produced similar trends in thermogram alteration, albeit to a lesser extent. The lowest extract concentration, 0.007 mg/mL, produced a thermogram closely resembling the control and appeared to have improved phytase activity as the first peak was larger in height than the control while the second peak was slightly sharper and appeared approximately three minutes sooner.

The inhibition of phytase with red sorghum (MR-Buster, Cracka) polyphenol extracts appeared more pronounced than activity in the presence of white sorghum (Liberty) polyphenol extract (**Figure 4.6A, B**).

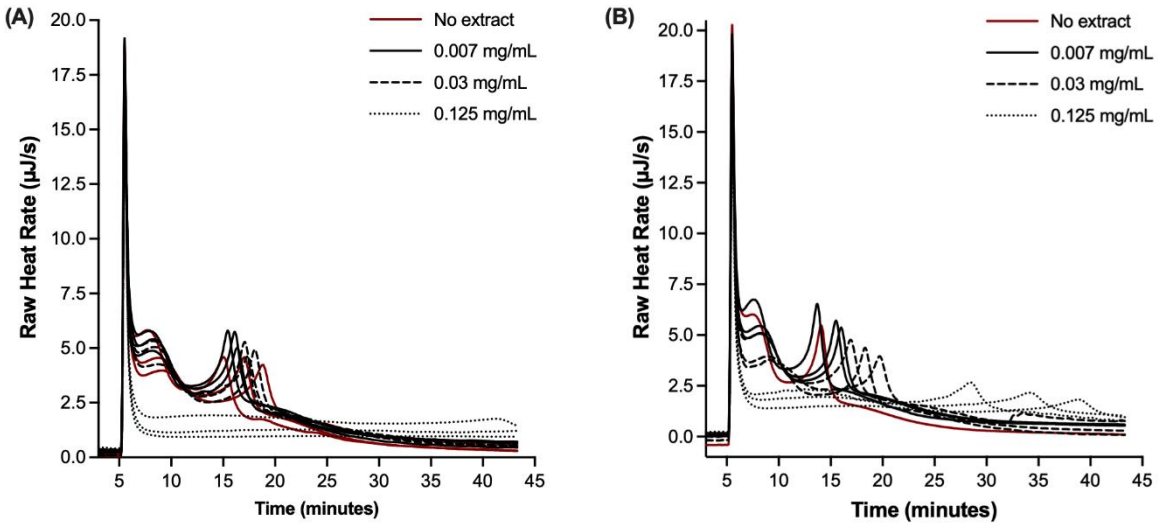

Figure 4.6 Phytase – phytate thermogram with red sorghum polyphenol extract
The raw heat rate (µJ/s) was measured for the titration of 20 mM phytic acid into a mixture of 32.6 FYT/mL phytase and **(A)** MR-Buster and **(B)** Cracka sorghum polyphenol extract. Three technical replicates were performed for each concentration of the sorghum polyphenol extract.

Inhibition of phytase activity by MR-Buster sorghum polyphenol extract was most prominent among the three sorghum polyphenol extracts tested. Incubation with the highest concentration of MR-Buster polyphenol extract (0.125 mg/mL) led to the elimination of any significant features associated with normal phytase activity. This result represented 100% inhibition of the enzyme's ability to degrade phytate. Activity was restored at the lower two concentrations, 0.03 and 0.007 mg/mL. The two lower concentrations produced thermograms very similar to each other. Comparable to the Liberty polyphenol extract, the highest concentration of the Cracka sorghum polyphenol extract extended the time to reach the second sharp peak but by more than double. The first peak had also been mostly eliminated at this high concentration of extract. A dose-response is observed with 0.03 and 0.007 mg/mL Cracka polyphenol extract as the thermogram shapes returned to normal, including the reappearance of the first peak. However, the second peaks for the two lower extract concentrations were very closely grouped, possibly indicating little difference in effect on the enzyme.

The two tannin extracts, grape seed and quebracho, had much greater effects on phytase activity than any sorghum polyphenol extract and at lower concentrations (**Figure 4.7A, B**).

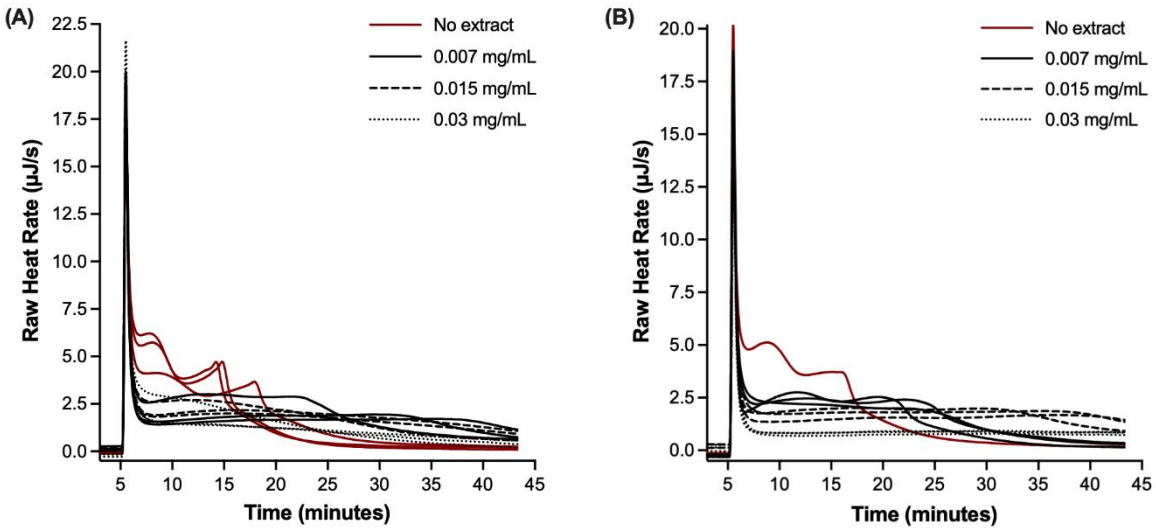

Figure 4.7 Phytase – phytate thermogram with tannin extracts
The raw heat rate (µJ/s) was measured for the titration of 20 mM phytic acid into a mixture of 32.6 FYT/mL phytase and **(A)** grape seed and **(B)** quebracho tannin extract. Three technical replicates were performed for each concentration of the tannin extract.

At the highest concentrations of both tannin extracts, 0.03 mg/mL, the expected thermogram representing phytase activity (see **Figure 4.4**) was not present and instead resembled the heat of dilution with equilibrium reached immediately following the initial peak. Similar to the result seen with MR-Buster sorghum polyphenol extract, this represented 100% inhibition of the enzyme's ability to degrade phytate. At the intermediate concentration, 0.015 mg/mL, the thermogram for grape seed tannin extract was essentially flat and devoid of any phytase activity features. Quebracho tannin extract at this concentration had some of the features of phytase activity including two subtle peaks. These two peaks were very small in size and lengthened considerably compared to the control. The differences in the thermograms here between the two tannin extracts indicated that grape seed tannin extract was a stronger inhibitor than quebracho tannin extract. At the lowest concentration, both tannin extracts displayed some of the phytase activity features but both peaks were smaller as compared to the control and lengthened.

A simplified analytical approach, previously optimised by Kempapidis et al. (2020), was then taken to quantify phytase activity inhibition by the sorghum polyphenol extracts and tannin extracts: 1) the area under the curve (AUC) for the control reaction was determined from the time of injection of phytate (5.15 minutes) until the point of equilibrium (35 minutes); 2) 50% of that value was determined for each thermogram; and 3) the time to reach that value

determined ($T_{50\%}$) (**Table 4.2**). The $T_{50\%}$ values were then compared to the control and expressed as percent inhibition values (**Figure 4.8**).

Table 4.2 Time (minutes) to 50% ($T_{50\%}$) phytate – phytase reaction completion in the presence of sorghum polyphenol extracts and tannin extracts (mg/mL)*

	0	0.007	0.015	0.03	0.06	0.125
Grape seed	11.14 ± 1.21	17.78 ± 1.29	N/A**	-----	-----	-----
Quebracho	11.30	15.23 ± 0.65	18.44 ± 0.24	-----	-----	-----
Liberty	11.25	12.03 ± 0.16	-----	13.87 ± 1.15	-----	16.49 ± 0.50
Cracka	10.33	12.46 ± 0.66	-----	13.18 ± 0.91	-----	17.05 ± 0.41
MR-Buster	12.96 ± 1.22	13.33 ± 0.17	-----	13.76 ± 0.20	-----	N/A**
Total	11.69 ± 1.32					

*Measurements with averaged replicates are shown with ± 1 SD, n = 3; Total 0 mg/mL is n = 9
** Indicates reaction thermograms in which the features of phytase activity were not clearly detected

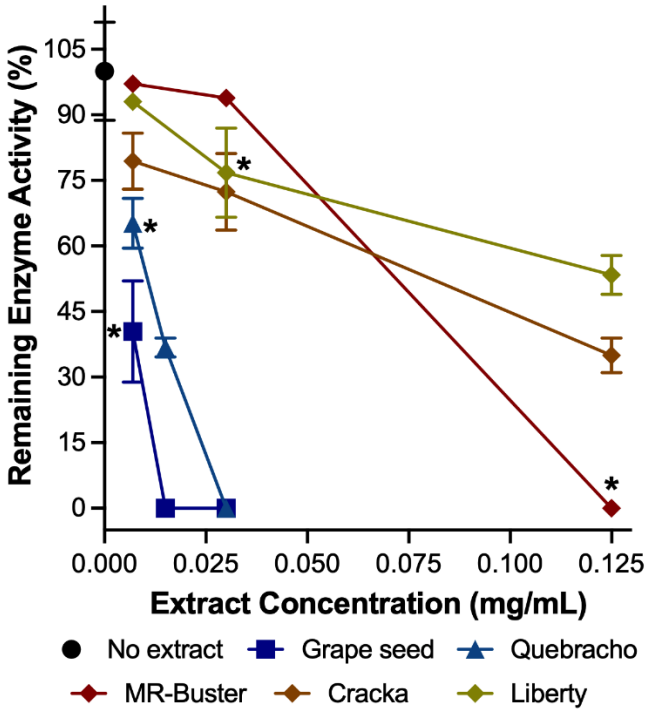

Figure 4.8 Remaining phytase activity with sorghum polyphenol extracts and tannin extracts
The remaining activity of the phytase enzyme in the presence of sorghum polyphenol extracts and tannin extracts was determined by comparing the $T_{50\%}$ values calculated for each thermogram and expressing them as percentages. Measurements are averaged replicates are shown with ± 1 SD, n = 3. All control activity values were averaged together, ± 1 SD, n = 9. * indicates values significantly different from normal enzyme activity; Grape seed $P < 0.0001$, Quebracho $P < 0.001$, MR-Buster $P < 0.0001$, Cracka $P < 0.001$, Liberty $P < 0.05$.

While previous studies (see **Section 4.2.2**) have utilised ITC in its traditional form to study polyphenol-protein interactions, this work sought to employ the technique in an understudied

way, following the work begun by Kempapidis (2019) and Kempapidis et al. (2020). In standard ITC enzyme experiments, the signal produced by either single or multiple injections is integrated with the AUC and equivalent to the total reaction enthalpy (ΔH_r). This value is directly proportional to enzymatic reaction rate (V_{max}) and kinetic constants (K_m, k_{cat}) can be further determined using a series of equations (Todd and Gomez, 2001). This approach can be a mathematically complex, especially in single injection studies assuming Michaelis-Menten kinetics (Hansen et al., 2016). Here, a rapid and simplified method to compare reaction rates and time was implemented by taking the $T_{50\%}$ and using that as a measure of phytase activity. The method used here (developed by Kempapidis, 2019; Kempapidis et al., 2020) allowed for the complex reaction mechanism of phytase to be accurately monitored and subsequently converted to a simplified output. The $T_{50\%}$ values calculated from the phytase-phytate reaction thermograms indicated that overall the phytase reaction time in the presence of sorghum polyphenol extracts and tannin extracts increased. The lengthening of this $T_{50\%}$ value was equivalent to phytase inhibition. The overall patterns observed here indicated that the two tannin extracts had greater inhibitory qualities than the three sorghum polyphenol extracts and are ranked: Grape seed > Quebracho >> MR-Buster > Cracka > Liberty. Remaining enzyme activity was significantly different between 0.007 mg/mL ($P < 0.05$) and 0.015 mg/mL ($P < 0.001$) grape seed and tannin extracts. For the sorghum polyphenol extracts, remaining enzyme activity was only significantly different between 0.125 mg/mL MR-Buster and Liberty extracts ($P < 0.0001$) and MR-Buster and Cracka extracts ($P < 0.01$).

The enzyme and enzyme-substrate structures demonstrated by Sanchez-Romero et al. (2013) from the closely related phytase from *Escherichia coli* (*E. coli*) provide insight into the phytase reaction mechanism and possible inhibition mechanisms by the sorghum polyphenol extracts and tannin extracts (Lim et al., 2000). The reaction to cleave one phosphorous from phytate is two-step involving a nucleophilic attack by a histidine in the highly positive, conserved active site, RHGXRXP, followed by hydrolysis of the inositol phosphate (IP) ester linkage. The products, phosphate and phytate minus phosphate, then dissociate and the process repeats itself depending on the number of IP groups remaining (Lim et al., 2000). The thermogram representing normal phytase activity (**Figure 4.4**) indicated that the conversion of IP6 to IP5 and IP5 to IP4 was relatively swift but was met with a 'bottleneck' as IP4 converted to IP3 (Kempapidis, 2019; Kempapidis et al., 2020). These initial conversions from IP6 to IP4 were seen on the ITC thermograms as the first peak at around 7.5 minutes. The 'bottleneck' appeared as the second peak at approximately 15 minutes.

The reduction in the height of the first peak with inclusion of sorghum polyphenol extracts and tannin extracts indicated that the extracts were most likely interfering with the initial conversions of IP6 to IP5 and IP5 to IP4, which delayed the appearance of the second peak, i.e. the 'bottleneck' (Kempapidis, 2019; Kempapidis et al., 2020). The structure described by Lim et al. (2000) was found to closely match several related species, including the exogenous feed phytase, and is described as having two domains, α and β, with a large cavity, containing the active site, dividing it in the middle. The α domain was found to have a unique β-hairpin structure, often rich in proline residues, opposite the active site (Hutchinson and Thornton, 1994). Polyphenols have been long established to bind strongly to proline-rich proteins and molecules (Hagerman and Butler, 1981). This structure may provide the compounds within the sorghum polyphenol extracts and tannin extracts a place to bind close to the active site. While not observed in the current study, polyphenols could interact with phytate *in vivo* possibly directly or indirectly through formation of phytate-starch/kafirin complexes. Polyphenols and phytate have been found to positively correlate, most likely due to their proximity in the aleurone layer (Selle et al., 2018).

4.4.3 Exogenous feed protease activity and inhibition

A kinetic, colourimetric assay for determining exogenous feed protease activity in the presence of sorghum polyphenol extracts and tannin extracts was developed based on a JECFA protocol (2012). A small, synthetic substrate, SAPNA, was hydrolysed in the presence of the enzyme to produce *p*NA, detectable at 405 nm. The assay was optimised to determine 1) maximum detectable limits; 2) the effects of ethanol concentration and incubation time on protease activity; and 3) whether sorghum polyphenol extracts interacted with the small, synthetic substrate as opposed to the protease (**Appendix Figures B.3 – B.5**). Seven protease standards were run as positive controls on each microtitre plate with the middle standard (150 mPROT/mL) chosen for inhibition studies (**Figure 4.9**).

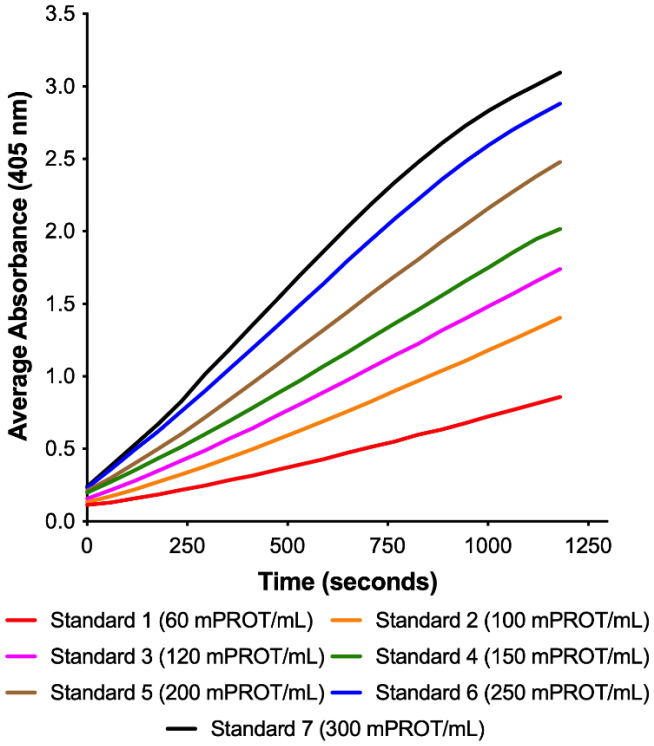

Figure 4.9 Activity of protease standards
The activity of the protease at seven different concentrations (mPROT/mL) was monitored at 405 nm for approximately 20 minutes. This was repeated in every microtitre plate used to ensure reproducibility.

The effect of sorghum polyphenol extracts and tannin extracts on protease activity was investigated by incubating varying concentrations of both extract types with the protease (150 mPROT/mL) for 25 minutes prior to adding the small, synthetic substrate SAPNA (**Figures 4.10 – 4.13**).

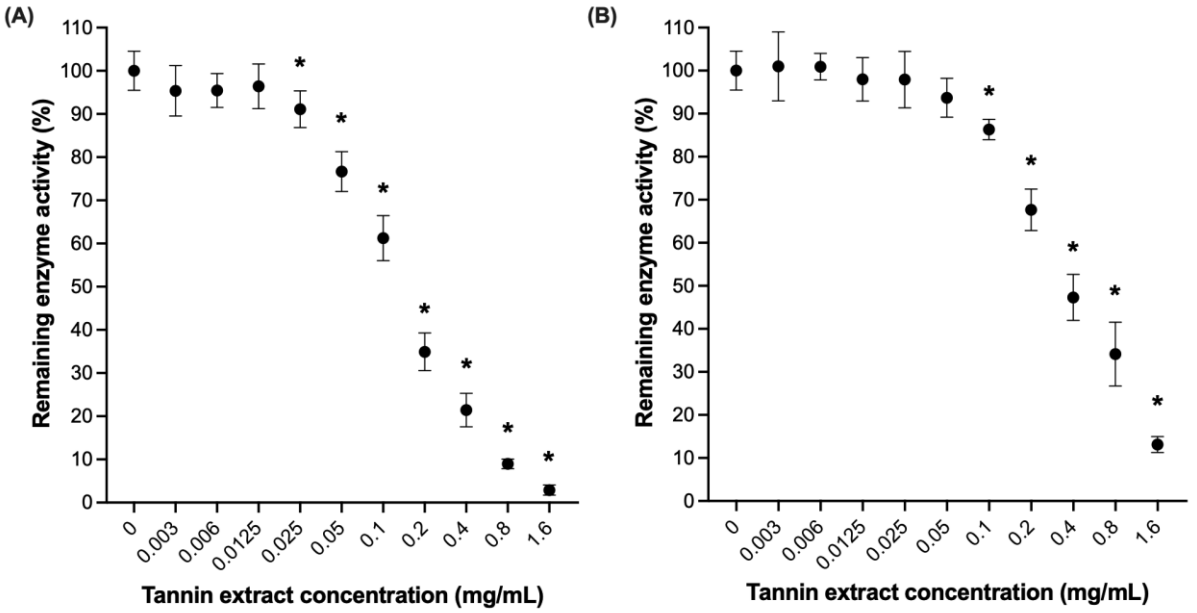

Figure 4.10 Protease activity in presence of grape seed and quebracho tannin extracts
(A) Grape seed and **(B)** quebracho tannin extracts were incubated with the exogenous feed protease (150 mPROT/mL) for 25 minutes before monitoring protease activity in the presence of the small, synthetic substrate SAPNA. Error bars plotted as ± 1 SD; n = 9. Asterisk (*) indicates a significant difference ($P < 0.0001$) from 0 mg/mL.

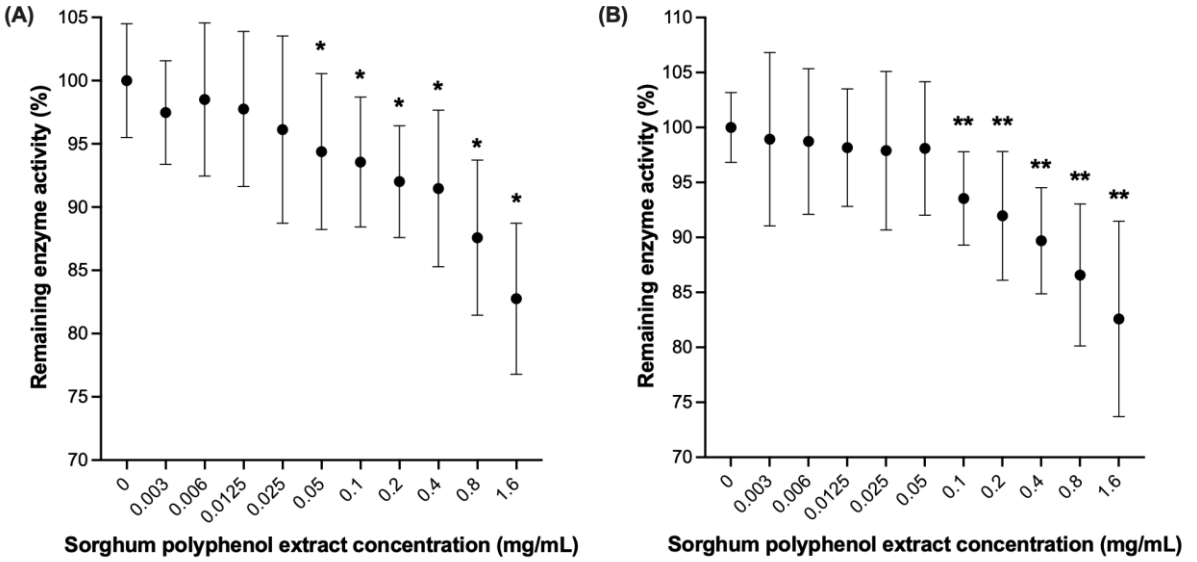

Figure 4.11 Protease activity in presence of red sorghum polyphenol extract
(A) MR-Buster and **(B)** Cracka sorghum polyphenol extracts were incubated with the exogenous feed protease (150 mPROT/mL) for 25 minutes before monitoring enzyme activity in the presence of the small, synthetic substrate SAPNA. Error bars plotted as ± 1 SD; n = 27 for each concentration, except for MR-Buster 1.6 mg/mL (n = 25). * indicates a significant difference ($P < 0.01$) from 0 mg/mL, **indicates a significant difference ($P < 0.001$) from 0 mg/mL.

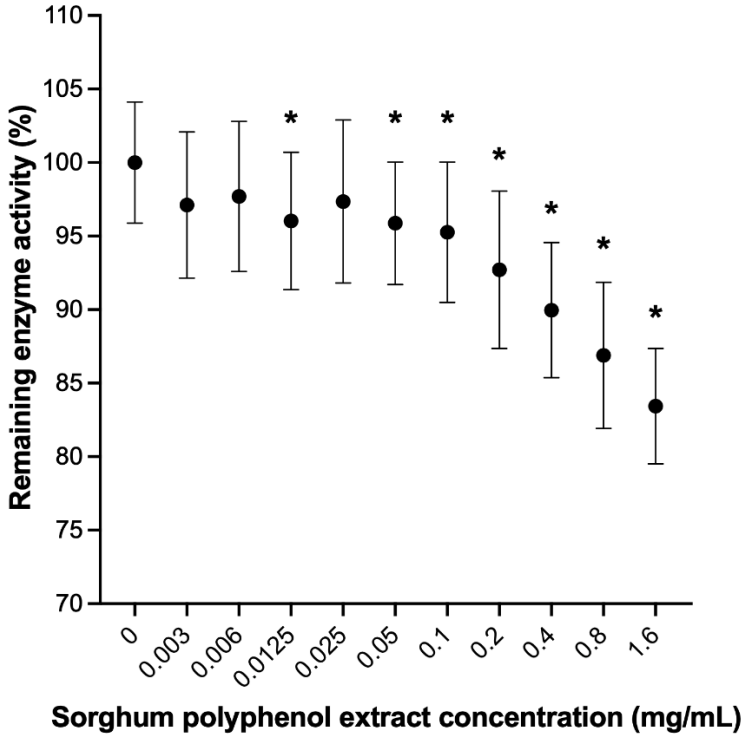

Figure 4.14 Protease activity in presence of white sorghum polyphenol extract
Liberty sorghum polyphenol extract was incubated with the exogenous feed protease (150 mPROT/mL) for 25 minutes before monitoring enzyme activity in the presence of the small, synthetic substrate SAPNA. Error bars plotted as ± 1 SD; n = 27 for each concentration. Asterisk (*) indicates a significant difference ($P < 0.05$) from 0 mg/mL.

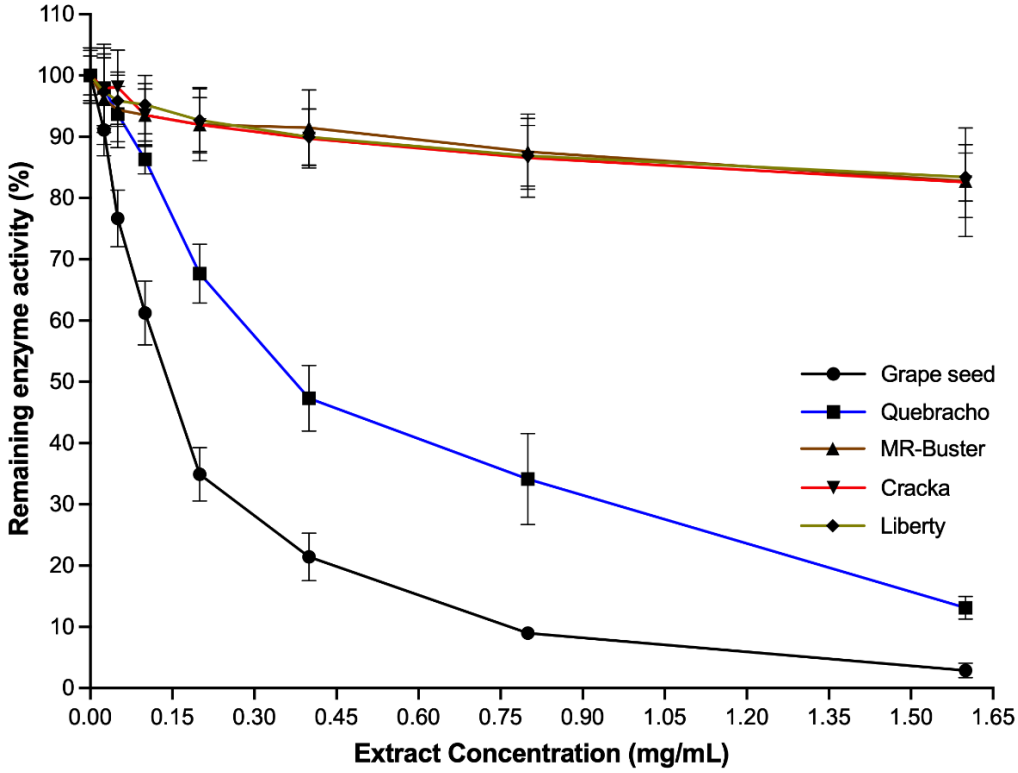

Figure 4.13 Protease activity with sorghum polyphenol extracts and tannin extracts
Error bars and n values are the same as in the figures above (Figures 4.10 – 4.12)

The level of protease inhibition was determined by calculating the average total rate of the reaction (Δabsorbance/Δtime). The presence of sorghum polyphenol extracts from all three varieties reduced protease activity by approximately 20% compared to the normal protease activity control. This is in stark contrast with grape seed and quebracho tannin extracts which inhibited protease activity by 98% and 85%, respectively. Protease activity was restored in a dose-dependent manner as the concentration of extract decreased. Grape seed and quebracho tannin extracts inhibited protease activity significantly ($P < 0.0001$) up until 0.025 and 0.1 mg/mL, respectively. Protease inhibition with grape seed tannin extract was significantly ($P < 0.0001$) different from quebracho tannin extract from 0.05 – 1.6 mg/mL. Slight variations occurred among the sorghum polyphenol extracts with MR-Buster and Cracka significantly inhibiting protease activity to concentrations of 0.05 mg/mL ($P < 0.01$) and 0.1 mg/mL ($P < 0.001$), respectively. Protease activity was significantly ($P < 0.05$) inhibited by Liberty polyphenol extract to 0.05 mg/mL as well as at 0.0125 mg/mL. There were no significant differences in inhibition between sorghum polyphenol extract types. There were clear differences between the sorghum polyphenol extracts and tannin extracts in their ability to inhibit the protease with almost 80% more inhibition gained by the two tannin extracts at their highest dose. These differences are most likely explained by the difference in purity and composition of the two tannin extracts. The crude sorghum polyphenol extracts were found to contain a wide variety of compounds including some sugars and fatty acids whereas the two tannin extracts clearly had large condensed tannins (see **Chapter 3**; Hodges et al., 2021). Sun et al. (2018) found the inhibitory effects of tannins towards porcine pancreatic α-amylase (PPA) to be reduced when plant sugars were mixed with them.

Kinetic studies were performed both with and without extracts to determine their impact on the protease reaction rate at different substrate concentrations (**Figure 4.14**). Michaelis-Menten kinetics were assumed and Lineweaver-Burk plots created from the calculated kinetic constants (**Figure 4.15**). The kinetic constants, V_{max} and $K_{m,}$ were then determined (**Table 4.3**).

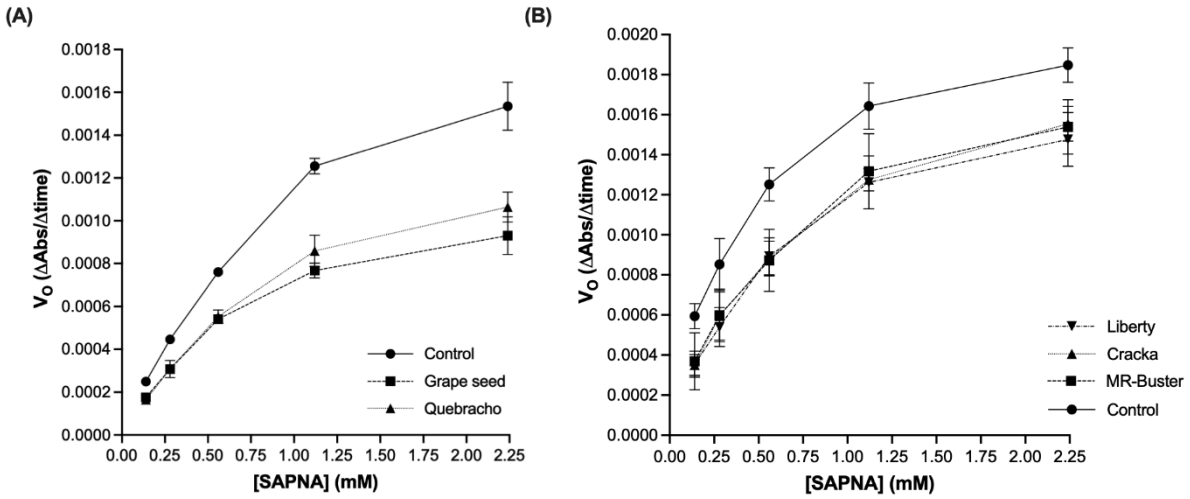

Figure 4.14 Effect of sorghum polyphenol extracts and tannin extracts on protease kinetics

The effect of sorghum polyphenol extracts and tannin extracts on protease reaction rate was tested at different SAPNA substrate concentrations (2.24, 1.12, 0.56, 0.28, 0.14 mM). The initial velocity (V_O) was determined for each substrate concentration. Error bars plotted as ± 1 SD, n = 9 for each concentration per sorghum extract, n = 3 for each commercial extract, n = 15 for the control (n = 14 for 1.12 mM).

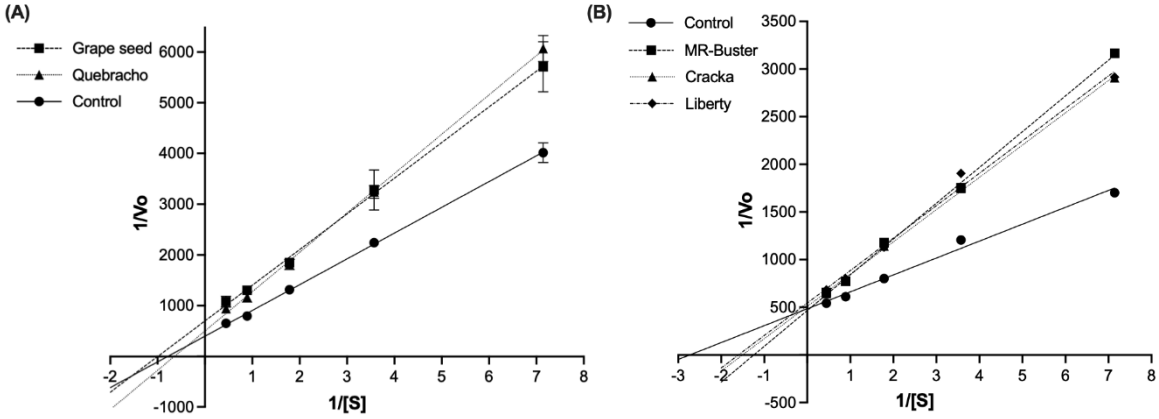

Figure 4.15 Lineweaver-Burk plots of protease reaction kinetics and mode of inhibition

The inverse of initial velocity ($1/V_O$) and substrate concentration (1/[S]) were plotted and linear regression was performed to determined the kinetic constants K_M and V_{max}. Error bars plotted as ± 1 SD, n = 9 for each concentration per sorghum polyphenol extract and n = 3 for the tannin extracts, n = 15 for the control (n = 14 for 1.488 mM^{-1}).

Table 4.3 Kinetic constants of protease with sorghum polyphenol extracts and tannin extracts

		Liberty	Cracka	MR-Buster	Grape seed	Quebracho
V_{max} (ΔAbs/Δt)	Control	0.00206	0.00206	0.00206	0.00251	0.00251
	Extract	0.00184	0.00196	0.00215	0.00143	0.00200
K_m (mM)	Control	0.366	0.366	0.366	1.273	1.273
	Extract	0.625	0.664	0.806	1.005	1.548

The sorghum polyphenol extracts and tannin extracts inhibited protease activity in a dose-dependent manner, similar to what was observed with the inhibition of phytase (see **Section 4.4.2**). Based on the Lineweaver-Burk plots and kinetic constants, the mode of inhibition for the sorghum polyphenol extracts was approximated to be competitive. Grape seed and quebracho tannin extracts proved more difficult to define and most likely were mixed uncompetitive and non-competitive inhibitors, respectively. Non-competitive inhibition, the most widely reported inhibition by polyphenolics, occurs as polyphenols cross-link on the surface of the protein thus preventing necessary conformational changes from occurring (Haslam, 1989). The protease in question is an enzyme from an *Actinomycetes* bacteria with an alkaline optimum pH but with acid stability as low as pH 2 (Dixit and Pant, 2000). The unique stability of this family of proteases is imparted by its structure, consisting of the characteristic double β-barrel structure, between which the catalytic triad of serine, histidine and arginine reside, as well as an unusual polyproline II fold which may provide more kinetic stability to the enzyme (Kelch et al., 2007; Rohamare et al., 2015). The higher levels of proline potentially found in this protease may allow for the binding of polyphenols and tannins resulting in a reduction in enzyme activity.

4.4.4 Relationship between sorghum polyphenol extract/tannin extract composition and exogenous feed enzyme inhibition

As the inhibition of both the exogenous feed protease and phytase did not correlate with total phenolic content within each extract type group (sorghum polyphenol vs. tannin), the differences observed among the extract types are most likely explained by the presence of unique compounds in each that might have varying affinities for the enzyme, substrate and/or enzyme-substrate complex. While no differences were determined between sorghum polyphenol extracts with regard to protease inhibition, MR-Buster, with an intermediate TPC, inhibited phytase the most. Grape seed and quebracho with similar TPC values, inhibited both

phytase and protease to slightly different degrees. However, both tannin extracts exhibited significant increases in inhibitory capacity over the three sorghum polyphenol extracts indicating that TPC did correlate with enzyme inhibition between the two major extract types. This result, alongside the previous characterisation completed (see **Chapter 3**; Hodges et al., 2021) strongly suggested that large tannins played a key role in *in vitro* enzyme inhibition. While the sorghum polyphenol extracts inhibited the enzymes to lesser degrees, significant inhibition from the controls was observed for all three sorghum grain varieties indicating that smaller polyphenols and other anti-nutrients may play an important role in compromising both endogenous and exogenous enzyme activity.

Among the sorghum polyphenol extracts, identifications were made for a wide variety of metabolites including polyphenols, lignin-like compounds, sugars and fatty acids. Phenylpropanoid glycosides, similar to those found in the sorghum polyphenol extracts, have been found to inhibit trypsin activity *in vitro*. Feng et al. (2018) tested the inhibitory effects of four different phenylpropanoid glycosides and found inhibition to increase as the number of phenolic hydroxyl groups increased. Taylor (2005) has suggested lignin-like compounds, similar to those identified in this thesis, might hinder normal digestion and thus potentially optimal exogenous feed enzyme activity. The sorghum polyphenol extracts were also found to contain high percentages of fatty acids, including linoleic and oleic acids. These compounds have been shown to inhibit enzymes *in vitro*. Matsushita et al. (1970) found linoleic acid to inhibit RNase, trypsin, chymotrypsin and pepsin to varying degrees dependant on temperature and pH, e.g., inhibition of trypsin greatly increased as pH increased. These authors speculated that binding was unspecific and based on hydrophobicity as well as the detergent-like nature of fatty acids. A wider range of fatty acids, including stearic, oleic, linoleic and linoleic acids, have also been shown to be potent inhibitors of a chymase (chymotrypsin-like protease) activity using a small, synthetic substrate, very similar to this work (Kido et al., 1984). More recently, crude hexane extracts from mushrooms, found to contain a mixture of fatty acids including linoleic and oleic acids, were shown to inhibit an HIV-1 protease between 13 – 23% (Sillapachaiyaporn et al., 2019).

Both MR-Buster and Cracka sorghum polyphenol extracts contained a series of masses of increasing size from 600 – 1300 Da which were determined to be either pyranoanthocyanins or unique polymerisations of smaller flavonoids. García-Estévez et al. (2017) studied the interaction of common pyranoanthocyanins from wine with salivary proteins and found they

exhibited similar tendencies as traditional tannins had in previous experimentation. While not identical to the traditional condensed tannins found in the grape seed and quebracho tannin extracts, these unknown polymers would have similar binding abilities as they are made up of comparable building blocks. Large tannins, such as those detected in the two tannin extracts here, are known to be strong enzyme inhibitors *in vitro* (Longstaff and McNab, 1991; Barrett et al., 2013).

Between the grape seed and quebracho tannin extracts, the most likely explanation for the variation in inhibitory effect are the differences in tannin structures. Variation in inhibition based on tannin type and extract has been previously described (Barrett et al., 2013; Tan and Chang, 2017). Grape seed and quebracho extracts are known to contain well-characterised condensed tannins. For grape seed, the primary structure type seen are repeating (epi)catechin units increasing 288 *m/z* when detected via MS (Monagas et al., 2003). Quebracho, on the other hand, is found to contain a mixture of repeating units, the most predominant being fisentinidin followed by (epi)catechin (Pasch et al., 2001). These structures, among others, were clearly identifiable when characterised (see **Chapter 3**).

The trends observed here for the inhibition of both phytase and protease were similar to those found across a host of enzymes and extract sources. Polyphenols and related compounds have been found to inhibit lipase (Griffiths, 1979; Boath et al., 2012), α-serine protease (Rohn et al., 2001), trypsin (Griffiths, 1979; Quesada et al., 1995; Gonçalves et al., 2007), α-amylase (Griffiths, 1979; Quesada et al., 1995; Boath et al., 2012; Cai et al., 2015), alkaline phosphatase (Blytt et al., 1988), 5'-nucleotide phosphodiesterase (Blytt et al., 1988), α-glucosidase (Boath et al., 2012) and bacterial cysteine proteases (Yamanaka et al., 2007) often in dose-dependent manners as seen here.

However, little research exists involving the *in vitro* inhibition of phytase caused specifically by polyphenols. Several compounds are known to inhibit phytase activity including various metal ions and phytate itself, in high enough concentrations. As found by this researcher, polyphenol inhibition of *in vitro* phytase activity appears once in the literature in a study conducted by Goel and Sharma (1979). They showed inhibition of a variety of plant phytases with 20 – 70 mM phloroglucinol, a relatively simple phenolic compound comprised of a benzene ring with a 1,3,5 hydroxylation pattern. Two related phenolic compounds, orcinol and resorcinol, were also tested but showed little to no inhibition indicating a role for the degree of

hydroxylation and thus hydrogen bonding in binding. A more recent study investigated grain protein extracts from several cereals and isolated a proteinase that inhibited phytase activity (Bekalu et al., 2017). The proteinase appeared to be related to the presence of *Fusarium graminearum* fungal infection in the grains.

Several proteases have been tested for polyphenol inhibition with similar results as found for the exogenous feed protease tested here. The effect of synthetic, grape and wine procyanidins on elastase, a serine protease, activity was measured through catalysis of the small synthetic, substrate Suc-$(Ala)_3$-*p*-nitroaniline, very similar to SAPNA used here (Brás et al., 2010). Elastase activity decreased in a dose-dependent manner regarding both concentration, 0-850 µM, and the size of procyanidin. These results suggest that larger procyanidin fractions have a greater ability to bond and interact non-covalently with the enzyme than smaller fractions. The procyanidins were found to competitively and reversibly inhibit the enzyme which matches the competitive inhibition type found for the sorghum polyphenol extracts in the present study. Gonçalves et al., (2007) studied procyanidins from grape seed and their inhibition of trypsin using another small, synthetic substrate, BAPNA, at physiological conditions of 37°C and a pH of 7.0 to mimic those of the duodenum. Similar to Brás et al. (2010), the rate of catalysis and initial rate decreased with more procyanidin and with molecular weight of compounds. They suggested that aggregates of enzyme-polyphenol were forming and become more favourable as the molecular weights of compounds increased.

Rohn et al. (2001, 2003) studied the oxidation products of phenolics and their subsequent inhibition of enzyme activity when derivatised to the enzyme. This appears to be the only research available which directly uses SAPNA substrate with phenolic compounds. Conditions were set to mimic those of food processing with an alkaline environment (pH 9). This alkaline pH was also chosen as to amplify the reactions and interactions of the phenolics and enzyme as covalent interactions are more likely to take place in these conditions. Derivatisation of the enzyme resulted in fewer free amino acids groups upon digestion with slight differences between phenolic compounds of different structures. Fluorescent quenching suggested the indole structure of tryptophan interacted with the phenolic compounds. Additionally, solubility decreased as a result of possible cross-linking and blocking of hydrophilic groups on the enzyme. This increased hydrophobicity also decreased the enzyme's isoelectric point. SDS-PAGE further confirmed aggregation with the presence of bands correlating to polymers of four α-serine protease enzymes bound by the phenolic compounds. These polymers were

shown to not be bound by disulphide bridges and the interactions were determined to be covalent. Enzyme activity as measured through SAPNA hydrolysis was significantly reduced from 30 – 60% depending on the phenolic compound tested. Interestingly, the greatest inhibition was caused by the smallest phenolic compounds. The results found in this current study echo what Rohn et al. (2001, 2003) found and also exhibited that the protease was susceptible to inhibition at much shorter incubation periods, 25 minutes versus 24 hours.

Several other studies of serine protease alone mention the use of much lower concentrations of SAPNA, including 0.5 mM (Kaspar et al., 1984), 0.1 mM (DelMar et al., 1979) and 20 µM (Louati et al., 2011). SAPNA was used as a substrate due to its small, synthetic nature. An issue that arises with using polyphenols in enzyme assays is the use of protein-based substrates, such as BSA and casein (Tamir and Alumot, 1969) as well as starches. The polyphenols in plant extracts often have higher affinities for the substrates than for the actual enzyme investigated. This is not necessarily a reason to not use them, however, researchers using these methods need to be clear in interpreting results and listing any or all caveats to the experiment. Interactions with substrates are quite useful and are telling in their own right as this does help mimic what is seen *in vivo* when an animal consumes feed. Polyphenols, in an animal digestive system, will never be truly isolated and free to interact with only one enzyme, protein or other nutrient. The goals and results of any experiment and work need to be clarified based on what interactions may or may not be occurring (see **Chapter 6**).

Blytt et al. (1988) argue that tannins are not necessarily as anti-nutritional as commonly accepted. This was investigated through the inhibition of alkaline phosphatase and 5'-nucleotide phosphodiesterase with condensed tannin extracts from quebracho and a bird-resistant sorghum hybrid called BR 64. The initial inhibition studies on the purified enzyme found a delayed inhibition after 15 minutes with 50% inhibition achieved with 20 µg/mL of extract for both enzymes and both extract types. Inhibition caused by the tannin extracts was able to be reversed through addition of Triton-X, a phospholipid compound and PVP. However, when repeated with freshly prepared, particulated enzyme from the intestine of a rat, the extracts were only able to achieve approximately 50% inhibition at a concentration of 50 µg/mL. Currently *in vivo* inhibition of these various proteases is uncertain, however, if interactions did occur they would be most likely in the duodenal region of the small intestine due to the higher pH (Velickovic and Stanic-Vucinic, 2018).

A discrepancy often seen in research involving polyphenol inhibition of enzymes is a lack of congruence between the concentrations and activities of enzymes used, particularly *in vitro*, and those that would be expected at applicable and relevant 'real-world' values. This is especially important when dealing with agricultural products/feed as inhibition values can distort the significance of what is occurring. In the current study, this aspect was considered and the *in vitro* values were converted to more relevant ones (**Figure 4.16**). These conversions helped to provide a better context for understanding the results.

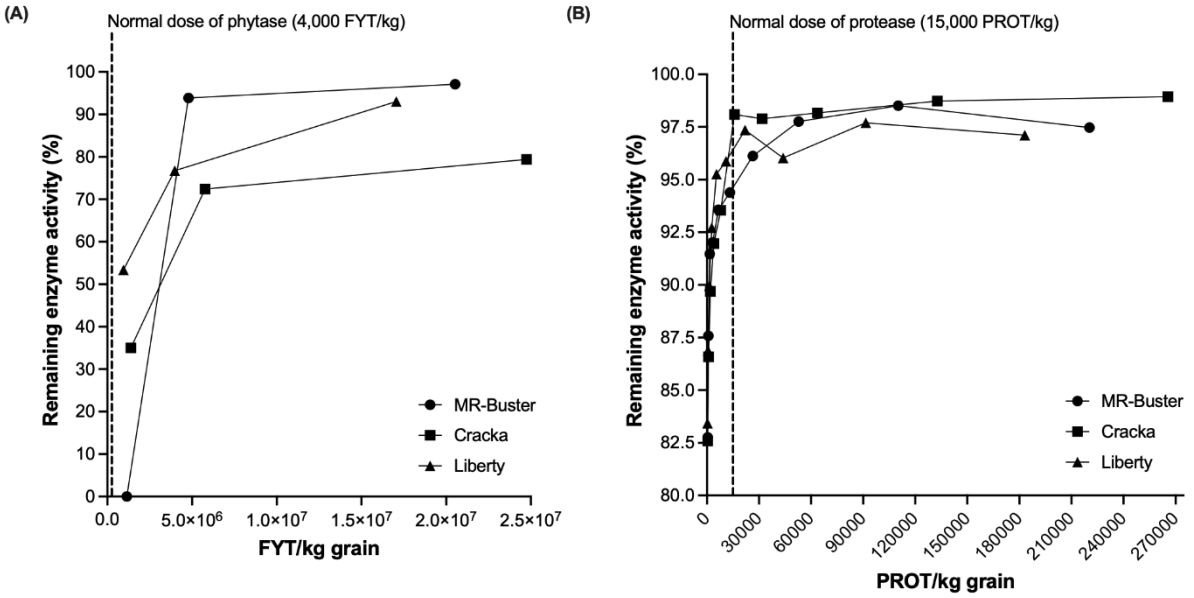

Figure 4.16 Conversion of *in vitro* inhibition results to commercial enzyme – sorghum inclusions
The relationships between the remaining activity of phytase and protease, when incubated with sorghum polyphenol-rich extracts, and enzyme activity units per kilogram of grain were determined.

While protease inhibition was significant *in vitro*, more relevant values based on enzyme inclusion in a 100% sorghum diet illustrated that the enzyme is robust and only shows inhibitory values at low enzyme:sorghum ratios and with higher tannin grains. Phytase, on the other hand, while seeing a full spectrum of inhibition in the ITC studies, was fully inhibited when evaluated at feed-relevant values.

4.5 Conclusions and future work

4.5.1 Conclusions

This work in this chapter sought to extract polyphenols from three modern Australian sorghum varieties (MR-Buster, Cracka, Liberty) routinely used in monogastric diets and test their effects on the activity of two commonly used exogenous feed enzymes, phytase and protease. Two more pure tannin extracts, known to contain large tannins, were tested alongside for comparison. Previous characterisation (see **Chapter 3**; Hodges et al., 2021) of the sorghum polyphenol extracts indicated that they contained a diverse range of polyphenols and other small metabolites. The total phenolic contents of the three sorghum polyphenol extracts were measured which indicated that the white coloured grain variety, Liberty, had the lowest levels of phenolic compounds while Cracka, a red coloured grain variety, had the highest. Both tannin extracts had significantly higher phenolic contents than all three sorghum polyphenol extracts but did not differ between themselves. Phytase proved susceptible to 100% inhibition with MR-Buster sorghum polyphenol extract at the highest concentration of extract tested, followed by Cracka and Liberty. Both tannin extracts also inhibited enzyme activity by 100% but at much lower concentrations than the sorghum polyphenol extracts. Inhibition of the protease with the sorghum polyphenol extracts approached 30% indicating that even at high levels of sorghum grain in diets this enzyme would remain robust and maintain sufficient activity. There was little difference in inhibition among the sorghum polyphenol extracts. The two tannin extracts, however, inhibited protease activity to almost 100% at the same concentrations tested as the sorghum polyphenol extracts. As the tannin extracts had phenolic contents much higher than the three sorghum extracts and contained large tannins, it stands to reason that these specific compounds contributed greatly to enzyme inhibition for both phytase and protease. These results indicate that grain variety and anti-nutrient content can play a key role in contributing to variability in nutrient digestibility and optimal function of exogenous feed enzymes.

4.5.2 Future work

There are several possible directions to take future work forward regarding the content in this chapter. The total phenolic content assay provided a useful benchmark for determining whether phenolic compounds contributed to and correlated with enzyme inhibition. It might be useful for the future to optimise several more ‘content’ assays for specific compounds groups, i.e. flavonoids, tannins and anthocyanins, within the sorghum polyphenol extracts.

These further assays might indicate that specific groups of compounds contribute towards the inhibitory effects seen here, rather than just total phenols.

Staying with the extracts generally, several options for further study exist and include optimising purification schemes and testing other grain/food extracts. As noted, the extracts tested in this chapter were classed as 'crude' because they were not further purified or separated after extraction. The development of a purification and separation regime could help to address specific research questions regarding inhibitory qualities of specific compounds and/or more specific groups of compounds. This optimisation would need to include the removal of various groups of sugars, fatty acids and other non-phenolic grain components before then trialling different separation strategies. These strategies are well-documented in the literature, especially in laboratories that specialise in grain and polyphenol research. While this thesis only investigated sorghum grain and its polyphenol extracts, grains with similar polyphenol content and profiles, including barley and millet, could also be studied in a similar manner. Beyond polyphenols, grains high in other anti-nutrients, e.g. canola or rapeseed meals which are high in complex sugars, could also be tested as feed enzyme inhibitors.

In addition to alternative grains and extract types, different feed enzymes could be researched for susceptibility to inhibition. Other feed enzymes include a host of carbohydrase enzymes, e.g. xylanase, β-glucanase, cellulase and xyloglucanase. The interactions the phytase and protease, as well as any other enzymes, have with anti-nutrients could be expanded to include specific binding interactions (ITC binding studies), structural features (NMR) and changes (fluorescence quenching) and precipitation studies.

Chapter 5 - A Study of the Interactions of Sorghum Polyphenol Extracts and Tannin Extracts with Exogenous Feed Enzymes in an *In Vitro* Simulated Digestion Model

5.1 Summary

Polyphenols are known to disrupt normal monogastric animal digestion through a variety of mechanisms including binding and cross-linking proteins and interrupting endogenous enzyme activity. As sorghum grain has higher than average concentrations of these compounds, they have long been stigmatised as being deleterious in monogastric animal feed. However, the effects polyphenols might have on exogenous feed enzymes is still unknown. In **Chapter 4**, polyphenol extracts from three modern Australian sorghum varieties and tannin extracts from grape seed and quebracho wood were tested, *in vitro*, as inhibitors of two commercially available exogenous feed enzymes, phytase and protease. When tested in these simple environments, all sorghum polyphenol extracts and both tannin extracts were found to inhibit phytase and protease activity, albeit in different ways and to varying extents.

In this chapter, an *in vitro* simulated digestion model was used to test the effects of the previously characterised sorghum polyphenol extracts and tannin extracts on endogenous and exogenous feed enzyme activity, as measured by their respective nutrient digestibility parameters. The extracts were added to a standard poultry diet of maize:soybean meal (70:30) which included endogenous enzymes commonly found in the poultry digestive tract. Half of the diets were supplemented with two exogenous feed enzymes, phytase and protease. The different sorghum and tannin extracts were found to affect measures of protein/nitrogen and phosphorous but in very different ways to each other. Protein/nitrogen parameters were more negatively affected than those for phosphorous indicating a role for the sorghum polyphenol extracts and tannin extracts in interrupting the endogenous and exogenous digestion of protein. While sorghum polyphenol extracts minimally affected protein/nitrogen measures, both tannin extracts significantly reduced these measures. Phosphorous digestibility was minimally affected by all extract types. These results indicated a role for polyphenols in limiting protein digestibility but with variability based on extract type. Finally, a rapid MALDI mass spectrometry metabolomic profiling method was tested to determine if such an approach was suitable to differentiate samples based on the metabolites present in the soluble portion of the digesta. When evaluated under specific filters, clear separations could be seen which allowed for groupings to be made based on certain parameters of the diet's composition including presence of exogenous feed enzymes, presence of polyphenol/tannin extracts and dose of polyphenol/tannin extracts. This kind of rapid assessment may be suitable when evaluating feed performance in full animal feeding trials.

5.2 Introduction

5.2.1 Sorghum's current role in animal feed

The intensification of the global meat industry has stimulated innovation in the animal feed sector. Advances in feed technology strive towards sustainable intensification through a reduction in feed conversion ratio (FCR), greater energy and nutrient utilisation, improved animal welfare and environmental sustainability, reduction in endogenous grain anti-nutrients and optimisation of costs (Makkar and Ankers, 2014; Hodges et al., 2021). Using poultry production as a specific example, the yield of chicken meat (with Australia as a model market) has exponentially increased from the 1970s until today where it has begun to level off (**Figure 5.1**).

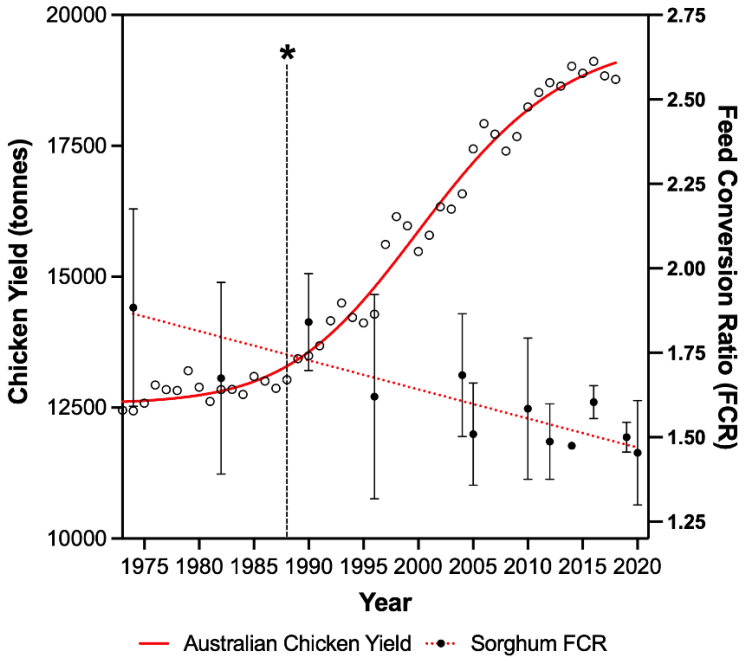

Figure 5.1 Historical chicken yield and feed conversion ratio data (from Hodges et al., 2021)
Data was gathered from FAOSTAT (Food and Agriculture Organization of the United Nations, 2020) on Australian chicken yield and global poultry feeding studies conducted from 1974 to 2020 that investigated the use of sorghum grain in broiler chicken feed (Armstrong et al., 1974; Hulan and Proudfoot, 1982; Banda-Nyirenda and Vohra, 1990; Nyachoti et al., 1996; Jacob et al., 1996; Black et al., 2005; Perez-Maldonado and Rodrigues, 2009; Selle et al., 2010b; Rodgers et al., 2012; Liu et al., 2014; Liu et al., 2016; Truong et al., 2016; Manyelo et al., 2019; Puntigam et al., 2020; Moss et al., 2020; Mabelebele et al., 2020). Chicken yield (asymmetric sigmoidal 5PL nonlinear model plotted as solid red line, individual values in open circles) and averaged FCR values were plotted for each year available and simple linear regression model (dotted red line) was fit over the averaged literature values. Asterisk (*) indicates when the first feed phytase was developed and when targeted sorghum breeding for tannin reduction began.

This increase in poultry meat production is mirrored by a similar decrease of FCR (increased efficiency) also with a levelling off phase. This gain in feed efficiency is due to several global innovations, including directed poultry and feed grain breeding, implementation of new feed additives and the use of higher quality grains and supplements in dietary formulations (Mottet and Tempio, 2017). Supplementation of monogastric feed with new feed additives, most notably exogenous feed enzymes, has become routine to support measures of performance, as well as to mitigate the effects of anti-nutrients, e.g., phytate, non-digestible starches and proteins and polyphenols (Cowieson et al., 2006; Hodges et al., 2021). Australia was chosen as the model market as this thesis and its contents are highly relevant to the monogastric feed industry, particularly poultry, in that country. Australia, a major sorghum producer, sees its poultry diets typically formulated with wheat, sorghum or a mix of the two. Sorghum in Australia is cheaper than wheat, has a higher energy density and is close at hand (Selle et al., 2010a).

Currently, maize and wheat are the primary base grains used in pig and poultry feed. These grains typically have a higher nutrient digestibility and bioavailability than other primary ingredients, including sorghum. Sorghum grain *in vitro* digestible energy and predicted digestible energy has been found to be lower than that of maize used in pig feed (Pan et al., 2021). Sorghum grain is however similar to maize and wheat in that it has comparable fibre and protein levels. Modern figures of sorghum grain viability in feed place its nutritional value at 98 – 99% of maize. This value has risen over the past 20 years from 96% (Goodband et al., 2016). Overall sorghum is a more cost-effective grain, grows in harsher conditions and can reduce the economic burden of growing maize and wheat exclusively for feed purposes (Bryden et al., 2009; Selle et al., 2010a). Both wheat and sorghum have been found to provide similar daily energy intakes for broilers, however, chickens fed wheat had overall better growth rates and ate approximately 17% less compared to those fed sorghum (Black et al., 2005). Bone abnormalities have also been reported in poultry fed sorghum grain, particularly those grains high in tannin content. This may be due to a complexing/chelating effect of the tannins with minerals necessary for bone and collagen formation (Gualtieri and Rapaccini, 1990). Polyphenols are well-established anti-nutrients, particularly to monogastrics, and routinely cause reduced feed intake and weight gain, increased FCR (reduced efficiency), and enzyme inhibition (Bravo, 1998; Cadogan and Finn, 2010; Pasquali et al., 2016; Alu'datt et al., 2018).

The inclusion of sorghum in growing pig feed formulations reduced feed intake and weight gain (Lizardo et al., 1995; Cadogan and Finn, 2010; Pasquali et al., 2016). Additionally, pig diets substituted with high-tannin sorghum over maize resulted in decreased energy digestibility and crude protein and increased faecal nitrogen and protein (Pan et al., 2021). Endogenous enzyme activity, including amylase, lipase and trypsin, were all decreased in diets made up of sorghum compared to those of maize. Increased FCR (decreased feed efficiency) values have been observed in broiler starter diets composed of sorghum grain versus maize (Batonon-Alavo et al., 2015). This group hypothesised that the depressed growth performance parameters observed with the substitution of maize with sorghum grain could be caused by a dose-response of anti-nutrients, including polyphenols and phytate found in sorghum. Torres et al. (2013) found that low-tannin sorghum (<0.5% tannin) could be substituted for maize up to 50% in broiler diets. Their results, however, were interesting as a 50% sorghum diet improved both FCR and weight gain over the 100% sorghum diet only at the 42-day finishing stage indicating that during the starter and grower phases 100% sorghum could be substituted with little to no loss in performance. Manyelo et al. (2019) found similar results with sorghum replacement of maize but broilers actually had an increase in body weight with a 50% replacement diet versus 100% maize. Nyachoti et al. (1996) studied maize replacement with high-tannin sorghum (2.5% tannin) and found broiler weight to increase with sorghum inclusion but only over the first nine days of feeding. High-tannin sorghum did result in lower average metabolisable energy (AME) versus maize. These conflicting results led these researchers to speculate as to whether the presence/amount of tannin was a good indicator for sorghum grain's suitability as a feed ingredient. Contradictory results in *in vivo* feeding trials are a common occurrence and can complicate any conclusions to be gained from the research.

Variation in sorghum grain feed performance has also been detected between different low-tannin sorghum varieties. Truong et al. (2016) tested six diets of equal nutritional value using various 'tannin-free' sorghum grains in broiler chicken diets. Average metabolisable energy (AME) recorded in the broiler chickens was less than that of the formulated value and the FCR value was higher than what was typically found and to be expected. As Truong et al. (2016) described reductions in predicted nutritional parameters, they found no differences in performance of the broiler chickens, i.e. FCR or weight gain, based on the sorghum variety but did find differences in nutrient utilisation between grain varieties. Liberty, the same white grain used in the current study, performed better than a red variety (Block I) regarding AME, metabolizable energy:gross energy (ME:GE) and nitrogen retention. Several negative

correlations were found linking phenolic acids, flavonols and kafirin protein to these measurements of digestibility. As the grains used here were 'tannin-free,' compounds other than traditional condensed tannins may have caused the anti-nutritional effects observed. The observed variations in the digestibility of sorghum grain were most likely caused by several intrinsic factors of the grain rather than one specific element.

A generalised view on sorghum grain's utilisation in monogastric animal feed, relating to polyphenol content, primarily divides the grain based on its colour. Brown and black coloured grain varieties are not typically used for animal feed purposes, primarily due to their connotations of having very high-tannin contents. High-tannin varieties were introduced with the aim to stop crop loss to birds, hence the term 'bird-resistant' (Davis and Hoseney, 1979). High-tannin sorghum varieties are not as commonly used in agriculture anymore as detrimental nutritional effects are often seen in animals fed these grains. This has led sorghum breeders and feed manufacturers to preferentially select low-tannin varieties for use in animal feed. Sorghum low in tannin content, i.e., most modern white and red coloured grain varieties, has been reported to have higher levels of digestible proteins thus implicating a role for polyphenols in binding protein leading to a reduction in bioavailability (Youssef, 1998). While there is some debate about equating nutrient content and polyphenol content with the colour of the kernel, today white coloured sorghum grain is widely accepted to be of a superior quality to similar red coloured grain varieties. White coloured grains, most commonly the Liberty variety in Australia, have been found to better support weight gain, FCR as well as growth performance in pigs and chickens than its red coloured counterparts (Cadogan and Finn, 2010; Liu et al., 2010). This may be due in part to the absence of large polyphenols, previously found in high concentrations in older varieties. While not routinely used in feed anymore, high-tannin varieties are important to alcohol production, particularly in China. Most of the sorghum grown in China is high in tannin content as this is required for liquor production (Diao, 2017).

Exogenous feed enzymes can be incorporated into feed formulations to increase nutrient utilisation. Animal feed formulations containing sorghum grain are often supplemented with exogenous enzymes to increase the bioavailability of nutrients, previously discussed in **Section 1.5.2**. Sorghum grain contains higher concentrations of lower quality and indigestible proteins, like kafirins, as well as phytate and can benefit from the inclusion of exogenous feed enzymes, like proteases and phytases (Cadogan and Finn, 2010). While the inclusion of sorghum grain in animal diets often leads to reduced body weight gain, the addition of exogenous enzymes,

e.g., phytases, proteases and carbohydrases, has been shown to increase those levels to that of a low- or non-sorghum diet (Avila et al., 2012; Pasquali et al., 2016). Typically any depression of nutritional parameters observed with sorghum is restored with the inclusion of enzymes (Cadogan and Finn, 2010; Selle et al., 2010b). This allows sorghum to replace other grains commonly used feed mixture and can reduce the overall cost of the feed. However, as Selle et al. (2010a) notes, phytase performance in sorghum can appear muted, especially given the grain's high phytate content. In addition to these direct 'phosphoric' effects to be gained with phytase supplementation, secondary or 'extra-phosphoric' effects have also been noted to be substandard. These 'extra-phosphoric' responses include improved energy utilisation through enhanced starch and protein digestibility. Previous studies have found diets with sorghum and supplemented with phytase to have lower metabolisable energy and amino acid digestibility compared to other cereals (Wu et al., 2004; Cervantes et al., 2011).

The reason for these muted responses is unknown but kafirin protein is noted as a possible culprit (Selle et al., 2010a; Liu et al., 2013). It is theorised that phytase produces beneficial impacts in energy and nutrient digestion partly due to the anti-nutritional nature of phytate. Phytate readily complexes with starch and protein and thus the degradation of phytate by phytase would enable those complexes to be full digested. However, kafirin protein's structure is not structured to readily bind to phytate which weakens this theory. Another endogenous component of sorghum grain might be causing this phenomenon and could include the wide range of polyphenolic compounds routinely found in the grain, even in low- or 'tannin-free' varieties (see **Chapter 3**; Hodges et al., 2021).

5.2.2 Use of simulated digestion models and *in vivo* feeding trials

While the use of simple *in vitro* techniques is useful for establishing the basic interactions and effects of inhibitors and anti-nutrients found in grains, more complex and realistic testing environments are needed to better understand the implications of anti-nutrients in animal feed. The clearest solution to this problem is through the use of animal feeding studies with specific diet and compounds of interest. Animal feeding studies, while providing the most realistic testing environment, are expensive, time-consuming and labour-intensive. The benefits of first conducting a simulated digestion study are to screen potential compounds of interest and to determine whether a follow-up feeding trial is necessary. Additionally, *in vitro* simulated models allow for the high-throughput screening of anti-nutrients and compounds of interest as

well as the determination of specific effects to various sections of the digestive system (Alminger et al., 2014). A limitation of *in vitro* models is that there are numerous variables to choose from, including but not limited to digestion time at each step, pH and temperature, ionic contents and enzyme type/activity (Alminger et al., 2014). While *in vivo* studies provide standard, robust measurable nutritional parameters, basic *in vitro* tests can help elucidate these findings and shed more light on their possible mechanisms. Chibber et al. (1980) tested a simple *in vitro* digestion model using sorghum grain with pepsin followed by incubation with trypsin and chymotrypsin. With this basic model, they found that pepsin was responsible for the majority of protein solubilisation. They concluded that the use of a simple model like this could help determine future *in vivo* findings.

Previous studies have investigated the effects of *in vitro* digestion on the bioavailability and degradation of polyphenols (Helal et al., 2014; Mandalari et al., 2016; He et al., 2017; Salazar-López et al., 2018). The bioavailability of polyphenols from cinnamon-based drinks were found to decrease by approximately 20% following gastro-pancreatic digestion due to tannin precipitation with pepsin (Helal et al., 2014). A similar reduction in phenolic content, this time with smaller phenolic acids in sorghum, was found after simulated digestion (Salazar-López et al., 2018). Interestingly, He et al. (2017) found simulated digestion to increase polyphenol and polysaccharide contents which in turn increased the inhibition of certain enzymes like amylase and glucosidase. However, the addition of simple sugars increased bioavailability. Little research has been done to determine the effects of the compounds themselves on measures of nutrient digestibility.

5.2.3 Research aims, hypotheses and methodology

Previously, both sorghum polyphenol extracts and tannin extracts were found, through basic *in vitro* testing, to inhibit exogenous feed phytase and protease activity, albeit to different degrees (see **Chapter 4**; Hodges et al., 2020). General characterisation of the three sorghum polyphenol extracts indicated that they contained polyphenols and other small metabolites like sugars and fatty acids (see **Chapter 3**; Hodges et al., 2021). Additionally, the two tannin extracts, from grape seed and quebracho wood, were characterised and found to contain traditional large tannin structures commonly associated with anti-nutrition. The purpose of this experimental chapter was to determine if these five different extracts compromised exogenous feed phytase and protease activity and efficiency when evaluated in a more realistic

in vitro model of simulated poultry digestion. The use of *in vitro* simulated digestion models can provide a useful intermediate step to predicting how animals might react in a full feeding trial.

As the direct inhibitory qualities of the sorghum polyphenol extracts and tannin extracts had been previously determined, it was necessary to understand whether these effects remained in a model of simulated poultry digestion or were mitigated. The five different extracts were incorporated into diets with and without exogenous feed phytase and protease, alongside several endogenous enzymes. After digestion, the soluble fractions of the digesta were analysed for measures of protein and phosphorous to determine any adverse effects from the inclusion of the extracts. A rapid metabolite profile fingerprinting method, using MALDI-ToF-MS, was also trialled as a potential tool to improve diet characterisation and detect relationships between different formulations. The results of the relationship of the extracts with enzymes alongside the previous chapter's results will help to build a better understanding for predicting diet and animal performance in feed containing high levels of polyphenols.

1. Sorghum polyphenol extracts and tannin extracts will significantly interfere with protein and nitrogen digestibility in a simulated digestion model **without** exogenous feed enzymes. Sorghum polyphenol extracts and tannin extracts will significantly interfere with protein and nitrogen digestibility in a simulated digestion model **with** exogenous feed enzymes.
    a. Protein and nitrogen digestibility were determined using a LECO nitrogen analyser and the *o*-phthaldialdehyde (OPA) assay for determining the degree of protein hydrolysis.

2. Sorghum polyphenol extracts and tannin extracts will not significantly interfere with phosphorous digestibility in a simulated digestion model **without** exogenous feed enzymes. Sorghum polyphenol extracts and tannin extracts will significantly interfere with phosphorous digestibility in a simulated digestion model **with** exogenous feed enzymes.
    a. Phosphorous digestibility was determined using the malachite green/molybdate assay for total phosphorous content.

3. The metabolite profiles of the digesta will be able to differentiate samples with and without exogenous feed enzymes and samples with and without sorghum polyphenol extracts/tannin extracts.
    a. Metabolite profiles were generated from MALDI-ToF-MS spectra of the digesta followed by multivariate analyses, i.e., PCA.

5.3 Materials and methods

5.3.1 Chemicals and materials

Sorghum grain and tannin extract information was previously described in **Section 3.3.1**. Exogenous feed enzymes, a phytase and protease, were used as previously described in **Section 4.3.1**.

5.3.2 Preparation of sorghum polyphenol extracts

Sorghum grain was extracted for polyphenols following Harbertson et al. (2014) with modifications and previously described in **Section 3.3.2**.

5.3.3 *In vitro* simulated poultry digestion model

A model to simulate poultry digestion *in vitro* was used as developed by Novozymes A/S (Bagsværd, Denmark) including pre-incubation, crop, gastric and intestinal phases (**Figure 5.2**).

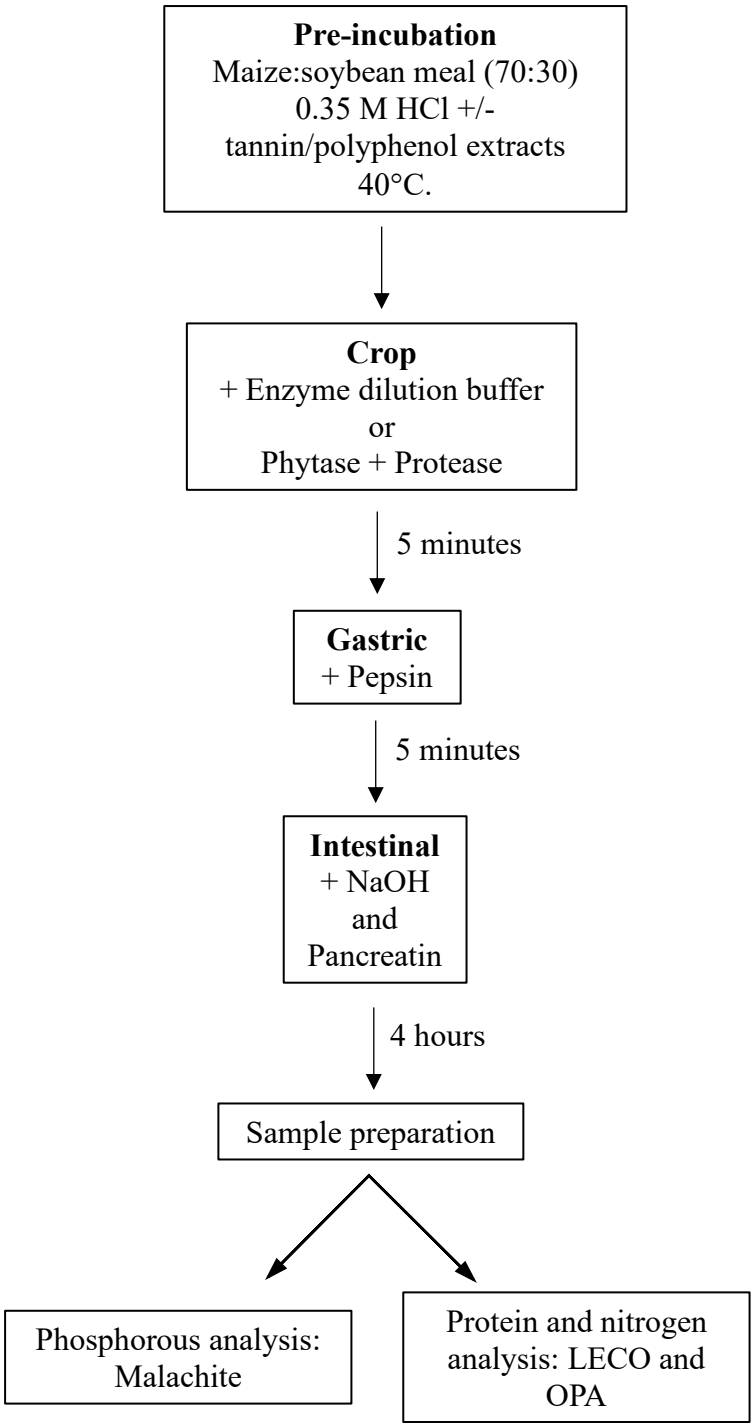

Figure 5.2 Stages of simulated digestion and nutrient analysis workflow

A standard poultry feed mixture of maize:soybean meal (SBM) (70:30) was used and 400 mg of ground material was added to each well of a 24 deep well-plate. Each sorghum polyphenol extract and each tannin extract were individually weighed, mixed with 0.035 M HCl and stirred until dissolved or a uniform slurry had formed. To the control (exogenous feed enzymes + endogenous enzymes) and blank (endogenous enzymes) sample wells, 2.05 mL of 0.035 M HCl was added to make four replicates. To wells containing sorghum polyphenol extracts or

tannin extracts, 2.05 mL of the previously prepared extract mixtures/slurries were added, also in four replicates. The amount of sorghum polyphenol extract or tannin extract added to each well was 5, 10, 17 or 20 mg and was converted to feed relevant values for the sorghum polyphenol extracts (**Table 5.1**). Stirring was continuous from this point and the temperature was set to approximately 40°C. Measurements were taken in the initial experiments to determine the effects of the extracts on digesta pH (**Appendix Table C.1**).

Table 5.1 Dosage conversion from extract (mg) to feed formulation (%)

Sorghum	**Red**	**White**	**Red**	**White**	**Red**	**White**	**Red**	**White**
% SBM:maize	100	100	50	41	33	27	23	17
% sorghum*	0	0	50	59	67	73	77	83
Extract (mg)	0		5		10		17	

*****Calculated from the extract yield from the bran of sorghum and not the whole grain (% sorghum values will increase if calculated from whole grain), see **Section 4.4.1**

Once the temperature had reached 40°C, 200 μL of an enzyme dilution buffer (EDB) was added to the wells without exogenous feed enzymes. EDB was prepared with 0.025 g BSA, 2.5 mL 1% Tween and 0.1 M acetate buffer with 5 mM calcium. The solution was pH adjusted to 6.0 (± 0.05). To wells with exogenous feed enzymes, 100 μL of phytase (1X commercial dose) and then 100 μL protease (20X commercial dose) were added. The 20X dose of the protease was used to ensure a measurable response was detected, as previously optimised by Novozymes. The mixtures were incubated for five minutes to simulate the crop phase in poultry.

Following the crop phase, the gastric phase was simulated by adding 200 μL pepsin (3000 U/g sample) to each well. Pepsin was prepared by dissolving 189.9 mg pepsin in 0.48 M HCl. The samples were then incubated for five minutes.

Next, the intestinal step was simulated by adding 500 μL NaOH to each well, followed by 100 μL pancreatin. Pancreatin was prepared by dissolving 320 mg pancreatin in 20 mL of 0.1 M $NaHCO_3$ to give activity of 4 mg pancreatin/g diet. This solution was centrifuged for 10 minutes at 3000 rpm and 5°C after which the supernatant was removed and set aside for use in the digestion. The pH of randomly selected wells was then measured within an hour of starting the intestinal phase. The samples were incubated at this stage for four hours.

At the end of the intestinal step, 500 μL from each well of the stirring digesta mixture was removed and placed in separate well-plates. To each of these aliquots, 500 μL 1 M HCl was added and the sample was extracted for three hours at 30°C. These samples were used for determination of phosphorous. Plates were then centrifuged for 10 minutes at 3000 rpm and 5°C. The remaining supernatants were removed, transferred to tubes and frozen until further analysis of protein content, protein hydrolysis and metabolite profile.

5.3.4 Protein and nitrogen content determination

A LECO FP628 nitrogen analyser (St Joseph, Michigan, USA) was used to determine nitrogen and protein contents in the supernatants obtained from simulated digestion as described above. Samples were prepared by adding 200 μL of supernatant to tin capsules and taking the total mass in grams. The capsules were left open, dried in an oven overnight at 60°C and closed using tweezers prior to analysis. Standards were prepared by weighing out 150 mg of ethylenediaminetetraacetic acid (EDTA) into tin capsules. Prior to analysis, ten blank measurements were taken, followed by the EDTA standards to ensure proper machine calibration. Samples were then loaded into the autosampler and analysed. Analysis, in brief, involved the combustion of the sample using pure oxygen. The combustion products underwent further oxidation after which water and carbon dioxide were removed from the analysis. Nitrogen oxides were then reduced to nitrogen (N_2) for final detection. Using the sample's mass and a pre-determined nitrogen factor for common feed proteins, the percent nitrogen was converted to percent protein. The nitrogen factor used in this work was that of soy protein, 6.25, as soybean meal was the principal source of protein in this diet. This value was determined based on the assumption that the average protein contains 16% nitrogen. Replicates were averaged and the standard deviation calculated.

5.3.5 Degree of protein hydrolysis determination

Protein hydrolysis of soluble protein was determined in the supernatants using the *o*-phthaldialdehyde (OPA) assay. The Novozymes protocol was followed which itself is based on previously published methods (Adler-Nissen, 1979; Nielsen et al., 2001). OPA reacts with α-amino groups produced upon peptide bond hydrolysis. The reaction of OPA with the α-amino group in the presence of a reducing agent, here dithiothreitol (DTT), formed a yellow-coloured complex that was detectable at 340 nm. Samples were prepared by diluting 150 μL

of supernatant 10 times and five times in MQ water. To a 96 well-plate, 25 µL of each sample was added in replicates of five. Eight replicates of the standard solution, L-serine (0.1 mg/mL), and a blank solution, water, were also added. To each well, 200 µL of OPA reagent was added. OPA reagent was prepared by dissolving 1.01 g $NaHCO_3$, 0.8586 g $NaCO_3 \bullet 10\ H_2O$, 150 mg SDS, 130 mg DTT and 120 mg OPA in 150 mL MQ water. The prepared reagent solution was kept covered in aluminium foil as it is light-sensitive. After the reagent was added, the plates were read in a Tecan spectrophotometer (Männedorf, Switzerland) at 340 nm following one minute of shaking at 650 rpm. Replicates were averaged and the standard deviation was calculated.

5.3.6 Total phosphorous determination

Total phosphorous in the supernatants was determined using the malachite green/molybdate assay as developed from a Quantichrom phosphate assay kit and from previously published sources (Van Veldhoven and Mannaerts, 1987). Inorganic phosphate forms a coloured complex, detectable at 610 nm, with malachite green and molybdate. Samples were taken from the previously described acid extracted digesta (see **Section 5.3.3**). Initially, diets containing the tannin extracts at 10 and 20 mg were trialled without the acid extraction step. While the values for phosphorous content were lower than with the acid extraction, the relative percent phosphorous digestibility was unchanged. To collate all results using the same measurement, phosphorus digestibility (%) was used instead of total phosphorous (mg P/g feed).

Samples, not containing phytase, were prepared by diluting them 500 times in 0.5 M HCl while samples containing phytase were diluted 1500 times in 0.5 M HCl. To a 96 well-plate, 125 µL of each sample was added in triplicate. A standard curve of KH_2PO_4 (0, 2.5, 5, 10, 15 and 20 µM), prepared with MQ water and 0.5 M HCl, was also added in triplicate to the well-plate. The assay reagent was prepared by mixing 5.7 mL of 28 mM ammonium heptamolybdate in 2.77 M H_2SO_4 with 4.3 mL of 0.82 mM malachite green in 0.35% polyvinyl alcohol in MQ water. To each well, 50 µL of the assay reagent was added and the plate placed in a shaker for 10 seconds at 1000 rpm. The plate was then allowed to incubate at 25°C for 20 minutes. Following incubation, the plate was transferred to a Tecan spectrophotometer and absorbance was measured at 610 nm. The concentration of phosphate (µM) was determined from the standard curve using linear regression. This value was then converted to the mass of phosphorous in milligrams. Replicates were averaged and the standard deviation calculated.

The results presented in this chapter were converted to percent (%) phosphorous digestibility. This was done by comparing the total phosphorous in each diet with sorghum polyphenol extracts or tannin extracts to the appropriate control diet.

5.3.7 MALDI analysis of soluble protein and data processing

The previously obtained untreated digesta were thawed on ice prior to analysis. From the thawed samples, 100 µL of digesta was diluted with 100 µL of acetonitrile:water:trifluoroacetic acid (TFA) (50:49.9:0.1). The diluted sample mixture was mixed in a 1:1 ratio with the matrix chemical CHCA in the same solvent composition. From this final mixture, 1 µL was plated onto a 96-spot steel MALDI plate and allowed to dry on a heating block. MALDI was performed on a Waters Synapt G2 ToF mass spectrometer (Waters Corporation). The MassLynx data system (Water Corporation) provided instrument control, data acquisition and data processing.

The spectra obtained from MALDI analysis were processed as described in **Section 3.3.9**.

5.3.8 Statistical analysis

Statistical differences in the data were evaluated using two-way analysis of variance (ANOVA) and the mean values were compared using a Tukey post-hoc test. All statistical analyses were performed using GraphPad Prism 8 (GraphPad Software, Inc.; San Diego, CA, USA).

5.4 Results and discussion

The direct effects of sorghum polyphenol extracts and tannin extracts on exogenous feed phytase and protease activity were previously determined in simple, *in vitro* environments (see **Chapter** 4; Hodges et al., 2020). While these results were key in determining the direct inhibitory effects of the extracts on the exogenous feed enzymes, studies in a more complex environment were needed to determine the impacts of the extracts in an environment closer to reality. In this experimental chapter, sorghum polyphenol extracts and tannin extracts, previously characterised (see **Chapter** 3; Hodges et al., 2021), were introduced to an *in vitro* simulated model of poultry digestion including crop, gastric and intestinal phases. Measures of exogenous feed enzyme efficacy, as determined by measuring their substrates, were taken as indicators of any anti-nutritional effects from the added sorghum polyphenol extracts and tannin extracts. Further, a rapid metabolite profiling method was trialled for use in separating

different diet formulations. This kind of experimental tool could be very useful in the high-throughput screening of diets and compounds of interest in animal feed.

5.4.1 Effects of sorghum polyphenol extracts and tannin extracts on protein digestibility

To determine the effects of the different extracts on the efficiency of the protein digestibility, two measures of protein/nitrogen content were used: LECO analysis for protein/nitrogen content and the OPA assay to measure the degree of hydrolysis of soluble protein (**Figures 5.3 – 5.7**).

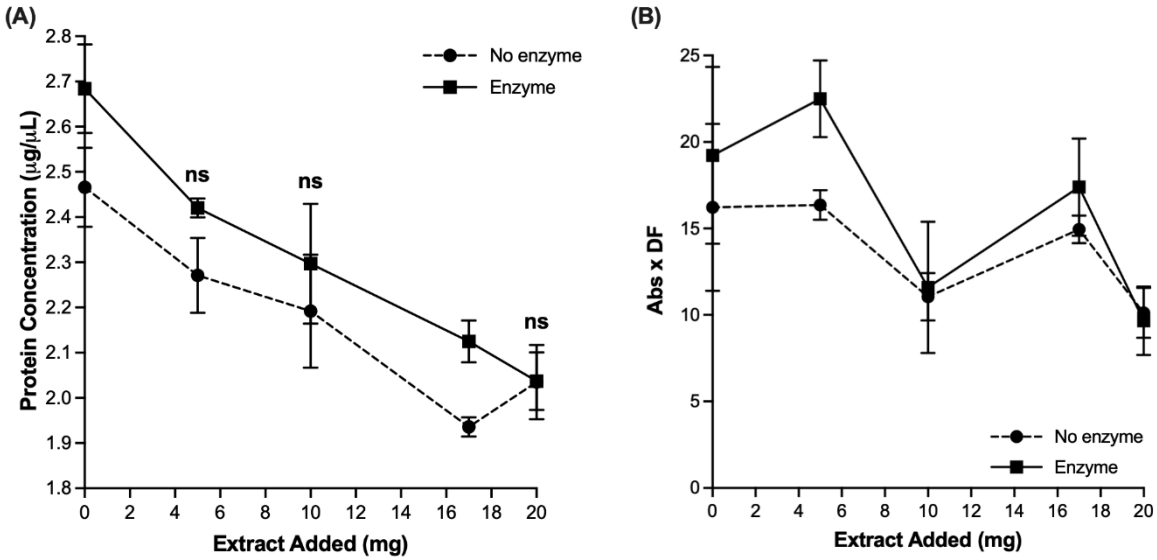

Figure 5.3 Measures of protein digestibility of digesta supernatant with grape seed tannin extract

(A) Protein concentration was determined, using LECO analysis, in the supernatant of the digesta with grape seed tannin extract included; diets without a label are statistically significant, $P < 0.05$; ns – no significant difference. Error bars represent ± 1 SD; n = 4 for extract trials, n = 12 for Enzyme – 0 mg, n = 11 for No enzyme – 0 mg. **(B)** OPA assay analysis of degree of protein hydrolysis; Abs – Absorbance, DF – dilution factor; there were no statistically significant differences between diets. Error bars represent ± 1 SD; n = 4 for extract trials, except 10 mg Enzyme, n = 12 for Enzyme – 0 mg, n = 16 for No enzyme – 0 mg.

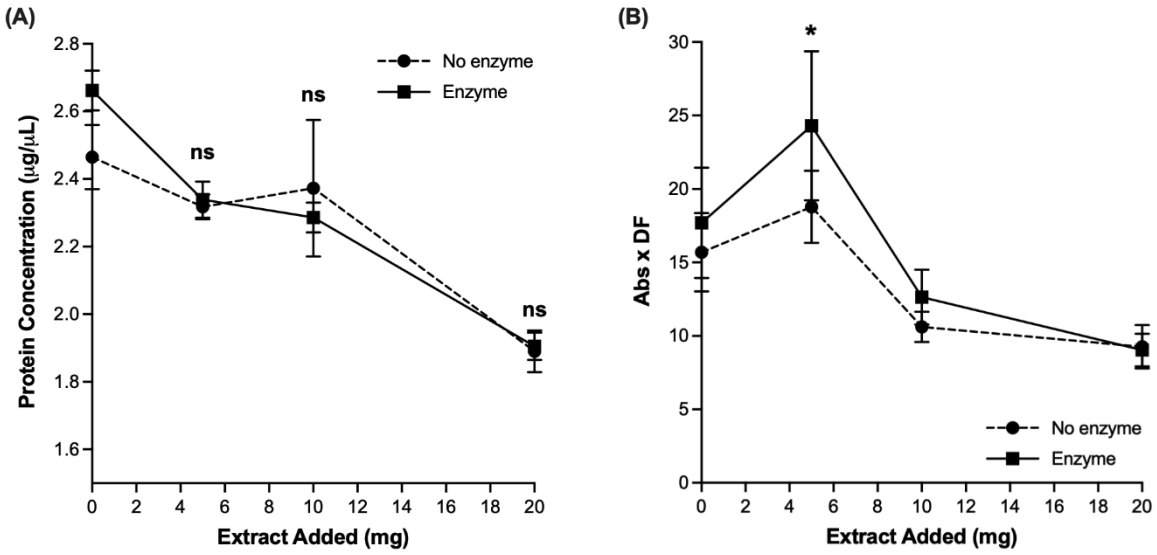

Figure 5.4 Measures of protein digestibility of digesta supernatant with quebracho tannin extract

A) Protein concentration was determined, using LECO analysis, in the supernatant of the digesta with quebracho tannin extract included; diets without a label are statistically significant, $P < 0.001$; ns – no significant difference. Error bars represent ± 1 SD; n = 4 for 5, 10, 20 mg, n = 8 for 0 mg. (**B)** OPA assay analysis of degree of protein hydrolysis; Abs – Absorbance, DF – dilution factor; * is $P < 0.05$, diets without a label are not significantly different. Error bars represent ± 1 SD; n = 4 for 5, 10, 20 mg, n = 8 for 0 mg.

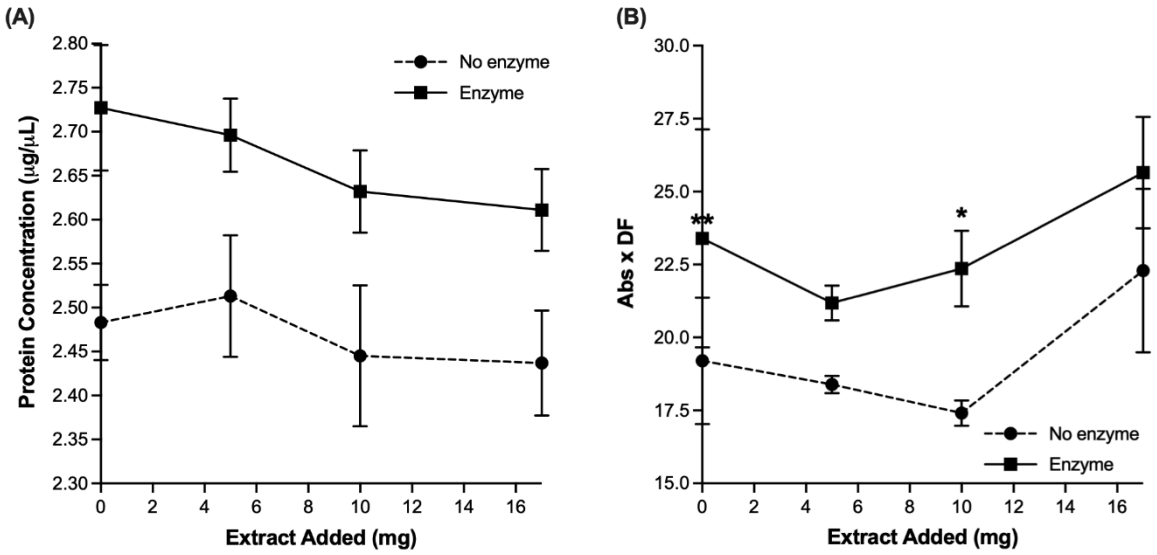

Figure 5.5 Measures of protein digestibility of digesta supernatant with MR-Buster sorghum polyphenol extract

(A) Protein concentration was determined, using LECO analysis, in the supernatant of the digesta with MR-Buster sorghum polyphenol extract included; diets without a label are statistically significant, $P < 0.001$. Error bars represent ± 1 SD; n = 4 for 5, 10 and 17 mg, n = 8 for 0 mg. (**B)** OPA assay analysis of degree of protein hydrolysis; Abs – Absorbance, DF – dilution factor; * is $P < 0.05$, ** is $P < 0.01$, diets without a label are not significantly different. Error bars represent ± 1 SD; n = 4 for 5, 10 and 17 mg, n = 8 for 0 mg.

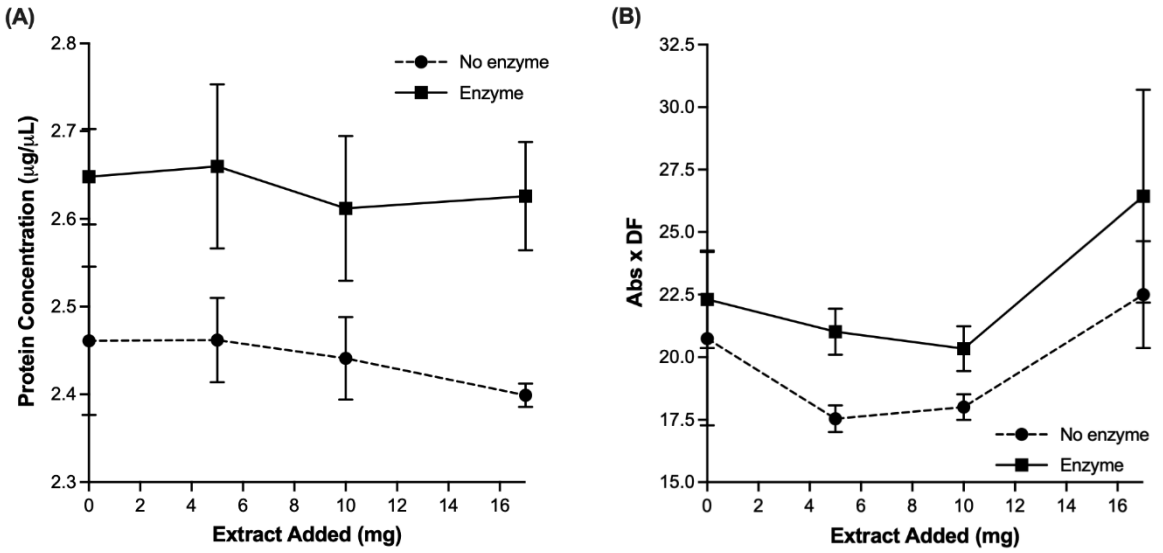

Figure 5.6 Measures of protein digestibility of digesta supernatant with Cracka sorghum polyphenol extract

(A) Protein concentration was determined, using LECO analysis, in the supernatant of the digesta with Cracka sorghum polyphenol extract included; diets without a label are statistically significant, $P < 0.01$. Error bars represent ± 1 SD; n = 4 for 5, 10, 17 mg, n = 7 for Enzyme – 0 mg, n = 8 for No enzyme – 0 mg. (**B)** OPA assay analysis of degree of protein hydrolysis; Abs – Absorbance, DF – dilution factor; diets without a label are not significantly different. Error bars represent ± 1 SD; n = 4 for 5, 10, 17 mg, n = 8 for 0 mg.

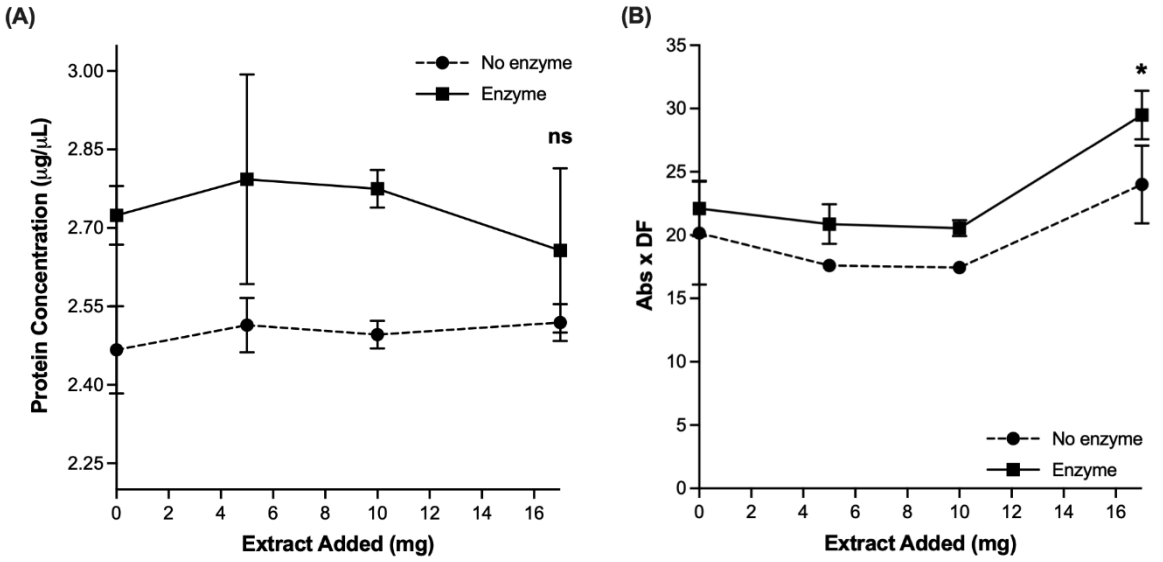

Figure 5.7 Measures of protein digestibility of digesta supernatant with Liberty sorghum polyphenol extract

(A) Protein concentration was determined, using LECO analysis, in the supernatant of the digesta with Liberty sorghum polyphenol extract included; diets without a label are statistically significant, $P < 0.001$. Error bars represent ± 1 SD; n = 4 for 5, 10, 17 mg, n = 8 for 0 mg. (**B)** OPA assay analysis of degree of protein hydrolysis; Abs – Absorbance, DF – dilution factor; * is $P < 0.05$, diets without a label are not significantly different. Error bars represent ± 1 SD; n = 4 for 5, 10, 17 mg, n = 8 for 0 mg.

Overall, the inclusion of both exogenous feed enzymes improved protein concentration by approximately 7 – 8% while the degree of hydrolysis of soluble protein improved 24% on average. These improvements in protein digestibility correlated with the industry reported gains of 3 – 8% protein digestibility with inclusion of a protease (Glitsø et al., 2012). It is important to note that the improvement in these measures of protein were brought about by the inclusion of both the protease and the phytase and not just the protease. However, the control diets, apart from **Figure 5.5B**, were not significantly different from each other regarding protein hydrolysis indicating no beneficial effects with the inclusion of exogenous feed enzymes. This result is most likely due to the nature of the OPA assay.

The inclusion of grape seed tannin extract reduced protein concentration in a dose-dependent manner (**Figure 5.3A**). This effect was observed in diets with and without exogenous feed enzymes. Without grape seed tannin extract, diets had approximately 2.7 ug/uL protein whereas at the highest level of grape seed tannin extract inclusion levels dropped to almost 2.0 ug/uL. At inclusion levels of 10 and 20 mg, there was no significant difference between diets with and without exogenous feed enzymes. This result indicated that the positive increases in protein concentration brought about by using the exogenous feed enzymes was eliminated. The inclusion of grape seed extract lowered the degree of hydrolysis of soluble protein in a roughly dose-dependent manner by up to 38% without feed enzymes and 50% with exogenous feed enzymes (**Figure 5.3B**). There were no significant differences between diets with and without exogenous feed enzymes indicating a role for grape seed tannins in disrupting protein hydrolysis.

In diets containing quebracho tannin extract, the positive impact of the exogenous feed enzymes was altered in a more significant manner than with grape seed tannin extract (**Figure 5.4**). There were no significant differences in protein concentration between diets with and without exogenous feed enzymes at all inclusion levels of quebracho tannin extract. Like grape seed tannin extract, all of the positive effects gained, with regard to protein concentration, were eliminated. The degree of hydrolysis of soluble protein also reduced in a roughly dose-dependent manner by up to 42% without exogenous feed enzymes and 49% with exogenous feed enzymes (**Figure 5.4B**). While the two diets containing 5 mg of quebracho tannin extract were significantly different, the remaining two were not indicating a role for quebracho tannins in the disruption of protein hydrolysis.

The inclusion of the three sorghum polyphenol extracts did not significantly affect protein concentration at any level of inclusion with reductions reaching a maximum of 4% without exogenous feed enzymes and 3% with exogenous feed enzymes included (**Figures 5.5A – 5.7A**). Protein concentration did decrease slightly in response to increased levels of sorghum polyphenol extract but only with the two red sorghum varieties, MR-Buster and Cracka. Liberty, the white sorghum variety, increased protein concentration. This indicated that Liberty sorghum polyphenol extract could contain high levels of small proteins and/or peptides. The sorghum polyphenol extracts had a small effect on the degree of hydrolysis of soluble protein measured in the diets. MR-Buster, Cracka and Liberty sorghum polyphenol extracts reduced hydrolysis by up to 10%, 15% and 14%, respectively, without exogenous feed enzymes and 10%, 9% and 7%, respectively, with exogenous feed enzymes added (**Figures 5.5B – 5.7B**). There did not appear to be a trend to this effect as at the highest dose, 17 mg, protein hydrolysis increased significantly.

The results above indicated that the negative effects associated with the two tannin extracts and protein digestibility were most likely caused by a mixture of interactions with both endogenous proteins/enzymes and the exogenous feed enzymes, phytase and protease. Using **Figure 5.3A** as a model, both diets with and without the exogenous feed enzymes had protein concentration decrease with increased grape seed tannin extract inclusion. This shared decrease in measured protein concentration demonstrated the effect of the tannins on endogenous sources of protein as well as those improved upon with the use of the exogenous feed enzymes. The two sets of data were parallel and decreased in a similar manner. However, this changed at the highest extract inclusion level of 20 mg. At this value, the protein concentration of both diets was approximately the same. The change at this point indicated that the tannins were influencing protein derived from the exogenous feed enzymes. This kind of direct interference with the exogenous feed enzymes was previously observed *in vitro* (see **Section 4.4.3**). In the previous chapter, both the exogenous feed protease and phytase were found to be significantly inhibited by both tannin extracts. While the impact on the exogenous feed protease could be greater considering the nature of its direct substrate, there might be negative effects on phytase's potential extra-phosphoric effects on protein and amino acid digestibility.

The inclusion of this kind of tannin extract is not directly comparable to a realistic monogastric feed scenario as the tannins found in grape seed are not present in appreciable quantities in modern feed-relevant sorghum grain. However, the grape seed tannin extract provided a useful

context as the compounds found within this extract were similar to those previously identified in high-tannin varieties of sorghum (Awika et al., 2003; Gu et al., 2003; Gu et al., 2004). These compounds include polymerised condensed tannins made up of (epi)catechin monomers. Traditional tannins, like those in the two tannin extracts, are known to bind proteins and form cross-links resulting in insoluble aggregates which may be resistant to hydrolysis. While these results provided useful insight into the negative impacts of certain tannin types, the use of quebracho tannin extract is not relatable to a normal monogastric feed environment. As quebracho extract comes from wood harvested in South America, it would not be found in the same form in any feed grain or supplement used (Venter et al., 2012). However, quebracho extracts have been utilised and tested in ruminant diets to improve various performance parameters (Díaz Carrasco et al., 2017; Aguerre et al., 2020).

Grape seed tannin extracts have been found to significantly reduce endogenous protease activity. Zhong et al. (2018) tested the effects of low (2-4 monomeric units) and high polymer (> 10 monomeric units) grape seed tannins in mice diets on endogenous enzyme activity and measures of nutrient digestibility. The activity of both trypsin and pepsin (included in the current experimental chapter) was significantly reduced by high polymer tannins but not by low polymer compounds. Activity was reduced with lower molecular weight compounds but not significantly. This was also matched with a decrease in apparent protein digestibility.

Similarly, sorghum grain has been shown to reduce endogenous protease activity. Nyamambi et al. (2000) found both low- and high-tannin sorghum varieties to inhibit trypsin. At an enzyme:polyphenol ratio of 1:1, trypsin was inhibited by the high-tannin varieties up to 50% *in vitro* and 35% in chickens. They noted a decrease in *in vivo* inhibition similar to what was found in the current work. Low-tannin sorghum grains affected enzyme activity to a lesser degree. Al-Mamary et al. (2001) found similar results in rabbits with trypsin inhibited 22 and 56% when fed low- and high-tannin sorghum, respectively. In pigs, Lizardo et al. (1995) found trypsin activity to reduce 10 – 25% with inclusion of low- and high-tannin sorghum in the diet. Interestingly, they found that serine protease activity increased. Mariscal-Landín et al. (2004) found that the addition of sorghum grain to pig diets with increasing tannin levels had no effect on endogenous trypsin and chymotrypsin activity or pancreas weight and protein content. Similar to Lizardo et al. (1995), this group found that high tannin levels actually increased duodenal trypsin activity by approximately 7%. *In vivo*, this effect has been suggested to be caused by stimulation of pancreatic enzyme secretion (Griffiths and Moseley,

1980). The improvements in protein concentration and protein hydrolysis in the current chapter are most likely caused by the sorghum polyphenol extracts themselves (**Appendix Figure C.1**). Dehulled high-tannin sorghum grain was found to improve protein digestibility as measured after digestion with pepsin, trypsin and chymotrypsin (Chibber et al., 1980). As more of the hull was removed from the grain, the tannin content was reduced. This reduction in tannin content resulted in improved solubilisation of sorghum protein.

The sorghum polyphenol extracts were previously found to inhibit the exogenous feed protease up to 20% *in vitro* which converted to minimal reductions when put into commercial settings (see **Chapter 4.4.3, Figure 4.16**). Here, in an *in vitro* simulated poultry digestion model, the effects, as measured by protein digestibility were greatly reduced, eliminated or even improved. Similar reductions in anti-nutritional effects were also reported by Blytt et al. (1988) and are most likely caused by the more realistic environment providing several potential proteinaceous targets for the polyphenols and tannins to bind to prior to interfering with enzyme activity. Griffiths and Moseley (1980) found that trypsin activity in rats was significantly depressed with the inclusion of field bean varieties with high tannin content (0.4% of diet). The resulting use of PVP to complex tannins increased trypsin activity indicating a clear role for polyphenols and tannins in reducing enzyme activity and protein digestion.

The inclusion of exogenous feed enzymes has been shown to be less impactful in diets containing sorghum. A cocktail of exogenous enzymes was included into both wheat- and sorghum-based broiler diets (Selle et al., 2010b). The broilers fed the sorghum diets including exogenous feed enzymes had no significant interactions regarding nutrient utilisation whereas the wheat diets had improved nutrient digestibility and growth performance. These authors focussed on the presence of sorghum's kafirin proteins as possible reasons for the enzyme underperformance.

Protein and starch characteristics are often thought to play a role in the lower nutrient digestibility of sorghum. As discussed in **Section 1.3**, the primary storage proteins in sorghum grain are kafirin and glutelin. While kafirin is known to have high levels of disulphide bonding, non-kafirin proteins, like glutelin, have also been found to have these deleterious bonds. High levels of disulphide bonds can lower protein digestibility (Wong et al., 2009). A diverse range of sorghum varieties was subject to *in vitro* pepsin digestion and *in vivo* feeding to broiler cockerels to determine the effects of tannin content on amino acid and protein digestibility

(Elkin et al., 1996). While they determined that tannin content (here specifically catechin equivalents) had an inverse relationship with amino acid digestibility, sorghum grains with similar tannin contents were observed to differ in their amino acid digestibility's and protein digestibility because of the *in vitro* digestion. This group suggested that other endogenous grain components, particularly kafirin proteins, could contribute to sorghum's nutritional variability.

The reduced protein digestibility and lower nutrient uptake commonly observed in animals fed sorghum might be indirectly controlled by polyphenol content. Kaufman et al. (2013) found that the tannin content of different sorghum varieties negatively correlated with both protein digestibility and kafirin availability. Tannins and other polyphenols have been well-established to bind selectively to proteins high in proline (Hagerman and Butler, 1981). This binding may also allow the large tannins in high-tannin sorghum varieties to escape initial digestion relatively unscathed as kafirin-bound tannins have been found to survive simulated digestion. The remaining tannins would then be free to inhibit digestive enzymes rather than bind to their substrates earlier on (Links et al., 2016). In a comparison between Buster and Liberty sorghum varieties, Buster was found to have not only a higher protein content, 11.5%, than Liberty, 9.0%, but to be higher overall in kafirin content (Cadogan and Finn, 2010). These differences in protein content might affect the overall availability of tannin and polyphenol content.

5.4.2 Effects of sorghum polyphenol extracts and tannin extracts on phosphorous digestibility

The effects of the sorghum polyphenol extracts and tannin extracts on phosphorus digestibility of the simulated digesta were determined using the malachite assay (**Figures 5.8 – 5.1**).

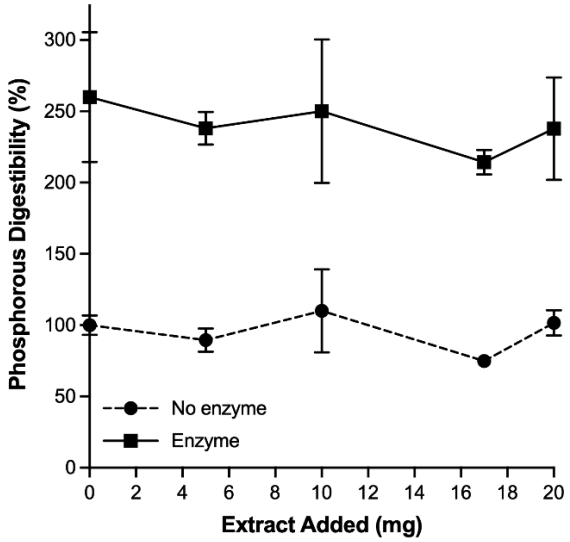

Figure 5.8 Phosphorous digestibility of simulated digesta with grape seed tannin extract
Phosphorous digestibility was determined, using the malachite assay, in the digesta with grape seed tannin extracts included with and without exogenous feed enzymes. Diets with exogenous feed enzymes included were significantly different from those without ($P < 0.0001$). Error bars represent ± 1 SD, n = 4 for extract trials, n = 12 for 0 mg.

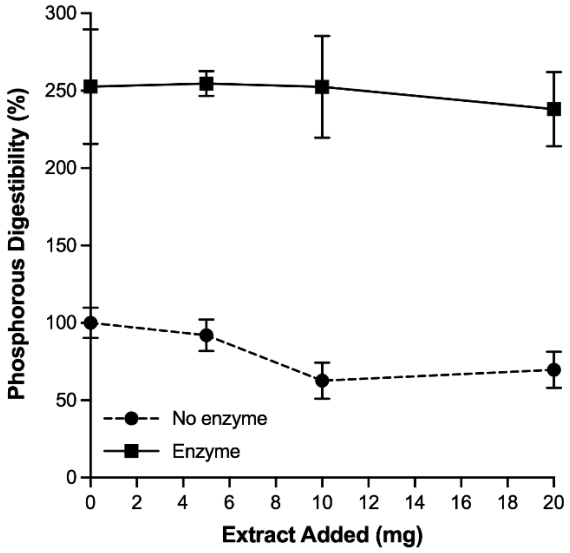

Figure 5.9 Phosphorous digestibility of simulated digesta with quebracho tannin extract
Phosphorous digestibility was determined, using the malachite assay, in the digesta with quebracho tannin extracts included with and without exogenous feed enzymes. Diets with exogenous feed enzymes included were significantly different from those without ($P < 0.0001$). Error bars represent ± 1 SD, n = 4 for extract trials, n = 8 for 0 mg.

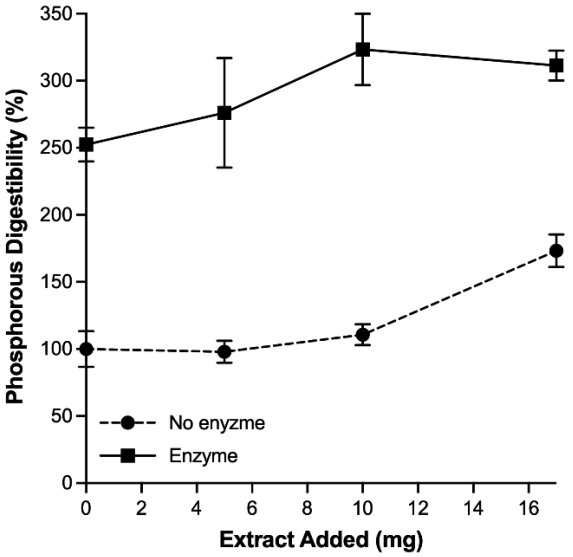

Figure 5.10 Phosphorous digestibility of simulated digesta with MR-Buster sorghum polyphenol extract

Phosphorous digestibility was determined, using the malachite assay, in the digesta with MR-Buster sorghum polyphenol extract included with and without exogenous feed enzymes. Diets with exogenous feed enzymes included were significantly different from those without ($P < 0.0001$). Error bars represent ± 1 SD, n = 4 for extract trials, n = 8 for 0 mg.

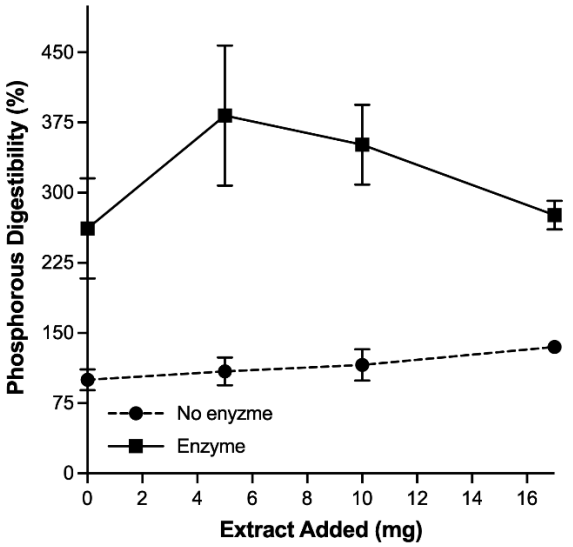

Figure 5.11 Phosphorous digestibility of simulated digesta with Cracka sorghum polyphenol extract

Phosphorous digestibility was determined, using the malachite assay, in the digesta with Cracka sorghum polyphenol extract included with and without exogenous feed enzymes. Diets with exogenous feed enzymes included were significantly different from those without ($P < 0.001$). Error bars represent ± 1 SD, n = 4 for extract trials, n = 8 for 0 mg.

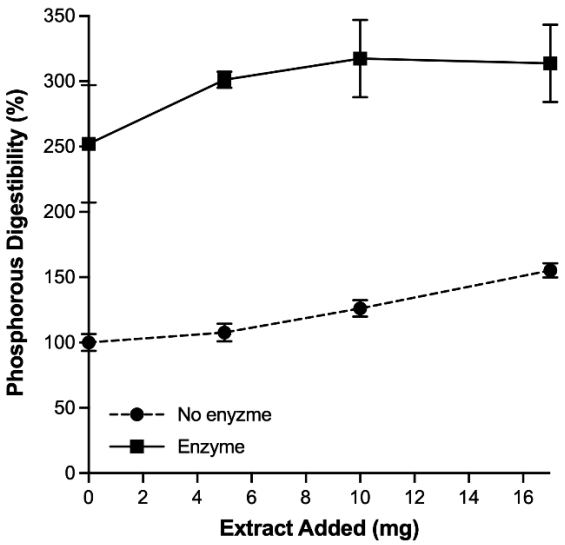

Figure 5.12 Phosphorous digestibility of simulated digesta with Liberty sorghum polyphenol extract
Phosphorous digestibility was determined, using the malachite assay, in the digesta with Liberty sorghum polyphenol extracts included with and without exogenous feed enzymes. Diets with exogenous feed enzymes included were significantly different from those without ($P < 0.0001$). Error bars represent ± 1 SD, n = 4 for extract trials, n = 8 for 0 mg.

The inclusion of both exogenous feed enzymes was demonstrated to be beneficial for the release of phosphorous from phytate as phosphorous digestibility increased by 162%, on average, compared to trials without the exogenous feed enzymes included. In diets containing grape seed and quebracho tannin extracts, phosphorous digestibility remained largely unchanged at any level of extract inclusion (**Figure 5.11, 5.12**). While there was a slight dose-response as the amount of tannin extract increased, this did not result in significant differences to the diets without tannin extract included. Similarly, the addition of the sorghum polyphenol extracts did not significantly lower phosphorous digestibility in trials both with and without exogenous feed enzymes (**Figures 5.13 – 5.15**). In fact, phosphorous digestibility slightly increased as more extract was added indicating that the sorghum polyphenol extracts themselves contributed to the total phosphorous in the digesta samples.

Total phosphorous of the five extracts alone were measured (**Appendix Figure C.2**) and indicated that the sorghum polyphenol extracts most likely contributed to the total phosphorous contents of digesta analysed. MR-Buster sorghum polyphenol extract was found to contain the highest concentration followed by Liberty and then Cracka polyphenol extracts. However, concentration did not seem to correlate directly with total phosphorous released in the trials as Cracka polyphenol extract inclusion had the highest value. The sorghum grain was soaked for

24 hours prior to grinding and extraction. It is possible that the soaking period may have activated endogenous phytases in the grain or increased soluble phytate thereby increasing phosphorous. However, Afify et al. (2011) found that soaked milled sorghum grain had no significant increase in phytase activity after being soaked for 20 hours. Kruger et al. (2014) found that soaked wholegrain sorghum had a lower phytate content than if not soaked, between 12 – 19% less. Afify et al. (2011) found that ground, sorghum grain was found to have a higher reduction in phytate content between 23 – 32%. Additionally, the crude nature of the extracts might mean that phospho-proteins and other such related compounds were present in the mixtures.

Salobir et al. (2005) tested the effects of added chestnut tannins on phytase activity in an *in vivo* feeding study with pigs. This kind of extract is very similar to the tannin extracts used throughout this thesis. They measured the effects of different doses of tannin on measures of mineral, protein and phosphorous digestibility. Phytase without tannin was shown to significantly increase phosphorous digestibility. In addition to improving phosphorous digestibility, protein/nitrogen utilisation was also increased with the addition of phytase, thus illustrating the extra-phosphoric effects this exogenous feed enzyme can have. With the addition of tannins to the diet, protein/nitrogen utilisation was most significantly affected and in a dose-dependent manner. Tannins at a high dose of 4.5 g/kg effectively eliminated the extra-phosphoric effects of phytase. Similar to what was found in the current work, added tannins did not have significant effects on phosphorous or mineral utilisation and were only able to reduce these measures to that of the control diet with no added phytase at the highest levels of added tannins. This group concluded by indicating that exogenous feed enzymes were effectively safe from inhibition from dietary tannins.

While not an exogenous feed phytase, intestinal alkaline phosphatase was also found to be unaffected by increasing levels of sorghum in broiler diets (Torres et al., 2013). Sorghum and quebracho tannins were also found to have minimal effect on alkaline phosphatase and 5'-nucleotide phosphodiesterase during *in vivo* simulated digestion (Blytt et al., 1988). The effects this group found closely mimic what was observed in this thesis. In basic *in vitro* inhibition environments, both extracts strongly inhibited the enzymes but these effects were lost when translated to complex, more realistic situations.

5.4.3 MALDI-ToF-MS metabolite profile analysis of simulated digesta

MALDI-ToF-MS and multivariate analysis were performed on the soluble fractions retained from the simulated digestion experiments. A rapid analytical method was tested to determine whether direct ionisation mass spectrometry method, i.e., MALDI, could be used to separate different diets and identify relationships among them. Like the approach taken in **Chapter 3**, principal component analysis (PCA) was performed on the MALDI spectra obtained from each digestion condition to determine if clear groupings and separation were present when viewed through the filter of enzyme/no enzyme (presence of exogenous feed enzymes or just endogenous enzymes). The analysis of the digestion conditions began with the broadest categories of including all digestion conditions (**Figure 5.13**).

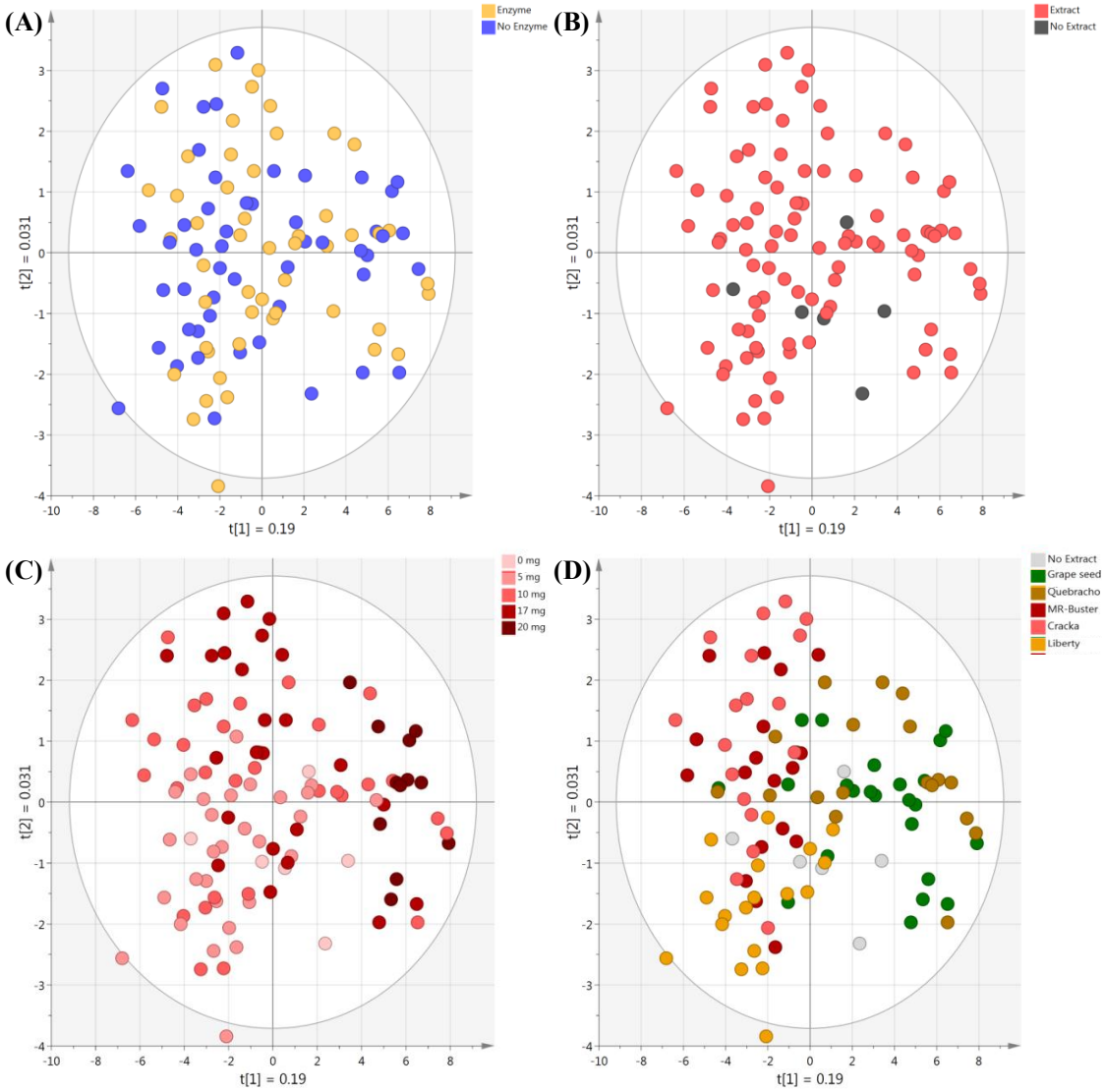

Figure 5.13 Principal component analysis (PCA) scores plots for MALDI spectra from all digestion conditions

PCA was performed on the MALDI spectra (50 – 1500 Da) to determine relationships and variance among the digestion conditions. **A** – Enzyme/No Enzyme (exogenous feed enzyme

presence/absence); **B** – Extract/No Extract; **C** – Extract inclusion level; **D** – Extract type. The ellipse represents a 95% CI. t(1) and t(2) represent principal components 1 and 2, respectively.

The first two principal components explained 22.1% of the variation among all digestion conditions. These initial analyses performed on the MALDI spectra showed little in the way of any clear separation and/or grouping among the different filters applied. This was particularly evident in the analyses of presence/absence of exogenous feed enzymes, presence/absence of sorghum polyphenol extracts/tannin extracts and extract type (**Figure 5.13A, B, D**). Some trends were observed in the plot of extract inclusion (**Figure 5.13C**). There was a general tendency observed as the lowest extract inclusion levels (0 and 5 mg) were primarily grouped in the lower left quadrant. Moving from the lower left to upper right quadrants, the higher extract inclusion levels (17 and 20 mg) were more abundant. These trends, while subtle, indicated a possible role for extract inclusion level in affecting the metabolite profile of the soluble fractions of the simulated digesta.

Moving towards more specific interactions, all digestion conditions containing exogenous feed enzymes were analysed for potential interactions and groupings (**Figure 5.14**). This analysis was broken down into evaluating conditions with or without sorghum polyphenol extracts/ tannin extracts and conditions based on the extract type included.

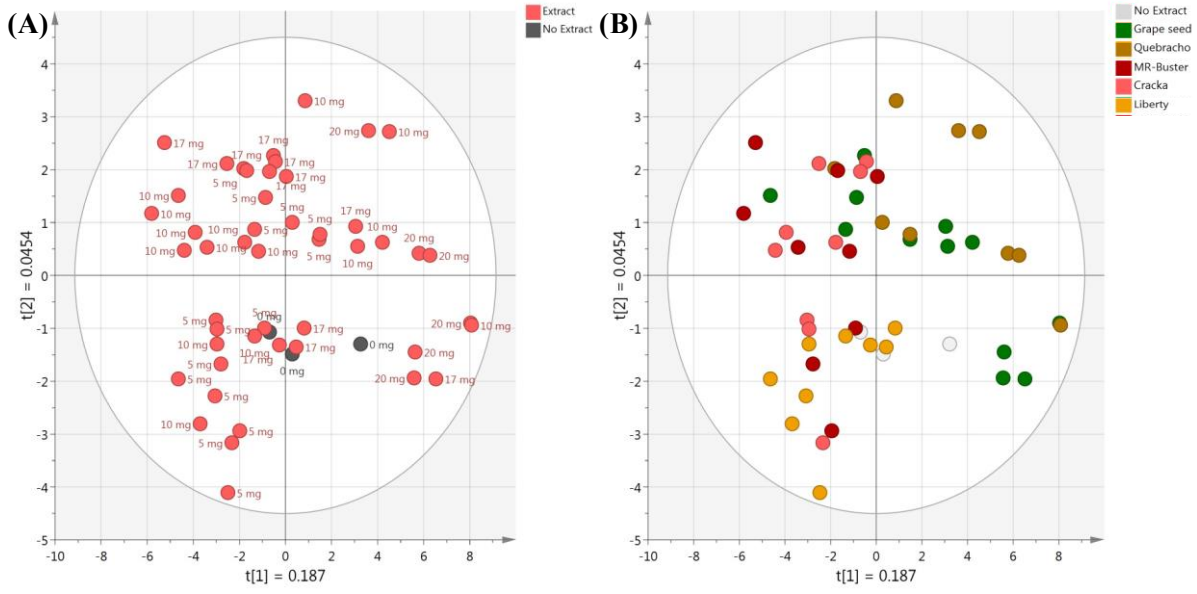

Figure 5.14 Principal component analysis (PCA) scores plots for MALDI spectra from all digestion conditions containing exogenous feed enzymes
PCA was performed on the MALDI spectra (50 – 1500 Da) to determine relationships and variance among the digestion conditions containing exogenous feed enzymes. **A** – Extract inclusion level; **B** – Extract type. The ellipse represents a 95% CI. t(1) and t(2) represent principal components 1 and 2, respectively.

The first two principal components explained 23.2% of the variation among the digestion conditions containing exogenous feed enzymes. No clear trends or separations were observed in the plot filtering based on presence of added sorghum polyphenol extract/tannin extract (**Figure 5.14A**). As the samples without any extract were not separated from the ones containing extracts, this result indicated that the presence of sorghum polyphenol extracts and/or tannin extracts might have a negative effect on the exogenous feed enzymes during digestion, especially at higher concentration levels. If the extracts had no effect on digestion, it would be expected that there would be clear separation and grouping of the samples. Similar to **Figure 5.13D**, the filter of extract type did show subtle grouping along the lines of tannin extracts versus sorghum polyphenol extracts (**Figure 5.14B**).

Digestion conditions containing only endogenous enzymes were next analysed for potential interactions and groupings (**Figure 5.15**).

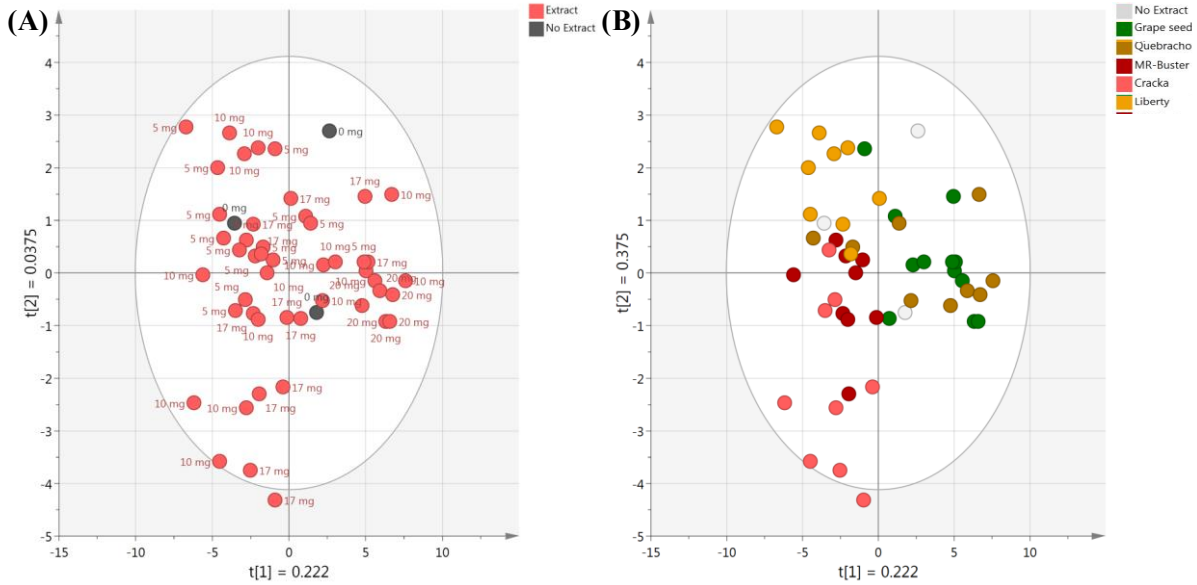

Figure 5.15 Principal component analysis (PCA) scores plots for MALDI spectra from all digestion conditions containing only endogenous enzymes
PCA was performed on the MALDI spectra (50 – 1500 Da) to determine relationships and variance among the digestion conditions containing only endogenous enzymes. **A** – Extract inclusion level; **B** – Extract type. The ellipse represents a 95% CI. t(1) and t(2) represent principal components 1 and 2, respectively.

The first two principal components explained 26.0% of the variation among all digestion conditions containing only endogenous enzymes. The trends observed were very similar to those of the conditions containing the exogenous feed enzymes alongside the endogenous

enzymes (**Figure 5.14**). However, the separation between sorghum polyphenol extracts and tannin extracts in diets containing only endogenous enzymes was slightly clearer.

These initial analyses of all the digestion conditions under very broad filters indicated that overall all of the samples were similar regarding their metabolite profiles as produced by MALDI-ToF-MS. The lack of grouping/separation between samples with and without tannin or sorghum polyphenol extract may indicate a negative effect of the extracts on digestion.

The control and blank diets, each containing the standard poultry diet of maize:SBM (70:30) and endogenous digestive enzymes were analysed alone. The control samples had both the exogenous feed protease and phytase included whereas the blank samples only had endogenous enzymes. These samples were included to determine the basal effects of both normal digestion and supplemented digestion without the inclusion of any tannin extract or sorghum polyphenol extract (**Figure 5.16**).

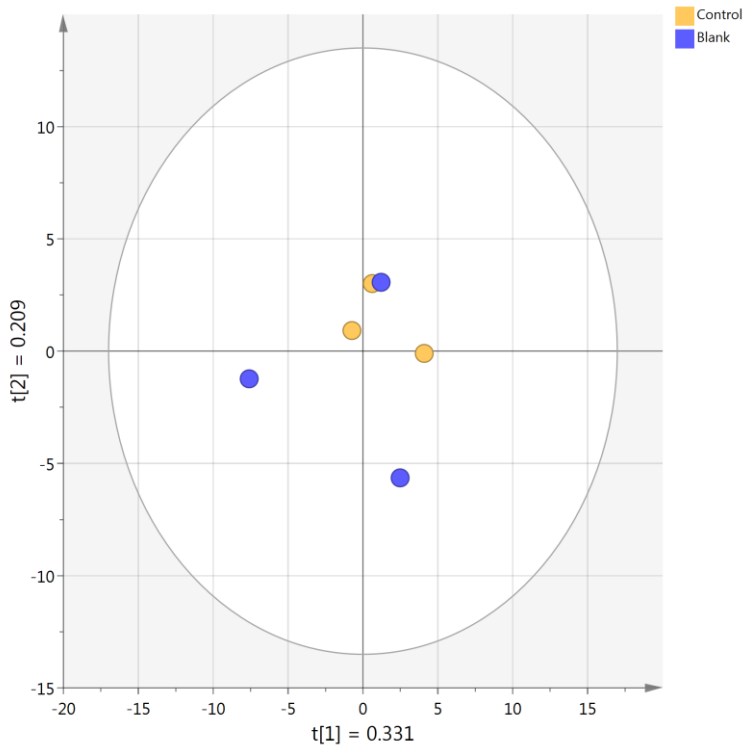

Figure 5.16 Principal component analysis (PCA) scores plots for MALDI spectra without tannin/sorghum polyphenol extracts
PCA was performed on the MALDI spectra (50 – 1500 Da) to determine relationships and variance among the digestion conditions. The ellipse represents a 95% CI. t(1) and t(2) represent principal components 1 and 2, respectively.

The first two principal components explained 54.0% of the variation among all digestion conditions. While the samples containing the two exogenous feed enzymes (Control) were closely grouped, there was some overlap with one samples containing only endogenous enzymes (Blank). This result indicated that, regarding metabolite profile, there was no significant difference between these two diets. The two exogenous feed enzymes were previously shown to significantly enhance protein concentration, protein hydrolysis and total phosphorous. The results here indicate that this effect is not reciprocated with respect to the metabolite profiles as obtained by MALDI-ToF-MS. However, more testing and sample numbers are needed to fully understand the results here.

More specific filters were then applied to the data and only digestion conditions containing tannin extracts or no extract were analysed (**Figure 5.17 – 5.19**).

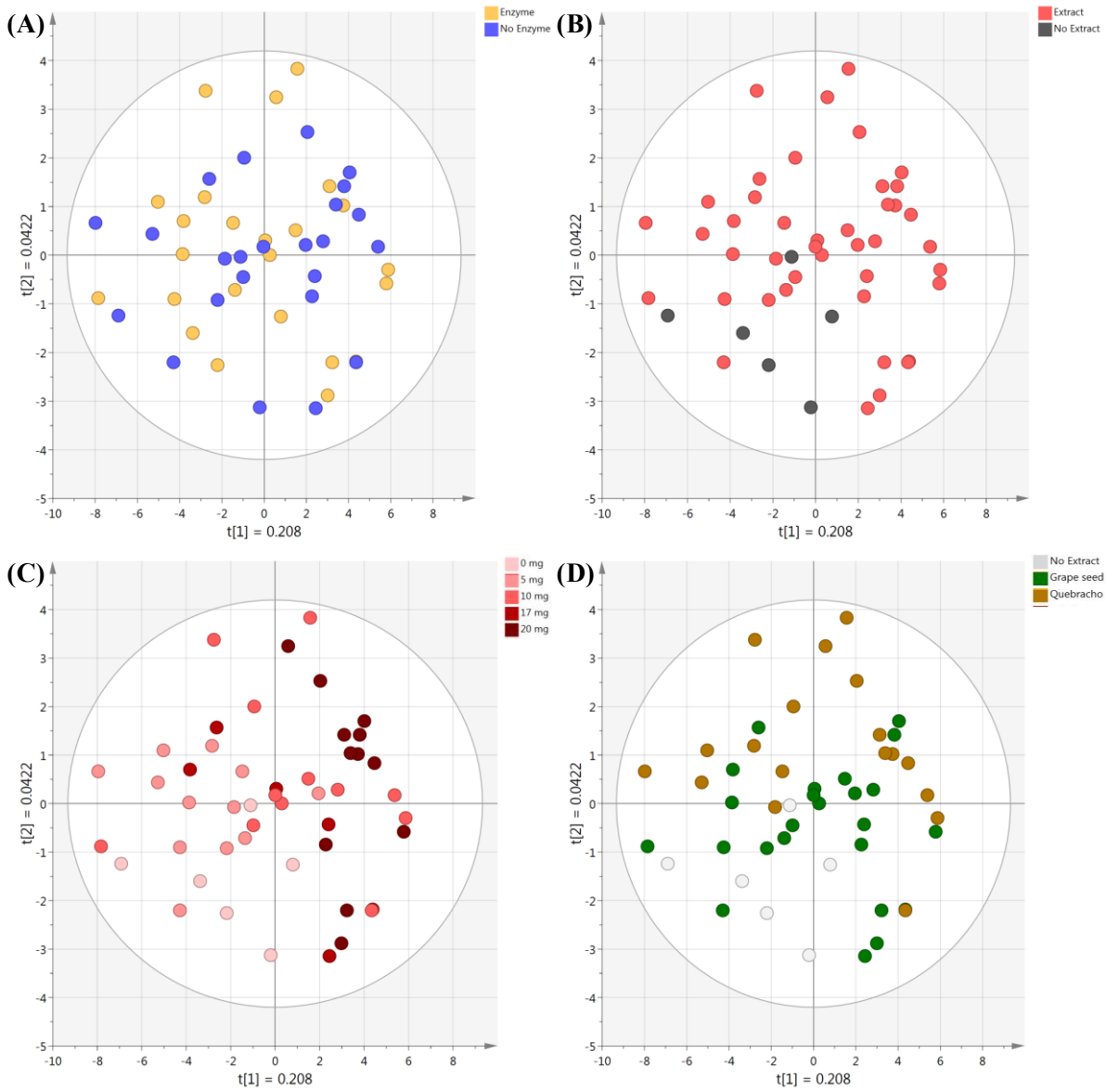

Figure 5.17 Principal component analysis (PCA) scores plots for MALDI spectra from digestion conditions containing tannin extract or no extract

PCA was performed on the MALDI spectra (50 – 1500 Da) to determine relationships and variance among the digestion conditions containing tannin extract or no extract. **A** – Enzyme/No Enzyme (exogenous feed enzyme presence/absence); **B** – Extract/No Extract; **C** – Extract inclusion level; **D** – Extract type. The ellipse represents a 95% CI. t(1) and t(2) represent principal components 1 and 2, respectively.

The first two principal components explained 25.0% of the variation among digestion conditions with tannin extracts or no extract. Among the four plots created, only the plot filtering for extract inclusion level appeared to have some subtle grouping (**Figure 5.17C**). This pattern was like that observed in **Figure 5.13C** describing the effect of extract inclusion level across all digestion condition.

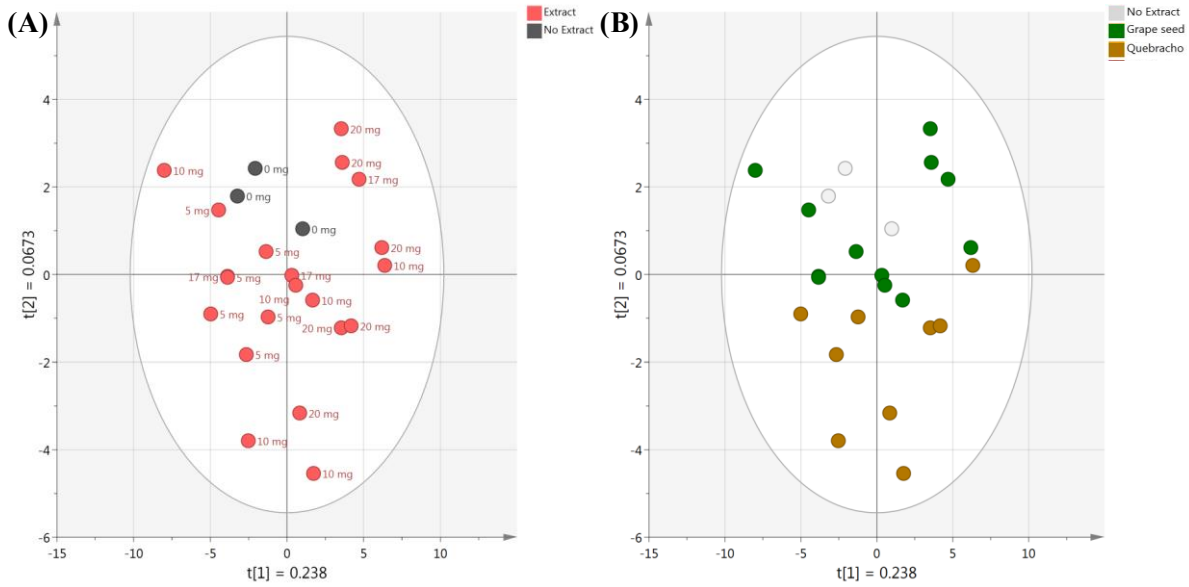

Figure 5.18 Principal component analysis (PCA) scores plots for MALDI spectra from digestion conditions containing tannin extract or no extract with exogenous feed enzymes
PCA was performed on the MALDI spectra (50 – 1500 Da) to determine relationships and variance among the digestion conditions. **A** – Extract inclusion level; **B** – Extract type. The ellipse represents a 95% CI. t(1) and t(2) represent principal components 1 and 2, respectively.

The first two principal components explained 30.5% of the variation among the conditions analysed. Between the two PCA plots, the one filtering extract type was the only one to indicate relatively clear separation. While the no extract samples were not discriminated clearly from those containing grape seed tannin extract, all the samples containing quebracho tannin extract were clearly separated from the other two conditions. This result indicated that the inclusion of quebracho tannin extract did compromise digestion in the presence of exogenous feed enzymes, as represented by the metabolite fingerprint created through MALDI-ToF-MS.

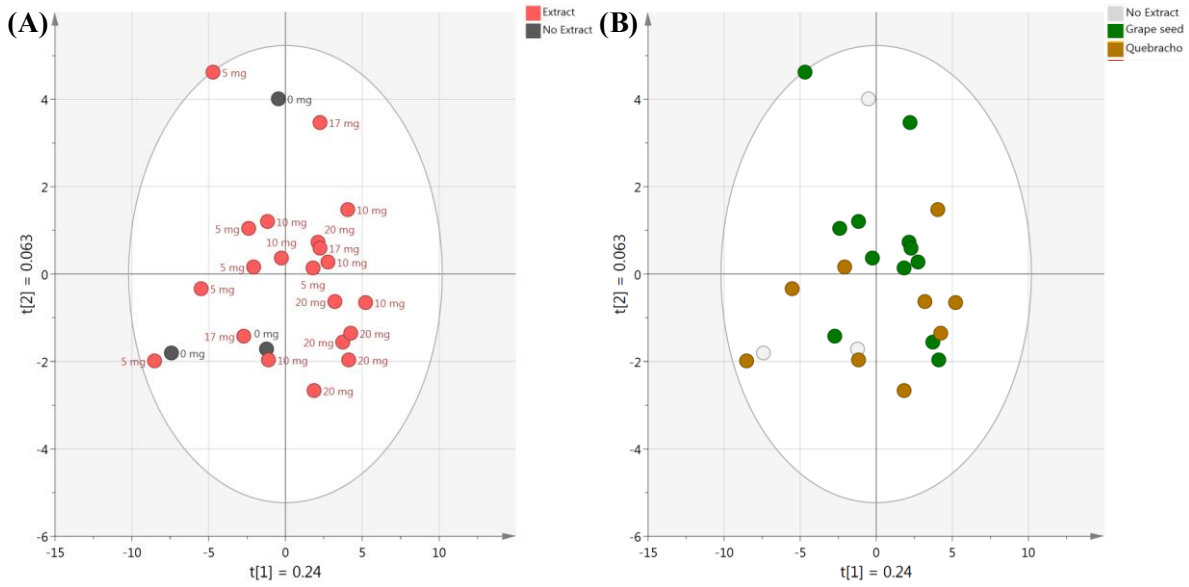

Figure 5.19 Principal component analysis (PCA) scores plots for MALDI spectra from digestion conditions containing tannin extract or no extract with only endogenous enzymes

PCA was performed on the MALDI spectra (50 – 1500 Da) to determine relationships and variance among the digestion conditions. **A** – Extract inclusion level; **B** – Extract type. The ellipse represents a 95% CI. t(1) and t(2) represent principal components 1 and 2, respectively.

The first two principal components explained 30.3% of the variation among the samples analysed. No clear trends or separations were identified in these plots which indicated no difference in digestion and thus the tannin extracts did not compromise normal digestion with endogenous enzymes.

The same analyses were conducted on samples containing sorghum polyphenol extracts or no extract (**Figures 5.20 – 5.22**).

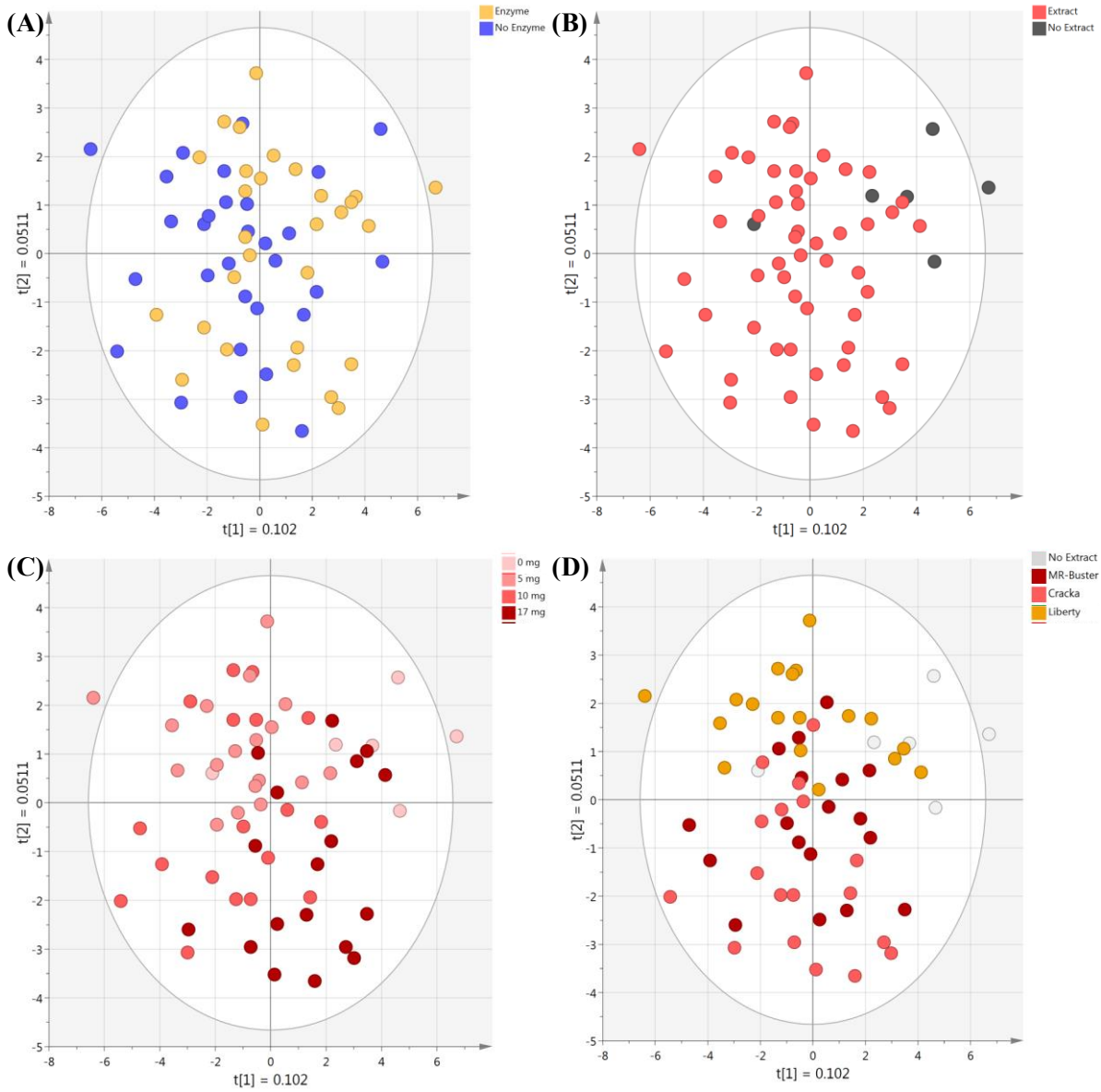

Figure 5.20 Principal component analysis (PCA) scores plots for MALDI spectra from digestion conditions containing sorghum polyphenol extracts/no extract
PCA was performed on the MALDI spectra (50 – 1500 Da) to determine relationships and variance among the digestion conditions. **A** – Enzyme/No Enzyme (exogenous feed enzyme presence/absence); **B** – Extract/No Extract; **C** – Extract inclusion level; **D** – Extract type. The ellipse represents a 95% CI. t(1) and t(2) represent principal components 1 and 2, respectively.

The first two principal components explained 15.3% of the variation among all digestion conditions. No clear trends or separations were identified in these plots.

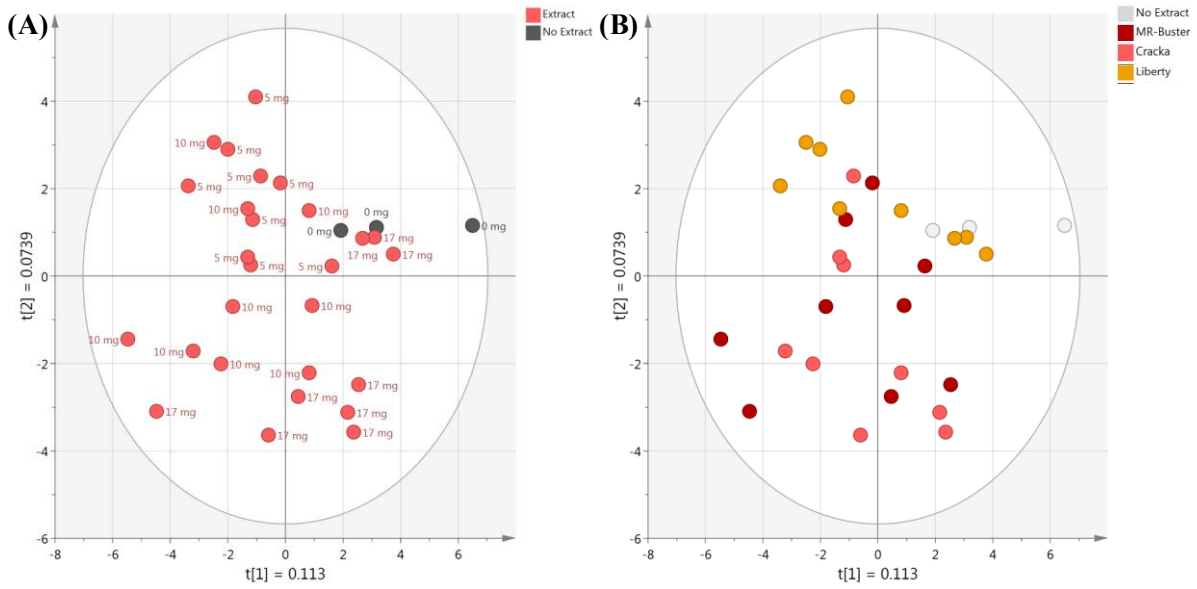

Figure 5.21 Principal component analysis (PCA) scores plots for MALDI spectra from digestion conditions containing sorghum polyphenol extracts/no extract with exogenous feed enzymes

PCA was performed on the MALDI spectra (50 – 1500 Da) to determine relationships and variance among the digestion conditions. **A** – Extract inclusion level; **B** – Extract type. The ellipse represents a 95% CI. t(1) and t(2) represent principal components 1 and 2, respectively.

The first two principal components explained 18.7% of the variation among all digestion conditions. No clear trends or separations were identified in these plots.

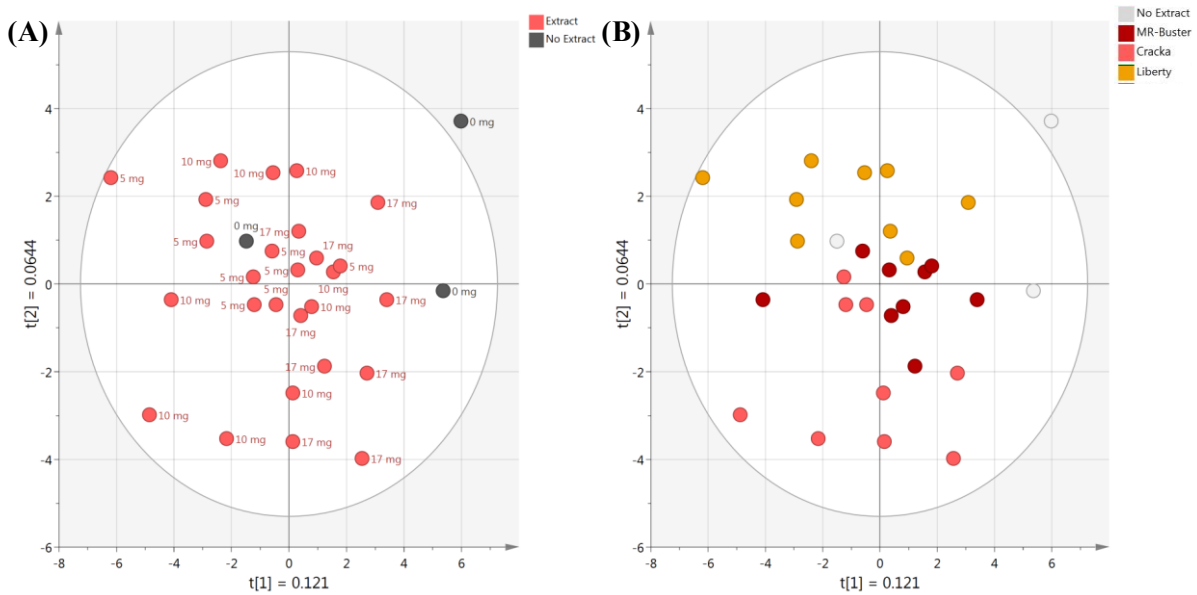

Figure 5.22 Principal component analysis (PCA) scores plots for MALDI spectra from digestion conditions containing sorghum polyphenol extracts/no extract with only endogenous enzymes

PCA was performed on the MALDI spectra (50 – 1500 Da) to determine relationships and variance among the digestion conditions. **A** – Extract inclusion level; **B** – Extract type. The ellipse represents a 95% CI. t(1) and t(2) represent principal components 1 and 2, respectively.

The first two principal components explained 18.5% of the variation among all digestion conditions. There was slight separation of the samples containing Liberty sorghum polyphenol extract from those containing red sorghum polyphenol extracts (**Figure 5.22B**). These analyses indicated that the inclusion of different sorghum polyphenol extracts alter the digestion fingerprint in different ways.

The individual extract types, beginning with grape seed tannin extract, were next evaluated using PCA to determine if separation could be observed at more specific levels (**Figure 5.23, 5.24**).

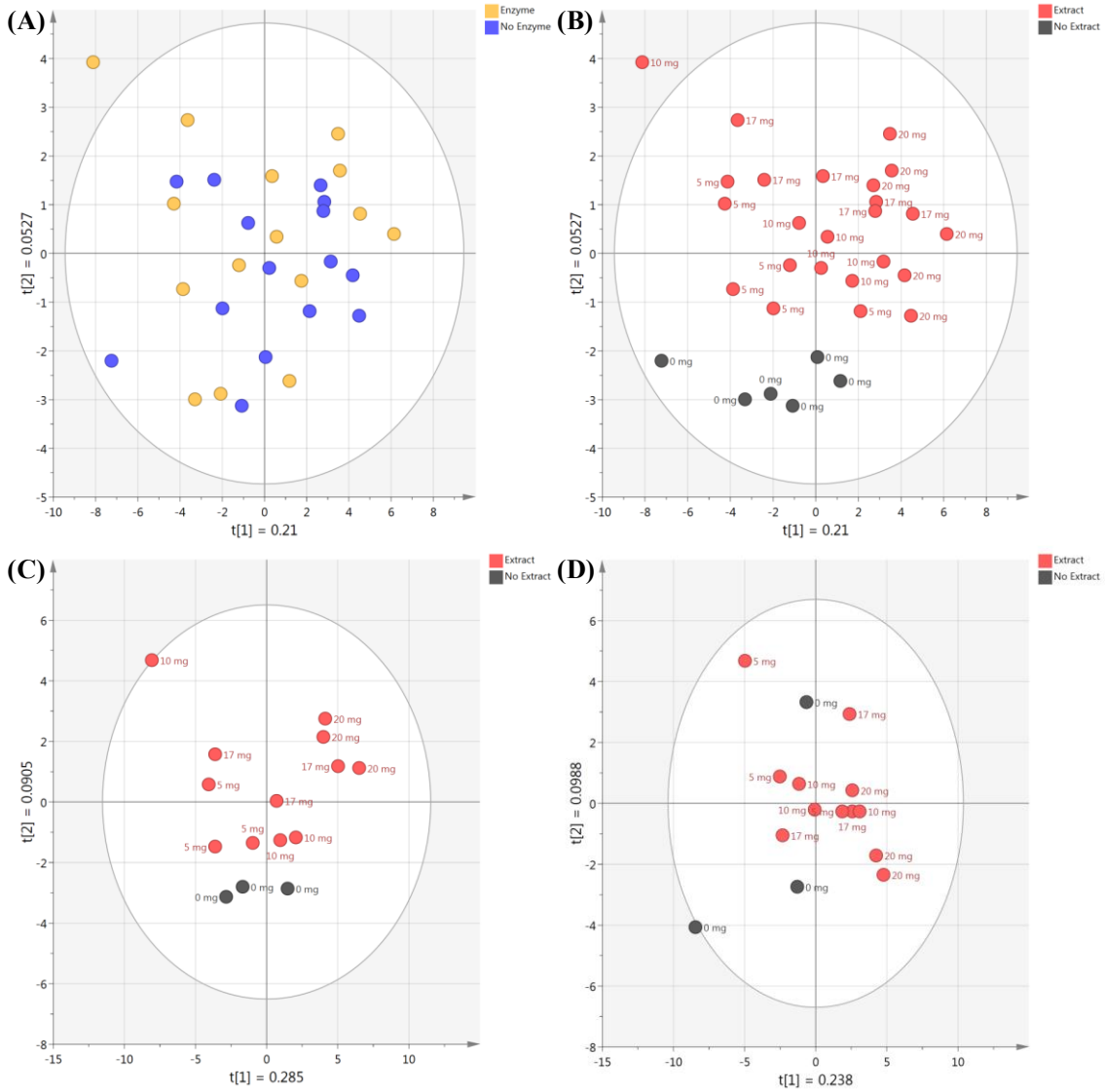

Figure 5.23 Principal component analysis (PCA) scores plots for MALDI spectra from digestion conditions containing grape seed tannin extract
PCA was performed on the MALDI spectra (50 – 1500 Da) to determine relationships and variance among the digestion conditions. **A, B** – All grape seed tannin extract conditions; **C** –

Grape seed tannin extract conditions with exogenous feed enzymes; **D** – Grape seed tannin extract conditions without exogenous feed enzymes. The ellipse represents a 95% CI. t(1) and t(2) represent principal components 1 and 2, respectively.

The first two principal components explained 26.3% of the variation among all digestion conditions containing grape seed tannin extract (**Figures 5.23A, B**). Among grape seed tannin extract samples with exogenous enzymes, the first two principal components explained 37.6% of the variation (**Figure 5.23C**). Among grape seed tannin extract samples with only endogenous enzymes, the first two principal components explained 33.7% of the variation (**Figure 5.23D**). When analysing all samples along the lines of extract content, clear separation was observed between samples containing grape seed tannin extract and those that did not (**Figure 5.23B**). The same pattern was also seen in the diets containing the two exogenous feed enzymes indicating that the grape seed tannin extract did alter the effect of the exogenous enzymes (**Figure 5.23C**). These results indicated that simple fingerprinting could be used to detect this type of tannin extract in diets compared to diets without the extract.

Grape seed tannin extract conditions were next evaluated based on the level of inclusion (5, 10, 17, 20 mg) (**Figures 5.24**).

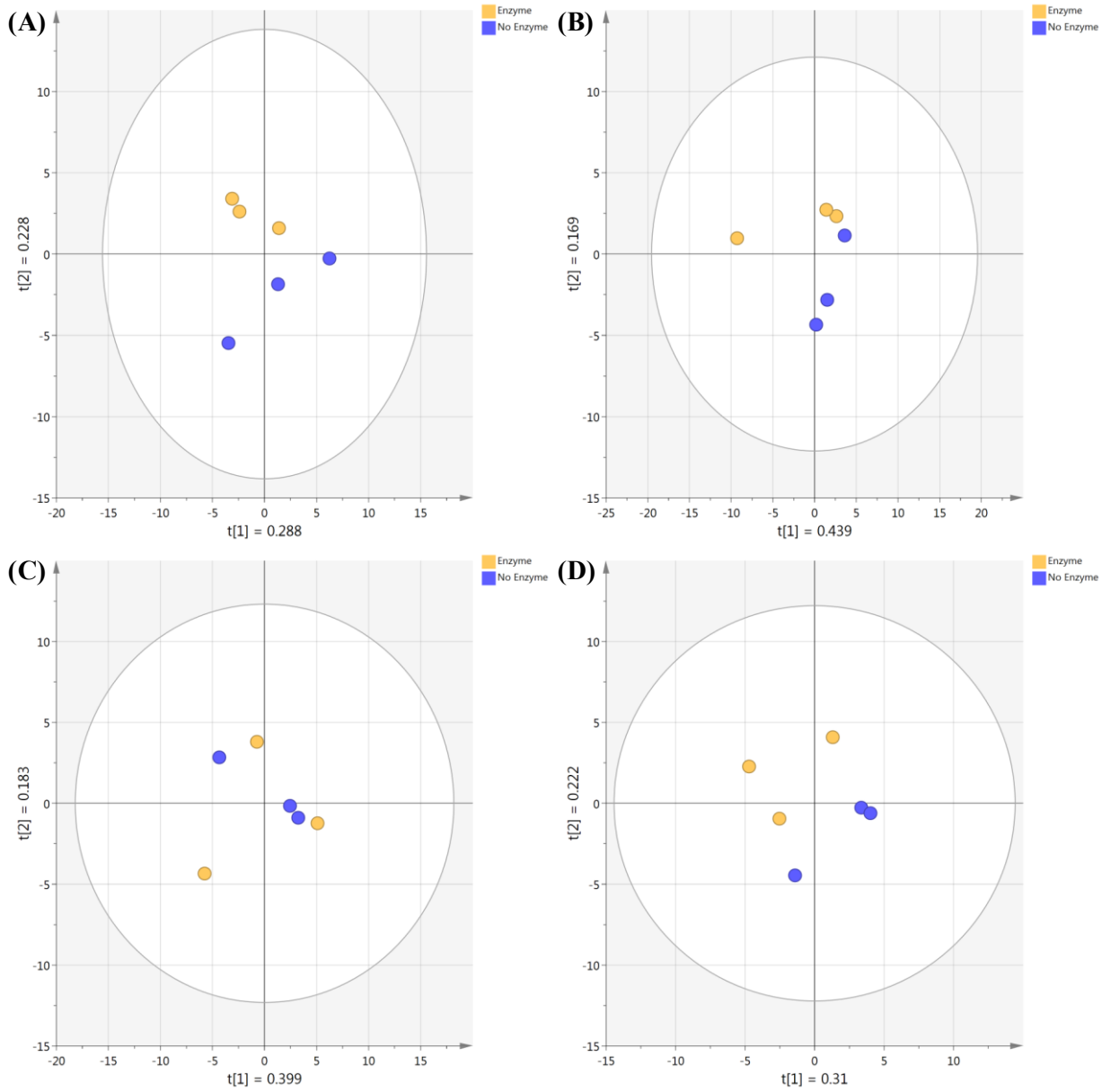

Figure 5.24 Principal component analysis (PCA) scores plots for MALDI spectra from digestion conditions containing grape seed tannin extract (extract dose)
PCA was performed on the MALDI spectra (50 – 1500 Da) to determine relationships and variance among the digestion conditions. **A** – 5 mg; **B** – 10 mg; **C** – 17 mg; **D** – 20 mg. The ellipse represents a 95% CI. t(1) and t(2) represent principal components 1 and 2, respectively.

The first two principal components explained 51.6%, 60.8%, 58.2% and 53.2% of the variation among the digestion conditions containing 5, 10, 17 and 20 mg grape seed tannin extract, respectively. Apart from **Figure 5.24C**, clear separations and grouping could be established in diets containing grape seed tannin extract. This result indicated that the metabolite profiles of the three diets (5, 10 and 20 mg) were significantly different when viewed through the filter of exogenous feed enzyme presence. The clear separation and grouping observed above for grape seed tannin, while very useful for quickly identifying sample types, indicated that the

inclusion of grape seed tannin extract, albeit **Figure 5.24C**, did not alter digestion when viewed through the filter of presence of exogenous feed enzymes.

Samples containing quebracho tannin extract were next analysed (**Figure 5.25**).

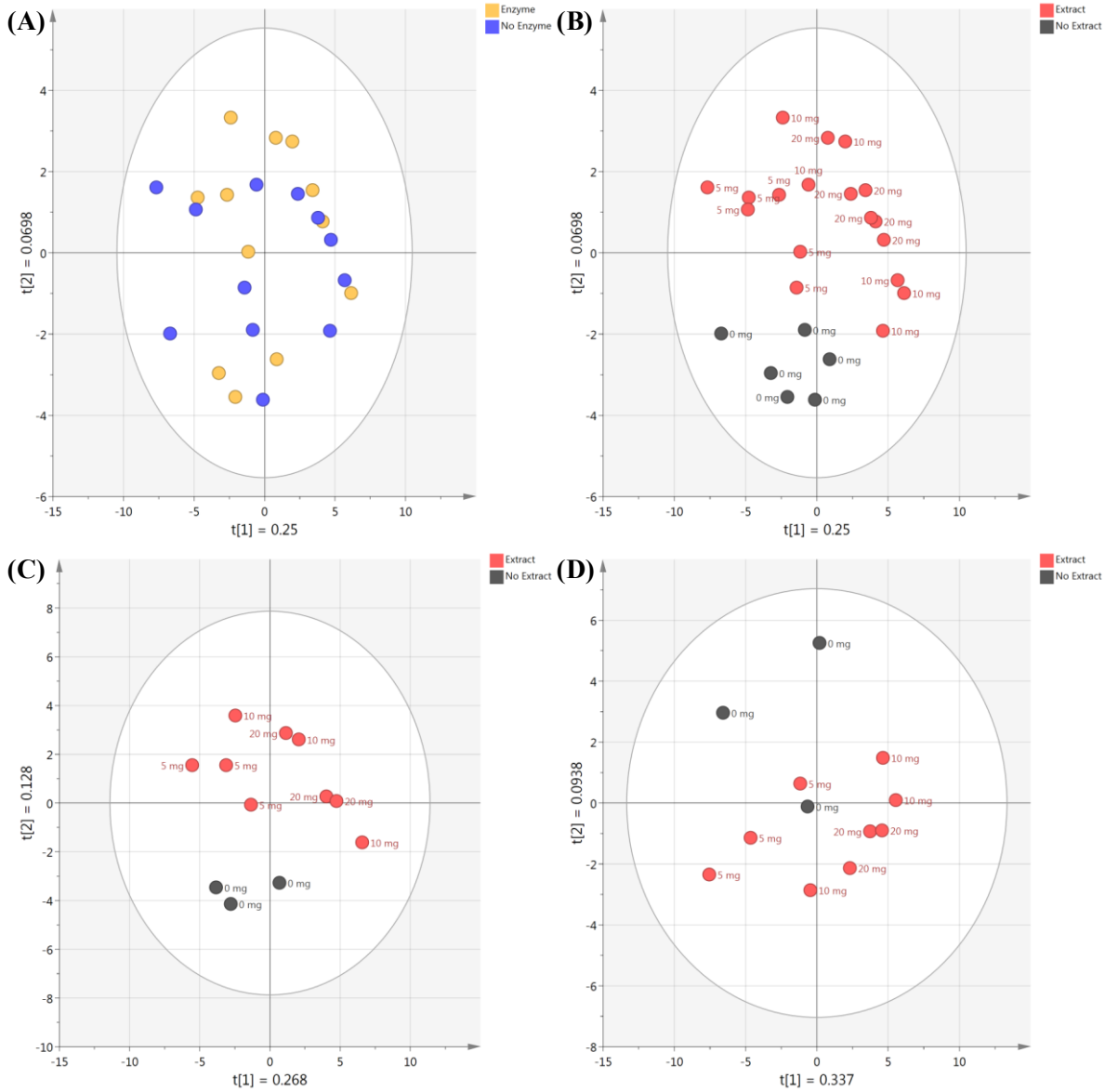

Figure 5.25 Principal component analysis (PCA) scores plots for MALDI spectra from digestion conditions containing quebracho tannin extract
PCA was performed on the MALDI spectra (50 – 1500 Da) to determine relationships and variance among the digestion conditions. **A, B** – All quebracho tannin extract conditions; **C** – Quebracho tannin extract conditions with exogenous feed enzymes; **D** – Quebracho tannin extract conditions without exogenous feed enzymes. The ellipse represents a 95% CI. t(1) and t(2) represent principal components 1 and 2, respectively.

The first two principal components explained 32.0% of the variation among all digestion conditions containing quebracho tannin extract (**Figures 5.25A, B**). Among quebracho tannin

extract conditions with exogenous enzymes, the first two principal components explained 39.6% of the variation (**Figure 5.25C**). Among quebracho tannin extract conditions with only endogenous enzymes, the first two principal components explained 43.1% of the variation (**Figure 5.25D**). Similar to the analysis of diets containing grape seed tannin extracts, clear separation was observed between samples containing quebracho tannin extracts and those that did not (**Figure 5.25B**). The same pattern was also seen in the diets containing the two exogenous feed enzymes indicating that quebracho tannins compromised exogenous enzyme action (**Figure 5.25C**). These results indicated that fingerprinting could be used to detect this type of tannin extract in diets.

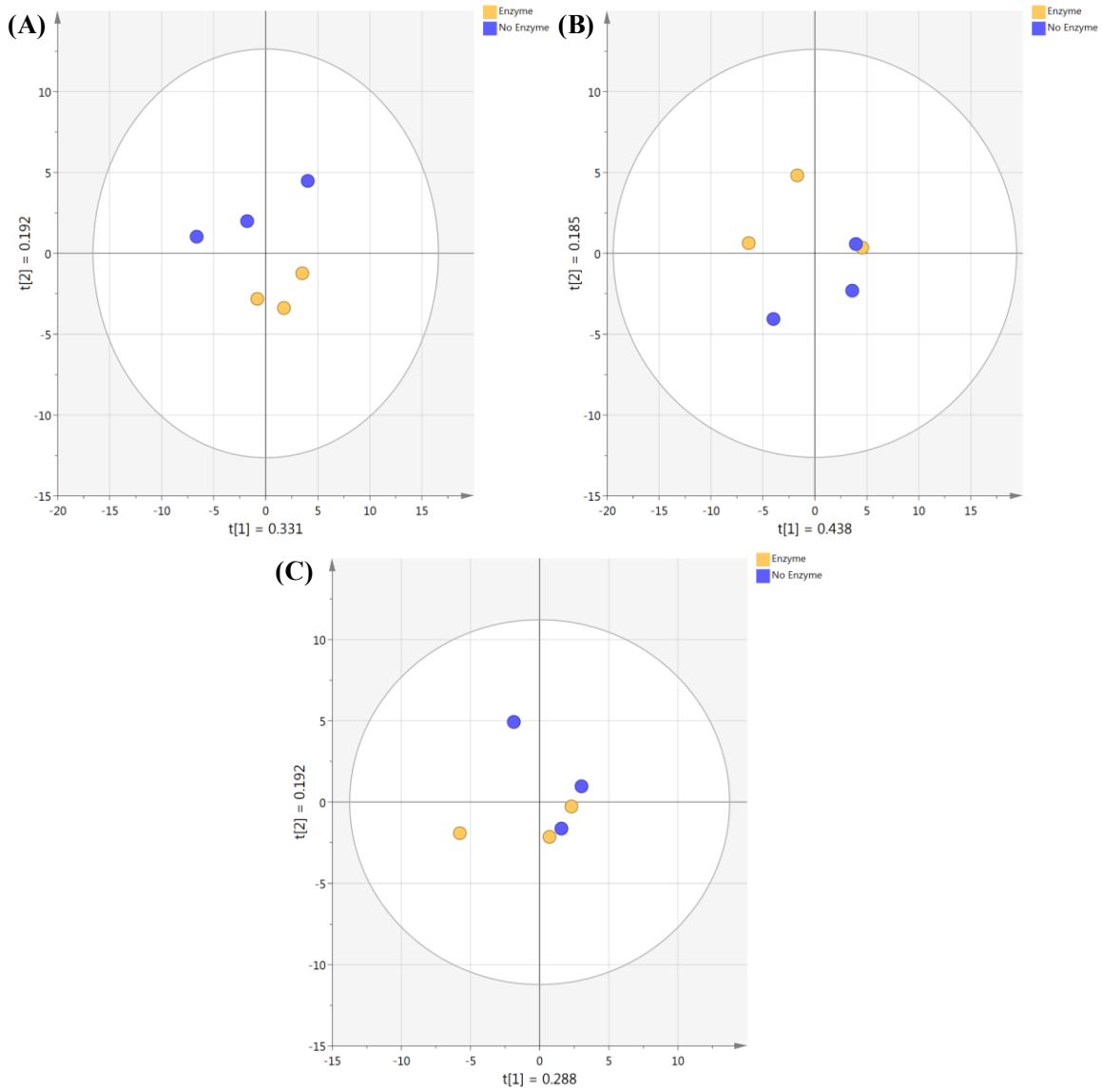

Figure 5.26 Principal component analysis (PCA) scores plots for MALDI spectra from digestion conditions containing quebracho tannin extract (extract dose)

PCA was performed on the MALDI spectra (50 – 1500 Da) to determine relationships and variance among the digestion conditions. **A** – 5 mg; **B** – 10 mg; **C** – 20 mg. The ellipse represents a 95% CI. t(1) and t(2) represent principal components 1 and 2, respectively.

The first two principal components explained 52.3%, 62.3% and 48.0% of the variation among the digestion conditions containing 5, 10 and 20 mg quebracho tannin extract, respectively. Clear separation of diets could only be observed in the diets with 5 mg of quebracho tannin extract (**Figure 5.26A**) indicating that at 10 and 20 mg inclusion quebracho tannin extract altered digestion when filtering based on presence of exogenous feed enzymes.

The samples containing sorghum polyphenol extracts (MR-Buster, Cracka, Liberty) were next evaluated (**Figures 5.27 – 5.32**).

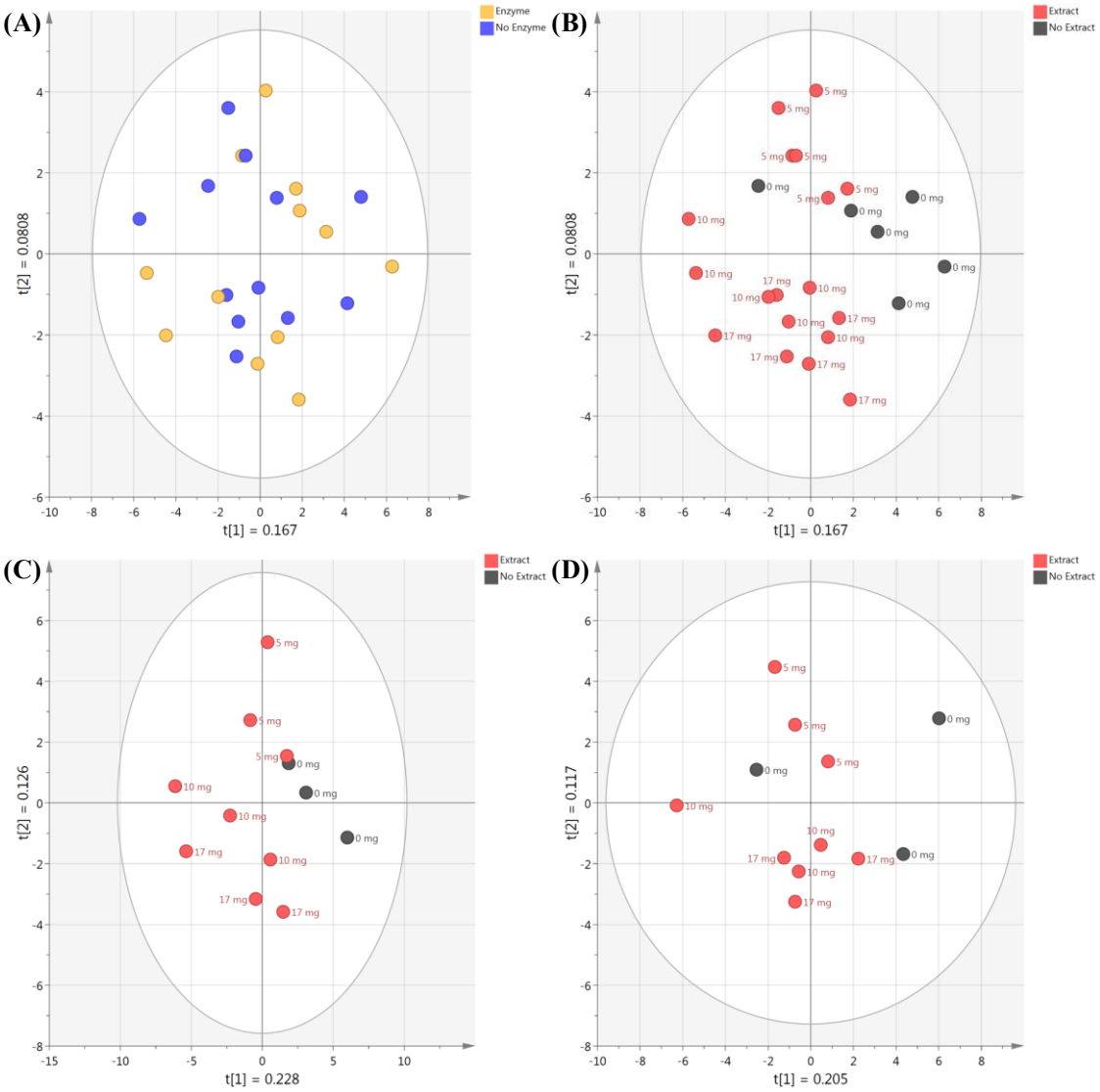

Figure 5.27 Principal component analysis (PCA) scores plots for MALDI spectra from digestion conditions containing MR-Buster sorghum polyphenol extract

PCA was performed on the MALDI spectra (50 – 1500 Da) to determine relationships and variance among the digestion conditions. **A, B** – All MR-Buster sorghum polyphenol extract conditions; **C** – MR-Buster sorghum polyphenol extract conditions with exogenous feed enzymes; **D** – MR-Buster sorghum polyphenol extract conditions without exogenous feed enzymes. The ellipse represents a 95% CI. t(1) and t(2) represent principal components 1 and 2, respectively.

The first two principal components explained 24.8% of the variation among all digestion conditions containing MR-Buster sorghum polyphenol extract (**Figures 5.27A, B**). Among MR-Buster sorghum polyphenol extract conditions with exogenous feed enzymes, the first two principal components explained 35.4% of the variation (**Figure 5.27C**). Among MR-Buster sorghum polyphenol extract conditions with only endogenous enzymes, the first two principal components explained 32.2% of the variation (**Figure 5.27D**). No clear separations or trends were identified at this level of analysis. MR-Buster sorghum polyphenol extracts appeared to have a minor effect on the positive impacts brought about by the exogenous feed enzymes.

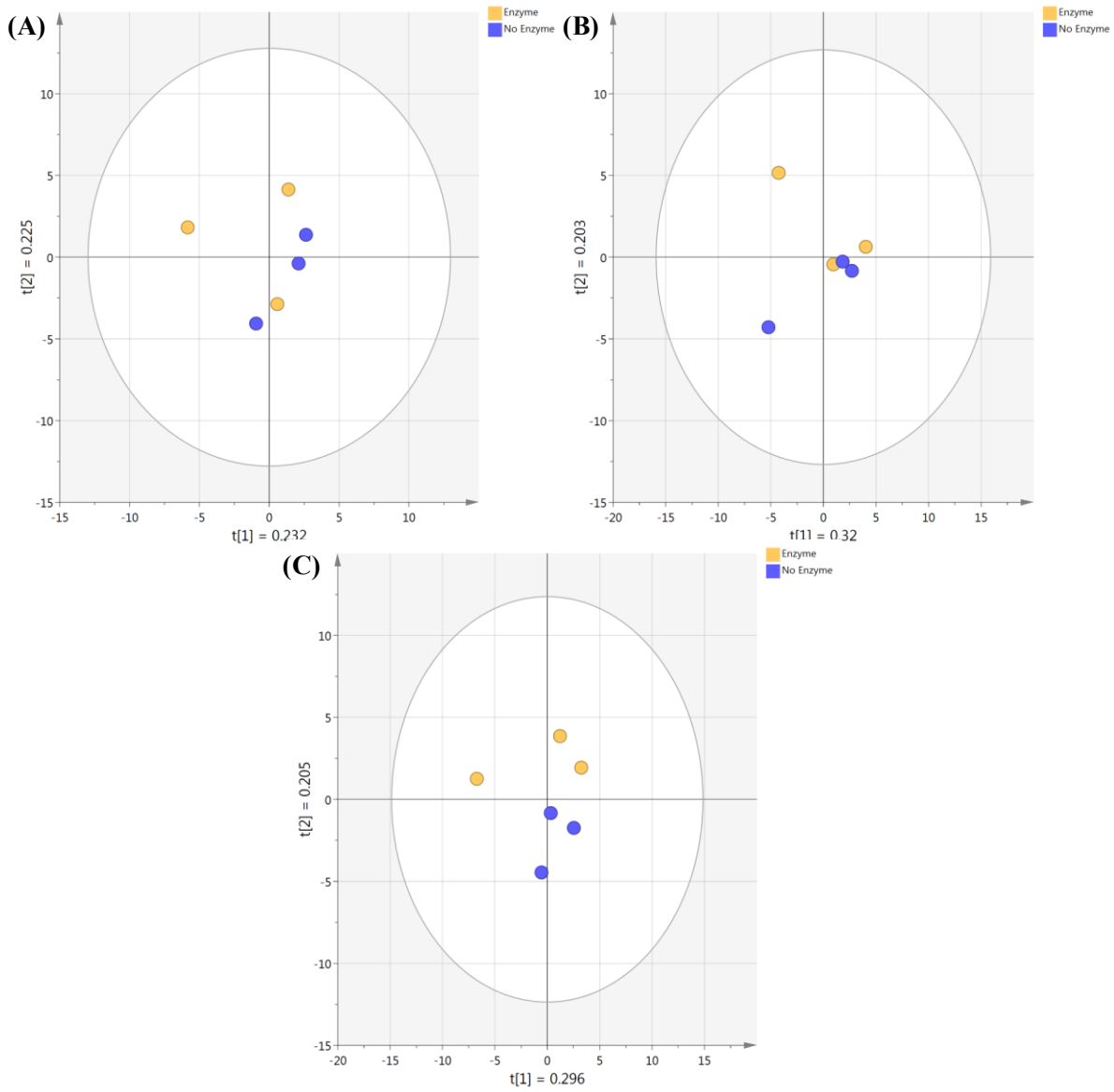

Figure 5.28 Principal component analysis (PCA) scores plots for MALDI spectra from digestion conditions containing MR-Buster sorghum polyphenol extract (extract dose)
PCA was performed on the MALDI spectra (50 – 1500 Da) to determine relationships and variance among the digestion conditions. **A** – 5 mg; **B** – 10 mg; **C** – 17 mg. The ellipse represents a 95% CI. t(1) and t(2) represent principal components 1 and 2, respectively.

The first two principal components explained 45.7%, 52.3% and 50.1% of the variation among the digestion conditions containing 5, 10 and 17 mg MR-Buster sorghum polyphenol extract, respectively. Clear separation of diets could only be observed in the diets with 17 mg of MR-Buster sorghum polyphenol extract (**Figure 5.28C**) and thus inclusion of 5 and 10 mg of MR-Buster extract changed the positive impact of the exogenous feed enzymes.

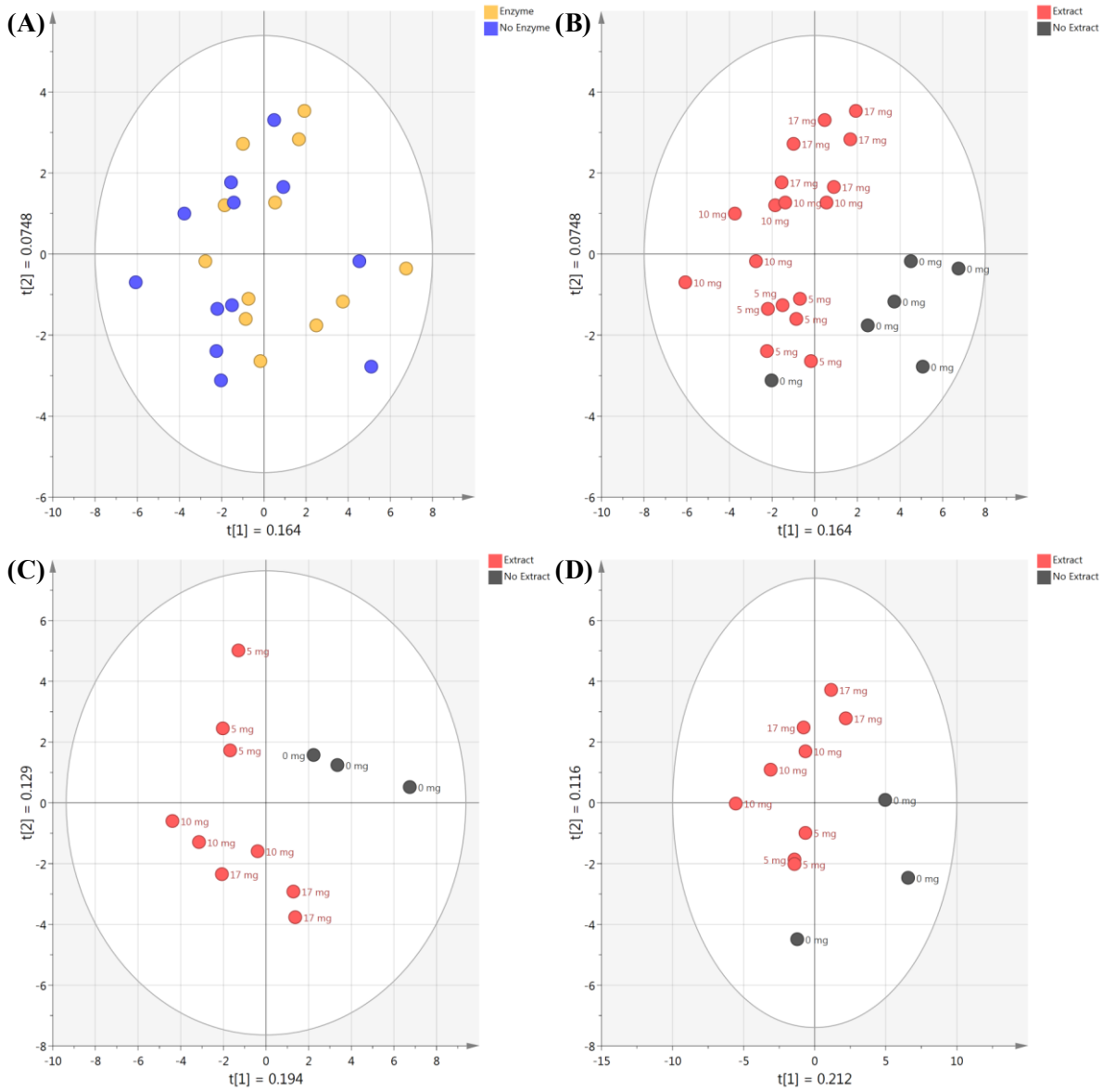

Figure 5.29 Principal component analysis (PCA) scores plots for MALDI spectra from digestion conditions containing Cracka sorghum polyphenol extract
PCA was performed on the MALDI spectra (50 – 1500 Da) to determine relationships and variance among the digestion conditions. **A, B** – All Cracka sorghum polyphenol extract conditions; **C** – Cracka sorghum polyphenol extract conditions with exogenous feed enzymes; **D** – Cracka sorghum polyphenol extract conditions without exogenous feed enzymes. The ellipse represents a 95% CI. t(1) and t(2) represent principal components 1 and 2, respectively.

The first two principal components explained 23.9% of the variation among all digestion conditions containing Cracka sorghum polyphenol extracts (**Figures 5.29A, B**). Cracka sorghum polyphenol extracts had an effect on the impacts brought about by the exogenous feed enzymes. Among Cracka sorghum polyphenol extract conditions with exogenous enzymes, the first two principal components explained 32.3% of the variation (**Figure 5.29C**). Among Cracka sorghum polyphenol extract conditions with only endogenous enzymes, the first two

principal components explained 32.8% of the variation (**Figure 5.29D**). Several important trends were observed in these analyses. When filtering based on extract presence, separation was clearly seen indicating significant differences in metabolite profiles (**Figures 5.29B-D**). Upon closer inspection, diets were clearly separated by the amount of Cracka sorghum polyphenol extract included in them.

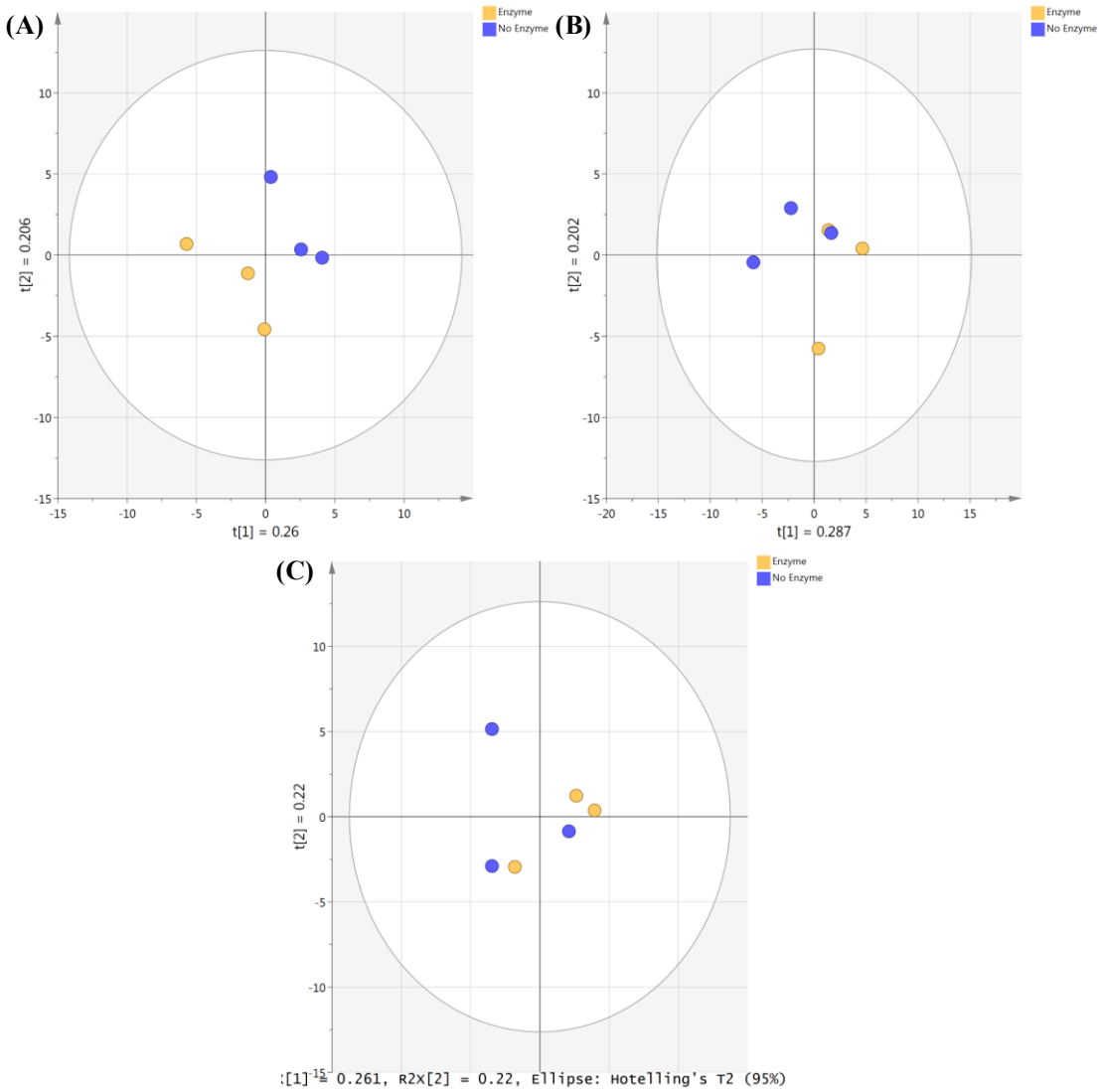

Figure 5.30 Principal component analysis (PCA) scores plots for MALDI spectra from digestion conditions containing Cracka sorghum polyphenol extract (extract dose)
PCA was performed on the MALDI spectra (50 – 1500 Da) to determine relationships and variance among the digestion conditions. **A** – 5 mg; **B** – 10 mg; **C** – 17 mg. The ellipse represents a 95% CI. t(1) and t(2) represent principal components 1 and 2, respectively.

The first two principal components explained 46.6%, 48.9% and 48.1% of the variation among the digestion conditions containing 5, 10 and 17 mg Cracka sorghum polyphenol extract, respectively. Clear separation of diets could only be observed in the diets with 5 mg of Cracka

sorghum polyphenol extract (**Figure 5.30C**) and thus 10 and 17 mg of Cracka polyphenol extract altered digestion in the presence of exogenous feed enzymes.

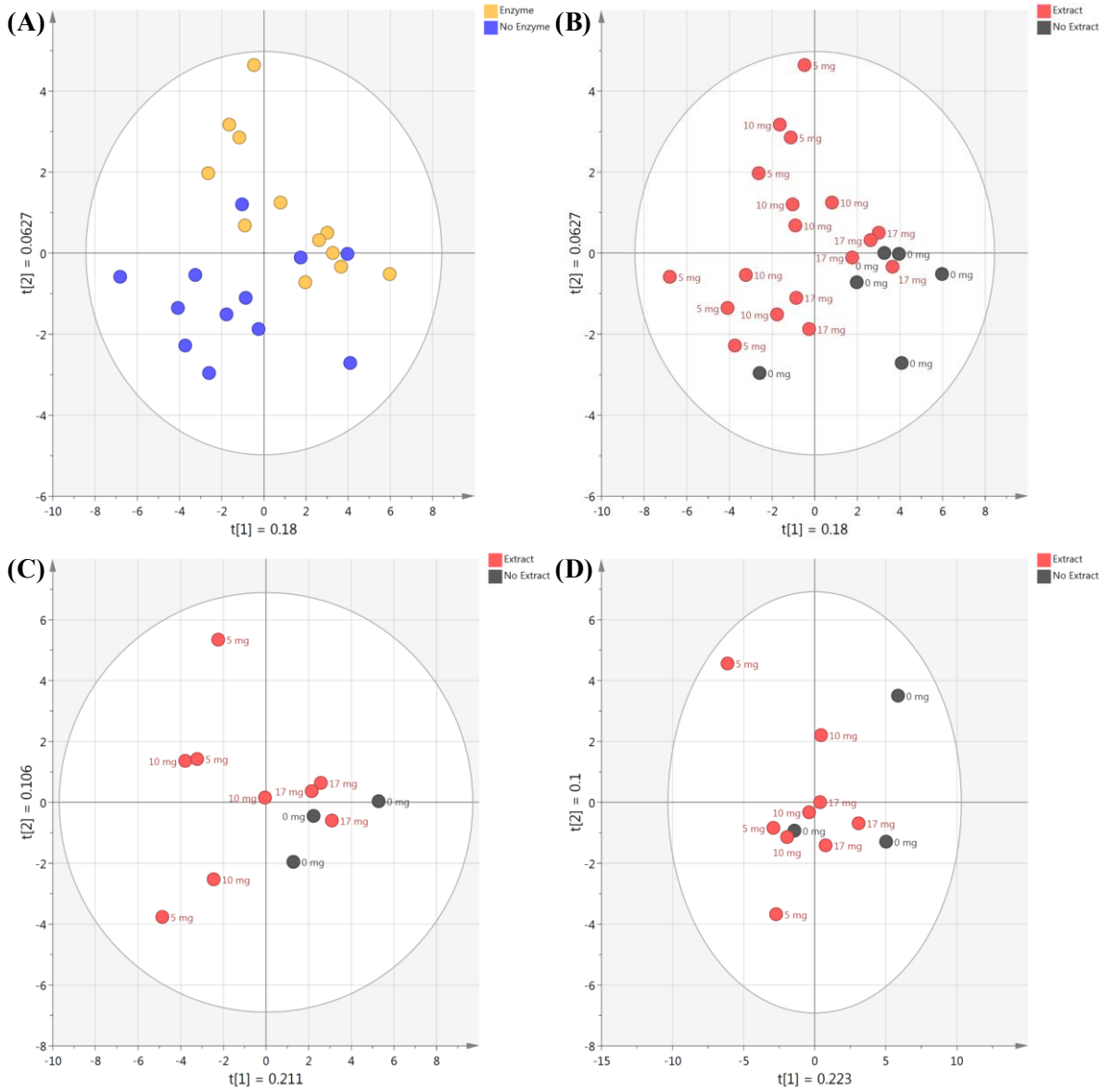

Figure 5.31 Principal component analysis (PCA) scores plots for MALDI spectra from digestion conditions containing Liberty sorghum polyphenol extract
PCA was performed on the MALDI spectra (50 – 1500 Da) to determine relationships and variance among the digestion conditions. **A, B** – All Liberty sorghum polyphenol extract conditions; **C** – Liberty sorghum polyphenol extract conditions with exogenous feed enzymes; **D** – Liberty sorghum polyphenol extract conditions without exogenous feed enzymes. The ellipse represents a 95% CI. t(1) and t(2) represent principal components 1 and 2, respectively.

The first two principal components explained 24.3% of the variation among all digestion conditions containing Liberty sorghum polyphenol extract (**Figures 5.31A, B**). Among Liberty sorghum polyphenol extract conditions with exogenous enzymes, the first two principal components explained 31.7% of the variation (**Figure 5.31C**). Among Liberty sorghum

polyphenol extract conditions with only endogenous enzymes, the first two principal components explained 32.3% of the variation (**Figure 5.31D**). No clear separations or trends were identified at this level of analysis. While **Figure 5.31A** showed no outright separation/grouping, there was a strong indication that grouping was occurring between samples with and without exogenous feed enzymes. This indicated that Liberty sorghum polyphenol extract did not have a large impact of digestion.

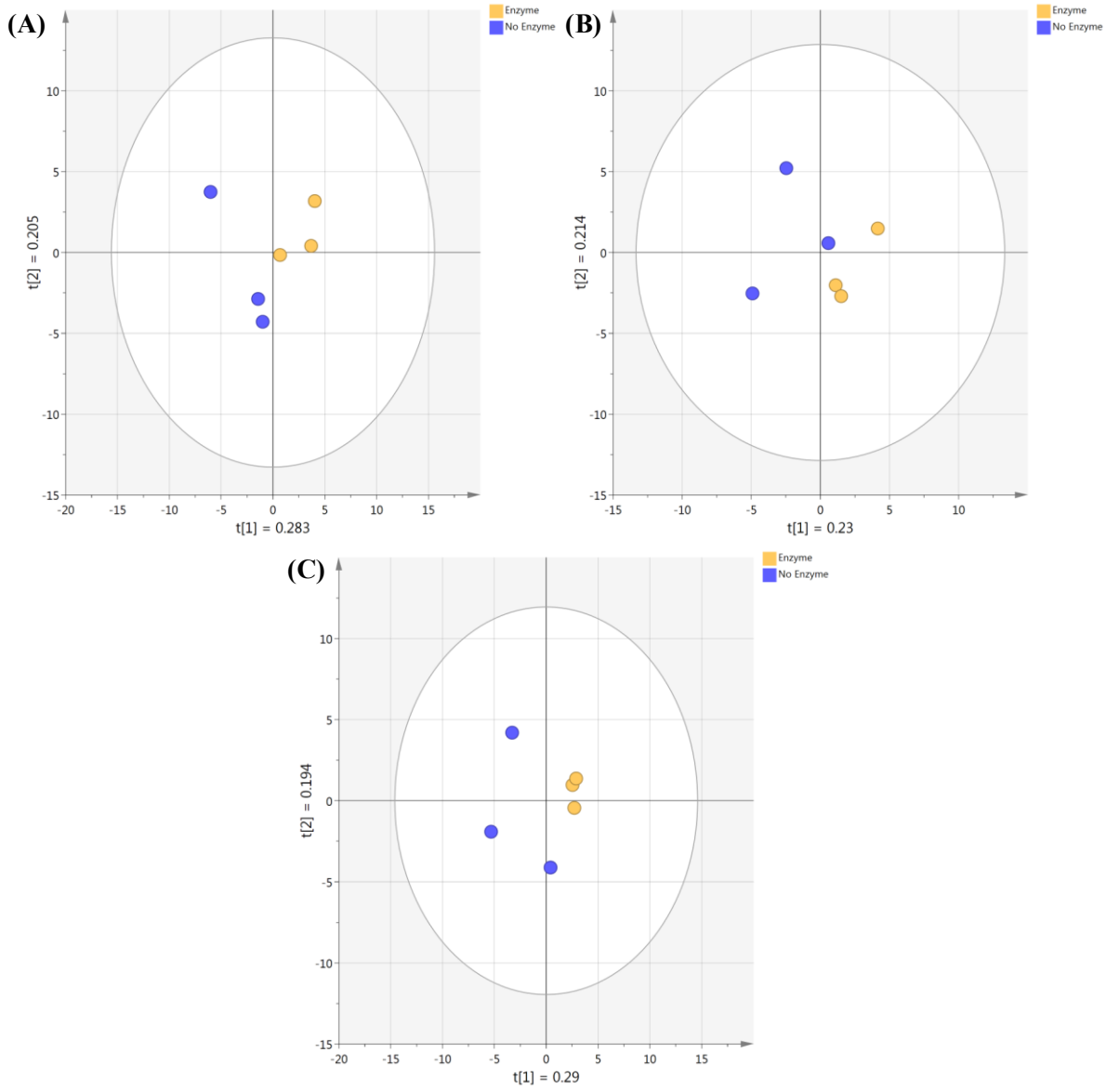

Figure 5.32 Principal component analysis (PCA) scores plots for MALDI spectra from digestion conditions containing Liberty sorghum polyphenol extract (extract dose)
PCA was performed on the MALDI spectra (50 – 1500 Da) to determine relationships and variance among the digestion conditions. **A** – 5 mg; **B** – 10 mg; **C** – 17 mg. The ellipse represents a 95% CI. t(1) and t(2) represent principal components 1 and 2, respectively.

The first two principal components explained 48.8%, 44.4% and 48.4% of the variation among the digestion conditions containing 5, 10 and 17 mg Liberty sorghum polyphenol extract, respectively. Clear separations of samples were observed in all three inclusion levels which indicated that the Liberty sorghum polyphenol extracts had a significant effect on the metabolite profiles obtained by MALDI mass spectrometry and did not have an impact of digestion in the presence of exogenous feed enzymes.

Overall, the multivariate analysis from MALDI-ToF-MS spectra indicated that the rapid profiling of the digesta samples could be useful when evaluating specific interactions with a low number of samples and different conditions. This kind of method could be beneficial in 1) evaluating a new feed formulation prior to *in vivo* testing; and 2) evaluating alterations in feed formulations currently in use prior to *in vivo* testing. Extensive studies reproducing a digestion and profiling method similar to this could be performed for a variety of feed formulations. This library of digestion profiles could then be used to evaluate new feed formulations rapidly.

A similar untargeted metabolomics method was used by Rocchetti et al. (2020) to identify compounds of interest in red and white sorghum grains that could play a role in modulating starch digestibility. This was tested in an *in vitro* simulated digestion model of human digestion consisting of oral (including amylase), gastric and pancreatic phases. They found that pigmented sorghums (red coloured grains) had the greatest effect on starch digestibility which was most likely caused by increased levels of anthocyanins and flavonols. This included lower starch hydrolysis which indicated the enzyme inhibition of amylase. During and after the different phases of digestion, multivariate analysis was conducted on the digesta to determine polyphenol markers which led to separation of samples and differentiated specific conditions. Using OPLS-DA without prior PCA, clear groupings appeared in the plots which separated samples based on their point of digestion, i.e., before and during.

Moving up in complexity, Cowieson et al. (2016) tested the use of proteomics for understanding the origins of digested peptides in an *in vivo* poultry feeding experiment. They tested a standard poultry diet (maize and soybean mean) against a diet including 20% raw soybean meal to determine if this diet change affected protein in the digesta. The digesta were extracted for proteins, tryptic digest performed on the concentrated protein and analysed using LC-MS. Through this analyses, several hundred peptides were identified and were able to be

sorted by their origin, i.e., endogenous, maize or soybean. The addition of the raw soybean did alter the ratios of protein origin identified. This proteomic analysis could then be linked to the nutritional parameters measured in the study as the addition of raw soybean negatively impacted nutritional markers. This study revealed the potential of incorporating proteomics methodologies into *in vivo* studies as a tool to better understanding the micro-changes occurring in relation to more macro-effects as observed in the various poultry nutritional parameters. This thesis sought to follow a similar route taken by Cowieson et al. (2016) in incorporating an '-omics' approach with more traditional methodologies. Overall the results in this section correlated with the effects measure in the *in vitro* enzyme assays and after simulated digestion. Metabolomics has the potential to become a key component of these kinds of feeding studies in order to help elucidate the biochemical pathways responsible for changes observed in whole animals.

Qi et al. (2016) studied tannin depolymerisation under multiple environmental conditions including pH, time and temperature. The material they analysed was purified bran powder from the sorghum variety called 'High Tannin.' They found that both increased temperature and lowered pH increased the rate of tannin depolymerisation. At 50°C and at pH 1.0, approximately 80% of the polymerised tannins were still intact after 5 minutes. While not exactly the same, these conditions are similar to those of the gastric phase of the simulated digestion model, 40°C and a pH of 3.0. This indicates that there is the possibility for degradation of large polyphenols within the extracts, like the condensed tannins identified in the grape seed and quebracho tannin extracts. However, this is likely to be minimal with most structures remaining whole. The remaining presence of these large tannins in the diets containing grape seed and quebracho extracts could explain the separation from diets without added extract.

5.5 Conclusions and future work

5.5.1 Conclusions

Sorghum has been stigmatised as being of lower nutritional value for monogastrics due to high levels of anti-nutrients. Sorghum is also thought to potentially limit the full benefits to be gained by using exogenous feed enzymes, like a protease or phytase. In this chapter, the goal was to determine the effects of sorghum polyphenol extracts on measures of protein and phosphorous in a model of simulated poultry digestion. Overall, the polyphenol extracts

obtained from feed-relevant sorghum varieties had minimal effect on protein or phosphorous digestibility when in the presence of exogenous feed enzymes. Tannin extracts from non-feed sources, grape seed and quebracho, significantly affected the positive impacts brought about by the exogenous feed enzymes on measures of protein. Like the sorghum polyphenol extracts, phosphorous digestibility was not affected by the inclusion of the tannin extracts. The anti-nutritional effects, regarding protein digestion, were most likely caused by both direct inhibition of endogenous and exogenous proteases and through indirect inhibition by binding protein substrate. The spectra obtained from MALDI-ToF-MS of the simulated digesta indicated that this rapid profiling method could be applied to certain digestion parameters and sample sizes for use in quickly distinguishing between diets containing specific ingredients/compounds of interest as well as anti-nutritional impact.

The impacts of sorghum grain on the full benefits of exogenous feed enzymes, i.e., 'extra-proteinaceous' and 'extra-phosphoric,' are most likely not solely due to the presence of small and medium sized polyphenols found in modern sorghum varieties. While sorghum polyphenol extracts were shown to significantly reduce enzyme activity directly, these effects were greatly diminished when evaluated in a simulated digestion model. However, this does not exclude the remaining anti-nutrients in sorghum, i.e., phytate and kafirin protein, and their complex interactions with various nutrients, i.e., other proteins, starches and lipids. The complex structures formed through these interactions might have significant effects on exogenous feed enzyme efficacy and may also provide opportunities for sorghum polyphenols to bind and further modify/enhance anti-nutritional behaviour. These results do no exclude all polyphenols from impacting exogenous feed enzyme efficacy as large polyphenols, i.e., condensed tannins, were shown to significantly reduce exogenous feed enzyme effectiveness in both simple and realistic models. This result indicates that care should still taken when formulating monogastric animal feed with grains known to contain high levels of polyphenols, especially larger compounds.

5.5.2 Future work

There remain many opportunities for further work on the material included in this experimental chapter. Regarding the simulated digestion, there are several parameters that could be modified to increase the realistic environment of the model as well as discern more specific effects by both exogenous feed enzymes. In the current chapter, sorghum polyphenols were incorporated

as a lyophilised extract into the ground maize:soybean meal diet. While the current method allowed the for the direct testing of specific polyphenol anti-nutrients, the model could be improved by incorporating ground sorghum grain instead. This could be done by blending in several percentages of each ingredient to test the dose-response of adding sorghum grain. This approach has been used many times in the literature but primarily limited to full *in vivo* feeding trials. A final variation to the digestion model would be to evaluate the individual diets with each exogenous feed enzyme incorporated separately as opposed to together. This would allow for more detail to be gained regarding specific anti-nutrient interaction with each enzyme as well as the individual contribution of each enzyme to the measures of protein and phosphorous digestibility.

Regarding the MALDI-ToF-MS study of the digesta from simulated digestion, there were several planned experiments intended to strengthen and supplement this data but were not completed (see **COVID-19 Impact Form**). A comprehensive proteomics approach was originally planned to fully understand the protein environment after digestion with the various polyphenol and tannin extracts and exogenous feed enzymes. This approach included protein extraction, SDS-PAGE to separate specific protein bands, tryptic digest of excised SDS-PAGE spots, MALDI-ToF-MS analysis of the tryptic digests and LC-MS studies of the protein extracts. This approach was based on a study of chicken endogenous proteins, maize proteins and soybean proteins in digesta from a chicken feeding trial (Cowieson et al., 2016). This type of analysis would have allowed for the identification of specific peptides produced upon digestion. This level of detail might have shown more subtle and nuanced effects of the sorghum polyphenol extracts on protein digestibility.

Chapter 6 – General Discussion

6.1 Paradigm shift in polyphenol and tannin chemistry methodology

The work from this thesis has identified areas for further study and research, including alterations to current research strategies in natural products research. As discussed throughout this work, polyphenols and related metabolites are routinely extracted, isolated and analysed for a variety of end purposes. Typically, this process involves three intensive steps including extraction, cleaning and purification of polyphenol extracts prior to liquid chromatography hyphenated to mass spectrometry (see **Chapter 2**). While the work presented in **Chapter 3** did not radically differ from this methodology, the analytical approach used aimed to reduce the amount of processing/analysis time and complexity. The work in this thesis represents the initial steps towards a paradigm shift in the way researchers could evaluate plant polyphenols and related anti-nutrients. The general focus of this shift would be to move research towards a more thoughtful and nuanced approach in evaluating these important metabolites and their relevant biological roles and functions.

For decades, natural products research has revolved around the extraction, purification, chromatographic separation and mass spectrometric identification of single compounds or specific groups of compounds. This approach has been widely successful and is still the gold-standard for natural products analysis (Kang et al., 2016; Jiang et al., 2020). However, this standard approach towards the characterisation and identification of polyphenols, as well as their interactions and behaviours, is not necessarily appropriate for all aspects of natural products research. As plant extracts are extremely complex, there is no universal methodology to extract and analyse all metabolites in a single sample (see **Chapter 2**; Djande et al., 2020). Within the suggested paradigm shift, more consideration should be taken when planning experimentation. A series of methodological questions and roadblocks could be utilised to allow for more precise and effective means of sample preparation, extraction, purification and analysis (**Table 6.1**).

Table 6.1 Experimental conditions/outcomes to evaluate prior to natural product research

Analytical outcome	*In vitro/vivo* testing	Compound identification	Metabolite profiling
Metabolite size	Small	Large	Broad
Testing outcome	Broad effects	Specific effects	
Extract purity	Crude	Cleaned	Purified
Level of identification*	Identified	Putatively annotated	Putatively characterised
Analytical approach	Untargeted	Semi-targeted	Targeted

*Levels of identification from Sumner et al. (2007) and the Metabolomics Standards Initiative

This thesis sought to explore the mechanisms for reduced enzyme efficacy through an underutilised analytical framework, both in polyphenol extract characterisation and in testing the biological effects of its inclusion.

Prior to polyphenol and metabolite extraction, there is a need to define the analytical outcomes/questions and how they relate to the extraction process. This question should be answered early in the method development process. Traditional *in vitro*, and often *in vivo*, studies of protein/enzyme – polyphenol interactions involve the inclusion of cleaned and/or purified polyphenol extracts. Specific compounds, or groups of compounds, are added in increasing concentrations to discern their biological effects on protein binding and enzyme inhibition, among other experimental measures. These experiments are very useful for determining the specific biological effect or toxicity of a single compound or certain group of compounds. Studies like these are necessary when determining the effects of potential active ingredients for therapeutics, particularly for human medicines (Gómez-Cordovés et al., 2001). As polyphenols are well-established antioxidants, they have long been known to have beneficial health properties. The *in vitro* action of these compounds on therapeutic targets is crucial for determining the mode of action of a proposed drug or active pharmaceutical ingredient. Additionally, the purified compounds/groups of compounds will be incorporated into the final drug directly, as opposed to a crude or unpurified extract.

This kind of approach using purified extracts is not as useful when evaluating animal feed ingredients. While the specific compounds of interest will still be bioavailable to some degree, they will not be in a form resembling that of a purified extract. The effects measured using refined extracts will be unrealistic and not comparable to actual feeding scenarios. There is a need to move away from the intensive purification of compounds to less intensive and invasive approaches that could allow for more realistic effects to be observed when tested both *in vitro* and *in vivo*.

Beyond the extraction and testing of polyphenol extracts, more emphasis could be put on developing robust metabolomic methodologies as an alternative analytical strategy to traditional identification protocols. Djande et al. (2020) reviewed the benefits of metabolomics-based approaches to helping guide crop grain cultivar selection and breeding. The study of plant metabolites is a complex area of research and involves balancing method

sensitivity, selectivity and reproducibility. Methods must be sensitive enough to detect low concentrations of metabolites, selective enough to target specific compound groups (or broad enough to catch multiple groups of compounds) and reproducible, not only for other researchers but if they are to be implemented into fieldwork and breeding efforts. Djande et al. (2020) highlights the room for technological growth and development in metabolomics, especially with regards to improving analytical power and integration with genomic approaches. Improvements to current practices include moving away from targeted, simple biomarker identifications to more complicated, untargeted pathway analyses capable of identifying possible drivers of important biological changes.

In sorghum grain specifically, breeding efforts have revolved around improving the grain's weather resistance, starch and protein characteristics and reducing the total concentration of polyphenols. With regards to polyphenol content, this has meant grain colour and genes associated with colour and polyphenol metabolism have been targeted. In the case of white sorghum varieties, colour has all but been eliminated along with any large polyphenol and tannin metabolites. In the case of red coloured grains, polyphenols and some larger metabolites are still present but the enhanced weathering features remain (Selle et al., 2021). The majority of sorghum polyphenol studies have focussed on concentrations of specific groups of compounds, including phenolic acids (Luthria and Liu, 2013), anthocyanins (Dykes et al., 2013) and condensed tannins (Kaufman et al., 2013). While these studies are successful in identifying clear quantitative changes in the concentrations of specific metabolites, they are limited in their overall scope. Studies like these could be supplemented and improved by using more broad metabolomics approaches including fingerprinting and pathway analysis.

6.2 Re-evaluation of plant and grain breeding practices

There is a growing need to evaluate and re-evaluate the possible unintended consequences of certain grain breeding practices. In this thesis, sorghum polyphenol extracts from three modern Australian varieties were found to contain a variety of metabolites, including polyphenols and related metabolites (see **Chapter 3**; Hodges et al., 2021). Interestingly, some of the most abundant compounds in some of the spectra were fatty acids, primarily linoleic acid, oleic acid and related fatty acids. This potential shift in metabolites was hypothesised by Xie et al. (2019) to be caused by the reduction of large tannins in sorghum grain. As bird-resistance was reduced, i.e., lower concentration of tannins, the concentration of fatty acids detected increased.

The characterisation methods employed in this thesis formulated a broad metabolomics approach, as opposed to a more directed study of specific compounds. As indicated in **Section 6.1**, metabolomics is underused in the study of grain metabolites, particularly sorghum polyphenols. The untapped potential of metabolomics in crop breeding could be met by marrying it with traditional genomic approaches (Alseekh et al., 2021; Djande et al., 2021). While genomic approaches allow for specific traits to be highlighted and studied, the responses of the plants are much more varied and dependent on other factors, including the environment. As genes and their products of transcription are the focus of most breeding and selection efforts, there is a lack of understanding about the effects these measures might have on the plant metabolome. These external effects produce significant changes in the primary and secondary metabolome which would be missed in traditional genomic approaches.

Beyond the effects of sorghum breeding and selection on polyphenols, much of the current conversation and research about sorghum revolves around the effects of breeding on proteins in the grain, particularly kafirin, and improving overall protein digestibility (Liu et al., 2019; Selle et al., 2020; Selle et al., 2021). Selle et al. (2020) analysed a wide selection of Australian sorghum varieties to analyse kafirin protein and amino acid composition. They also evaluated previous studies and unpublished data from 1996 to 2016 and found that overall kafirin content in sorghum was rising as leucine, a primary component of kafirin, was found to significantly increase over time. This effect was most likely due to breeding for higher yield and through use of nitrogen fertilisers. This unintentional effect of breeding on kafirin content in sorghum has also been attributed to breeder selection (Selle et al., 2021). Red sorghum grains, the most common feed variety, have been selected based on their environmental durability. This durability comes from the corneous section of the endosperm and so by selecting varieties with enhanced weathering capacity kafirin content has inadvertently risen as well. Moving forwards, there is the potential for successful cultivars to be neither red nor white but pink. This pink variety would have the weathering capacity of red sorghum grains with the lower kafirin and polyphenol levels of white cultivars (Selle et al., 2021).

Liu et al. (2019) took a direct approach to solving sorghum's protein issue. This group inserted a synthetic β-kafirin gene into a sorghum cultivar with the aim of improving proteolysis. The transgenic lines produced using this synthetic biology approach not only had up to 25% increased proteolysis but had increased protein content both visibly via a microscope and

quantitatively when measured. Similarly, Li et al. (2018) used a Crispr/Cas9 gene editing approach to induce mutations in the gene encoding for α-kafirins which make up the majority of kafirin protein found in sorghum grain. They were able to significantly increase protein digestibility while also increasing the amount of lysine, an essential amino acid, available. These recent innovations in gene editing may be the best way forward regarding targeted breeding efforts; however, significant regulatory challenges remain for these methods as they would produce 'GMO,' or genetically modified organism status crops. GMO is still a contentious issue, especially in the eye of the public, but may be the best solution to solving important agricultural issues as humanity moves towards sustainable innovations in an ever-uncertain environmental climate.

As the value and nutritive content of sorghum grain is no longer dictated by large tannins and specific polyphenols, alternative methods of evaluating sorghum's use in feed are needed that can incorporate other important measures of viability like protein content and type. Similar to the approach here, Lin et al. (2021) used FT-IR to evaluate non-tannin and tannin sorghum varieties but also applied it to major nutrient groups in the grain. Using a calibration curve, they were able to accurate predict protein content, in addition to identifying protein secondary structures. Moving to more broad measures of analysis, Akın et al. (2021) applied spectroscopy to rapidly profile feed ingredients and mixtures. They used a technique called laser-induced breakdown spectroscopy (LIBS) to differentiate mixtures of corn and sorghum. LIBS is a rapid profiling method requiring little to no sample preparation and is available as a handheld device. Tools like this could be used to differentiate/validate feed ingredients against databases and known standards.

6.3 Modification of current animal feeding practices

The sustainable intensification of animal production is crucial to meeting global demands for inexpensive meat products. Globally, current agricultural practices are at a crossroads with regards to climate change and sustainability while also preparing for populations worldwide to increase to approximately 10 billion people by 2050. The issue is two-fold and solutions must address both changing environments and increased production requirements. Solutions must make economic sense and be feasible within reasonable time frames. Several paths forward remain available for food production and eating habits and include maintaining current practices, reducing meat consumption/industrialisation of livestock and the elimination of meat

consumption. Realistically, the elimination of meat and worldwide adoption of vegetarian and/or vegan diets is currently unattainable. Likewise, the continuation of current practices, such as intensive farming and livestock rearing, is not sustainable and poses many risks to climate health. These issues are multi-faceted and involve input from not only the agricultural/animal sciences but economics, nutrition, sustainability, environmental and government sectors. The benefits of a middle-ground approach involving the reduction in daily consumption of meat and scaling back of industrial livestock practices are well-documented and reviewed (McMichael et al., 2007).

Two current solutions to reducing the climate impacts of agriculture already exist and are currently implemented in Europe but have the ability to be greatly expanded through incentive and education. They include the increased use of less commonly harvested grains such as sorghum, alongside the expanded use of enzymes in animal feed using these grains.

Arable land is decreasing throughout Europe due to increased urbanisation; however, future climate changes will accelerate this (EU Agriculture and Rural Development, 2017). As arable land decreases, practices must adapt to better utilise shrinking spaces while maintaining productivity. While wheat is currently the most harvested cereal in Europe, sorghum and other minor cereals are poised to alleviate this burden and perform well in a turbulent future climate (EU Agriculture and Rural Development, 2017). Sorghum has the ability to take root in areas of land not previously used or thought to be arable. While sorghum harvesting and planting is on the rise in Europe, other parts of the world have consistently utilised the grain and worldwide ranks fifth in importance. This production has been traditionally limited to tropical and arid climates, as sorghum is particularly well-suited to these drought-like conditions. While these climates are, for the most part, not typical for Europe, they are potentially the future.

As discussed throughout this thesis, enzyme supplements have been included in animal feed for approximately 40 years. Their primary role as a supplement is to increase the availability of nutrients and reduce antinutritional components in feed, often lower quality grain, which allows for more predictable growth, better utilisation of feed components and optimisation of costs (Walsh et al., 1994). There is also a growing need to reduce the use of animal protein meal in feed due to ethical and health concerns. This loss of protein rich mixture must be substituted by either an amino acid supplement, increased vegetable protein or protease enzyme supplementation. Increased use of vegetable proteins, through grains, has been observed to

lower digestibility and nutrient uptake (Brufau et al., 2006). Exogenous proteases allow the use of grains lower in digestibility thus decreasing the cost of the feed. Similarly, the addition of exogenous phytase is thought to increase overall nutrient utilisation and digestibility through the degradation of anti-nutritional complexes (Liu et al., 2013). An additional benefit beyond nutrition is that phytase increases the availability of phosphorous to animals thus decreasing its excretion into the environment (Kies et al., 2001). European farmers could be encouraged to use feed enzymes more frequently, especially when using potentially lower quality and cost grains. There also remain unexplored opportunities for use of enzymes and additives in feed including more targeted anti-nutrient, lipid and protease products. These solutions include, but are not limited to: polyphenol oxidase, tannase (Schons et al., 2011; Schons et al., 2012; Weihua et al., 2015), laccase, lipid emulsifiers and/or exogenous lipases and proteases to breakdown specific indigestible proteins like kafirin, e.g., subtilisin. Recently, DSM and Novozymes launched the release of their second-generation exogenous feed protease, ProAct 360™ (DSM Animal Nutrition and Health, 2021). This new product contains a completely new enzyme with a broad specificity and the ability to work with endogenous enzyme as well as other exogenous feed enzymes. The enzyme is improved over the first-generation product through more reliable FCR reduction, better amino acid digestibility, enhanced action against anti-nutrient trypsin inhibitors and more effective protein hydrolysis. These improvement to ProAct should enable producers to lower production costs, improve feed efficiency, improve animal welfare and health and continue to lower nitrogen environmental emissions (DSM, 2021). The development and increased use of products like these could indirectly unlock greater animal production gains, increased animal health, decreased environment emissions and improved nutrient utilisation.

Precision agriculture and its associated techniques are another promising area of innovation to help future-proof arable and livestock farming. These technologies involve collecting large amounts of data, using automated machinery and incorporating artificial intelligence/computer modelling/machine learning with the aim of improving efficiency and reducing waste. The arable sector of farming has already benefited greatly from precision agriculture technologies including automated crop robots, soil health monitors and crop monitoring. The uptake in the livestock production sector has been slower, potentially due to the complexities surrounding this kind of farming, namely: animal health and welfare monitoring, diet and nutrition optimisation and production efficiency.

In a comprehensive review of current precision feeding systems, research and thoughts for the future, Moss et al. (2021) provided a strong vision for the future of poultry production, with Australia as a model country. The current state of broiler diet formulation and feeding is based on the principles of having distinct feeding phases for different stages of growth of the bird. These phases are starter, grower, finisher and withdrawal. However, the use of these discrete steps can lead to increased ingredient waste, depression of bird growth and inefficient use of resources. These authors propose a paradigm shift in the way poultry, particularly broiler, diets could be formulated. This shift would involve the daily blending of protein-dense and energy-dense ingredient mixtures formulated on predicted broiler nutrient requirements. The thinking behind this shift revolves around identifying minimum daily nutrient requirements of birds and then tailoring the diet based on that calculation to minimise resource and ingredient loss. This increase in efficiency has environmental benefits as unused nutrients are not wasted, e.g., too much crude protein in diets often ends up as excreted ammonia. While it's not certain whether this change in diet formulation would necessarily improve bird efficiency, i.e., FCR, it would improve nutritional digestibility, overall operating efficiency and reduce the costs of the meat end-product. These tailored diets could be further improved with the addition of ingredient analysis using NIR to assess individual feed components on-site, as opposed to relying on historical values. As Moss et al. (2021) notes, many farms already have the infrastructure in place to allow for precision nutrition but just need slight alterations to current functionalities.

Feed additives, due to their complex natures and formulation requirements, are not currently suitable to this shift in formulation but could become viable in the future. However, this on-demand diet formulation scheme could be applied to the use and inclusion of feed additives like exogenous enzymes. For example, ingredients could be rapidly evaluated for phytate content using NIR spectroscopy (Aureli et al., 2017). Based on the levels detected and the phosphorus requirements of the bird on the current day of growth, the exact amount of exogenous phytase could be included to maximise the degradation of phytate, reduce waste and lower costs.

A decrease in FCR can be realised by directed animal breeding efforts but is most easily controlled and affected through diet manipulation. Challenges that emerge in diet formulation include the management of ingredient components which may compromise digestion and thus limit the ability to lower FCR. These components, anti-nutrients, include phenolics, phytate and indigestible proteins, and can be limited through directed grain breeding programs;

however, these strategies do not always work in the intended way as latent anti-nutrients may remain.

6.4 Conclusions

The goal of this thesis was to investigate the anti-nutritional components of sorghum grain in the context of monogastric animal feed, particularly as it relates to modern poultry production and exogenous feed additives. Sorghum grain can show nutritional variation when formulated into animal diets with exogenous feed enzymes which is only partly understood. This problem is thought to revolve around three unique intrinsic components of the grain: kafirin protein, high levels of phytate and high levels of polyphenols. This thesis focussed on the role polyphenols might play in reducing the quality of modern sorghum-based feeds. Historically, sorghum has long been known to contain very high levels of polyphenols, including large, condensed tannins, which have been clearly linked to anti-nutrition as they bind protein and inhibit endogenous enzyme activity. Because of these clear negative interactions, decades of breeding and selection has resulted in modern sorghum grains being free of large condensed tannins. The full implications of breeding programs on the phenolic profiles of modern grains have not been fully explored. However, formulations containing modern varieties still present with sub-optimal results, often when exogenous feed enzyme supplements are included. The effects of polyphenols, in any kind of grain, on these exogenous enzymes was unknown prior to the work in this thesis.

This thesis sought to better understand what role sorghum non-tannin polyphenols play in suboptimal sorghum feed efficiency and muted exogenous enzyme response. Characterisation of the grain polyphenol extracts indicated possible unintentional consequences of sorghum breeding and selection. Metabolomics is a powerful tool that could be better incorporated into crop breeding methodologies. For the first time, exogenous feed enzymes were found to be directly inhibited by sorghum polyphenol extracts, as well as two tannin extracts. These results provide one possibility for the suboptimal results often observed in poultry fed sorghum diets. Although modern sorghum varieties contain little to no large tannin anti-nutrients, care should be taken when adding exogenous feed enzymes to sorghum-based feed formulations. A more realistic *in vitro* simulated digestion model was used to further evaluate the effects of the sorghum polyphenol extracts and tannin extracts on the efficacy of the two feed enzymes. In

the more complex environment, the negative impacts of the extracts were greatly reduced and eliminated in some cases. However, some negative effects remained, again impressing the importance of taking care when incorporating exogenous enzymes into sorghum diets. While in true feeding scenarios effects may be quite variable with some animals responding positively to sorghum diets and others negatively, the results presented here support the notion that animal feed diets are not constant and immovable parameters but constantly evolving and shifting components of a crucial agricultural system needed to feed billions across the globe.

References

Acamovic, T., (2001). Commercial application of enzyme technology for poultry production. *World's Poultry Science Journal* [online]. **57**(3), 225-242. [16/07/2018]. Available from: doi: 10.1079/WPS20010016.

Acquisgrana, M. del R., Benítez, E.I., Pamies, L.C.G., Sosa, G.L., Peruchena, N.M., Lozano, J.E., (2016). Total polyphenol extraction from red sorghum grain and effects on the morphological structure of starch granules. *International Journal of Food Science and Technology* [online]. **51**(10), 2151-2156. [10/07/2019]. Available from: doi: 10.1111/ijfs.13194.

Adler-Nissen, J., (1979). Determination of the degree of hydrolysis of food protein hydrolysates by trinitrobenzenesulfonic acid. *Journal of Agricultural and Food Chemistry* [online]. **27**(6), 1256-1262. [21/07/2021]. Available from: doi: 10.1021/jf60226a042.

Afify, A.E.-M.M.R., El-Beltagi, S., El-Salam, S.M.A., Omran, A.A. (2011). Bioavailability of Iron, Zinc, Phytate and Phytase Activity during Soaking and Germination of White Sorghum Varieties. *PLoS ONE* [online]. **6**(10), 1-7. [13/11/2019]. Available from: doi: 10.1371/journal.pone.0025512.

Agricultural and Rural Development, Joint Research Centre, (2017). EU Agricultural Outlook for the Agricultural Markets and Income 2017-2030 [online]. European Commission. [01/04/2019] Available from: https://ec.europa.eu/info/sites/info/files/food-farming-fisheries/farming/documents/agricultural-outlook-2017-30_en.pdf.

Aguerre, M.J., Duval, B., Powell, J.M., Vadas, P.A., Wattiaux, M.A., (2020). Effects of feeding a quebracho–chestnut tannin extract on lactating cow performance and nitrogen utilization efficiency. *Journal of Dairy Science* [online]. **103**(3), 2264-2271. [03/05/2021]. Available from: doi: 10.3168/jds.2019-17442.

Ainsworth, E.A., Gillespie, K.M., (2007). Estimation of total phenolic content and other oxidation substrates in plant tissues using Folin–Ciocalteu reagent. *Nature Protocols* [online]. **2**(4), 875-877. [07/16/2018]. Available from: doi: 10.1038/nprot.2007.102.

Aizpurua-Olaizola, O., Ormazabal, M., Vallejo, A., Olivares, M., Navarro, P., Etxebarria, N., Usobiaga, A., (2015). Optimization of Supercritical Fluid Consecutive Extractions of Fatty Acids and Polyphenols from *Vitis Vinifera* Grape Wastes. *Journal of Food Science* [online]. **80**(1), E101-E107. [28/09/2017]. Available from: doi: 10.1111/1750-3841.12715.

Ajila, C.M., Brar, S.K., Verma, M., Tyagi, R.D., Godbout, S., Valéro, J.R., (2011). Extraction and Analysis of Polyphenols: Recent trends. *Critical Reviews in Biotechnology* [online]. **31**(3), 227-249. [02/10/2017]. Available from: doi: 10.3109/07388551.2010.513677.

Akın, P.A., Sezer, B., Bean, S.R., Peiris, K., Tilley, M., Apaydın, H., Boyacı, İ.H., (2021). Analysis of corn and sorghum flour mixtures using laser-induced breakdown spectroscopy. *Journal of the Science of Food and Agriculture* [online]. **101**(3), 1076-1084. [22/03/2021]. Available from: doi: 10.1002/jsfa.10717.

Alhotan, R.A., (2021). Commercial poultry feed formulation: current status, challenges, and future expectations. *World's Poultry Science Journal* [online]. 1-21. [26/04/2021]. Available from: doi: 10.1080/00439339.2021.1891400.

Al-Mamary, M., Al-Habori, M., Al-Aghbari, A., Al-Obeidi, A., (2001). In vivo effects of dietary sorghum tannins on rabbit digestive enzymes and mineral absorption. *Nutrition Research* [online]. **21**(10), 1393-1401. [30/05/2018]. Available from: doi: 10.1016/S0271-5317(01)00334-7.

Alminger, M., Aura, A.-M., Bohn, T., Dufour, C., El, S.N., Gomes, A., Karakaya, S., Martínez-Cuesta, M.C., McDougall, G.J., Requena, T, Santos, C.N., (2014). *In Vitro* Models for Studying Secondary Plant Metabolite Digestion and Bioaccessibility. *Comprehensive Reviews in Food Science and Food Safety* [online]. **13**(4), 413-436. [12/06/2018]. Available from: doi: 10.1111/1541-4337.12081.

Alseekh, S., Scossa, F., Wen, W., Luo, J., Yan, J., Beleggia, R., Klee, H.J., Huang, S., Papa, R., Fernie, A.R., (2021). Domestication of Crop Metabolomes: Desired and Unintended Consequences. *Trends in Plant Science* [online]. **26**(6), 650-661. [13/05/2021]. Available from: doi: 10.1016/j.tplants.2021.02.005.

Alu'datt, M.H., Rababah, T., Alhamad, M.N., Al-Rabadi, G.J., Tranchant, C.C., Almajwal, A., Kubow, S., Alli, I., (2017). Occurrence, types, properties and interactions of phenolic compounds with other food constituents in oil-bearing plants. *Critical Reviews in Food Science and Nutrition* [online]. **8398**, 1-10 [23/07/2018]. Available from: doi: 10.1080/10408398.2017.1391169.

Antal, D.S., Schwaiger, S., Ellmerer-Müller, E.P., Stuppner, H., (2010). *Cotinus coggygria* Wood: Novel Flavanone Dimer and Development of an HPLC/UV/MS Method for the Simultaneous Determination of Fourteen Phenolic Constituents. *Planta Medica* [online]. **76**(15), 1765-1772. [10/02/2020]. Available from: doi: 10.1055/s-0030-1249878.

Arancibia-Avila, P., Namiesnik, J., Toledo, F., Werner, E., Martinez-Ayala, A.L., Rocha-Guzmán, N.E., Gallegos-Infante, J.A., Gorinstein, S., (2012). The influence of different time durations of thermal processing on berries quality. *Food Control* [online]. **26**(2), 587-593. [26/05/2021]. Available from: doi: 10.1016/j.foodcont.2012.01.036.

Armstrong, W.D., Featherston, W.R., Rogler, J.C., (1974). Effects of Bird Resistant Sorghum Grain and Various Commercial Tannins on Chick Performance. *Poultry Science* [online]. **53**(6), 2137-2142. [12/10/2020]. Available from: doi: 10.3382/ps.0532137.

Ashraf-Khorassani, M., Taylor, L.T., (2004). Sequential Fractionation of Grape Seeds into Oils, Polyphenols, and Procyanidins via a Single System Employing CO_2-Based Fluids. *Journal of Agricultural and Food Chemistry* [online]. **52**(9), 2440-2444. [30/05/2018]. Available from: doi: 10.1021/jf030510n.

Asquith, T.N., Izuno, C.C., Butler, L.G., (1983). Characterization of the Condensed Tannin (Proanthocyanidin) from a Group II Sorghum. *Journal of Agricultural and Food Chemistry* [online]. **31**(6), 1299-1303. [10/07/2019]. Available from: doi: 10.1021/jf00120a038.

Aureli, R., Ueberschlag, Q., Klein, F., Noël, C., Guggenbuhl, P., (2017). Use of near infrared reflectance spectroscopy to predict phytate phosphorus, total phosphorus, and crude protein of common poultry feed ingredients. *Poultry Science* [online]. **96**(1), 160-168. [11/05/2021]. Available from: doi: 10.3382/ps/pew214.

Austen, N., (2016). Understanding the Dynamics and Regulation of Biogenic Volatile Organic Compound Emissions by Woody Plants. Ph.D. Thesis, University of Sheffield. [03/04/2020]. Available from: https://ethos.bl.uk/OrderDetails.do?uin=uk.bl.ethos.721851.

Austen, N., Walker, H.J., Lake, J.A., Phoenix, G.K., Cameron, D.D., (2019). The Regulation of Plant Secondary Metabolism in Response to Abiotic Stress: Interactions Between Heat Shock and Elevated CO_2. *Frontiers in Plant Science* [online]. **10**(November), 1-12. [26/03/2020]. Available from: doi: 10.3389/fpls.2019.01463.

Avila, E., Arce, J., Soto, C., Rosas, F., Ceccantini, M., McIntyre, D.R., (2012). Evaluation of an enzyme complex containing nonstarch polysaccharide enzymes and phytase on the performance of broilers fed a sorghum and soybean meal diet. *Journal of Applied Poultry Research* [online]. **21**(2), 279-286. [04/06/2018]. Available from: doi: 10.3382/japr.2011-00382.

Awika, J.M., Dykes, L., Gu, L., Rooney, L.W., Prior, R.L., (2003). Processing of Sorghum (*Sorghum bicolor*) and Sorghum Products Alters Procyanidin Oligomer and Polymer Distribution and Content. *Journal of Agricultural and Food Chemistry* [online]. **51**(18), 5516-5521. [02/11/2017]. Available from: doi: 10.1021/jf0343128.

Awika, J.M., Rooney, L.W., (2004a). Sorghum phytochemicals and their potential impact on human health. *Phytochemistry* [online]. **65**(9), 1199-1221. [10/07/2019]. Available from: doi: 10.1016/j.phytochem.2004.04.001.

Awika, J.M., Rooney, L.W., Waniska, R.D., (2004b). Properties of 3-Deoxyanthocyanins from Sorghum. *Journal of Agricultural and Food Chemistry* [online]. **52**(14), 4388-4394. [09/10/2017]. Available from: doi: 10.1021/jf049653f.

Awika, J.M., McDonough, C.M., Rooney, L.W., (2005). Decorticating Sorghum To Concentrate Healthy Phytochemicals. *Journal of Agricultural and Food Chemistry* [online]. **53**(16), 6230-6234. [09/10/2017]. Available from: doi: 10.1021/jf0510384.

Ayala-Soto, F.E., Serna-Saldívar, S.O., Welti-Chanes, J., Gutierrez-Uribe, J.A., (2015). Phenolic compounds, antioxidant capacity and gelling properties of glucoarabinoxylans from three types of sorghum brans. *Journal of Cereal Science*. [online]. **65**, 277-284. [07/11/2017]. Available from: doi: 10.1016/j.jcs.2015.08.004.

Banda-Nyirenda, D.B.C., Vohra, P., (1990). Nutritional Improvement of Tannin-Containing Sorghums (*Sorghum bicolor*) by Sodium Bicarbonate. *Cereal Chemistry* [online]. **67**(6), 533-537. [26/11/2018]. Available from: https://www.cerealsgrains.org/publications/cc/backissues/1990/Documents/67_533.pdf.

Barrett, A.H., Farhadi, N.F., Smith, T.J., (2018). Slowing starch digestion and inhibiting digestive enzyme activity using plant flavanols/tannins – A review of efficacy and mechanisms. *LWT – Food Science and Technology* [online]. **87**, 394-399. [07/06/2018]. Available from: doi: 10.1016/j.lwt.2017.09.002.

Barros, F., Dykes, L., Awika, J.M., Rooney, L.W., (2013). Accelerated solvent extraction of phenolic compounds from sorghum brans. *Journal of Cereal Science* [online]. **58**(2), 305-312. [19/10/2017]. Available from: doi: 10.1016/j.jcs.2013.05.011.

Batonon-Alavo, D.I., Faruk, M.U., Lescoat, P., Weber, G.M., Bastianelli, D., (2015). Inclusion of sorghum, millet and cottonseed meal in broiler diets: a meta-analysis of effects on performance. *Animal* [online]. **9**(7), 1120-1130. [26/11/2018]. Available from: doi: 10.1017/S1751731115000282.

Baxter, N.J., Lilley, T.H., Haslam, E., Williamson, M.P., (1997). Multiple Interactions between Polyphenols and a Salivary Proline-Rich Protein Repeat Result in Complexation and Precipitation. *Biochemistry* [online]. **36**(18), 5566-5577. [07/06/2018]. Available from: doi: 10.1021/bi9700328.

Bean, S.R., Ioerger, B.P., Wilson, J.D., Tilley, M., Rhodes, D., Herald, T.J., (2018). Structure and chemistry of sorghum grain: *Achieving sustainable cultivation of sorghum, Volume 2: Sorghum utilization around the world.* 1-27. Edited by Rooney, W., Texas A&M University, USA, Burleigh Dodds Science Publishing Ltd.

Bedford, M.R., (1996). Interaction between ingested feed and the digestive system in poultry. *Journal of Applied Poultry Research* [online]. **5**, 86-95. [26/03/2021]. Available from: doi: 10.1093/japr/5.1.86.

Bedford, M.R., Schulze, H., (1998). Exogenous enzymes for pigs and poultry. *Nutrition Research Reviews* [online]. **11**(1), 91-114. [16/07/2018]. Available from: doi: 10.1079/NRR19980007.

Bekalu, Z.E., Madsen, C.K., Dionisio, G., Brinch-Pederson, H., (2017). Aspergillus ficuum phytase activity is inhibited by cereal grain components. *PLoS ONE* [online]. **12**(5), 1-13. [25/02/2018]. Available from: doi: 10.1371/journal.pone.0176838.

Berenji, J., Dahlberg, J., Sikora, V., Latković, D., (2011). Origin, History, Morphology, Production, Improvement, and Utilization of Broomcorn [*Sorghum bicolor* (L.) Moench] in Serbia. *Economic Botany* [online]. **65**(2), 190-208. [12/09/2019]. Available from: doi: 10.1007/s12231-011-9155-2.

Bianchi, S., Kroslakova, I., Janzon, R., Mayer, I., Saake, B., Pichelin, F., (2015). Characterization of condensed tannins and carbohydrates in hot water bark extracts of European softwood species. *Phytochemistry* [online]. **120**, 53-61. [10/11/2017]. Available from: doi: 10.1016/j.phytochem.2015.10.006.

Bianchi, S., Kroslakova, I., Mayer, I., (2016). Determination of Molecular Structures of Condensed Tannins from Plant Tissues Using HPLC-UV Combined with Thiolysis and MALDI-TOF Mass Spectrometry. *Bio-Protocol* [online]. **6**(20), 1-14. [02/11/2017]. Available from: doi: 10.21769/BioProtoc.1975.

Black, J.L., Hughes, R.J., Nielsen, S.G., Tredrea, A.M., MacAlpine, R., van Barneveld, R.J., (2005). The energy value of cereal grains, particularly wheat and sorghum, for poultry. *Proceedings of the Australian Poultry Science Symposium* [online]. **17**, 21-29. [14/06/2018]. Available from: doi: https://ses.library.usyd.edu.au/handle/2123/2284.

Blytt, H.J., Guscar, T.K., Butler, L.G., (1988). Antinutritional effects and ecological significance of dietary condensed tannins may not be due to binding and inhibiting digestive enzymes. *Journal of Chemical Ecology* [online]. **14**(6), 1455-1465. [28/09/2017]. Available from: doi: 10.1007/BF01012417.

Boath, A.S., Grussu, D., Stewart, D., McDougall, G.J., (2012). Berry Polyphenols Inhibit Digestive Enzymes: a Source of Potential Health Benefits? *Food Digestion* [online]. **3**(1-3), 1-7. [28/09/2017]. Available from: doi: 10.1007/s13228-012-0022-0.

Boddu, J., Svabek, C., Sekhon, R., Gevens, A., Nicholson, R.L., Jones, A.D., Pedersen, J.F., Gustine, D.L., Chopra, S., (2004). Expression of a putative *flavonoid 3'-hydroxylase* in sorghum mesocotyls synthesizing 3-deoxyanthocyanidin phytoalexins. *Physiological and Molecular Plant Pathology*. [online]. **65**(2), 101-113. [19/11/2017]. Available from: doi: 10.1016/j.pmpp.2004.11.007.

Bordenave, N., Hamaker, B.R., Ferruzzi, M.G., (2014). Nature and consequences of non-covalent interactions between flavonoids and macronutrients in foods. *Food & Function* [online]. **5**(1), 18-34. [10/11/2017]. Available from: doi: 10.1039/C3FO60263J.

Brandon, M.J., Foo, L.Y., Porter, L.J., Meredith, P., (1982). Proanthocyanidins of barley and sorghum; composition as a function of maturity of barley ears. *Phytochemistry* [online]. **21**(12), 2953-2957. [31/10/2017]. Available from: doi: 10.1016/0031-9422(80)85076-X.

Brás, N.F., Gonçalves, R., Mateus, N., Fernandes, P.A., Ramos, M.J., De Freitas, V., (2010). Inhibition of Pancreatic Elastase by Polyphenolic Compounds. *Journal of Agricultural and Food Chemistry* [online]. **58**(19), 10668-10676. [28/09/2017]. Available from: doi: 10.1021/jf1017934.

Bravo, L., (1998). Polyphenols: Chemistry, Dietary Sources, Metabolism, and Nutritional Significance. *Nutrition Reviews* [online]. **56**(11), 317-333. [28/09/2017]. Available from: doi: 10.1111/j.1753-4887.1998.tb01670.x.

Brufau, J., Francesch, M., Pérez-Vendrell, A.M., (2006). The use of enzymes to improve cereal diets for animal feeding. *Journal of the Science of Food and Agriculture* [online]. **86**, 1705-1713. [24/10/2018]. Available from: doi: 10.1002/jsfa.2557.

Bryden, W.L., Selle, P.H., Cadogan, D.J., Li, X., Muller, N.D., Jordan, D.R., Gidley, M.J., Hamilton, W.D., (2009). *A review of the nutritive value of sorghum for broilers* [online]. Australian Government, Rural Industries Research and Development Corporation [30/05/2018]. Available from: http://www.agrifutures.com.au/wp-content/uploads/publications/09-077.pdf.

Bullard, R.W., Garrison, M.V., Kilburn, S.R., York, J.O., (1980). Laboratory Comparisons of Polyphenols and Their Repellent Characteristics in Bird-Resistant Sorghum Grains. *Journal of Agricultural and Food Chemistry* [online]. **28**(5), 1006-1011. [19/10/2017]. Available from: doi: 10.1021/jf60231a015.

Bullard, R.W., (1988). Characteristics of Bird-Resistance in Agricultural Crops. *Proceedings of the Thirteenth Vertebrate Pest Conference* [online]. **13**, 305-309. [26/11/2018]. Available from: https://escholarship.org/uc/item/0qq0w2fs.

Butler, L. G., (1982). Relative Degree of Polymerization of Sorghum Tannin during Seed Development and Maturation. *Journal of Agricultural and Food* Chemistry. [online]. **30**(6), 1090–1094. [31/10/2017]. Available from: doi: 10.1021/jf00114a021.

Bye, J.W., Cowieson, N.P., Cowieson, A.J., Selle, P.H., Falconer, R.J., (2013). Dual Effects of Sodium Phytate on the Structural Stability and Solubility of Proteins. *Journal of Agricultural and Food Chemistry* [online]. **61**(2), 290-295. [28/09/2017]. Available from: doi: 10.1021/jf303926v.

Cadogan, D., Finn, A., (2010). *Influence of increasing protease supplementation on two different types of sorghum* [online]. Co-operative Research Centre for an Internationally Competitive Pork Industry [02/10/2018].

Cai, X., Yu, J., Xu, L., Liu, R., Yang, J., (2015). The mechanism study in the interactions of sorghum procyanidins trimer with porcine pancreatic α-amylase. *Food Chemistry* [online]. **174**, 291-298. [26/10/2017]. Available from: doi: 10.1016/j.foodchem.2014.10.131.

Cameron, D.D., Coats, A.M., Seel, W.E., (2006). Differential Resistance among Host and Non-host Species Underlies the Variable Success of the Hemi-parasitic Plant *Rhinanthus minor*. *Annals of Botany* [online]. **98**(6), 1289-1299. [15/11/2017]. Available from: doi: 10.1093/aob/mcl218.

Cao, Y., Zhang, X., (2013). Production of long-chain hydroxy fatty acids by microbial conversion. *Applied Microbiology and Biotechnology* [online]. **97**, 3323–3331. [26/05/2021]. Available from: doi: 10.1007/s00253-013-4815-z.

Carrasco, J.M.D., Cabral, C., Redondo, L.M., Viso, N.D.P., Colombatto, D., Farber, M.D., Miyakawa, M.E.F., (2017). Impact of Chestnut and Quebracho Tannins on Rumen Microbiota of Bovines. *BioMed Research International* [online]. **2017**, 9610810. [26/05/2021]. Available from: 10.1155/2017/9610810.

Cervantes, M., Gómez, R., Fierro, S., Barrera, M.A., Morales, A., Araiza, B.A., Zijlstra, R.T., Sánchez, W., Sauer, C., (2011). Ileal digestibility of amino acids, phosphorus, phytate and energy in pigs fed sorghum-based diets supplemented with phytase and Pancreatin®. *Journal of Animal Physiology and Animal Nutrition* [online]. **95**(2), 179-186. [29/04/2021]. Available from: doi: 10.1111/j.1439-0396.2010.01038.x.

Charlton, A.J., Baxter, N.J., Lilley, T.H., Haslam, E., McDonald, C.J., Williamson, M.P., (1996). Tannin interactions with a full-length human salivary proline-rich protein display a stronger affinity than with single proline-rich repeats. *FEBS Letters* [online]. **382**(3), 289-292. [15/11/2017]. Avaliable from: doi: 10.1016/0014-5793(96)00186-X.

Chen, Y.M., Tsao, T.M., Liu, C.C., Huang, P.M., Wang, M.K., (2010). Polymerization of catechin catalyzed by Mn-, Fe- and Al-oxides. *Colloids and Surfaces B: Biointerfaces* [online]. **81**(1), 217-223. [20/07/2021]. Available from: doi: 10.1016/j.colsurfb.2010.07.012.

Cheryan, M., Rackis, J.,(1980). Phytic acid interactions in food systems. *C R C Critical Reviews in Food Science and Nutrition* [online]. **13**(4), 297-335. [21/02/2019]. Available from: doi: 10.1080/10408398009527293.

Chibber, B.A.K., Mertz, E.T., Axtell, J.D., (1980). In Vitro Digestibility of High-Tannin Sorghum at Different Stages of Dehulling. *Journal of Agricultural and Food Chemistry* [online]. **28**(1), 160-161. [12/10/2020]. Available from: doi: 10.1021/jf60227a035.

Childers, D.L., Corman, J., Edwards, M., Elser, J.L., (2011). Sustainability Challenges of Phosphorus and Food: Solutions from Closing the Human Phosphorus Cycle. *BioScience* [online]. **61**(2), 117-124. [27/07/2018]. Available from: doi: 10.1525/bio.2011.61.2.6.

Choct, M., (2006). Enzymes for the feed industry: past, present and future. *World's Poultry Science Journal* [online]. **62**(1), 5-16. [23/07/2018]. Available from: doi: 10.1079/WPS200480.

Chong J., Wishart D.S., Xia J., (2019). Using MetaboAnalyst 4.0 for Comprehensive and Integrative Metabolomics Data Analysis. Current Protocols in Bioinformatics. **68**(1), e86. [25/05/2021]. Available from: doi: 10.1002/cpbi.86.

Cork, S.J., Krockenberger, A.K., (1991). Methods and pitfalls of extracting condensed tannins and other phenolics from plants: Insights from investigations on *Eucalyptus* leaves. *Journal of Chemical Ecology* [online]. **17**(1), 123-134. [15/06/2018]. Available from: doi: 10.1007/BF00994426.

Cowieson, A.J., Hruby, M., Pierson, E.E.M., (2006). Evolving enzyme technology: impact on commercial poultry nutrition. *Nutrition Research Reviews* [online]. **19**(1), 90-103. [28/09/2017]. Available from: doi: 10.1079/NRR2006121.

Cowieson, A.J., Ravindran, V., Selle, P.H., (2008). Influence of Dietary Phytic Acid and Source of Microbial Phytase on Ileal Endogenous Amino Acid Flows in Broiler Chickens. *Poultry Science* [online]. **87**, 2287-2299. [06/05/2020]. Available from: doi: 10.3382/ps.2008-00096.

Cowieson, A.J., Bedford, M.R., Selle, P.H., Ravindran, V., (2009). Phytate and microbial phytase: implications for endogenous nitrogen losses and nutrient availability. *World's Poultry Science Journal* [online]. **65**(3), 401-418. [28/09/2017]. Available from: doi: 10.1017/S0043933909000294.

Cowieson, A.J., Wilcock, P., Bedford, M.R., (2011). Super-dosing effects of phytase in poultry and other monogastrics. *World's Poultry Science Journal* [online]. **67**(2), 225-236. [21/02/2019]. Available from: doi: 10.1017/s0043933911000250.

Cowieson, A.J., Bhuiyan, M.M., Sorbara, J.O.B., Pappenberger, G., Pedersen, M.B., Choct, M., (2020). Contribution of individual broilers to variation in amino acid digestibility in soybean meal and the efficacy of an exogenous monocomponent protease. *Poultry Science* [online]. **99**(2), 1075-1083. [25/02/2020]. Available from: doi: 10.1016/j.psj.2019.10.001.

Dai, J., Mumper, R.J., (2010). Plant Phenolics: Extraction, Analysis and Their Antioxidant and Anticancer Properties. *Molecules* [online]. **15**(10), 7313-7352. [20/04/2018]. Available from: doi: 10.3390/molecules15107313.

Darby, S.J., (2016). An Isothermal Titration Calorimetry Study: Complex Binding Isotherms obtained from the Interaction between Phytate and Tannins with Proteins. PhD Thesis, University of Sheffield. Available from: http://etheses.whiterose.ac.uk/13841/.

Davis, A.B., Hoseney, R.C., (1979). Grain Sorghum Condensed Tannins. I. Isolation, Estimation, and Selective Adsorption by Starch. *Cereal Chemistry* [online]. **56**(4), 310-314. [27/09/2018]. Available from: https://www.cerealsgrains.org/publications/cc/backissues/1979/Documents/chem56_310.pdf.

de Freitas, V., Mateus, N., (2011). Formation of pyranoanthocyanins in red wines: a new and diverse class of anthocyanin derivatives. *Analytical and Bioanalytical Chemistry* [online]. **401**(5), 1467-1477. [10/02/2020]. Available from: doi: 10.1007/s00216-010-4479-9.

DelMar, E.G., Largman, C., Brodrick, J.W., Geokas, M.C., (1979). A Sensitive New Substrate For Chymotrypsin. *Analytical Biochemistry* [online]. **99**(2), 316-320. [10/07/2019]. Available from: doi: 10.1016/S0003-2697(79)80013-5.

de O. Buanafina, M.M., (2009). Feruloylation in Grasses: Current and Future Perspectives. *Molecular Plant* [online]. **2**(5), 861-872. [27/09/2019]. Available from: doi: 10.1093/mp/ssp067.

Dersjant-Li, Y., Awati, A., Schulze, H., Partridge, G., (2015). Phytase in non-ruminant animal nutrition: a critical review on phytase activities in the gastrointestinal tract and influencing factors. *Journal of the Science of Food and Agriculture* [online]. **95**(5), 878-896. [11/01/2018]. Available from: doi: 10.1002/jsfa.6998.

de Villiers, A., Venter, P., Pasch, H., (2016). Recent advances and trends in the liquid-chromatography–mass spectrometry analysis of flavonoids. *Journal of Chromatography A* [online]. **1430**, 16-78. [31/10/2017]. Available from: doi: 10.1016/j.chroma.2015.11.077.

Diao, X., (2017). Production and genetic improvement of minor cereals in China. *The Crop Journal* [online]. **5**(2), 103-114. [29/04/2021]. Available from: doi: 10.1016/j.cj.2016.06.004.

Díaz-Reinoso, B., Moure, A., Domínguez, H., Parajó, J.C., (2006). Supercritical CO_2 Extraction and Purification of Compounds with Antioxidant Activity. *Journal of Agricultural and Food Chemistry* [online]. **54**(7), 2441-2469. [02/10/2017]. Available from: doi: 10.1021/jf052858j.

Dicko, M.H., Hilhorst, R., Gruppen, H., Traore, A.S., Laane, C., van Berkey, W.J.H., Voragen, A.G.J., (2002). Comparison of Content in Phenolic Compounds, Polyphenol Oxidase, and Peroxidase in Grains of Fifty Sorghum Varieties from Burkina Faso. *Journal of Agriculture and Food Chemistry*. [online]. **50**(13), 3780-3788. [19/10/2017]. Available from: doi: 10.1021/jf011642o.

Dixit, V.S., Pant, A., (2000). Comparative characterization of two serine endopeptidases from *Nocardiopsis* sp. NCIM 5124. *Biochimica et Biophysica Acta – General Subjects* [online]. **1523**(2-3), 261-268. [26/03/2018]. Available from: doi: 10.1016/S0304-4165(00)00132-X.

Djande, C.Y.H., Pretorius, C., Tugizimana, F., Piater, L.A., Dubery, I.A., (2020). Metabolomics: A Tool for Cultivar Phenotyping and Investigation of Grain Crops. *Agronomy* [online]. **10**(831), 1-28. [09/03/2021]. Available from: doi: 10.3390/agronomy10060831.

Dosković, V., Bogosavljević-Bosković, S., Pavlovski, Z., Milošević, B., Škrbić, Z., Rakonjac, S., Petričević, V., (2013). Enzymes in broiler diets with special reference to protease. *World's Poultry Science Journal* [online]. **69**(2), 343-360. [23/07/2018]. Available from: doi: 10.1017/S0043933913000342.

dos Santos, T.T., O'Neil, H.V.M, González-Ortiz, G., Camacho-Fernández, D., López-Coello, C., (2017). Xylanase, protease and superdosing phytase interactions in broiler performance, carcass yield and digesta transit time. *Animal Nutrition* [online]. **3**(2), 121-126. [28/09/2017] Available from: doi: 10.1016/j.aninu.2017.02.001.

DSM Animal Nutrition and Health, (2021). ProAct 360™ [Viewed 21 July 2021]. Available from: https://www.dsm.com/anh/en_US/products/feed-enzymes/protease/proact-360.html.

Duodu, K.G., Tang, H., Grant, A., Wellner, N., Belton, P.S., Taylor, J.R.N., (2001). FTIR and Solid State ^{13}C NMR Spectroscopy of Proteins of Wet Cooked and Popped Sorghum and Maize. *Journal of Cereal Science*. [online] **33**(3), 261-269. [24/05/2019]. Available from: doi: 10.1006/jcrs.2000.0352.

du Plessis, I.J., (2014). Flavonoid compounds of sorghum and maize bran and their inhibitory effects against alpha-amylase. MSc. Thesis, University of Pretoria. [17/10/2017]. Available from: doi: http://hdl.handle.net/2263/43324.

Dykes, L., Rooney, L.W., (2007). Phenolic Compounds in Cereal Grains and Their Health Benefits. *Cereal Foods World* [online]. **52**(3), 105-111. [24/08/2018]. Available from: doi: 10.1094/CFW-52-3-0105.

Dykes, L., Rooney, W.L., Rooney, L.W., (2013). Evaluation of phenolics and antioxidant activity of black sorghum hybrids. *Journal of Cereal Science* [online]. **58**(2), 278-283. [31/10/2017]. Available from: doi: 0.1016/j.jcs.2013.06.006.

Dykes, L., Hoffmann Jr., L., Portillo-Rodriguez, O., Rooney, W.L., Rooney, L.W., (2014). Prediction of total phenols, condensed tannins, and 3-deoxyanthocyanidins in sorghum grain using near-infrared (NIR) spectroscopy. *Journal of Cereal Science* [online]. **60**, 138-142. [11/01/2018]. Available from: doi: 10.1016/j.jcs.2014.02.002.

Eisath, N.G., Sturm, S., Stuppner, H., (2017). Supercritical Fluid Chromatography in Natural Product Analysis – An Update. *European Journal of Integrative Medicine* [online]. **6**(6), 1-11. [14/10/2017]. Available from: doi: 10.1016/j.eujim.2014.09.033.

Elkin, R.G., Freed, M.B., Hamaker, B.R., Zhang, Y., Parsons, C.M., (1996). Condensed Tannins Are Only Partially Responsible for Variations in Nutrient Digestibilities of Sorghum Grain Cultivars. *Journal of Agricultural and Food Chemistry* [online]. **44**(3), 848-853. [12/10/2020]. Available from: doi: 10.1021/jf950489t.

Erdaw, M.M., Perez-Maldonado, R.A., Iji, P.A., (2017). Apparent and standardized ileal nutrient digestibility of broiler diets containing varying levels of raw full-fat soybean and microbial protease. *Journal of Animal Science and Technology* [online]. **59**, 23. [10/07/2019]. Available from: doi: 10.1186/s40781-017-0148-2.

Falcão, L., Araújo, M.E.M., (2013). Tannins characterization in historic leathers by complementary analytical techniques ATR-FTIR, UV-Vis and chemical tests. *Journal of Cultural Heritage* [online]. **14**(6), 499-508. [07/10/2020]. Available from: doi: 10.1016/j.culher.2012.11.003.

Falcão, L., Araújo, M.E.M., (2014). Application of ATR-FTIR spectroscopy to the analysis of tannins in historic leathers: The case study of the upholstery from the 19th century Portuguese Royal Train. *Vibrational Spectroscopy* [online]. **74**, 98-103. [24/05/2019]. Available from: doi: 10.1016/j.vibspec.2014.08.001.

Falconer, R.J., Penkova, A., Jelesarov, I., Collins, B.M., (2010). Survey of the year 2008: Applications of isothermal titration calorimetry. *Journal of Molecular Recognition* [online]. **23**(5), 395-413. [28/09/2017]. Available from: doi: 10.1002/jmr.1025

Falconer, R.J., Collins, B.M., (2011). Survey of the year 2009: applications of isothermal titration calorimetry. *Journal of Molecular Recognition* [online]. **24**(1), 1-16. [28/09/2017]. Available from: doi: 10.1002/jmr.1073.

Falconer, R.J., (2016). Applications of isothermal titration calorimetry – the research and technical developments from 2011 to 2015. *Journal of Molecular Recognition* [online]. **29**(May), 504-515. [28/09/2017]. Available from: doi: 10.1002/jmr.2550.

Feng, Y., Lv, M., Lu, Y., Liu, K., Liu, L., He, Z., Wu, K., Wang, X., Zhang, B., Wu, X., (2018). Characterization of binding interactions between selected phenylpropanoid glycosides and trypsin. *Food Chemistry* [online]. **243**(August 2017), 118-124. [26/10/2017]. Available from: doi: 10.1016/j.foodchem.2017.09.118.

Fernández-Ponce, M.T., Casas, L., Mantell, C., de la Ossa, E.M., (2014). Fractionation of *Mangifera indica Linn* polyphenols by reverse phase supercritical fluid chromatography (RP-SFC) at pilot plant scale. *Journal of Supercritical Fluids* [online]. **95**, 444-456. [04/10/2017]. Available from: doi: 10.1016/j.supflu.2014.10.005.

Foo, L., Porter, L.J, (1980). The phytochemistry of proanthocyanidin polymers. *Phytochemistry* [online]. **19**(8), 1747-1754. [31/10/2017]. Available from: doi: 10.1016/S0031-9422(00)83807-8.

Food and Agriculture Organization of the United Nations, (2019). FAOSTAT [Viewed 25 May 2021]. Available from: http://www.fao.org/faostat/en/#data.

Frazier, R.A., Papadopoulou, A., Green, R.J., (2006). Isothermal titration calorimetry study of epicatechin binding to serum albumin. *Journal of Pharmaceutical and Biomedical Analysis* [online]. **41**(5), 1602-1605. [28/09/2017]. Available from: doi: 10.1016/j.jpba.2006.02.004.

Ganzera, M., (2015). Supercritical fluid chromatography for the separation of isoflavones. *Journal of Pharmaceutical and Biomedical Analysis* [online]. **107**, 364-369. [17/10/2017]. Available from: doi: 10.1016/j.jpba.2015.01.013.

García-Estévez, I., Cruz, L., Oliveira, J., Mateus, N., de Freitas, V., Soares, S., (2017). First evidences of interaction between pyranoanthocyanins and salivary proline-rich proteins. *Food Chemistry* [online]. **228**, 574-581. [30/05/2018]. Available from: doi: 10.1016/j.foodchem.2017.02.030.

Geera, B., Ojwang, L.O., Awika, J.M., (2012). New Highly Stable Dimeric 3-Deoxyanthocyanidin Pigments from *Sorghum bicolor* Leaf Sheath. *Journal of Food Science* [online]. **77**(5), C566-C572. [26/11/2018]. Available from: doi: 10.1111/j.1750-3841.2012.02668.x.

Ghai, R., Falconer, R.J., Collins, B.M., (2012). Applications of isothermal titration calorimetry in pure and applied research-survey of the literature from 2010. *Journal of Molecular Recognition* [online]. **25**, 32-52. [28/09/2017]. Available from: doi: 10.1002/jmr.1167.

Gilani, G.S., Xiao, C.W., Cockell, K.A., (2012). Impact of Antinutritional Factors in Food Proteins on the Digestibility of Protein and the Bioavailability of Amino Acids and on Protein Quality. *British Journal*

of Nutrition [online]. **108**(Suppl 2), S315-S332. [10/07/2019]. Available from: doi: 10.1017/S0007114512002371.

Glennie, C.W., Kaluza, W.Z., van Niekerk, P.J., (1981). High-Performance Liquid Chromatography of Procyanidins in Developing Sorghum Grain. *Journal of Agricultural and Food Chemistry* [online]. **29**(5), 965-968. [10/11/2017]. Available from: doi: 10.1021/jf00107a020.

Glitsø, V., Pontoppidan, K., Knap, I., Ward, N., (2012). Catalyzing Innovation – Development of a Feed Protease. *Industrial Biotechnology* [online]. **8**(4), 172-175. [05/08/2019]. Available from: doi: 10.1089/ind.2012.1531.

Goel, M., Sharma, C.B., (1979). Inhibition of plant phytases by phloroglucinol. *Phytochemistry* [online]. **18**(6), 939-942. [30/05/2018]. Available from: doi: 10.1016/S0031-9422(00)91453-5.

Goldstein, J.L., Swain, T., (1965). The Inhibition of Enzymes by Tannins. *Phytochemistry* [online]. **4**, 185-192. [27/09/2018]. Available from: doi: 10.1016/S0031-9422(00)86162-2.

Gómez-Cordovés, C., Bartolomé, B., Vieira, W., Virador, V. M., (2001). Effects of wine phenolics and sorghum tannins on tyrosinase activity and growth of melanoma cells. *Journal of Agricultural and Food Chemistry* [online]. **49**(3), 1620-1624. [30/05/2018]. Available from: doi: 10.1021/jf001116h.

Gonçalves, R., Soares, S., Mateus, N., De Freitas, V., (2007). Inhibition of Trypsin by Condensed Tannins and Wine. *Journal of Agricultural and Food Chemistry* [online]. **55**(18), 7596-7601. [28/09/2017]. Available from: doi: 10.1021/jf071490i.

Grasel, F., Ferrao, M.F., Wolf, C.R., (2016). Ultraviolet spectroscopy and chemometrics for the identification of vegetable tannins. *Industrial Crops and Products* [online]. **91**, 279-285. [30/05/2019]. Available from: doi: 10.1016/j.indcrop.2016.07.022.

Griffiths, D.W., (1979). The Inhibition of Digestive Enzymes by Extracts of Field Bean (*Vicia faba*). *Journal of the Science of Food and Agriculture* [online]. **30**(5), 458-462. [05/06/2020]. Available from: doi: 10.1002/jsfa.2740300503.

Griffiths, D.W., Moseley, G., (1980). The Effect of Diets Containing Field Beans of High or Low Polyphenolic Content on the Activity of Digestive Enzymes in the Intestines of Rats. *Journal of the Science of Food and Agriculture* [online]. 31, 255-259. [22/03/2018]. Available from: doi: 10.1002/jsfa.2740310307.

Gu, L., Kelm, M., Hammerstone, J.F., Beecher, G., Cunningham, D., Vannozzi, S., Prior, R.L., (2002). Fractionation of Polymeric Procyanidins from Lowbush Blueberry and Quantification of Procyanidins in Selected Foods with an Optimized Normal-Phase HPLC−MS Fluorescent Detection Method. *Journal of Agricultural and Food Chemistry* [online]. **50**(17), 4852-4860. [10/11/2017]. Available from: doi: 10.1021/jf020214v.

Gu, L., Kelm, M.A., Hammerstone, J.F., Beecher, G., Holden, J., Haytowitz, D., Prior, R.L., (2003). Screening of Foods Containing Proanthocyanidins and Their Structural Characterization Using LC-MS/MS and Thiolytic Degradation. *Journal of Agricultural and Food Chemistry* [online]. **51**(25), 7513-7531. [10/11/2017]. Available from: doi: 10.1021/jf034815d.

Gu, L., Kelm, M.A., Hammerstone, J.F., Beecher, G., Holden, J., Haytowitz, D., Gebhardt, S., Prior, R.L., (2004). Concentrations of Proanthocyanidins in Common Foods and Estimations of Normal Consumption. *The Journal of Nutrition* [online]. **134**(3), 613-617. [02/11/2017]. Available from: doi: 10.1093/jn/134.3.613.

Gualtieri, M., Rappaccini, S., (1990). Sorghum grain in poultry feeding. *World's Poultry Science Journal* [online]. **46**(3), 246-254. [07/06/2018]. Available from: doi: 10.1079/WPS19900024.

Gujer, R., Magnolato, D., Self, R., (1986). Glucosylated flavonoids and other phenolic compounds from sorghum. *Phytochemistry*. [online]. **25**(6), 1431-1436. [31/10/2017]. Available from: doi: 10.1016/S0031-9422(00)81304-7.

Hagerman, A.E., Butler, L.G., (1981). The Specificity of Proanthocyanidin-Protein Interactions. *Journal of Biological Chemistry* [online]. **256**(9), 4494-4497. [31/10/2017]. Available from: https://www.jbc.org/content/256/9/4494.long.

Hagerman, A.E., Rice, M.E., Ritchard, N.T., (1998). Mechanisms of protein precipitation for two tannins, pentagalloyl glucose and epicatechin$_{16}$ (4→8) catechin (procyanidin). *Journal of Agricultural and Food Chemistry* [online]. **46**(7), 2590-2595. [10/11/2017]. Available from: doi: 10.1021/jf971097k.

Hahn, D.H., Faubion, J.M., Rooney, L.W., (1983). Sorghum Phenolic Acids, Their High Performance Liquid Chromatography Separation and Their Relation to Fungal Resistance. *Cereal Chemistry* [online]. **60**(4), 255-259. [31/10/2017]. Available from: https://www.cerealsgrains.org/publications/cc/backissues/1983/Documents/chem60_255.pdf.

Hammerstone J.F., Lazarus S.A., Mitchell A.E., Rucker R., Schmitz H.H., (1999). Identification of procyanidins in cocoa (*Theobroma cacao*) and chocolate using high-performance liquid chromatography/mass spectrometry. *Journal of Agricultural and Food Chemistry* [online]. **47**(2), 490-496. [25/05/2021]. Available from: doi: 10.1021/jf980760h.

Hansen, L.D., Transtrum, M.K., Quinn, C., Demarse, N., (2016). Enzyme-catalyzed and binding reaction kinetics determined by titration calorimetry. *Biochimica et Biophysica Acta – General Subjects* [online]. **1860**(5), 957-966. [30/11/2017]. Available from: doi: 10.1016/j.bbagen.2015.12.018.

Harbertson, J.F., Kilmister, R.L., Kelm, M.A., Downey, M.O., (2014). Impact of condensed tannin size as individual and mixed polymers on bovine serum albumin precipitation. *Food Chemistry* [online]. **160**(October), 16-21. [19/11/2017]. Available from: doi: 10.1016/j.foodchem.2014.03.026.

Haskins, F.A., Gorz, H.J., (1985). Dhurrin and *p*-hydroxybenzaldehyde in seedlings of various *sorghum* species. *Phytochemistry* [online]. **24**(3), 597-598. [17/10/2017]. Available from: doi: 10.1016/S0031-9422(00)80775-X.

Haslam, E., (1989). *Plant polyphenols: Vegetable tannins revisited*. Cambridge: Cambridge University Press.

Hatfield, R.D., Rancour, D.M., Marita, J.M., (2017). Grass Cell Walls: A Story of Cross-Linking. *Frontiers in Plant Science* [online]. **7**(2056), 1-15. [12/09/2019]. Available from: doi: 10.3389/fpls.2016.02056.

Hayasaka, Y., Waters, E.J., Cheynier, V., Herderich, M.J., Vidal, S., (2003). Characterization of proanthocyanidins in grape seeds using electrospray mass spectrometry. *Rapid Communications in Mass Spectrometry* [online]. **17**(1), 9-16. [10/07/2019]. Available from: doi: 10.1002/rcm.869.

He, M., Zeng, J., Zhai, L., Liu, Y., Wu, H., Zhang, R., Li, Z., Xia, E., (2017). Effect of *in vitro* simulated gastrointestinal digestion on polyphenol and polysaccharide content and their biological activities among 22 fruit juices. *Food Research International* [online]. **102**(June), 156-162. [25/10/2018]. Available from: doi: 10.1016/j.foodres.2017.10.001.

Helal, A., Tagliazucchi, D., Verzelloni, E., Conte, A., (2014). Bioaccessibility of polyphenols and cinnamaldehyde in cinnamon beverages subjected to in vitro gastro-pancreatic digestion. *Journal of Functional Foods* [online]. **7**(1), 506-516. [07/09/2018]. Available from: doi: 10.1016/j.jff.2014.01.005.

Hodges, H., Cowieson, A., Falconer, R., Cameron, D., (2020). Chemical profile and effects of modern Australian sorghum polyphenolic-rich extracts on feed phytase and protease activity. *Proceedings of the Australian Poultry Science Symposium* [online]. **31**, 76-79. [28/05/2020]. Available from: doi: https://az659834.vo.msecnd.net/eventsairaueprod/production-usyd-public/8f563f4140d24984879bd01be567dfc2.

Hodges, H.E., Walker, H.J., Cowieson, A.J., Falconer, R.J., Cameron, D.D., (2021). Latent Anti-nutrients and Unintentional Breeding Consequences in Australian *Sorghum bicolor* Varieties. *Frontiers in Plant Science* [online]. **12**(625260), 1-12. [01/03/2021]. Available from: doi:10.3389/fpls.2021.625260.

Horigome, T., Kumar, R., Okamoto, K., (1988). Effects of condensed tannins prepared from leaves of fodder plants on digestive enzymes in vitro and in the intestine of rats. *The British Journal of Nutrition* [online]. **60**(2), 275-285. [19/03/2018]. Available from: 10.1079/BJN19880099.

Howell, H., Malan, E., Brand, D.J., Kamara, B.I., Bezuidenhoudt, B.C.B., Marais, C., Steenkamp, J.A., (2007). Two new promelacacinidin dimers, including a novel flavanone-flavanol dimer characterized by a unique c(3)-c(4) linkage, from the heartwood of *Acacia nigrescens. Chemistry of Natural Compounds* [online]. **43**(5), 533-538. [10/02/2020]. Available from: doi: 10.1007/s10600-007-0184-0.

Huang, H., Zhao, M., (2008). Changes of trypsin in activity and secondary structure induced by complex with trypsin inhibitors and tea polyphenol. *European Food Research and Technology*. **227**, 2, 361-365. [25/07/2018]. Available from: doi: 10.1007/s00217-007-0729-2.

Hulan, H.W., Proudfoot, F.G., (1982). Nutritive value of sorghum grain for broiler chickens. *Canadian Journal of Animal Science* [online]. **62**, 869-875. [01/06/2020]. Avaliable from: https://www.nrcresearchpress.com/doi/pdfplus/10.4141/cjas82-105.

Hutchinson, E.G., Thornton, J.M., (1994). A revised set of potential for β-turn formation in proteins. *Protein Science* [online]. **3**(12), 2207-2216. [12/04/2019]. Available from: doi: 10.1002/pro.5560031206.

Ignat, I., Volf, I., Popa, V.I., (2011). A critical review of methods for characterisation of polyphenolic compounds in fruits and vegetables. *Food Chemistry* [online]. **126**(4), 1821-1835. [14/11/2017]. Available from: doi: 10.1016/j.foodchem.2010.12.026.

Irondi, E.A., Adegoke, B.M., Effion, E.S., Oyewo, S.O., Alamu, E.O., Boligon, A.A., (2019). Enzymes inhibitory property, antioxidant activity and phenolics profile of raw and roasted red sorghum grains *in vitro*. *Food Science and Human Wellness* [online]. **8**(2), 142-148. [07/01/2020]. Available from: doi: 10.1016/j.fshw.2019.03.012.

Jacob, J.P., Mitaru, B.N., Mbugua, P.N., Blair, R., (1996). The effect of substituting Kenyan Serena sorghum for maize in broiler starter diets with different dietary crude protein and methionine levels. *Animal Feed Science and Technology* [online]. **61**, 27-39. [14/10/2020]. Available from: doi: 10.1016/0377-8401(96)00955-8.

Jambunathan, R., Mertz, E.T., (1973). Relationship between Tannin Levels, Rat Growth, and Distribution of Proteins in Sorghum. *Journal of Agricultural and Food Chemistry* [online]. **21**(4), 692-696. [31/10/2017]. Available from: doi: 10.1021/jf60188a027.

Jansman, A.J.M., (1993). Tannins in Feedstuffs for Simple-Stomached Animals. *Nutrition Research Reviews* [online]. **6**, 209-236. [10/07/2019]. Available from: doi: 10.1079/NRR19930013.

Jensen, J.S., Egebo, M., Meyer, A.S., (2008). Identification of Spectral Regions for the Quantification of Red Wine Tannins with Fourier Transform Mid-Infrared Spectroscopy. *Journal of Agricultural and Food Chemistry* [online]. **56**(10), 3493-3499. [26/05/2021]. Available from: doi: 10.1021/jf703573f.

Jiang, Y., Zhang, H., Qi, X., Wu, G., (2020). Structural characterization and antioxidant activity of condensed tannins fractionated from sorghum grain. *Journal of Cereal Science* [online]. **92**(102918), 1-9. [28/01/2020]. Available from: doi: 10.1016/j.jcs.2020.102918.

Joint Food and Agriculture Organisation of the United Nation/World Health Organisation Expert Committee on Food Additives, (2013). *Compendium of Food Additive Specifications* 13 [online]. Rome: Food and Agriculture Organization of the United Nations. [19/02/2018]. Available from: http://www.fao.org/fileadmin/user_upload/agns/pdf/JECFA_Monograph_13.pdf.

Juhaimi, F.A., Şimşek, S., Ghafoor, K., Babiker, E.E., Özcan, M.M., Ahmed, I.A.M., Alsawmahi, O., (2019). Effect of Varieties on Bioactive Properties and Mineral Contents of Some Sorghum, Millet and Lupin Seeds. *Journal of Oleo Science* [online]. **68**(11), 1063-1071. [04/06/2020]. Available from: doi: 10.5650/jos.ess19113.

Kamangerpour, A., Ashraf-Khorassani, M., Taylor, L.T., McNair, H.M., Chorida, L., (2002). Supercritical Fluid Chromatography of Polyphenolic Compounds in Grape Seed Extract. *Chromatographia* [online]. **55**, 417-421. [04/10/2017]. Available from: doi: 10.1007/BF02492270.

Kanehisa M., Goto S., (2000). KEGG: Kyoto Encyclopedia of genes and genomes. *Nucleic Acids Research* [online]. **28**(1), 27-30. [25/05/2021]. Available from: doi: 10.1093/nar/28.1.27.

Kang, J., Price, W.E., Ashton, J., Tapsell, L.C., Johnson, S., (2016). Identification and characterization of phenolic compounds in hydromethanolic extracts of sorghum wholegrains by LC-ESI-MS^n. *Food Chemistry* [online]. **211**, 215-226. [19/10/2017]. Available from: doi: 10.1016/j.foodchem.2016.05.052.

Karonen, M., Oraviita, M., Mueller-Harvey, I., Salminen, J-P., Green, R.J., (2015). Binding of an Oligomeric Ellagitannin Series to Bovine Serum Albumin (BSA): Analysis by Isothermal Titration Calorimetry (ITC). *Journal of Agricultural and Food Chemistry* [online]. **63**(49), 10647-10654. [19/11/2017]. Available from: doi: 10.1021/acs.jafc.5b04843.

Kaspar, P., Möller, G., Wahlefeld, A., (1984). New Photometric Assay for Chymotrypsin in Stool. *Clinical Chemistry* [online]. **30**(11), 1753-1757. [10/07/2019]. Available from: doi: 10.1093/clinchem/30.11.1753.

Kaspchak, E., Mafra, L.I., Mafra, M.R., (2018). Effect of heating and ionic strength on the interaction of bovine serum albumin and the antinutrients tannic and phytic acids, and its influence on in vitro protein digestibility. *Food Chemistry* [online]. **252**, 1-8. [18/01/2018]. Available from: doi: 10.1016/j.foodchem.2018.01.089.

Kaufman, R.C., Tilley, M., Bean, S.R., Tuinstra, M.R., (2009). Improved Characterization of Sorghum Tannins Using Size-Exclusion Chromatography. *Cereal Chemistry* [online]. **86(**4), 369-371. [02/11/2017]. Available from: doi: 10.1094/CCHEM-86-4-0369.

Kaufman, R.C., Herald, T.J., Bean, S.R., Wilson, J.D., Tuinstra, M.R., (2013). Variability in tannin content, chemistry and activity in a diverse group of tannin containing sorghum cultivars. *Journal of the Science of Food and Agriculture* [online]. **93**(5), 1233-1241. [07/11/2017]. Available from: doi: 10.1002/jsfa.5890.

Kebreab, E., Hansen, A.V., Strathe, A.B., (2012). Animal production for efficient phosphate utilization: from optimized feed to high efficiency livestock. *Current Opinion in Biotechnology* [online]. **23**(6), 872-877. [16/07/2018]. Available from: doi: 10.1016/j.copbio.2012.06.001.

Kelch, B.A., Eagen, K.P., Erciyas, F.P., Humphris, E.L., Thomason, A.R., Mitsuiki, S., Agard, D.A., (2007). Structural and Mechanistic Exploration of Acid Resistance: Kinetic Stability Facilitates Evolution of Extremophilic Behavior. *Journal of Molecular Biology* [online]. **368**(3), 870-883. [26/03/2018]. Available from: doi: 10.1016/j.jmb.2007.02.032.

Kempapidis, T., (2019). Relationship between digestive enzymes, proteins and anti-nutritive factors in monogastric digestion. Ph.D. Thesis, University of Sheffield. [10/02/2020].

Kempapidis, T., Bradshaw, N.J., Hodges, H.E., Cowieson, A.J., Cameron, D.D., Falconer, R.J., (2020). Phytase Catalysis of Dephosphorylation Studied using Isothermal Titration Calorimetry and Electrospray Ionization Time-of-Flight Mass Spectroscopy. *Analytical Biochemistry* [online]. **606**, 113859. [07/08/2020]. Available from: doi: 10.1016/j.ab.2020.113859.

Khalil, A., Baltenweck-Guyot, R., Ocampo-Torres, R., Albrecht, P., (2010). A novel symmetrical pyrano-3-deoxyanthocyanidin from a *Sorghum* species. *Phytochemistry Letters*. [online]. **3**(2), 93-95. [19/10/2017]. Available from: doi: 10.1016/j.phytol.2010.02.003.

Khoddami, A., Mohammadrezaei, M., Robert, T.H., (2017). Effects of Sorghum Malting on Colour, Major Classes of Phenolics and Individual Anthocyanins. *Molecules* [online]. **22**(10), 1713-1729. [31/10/2017]. Available from: doi: 10.3390/molecules22101713.

Kido, H., Fukusen, N., Katunuma, N., (1984). Inhibition of Chymase Activity by Long Chain Fatty Acids. *Archives of Biochemistry and Biophysics* [online]. **230**(2), 610-614. [04/06/2020]. Available from: doi: 10.1016/0003-9861(84)90442-9.

Kies, A.K., Van Hemert, K.H.F., Sauer, W.C., (2001). Effect of phytase on protein and amino acid digestibility and energy utilisation. *World's Poultry Science Journal* [online]. **57**(2), 109-126. [16/07/2018]. Available from: doi: 10.1079/WPS20010009.

Kies, A.K., De Jonge, L.H., Kemme, P.A., Jongbloed, A.G., (2006). Interaction between Protein, Phytate, and Microbial Phytase. In Vitro Studies. *Journal of Agricultural and Food Chemistry* [online]. **54**(5), 1753-1758. [19/06/2019]. Avaliable from: doi: 10.1021/jf0518554.

Kilmister, R.L., Faulkner, P., Downey, M.O., Darby, S.J., Falconer, R.J., (2016). The complexity of condensed tannin binding to bovine serum albumin – An isothermal titration calorimetry study. *Food Chemistry* [online]. **190**, 173-178. [28/09/2017]. Available from: doi: 10.1016/j.foodchem.2015.04.144.

Krueger, C.G., Vestling, M.M., Reed, J.D., (2003). Matrix-Assisted Laser Desorption/Ionization Time-of-Flight Mass Spectrometry of Heteropolyflavan-3-ols and Glucosylated Heteropolyflavans in Sorghum [*Sorghum bicolor* (L.) Moench]. *Journal of Agricultural and Food Chemistry*. [online] **51**(3), 538-543. [30/05/2018]. Available from: doi: 10.1021/jf020746b.

Kruger, J., Oelofse, A., Taylor, J.R.N., (2014). Effects of aqueous soaking on the phytate and mineral contents and phytate:mineral ratios of wholegrain normal sorghum and maize and low phytate sorghum. *International Journal of Food Sciences and Nutrition* [online]. **65**(5), 539-546. [13/11/2019]. Available from: doi: 10.3109/09637486.2014.886182.

Kumar, R., Singh, M., (1984). Tannins: Their Adverse Role in Ruminant Nutrition. *Journal of Agricultural and Food Chemistry* [online]. **32**(3), 447-453. [06/05/2020]. Available from: doi: 10.1021/jf00123a006.

Laghi, L., Parpinello, G.P., Del Rio, D., Calani, L., Mattioli, A.U., Versari, A., (2010). Fingerprint of enological tannins by multiple techniques approach. *Food Chemistry* [online]. **121**(3), 783-788. [30/05/2019]. Available from: doi: 10.1016/j.foodchem.2010.01.002.

Langer, S., Marshall, L.J., Day, A.J., Morgan, M.R.A., Flavanols and Methylxanthines in Commercially Available Dark Chocolate: A Study of the Correlation with Nonfat Cocoa Solids. *Journal of Agricultural and Food Chemistry* [online]. 59(15), 8435-8441. [25/05/2021]. Available from: doi: 10.1021/jf201398t.

Li, A., Jia, S., Yobi, A., Ge, Z., Sato, S.J., Zhang, C., Angelovici, R., Clemente, T.E., Holding, D.R., (2018). Editing of an alpha-kafirin gene family increases digestibility and protein quality in sorghum. *Plant Physiology* [online]. **177**(4), 1425-1438. [22/11/2019]. Available from: doi: 10.1104/pp.18.00200.

Lim, D., Golovan, S., Forsberg, C.W., Jia, Z., (2000). Crystal structures of *Escherichia coli* phytase and its complex with phytate. *Nature Structural Biology* [online]. **7**(2), 108-113. [25/03/2019]. Available from: doi: 10.1038/72371.

Lin, H., Bean, S.R., Tilley, M., Peiris, K.H.S., Brabec, D., (2021). Qualitative and Quantitative Analysis of Sorghum Grain Composition Including Protein and Tannins Using ATR-FTIR Spectroscopy. *Food Analytical Methods* [online]. **14**(2), 268-279. [06/04/2021]. Available from: doi: 10.1007/s12161-020-01874-5.

Links, M.R., Taylor, J., Kruger, M.C., Naidoo, V., Taylor, J.R.N., (2016). Kafirin microparticle encapsulated sorghum condensed tannins exhibit potential as an anti-hyperglycaemic agent in a small animal model. *Journal of Functional Foods* [online]. **20**, 394-399. [16/06/2021]. Available from: doi: 10.1016/j.jff.2015.11.015.

Lipiński, K., Mazur, M., Antoszkiewicz, Z., Purwin, C., (2016). Polyphenols in monogastric nutrition – A review. *Annals of Animal Science* [online]. **17**(1), 41-58. [23/07/2018]. Available from: doi: 10.1515/aoas-2016-0042.

Liu, Z., Zhao, S., Wang, R., Yang, G., (1999). Separation of Polyhydroxylflavonoids by Packed-Column Supercritical Fluid Chromatography. *Journal of Chromatographic Science* [online]. **37**(5), 155-158. [10/10/2017]. Available from: doi: 10.1093/chromsci/37.5.155.

Liu, S., Truong, H., Selle, P., (2010). Red versus white sorghums Part I Is white sorghum really better then red? *Sorghum TechNote – Poultry Research Foundation* [online]. [02/10/2018]. Available from: http://www.feedgrainpartnership.com.au/items/897/Sorghum%20TechNote%20PRF%203-14A.pdf.

Liu, S.Y., Selle, P.H., Cowieson, A.J., (2013). Strategies to enhance the performance of pigs and poultry on sorghum-based diets. *Animal Feed Science and Technology* [online]. **181**(1-4), 1-14. [04/06/2018]. Available from: doi: 10.1016/j.anifeedsci.2013.01.008.

Liu, S.Y., Cadogan, D.J., Péron, A., Truong, H.H., Selle, P.H., (2014). Effects of phytase supplementation on growth performance, nutrient utilization and digestive dynamics of starch and protein in broiler chickens offered maize-, sorghum- and wheat-based diets. *Animal Feed Science and Technology* [online]. **197**, 164-175. [14/10/2020]. Available from: doi: 10.1016/j.anifeedsci.2014.08.005.

Liu, S.Y., Fox, G., Khoddami, A., Neilson, K.A., Truong, H.H., Moss, A.F., Selle, P.H., (2015). Grain Sorghum: A Conundrum for Chicken-Meat Production. *Agriculture* [online]. **5**(4), 1224-1251. [07/01/2018]. Available from: doi: 10.3390/agriculture5041224.

Liu, S.Y., Truong, H.H., Khoddami, A., Moss, A.F., Thomson, P.C., Roberts, T.H., Selle, P.H., (2016). Comparative performance of broiler chickens offered ten equivalent diets based on three grain sorghum varieties as determined by response surface mixture design. *Animal Feed Science and Technology* [online]. **218**, 70-83. [15/10/2020]. Available from: doi: 10.1016/j.anifeedsci.2016.05.008.

Liu, N., Wang, J.Q., Gu, K.T., Deng, Q.Q., Wang, J.P., (2017). Effects of dietary protein levels and multienzyme supplementation on growth performance and markers of gut health of broilers fed a miscellaneous meal based diet. *Animal Feed Science and Technology* [online]. **234**, 110-117. [04/06/2018]. Available from: doi: 10.1016/j.anifeedsci.2017.09.013.

Liu, G., Gilding, E.K., Kerr, E.D., Schulz, B.L., Tabet, B., Hamaker, B.R., Godwin, I.D., (2019). Increasing protein content and digestibility in sorghum grain with a synthetic biology approach. *Journal of Cereal Science* [online]. **85**, 27-34. [19/06/2019]. Available from: doi: 10.1016/j.jcs.2018.11.001.

Lizardo, R., Peiniau, J., Aumaitre, A. (1995). Effect of sorghum on performance, digestibility of dietary components and activities of pancreatic and intestinal enzymes in the weaned piglet. *Animal Feed Science and Technology* [online]. **56**(1-2), 67-82. [30/05/2018]. Available from: doi: 10.1016/0377-8401(95)00813-3.

Longstaff, M., McNab, J.M., (1991). The inhibitory effects of hull polysaccharides and tannins of field beans (*Vicia faba* L.) on the digestion of amino acids, starch and lipid and on digestive enzyme activities in young chicks. *British Journal of Nutrition* [online]. **65**(2), 199-216. [30/05/2018]. Available from: doi: 10.1079/BJN19910081.

Losso, J.N., (2008) The Biochemical and Functional Food Properties of the Bowman-Birk Inhibitor. *Critical Reviews in Food Science and Nutrition* [online]. **48**(1), 94-118. [25/05/2021]. Available from: doi: 10.1080/10408390601177589.

Louati, H., Zouari, N., Miled, N., Gargouri, Y., (2011). A new chymotrypsin-like serine protease involved in dietary protein digestion in a primitive animal, *Scorpio maurus*: purification and biochemical characterization. *Lipids in Health and Disease* [online]. **10**(1), 121-128. [10/07/2019]. Available from: doi: 10.1186/1476-511X-10-121.

Lu, Y., Sun, Y., Foo, L.Y., (2000). Novel pyranoanthocyanins from black currant seed. *Tetrahedron Letters* [online]. **41**(31), 5975-5978. [11/05/2020]. Available from: doi: 10.1016/S0040-4039(00)00954-0.

Lu, Y., Foo, L.Y., (2001). Unusual anthocyanin reaction with acetone leading to pyranoanthocyanin formation. *Tetrahedron Letters* [online]. **42**(7), 1371-1373. [10/05/2020]. Available from: doi: 10.1016/S0040-4039(00)02246-2.

Luthria, D.L., Liu, K., (2013). Localization of phenolic acids and antioxidant activity in sorghum kernels. *Journal of Functional Foods* [online]. **5**(4), 1751-1760. [19/10/2017]. Available from: doi: 10.1016/j.jff.2013.08.001.

Mabelebele, M., Gous, R.M., O'Neil, H.M., Iji, P.A., (2020). The effect of age of introducing whole sorghum grain on performance of broiler chickens. *Journal of Animal and Feed Sciences* [online]. **29**(2), 151-157. [14/10/2020]. Available from: doi: 10.22358/jafs/124045/2020.

Makkar, H. P. S., Ankers, P., (2014). Towards sustainable animal diets: a survey-based study. *Animal Feed Science and Technology* [online]. **198**, 309–322. [26/05/2021]. Available from: doi: 10.1016/j.anifeedsci.2014.09.018.

Mandalari, G., Vardakou, M., Faulks, R., Bisignano, C., Martorana, M., Smeriglio, A., Trombetta, D., (2016). Food matrix effects of polyphenol bioaccessibility from almond skin during simulated human digestion. *Nutrients* [online]. **8**(568), 1-17. [07/09/2018]. Available from: doi: 10.3390/nu8090568.

Mané, C., Sommerer, N., Yalcin, T., Cheynier, V., Cole, R.B., Fulcrand, H., (2007). Assessment of the Molecular Weight Distribution of Tannin Fractions through MALDI-TOF MS Analysis of Protein-Tannin Complexes. *Analytical Chemistry* [online]. **79**(6), 2239-2248. [07/09/2018]. Available from: doi: 10.1021/ac061685.

Manuhara, G.J., Amanto, B.S., Astuti, T.A., (2017). Effect of drying temperatures on physical characteristics of sorghum flour modified with lactic acid. *International Conference on Food Science and Engineering* [online]. **193**, 1-6. [24/05/2019]. Available from: doi: 10.1088/1757-899X/193/1/012024.

Manyelo, T.G., Ng'ambi, J.W., Norris, D., Mabelebele, M., (2019). Substitution of *Zea mays* by *Sorghum bicolor* on Performance and Gut Histo-Morphology of Ross 308 Broiler Chickens Aged 1–42. *Journal of Applied Poultry Research* [online]. **28**(3), 647-657. [07/01/2020]. Available from: doi: 10.3382/japr/pfz015.

Mareya, C.R., Tugizimana, F., Piater, L.A., Madala, N.E., Steenkamp, P.A., Dubery, I.A., (2019). Untargeted metabolomics reveal defensome-related metabolic reprogramming in *Sorghum bicolor* against infection by *Burkholderia andropogonis*. *Metabolites* [online]. **9**(8), 1-23. [08/04/2020]. Available from: doi: 10.3390/metabo9010008.

Mariscal-Landín, G., Avellaneda, J.H., de Souza, T.C.R., Aguilera, A., Borbolla, G.A., Mar, B., (2004). Effect of tannins in sorghum on amino acid ileal digestibility and on trypsin (E.C.2.4.21.4) and chymotrypsin (E.C.2.4.21.1) activity of growing pigs. *Animal Feed Science and Technology* [online]. **117**(3-4), 245-264. [05/02/2018]. Available from: doi: 10.1016/j.anifeedsci.2004.09.001.

Matsushita, S., Kobayashi, M., Nitta, Y., (1970). Inactivation of Enzymes by Linoleic Acid Hydroperoxides and Linoleic Acid. *Agricultural and Biological Chemistry* [online]. **34**(6), 817-824. [04/06/2020]. Available from: doi 10.1080/00021369.1970.10859695.

Mazur, B., Krebbers, E., Tingey, S., (1999). Gene discovery and product development for grain quality traits. *Science* [online]. **285**(5426), 372-375. [26/05/2021]. Available from: doi: 10.1126/science.285.5426.372.

McMichael, A.J., Powles, J.W., Butler, C.D., Uauy, R., (2007). Food, livestock production, energy, climate change, and health. *The Lancet* [online]. **370**(9594), 1253-1263. [26/05/2021]. Available from: doi: 10.1016/S0140-6736(07)61256-2.

Mehmood, S., Orhan, I., Ahsan, Z., Aslan, S., Gulfraz, M., (2008). Fatty acid composition of seed oil of different Sorghum bicolor varieties. *Food Chemistry* [online]. **109**(4), 855-859. [22/02/2020]. Available from: doi: 10.1016/j.foodchem.2008.01.014.

Mohapatra, D., Patel, A.V., Kar, A., Deshpande, S.S., Tripathi, M.K., (2019). Effect of different processing conditions on proximate composition, anti-oxidants, anti-nutrients and amino acid profile of grain

sorghum. *Food Chemistry* [online]. **271**, 129-135. [01/11/2018]. Available from: doi: 10.1016/j.foodchem.2018.07.196.

Mojzer, E.B., Hrnčič, M.K., Škerget, M., Knez, Z., Bren, U., (2016). Polyphenols: Extraction Methods, Antioxidative Action, Bioavailability and Anticarcinogenic Effects. *Molecules* [online]. **21**(7), 1-38. [30/05/2018]. Available from: doi: 10.3390/molecules21070901.

Monagas, M., Quintanilla-López, J.E., Gómez-Cordovés, C., Bartolomé, B., Lebrón-Aguilar, R., (2010). MALDI-TOF MS analysis of plant proanthocyanidins. *Journal of Pharmaceutical and Biomedical Analysis* [online]. **51**(2), 358-372. [10/11/2017]. Available from: doi: 10.1016/j.jpba.2009.03.035.

Moss, A.F., Khoddami, A., Chrystal, P.V., Sorbara, J.-O.B., Cowieson, A.J., Selle, P.H., Liu, S.Y., (2020). Starch digestibility and energy utilisation of maize- and wheat-based diets is superior to sorghum-based diets in broiler chickens offered diets supplemented with phytase and xylanase. *Animal Feed Science and Technology* [online]. **264**, 114475. [14/10/2020]. Available from: doi: 10.1016/j.anifeedsci.2020.114475

Moss, A.F., Chrystal, P.V., Cadogan, D.J., Wilkinson, S.J., Crowley, T.M., Choct, M., (2021). Precision feeding and precision nutrition: a paradigm shift in broiler feed formulation? *Animal Bioscience* [online]. **34**(3), 354-362. [26/04/2021]. Available from: doi: 10.5713/ab.21.0034.

Mottet, A., Tempio, G., (2017). Global poultry production: current state and future outlook and challenges. *Worlds Poultry Science Journal* [online]. **73**, 245–256. [26/05/2021]. Available from: doi: 10.1017/S0043933917000071.

Mouls, L., Mazauric, J-P, Sommerer, N., Fulcrand, H., Mazerolles, G., (2011). Comprehensive study of condensed tannins by ESI mass spectrometry: average degree of polymerisation and polymer distribution determination from mass spectra. *Analytical and Bioanalytical Chemistry* [online]. **400**(2), 613-623. [02/11/2017]. Available from: doi: 10.1007/s00216-011-4751-7.

Naczk, M., Shahidi, F., (2006). Phenolics in cereals, fruits and vegetables: Occurrence, extraction and analysis. *Journal of Pharmaceutical and Biomedical Analysis* [online]. **41**(5), 1523-1542. [28/09/2017]. Available from: doi: 10.1016/j.jpba.2006.04.002.

National Research Council. 1994. Nutrient Requirements of Poultry: Ninth Revised Edition, 1994. Washington, DC: The National Academies Press. https://doi.org/10.17226/2114.

Ncube, B., Van Staden, J., (2015). Tilting Plant Metabolism for Improved Metabolite Biosynthesis and Enhanced Human Benefit. *Molecules* [online]. **20**, 12698-12731. [30/10/2020]. Available from: doi.org/10.3390/molecules200712698.

Nielsen, P.M., Petersen, D., Dambmann, C., (2001). Improved Method for Determining Food Protein Degree of Hydrolysis. *Journal of Food Science* [online]. **66**(5), 642-646. [21/07/2021]. Available from: doi: 10.1111/j.1365-2621.2001.tb04614.x.

Nielsen, P.H., Wenzel, H., (2006). Environmental Assessment of Ronozyme® P5000 CT Phytase as an Alternative to Inorganic Phosphate Supplementation to Pig Feed Used in Intensive Pig Production. *International Journal of Life Cycle Assessment* [online]. **12**, 1-7. [01/06/2020]. Available from: doi: 10.1065/lca2006.08.265.2.

Nyachoti, C.M., Atkinson, J.L., Leeson, S., (1996). Response of broiler chicks fed a high-tannin sorghum diet. *Journal of Applied Poultry Research* [online]. **5**(3), 239-245. [07/01/2018]. Available from: doi: 10.1093/japr/5.3.239.

Nyamambi, B., Ndlovu, L.R., Read, J.S., Reed, J.D., (2000). The effects of sorghum proanthocyanidins on digestive enzyme activity *in vitro* and in the digestive tract of chicken. *Journal of the Science of Food and Agriculture* [online]. **80**(15), 2223-2231. [07/06/2018]. Available from: doi: 10.1002/1097-0010(200012)80:15<2223::AID-JSFA768>3.0.CO;2-I.

Ohnishi-Kameyama, M., Yanagida, A., Kanda, T., Nagata, T., (1997). Identification of Catechin Oligomers from Apple (*Malus pumila* cv. Fuji) in Matrix-assisted Laser Desorption/Ionization Time-of-flight Mass Spectrometry and Fast-atom Bombardment Mass Spectrometry. *Rapid Communications in Mass Spectrometry* [online]. **11**(1), 31-36. [14/11/2018]. Available from: doi: 10.1002/(SICI)1097-0231(19970115)11:1<31::AID-RCM784>3.0.CO;2-T.

Oladoja, N.A., Alliu, Y.B., Ofomaja, A.E., Unuabonah, I.E., (2011). Synchronous attenuation of metal ions and colour in aqua stream using tannin–alum synergy. *Desalination* [online]. **271**(1-3), 34-40. [30/05/2019]. Available from: doi: 10.1016/j.desal.2010.12.008.

Olukosi, O.A., Cowieson, A.J., Adeola, O., (2007). Age-Related Influence of a Cocktail of Xylanase, Amylase, and Protease or Phytase Individually or in Combination in Broilers. *Poultry Science* [online]. **86**(1), 77-86. [28/09/2017]. Available from: doi: 10.1093/ps/86.1.77.

Oroian, M., Escriche, I., (2015). Antioxidants: Characterization, natural sources, extraction and analysis. *Food Research International* [online]. **74**, 10-36. [31/10/2017]. Available from: doi: 10.1016/j.foodres.2015.04.018.

Osuntogun, B.A., Adewusi, S.R.A., Ogundiwin, J.O., Nwasike, C.C., (1989). Effect of Cultivar, Steeping, and Malting on Tannin, Total Polyphenol, and Cyanide Content of Nigerian Sorghum. *Cereal Chemistry* [online]. **66**(2), 87-89. [16/10/2017]. Available from: https://www.cerealsgrains.org/publications/cc/backissues/1989/Documents/66_87.pdf.

Overy, S.A., Walker, H.J., Malone, S., Howard, T.P., Baxter, C.J., Sweetlove, L.J., Hill, S.A., Quick, W.P., (2005). Application of metabolite profiling to the identification of traits in a population of tomato introgression lines. *Journal of Experimental Botany* [online]. **56**(10), 287-296. [20/06/2019]. Available from: doi: 10.1093/jxb/eri070.

Oxenboll, K.M., Pontoppidan, K., Fru-Nji, F., (2011). Use of a Protease in Poultry Feed Offers Promising Environmental Benefits. *International Journal of Poultry Science* [online]. **10**(11), 842-848. [11/07/2019]. Available from: doi: 10.3923/ijps.2011.842.848.

Palma, A.S., Ricci, A., Parpinello, G.P., Versari, A., (2017). Rapid screening method to assess tannin antioxidant activity in food-grade botanical extract. *Italian Journal of Food Science* [online]. **29**(3), 559-564. [25/05/2021]. Available from: doi: 10.14674/IJFS-671.

Pan, L., An, D., Zhu, W.Y., (2021). Sorghum as a dietary substitute for corn reduces the activities of digestive enzymes and antioxidant enzymes in pigs. *Animal Feed Science and Technology* [online]. **273**(June 2020), 1-9. [06/04/2021]. Available from: doi: 10.1016/j.anifeedsci.2021.114831.

Park, J., Yuk, H.J., Ryu, H.W., Lim, S.H., Kim, K.S., Park, K.H., Ryu, Y.B., Lee, W.S., (2017). Evaluation of polyphenols from Broussonetia papyrifera as coronavirus protease inhibitors. *Journal of Enzyme Inhibition and Medicinal Chemistry* [online]. **32**(1), 504-512. [05/12/2017]. Available from: doi: 10.1080/14756366.2016.1265519.

Pasch, H., Pizzi, A., Rode, K., (2001). MALDI-TOF mass spectrometry of polyflavonoid tannins. *Polymer* [online]. **42**, 7531-7539. [10/11/2017]. Available from: doi: 0.1016/S0032-3861(01)00216-6.

Pasquali, G.A.M., Fascina, V.B., Silva, A.L., Aoyagi, M.M., Muro, E.M., Serpa, P.G., Berto, D.A., Saldanha, E.S.P.B., Sartori, J.R., (2016). Maize replacement with sorghum and a combination of protease, xylanase, and phytase on performance, nutrient utilization, litter moisture, and digestive organ size in broiler chicken. *Canadian Journal of Animal Science* [online]. **97**, 328-337. [02/10/2018]. Available from: doi: 10.1139/CJAS-2016-0133.

Paterson, A.H., Bowers, J.E., Bruggmann, R., Dubchak, I., Grimwood, J., Gundlach, H., Haberer, G., Hellsten, U., Mitros, T., Poliakov, A., Schmutz, J., Spannagl, M., Tang, H., Wang, X., Wicker, T., Bharti, A.K., Chapman, J., Feltus, F.A., Gowik, U., Grigoriev, I.V., Lyons, E., Maher, C.A., Martis, M., Narechania, A., Otillar, R.P., Penning, B.W., Salamov, A.A., Wang, Y., Zhang, L., Carpita, N.C., Freeling, M., Gingle, A.R., Hash, C.T., Keller, B., Klein, P., Kresovich, S., McCann, M.C., Ming, R., Peterson, D.G., ur-Rahman, M., Ware, D., Westhoff, P., Mayer, K.F.X, Messing, J., Rokhsar, D.S., (2009). The

Sorghum bicolor genome and the diversification of grasses. *Nature* [online]. **457**(7229), 551-556. [26/11/2018]. Available from: doi: 10.1038/nature07723.

Perez-Maldonado, R.A., Rodrigues, H.D., (2007). *Nutritional Characteristics of Sorghums from Queensland and New South Wales for Chicken Meat Production* [online]. Canberra: Rural Industries Research and Development Corporation. [05/01/18]. Available from: www.rirdc.gov.au.

Poncet-Legrand, C., Gautier, C., Cheynier, V., Imberty, A., (2007). Interactions between Flavan-3-ols and Poly(L-proline) Studied by Isothermal Titration Calorimetry: Effect of the Tannin Structure. *Journal of Agricultural and Food Chemistry* [online]. **55**, 9235-9240. [05/10/2017]. Available from: 10.1021/jf071297o.

Pontoppidan, K., Pettersson, D., Sandberg, A.-S., (2007). *Peniophora lycii* phytase is stabile and degrades phytate and solubilises minerals *in vitro* during simulation of gastrointestinal digestion in the pig. *Journal of the Science of Food and Agriculture* [online]. **87**(2), 930-944. [10/07/2019]. Available from: doi: 10.1002/jsfa.

Poontawee, W., Natakankitkul, S., Wongmekiat, O., (2015) Enhancing Phenolic Contents and Antioxidant Potentials of *Antidesma thwaitesianum* by Supercritical Carbon Dioxide Extraction. *Journal of Analytical Methods in Chemistry* [online]. **2015**, 1-7. [02/10/2017]. Available from: doi: 10.1155/2015/956298.

Puntigam, R., Brugger, D., Slama, J., Inhuber, V., Boden, B., Krammer, V., Schedle, K., Wetscherek-Seipelt, G., Wetscherek, W., (2020). The effects of a partial or total replacement of ground corn with ground and whole-grain low-tannin sorghum (*Sorghum bicolor* (L.) Moench) on zootechnical performance, carcass traits and apparent ileal amino acid digestibility of broiler chickens. *Livestock Science* [online]. **241**, 104187. [14/10/2020]. Available from: doi: 10.1016/j.livsci.2020.104187.

Qi, Y., Zhang, H., Awika, J.M., Wang, L., Qian, H., Gu, L., (2016). Depolymerization of sorghum procyanidin polymers into oligomers using HCl and epicatechin: Reaction kinetics and optimization. *Journal of Cereal Science* [online]. **70**, 170-176. [31/10/2018]. Available from: doi: 10.1016/j.jcs.2016.06.002.

Qi, Y., Zhang, H., Wu, G., Zhang, H., Gu, L., Wang, L., Qian, H., Qi, X., (2018). Mitigation effects of proanthocyanidins with different structures on acrylamide formation in chemical and fried potato crisp models. *Food Chemistry* [online]. **250**(January), 98-104. [24/09/2018]. Available from: doi: 10.1016/j.foodchem.2018.01.012.

Quesada, C., Bartolomé, B., Nieto, O., Gómez-Cordovés, C., Hernández, T., Estrella, I., (1996). Phenolic Inhibitors of α-Amylase and Trypsin Enzymes by Extracts From Pears, Lentils, and Cocoa. *Journal of Food Protection* [online]. **59**(2), 185-192. [30/05/2018]. Available from: doi: 10.4315/0362-028X-59.2.185.

Quideau, S., Deffieux, D., Douat-Casassus, C., Pouységu, L., (2011). Plant Polyphenols: Chemical Properties, Biological Activities, and Synthesis. *Angewandte Chemie - International Edition* [online]. **50**(3), 586-621. [25/07/2018]. Available from: doi: 10.1002/anie.201000044.

Ramírez P., García-Risco, M.R., Santoyo, S., Señoráns, F.J., Ibáñez, E., Reglero, G., (2006). Isolation of functional ingredients from rosemary by preparative-supercritical fluid chromatography (Prep-SFC). *Journal of Pharmaceutical and Biomedical Analysis* [online]. **41**(5), 1606-1613. [25/05/2021]. Available from: doi: 10.1016/j.jpba.2006.02.001.

Rao, S., Santhakumar, A.B., Chinkwo, K.A., Wu, G., Johnson, S.K., Blanchard, C.L., (2018). Characterization of phenolic compounds and antioxidant activity in sorghum grains. *Journal of Cereal Science* [online]. **84**(June), 103-111. [01/11/2018]. Available from: doi: 10.1016/j.jcs.2018.07.013.

Ravindran, V., (2013). Feed enzymes: The science, practice, and metabolic realities. *Journal of Applied Poultry Research* [online]. **22**(3), 628-636. [04/06/2018]. Available from: doi: 10.3382/japr.2013-00739.

Reeves, S.G., Somogyi, A., Zeller, W.E., Ramelot, T.A., Wrighton, K.C., Hagerman, A.E., (2020). Proanthocyanidin Structural Details Revealed by Ultrahigh Resolution FT-ICR MALDI-Mass

Spectrometry, ^{1}H-^{13}C HSQC NMR, and Thiolysis-HPLC-DAD. *Journal of Agricultural and Food Chemistry* [online]. **68**, 14038-14048. [04/01/2021]. Available from: doi: 10.1021/acs.jafc.0c04877.

Rhodes, D.H., Hoffman Jr., L., Rooney, W.L., Ramu, P., Morris, G.P., Kresovich, S., (2014). Genome-Wide Association Study of Grain Polyphenol Concentrations in Global Sorghum [*Sorghum bicolor* (L.) Moench] Germplasm. *Journal of Agricultural and Food Chemistry* [online]. **62**(45), 10916-10927. [12/09/2019]. Available from: doi: 10.1021/jf503651t.

Ricci, A., Olejar, K.J., Parpinello, G.P., Kilmartin, P.A., Versari, A., (2015). Application of Fourier Transform Infrared (FTIR) Spectroscopy in the Characterization of Tannins. *Applied Spectroscopy Reviews* [online]. **50**(5), 407-442. [05/04/2019]. Available from: doi: 10.1080/05704928.2014.1000461.

Ricci, A., Lagel, M.-C., Parpinello, G.P., Pizzi, A., Kilmartin, P.A., Versari, A., (2016). Spectroscopy analysis of phenolic and sugar patterns in a food grade chestnut tannin. *Food Chemistry* [online]. **203**, 425-429. [30/05/2019]. Available from: doi: 10.1016/j.foodchem.2016.02.105.

Rocchetti, G., Giuberti, G., Busconi, M., Marocco, A., Trevisan, M., Lucini, L., (2020). Pigmented sorghum polyphenols as potential inhibitors of starch digestibility: An in vitro study combining starch digestion and untargeted metabolomics. *Food Chemistry* [online]. **312**(126076), 1-8. [08/04/2020]. Available from: doi: 10.1016/j.foodchem.2019.126077.

Rodgers, N. J., Choct, M., Hetland, H., Sundby, F., and Svihus, B. (2012). Extent and method of grinding of sorghum prior to inclusion in complete pelleted broiler chicken diets affects broiler gut development and performance. *Animal Feed Science and Technology* [online. **171**, 60–67. [14/10/2020]. Available from: doi: 10.1016/j.anifeedsci.2011.09.020

Rohamare, S., Javdekar, V., Dalal, S., Nareddy, P.K., Swamy, M.J., Gaikwad, S.M., (2015). Acid Stability of the Kinetically Stable Alkaline Serine Protease Possessing Polyproline II Fold. *Protein Journal* [online]. **34**(1), 60-67. [12/04/2019]. Available from: doi: 10.1007/s10930-014-9597-3.

Rohn, S., Rawel, H.M., Pietruschinski, N., Kroll, J., (2001). *In vitro* inhibition of α-chymotryptic activity by phenolic compounds. *Journal of the Science of Food and Agriculture* [online]. **81**(15), 1512-1521. [05/02/2018]. Available from: doi: 10.1002/jsfa.977.

Rohn, S., Rawel, H.M., Wollenberger, U., Kroll, U., (2003). Enzyme activity of α-chymotrypsin after derivatization with phenolic compounds. *Nahrung/Food* [online]. **47**(5), 325-329. [07/06/2018]. Available from: doi: 10.1002/food.200390075.

Rooney, L.W., Miller, F.R., (1982). Variation in the structure and kernel characteristics of sorghum. *ICRISAT (International Crops Research Institute for the Semi-Arid Tropics) Proceedings of the International Symposium on Sorghum Grain Quality* [online]. 143–162. [25/05/2021]. Available from: https://pdf.usaid.gov/pdf_docs/PNAAQ780.pdf.

Rue, E.A., Rush, M.D., van Breeman, R.B., (2018). Procyanidins: a comprehensive review encompassing structure elucidation via mass spectrometry. *Phytochemistry Reviews* [online]. **17**(1), 1-16. [17/09/2018]. Available from: doi: 10.1007/s11101-017-9507-3.

Saad, H., Khoukh, A., Ayed, N., Charrier, B., Bouhtoury, F.C-El., (2014). Characterization of Tunisian Aleppo pine tannins for a potential use in wood adhesive formulation. *Industrial Crops and Products* [online]. **61**, 517-525. [30/05/2019]. Available from: doi: 10.1016/j.indcrop.2014.07.035.

Salazar-López, N.J., González-Aguilar, G.A., Rouzaud-Sández, O., Robles-Sánchez, M., (2018). Bioaccessibility of hydroxycinnamic acids and antioxidant capacity from sorghum bran thermally processed during simulated in vitro gastrointestinal digestion. *Journal of Food Science and Technology* [online]. **55**(6), 2021-2030. [13/07/2018]. Available from: doi: 10.1007/s13197-018-3116-z.

Salobir, J., Kostanjevec, B., Štruklec, M., Salobir, K., (2005). Tannins reduce protein but not phosphorous utilization of diet with added phytase in pigs. *Journal of Animal and Feed Sciences* [online]. **14**(2), 277-282. [28/09/2017]. Available from: doi: 10.22358/jafs/67013/2005.

Sanchez-Romero, I., Ariza, A., Wilson, K.S., Skjøt, M., Vind, J., De Maria, L., Skov, L.K., Sanchez-Ruiz, J.M., (2013). Mechanism of Protein Kinetic Stabilization by Engineered Disulfide Crosslinks. *PLoS ONE* [online]. **8**(7), 1-9. [24/11/2017]. Available from: doi: 10.1371/journal.pone.0070013.

Sarni-Manchado, P., Cheynier, V., Moutounet, M., (1999). Interactions of Grape Seed Tannins with Salivary Proteins. *Journal of Agricultural and Food Chemistry* [online]. **47**(1), 42-47. [06/05/2020]. Available from: doi: 10.1021/jf9805146.

Schons, P.F., Ries, E.F., Battestin, V., Macedo, G.A., (2011). Effect of enzymatic treatment on tannins and phytate in sorghum (*Sorghum bicolor*) and its nutritional study in rats. *International Journal of Food Science and Technology* [online]. **46**, 1253-1258. [07/06/2018]. Available from: doi: 10.1111/j.1365-2621.2011.02620.x.

Schons, P.F., Battestin, V., Macedo, G.A., (2012). Fermentation and enzyme treatments for sorghum. *Brazilian Journal of Microbiology* [online]. **43**, 89-97. [10/07/2019]. Available from: doi: 10.1590/S1517-83822012000100010.

Scripps Center for Metabolomics. (2019). Metlin: Metabolite Search. https://metlin.scripps.edu/index.php [Accessed: 15th October 2019].

Selle, P.H., Ravindran, V., Caldwell, R.A., Bryden, W.L., (2000). Phytate and phytase: consequences for protein utilisation. *Nutrition Research Reviews* [online]. **13**(2), 255-278. [28/09/2017]. Available from: doi: 10.1079/095442200108729098.

Selle, P.H., Cadogan, D.J., Li, X., Bryden, W.L., (2010a). Implications of sorghum in broiler chicken nutrition. *Animal Feed Science Technology* [online]. **156**(3-4), 57-74. [26/10/2017]. Available from: doi: 10.1016/j.anifeedsci.2010.01.004.

Selle, P.H., Cadogan, D.J., Ru, Y.J., Partridge, G.G., (2010b). Impact of exogenous enzymes in sorghum- or wheat based broiler diets on nutrient utilization and growth performance. *International Journal of Poultry Science* [online]. **9**(1), 53-58. [02/10/2018]. Available from: doi: 10.3923/ijps.2010.53.58.

Selle, P.H., Cowieson, A.J., Cowieson, N.P., Ravindran, V., (2012). Protein–phytate interactions in pig and poultry nutrition: a reappraisal. *Nutrition Research Reviews* [online]. **25**(1), 1-17. [28/09/2017]. Available from: doi: 10.1017/S0954422411000151.

Selle, P.H., Moss, A.F., Truong, H.H., Khoddami, A., Cadogan, D.J., Godwin, I.D., Liu, S.Y., (2018). Outlook: Sorghum as a feed grain for Australian chicken-meat production. *Animal Nutrition* [online]. **4**(1), 17-30. [10/06/2020]. Available from: doi: 10.1016/j.aninu.2017.08.007.

Selle, P.H., McInerney, B.V., McQuade, L.R., Khoddami, A., Chrystal, P.V., Hughes, R.J., Liu, S.Y., (2020). Composition and characterisation of kafirin, the dominant protein fraction in grain sorghum. *Animal Production Science* [online]. **60**(9), 1163-1172. [27/02/2020]. Available from: doi: 10.1071/AN19393.

Selle, P.H., Hughes, R.J., Godwin, I.D., Khoddami, A., Chrystal, P.V., Liu, S.Y., (2021). Addressing the shortfalls of sorghum as a feed grain for chicken-meat production. *World's Poultry Science Journal* [online]. **77**(1), 29-41. [16/03/2021]. Available from: doi: 10.1080/00439339.2020.1866966.

Shapaval, V., Afseth, N. K., Vogt, G., Kohler, A., (2014). Fourier transform infrared spectroscopy for the prediction of fatty acid profiles in *Mucor* fungi grown in media with different carbon sources. *Microbial Cell Factories* [online]. 13, 86. [26/05/2021]. Available from: doi: 10.1186/1475-2859-13-86.

She, D., Xu, F., Geng, Z., Sun, R., Jones, G.L., Baird, M.S., (2010). Physiochemical characterization of extracted lignin from sweet sorghum stem. *Industrial Crops and Products* [online]. **32**(1), 21-28. [24/05/2019]. Available from: doi: 10.1016/j.indcrop.2010.02.008.

Sillapachaiyaporn, C., Nilkhet, S., Ung, A.T., Chuchawankul, S., (2019). Anti-HIV-1 protease activity of the crude extracts and isolated compounds from *Auricularia polytricha*. *BMC Complementary and*

Alternative Medicine [online]. **19**, 1-10. [04/06/2020]. Available from: doi: 10.1186/s12906-019-2766-3.

Slominski, B.A., (2011). Recent advances in research on enzymes for poultry diets. *Poultry Science* [online]. **90**(9), 2013-2023. [28/09/2017]. Available from: doi: 10.3382/ps.2011-01372.

Smith, A., (2011). Using proteases in broiler diets – careful selection is key. *International Poultry Production* [online]. **19**(7), 15-17. [01/06/2020]. Available from: http://www.positiveaction.info/pdfs/articles/pp19.7p15.pdf.

Stafford, H.A., (1965). Flavonoids and Related Phenolic Compounds Produced in the First Internode of Sorghum vulgare Pers. in Darkness and in Light. *Plant Physiology* [online]. **40**, 130-138. [02/11/2017]. Available from: doi: 0.1104/pp.40.1.130.

Stefanello, C., Vieira, S.L., Santiago, G.O., Kindlein, L., Sorbara, J.O.B., Cowieson, A.J., (2015). Starch digestibility, energy utilization, and growth performance of broilers fed corn-soybean basal diets supplemented with enzymes. *Poultry Science* [online]. **94**(10), 2472-2479. [28/09/2017]. Available from: doi: 10.3382/ps/pev244.

Stefoska-Needham, A., Beck, E.J., Johnson, S.K., Tapsell L.C., (2015). Sorghum: An Underutilized Cereal Whole Grain with the Potential to Assist in the Prevention of Chronic Disease. *Food Reviews International* [online]. **31**(4), 401-437. [17/10/2017]. Available from: doi: 10.1080/87559129.2015.1022832.

Sumner, L.W., Amberg, A., Barrett, D., Beale, M.H., Beger, R., Daykin, C.A., Fan, T.W.-M., Fiehn, O., Goodacre, R., Griffin, J.L., Hankemeier, T., Hardy, N., Harnly, J., Higashi, R., Kopka, J., Lane, A.N., Lindon, J.C., Marriott, P., Nicholls, A.W., Reily, M.D., Thaden, J.J., Viant, M.R., (2007). Proposed minimum reporting standards for chemical analysis Chemical Analysis Working Group (CAWG) Metabolomics Standards Initiative (MSI). *Metabolomics* [online]. **3**(3), 211-221. [26/03/2020]. Available from: doi: 10.1007/s11306-007-0082-2.Proposed.

Sun, L., Warren, F.J., Gidley, M.J., (2018). Soluble polysaccharides reduce binding and inhibitory activity of tea polyphenols against porcine pancreatic a-amylase. *Food Hydrocolloids* [online]. **79**, 63-70. [11/06/2019]. Available from: doi: 10.1016/j.foodhyd.2017.12.011.

Svensson, L., Sekwati-Monang, B., Lutz, D.L., Schieber, A., Gänzle, M.G., (2010). Phenolic Acids and Flavonoids in Nonfermented and Fermented Red Sorghum (Sorghum bicolor (L.) Moench). *Journal of Agricultural and Food Chemistry* [online]. **58**(16), 9214-9220. [17/10/2017]. Available from: doi: 10.1021/jf101504v.

Svihus, B., (2014). Function of the digestive system. *Journal of Applied Poultry Research* [online]. **23**(2), 306-314. [19/07/2018]. Available from: doi: 10.3382/japr.2014-00937.

Taleon, V., Dykes, L., Rooney, W.L., Rooney, L.W., (2012). Effect of genotype and environment on flavonoid concentration and profile of black sorghum grains. *Journal of Cereal Science*. [online]. **56**(2), 470-475. [31/10/2017]. Available from: doi: 10.1016/j.jcs.2012.05.001.

Taleon, V., Dykes, L., Rooney, W.L., Rooney, L.W., (2014). Environmental effect on flavonoid concentrations and profiles of red and lemon-yellow sorghum grains. *Journal of Food Composition and Analysis* [online]. **34**(2), 178-185. [07/06/2018]. Available from: doi: 10.1016/j.jfca.2014.03.003.

Tamir, M., Alumot, E., (1969). Inhibition of digestive enzymes by condensed tannins from green and ripe carobs. *Journal of the Science of Food and Agriculture* [online]. **20**(4), 199-202. [25/02/2018]. Available from: doi: 10.1002/jsfa.2740200402.

Tan, Y., Chang, S.K.C., (2017). Digestive enzyme inhibition activity of the phenolic substances in selected fruits, vegetables and tea as compared to black legumes. *Journal of Functional Foods* [online]. **38**, 644-655. [25/10/2018]. Available from: doi: 10.1016/j.jff.2017.04.005.

Taylor, J.R.N., (2005). Non-starch polysaccharides, protein and starch: form function and feed - highlight on sorghum. *Proceedings of the 17th Australian Poultry Science Symposium* [online]. **17**, 9-16. [12/09/2019]. Available from: https://www.cabdirect.org/cabdirect/abstract/20073008821.

Taylor, J.R.N., Emmambux, M.N., (2008). Products containing other speciality grains: sorghum, the millets and pseudocereals: *Woodhead Publishing Series in Food Science, Technology and Nutrition, Technology of Functional Cereal Products*. 281-335. Edited by Hamaker, B.R., Woodhead Publishing.

Taylor, J.R.N., Belton, P.S., Beta, T., Duodu, K.G., (2014). Increasing the utilisation of sorghum, millets and pseudocereals: Developments in the science of their phenolic phytochemicals, biofortification and protein functionality. *Journal of Cereal Science* [online]. **59**(3), 257-275. [07/09/2018]. Available from: doi: 10.1016/j.jcs.2013.10.009.

Todd, M.J., Gomez, J., (2001). Enzyme Kinetics Determined Using Calorimetry: A General Assay for Enzyme Activity? *Analytical Biochemistry* [online]. **296**(2), 179-187. [25/07/2018]. Available from: doi: 10.1006/abio.2001.5218.

Toomer, O.T., Livingston, M., Wall, B., Sanders, E., Vu, T., Malheiros, R.D., Livingston, K.A., Carvalho, L.V., Ferket, P.R., Dean, L.L., (2003). Feeding high-oleic peanuts to meat-type broiler chickens enhances the fatty acid profile of the meat produced. *Poultry Science* [online]. **99**(4), 2236-2245. [04/06/2020]. Available from: doi: 10.1016/j.psj.2019.11.015.

Torres, K.A.A., Pizauro, J.M., Soares, C.P., Silva, T.G.A., Nogueira, W.C.L., Campos, D.M.B., Furlan, R.L., Macari, M., (2013). Effects of corn replacement by sorghum in broiler diets on performance and intestinal mucosa integrity. *Poultry Science* [online]. **92**(6), 1564-1571. [26/11/2018]. Available from: doi: 10.3382/ps.2012-02422.

Troesch, B., Jing, H., Laillou, A., Fowler, A., (2013). Absorption studies show that phytase from *Aspergillus niger* significantly increases iron and zinc bioavailability from phytate-rich foods. *Food and Nutrition Bulletin* [online]. **34**(2 Suppl), 90-101. [06/05/2020]. Available from: doi: 10.1177/15648265130342s111.

Truong, H.H., Yu, S., Péron, A., Cadogan, D.J., Khoddami, A., Robert, T.H., Liu, S.Y., Selle, P.H., (2014). Phytase supplementation of maize-, sorghum- and wheat-based broiler diets with identified starch pasting properties influences phytate (IP_6) and sodium jejunal and ileal digestibility. *Animal Feed Science and Technology* [online]. **198**, 248-256. [24/07/2020]. Available from: doi: 10.1016/j.anifeedsci.2014.10.007.

Truong, H.H., Neilson, K.A., McInerney, B.V., Khoddami, A., Robert, T.H., Cadogan, D.J., Liu, S.Y., Selle, P.H., (2016). Comparative performance of broiler chickens offered nutritionally equivalent diets based on six diverse, 'tannin- free' sorghum varieties with quantified concentrations of phenolic compounds, kafirin, and phytate. *Animal Production Science* [online]. **57**(5), 828-838. [08/06/2020]. Available from: doi: 10.1071/AN16073.

Tsao, R., (2010). Chemistry and biochemistry of dietary polyphenols. *Nutrients* [online]. **2**(12), 1231-1246. [28/09/2017]. Available from: doi: 10.3390/nu2121231.

Tugizimana, F., Djami-Tchatchou, A.T., Steenkamp, P.A., Piater, L.A., Dubery, I.A., (2019). Metabolomic analysis of defense-related reprogramming in *Sorghum bicolor* in response to *Colletotrichum sublineolum* infection reveals a functional metabolic web of phenylpropanoid and flavonoid pathways. *Frontiers in Plant Science* [online]. **9**, 1840. [08/04/2020]. Available from: doi: 10.3389/fpls.2018.01840.

Van Veldhoven, P.P., Mannaerts, G.P., (1987). Inorganic and organic phosphate measurements in the nanomolar range. *Analyical Biochemistry* [online]. **161**(1), 45-48. [21/07/2021]. Available from: doi: 10.1016/0003-2697(87)90649-x.

Velickovic, T.J.C., Stanic-Vucinic, D.J., (2018). The Role of Dietary Phenolic Compounds in Protein Digestion and Processing Technologies to Improve Their Antinutritive Properties. *Comprehensive Reviews in*

Food Science and Food Safety [online]. **17**, 82-103. [24/08/2018]. Available from: doi: 10.1111/1541-4337.12320.

Venter, P.B., Sisa, M., van der Merwe, M.J., Bonnet, S.L., van der Westhuizen, J.H., (2012). Analysis of commercial proanthocyanidins. Part 1: The chemical composition of quebracho (*Schinopsis lorentzii* and *Schinopsis balansae*) heartwood extract. *Phytochemistry* [online]. **78**, 156-169. [09/06/2020]. Available from: doi: 10.1016/j.phytochem.2012.01.027.

Venter, P., Muller, M., Vestner, J., Stander, M.A., Tredoux, A.G.J., Pasch, H., de Villiers, A., (2018). Comprehensive Three-Dimensional LC × LC × Ion Mobility Spectrometry Separation Combined with High-Resolution MS for the Analysis of Complex Samples. *Analytical Chemistry* [online]. **90**(19), 11643-11650. [05/08/2019]. Available from: doi: 10.1021/acs.analchem.8b03234.

Vivas, N., Nonier, M., de Gaulejac, N.V., Absalon, C., Bertrand, A., Mirabel, M., (2004). Differentiation of proanthocyanidin tannins from seeds, skins and stems of grapes (Vitis vinifera) and heartwood of Quebracho (*Schinopsis balansae*) by matrix-assisted laser desorption/ionization time-of-flight mass spectrometry and thioacidolysis/liquid chromatography/electrospray ionization mass spectrometry. *Analytica Chimica Acta* [online]. **513**(1), 247-256. [12/11/2018]. Available from: doi: 10.1016/j.aca.2003.11.085.

Wall, J.S., Blessin, C.W., (1969). Composition of Sorghum Plant and Grain: *Sorghum Production and Utilization*. 118-166. Edited by Wall, J.S., Ross, W.M., AVI Publishing Company, Westport, CT, USA.

Walsh, G.A., Power, R.F., Headon, D.R., (1994). Enzymes in the animal-feed industry. *Trends in Food Science and Technology* [online]. **5**(3), 81-87. [04/06/2018]. Available from: doi: 10.1016/0924-2244(94)90242-9.

Wang, L., Weller, C.L., Schlegel, V.L., Carr, T.P., Cuppett, S.L., (2007). Comparison of supercritical CO_2 and hexane extraction of lipids from sorghum distillers grains. *European Journal of Lipid Science and Technology*. [online]. **109**(6), 567-574. [07/11/2017]. Available from: doi: 10.1002/ejlt.200700018.

Waterman, P.G., Mole, S., (1994). *Analysis of Phenolic Plant Metabolites*. Oxford: Blackwell Scientific Publications.

Weihua, X., Miao, Z., Jing, L., Chuanxiu, X., Yuwei, L., (2015). Effects of phytase and tannase on *in vivo* nutritive utilisation of faba bean (*Vicia faba* L.) flour. *International Food Research Journal* [online]. **22**(4), 1550-1556. [24/09/2017]. Available from: https://www.cabdirect.org/cabdirect/abstract/20153264714.

Williams, P.E.V., (1997). Poultry production and science: future directions in nutrition. *World's Poultry Science Journal* [online]. **53**(1), 33-48. [23/07/2018]. Available from: doi: 10.1079/WPS19970004.

Wong, J.H., Lau, T., Cai, N., Singh, J., Pedersen, J.F., Vensel, W.H., Hurkman, W.J., Wilson, J.D., Lemaux, P.G., Buchana, B.B., (2009). Digestibility of protein and starch from sorghum (Sorghum bicolor) is linked to biochemical and structural features of grain endosperm. *Journal of Cereal Science* [online]. **49**(1), 73-82. [25/07/2018]. Available from: doi: 10.1016/j.jcs.2008.07.013.

Woodhead, S., Galeffi, C., Bettolo, G.B.M., (1982). *p*-Hydroxybenzaldehyde as a major constituent of the epicuticular wax of seedling *Sorghum Bicolor*. *Phytochemistry* [online]. **21**(2), 455-456. [31/10/2017]. Available from: doi: 10.1016/S0031-9422(00)95288-9.

Wu, Y.B., Ravindran, V., Hendriks, W.H., (2004). Influence of exogenous enzyme supplementation on energy utilisation and nutrient digestibility of cereals for broilers. *Journal of the Science of Food and Agriculture* [online]. **84**(14), 1817-1822. [29/04/2021]. Available from: doi: 10.1002/jsfa.1892.

Wu, Y., Li, X., Xiang, W., Zhu, C., Lin, Z., Wu, Y., Li, J., Pandravada, S., Ridder, D.D., Bai, G., Wang, M.L., Trick, H.N., Bean, S.R., Tuinstra, M.R., Tesso, T.T., Yu, J., (2012). Presence of tannins in sorghum grains is conditioned by different natural alleles of *Tannin1*. *Proceedings of the National Academy of*

Sciences [online]. **109**(26), 10281-10286. [26/11/2018]. Available from: doi: 10.1073/pnas.1201700109.

Wu, G., Johnson, S.K., Bornman, J.F., Bennett, S.J., Clarke, M.W., Singh, V., Fang, X., (2016). Growth temperature and genotype both play important roles in sorghum grain phenolic composition. *Scientific Reports* [online]. **6**(November 2015), 1-10. [20/10/2017]. Avaliable from: doi: 10.1038/srep21835.

Wu, G., Bornman, J.F., Bennett, S.J., Clarke, M.W., Fang, Z., Johnson, S.K., (2017). Individual polyphenolic profiles and antioxidant activity in sorghum grains are influenced by very low and high solar UV radiation and genotype. *Journal of Cereal Science* [online]. **77**, 17-23. [14/11/2017]. Available from: doi: 10.1016/j.jcs.2017.07.014.

Xia, B., Feng, M., Ding, L., Zhou, Y., (2014). Fast Separation Method Development for Supercritical Fluid Chromatography Using an Autoblending Protocol. *Chromatographia* [online]. **77**(11-12), 783-791. [06/10/2017]. Available from: doi: 10.1007/s10337-014-2684-y.

Xie, P., Shi, J., Tang, S., Chen, C., Khan, A., Zhang, F., Xiong, Y., Li, C., He, W., Wang, G., Lei, F., Wu, Y., Xie, Q., (2019). Control of Bird Feeding Behavior by *Tannin1* through Modulating the Biosynthesis of Polyphenols and Fatty Acid-Derived Volatiles in Sorghum. *Molecular Plant*. [online]. **12**(10), 1315-1324. [29/04/2020]. Available from: doi: 10.1016/j.molp.2019.08.004.

Yamanaka, A., Kouchi, T., Kasai, K., Kato, T., Ishihara, K., Okuda, K., (2007). Inhibitory effect of cranberry polyphenol on biofilm formation and cysteine proteases of *Porphyromonas gingivalis*. *Journal of Periodontal Research* [online]. **42**(6), 589-592. [19/01/2018]. Available from: doi: 10.1111/j.1600-0765.2007.00982.x.

Yang, L., Browning, J.D., Awika, J.M., (2009). Sorghum 3-Deoxyanthocyanins Possess Strong Phase II Enzyme Inducer Activity and Cancer Cell Growth Inhibition Properties. *Journal of Agricultural and Food Chemistry* [online]. **57**(5), 1797-1804. [26/11/2018]. Available from: doi: 10.1021/jf8035066.

Yang, L., (2013). Estrogenic properties of sorghum phenolics: possible role in colon cancer prevention. Ph.D. Thesis, Texas A&M University. [10/02/2020]. Available from: http://hdl.handle.net/1969.1/151237.

Youssef, A.M., (1998). Extractability, fractionation and nutritional value of low and high tannin sorghum proteins. *Food Chemistry* [online]. **63**(3), 325-329. [07/11/2017]. Available from: doi: 10.1016/S0308-8146(98)00028-4.

Yu, S., Cowieson, A., Gilbert, C., Plumstead, P., Dalsgaard, S., (2012). Interactions of phytate and myo-inositol phosphate esters (IP_{1-5}) including IP5 isomers with dietary protein and iron and inhibition of pepsin. *Journal of Animal Science* [online]. **90**(6), 1824-1832. [01/05/2020]. Available from: doi: 10.2527/jas.2011-3866.

Zhang, Y., Li, M., Gao, H., Wang, B., Tongcheng, X., Gao, B., Yu, L., (2019). Triacylglycerol, fatty acid, and phytochemical profiles in a new red sorghum variety (Ji Liang No. 1) and its antioxidant and anti-inflammatory properties. *Food Science and Nutrition* [online]. **7**(3), 949-958. [07/01/2020]. Available from: doi: 10.1002/fsn3.886.

Zhong, H., Xue, Y., Lu, X., Shao, Q., Cao, Y., Wu, Z., Chen, G., (2018). The Effects of Different Degrees of Procyanidin Polymerization on the Nutrient Absorption and Digestive Enzyme Activity in Mice. *Molecules* [online]. **23**(11), 1-11. [22/03/2019]. Available from: doi: 10.3390/molecules23112916.

Zhou, Y., Wang, Z., Li, Y., Li, Z., Liu, H., Zhou, W., (2020). Metabolite Profiling of Sorghum Seeds of Different Colors from Different Sweet Sorghum Cultivars Using a Widely Targeted Metabolomics Approach. *International Journal of Genomics*. [online]. **2020**, 1-13. [08/04/2020]. Available from: doi: 10.1155/2020/6247429.

Appendix

Appendix A

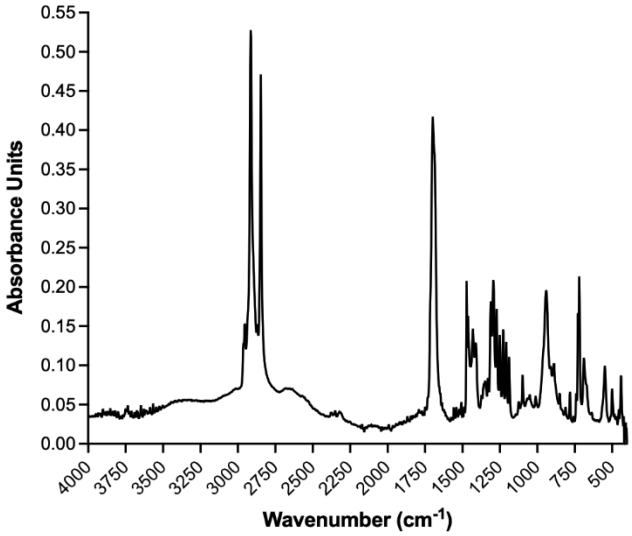

Figure A.1 Palmitic acid standard FT-IR spectra
Spectra were obtained from 4000 – 400 cm^{-1} and baseline corrected using a multi-point method. Three replicate spectra were averaged.

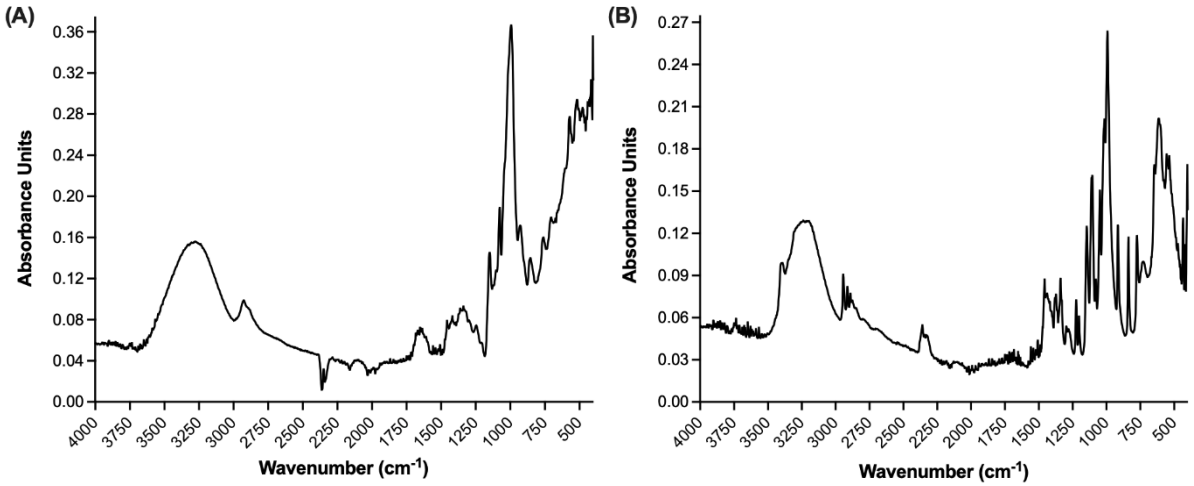

Figure A.2 Starch and glucose standard FT-IR spectra
Spectra were obtained from **(A)** starch and **(B)** glucose standards between 4000 – 400 cm^{-1} and baseline corrected using a multi-point method. Three replicate spectra were averaged.

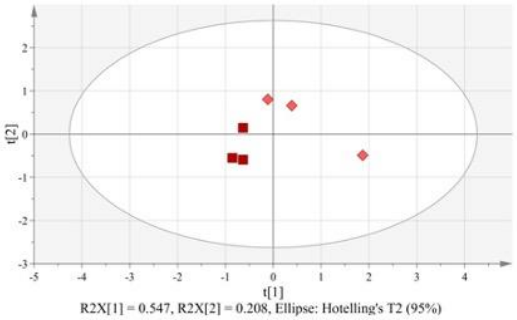

MR-Buster

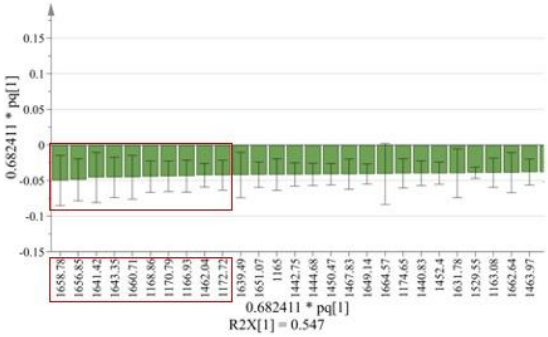

Cracka

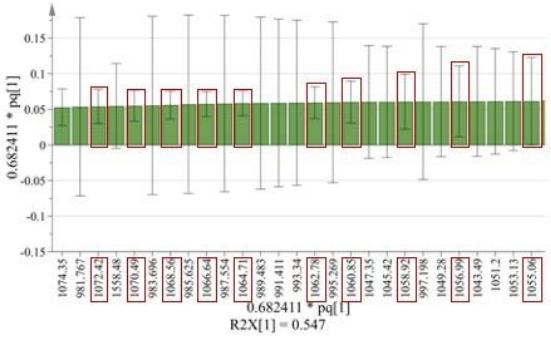

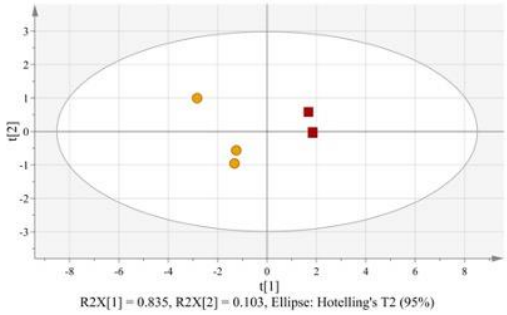

Liberty

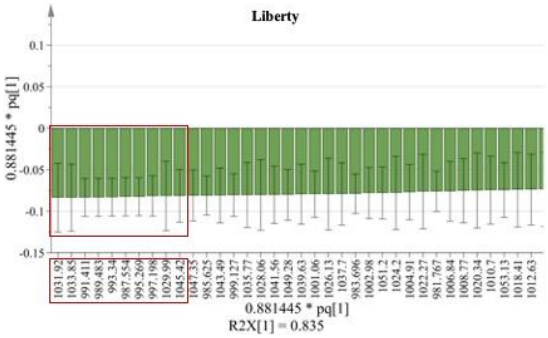

MR-Buster

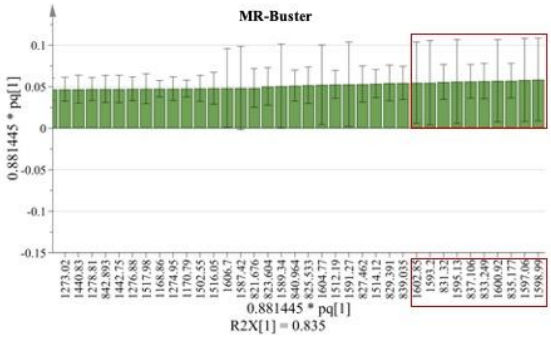

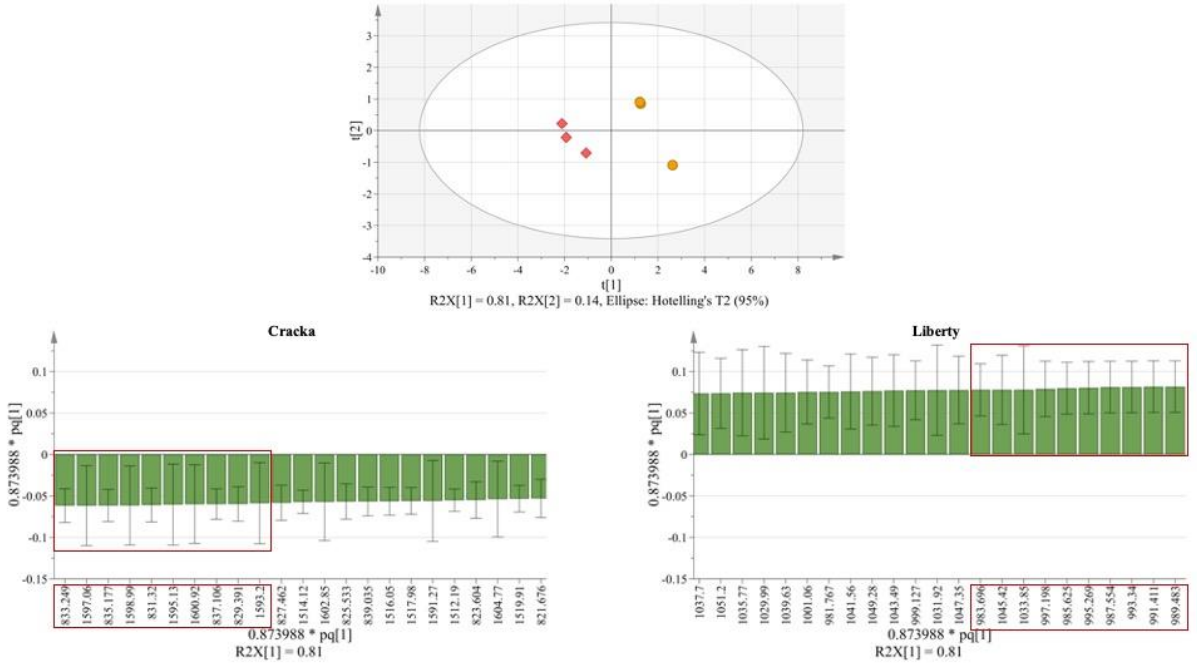

Figure A.3 FT-IR Fingerprint Spectra OPLS-DA and loadings plots of sorghum polyphenol extracts

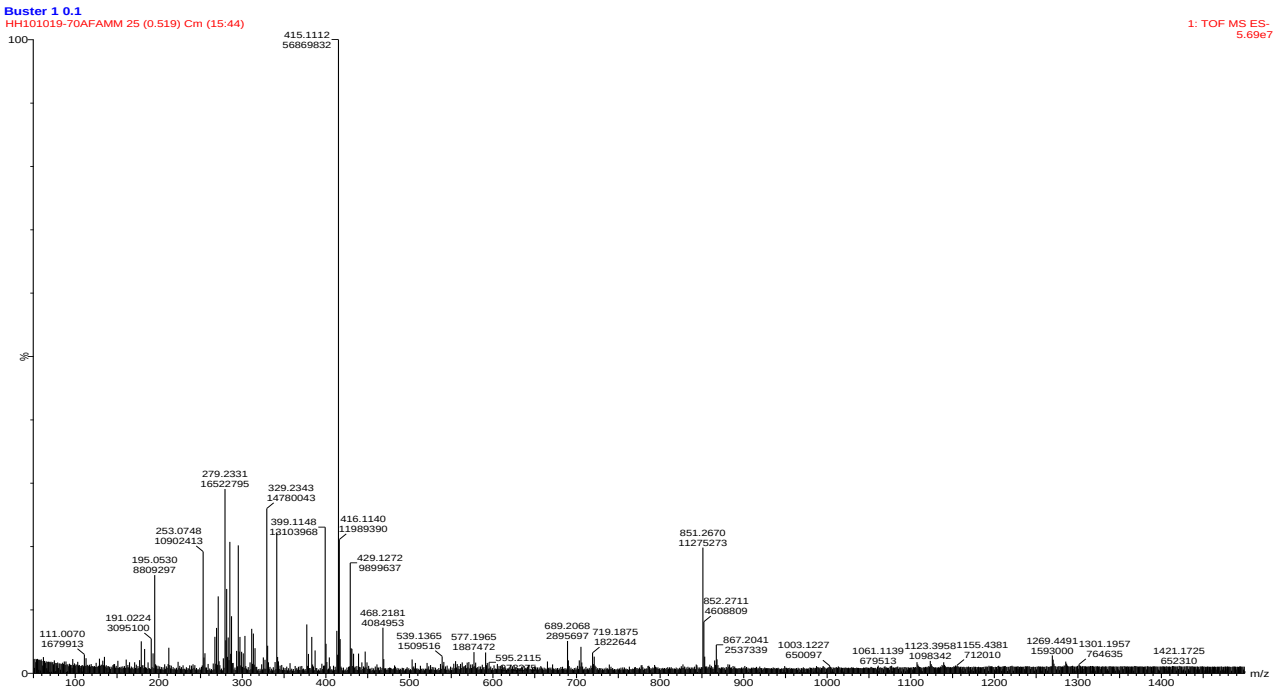

Figure A.4A Sample ESI-MS (–) spectrum of MR-Buster sorghum polyphenol extract

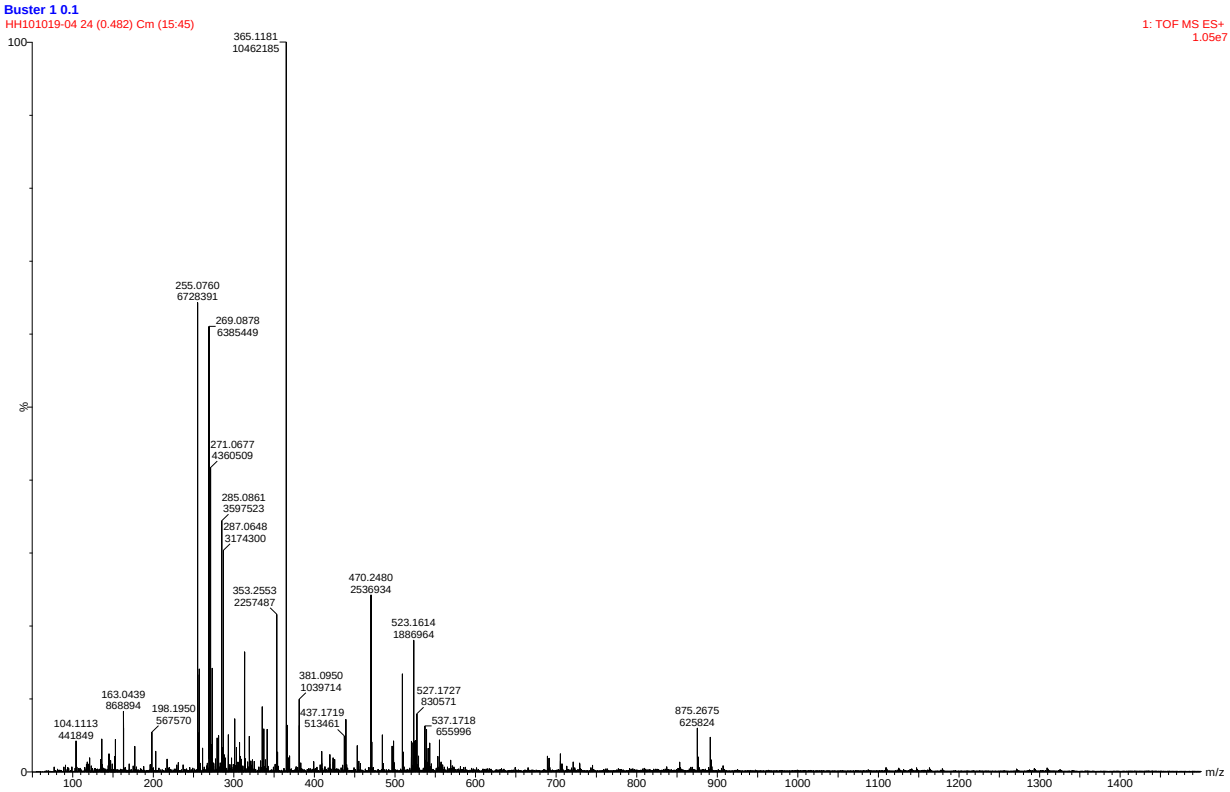

Figure A.4B Sample ESI-MS (+) spectrum of MR-Buster sorghum polyphenol extract

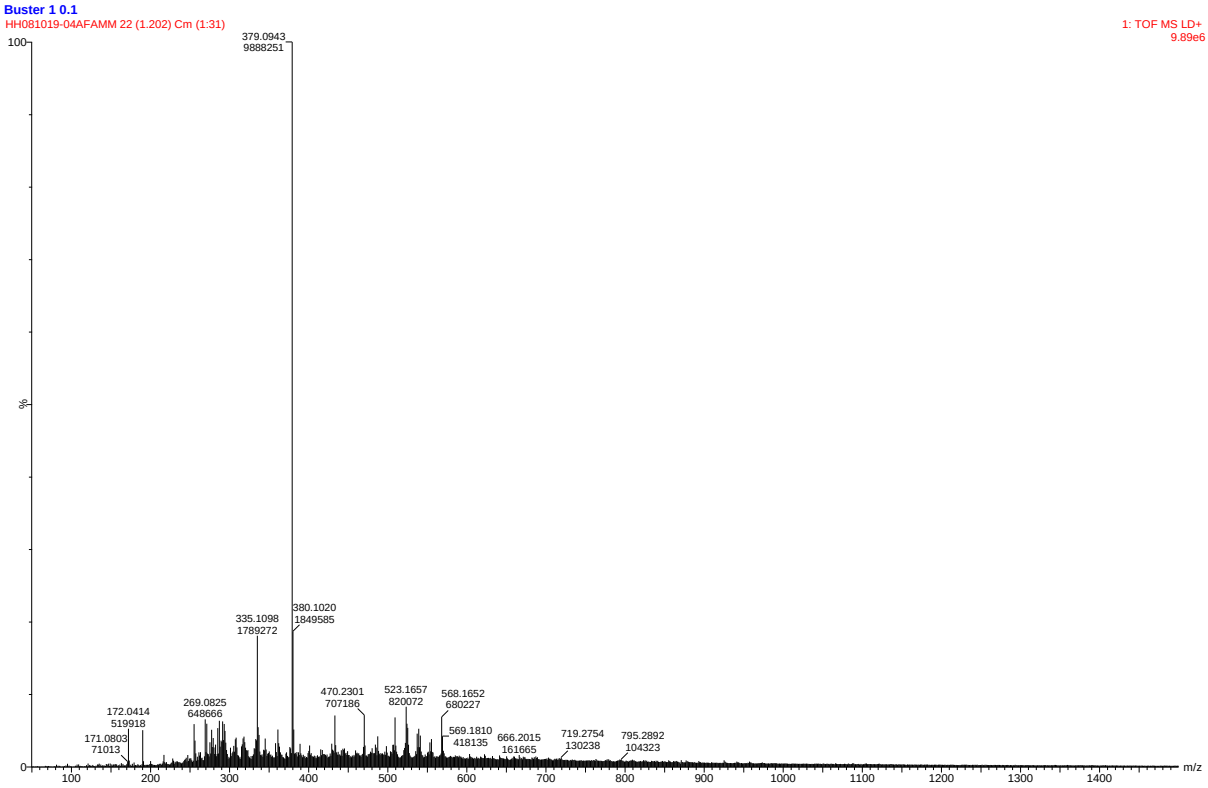

Figure A.4C Sample MALDI (+) spectrum of MR-Buster sorghum polyphenol extract

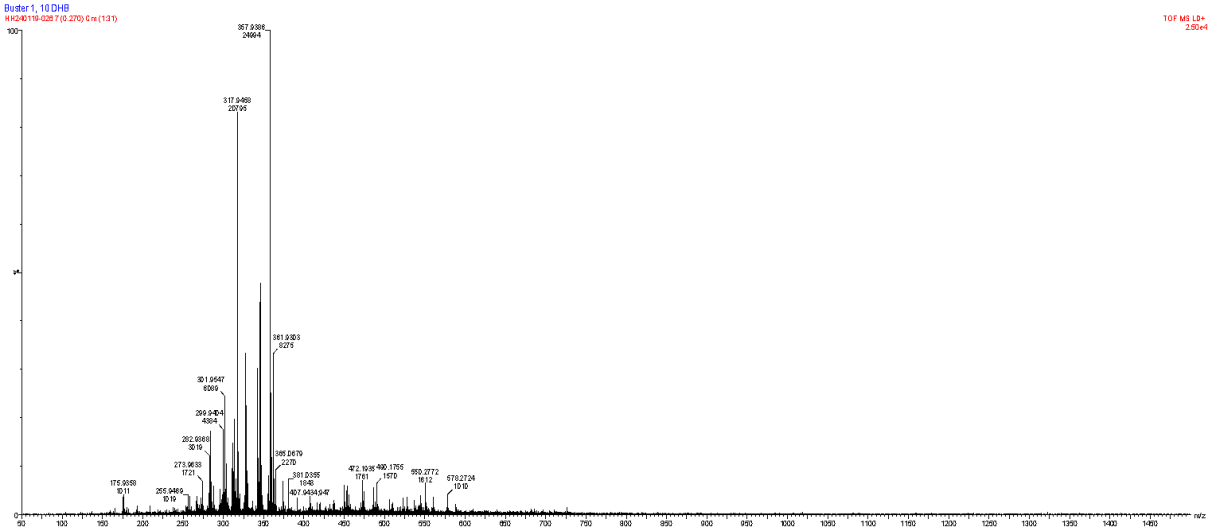

Figure A.5 MALDI (+) spectrum of MR-Buster sorghum polyphenol extract containing DHB matrix chemical

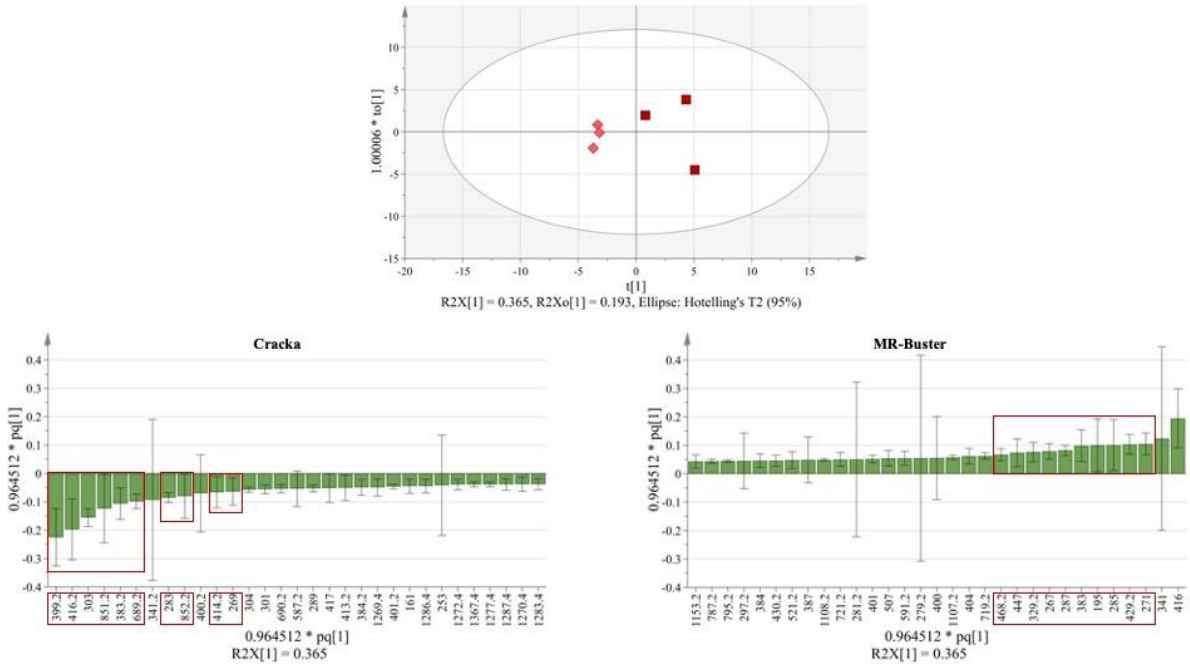

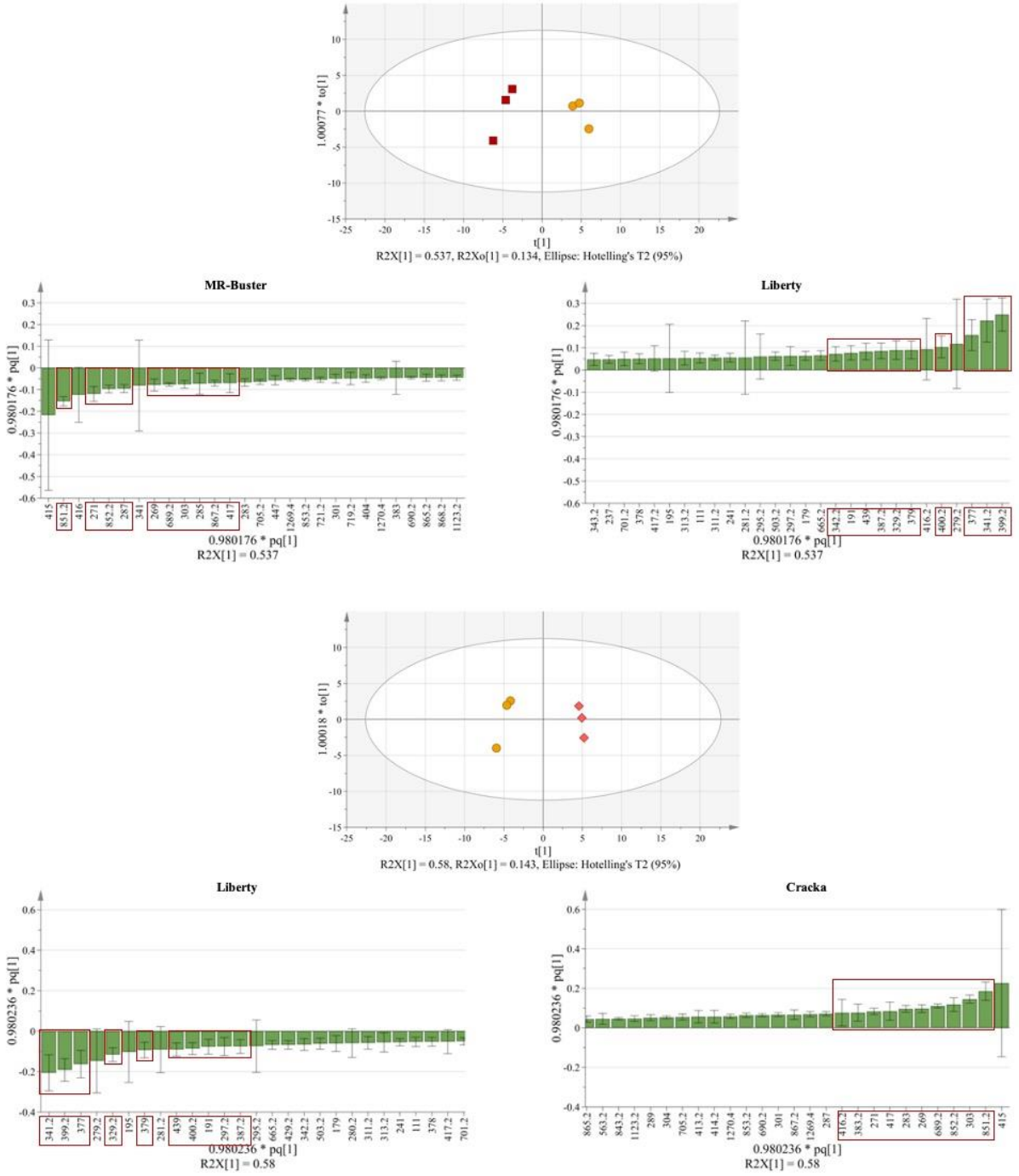

Figure A.6 ESI (-) OPLS-DA and loadings plots of sorghum polyphenol extracts

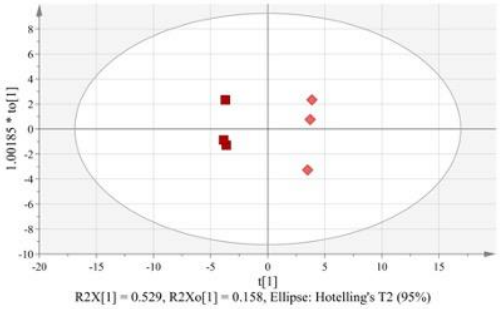
1.00185 * to[1]
t[1]
R2X[1] = 0.529, R2Xo[1] = 0.158, Ellipse: Hotelling's T2 (95%)

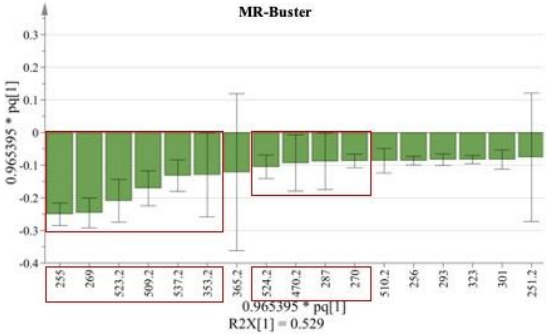
MR-Buster
0.965395 * pq[1]
R2X[1] = 0.529

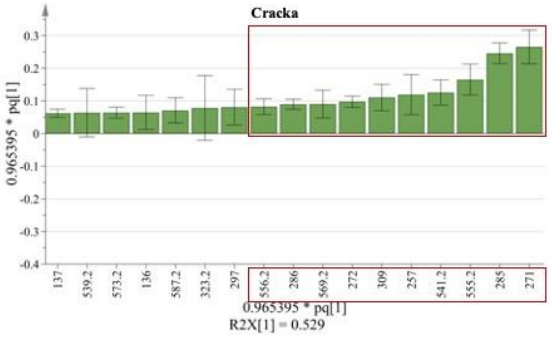
Cracka
0.965395 * pq[1]
R2X[1] = 0.529

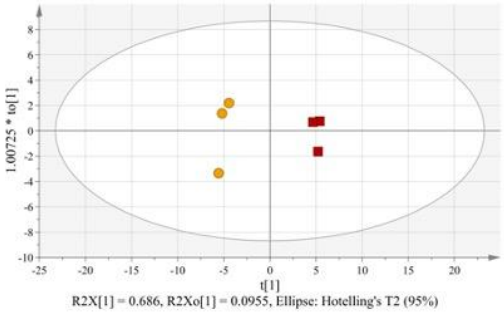
1.00725 * to[1]
t[1]
R2X[1] = 0.686, R2Xo[1] = 0.0955, Ellipse: Hotelling's T2 (95%)

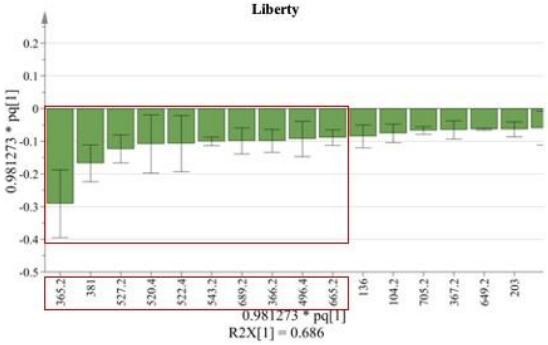
Liberty
0.981273 * pq[1]
R2X[1] = 0.686

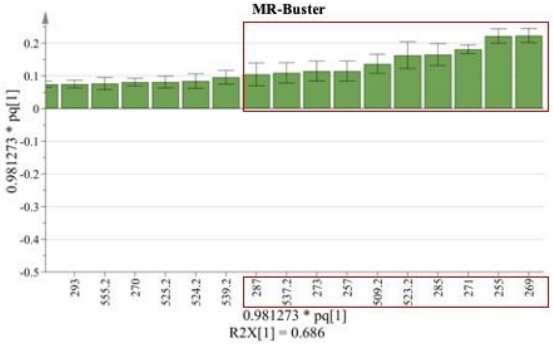
MR-Buster
0.981273 * pq[1]
R2X[1] = 0.686

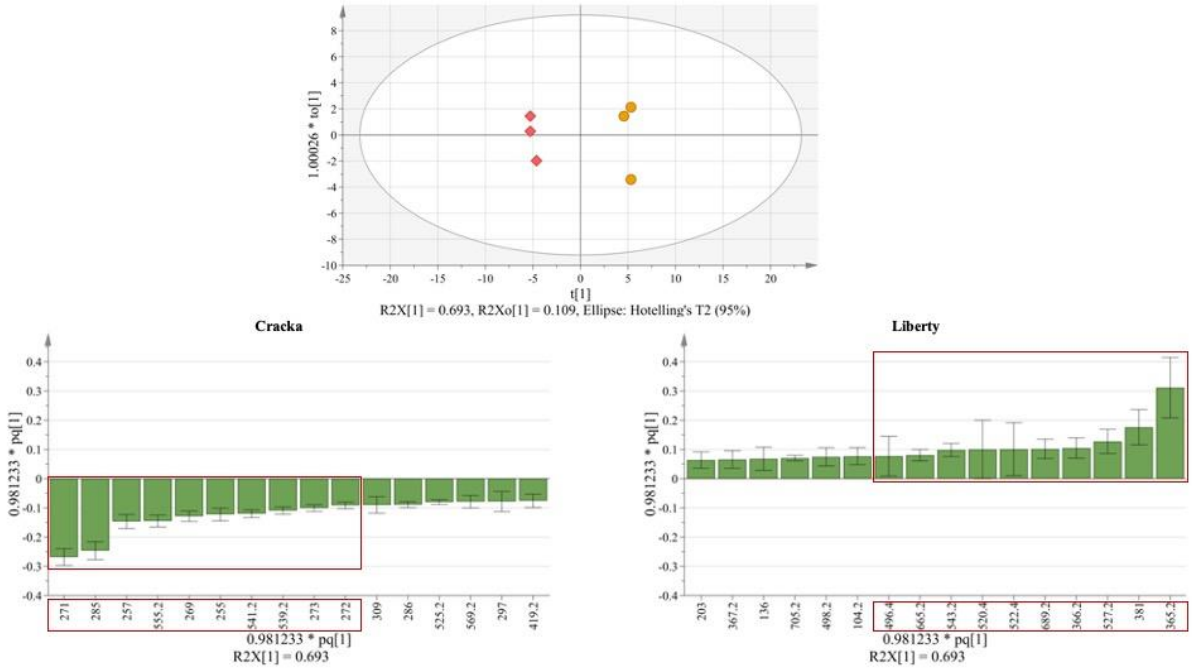

Figure A.7 ESI (+) OPLS-DA and loadings plots of sorghum polyphenol extracts

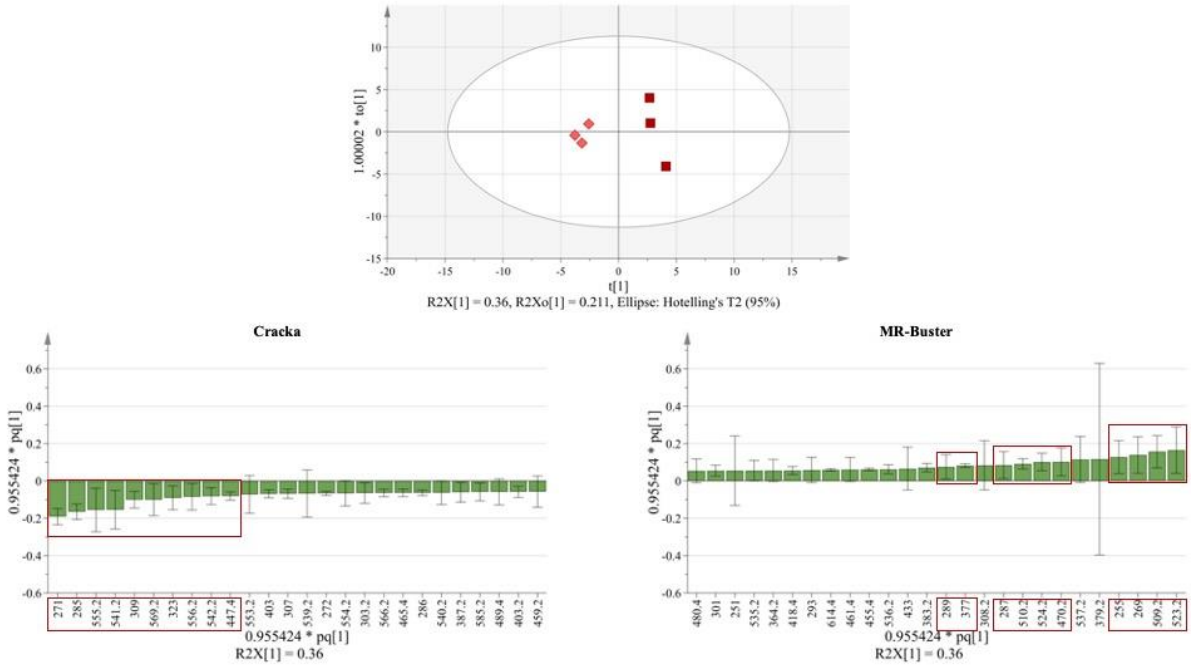

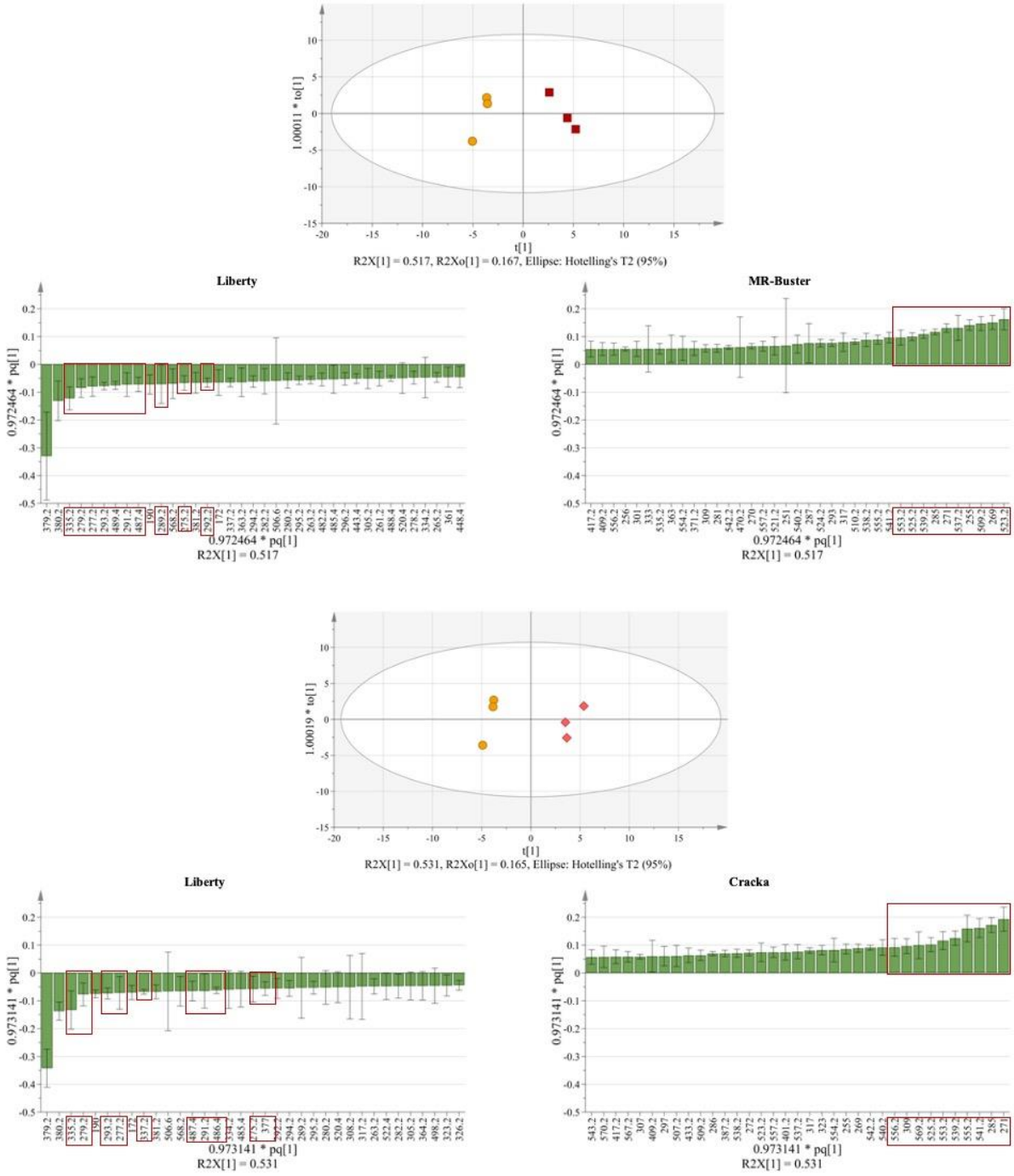

Figure A.8 MALDI (+) OPLS-DA and loadings plots of sorghum polyphenol extracts

(A)

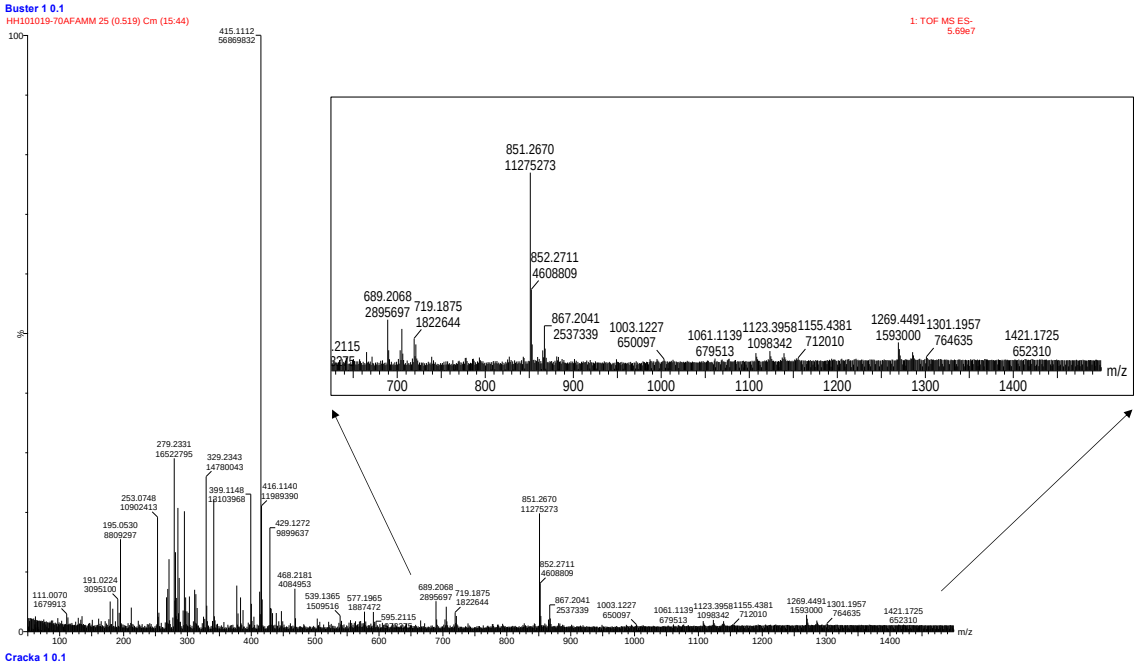
Buster 1 0.1
HH101019-70AFAMM 25 (0.519) Cm (15:44)
1: TOF MS ES-
5.69e7
415.1112
56869832
851.2670
11275273
852.2711
4608809
689.2068
2895697
719.1875
1822644
867.2041
2537339
1003.1227
650097
1061.1139
679513
1123.3958
1098342
1155.4381
712010
1269.4491
1593000
1301.1957
764635
1421.1725
652310
m/z
279.2331
16522795
329.2343
14780043
253.0748
10902413
399.1148
18103968
416.1140
11989390
195.0530
8809297
429.1272
9899637
191.0224
3095100
468.2181
4084953
111.0070
1679913
539.1365
1509516
577.1965
1887472
595.2115

(B)

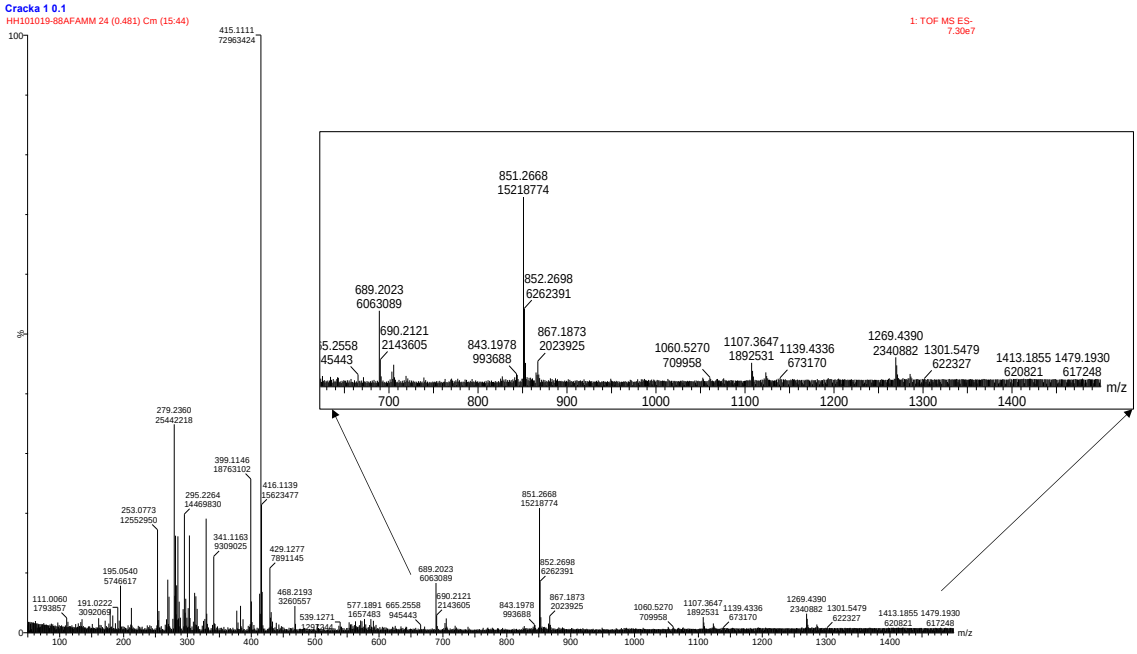
Cracka 1 0.1
HH101019-88AFAMM 24 (0.481) Cm (15:44)
1: TOF MS ES-
7.30e7
415.1111
72963424
851.2668
15218774
852.2698
6262391
689.2023
6063089
690.2121
2143605
843.1978
993688
867.1873
2023925
1060.5270
709958
1107.3647
1892531
1139.4336
673170
1269.4390
2340882
1301.5479
622327
1413.1855
620821
1479.1930
617248
m/z
279.2360
25442218
399.1146
18763102
416.1139
15623477
295.2264
14469830
253.0773
12552950
341.1163
9309025
429.1277
7891145
195.0540
5746617
468.2193
3260557
111.0060
1793857
191.0222
3092069
539.1271
577.1891
1657483
665.2558
945443

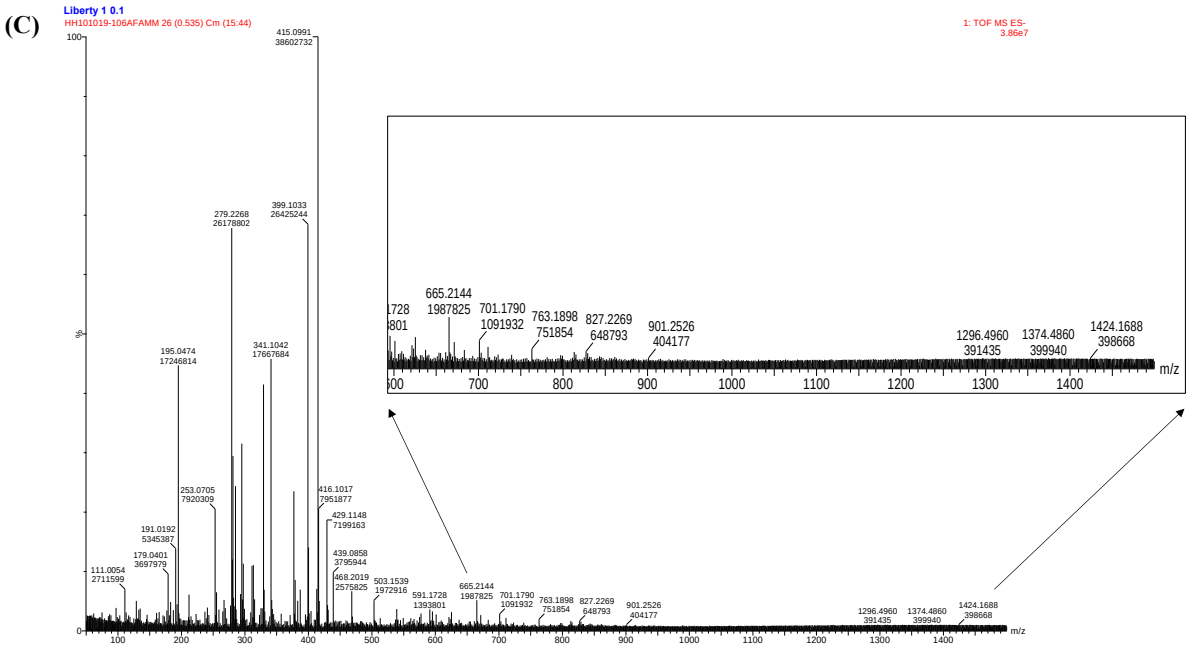

Figure A.9 Unresolved high molecular weight compounds in sorghum polyphenol extracts identified using ESI (–)

Table A.1 MR-Buster sorghum polyphenol extract putative identifications from OPLS-DA (ESI [-])

Bin	Detected Mass	Accurate Mass	Δppm	Name	Formula	Chemical Group	Pathway
329.2	329.224	330.232	35	Jasmolin I	C21H30O3	Monoterpene	
			28	9,10-Dihydroxy-12,13-epoxyoctadecanoic acid	C18H34O5	Fatty acid	Linoleic acid metabolism
			28	9,10,13-Trihydroxyoctadec-11-enoic acid	C18H34O5	Fatty acid	Linoleic acid metabolism
			28	9(S),12(S),13(S)-Trihydroxy-10(E)-octadecenoic acid	C18H34O5	Fatty acid	Linoleic acid metabolism
			35	Turricolol E	C21H30O3	Sesquiterpenoid	
	329.2272333	330.2352333	18	9,10-Dihydroxy-12,13-epoxyoctadecanoic acid	C18H34O5	Fatty acid	Linoleic acid metabolism
			18	9,10,13-Trihydroxyoctadec-11-enoic acid	C18H34O5	Fatty acid	Linoleic acid metabolism
			18	9(S),12(S),13(S)-Trihydroxy-10(E)-octadecenoic acid	C18H34O5	Fatty acid	Linoleic acid metabolism
	329.2284667	330.2364667	14	9,10-Dihydroxy-12,13-epoxyoctadecanoic acid	C18H34O5	Fatty acid	Linoleic acid metabolism
			14	9,10,13-Trihydroxyoctadec-11-enoic acid	C18H34O5	Fatty acid	Linoleic acid metabolism
			14	9(S),12(S),13(S)-Trihydroxy-10(E)-octadecenoic acid	C18H34O5	Fatty acid	Linoleic acid metabolism
416	416.0964	417.1044	34	Apigeninidin 5-O-glucoside	C21H20O9	3-deoxyanthocyanidin	
	416.1006667	417.1086667	24	Apigeninidin 5-O-glucoside	C21H20O9	3-deoxyanthocyanidin	
	416.1015333	417.1095333	22	Apigeninidin 5-O-glucoside	C21H20O9	3-deoxyanthocyanidin	
	416.2851	417.2931					
285	285.0319333	286.0399333	29	Orobol	C15H10O6	Isoflavone	
			29	6-Hydroxyapigenin	C15H10O6	Flavone	
			29	8-Hydroxyapigenin	C15H10O6	Flavone	
			29	Fisetin	C15H10O6	Flavonol	
			29	Datiscetin	C15H10O6	Flavonol	
			29	Maritimetin	C15H10O6	Aurone	
			29	Aureusidin	C15H10O6	Aurone	
			29	Kaempferol	C15H10O6	Flavonol	Flavonoid, flavone and flavonol and phenylpropanoid biosynthesis
			29	Luteolin	C15H10O6	Flavone	Flavonoid, flavone and flavonol biosynthesis
			29	2'-Hydroxygenistein	C15H10O6	Isoflavone	Isoflavonoid biosynthesis
	285.0779667	286.0859667	3	2,7-Dihydroxy-4'-methoxyisoflavanone	C16H14O5	Isoflavanone	Isoflavonoid biosynthesis
			3	(-)-Nissolin	C16H14O5	Pterocarpan	
			3	Phyllodulcin	C16H14O5	Stilbenoid	
			3	2',4',6'-Trihydroxy-3'-formyldihydrochalcone	C16H14O5	Dihydrochalcone	
			3	Brazilin	C16H14O5	Neoflavonoid	
			3	Sakuranetin	C16H14O5	Flavanone	Flavonoid biosynthesis
			3	Oxypeucedanin	C16H14O5	Furanocoumarin	
			3	Quinquangulin	C16H14O5	Naphthopyrone	
			3	Sainfuran	C16H14O5	2-Arylbenzofuran	
			3	Moracin A	C16H14O5	2-Arylbenzofuran	
			3	4'-Methylnaringenin	C16H14O5	Flavanone	Flavonoid biosynthesis
			3	2'-O-Methyllicodione	C16H14O5	Dihydrochalcone	
			3	Dihydrobiochanin A	C16H14O5	Isoflavanone	Isoflavonoid biosynthesis

			3	Vestitone	C16H14O5	Isoflavanone	Isoflavonoid biosynthesis
	284.9164333	285.9244333					
	285.0353667	286.0433667	17	Orobol	C15H10O6	Isoflavone	
			17	6-Hydroxyapigenin	C15H10O6	Flavone	
			17	8-Hydroxyapigenin	C15H10O6	Flavone	
			17	Fisetin	C15H10O6	Flavonol	
			17	Datiscetin	C15H10O6	Flavonol	
			17	Maritimetin	C15H10O6	Aurone	
			17	Aureusidin	C15H10O6	Aurone	
			17	Kaempferol	C15H10O6	Flavonol	Flavonoid, flavone and flavonol and phenylpropanoid biosynthesis
			17	Luteolin	C15H10O6	Flavone	Flavonoid, flavone and flavonol biosynthesis
			17	2'-Hydroxygenistein	C15H10O6	Isoflavone	Isoflavonoid biosynthesis
	285.082	286.09	18	2,7-Dihydroxy-4'-methoxyisoflavanone	C16H14O5	Isoflavanone	Isoflavonoid biosynthesis
			18	(-)-Nissolin	C16H14O5	Pterocarpan	
			18	Phyllodulcin	C16H14O5	Stilbenoid	
			18	2',4',6'-Trihydroxy-3'-formyldihydrochalcone	C16H14O5	Dihydrochalcone	
			18	Brazilin	C16H14O5	Neoflavonoid	
			18	Sakuranetin	C16H14O5	Flavanone	Flavonoid biosynthesis
			18	Oxypeucedanin	C16H14O5	Furanocoumarin	
			18	Quinquangulin	C16H14O5	Naphthopyrone	
			18	Sainfuran	C16H14O5	2-Arylbenzofuran	
			18	Moracin A	C16H14O5	2-Arylbenzofuran	
			18	4'-Methylnaringenin	C16H14O5	Flavanone	Flavonoid biosynthesis
			18	2'-O-Methyllicodione	C16H14O5	Dihydrochalcone	
			18	Dihydrobiochanin A	C16H14O5	Isoflavanone	Isoflavonoid biosynthesis
			18	Vestitone	C16H14O5	Isoflavanone	Isoflavonoid biosynthesis
	285.0359667	286.0439667	15	Orobol	C15H10O6	Isoflavone	
			15	6-Hydroxyapigenin	C15H10O6	Flavone	
			15	8-Hydroxyapigenin	C15H10O6	Flavone	
			15	Fisetin	C15H10O6	Flavonol	
			15	Datiscetin	C15H10O6	Flavonol	
			15	Maritimetin	C15H10O6	Aurone	
			15	Aureusidin	C15H10O6	Aurone	
			15	Kaempferol	C15H10O6	Flavonol	Flavonoid, flavone and flavonol and phenylpropanoid biosynthesis
			15	Luteolin	C15H10O6	Flavone	Flavonoid, flavone and flavonol biosynthesis
			15	2'-Hydroxygenistein	C15H10O6	Isoflavone	Isoflavonoid biosynthesis
	285.0832	286.0912	22	2,7-Dihydroxy-4'-methoxyisoflavanone	C16H14O5	Isoflavanone	Isoflavonoid biosynthesis
			22	(-)-Nissolin	C16H14O5	Pterocarpan	
			22	Phyllodulcin	C16H14O5	Stilbenoid	

			22	2',4',6'-Trihydroxy-3'-formyldihydrochalcone	C16H14O5	Dihydrochalcone	
			22	Brazilin	C16H14O5	Neoflavonoid	
			22	Sakuranetin	C16H14O5	Flavanone	Flavonoid biosynthesis
			22	Oxypeucedanin	C16H14O5	Furanocoumarin	
			22	Quinquangulin	C16H14O5	Naphthopyrone	
			22	Sainfuran	C16H14O5	2-Arylbenzofuran	
			22	Moracin A	C16H14O5	2-Arylbenzofuran	
			22	4'-Methylnaringenin	C16H14O5	Flavanone	Flavonoid biosynthesis
			22	2'-O-Methyllicodione	C16H14O5	Dihydrochalcone	
			22	Dihydrobiochanin A	C16H14O5	Isoflavanone	Isoflavonoid biosynthesis
			22	Vestitone	C16H14O5	Isoflavanone	Isoflavonoid biosynthesis
	851.21877	852.22677					
	851.2274	852.2354					
851.2	851.2301	852.2381					
	271.0532333	272.0612333	29	Toralactone	C15H12O5	Naphthopyrone	
			29	6,7,4'-Trihydroxyflavanone	C15H12O5	Flavanone	Isoflavonoid biosynthesis
271			29	2,7,4'-Trihydroxyisoflavanone	C15H12O5	Isoflavanone	Isoflavonoid biosynthesis
			29	Dihydrogenistein	C15H12O5	Flavanone	
			29	p-Coumaroyltriacetic acid lactone	C15H12O5	Chalcone	
			29	Pinobanksin	C15H12O5	Dihydroflavonol	Flavonoid biosynthesis
			29	Garbanzol	C15H12O5	Dihydroflavonol	Flavonoid biosynthesis
			29	Butin	C15H12O5	Flavanone	Flavonoid biosynthesis
			29	Rubrofusarin	C15H12O5	Naphthopyrones	
			29	Butein	C15H12O5	Chalcone	Flavonoid biosynthesis
			29	Naringenin chalcone	C15H12O5	Chalcone	Flavonoid biosynthesis
			29	2'-Hydroxydihydrodaidzein	C15H12O5	Isoflavanone	Isoflavonoid biosynthesis
			29	Licodione	C15H12O5	Chalcone	
			29	(-)-Glycinol	C15H12O5	Pterocarpan	Isoflavonoid biosynthesis
			29	Naringenin	C15H12O5	Flavanone	Flavonoid, isoflavonoid and phenylpropanoid biosynthesis
	271.0556333	272.0636333	20	Toralactone	C15H12O5	Naphthopyrone	
			20	6,7,4'-Trihydroxyflavanone	C15H12O5	Flavanone	Isoflavonoid biosynthesis
			20	2,7,4'-Trihydroxyisoflavanone	C15H12O5	Isoflavanone	Isoflavonoid biosynthesis
			20	Dihydrogenistein	C15H12O5	Flavanone	
			20	p-Coumaroyltriacetic acid lactone	C15H12O5	Chalcone	
			20	Pinobanksin	C15H12O5	Dihydroflavonol	Flavonoid biosynthesis
			20	Garbanzol	C15H12O5	Dihydroflavonol	Flavonoid biosynthesis
			20	Butin	C15H12O5	Flavanone	Flavonoid biosynthesis
			20	Rubrofusarin	C15H12O5	Naphthopyrones	
			20	Butein	C15H12O5	Chalcone	Flavonoid biosynthesis
			20	Naringenin chalcone	C15H12O5	Chalcone	Flavonoid biosynthesis
			20	2'-Hydroxydihydrodaidzein	C15H12O5	Isoflavanone	Isoflavonoid biosynthesis
			20	Licodione	C15H12O5	Chalcone	
			20	(-)-Glycinol	C15H12O5	Pterocarpan	Isoflavonoid biosynthesis

			20	Naringenin	C15H12O5	Flavanone	Flavonoid, isoflavonoid and phenylpropanoid biosynthesis
	270.9482	271.9562					
	271.0566	272.0646	16	Toralactone	C15H12O5	Naphthopyrone	
			16	6,7,4'-Trihydroxyflavanone	C15H12O5	Flavanone	Isoflavonoid biosynthesis
			16	2,7,4'-Trihydroxyisoflavanone	C15H12O5	Isoflavanone	Isoflavonoid biosynthesis
			16	Dihydrogenistein	C15H12O5	Flavanone	
			16	p-Coumaroyltriacetic acid lactone	C15H12O5	Chalcone	
			16	Pinobanksin	C15H12O5	Dihydroflavonol	Flavonoid biosynthesis
			16	Garbanzol	C15H12O5	Dihydroflavonol	Flavonoid biosynthesis
			16	Butin	C15H12O5	Flavanone	Flavonoid biosynthesis
			16	Rubrofusarin	C15H12O5	Naphthopyrones	
			16	Butein	C15H12O5	Chalcone	Flavonoid biosynthesis
			16	Naringenin chalcone	C15H12O5	Chalcone	Flavonoid biosynthesis
			16	2'-Hydroxydihydrodaidzein	C15H12O5	Isoflavanone	Isoflavonoid biosynthesis
			16	Licodione	C15H12O5	Chalcone	
			16	(-)-Glycinol	C15H12O5	Pterocarpan	Isoflavonoid biosynthesis
			16	Naringenin	C15H12O5	Flavanone	Flavonoid, isoflavonoid and phenylpropanoid biosynthesis
429.2	429.1054	430.1134	7	N-Ethylmaleimide-S-glutathione	C16H22N4O8S	Peptide	
			31	Formononetin 7-O-glucoside	C22H22O9	Isoflavone	Isoflavonoid biosynthesis
	429.2057	430.2137	6	Cinegalline	C23H30N2O6	Quinolizidine alkaloid	
			32	Athamantin	C24H30O7	Furanocoumarin	
	429.1094	430.1174	1	N-Ethylmaleimide-S-glutathione	C16H22N4O8S	Peptide	
			22	Formononetin 7-O-glucoside	C22H22O9	Isoflavone	Isoflavonoid biosynthesis
	429.2095333	430.2175333	14	Cinegalline	C23H30N2O6	Quinolizidine alkaloid	
	429.1109	430.1189	5	N-Ethylmaleimide-S-glutathione	C16H22N4O8S	Peptide	
			19	Formononetin 7-O-glucoside	C22H22O9	Isoflavone	Isoflavonoid biosynthesis
	429.2119333	430.2199333	20	Cinegalline	C23H30N2O6	Quinolizidine alkaloid	
383	383.0993333	384.1073333	37	4'-Demethyldeoxypodophyllotoxin	C21H20O7	Lignan	
			39	S-Adenosylhomocysteine	C14H20N6O5S	Amino acid	Cysteine and methionine metabolism
	383.1009	384.1089	33	4'-Demethyldeoxypodophyllotoxin	C21H20O7	Lignan	
			35	S-Adenosylhomocysteine	C14H20N6O5S	Amino acid	Cysteine and methionine metabolism
	383.1050667	384.1130667	22	4'-Demethyldeoxypodophyllotoxin	C21H20O7	Lignan	
			24	S-Adenosylhomocysteine	C14H20N6O5S	Amino acid	Cysteine and methionine metabolism
			37	Acetyl-maltose	C14H24O12	Disaccharide	
	383.2344333	384.2424333					
	286.9263667	287.9343667					
	287.0408	288.0488					
	287.0836333	288.0916333	30	Shikonin	C16H16O5	Naphthoquinone	Ubiquinone and terpenoid-quinone biosynthesis
			30	7,2'-Dihydroxy-4'-methoxy-isoflavanol	C16H16O5	Isoflavone	Isoflavonoid biosynthesis
			30	Asebogenin	C16H16O5	Dihydrochalcone	

287	286.9290333	287.9370333					
	287.0444	288.0524					
	287.0867667	288.0947667	19	Shikonin	C16H16O5	Naphthoquinone	Ubiquinone and terpenoid-quinone biosynthesis
			19	7,2'-Dihydroxy-4'-methoxy-isoflavanol	C16H16O5	Isoflavone	Isoflavonoid biosynthesis
			19	Asebogenin	C16H16O5	Dihydrochalcone	
	287.0476333	288.0556333	29	Carthamidin	C15H12O6	Flavanone	
			29	2,6,7,4'-Tetrahydroxyisoflavanone	C15H12O6	Isoflavanone	Isoflavonoid biosynthesis
			29	Eriodictyol chalcone	C15H12O6	Chalcone	Flavonoid biosynthesis
			29	2-Hydroxy-2,3-dihydrogenistein	C15H12O6	Isoflavanone	Isoflavonoid biosynthesis
			29	(+-)-Dalbergioidin	C15H12O6	Isoflavanone	
			29	Swerchirin	C15H12O6	Xanthene	
			29	2-O-Methylswertianin	C15H12O6	Xanthene	
			29	Gentiacaulein	C15H12O6	Xanthene	
			29	3,5-Dimethoxy-1,6-dihydroxyxanthone	C15H12O6	Xanthene	
			29	Micromelin	C15H12O6	Coumarin	
			29	Okanin	C15H12O6	Chalcone	
			29	Eriodictyol	C15H12O6	Flavanone	Flavonoid biosynthesis
			29	Fustin	C15H12O6	Dihydroflavonol	Flavonoid biosynthesis
			29	Dihydrokaempferol	C15H12O6	Dihydroflavonol	Flavonoid and phenylpropanoid biosynthesis
	287.0880667	288.0960667	15	Shikonin	C16H16O5	Naphthoquinone	Ubiquinone and terpenoid-quinone biosynthesis
			15	7,2'-Dihydroxy-4'-methoxy-isoflavanol	C16H16O5	Isoflavane	Isoflavonoid biosynthesis
			15	Asebogenin	C16H16O5	Dihydrochalcone	
267	266.9587667	267.9667667					
	267.0595667	268.0675667	25	6-Hydroxy-2'-methoxyflavone	C16H12O4	Flavone	
			25	Isoformononetin	C16H12O4	Isoflavone	Isoflavonoid biosynthesis
			25	Tectochrysin	C16H12O4	Flavone	
			25	Dalbergin	C16H12O4	Neoflavonoid	
			10	Portulacaxanthin III	C11H12N2O6	Amino acid	
			25	Formononetin	C16H12O4	Isoflavone	Isoflavonoid and phenylpropanoid biosynthesis
	266.9636	267.9716					
	267.0618	268.0698	16	6-Hydroxy-2'-methoxyflavone	C16H12O4	Flavone	
			16	Isoformononetin	C16H12O4	Isoflavone	Isoflavonoid biosynthesis
			16	Tectochrysin	C16H12O4	Flavone	
			16	Dalbergin	C16H12O4	Neoflavonoid	
			1	Portulacaxanthin III	C11H12N2O6	Amino acid	
			16	Formononetin	C16H12O4	Isoflavone	Isoflavonoid and phenylpropanoid biosynthesis
			38	2-O-(alpha-D-Mannosyl)-D-glycerate	C9H16O9	Sugar	Fructose and mannose metabolism
	267.0626333	268.0706333	13	6-Hydroxy-2'-methoxyflavone	C16H12O4	Flavone	
			13	Isoformononetin	C16H12O4	Isoflavone	Isoflavonoid biosynthesis
			13	Tectochrysin	C16H12O4	Flavone	

			13	Dalbergin	C16H12O4	Neoflavonoid	
			1	Portulacaxanthin III	C11H12N2O6	Amino acid	
			13	Formononetin	C16H12O4	Isoflavone	Isoflavonoid and phenylpropanoid biosynthesis
			35	2-O-(alpha-D-Mannosyl)-D-glycerate	C9H16O9	Sugar	Fructose and mannose metabolism
447	447.0869	448.0949	14	Scutellarein 7beta-D-glucopyranoside	C21H20O11	Flavanone	
			14	Aureusidin 6-O-glucoside	C21H20O11	Aurone	Flavonoid biosynthesis
			14	Cyanidin 5-O-glucoside	C21H20O11	Anthocyanin	Anthocyanin biosynthesis
			14	Kaempferol-3-O-galactoside	C21H20O11	Flavonol	Flavone and flavonol biosynthesis
			14	Kaempferol 3-O-glucoside	C21H20O11	Flavonol	Flavone and flavonol biosynthesis
			14	Luteolin 8-C-glucoside	C21H20O11	Flavone	
			14	Fisetin 8-C-glucoside	C21H20O11	Flavonoid	
			14	Cyanidin 3-O-glucoside	C21H20O11	Anthocyanin	Anthocyanin biosynthesis
			14	Carthamone	C21H20O11	Chalcone	
			14	Luteolin 7-O-glucoside	C21H20O11	Flavone	Flavone and flavonol biosynthesis
			14	Isoorientin	C21H20O11	Flavone	
			14	Quercitrin	C21H20O11	Flavonol	Flavone and flavonol biosynthesis
	447.0922	448.1002	2	Scutellarein 7beta-D-glucopyranoside	C21H20O11	Flavanone	
			2	Aureusidin 6-O-glucoside	C21H20O11	Aurone	Flavonoid biosynthesis
			2	Cyanidin 5-O-glucoside	C21H20O11	Anthocyanin	Anthocyanin biosynthesis
			2	Kaempferol-3-O-galactoside	C21H20O11	Flavonol	Flavone and flavonol biosynthesis
			2	Kaempferol 3-O-glucoside	C21H20O11	Flavonol	Flavone and flavonol biosynthesis
			2	Luteolin 8-C-glucoside	C21H20O11	Flavone	
			2	Fisetin 8-C-glucoside	C21H20O11	Flavonoid	
			2	Cyanidin 3-O-glucoside	C21H20O11	Anthocyanin	Anthocyanin biosynthesis
			2	Carthamone	C21H20O11	Chalcone	
			2	Luteolin 7-O-glucoside	C21H20O11	Flavone	Flavone and flavonol biosynthesis
			2	Isoorientin	C21H20O11	Flavone	
			2	Quercitrin	C21H20O11	Flavonol	Flavone and flavonol biosynthesis
	447.0954667	448.1034667	4	Scutellarein 7beta-D-glucopyranoside	C21H20O11	Flavanone	
			4	Aureusidin 6-O-glucoside	C21H20O11	Aurone	Flavonoid biosynthesis
			4	Cyanidin 5-O-glucoside	C21H20O11	Anthocyanin	Anthocyanin biosynthesis
			4	Kaempferol-3-O-galactoside	C21H20O11	Flavonol	Flavone and flavonol biosynthesis
			4	Kaempferol 3-O-glucoside	C21H20O11	Flavonol	Flavone and flavonol biosynthesis

			4	Luteolin 8-C-glucoside	C21H20O11	Flavone	
			4	Fisetin 8-C-glucoside	C21H20O11	Flavonoid	
			4	Cyanidin 3-O-glucoside	C21H20O11	Anthocyanin	Anthocyanin biosynthesis
			4	Carthamone	C21H20O11	Chalcone	
			4	Luteolin 7-O-glucoside	C21H20O11	Flavone	Flavone and flavonol biosynthesis
			4	Isoorientin	C21H20O11	Flavone	
			4	Quercitrin	C21H20O11	Flavonol	Flavone and flavonol biosynthesis
468.2	468.1999667	469.2079667	0	Peptide	C22H27N7O5	Peptide	
	468.2045333	469.2125333	9	Peptide	C22H27N7O5	Peptide	
	468.2069333	469.2149333	6	Peptide	C20H31N5O8	Peptide	
719.2	719.1460667	720.1540667	21	Sagerinic acid	C36H32O16	Lignan	
			21	Xanthochymuside	C36H32O16	Chalcone	
			28	Swertifrancheside	C35H28O17	Flavone-xanthone	
	719.1511333	720.1591333	14	Sagerinic acid	C36H32O16	Lignan	
			14	Xanthochymuside	C36H32O16	Chalcone	
			35	Swertifrancheside	C35H28O17	Flavone-xanthone	
	719.1530667	720.1610667	12	Sagerinic acid	C36H32O16	Lignan	
			12	Xanthochymuside	C36H32O16	Chalcone	
			38	Swertifrancheside	C35H28O17	Flavone-xanthone	
1107.2	1107.270667	1108.278667	25	Malvidin 3-O-[6-O-(4-O-(4-O-(6-O-(trans-caffeoyl)-beta-D-glucopyranosyl)-trans-p-coumaroyl)-alpha-L-rhamnopyranosyl)-beta-D-glucopyranoside]	C53H56O26	Anthocyanin	
			25	Pelargonidin 3-(6"-ferulyl-2"'-sinapylsambubioside)-5-glucoside	C53H56O26	Anthocyanin	
			25	Pelargonidin 3-O-[2-O-(2-(E)-feruloyl-beta-D-glucopyranosyl)-6-O-(E)-feruloyl-beta-D-glucopyranoside]-5-O-(beta-D-glucopyranoside)	C53H56O26	Anthocyanin	
			25	Pelargonidin 3-O-[2-O-(6-(E)-feruloyl-beta-D-glucopyranosyl)-6-O-(E)-feruloyl-beta-D-glucopyranoside]-5-O-(beta-D-glucopyranoside)	C53H56O26	Anthocyanin	
	1107.282333	1108.290333	14	Malvidin 3-O-[6-O-(4-O-(4-O-(6-O-(trans-caffeoyl)-beta-D-glucopyranosyl)-trans-p-coumaroyl)-alpha-L-rhamnopyranosyl)-beta-D-glucopyranoside]	C53H56O26	Anthocyanin	
			14	Pelargonidin 3-(6"-ferulyl-2"'-sinapylsambubioside)-5-glucoside	C53H56O26	Anthocyanin	
			14	Pelargonidin 3-O-[2-O-(2-(E)-feruloyl-beta-D-glucopyranosyl)-6-O-(E)-feruloyl-beta-D-glucopyranoside]-5-O-(beta-D-glucopyranoside)	C53H56O26	Anthocyanin	
			14	Pelargonidin 3-O-[2-O-(6-(E)-feruloyl-beta-D-glucopyranosyl)-6-O-(E)-feruloyl-beta-D-glucopyranoside]-5-O-(beta-D-glucopyranoside)	C53H56O26	Anthocyanin	
	1107.288333	1108.296333	9	Malvidin 3-O-[6-O-(4-O-(4-O-(6-O-(trans-caffeoyl)-beta-D-glucopyranosyl)-trans-p-	C53H56O26	Anthocyanin	

				coumaroyl)-alpha-L-rhamnopyranosyl)-beta-D-glucopyranoside]			
			9	Pelargonidin 3-(6"-ferulyl-2"'-sinapylsambubioside)-5-glucoside	C53H56O26	Anthocyanin	
			9	Pelargonidin 3-O-[2-O-(2-(E)-feruloyl-beta-D-glucopyranosyl)-6-O-(E)-feruloyl-beta-D-glucopyranoside]-5-O-(beta-D-glucopyranoside)	C53H56O26	Anthocyanin	
			9	Pelargonidin 3-O-[2-O-(6-(E)-feruloyl-beta-D-glucopyranosyl)-6-O-(E)-feruloyl-beta-D-glucopyranoside]-5-O-(beta-D-glucopyranoside)	C53H56O26	Anthocyanin	
404	404.0922667	405.1002667					
	404.0941667	405.1021667					
	404.099	405.107					
852.2	852.22193	853.22993					
	852.2286333	853.2366333					
	852.2332667	853.2412667					
269	268.9246667	269.9326667					
	269.0388	270.0468	25	Islandicin	C15H10O5	Anthraquinone	
			25	3,6,4'-Trihydroxyflavone	C15H10O5	Flavone	
			25	6-Hydroxydaidzein	C15H10O5	Isoflavone	Isoflavonoid biosynthesis
			25	3',4',7-Trihydroxyisoflavone	C15H10O5	Isoflavone	
			25	Purpurin 1-methyl ether	C15H10O5	Anthraquinone	
			25	2-Hydroxychrysophanol	C15H10O5	Anthraquinone	
			25	Morindone	C15H10O5	Anthraquinone	
			25	Lucidin	C15H10O5	Anthraquinone	
			25	Emodin	C15H10O5	Anthraquinone	
			25	Aloe-emodin	C15H10O5	Anthraquinone	
			25	Norwogonin	C15H10O5	Flavone	
			25	Galangin	C15H10O5	Flavone	Flavonoid biosynthesis
			25	5-Deoxykaempferol	C15H10O5	Flavone	
			25	Baicalein	C15H10O5	Flavone	
			25	Sulphuretin	C15H10O5	Aurone	
			25	Genistein	C15H10O5	Isoflavone	Isoflavonoid and phenylpropanoid biosynthesis
			25	Pelargonidin	C15H10O5	Anthocyanidin	Flavonoid and anthocyanin biosynthesis
			25	2'-Hydroxydaidzein	C15H10O5	Isoflavone	Isoflavonoid biosynthesis
			25	Apigenin	C15H10O5	Flavone	Flavonoid, isoflavonoid, flavone, flavonol and phenylpropanoid biosynthesis
	269.0411333	270.0491333	16	Islandicin	C15H10O5	Anthraquinone	
			16	3,6,4'-Trihydroxyflavone	C15H10O5	Flavone	
			16	6-Hydroxydaidzein	C15H10O5	Isoflavone	Isoflavonoid biosynthesis
			16	3',4',7-Trihydroxyisoflavone	C15H10O5	Isoflavone	
			16	Purpurin 1-methyl ether	C15H10O5	Anthraquinone	
			16	2-Hydroxychrysophanol	C15H10O5	Anthraquinone	

			16	Morindone	C15H10O5	Anthraquinone	
			16	Lucidin	C15H10O5	Anthraquinone	
			16	Emodin	C15H10O5	Anthraquinone	
			16	Aloe-emodin	C15H10O5	Anthraquinone	
			16	Norwogonin	C15H10O5	Flavone	
			16	Galangin	C15H10O5	Flavone	Flavonoid biosynthesis
			16	5-Deoxykaempferol	C15H10O5	Flavone	
			16	Baicalein	C15H10O5	Flavone	
			16	Sulphuretin	C15H10O5	Aurone	
			16	Genistein	C15H10O5	Isoflavone	Isoflavonoid and phenylpropanoid biosynthesis
			16	Pelargonidin	C15H10O5	Anthocyanidin	Flavonoid and anthocyanin biosynthesis
			16	2'-Hydroxydaidzein	C15H10O5	Isoflavone	Isoflavonoid biosynthesis
			16	Apigenin	C15H10O5	Flavone	Flavonoid, isoflavonoid, flavone, flavonol and phenylpropanoid biosynthesis
	268.9129	269.9209					
	269.0418667	270.0498667	13	Islandicin	C15H10O5	Anthraquinone	
			13	3,6,4'-Trihydroxyflavone	C15H10O5	Flavone	
			13	6-Hydroxydaidzein	C15H10O5	Isoflavone	Isoflavonoid biosynthesis
			13	3',4',7-Trihydroxyisoflavone	C15H10O5	Isoflavone	
			13	Purpurin 1-methyl ether	C15H10O5	Anthraquinone	
			13	2-Hydroxychrysophanol	C15H10O5	Anthraquinone	
			13	Morindone	C15H10O5	Anthraquinone	
			13	Lucidin	C15H10O5	Anthraquinone	
			13	Emodin	C15H10O5	Anthraquinone	
			13	Aloe-emodin	C15H10O5	Anthraquinone	
			13	Norwogonin	C15H10O5	Flavone	
			13	Galangin	C15H10O5	Flavone	Flavonoid biosynthesis
			13	5-Deoxykaempferol	C15H10O5	Flavone	
			13	Baicalein	C15H10O5	Flavone	
			13	Sulphuretin	C15H10O5	Aurone	
			13	Genistein	C15H10O5	Isoflavone	Isoflavonoid and phenylpropanoid biosynthesis
			13	Pelargonidin	C15H10O5	Anthocyanidin	Flavonoid and anthocyanin biosynthesis
			13	2'-Hydroxydaidzein	C15H10O5	Isoflavone	Isoflavonoid biosynthesis
			13	Apigenin	C15H10O5	Flavone	Flavonoid, isoflavonoid, flavone, flavonol and phenylpropanoid biosynthesis
689.2	689.1665667	690.1745667					
	689.1740667	690.1820667					
	689.1764	690.1844					
303	303.0751	304.0831	27	N-Acetylaspartylglutamate	C11H16N2O8	Amino acid	Alanine, aspartate and glutamate metabolism

	302.9024667	303.9104667					
	302.9668	303.9748					
	303.0785	304.0865	16	N-Acetylaspartylglutamate	C11H16N2O8	Amino acid	Alanine, aspartate and glutamate metabolism
			29	Griseophenone C	C16H16O6	Benzophenone	
			29	beta-Cotonefuran	C16H16O6	2-arylbenzofuran flavonoid	
			29	7-Hydroxy-6-methoxy-alpha-pyrufuran	C16H16O6	Hydrolyzable tannin	
	302.8983	303.9063					
	303.0792333	304.0872333	26	Griseophenone C	C16H16O6	Benzophenone	
			13	N-Acetylaspartylglutamate	C11H16N2O8	Amino acid	Alanine, aspartate and glutamate metabolism
			26	beta-Cotonefuran	C16H16O6	2-arylbenzofuran flavonoid	
			26	7-Hydroxy-6-methoxy-alpha-pyrufuran	C16H16O6	Hydrolyzable tannin	
	867.2130667	868.2210667					
867.2	867.2217333	868.2297333					
	867.2270667	868.2350667					
417	416.9540333	417.9620333					
	417.0945667	418.1025667	28	Luteolin 3'-xyloside	C20H18O10	Flavone	
			28	Luteolin 7-xyloside	C20H18O10	Flavone	
			28	6-C-beta-D-Xylopyranosylluteolin	C20H18O10	Flavone	
			28	Kaempferol 7-alpha-L-arabinoside	C20H18O10	Flavone	
			28	Kaempferol 7-xyloside	C20H18O10	Flavone	
			28	Kaempferol 3-alpha-L-arabinopyranoside	C20H18O10	Flavone	
			28	Scutellarein 6-xyloside	C20H18O10	Flavone	
			28	Juglanin	C20H18O10	Flavone	
			28	Isoscutellarein 7-xyloside	C20H18O10	Flavone	
			28	Kaempferol 3-O-arabinoside	C20H18O10	Flavone	
			28	Kaempferol 3-xyloside	C20H18O10	Flavone	
			28	Salvianolic acid G	C20H18O10	Stilbenoid	
			28	Luteolin 6-C-alpha-L-arabinopyranoside	C20H18O10	Flavone	
			28	8-C-alpha-L-Arabinosylluteolin	C20H18O10	Flavone	
			28	Kaempferol 3-alpha-L-arabinofuranoside	C20H18O10	Flavone	
			28	5,3'-Dihydroxy-3,8,4',5'-tetramethoxy-6,7-methylenedioxyflavone	C20H18O10	Flavone	
	416.9556667	417.9636667					
	417.0982333	418.1062333	0	8-Caffeoyl-3,4-dihydro-5,7-dihydroxy-4-phenylcoumarin	C24H18O7	Coumarin	
			37	Luteolin 3'-xyloside	C20H18O10	Flavone	
			37	Luteolin 7-xyloside	C20H18O10	Flavone	
			37	6-C-beta-D-Xylopyranosylluteolin	C20H18O10	Flavone	
			37	Kaempferol 7-alpha-L-arabinoside	C20H18O10	Flavone	
			37	Kaempferol 7-xyloside	C20H18O10	Flavone	
			37	Kaempferol 3-alpha-L-arabinopyranoside	C20H18O10	Flavone	
			37	Scutellarein 6-xyloside	C20H18O10	Flavone	
			37	Juglanin	C20H18O10	Flavone	

			37	Isoscutellarein 7-xyloside	C20H18O10	Flavone	
			37	Kaempferol 3-O-arabinoside	C20H18O10	Flavone	
			37	Kaempferol 3-xyloside	C20H18O10	Flavone	
			37	Salvianolic acid G	C20H18O10	Stilbenoid	
			37	Luteolin 6-C-alpha-L-arabinopyranoside	C20H18O10	Flavone	
			37	8-C-alpha-L-Arabinosylluteolin	C20H18O10	Flavone	
			37	Kaempferol 3-alpha-L-arabinofuranoside	C20H18O10	Flavone	
			37	5,3'-Dihydroxy-3,8,4',5'-tetramethoxy-6,7-methylenedioxyflavone	C20H18O10	Flavone	
	417.0996667	418.1076667	4	8-Caffeoyl-3,4-dihydro-5,7-dihydroxy-4-phenylcoumarin	C24H18O7	Coumarin	
283	282.9759	283.9839					
	283.0518333	284.0598333	33	Emodin monomethyl ether	C16H12O5	Anthraquinone	
			33	Obtusifolin	C16H12O5	Anthraquinone	
			33	(+)-Maackiain	C16H12O5	Pterocarpan	Isoflavonoid biosynthesis
			33	Glycitein	C16H12O5	Isoflavone	Isoflavonoid biosynthesis
			33	3-Methylgalangin	C16H12O5	Flavonol	
			33	Texasin	C16H12O5	Isoflavone	
			33	Prunetin	C16H12O5	Isoflavone	Isoflavonoid biosynthesis
			33	Melannin	C16H12O5	Neoflavonoid	
			33	(-)-Maackiain	C16H12O5	Pterocarpan	Isoflavonoid biosynthesis
			33	Lucidin omega-methyl ether	C16H12O5	Anthraquinone	
			33	Cypripedin	C16H12O5	Anthraquinone	
			33	Wogonin	C16H12O5	Flavone	
			33	5-Deoxychrysoeriol	C16H12O5	Flavone	
			33	Apigenin 7-methyl ether	C16H12O5	Flavone	
			33	2'-Hydroxyformononetin	C16H12O5	Isoflavone	Isoflavonoid biosynthesis
			33	3'-Hydroxyformononetin	C16H12O5	Isoflavone	Isoflavonoid biosynthesis
			33	Acacetin	C16H12O5	Flavone	Flavone and flavonol biosynthesis
			33	Questin	C16H12O5	Anthraquinone	
			33	Biochanin A	C16H12O5	Isoflavone	Isoflavonoid and phenylpropanoid biosynthesis
	282.9107333	283.9187333					
	283.0524333	284.0604333	30	Emodin monomethyl ether	C16H12O5	Anthraquinone	
			30	Obtusifolin	C16H12O5	Anthraquinone	
			30	(+)-Maackiain	C16H12O5	Pterocarpan	Isoflavonoid biosynthesis
			30	Glycitein	C16H12O5	Isoflavone	Isoflavonoid biosynthesis
			30	3-Methylgalangin	C16H12O5	Flavonol	
			30	Texasin	C16H12O5	Isoflavone	
			30	Prunetin	C16H12O5	Isoflavone	Isoflavonoid biosynthesis
			30	Melannin	C16H12O5	Neoflavonoid	
			30	(-)-Maackiain	C16H12O5	Pterocarpan	Isoflavonoid biosynthesis
			30	Lucidin omega-methyl ether	C16H12O5	Anthraquinone	
			30	Cypripedin	C16H12O5	Anthraquinone	
			30	Wogonin	C16H12O5	Flavone	

			30	5-Deoxychrysoeriol	C16H12O5	Flavone	
			30	Apigenin 7-methyl ether	C16H12O5	Flavone	
			30	2'-Hydroxyformononetin	C16H12O5	Isoflavone	Isoflavonoid biosynthesis
			30	3'-Hydroxyformononetin	C16H12O5	Isoflavone	Isoflavonoid biosynthesis
			30	Acacetin	C16H12O5	Flavone	Flavone and flavonol biosynthesis
			30	Questin	C16H12O5	Anthraquinone	
			30	Biochanin A	C16H12O5	Isoflavone	Isoflavonoid and phenylpropanoid biosynthesis
	282.9211667	283.9291667					
	282.9765333	283.9845333					
	283.0550667	284.0630667	21	Emodin monomethyl ether	C16H12O5	Anthraquinone	
			21	Obtusifolin	C16H12O5	Anthraquinone	
			21	(+)-Maackiain	C16H12O5	Pterocarpan	Isoflavonoid biosynthesis
			21	Glycitein	C16H12O5	Isoflavone	Isoflavonoid biosynthesis
			21	3-Methylgalangin	C16H12O5	Flavonol	
			21	Texasin	C16H12O5	Isoflavone	
			21	Prunetin	C16H12O5	Isoflavone	Isoflavonoid biosynthesis
			21	Melannin	C16H12O5	Neoflavonoid	
			21	(-)-Maackiain	C16H12O5	Pterocarpan	Isoflavonoid biosynthesis
			21	Lucidin omega-methyl ether	C16H12O5	Anthraquinone	
			21	Cypripedin	C16H12O5	Anthraquinone	
			21	Wogonin	C16H12O5	Flavone	
			21	5-Deoxychrysoeriol	C16H12O5	Flavone	
			21	Apigenin 7-methyl ether	C16H12O5	Flavone	
			21	2'-Hydroxyformononetin	C16H12O5	Isoflavone	Isoflavonoid biosynthesis
			21	3'-Hydroxyformononetin	C16H12O5	Isoflavone	Isoflavonoid biosynthesis
			21	Acacetin	C16H12O5	Flavone	Flavone and flavonol biosynthesis
			21	Questin	C16H12O5	Anthraquinone	
			21	Biochanin A	C16H12O5	Isoflavone	Isoflavonoid and phenylpropanoid biosynthesis

Table A.2 Cracka sorghum polyphenol extract putative identifications from OPLS-DA (ESI [-])

Bin	Detected Mass	Accurate Mass	Δppm	Name	Formula	Chemical Group	Pathway
399.2	399.1028333	400.1108333	14	alpha-Peltatin	C21H20O8	Lignan	Phenylpropanoid biosynthesis
			14	2-[4-(Acetyloxy)phenyl]-5,6,7,8-tetramethoxy-4H-1-benzopyran-4-one	C21H20O8	Flavone	
			14	4'-Demethylpodophyllotoxin	C21H20O8	Lignan	Phenylpropanoid biosynthesis
			14	Isoflavone 7-O-beta-D-glucoside	C21H20O8	Isoflavone	
			14	Flavonol 3-O-D-glucoside	C21H20O8	Flavonol	
			14	Flavonol 3-O-D-galactoside	C21H20O8	Flavonol	
			14	Flavonol 3-O-D-glycoside	C21H20O8	Flavonol	
	399.2818667	400.2898667					
	399.104	400.112	11	alpha-Peltatin	C21H20O8	Lignan	Phenylpropanoid biosynthesis
			11	2-[4-(Acetyloxy)phenyl]-5,6,7,8-tetramethoxy-4H-1-benzopyran-4-one	C21H20O8	Flavone	
			11	4'-Demethylpodophyllotoxin	C21H20O8	Lignan	Phenylpropanoid biosynthesis
			11	Isoflavone 7-O-beta-D-glucoside	C21H20O8	Isoflavone	
			11	Flavonol 3-O-D-glucoside	C21H20O8	Flavonol	
			11	Flavonol 3-O-D-galactoside	C21H20O8	Flavonol	
			11	Flavonol 3-O-D-glycoside	C21H20O8	Flavonol	
	399.1046333	400.1126333	9	alpha-Peltatin	C21H20O8	Lignan	Phenylpropanoid biosynthesis
			9	2-[4-(Acetyloxy)phenyl]-5,6,7,8-tetramethoxy-4H-1-benzopyran-4-one	C21H20O8	Flavone	
			9	4'-Demethylpodophyllotoxin	C21H20O8	Lignan	Phenylpropanoid biosynthesis
			9	Isoflavone 7-O-beta-D-glucoside	C21H20O8	Isoflavone	
			9	Flavonol 3-O-D-glucoside	C21H20O8	Flavonol	
			9	Flavonol 3-O-D-galactoside	C21H20O8	Flavonol	
			9	Flavonol 3-O-D-glycoside	C21H20O8	Flavonol	
416.2	416.1018667	417.1098667	21	Apigeninidin 5-O-glucoside	C21H20O9	3-deoxyanthocyanidin	
	416.283	417.291					
	416.1020333	417.1100333	20	Apigeninidin 5-O-glucoside	C21H20O9	3-deoxyanthocyanidin	
	416.2944333	417.3024333					
	416.1032	417.1112	18	Apigeninidin 5-O-glucoside	C21H20O9	3-deoxyanthocyanidin	
	416.2953333	417.3033333					
851.2	851.2315333	852.2395333					
	851.2322667	852.2402667					
	851.2336	852.2416					
303	303.0149667	304.0229667					
	303.0828667	304.0908667	14	Griseophenone C	C16H16O6	Benzophenone	
			1	N-Acetylaspartylglutamate	C11H16N2O8	Amino acid	Alanine, aspartate and glutamate metabolism
			14	beta-Cotonefuran	C16H16O6	2-arylbenzofuran flavonoid	
			14	7-Hydroxy-6-methoxy-alpha-pyrufuran	C16H16O6	Hydrolyzable tannin	
	302.9649	303.9729					
	303.0304667	304.0384667					
	303.0832	304.0912	13	Griseophenone C	C16H16O6	Benzophenone	

			0	N-Acetylaspartylglutamate	C11H16N2O8	Amino acid	Alanine, aspartate and glutamate metabolism
			13	beta-Cotonefuran	C16H16O6	2-arylbenzofuran flavonoid	
			13	7-Hydroxy-6-methoxy-alpha-pyrufuran	C16H16O6	Hydrolyzable tannin	
			37	Vicine	C10H16N4O7	Alkaloid	
	303.0833	304.0913	13	Griseophenone C	C16H16O6	Benzophenone	
			0	N-Acetylaspartylglutamate	C11H16N2O8	Amino acid	Alanine, aspartate and glutamate metabolism
			13	beta-Cotonefuran	C16H16O6	2-arylbenzofuran flavonoid	
			13	7-Hydroxy-6-methoxy-alpha-pyrufuran	C16H16O6	Hydrolyzable tannin	
			37	Vicine	C10H16N4O7	Alkaloid	
383.2	383.1050333	384.1130333	22	4'-Demethyldeoxypodophyllotoxin	C21H20O7	Lignan	
			24	S-Adenosylhomocysteine	C14H20N6O5S	Amino acid	Cysteine and methionine metabolism
			37	Acetyl-maltose	C14H24O12	Disaccharide	
	383.2235333	384.2315333					
	383.1064	384.1144	18	4'-Demethyldeoxypodophyllotoxin	C21H20O7	Lignan	
			20	S-Adenosylhomocysteine	C14H20N6O5S	Amino acid	Cysteine and methionine metabolism
			34	Acetyl-maltose	C14H24O12	Disaccharide	
	383.1059	384.1139	20	4'-Demethyldeoxypodophyllotoxin	C21H20O7	Lignan	
			21	S-Adenosylhomocysteine	C14H20N6O5S	Amino acid	Cysteine and methionine metabolism
			35	Acetyl-maltose	C14H24O12	Disaccharide	
689.2	689.1786667	690.1866667					
	689.1789333	690.1869333					
	689.1798333	690.1878333					
283	283.0552333	284.0632333	21	Emodin monomethyl ether	C16H12O5	Anthraquinone	
			21	Obtusifolin	C16H12O5	Anthraquinone	
			21	(+)-Maackiain	C16H12O5	Pterocarpan	Isoflavonoid biosynthesis
			21	Glycitein	C16H12O5	Isoflavone	Isoflavonoid biosynthesis
			21	3-Methylgalangin	C16H12O5	Flavonol	
			21	Texasin	C16H12O5	Isoflavone	
			21	Prunetin	C16H12O5	Isoflavone	Isoflavonoid biosynthesis
			21	Melannin	C16H12O5	Neoflavonoid	
			21	(-)-Maackiain	C16H12O5	Pterocarpan	Isoflavonoid biosynthesis
			21	Lucidin omega-methyl ether	C16H12O5	Anthraquinone	
			21	Cypripedin	C16H12O5	Anthraquinone	
			21	Wogonin	C16H12O5	Flavone	
			21	5-Deoxychrysoeriol	C16H12O5	Flavone	
			21	Apigenin 7-methyl ether	C16H12O5	Flavone	
			21	2'-Hydroxyformononetin	C16H12O5	Isoflavone	Isoflavonoid biosynthesis
			21	3'-Hydroxyformononetin	C16H12O5	Isoflavone	Isoflavonoid biosynthesis
			21	Acacetin	C16H12O5	Flavone	Flavone and flavonol biosynthesis
			21	Questin	C16H12O5	Anthraquinone	

			21	Biochanin A	C16H12O5	Isoflavone	Isoflavonoid and phenylpropanoid biosynthesis
	282.9021667	283.9101667					
	283.0554	284.0634	20	Emodin monomethyl ether	C16H12O5	Anthraquinone	
			20	Obtusifolin	C16H12O5	Anthraquinone	
			20	(+)-Maackiain	C16H12O5	Pterocarpan	Isoflavonoid biosynthesis
			20	Glycitein	C16H12O5	Isoflavone	Isoflavonoid biosynthesis
			20	3-Methylgalangin	C16H12O5	Flavonol	
			20	Texasin	C16H12O5	Isoflavone	
			20	Prunetin	C16H12O5	Isoflavone	Isoflavonoid biosynthesis
			20	Melannin	C16H12O5	Neoflavonoid	
			20	(-)-Maackiain	C16H12O5	Pterocarpan	Isoflavonoid biosynthesis
			20	Lucidin omega-methyl ether	C16H12O5	Anthraquinone	
			20	Cypripedin	C16H12O5	Anthraquinone	
			20	Wogonin	C16H12O5	Flavone	
			20	5-Deoxychrysoeriol	C16H12O5	Flavone	
			20	Apigenin 7-methyl ether	C16H12O5	Flavone	
			20	2'-Hydroxyformononetin	C16H12O5	Isoflavone	Isoflavonoid biosynthesis
			20	3'-Hydroxyformononetin	C16H12O5	Isoflavone	Isoflavonoid biosynthesis
			20	Acacetin	C16H12O5	Flavone	Flavone and flavonol biosynthesis
			20	Questin	C16H12O5	Anthraquinone	
			20	Biochanin A	C16H12O5	Isoflavone	Isoflavonoid and phenylpropanoid biosynthesis
	283.0562	284.0642	17	Emodin monomethyl ether	C16H12O5	Anthraquinone	
			17	Obtusifolin	C16H12O5	Anthraquinone	
			17	(+)-Maackiain	C16H12O5	Pterocarpan	Isoflavonoid biosynthesis
			17	Glycitein	C16H12O5	Isoflavone	Isoflavonoid biosynthesis
			17	3-Methylgalangin	C16H12O5	Flavonol	
			17	Texasin	C16H12O5	Isoflavone	
			17	Prunetin	C16H12O5	Isoflavone	Isoflavonoid biosynthesis
			17	Melannin	C16H12O5	Neoflavonoid	
			17	(-)-Maackiain	C16H12O5	Pterocarpan	Isoflavonoid biosynthesis
			17	Lucidin omega-methyl ether	C16H12O5	Anthraquinone	
			17	Cypripedin	C16H12O5	Anthraquinone	
			17	Wogonin	C16H12O5	Flavone	
			17	5-Deoxychrysoeriol	C16H12O5	Flavone	
			17	Apigenin 7-methyl ether	C16H12O5	Flavone	
			17	2'-Hydroxyformononetin	C16H12O5	Isoflavone	Isoflavonoid biosynthesis
			17	3'-Hydroxyformononetin	C16H12O5	Isoflavone	Isoflavonoid biosynthesis
			17	Acacetin	C16H12O5	Flavone	Flavone and flavonol biosynthesis
			17	Questin	C16H12O5	Anthraquinone	
			17	Biochanin A	C16H12O5	Isoflavone	Isoflavonoid and phenylpropanoid biosynthesis
852.2	852.2343667	853.2423667					

	852.2355667	853.2435667					
	852.2361667	853.2441667					
414.2	414.1031667	415.1111667	36	N6-(Dimethylallyl)adenosine 5'-phosphate	C15H22N5O7P	Nucleotide	Zeatin biosynthesis
	414.2089667	415.2169667					
	414.1075667	415.1155667	26	N6-(Dimethylallyl)adenosine 5'-phosphate	C15H22N5O7P	Nucleotide	Zeatin biosynthesis
	414.2128	415.2208					
	414.1076667	415.1156667	25	N6-(Dimethylallyl)adenosine 5'-phosphate	C15H22N5O7P	Nucleotide	Zeatin biosynthesis
	414.2128	415.2208					
269	268.9201	269.9281					
	269.042	270.05	13	Islandicin	C15H10O5	Anthraquinone	
			13	3,6,4'-Trihydroxyflavone	C15H10O5	Flavone	
			13	6-Hydroxydaidzein	C15H10O5	Isoflavone	Isoflavonoid biosynthesis
			13	3',4',7-Trihydroxyisoflavone	C15H10O5	Isoflavone	
			13	Purpurin 1-methyl ether	C15H10O5	Anthraquinone	
			13	2-Hydroxychrysophanol	C15H10O5	Anthraquinone	
			13	Morindone	C15H10O5	Anthraquinone	
			13	Lucidin	C15H10O5	Anthraquinone	
			13	Emodin	C15H10O5	Anthraquinone	
			13	Aloe-emodin	C15H10O5	Anthraquinone	
			13	Norwogonin	C15H10O5	Flavone	
			13	Galangin	C15H10O5	Flavone	Flavonoid biosynthesis
			13	5-Deoxykaempferol	C15H10O5	Flavone	
			13	Baicalein	C15H10O5	Flavone	
			13	Sulphuretin	C15H10O5	Aurone	
			13	Genistein	C15H10O5	Isoflavone	Isoflavonoid and phenylpropanoid biosynthesis
			13	Pelargonidin	C15H10O5	Anthocyanidin	Flavonoid and anthocyanin biosynthesis
			13	2'-Hydroxydaidzein	C15H10O5	Isoflavone	Isoflavonoid biosynthesis
			13	Apigenin	C15H10O5	Flavone	Flavonoid, isoflavonoid, flavone, flavonol and phenylpropanoid biosynthesis
	268.9195	269.9275					
	269.0423	270.0503	12	Islandicin	C15H10O5	Anthraquinone	
			12	3,6,4'-Trihydroxyflavone	C15H10O5	Flavone	
			12	6-Hydroxydaidzein	C15H10O5	Isoflavone	Isoflavonoid biosynthesis
			12	3',4',7-Trihydroxyisoflavone	C15H10O5	Isoflavone	
			12	Purpurin 1-methyl ether	C15H10O5	Anthraquinone	
			12	2-Hydroxychrysophanol	C15H10O5	Anthraquinone	
			12	Morindone	C15H10O5	Anthraquinone	
			12	Lucidin	C15H10O5	Anthraquinone	
			12	Emodin	C15H10O5	Anthraquinone	
			12	Aloe-emodin	C15H10O5	Anthraquinone	
			12	Norwogonin	C15H10O5	Flavone	
			12	Galangin	C15H10O5	Flavone	Flavonoid biosynthesis
			12	5-Deoxykaempferol	C15H10O5	Flavone	

			12	Baicalein	C15H10O5	Flavone	
			12	Sulphuretin	C15H10O5	Aurone	
			12	Genistein	C15H10O5	Isoflavone	Isoflavonoid and phenylpropanoid biosynthesis
			12	Pelargonidin	C15H10O5	Anthocyanidin	Flavonoid and anthocyanin biosynthesis
			12	2'-Hydroxydaidzein	C15H10O5	Isoflavone	Isoflavonoid biosynthesis
			12	Apigenin	C15H10O5	Flavone	Flavonoid, isoflavonoid, flavone, flavonol and phenylpropanoid biosynthesis
	268.927	269.935					
	269.0431333	270.0511333	8	Islandicin	C15H10O5	Anthraquinone	
			8	3,6,4'-Trihydroxyflavone	C15H10O5	Flavone	
			8	6-Hydroxydaidzein	C15H10O5	Isoflavone	Isoflavonoid biosynthesis
			8	3',4',7-Trihydroxyisoflavone	C15H10O5	Isoflavone	
			8	Purpurin 1-methyl ether	C15H10O5	Anthraquinone	
			8	2-Hydroxychrysophanol	C15H10O5	Anthraquinone	
			8	Morindone	C15H10O5	Anthraquinone	
			8	Lucidin	C15H10O5	Anthraquinone	
			8	Emodin	C15H10O5	Anthraquinone	
			8	Aloe-emodin	C15H10O5	Anthraquinone	
			8	Norwogonin	C15H10O5	Flavone	
			8	Galangin	C15H10O5	Flavone	Flavonoid biosynthesis
			8	5-Deoxykaempferol	C15H10O5	Flavone	
			8	Baicalein	C15H10O5	Flavone	
			8	Sulphuretin	C15H10O5	Aurone	
			8	Genistein	C15H10O5	Isoflavone	Isoflavonoid and phenylpropanoid biosynthesis
			8	Pelargonidin	C15H10O5	Anthocyanidin	Flavonoid and anthocyanin biosynthesis
			8	2'-Hydroxydaidzein	C15H10O5	Isoflavone	Isoflavonoid biosynthesis
			8	Apigenin	C15H10O5	Flavone	Flavonoid, isoflavonoid, flavone, flavonol and phenylpropanoid biosynthesis
304	304.0837333	305.0917333	16	Convicine	C10H15N3O8	Alkaloid	
	304.0845667	305.0925667	19	Convicine	C10H15N3O8	Alkaloid	
	303.9019	304.9099					
	304.0828667	305.0908667	13	Convicine	C10H15N3O8	Alkaloid	
301	301.0125333	302.0205333					
	301.0676333	302.0756333	13	Homoeriodictyol chalcone	C16H14O6	Chalcone	Flavonoid biosynthesis
			13	Dihydrokalafungin	C16H14O6	Anthraquinone	
			13	Ferreirin	C16H14O6	Isoflavanone	
			13	Haematoxylin	C16H14O6	Neoflavonoid	
			13	Homoeriodictyol	C16H14O6	Flavanone	Flavonoid biosynthesis
			13	Hesperetin	C16H14O6	Flavanone	Flavonoid biosynthesis
	301.0666667	302.0746667	16	Homoeriodictyol chalcone	C16H14O6	Chalcone	Flavonoid biosynthesis

			16	Dihydrokalafungin	C16H14O6	Anthraquinone	
			16	Ferreirin	C16H14O6	Isoflavanone	
			16	Haematoxylin	C16H14O6	Neoflavonoid	
			16	Homoeriodictyol	C16H14O6	Flavanone	Flavonoid biosynthesis
			16	Hesperetin	C16H14O6	Flavanone	Flavonoid biosynthesis
	301.0678333	302.0758333	13	Homoeriodictyol chalcone	C16H14O6	Chalcone	Flavonoid biosynthesis
			13	Dihydrokalafungin	C16H14O6	Anthraquinone	
			13	Ferreirin	C16H14O6	Isoflavanone	
			13	Haematoxylin	C16H14O6	Neoflavonoid	
			13	Homoeriodictyol	C16H14O6	Flavanone	Flavonoid biosynthesis
			13	Hesperetin	C16H14O6	Flavanone	Flavonoid biosynthesis
417	417.0985333	418.1065333	37	Luteolin 3'-xyloside	C20H18O10	Flavone	
			37	Luteolin 7-xyloside	C20H18O10	Flavone	
			37	6-C-beta-D-Xylopyranosylluteolin	C20H18O10	Flavone	
			37	Kaempferol 7-alpha-L-arabinoside	C20H18O10	Flavone	
			37	Kaempferol 7-xyloside	C20H18O10	Flavone	
			37	Kaempferol 3-alpha-L-arabinopyranoside	C20H18O10	Flavone	
			37	Scutellarein 6-xyloside	C20H18O10	Flavone	
			37	Juglanin	C20H18O10	Flavone	
			37	Isoscutellarein 7-xyloside	C20H18O10	Flavone	
			37	Kaempferol 3-O-arabinoside	C20H18O10	Flavone	
			37	Kaempferol 3-xyloside	C20H18O10	Flavone	
			37	Salvianolic acid G	C20H18O10	Stilbenoid	
			37	Luteolin 6-C-alpha-L-arabinopyranoside	C20H18O10	Flavone	
			37	8-C-alpha-L-Arabinosylluteolin	C20H18O10	Flavone	
			37	Kaempferol 3-alpha-L-arabinofuranoside	C20H18O10	Flavone	
			37	5,3'-Dihydroxy-3,8,4',5'-tetramethoxy-6,7-methylenedioxyflavone	C20H18O10	Flavone	
			1	8-Caffeoyl-3,4-dihydro-5,7-dihydroxy-4-phenylcoumarin	C24H18O7	Coumarin	
	417.0988333	418.1068333	38	Luteolin 3'-xyloside	C20H18O10	Flavone	
			38	Luteolin 7-xyloside	C20H18O10	Flavone	
			38	6-C-beta-D-Xylopyranosylluteolin	C20H18O10	Flavone	
			38	Kaempferol 7-alpha-L-arabinoside	C20H18O10	Flavone	
			38	Kaempferol 7-xyloside	C20H18O10	Flavone	
			38	Kaempferol 3-alpha-L-arabinopyranoside	C20H18O10	Flavone	
			38	Scutellarein 6-xyloside	C20H18O10	Flavone	
			38	Juglanin	C20H18O10	Flavone	
			38	Isoscutellarein 7-xyloside	C20H18O10	Flavone	
			38	Kaempferol 3-O-arabinoside	C20H18O10	Flavone	
			38	Kaempferol 3-xyloside	C20H18O10	Flavone	
			38	Salvianolic acid G	C20H18O10	Stilbenoid	
			38	Luteolin 6-C-alpha-L-arabinopyranoside	C20H18O10	Flavone	
			38	8-C-alpha-L-Arabinosylluteolin	C20H18O10	Flavone	
			38	Kaempferol 3-alpha-L-arabinofuranoside	C20H18O10	Flavone	

			38	5,3'-Dihydroxy-3,8,4',5'-tetramethoxy-6,7-methylenedioxyflavone	C20H18O10	Flavone	
			2	8-Caffeoyl-3,4-dihydro-5,7-dihydroxy-4-phenylcoumarin	C24H18O7	Coumarin	
	417.0989667	418.1069667	38	Luteolin 3'-xyloside	C20H18O10	Flavone	
			38	Luteolin 7-xyloside	C20H18O10	Flavone	
			38	6-C-beta-D-Xylopyranosylluteolin	C20H18O10	Flavone	
			38	Kaempferol 7-alpha-L-arabinoside	C20H18O10	Flavone	
			38	Kaempferol 7-xyloside	C20H18O10	Flavone	
			38	Kaempferol 3-alpha-L-arabinopyranoside	C20H18O10	Flavone	
			38	Scutellarein 6-xyloside	C20H18O10	Flavone	
			38	Juglanin	C20H18O10	Flavone	
			38	Isoscutellarein 7-xyloside	C20H18O10	Flavone	
			38	Kaempferol 3-O-arabinoside	C20H18O10	Flavone	
			38	Kaempferol 3-xyloside	C20H18O10	Flavone	
			38	Salvianolic acid G	C20H18O10	Stilbenoid	
			38	Luteolin 6-C-alpha-L-arabinopyranoside	C20H18O10	Flavone	
			38	8-C-alpha-L-Arabinosylluteolin	C20H18O10	Flavone	
			38	Kaempferol 3-alpha-L-arabinofuranoside	C20H18O10	Flavone	
			38	5,3'-Dihydroxy-3,8,4',5'-tetramethoxy-6,7-methylenedioxyflavone	C20H18O10	Flavone	
			2	8-Caffeoyl-3,4-dihydro-5,7-dihydroxy-4-phenylcoumarin	C24H18O7	Coumarin	
271	270.9415667	271.9495667					
	271.0566333	272.0646333	16	Toralactone	C15H12O5	Naphthopyrone	
			16	6,7,4'-Trihydroxyflavanone	C15H12O5	Flavanone	Isoflavonoid biosynthesis
			16	2,7,4'-Trihydroxyisoflavanone	C15H12O5	Isoflavanone	Isoflavonoid biosynthesis
			16	Dihydrogenistein	C15H12O5	Flavanone	
			16	p-Coumaroyltriacetic acid lactone	C15H12O5	Chalcone	
			16	Pinobanksin	C15H12O5	Dihydroflavonol	Flavonoid biosynthesis
			16	Garbanzol	C15H12O5	Dihydroflavonol	Flavonoid biosynthesis
			16	Butin	C15H12O5	Flavanone	Flavonoid biosynthesis
			16	Rubrofusarin	C15H12O5	Naphthopyrones	
			16	Butein	C15H12O5	Chalcone	Flavonoid biosynthesis
			16	Naringenin chalcone	C15H12O5	Chalcone	Flavonoid biosynthesis
			16	2'-Hydroxydihydrodaidzein	C15H12O5	Isoflavanone	Isoflavonoid biosynthesis
			16	Licodione	C15H12O5	Chalcone	
			16	(-)-Glycinol	C15H12O5	Pterocarpan	Isoflavonoid biosynthesis
			16	Naringenin	C15H12O5	Flavanone	Flavonoid, isoflavonoid and phenylpropanoid biosynthesis
	270.952	271.96					
	271.0566667	272.0646667	16	Toralactone	C15H12O5	Naphthopyrone	
			16	6,7,4'-Trihydroxyflavanone	C15H12O5	Flavanone	Isoflavonoid biosynthesis
			16	2,7,4'-Trihydroxyisoflavanone	C15H12O5	Isoflavanone	Isoflavonoid biosynthesis
			16	Dihydrogenistein	C15H12O5	Flavanone	
			16	p-Coumaroyltriacetic acid lactone	C15H12O5	Chalcone	

			16	Pinobanksin	C15H12O5	Dihydroflavonol	Flavonoid biosynthesis
			16	Garbanzol	C15H12O5	Dihydroflavonol	Flavonoid biosynthesis
			16	Butin	C15H12O5	Flavanone	Flavonoid biosynthesis
			16	Rubrofusarin	C15H12O5	Naphthopyrones	
			16	Butein	C15H12O5	Chalcone	Flavonoid biosynthesis
			16	Naringenin chalcone	C15H12O5	Chalcone	Flavonoid biosynthesis
			16	2'-Hydroxydihydrodaidzein	C15H12O5	Isoflavanone	Isoflavonoid biosynthesis
			16	Licodione	C15H12O5	Chalcone	
			16	(-)-Glycinol	C15H12O5	Pterocarpan	Isoflavonoid biosynthesis
			16	Naringenin	C15H12O5	Flavanone	Flavonoid, isoflavonoid and phenylpropanoid biosynthesis
	270.9515667	271.9595667					
	271.0573667	272.0653667	14	Toralactone	C15H12O5	Naphthopyrone	
			14	6,7,4'-Trihydroxyflavanone	C15H12O5	Flavanone	Isoflavonoid biosynthesis
			14	2,7,4'-Trihydroxyisoflavanone	C15H12O5	Isoflavanone	Isoflavonoid biosynthesis
			14	Dihydrogenistein	C15H12O5	Flavanone	
			14	p-Coumaroyltriacetic acid lactone	C15H12O5	Chalcone	
			14	Pinobanksin	C15H12O5	Dihydroflavonol	Flavonoid biosynthesis
			14	Garbanzol	C15H12O5	Dihydroflavonol	Flavonoid biosynthesis
			14	Butin	C15H12O5	Flavanone	Flavonoid biosynthesis
			14	Rubrofusarin	C15H12O5	Naphthopyrones	
			14	Butein	C15H12O5	Chalcone	Flavonoid biosynthesis
			14	Naringenin chalcone	C15H12O5	Chalcone	Flavonoid biosynthesis
			14	2'-Hydroxydihydrodaidzein	C15H12O5	Isoflavanone	Isoflavonoid biosynthesis
			14	Licodione	C15H12O5	Chalcone	
			14	(-)-Glycinol	C15H12O5	Pterocarpan	Isoflavonoid biosynthesis
			14	Naringenin	C15H12O5	Flavanone	Flavonoid, isoflavonoid and phenylpropanoid biosynthesis
287	287.0465	288.0545	33	Carthamidin	C15H12O6	Flavanone	
			33	2,6,7,4'-Tetrahydroxyisoflavanone	C15H12O6	Isoflavanone	Isoflavonoid biosynthesis
			33	Eriodictyol chalcone	C15H12O6	Chalcone	Flavonoid biosynthesis
			33	2-Hydroxy-2,3-dihydrogenistein	C15H12O6	Isoflavanone	Isoflavonoid biosynthesis
			33	(+-)-Dalbergioidin	C15H12O6	Isoflavanone	
			33	Swerchirin	C15H12O6	Xanthene	
			33	2-O-Methylswertianin	C15H12O6	Xanthene	
			33	Gentiacaulein	C15H12O6	Xanthene	
			33	3,5-Dimethoxy-1,6-dihydroxyxanthone	C15H12O6	Xanthene	
			33	Micromelin	C15H12O6	Coumarin	
			33	Okanin	C15H12O6	Chalcone	
			33	Eriodictyol	C15H12O6	Flavanone	Flavonoid biosynthesis
			33	Fustin	C15H12O6	Dihydroflavonol	Flavonoid biosynthesis
			33	Dihydrokaempferol	C15H12O6	Dihydroflavonol	Flavonoid and phenylpropanoid biosynthesis
	287.0878	288.0958	16	Shikonin	C16H16O5	Naphthoquinone	Ubiquinone and terpenoid-quinone biosynthesis
			16	7,2'-Dihydroxy-4'-methoxy-isoflavanol	C16H16O5	Isoflavone	Isoflavonoid biosynthesis

			16	Asebogenin	C16H16O5	Dihydrochalcone	
	287.0470667	288.0550667	31	Carthamidin	C15H12O6	Flavanone	
			31	2,6,7,4'-Tetrahydroxyisoflavanone	C15H12O6	Isoflavanone	Isoflavonoid biosynthesis
			31	Eriodictyol chalcone	C15H12O6	Chalcone	Flavonoid biosynthesis
			31	2-Hydroxy-2,3-dihydrogenistein	C15H12O6	Isoflavanone	Isoflavonoid biosynthesis
			31	(+-)-Dalbergioidin	C15H12O6	Isoflavanone	
			31	Swerchirin	C15H12O6	Xanthene	
			31	2-O-Methylswertianin	C15H12O6	Xanthene	
			31	Gentiacaulein	C15H12O6	Xanthene	
			31	3,5-Dimethoxy-1,6-dihydroxyxanthone	C15H12O6	Xanthene	
			31	Micromelin	C15H12O6	Coumarin	
			31	Okanin	C15H12O6	Chalcone	
			31	Eriodictyol	C15H12O6	Flavanone	Flavonoid biosynthesis
			31	Fustin	C15H12O6	Dihydroflavonol	Flavonoid biosynthesis
			31	Dihydrokaempferol	C15H12O6	Dihydroflavonol	Flavonoid and phenylpropanoid biosynthesis
	287.0884333	288.0964333	14	Shikonin	C16H16O5	Naphthoquinone	Ubiquinone and terpenoid-quinone biosynthesis
			14	7,2'-Dihydroxy-4'-methoxy-isoflavanol	C16H16O5	Isoflavane	Isoflavonoid biosynthesis
			14	Asebogenin	C16H16O5	Dihydrochalcone	
	286.9252333	287.9332333					
	287.046	288.054	35	Carthamidin	C15H12O6	Flavanone	
			35	2,6,7,4'-Tetrahydroxyisoflavanone	C15H12O6	Isoflavanone	Isoflavonoid biosynthesis
			35	Eriodictyol chalcone	C15H12O6	Chalcone	Flavonoid biosynthesis
			35	2-Hydroxy-2,3-dihydrogenistein	C15H12O6	Isoflavanone	Isoflavonoid biosynthesis
			35	(+-)-Dalbergioidin	C15H12O6	Isoflavanone	
			35	Swerchirin	C15H12O6	Xanthene	
			35	2-O-Methylswertianin	C15H12O6	Xanthene	
			35	Gentiacaulein	C15H12O6	Xanthene	
			35	3,5-Dimethoxy-1,6-dihydroxyxanthone	C15H12O6	Xanthene	
			35	Micromelin	C15H12O6	Coumarin	
			35	Okanin	C15H12O6	Chalcone	
			35	Eriodictyol	C15H12O6	Flavanone	Flavonoid biosynthesis
			35	Fustin	C15H12O6	Dihydroflavonol	Flavonoid biosynthesis
			35	Dihydrokaempferol	C15H12O6	Dihydroflavonol	Flavonoid and phenylpropanoid biosynthesis
	287.0882333	288.0962333	14	Shikonin	C16H16O5	Naphthoquinone	Ubiquinone and terpenoid-quinone biosynthesis
			14	7,2'-Dihydroxy-4'-methoxy-isoflavanol	C16H16O5	Isoflavane	Isoflavonoid biosynthesis
			14	Asebogenin	C16H16O5	Dihydrochalcone	
1269.4	1269.340333	1270.348333	8	Malvidin 3-O-[6-O-[4-O-[4-O-(6-O-caffeoyl-beta-D-glucopyranosyl)-p-coumaroyl]-alpha-L-rhamnosyl]-beta-D-glucopyranoside]-5-O-beta-D-glucopyranoside	C59H66O31	Anthocyanidin	

			19	Cyanidin 3-O-[6-O-(malonyl)-beta-D-glucopyranoside]-7,3'-di-O-[6-O-(sinapyl)-beta-D-glucopyranoside]	C58H62O32	Anthocyanidin	
	1269.341	1270.349	8	Malvidin 3-O-[6-O-[4-O-[4-O-(6-O-caffeoyl-beta-D-glucopyranosyl)-p-coumaroyl]-alpha-L-rhamnosyl]-beta-D-glucopyranoside]-5-O-beta-D-glucopyranoside	C59H66O31	Anthocyanidin	
			20	Cyanidin 3-O-[6-O-(malonyl)-beta-D-glucopyranoside]-7,3'-di-O-[6-O-(sinapyl)-beta-D-glucopyranoside]	C58H62O32	Anthocyanidin	
	1269.341	1270.349	8	Malvidin 3-O-[6-O-[4-O-[4-O-(6-O-caffeoyl-beta-D-glucopyranosyl)-p-coumaroyl]-alpha-L-rhamnosyl]-beta-D-glucopyranoside]-5-O-beta-D-glucopyranoside	C59H66O31	Anthocyanidin	
			20	Cyanidin 3-O-[6-O-(malonyl)-beta-D-glucopyranoside]-7,3'-di-O-[6-O-(sinapyl)-beta-D-glucopyranoside]	C58H62O32	Anthocyanidin	

Table A.3 Liberty sorghum polyphenol extract putative identifications from OPLS-DA (ESI [-])

Bin	Detected Mass	Accurate Mass	Δppm	Name	Formula	Chemical Group	Pathway
399.2	399.1035667	400.1115667	12	alpha-Peltatin	C21H20O8	Lignan	Phenylpropanoid biosynthesis
			12	2-[4-(Acetyloxy)phenyl]-5,6,7,8-tetramethoxy-4H-1-benzopyran-4-one	C21H20O8	Flavone	
			12	4'-Demethylpodophyllotoxin	C21H20O8	Lignan	Phenylpropanoid biosynthesis
			12	Isoflavone 7-O-beta-D-glucoside	C21H20O8	Isoflavone	
			12	Flavonol 3-O-D-glucoside	C21H20O8	Flavonol	
			12	Flavonol 3-O-D-galactoside	C21H20O8	Flavonol	
			12	Flavonol 3-O-D-glycoside	C21H20O8	Flavonol	
	399.1808	400.1888	1	(+)-gamma-Schizandrin	C23H28O6	Lignan	
			1	(-)-gamma-Schizandrin	C23H28O6	Lignan	
			29	11-O-Demethyl-17-O-deacetylvindoline	C22H28N2O5	Alkaloid	
	399.1033	400.1113	13	alpha-Peltatin	C21H20O8	Lignan	Phenylpropanoid biosynthesis
			13	2-[4-(Acetyloxy)phenyl]-5,6,7,8-tetramethoxy-4H-1-benzopyran-4-one	C21H20O8	Flavone	
			13	4'-Demethylpodophyllotoxin	C21H20O8	Lignan	Phenylpropanoid biosynthesis
			13	Isoflavone 7-O-beta-D-glucoside	C21H20O8	Isoflavone	
			13	Flavonol 3-O-D-glucoside	C21H20O8	Flavonol	
			13	Flavonol 3-O-D-galactoside	C21H20O8	Flavonol	
			13	Flavonol 3-O-D-glycoside	C21H20O8	Flavonol	
	399.1827333	400.1907333	3	(+)-gamma-Schizandrin	C23H28O6	Lignan	
			3	(-)-gamma-Schizandrin	C23H28O6	Lignan	
			24	11-O-Demethyl-17-O-deacetylvindoline	C22H28N2O5	Alkaloid	

	399.28	400.288					
	399.1032	400.1112	13	alpha-Peltatin	C21H20O8	Lignan	Phenylpropanoid biosynthesis
			13	2-[4-(Acetyloxy)phenyl]-5,6,7,8-tetramethoxy-4H-1-benzopyran-4-one	C21H20O8	Flavone	
			13	4'-Demethylpodophyllotoxin	C21H20O8	Lignan	Phenylpropanoid biosynthesis
			13	Isoflavone 7-O-beta-D-glucoside	C21H20O8	Isoflavone	
			13	Flavonol 3-O-D-glucoside	C21H20O8	Flavonol	
			13	Flavonol 3-O-D-galactoside	C21H20O8	Flavonol	
			13	Flavonol 3-O-D-glycoside	C21H20O8	Flavonol	
	399.1834333	400.1914333	5	(+)-gamma-Schizandrin	C23H28O6	Lignan	
			5	(-)-gamma-Schizandrin	C23H28O6	Lignan	
			22	11-O-Demethyl-17-O-deacetylvindoline	C22H28N2O5	Alkaloid	
	399.2784667	400.2864667					
341.2	341.1040333	342.1120333	14	3-O-alpha-D-Mannopyranosyl-alpha-D-mannopyranose	C12H22O11	Disaccharide	
			14	Turanose	C12H22O11	Disaccharide	
			14	Melibiulose	C12H22O11	Disaccharide	
			14	Maltulose	C12H22O11	Disaccharide	
			14	Kojibiose	C12H22O11	Disaccharide	
			14	2-alpha-D-Glucosyl-D-glucose	C12H22O11	Disaccharide	
			2	5,6,7,4'-Tetramethoxyisoflavone	C19H18O6	Isoflavone	
			2	Tetra-O-methylscutellarein	C19H18O6	Flavone	
			14	Nigerose	C12H22O11	Disaccharide	
			14	Galactinol	C12H22O11	Disaccharide	Galactose metabolism
			14	Trehalose	C12H22O11	Disaccharide	Starch and sucrose metabolism
			14	Isomaltose	C12H22O11	Disaccharide	Starch and sucrose metabolism
			14	Lactose	C12H22O11	Disaccharide	Galactose metabolism
			14	Maltose	C12H22O11	Disaccharide	Starch and sucrose metabolism
			14	Sucrose	C12H22O11	Disaccharide	Galactose metabolism; Starch and sucrose metabolism
			14	Cellobiose	C12H22O11	Disaccharide	Starch and sucrose metabolism
			14	Sophorose	C12H22O11	Disaccharide	
			14	Gentiobiose	C12H22O11	Disaccharide	
			14	Melibiose	C12H22O11	Disaccharide	Galactose metabolism
			14	Epimelibiose	C12H22O11	Disaccharide	Galactose metabolism
			14	alpha-D-Glucosyl-(1,3)-D-mannose	C12H22O11	Disaccharide	
			14	Laminaribiose	C12H22O11	Disaccharide	
			14	beta-Lactose	C12H22O11	Disaccharide	
			14	Palatinose	C12H22O11	Disaccharide	
			14	Levanbiose	C12H22O11	Disaccharide	Starch and sucrose metabolism
			14	Inulobiose	C12H22O11	Disaccharide	
	341.2742333	342.2822333					
	341.1039333	342.1119333	14	3-O-alpha-D-Mannopyranosyl-alpha-D-mannopyranose	C12H22O11	Disaccharide	
			14	Turanose	C12H22O11	Disaccharide	
			14	Melibiulose	C12H22O11	Disaccharide	

			14	Maltulose	C12H22O11	Disaccharide	
			14	Kojibiose	C12H22O11	Disaccharide	
			14	2-alpha-D-Glucosyl-D-glucose	C12H22O11	Disaccharide	
			2	5,6,7,4'-Tetramethoxyisoflavone	C19H18O6	Isoflavone	
			2	Tetra-O-methylscutellarein	C19H18O6	Flavone	
			14	Nigerose	C12H22O11	Disaccharide	
			14	Galactinol	C12H22O11	Disaccharide	Galactose metabolism
			14	Trehalose	C12H22O11	Disaccharide	Starch and sucrose metabolism
			14	Isomaltose	C12H22O11	Disaccharide	Starch and sucrose metabolism
			14	Lactose	C12H22O11	Disaccharide	Galactose metabolism
			14	Maltose	C12H22O11	Disaccharide	Starch and sucrose metabolism
			14	Sucrose	C12H22O11	Disaccharide	Galactose metabolism; Starch and sucrose metabolism
			14	Cellobiose	C12H22O11	Disaccharide	Starch and sucrose metabolism
			14	Sophorose	C12H22O11	Disaccharide	
			14	Gentiobiose	C12H22O11	Disaccharide	
			14	Melibiose	C12H22O11	Disaccharide	Galactose metabolism
			14	Epimelibiose	C12H22O11	Disaccharide	Galactose metabolism
			14	alpha-D-Glucosyl-(1,3)-D-mannose	C12H22O11	Disaccharide	
			14	Laminaribiose	C12H22O11	Disaccharide	
			14	beta-Lactose	C12H22O11	Disaccharide	
			14	Palatinose	C12H22O11	Disaccharide	
			14	Levanbiose	C12H22O11	Disaccharide	Starch and sucrose metabolism
			14	Inulobiose	C12H22O11	Disaccharide	
	341.1800333	342.1880333					
	341.2694333	342.2774333					
	341.1039667	342.1119667	14	3-O-alpha-D-Mannopyranosyl-alpha-D-mannopyranose	C12H22O11	Disaccharide	
			14	Turanose	C12H22O11	Disaccharide	
			14	Melibiulose	C12H22O11	Disaccharide	
			14	Maltulose	C12H22O11	Disaccharide	
			14	Kojibiose	C12H22O11	Disaccharide	
			14	2-alpha-D-Glucosyl-D-glucose	C12H22O11	Disaccharide	
			2	5,6,7,4'-Tetramethoxyisoflavone	C19H18O6	Isoflavone	
			2	Tetra-O-methylscutellarein	C19H18O6	Flavone	
			14	Nigerose	C12H22O11	Disaccharide	
			14	Galactinol	C12H22O11	Disaccharide	Galactose metabolism
			14	Trehalose	C12H22O11	Disaccharide	Starch and sucrose metabolism
			14	Isomaltose	C12H22O11	Disaccharide	Starch and sucrose metabolism
			14	Lactose	C12H22O11	Disaccharide	Galactose metabolism
			14	Maltose	C12H22O11	Disaccharide	Starch and sucrose metabolism
			14	Sucrose	C12H22O11	Disaccharide	Galactose metabolism; Starch and sucrose metabolism
			14	Cellobiose	C12H22O11	Disaccharide	Starch and sucrose metabolism
			14	Sophorose	C12H22O11	Disaccharide	
			14	Gentiobiose	C12H22O11	Disaccharide	

			14	Melibiose	C12H22O11	Disaccharide	Galactose metabolism
			14	Epimelibiose	C12H22O11	Disaccharide	Galactose metabolism
			14	alpha-D-Glucosyl-(1,3)-D-mannose	C12H22O11	Disaccharide	
			14	Laminaribiose	C12H22O11	Disaccharide	
			14	beta-Lactose	C12H22O11	Disaccharide	
			14	Palatinose	C12H22O11	Disaccharide	
			14	Levanbiose	C12H22O11	Disaccharide	Starch and sucrose metabolism
			14	Inulobiose	C12H22O11	Disaccharide	
	341.1797	342.1877					
	341.2701667	342.2781667					
329.2	329.2294667	330.2374667	11	9,10-Dihydroxy-12,13-epoxyoctadecanoic acid	C18H34O5	Fatty acid	Linoleic acid metabolism
			11	9,10,13-Trihydroxyoctadec-11-enoic acid	C18H34O5	Fatty acid	Linoleic acid metabolism
			11	9(S),12(S),13(S)-Trihydroxy-10(E)-octadecenoic acid	C18H34O5	Fatty acid	Linoleic acid metabolism
	329.2293	330.2373	12	9,10-Dihydroxy-12,13-epoxyoctadecanoic acid	C18H34O5	Fatty acid	Linoleic acid metabolism
			12	9,10,13-Trihydroxyoctadec-11-enoic acid	C18H34O5	Fatty acid	Linoleic acid metabolism
			12	9(S),12(S),13(S)-Trihydroxy-10(E)-octadecenoic acid	C18H34O5	Fatty acid	Linoleic acid metabolism
	329.2292	330.2372	12	9,10-Dihydroxy-12,13-epoxyoctadecanoic acid	C18H34O5	Fatty acid	Linoleic acid metabolism
			12	9,10,13-Trihydroxyoctadec-11-enoic acid	C18H34O5	Fatty acid	Linoleic acid metabolism
			12	9(S),12(S),13(S)-Trihydroxy-10(E)-octadecenoic acid	C18H34O5	Fatty acid	Linoleic acid metabolism
377	377.0809667	378.0889667					
	376.9605	377.9685					
	377.0810333	378.0890333					
	377.0807	378.0887					
400.2	400.1078333	401.1158333					
	400.1082	401.1162					
	400.1076667	401.1156667					
379	378.9617667	379.9697667					
	379.0789333	380.0869333	8	Diphyllin	C21H16O7	Lignan	
			36	S-(N-Hydroxy-N-methylcarbamoyl)glutathione	C12H20N4O8S	Amino acid	
	378.9690333	379.9770333					
	379.0786667	380.0866667	9	Diphyllin	C21H16O7	Lignan	
			37	S-(N-Hydroxy-N-methylcarbamoyl)glutathione	C12H20N4O8S	Amino acid	
	378.9622333	379.9702333					
	379.0789667	380.0869667	8	Diphyllin	C21H16O7	Lignan	
			36	S-(N-Hydroxy-N-methylcarbamoyl)glutathione	C12H20N4O8S	Amino acid	
387.2	387.1077667	388.1157667	2	Hydroxypentamethoxyflavone	C20H20O8	Flavone	
	387.1900333	388.1980333	32	Rehmaionoside C	C19H32O8	Iridoid	
			22	Surinamensin	C22H28O6	Neolignan	
			22	Nigakilactone D	C22H28O6	Terpenoid	
	387.2805667	388.2885667					
	387.1078333	388.1158333	1	Hydroxypentamethoxyflavone	C20H20O8	Flavone	
	387.1892	388.1972	34	Rehmaionoside C	C19H32O8	Iridoid	
			20	Surinamensin	C22H28O6	Neolignan	

			20	Nigakilactone D	C22H28O6	Terpenoid	
	387.2848	388.2928					
	387.1081333	388.1161333	1	Hydroxypentamethoxyflavone	C20H20O8	Flavone	
	387.189	388.197	33	Rehmaionoside C	C19H32O8	Iridoid	
			20	Surinamensin	C22H28O6	Neolignan	
			20	Nigakilactone D	C22H28O6	Terpenoid	
	387.2841667	388.2921667					
439	439.0797	440.0877					
	439.0785	440.0865					
	438.9003333	439.9083333					
	439.0790333	440.0870333					
191	190.9119333	191.9199333					
	191.0164	192.0244	17	D-erythro-Isocitric acid	C6H8O7	Tricarboxylic acid	
			17	2,3-Diketo-L-gulonate	C6H8O7	Tricarboxylic acid	Pentose and glucuronate interconversions, ascorbate and aldarate metabolism
			17	2-Dehydro-3-deoxy-D-glucarate	C6H8O7	Tricarboxylic acid	Ascorbate and aldarate metabolism
			17	Carboxymethyloxysuccinate	C6H8O7	Tricarboxylic acid	
			17	2,5-Diketogluconic acid	C6H8O7	Tricarboxylic acid	
			17	5-Dehydro-4-deoxy-D-glucarate	C6H8O7	Tricarboxylic acid	Ascorbate and aldarate metabolism
			17	Isocitrate	C6H8O7	Tricarboxylic acid	Lots
			17	Citrate	C6H8O7	Tricarboxylic acid	Lots
	191.0565	192.0645	2	Quinic acid	C7H12O6	Cyclic polyol	Phenylalanine, tyrosine and tryptophan biosynthesis
			2	Valiolone	C7H12O6	Cyclic polyol	
			2	2D-5-O-Methyl-2,3,5/4,6-pentahydroxycyclohexanone	C7H12O6	Cyclic polyol	
	190.9137	191.9217					
	191.016	192.024	19	D-erythro-Isocitric acid	C6H8O7	Tricarboxylic acid	
			19	2,3-Diketo-L-gulonate	C6H8O7	Tricarboxylic acid	Pentose and glucuronate interconversions, ascorbate and aldarate metabolism
			19	2-Dehydro-3-deoxy-D-glucarate	C6H8O7	Tricarboxylic acid	Ascorbate and aldarate metabolism
			19	Carboxymethyloxysuccinate	C6H8O7	Tricarboxylic acid	
			19	2,5-Diketogluconic acid	C6H8O7	Tricarboxylic acid	
			19	5-Dehydro-4-deoxy-D-glucarate	C6H8O7	Tricarboxylic acid	Ascorbate and aldarate metabolism
			19	Isocitrate	C6H8O7	Tricarboxylic acid	Lots
			19	Citrate	C6H8O7	Tricarboxylic acid	Lots
	191.0555	192.0635	3	Quinic acid	C7H12O6	Cyclic polyol	Phenylalanine, tyrosine and tryptophan biosynthesis
			3	Valiolone	C7H12O6	Cyclic polyol	
			3	2D-5-O-Methyl-2,3,5/4,6-pentahydroxycyclohexanone	C7H12O6	Cyclic polyol	

	190.9237667	191.9317667					
	191.0158667	192.0238667	20	D-erythro-Isocitric acid	C6H8O7	Tricarboxylic acid	
			20	2,3-Diketo-L-gulonate	C6H8O7	Tricarboxylic acid	Pentose and glucuronate interconversions, ascorbate and aldarate metabolism
			20	2-Dehydro-3-deoxy-D-glucarate	C6H8O7	Tricarboxylic acid	Ascorbate and aldarate metabolism
			20	Carboxymethyloxysuccinate	C6H8O7	Tricarboxylic acid	
			20	2,5-Diketogluconic acid	C6H8O7	Tricarboxylic acid	
			20	5-Dehydro-4-deoxy-D-glucarate	C6H8O7	Tricarboxylic acid	Ascorbate and aldarate metabolism
			20	Isocitrate	C6H8O7	Tricarboxylic acid	Lots
			20	Citrate	C6H8O7	Tricarboxylic acid	Lots
	191.0552	192.0632	4	Quinic acid	C7H12O6	Cyclic polyol	Phenylalanine, tyrosine and tryptophan biosynthesis
			4	Valiolone	C7H12O6	Cyclic polyol	
			4	2D-5-O-Methyl-2,3,5/4,6-pentahydroxycyclohexanone	C7H12O6	Cyclic polyol	
297.2	297.1321333	298.1401333					
	297.2393	298.2473	14	18-Hydroxyoleate	C18H34O3	Fatty acid	Cutin, suberine and wax biosynthesis
			14	cis-9,10-Epoxystearic acid	C18H34O3	Fatty acid	Cutin, suberine and wax biosynthesis
			14	Ricinoleic acid	C18H34O3	Fatty acid	
	297.1336	298.1416					
	297.2391667	298.2471667	14	18-Hydroxyoleate	C18H34O3	Fatty acid	Cutin, suberine and wax biosynthesis
			14	cis-9,10-Epoxystearic acid	C18H34O3	Fatty acid	Cutin, suberine and wax biosynthesis
			14	Ricinoleic acid	C18H34O3	Fatty acid	
	297.1381667	298.1461667	38	Ostruthin	C19H22O3	Coumarin	
			38	Glepidotin C	C19H22O3	Stilbenoid	
	297.2389333	298.2469333	15	18-Hydroxyoleate	C18H34O3	Fatty acid	Cutin, suberine and wax biosynthesis
			15	cis-9,10-Epoxystearic acid	C18H34O3	Fatty acid	Cutin, suberine and wax biosynthesis
			15	Ricinoleic acid	C18H34O3	Fatty acid	
342.2	342.107	343.115					
	342.2063	343.2143					
	342.1073667	343.1153667					
	342.2036667	343.2116667					
	342.267	343.275					
	342.1073667	343.1153667					
	342.206	343.214					
	342.2669667	343.2749667					
665.2	665.2044	666.2124	15	Sesamose	C24H42O21	Tetrasaccharide	
			15	Lychnose	C24H42O21	Tetrasaccharide	

			15	1,3-alpha-D-Mannosyl-1,2-alpha-D-mannosyl-1,2-alpha-D-mannosyl-D-mannose	C24H42O21	Tetrasaccharide	
			15	Isolychnose	C24H42O21	Tetrasaccharide	
			15	Maltotetraose	C24H42O21	Tetrasaccharide	
			15	Cellotetraose	C24H42O21	Tetrasaccharide	
			15	Stachyose	C24H42O21	Tetrasaccharide	Galactose metabolism
			15	Glycogen	C24H42O21	Tetrasaccharide	Glucagon signalling pathway
			6	Quercetin 5,7,3',4'-tetramethyl ether 3-rutinoside	C31H38O16	Flavonol	
	665.2057	666.2137	13	Sesamose	C24H42O21	Tetrasaccharide	
			13	Lychnose	C24H42O21	Tetrasaccharide	
			13	1,3-alpha-D-Mannosyl-1,2-alpha-D-mannosyl-1,2-alpha-D-mannosyl-D-mannose	C24H42O21	Tetrasaccharide	
			13	Isolychnose	C24H42O21	Tetrasaccharide	
			13	Maltotetraose	C24H42O21	Tetrasaccharide	
			13	Cellotetraose	C24H42O21	Tetrasaccharide	
			13	Stachyose	C24H42O21	Tetrasaccharide	Galactose metabolism
			13	Glycogen	C24H42O21	Tetrasaccharide	Glucagon signalling pathway
			4	Quercetin 5,7,3',4'-tetramethyl ether 3-rutinoside	C31H38O16	Flavonol	
	665.2041333	666.2121333	15	Sesamose	C24H42O21	Tetrasaccharide	
			15	Lychnose	C24H42O21	Tetrasaccharide	
			15	1,3-alpha-D-Mannosyl-1,2-alpha-D-mannosyl-1,2-alpha-D-mannosyl-D-mannose	C24H42O21	Tetrasaccharide	
			15	Isolychnose	C24H42O21	Tetrasaccharide	
			15	Maltotetraose	C24H42O21	Tetrasaccharide	
			15	Cellotetraose	C24H42O21	Tetrasaccharide	
			15	Stachyose	C24H42O21	Tetrasaccharide	Galactose metabolism
			15	Glycogen	C24H42O21	Tetrasaccharide	Glucagon signalling pathway
			6	Quercetin 5,7,3',4'-tetramethyl ether 3-rutinoside	C31H38O16	Flavonol	
179	178.9634	179.9714					
	179.0296667	180.0376667	29	trans-2,3-Dihydroxycinnamate	C9H8O4	Phenolic acid	Phenylalanine metabolism
			29	2-Hydroxy-3-(4-hydroxyphenyl)propenoate	C9H8O4	Phenolic acid	Tyrosine metabolism
			29	Caffeic acid	C9H8O4	Phenolic acid	Phenylpropanoid biosynthesis
			29	p-Hydroxyphenylpyruvic acid	C9H8O4	Phenolic acid	Lots
	179.0531333	180.0611333	16	1,4-beta-D-Mannooligosaccharide	H2O(C6H10O5)n	Sugar	
			16	L-Gulose	C6H12O6	Sugar	Ascorbate and aldorate metabolism
			16	D-Fructose	C6H12O6	Sugar	
			16	beta-D-Hamamelopyranose	C6H12O6	Sugar	
			16	2-Deoxy-D-gluconate	C6H12O6	Sugar	

			16	beta-D-Fructose	C6H12O6	Sugar	Amino and nucleotide sugar metabolism
			16	L-Rhamnonate	C6H12O6	Sugar	Fructose and mannose metabolism
			16	D-Hamamelose	C6H12O6	Sugar	
			16	L-Galactose	C6H12O6	Sugar	Ascorbate and aldarate metabolism
			16	D-Fuconate	C6H12O6	Sugar	
			16	Galactose	C6H12O6	Sugar	
			16	Sorbose	C6H12O6	Sugar	
			16	D-Tagatose	C6H12O6	Sugar	Galactose metabolism
			16	alpha-D-Glucose	C6H12O6	Sugar	Lots
			16	beta-D-Glucose	C6H12O6	Sugar	Glycolysis and pentose phosphate pathway
			16	D-Mannose	C6H12O6	Sugar	Lots
			16	myo-Inositol	C6H12O6	Sugar	Lots
			16	D-Galactose	C6H12O6	Sugar	Lots
			16	D-Fructose	C6H12O6	Sugar	Lots
			24	Paraxanthine	C7H8N4O2	Purine alkaloid	Caffeine metabolism
			24	Theobromine	C7H8N4O2	Purine alkaloid	Caffeine and alkaloid metabolism
			24	Theophylline	C7H8N4O2	Purine alkaloid	Caffeine and alkaloid metabolism
	178.9163333	179.9243333					
	178.9724667	179.9804667					
	179.0296333	180.0376333	29	trans-2,3-Dihydroxycinnamate	C9H8O4	Phenolic acid	Phenylalanine metabolism
			29	2-Hydroxy-3-(4-hydroxyphenyl)propenoate	C9H8O4	Phenolic acid	Tyrosine metabolism
			29	Caffeic acid	C9H8O4	Phenolic acid	Phenylpropanoid biosynthesis
			29	p-Hydroxyphenylpyruvic acid	C9H8O4	Phenolic acid	Lots
	179.0530667	180.0610667	17	1,4-beta-D-Mannooligosaccharide	H2O(C6H10O5)n	Sugar	
			17	L-Gulose	C6H12O6	Sugar	Ascorbate and aldorate metabolism
			17	D-Fructose	C6H12O6	Sugar	
			17	beta-D-Hamamelopyranose	C6H12O6	Sugar	
			17	2-Deoxy-D-gluconate	C6H12O6	Sugar	
			17	beta-D-Fructose	C6H12O6	Sugar	Amino and nucleotide sugar metabolism
			17	L-Rhamnonate	C6H12O6	Sugar	Fructose and mannose metabolism
			17	D-Hamamelose	C6H12O6	Sugar	
			17	L-Galactose	C6H12O6	Sugar	Ascorbate and aldorate metabolism
			17	D-Fuconate	C6H12O6	Sugar	
			17	Galactose	C6H12O6	Sugar	
			17	Sorbose	C6H12O6	Sugar	
			17	D-Tagatose	C6H12O6	Sugar	Galactose metabolism

			17	alpha-D-Glucose	C6H12O6	Sugar	Lots
			17	beta-D-Glucose	C6H12O6	Sugar	Glycolysis and pentose phosphate pathway
			17	D-Mannose	C6H12O6	Sugar	Lots
			17	myo-Inositol	C6H12O6	Sugar	Lots
			17	D-Galactose	C6H12O6	Sugar	Lots
			17	D-Fructose	C6H12O6	Sugar	Lots
			24	Paraxanthine	C7H8N4O2	Purine alkaloid	Caffeine metabolism
			24	Theobromine	C7H8N4O2	Purine alkaloid	Caffeine and alkaloid metabolism
			24	Theophylline	C7H8N4O2	Purine alkaloid	Caffeine and alkaloid metabolism
	178.974	179.982					
	179.0295	180.0375	30	trans-2,3-Dihydroxycinnamate	C9H8O4	Phenolic acid	Phenylalanine metabolism
			30	2-Hydroxy-3-(4-hydroxyphenyl)propenoate	C9H8O4	Phenolic acid	Tyrosine metabolism
			30	Caffeic acid	C9H8O4	Phenolic acid	Phenylpropanoid biosynthesis
			30	p-Hydroxyphenylpyruvic acid	C9H8O4	Phenolic acid	Lots
	179.0532333	180.0612333	16	1,4-beta-D-Mannooligosaccharide	H2O(C6H10O5)n	Sugar	
			16	L-Gulose	C6H12O6	Sugar	Ascorbate and aldorate metabolism
			16	D-Fructose	C6H12O6	Sugar	
			16	beta-D-Hamamelopyranose	C6H12O6	Sugar	
			16	2-Deoxy-D-gluconate	C6H12O6	Sugar	
			16	beta-D-Fructose	C6H12O6	Sugar	Amino and nucleotide sugar metabolism
			16	L-Rhamnonate	C6H12O6	Sugar	Fructose and mannose metabolism
			16	D-Hamamelose	C6H12O6	Sugar	
			16	L-Galactose	C6H12O6	Sugar	Ascorbate and aldorate metabolism
			16	D-Fuconate	C6H12O6	Sugar	
			16	Galactose	C6H12O6	Sugar	
			16	Sorbose	C6H12O6	Sugar	
			16	D-Tagatose	C6H12O6	Sugar	Galactose metabolism
			16	alpha-D-Glucose	C6H12O6	Sugar	Lots
			16	beta-D-Glucose	C6H12O6	Sugar	Glycolysis and pentose phosphate pathway
			16	D-Mannose	C6H12O6	Sugar	Lots
			16	myo-Inositol	C6H12O6	Sugar	Lots
			16	D-Galactose	C6H12O6	Sugar	Lots
			16	D-Fructose	C6H12O6	Sugar	Lots
			23	Paraxanthine	C7H8N4O2	Purine alkaloid	Caffeine metabolism
			23	Theobromine	C7H8N4O2	Purine alkaloid	Caffeine and alkaloid metabolism
			23	Theophylline	C7H8N4O2	Purine alkaloid	Caffeine and alkaloid metabolism

429.2	429.1129	430.1209	10	N-Ethylmaleimide-S-glutathione	C16H22N4O8S	Peptide	
			14	Formononetin 7-O-glucoside	C22H22O9	Isoflavone	Isoflavonoid biosynthesis
	429.2127	430.2207	22	Cinegalline	C23H30N2O6	Quinolizidine alkaloid	
	429.2913667	430.2993667					
	429.1132333	430.1212333	10	N-Ethylmaleimide-S-glutathione	C16H22N4O8S	Peptide	
			13	Formononetin 7-O-glucoside	C22H22O9	Isoflavone	Isoflavonoid biosynthesis
	429.2141	430.2221	25	Cinegalline	C23H30N2O6	Quinolizidine alkaloid	
	429.1127333	430.1207333	9	N-Ethylmaleimide-S-glutathione	C16H22N4O8S	Peptide	
			14	Formononetin 7-O-glucoside	C22H22O9	Isoflavone	Isoflavonoid biosynthesis
	429.2118333	430.2198333	20	Cinegalline	C23H30N2O6	Quinolizidine alkaloid	

Table A.4 MR-Buster sorghum polyphenol extract putative identifications from OPLS-DA (ESI [+])

Bin	Detected Mass	Accurate Mass	Adduct	Δppm	Name	Formula	Chemical Group	Pathway
255	254.977	253.969	H+					
		231.987	Na+					
		215.877	K+					
	255.0744333	254.0664333	H+	20	S-(Phenylacetothiohydroximoyl)-L-cysteine	C11H14N2O3S	Amino acid	Glucosinolate and 2-oxocarboxylic acid biosynthesis and metabolism
				36	4',6-Dihydroxyflavone	C15H10O4	Flavone	
				36	7,4'-Dihydroxyflavone	C15H10O4	Flavone	Flavonoid and isoflavonoid biosynthesis
				36	Rubiadin	C15H10O4	Anthraquinone	
				36	1,4-Dihydroxy-2-methylanthraquinone	C15H10O4	Anthraquinone	
				36	Digiferrugineol	C15H10O4	Anthraquinone	
				36	Chrysophanol	C15H10O4	Anthraquinone	
				36	Alizarin 2-methyl ether	C15H10O4	Anthraquinone	
				36	Daidzein	C15H10O4	Isoflavone	Isoflavonoid and phenylpropanoid biosynthesis
				36	Anhydroglycinol	C15H10O4	Pterocarpan	Isoflavonoid biosynthesis
				36	Primetin	C15H10O4	Flavone	
				36	Chrysin	C15H10O4	Flavone	Flavonoid biosynthesis
				36	Hispidol	C15H10O4	Aurone	
				38	5-Glutamyl-taurine	C7H14N2O6S	Dipeptide	Taurine and hypotaurine metabolism
		232.0844333	Na+					
		215.9744333	K+	1	gamma-Glutamyl-gamma-aminobutyraldehyde	C9H16N2O4	Amino acid	Arginine and proline metabolism
	254.9394667	253.9314667	H+					
		231.9494667	Na+					
		215.8394667	K+					
	254.9953	253.9873	H+					
		232.0053	Na+					
		215.8953	K+	39	Isobergapten	C12H8O4	Furanocoumarin	
				39	Sphondin	C12H8O4	Furanocoumarin	

				39	Norvisnagin	C12H8O4	Furanocoumarin	
				30	2-C-Methyl-D-erythritol 4-phosphate	C5H13O7P	Isoprenoid precursor	Terpenoid, steroid and plant hormone biosynthesis
				39	Xanthotoxin	C12H8O4	Furanocoumarin	
				39	Bergapten	C12H8O4	Furanocoumarin	Phenylpropanoid biosynthesis
	255.0748	254.0668	H+	19	S-(Phenylacetothiohydroximoyl)-L-cysteine	C11H14N2O3S	Amino acid	Glucosinolate and 2-oxocarboxylic acid biosynthesis and metabolism
				37	4',6-Dihydroxyflavone	C15H10O4	Flavone	
				37	7,4'-Dihydroxyflavone	C15H10O4	Flavone	Flavonoid and isoflavonoid biosynthesis
				37	Rubiadin	C15H10O4	Anthraquinone	
				37	1,4-Dihydroxy-2-methylanthraquinone	C15H10O4	Anthraquinone	
				37	Digiferrugineol	C15H10O4	Anthraquinone	
				37	Chrysophanol	C15H10O4	Anthraquinone	
				37	Alizarin 2-methyl ether	C15H10O4	Anthraquinone	
				37	Daidzein	C15H10O4	Isoflavone	Isoflavonoid and phenylpropanoid biosynthesis
				37	Anhydroglycinol	C15H10O4	Pterocarpan	Isoflavonoid biosynthesis
				37	Primetin	C15H10O4	Flavone	
				37	Chrysin	C15H10O4	Flavone	Flavonoid biosynthesis
				37	Hispidol	C15H10O4	Aurone	
		232.0848	Na+					
		215.9748	K+	2	gamma-Glutamyl-gamma-aminobutyraldehyde	C9H16N2O4	Amino acid	Arginine and proline metabolism
	254.9833	253.9753	H+					
		231.9933	Na+					
		215.8833	K+					
	255.0751333	254.0671333	H+	18	S-(Phenylacetothiohydroximoyl)-L-cysteine	C11H14N2O3S	Amino acid	Glucosinolate and 2-oxocarboxylic acid biosynthesis and metabolism
				39	4',6-Dihydroxyflavone	C15H10O4	Flavone	
				39	7,4'-Dihydroxyflavone	C15H10O4	Flavone	Flavonoid and isoflavonoid biosynthesis
				39	Rubiadin	C15H10O4	Anthraquinone	
				39	1,4-Dihydroxy-2-methylanthraquinone	C15H10O4	Anthraquinone	
				39	Digiferrugineol	C15H10O4	Anthraquinone	
				39	Chrysophanol	C15H10O4	Anthraquinone	
				39	Alizarin 2-methyl ether	C15H10O4	Anthraquinone	
				39	Daidzein	C15H10O4	Isoflavone	Isoflavonoid and phenylpropanoid biosynthesis
				39	Anhydroglycinol	C15H10O4	Pterocarpan	Isoflavonoid biosynthesis
				39	Primetin	C15H10O4	Flavone	
				39	Chrysin	C15H10O4	Flavone	Flavonoid biosynthesis
				39	Hispidol	C15H10O4	Aurone	
		232.0851333	Na+					
		215.9751333	K+	3	gamma-Glutamyl-gamma-aminobutyraldehyde	C9H16N2O4	Amino acid	Arginine and proline metabolism

269	268.9808333	267.9728333	H+					
		245.9908333	Na+					
		229.8808333	K+	5	D-Xylose-5-phosphate	C5H11O8P	Sugar	
				5	L-Xylulose 1-phosphate	C5H11O8P	Sugar	Pentose and glucuronate interconversions
				5	beta-L-Arabinose 1-phosphate	C5H11O8P	Sugar	Amino acid and nucleotide sugar metabolism
				5	alpha-D-Xylose 1-phosphate	C5H11O8P	Sugar	
				5	D-Arabinose 5-phosphate	C5H11O8P	Sugar	Lipopolysaccharide biosynthesis
				5	L-Ribulose 5-phosphate	C5H11O8P	Sugar	Ascorbate and aldarate metabolism; pentose and glucuronate interconversions
				5	Ribose 1-phosphate	C5H11O8P	Sugar	Pentose phosphate pathway; purine metabolism
				5	D-Xylulose 5-phosphate	C5H11O8P	Sugar	Lots
				5	D-Ribulose 5-phosphate	C5H11O8P	Sugar	Lots
				5	Ribose 5-phosphate	C5H11O8P	Sugar	Lots
	269.0905667	268.0825667	H+	36	6-Hydroxy-2'-methoxyflavone	C16H12O4	Flavone	
				36	Isoformononetin	C16H12O4	Isoflavone	Isoflavonoid and phenylpropanoid biosynthesis
				36	Tectochrysin	C16H12O4	Flavone	
				5	Saphenic acid	C15H12N2O3	Alkaloid	
				14	2-O-(alpha-D-Mannosyl)-D-glycerate	C9H16O9	Sugar	Fructose and mannose metabolism
				36	Dalbergin	C16H12O4	Neoflavonoid	
				36	Formononetin	C16H12O4	Isoflavone	Isoflavonoid and phenylpropanoid biosynthesis
		246.1005667	Na+					
		229.9905667	K+	12	Isodehydrocostus lactone	C15H18O2	Sesquiterpenoid	
				12	Linderenol	C15H18O2	Sesquiterpenoid	
				12	Furanodienone	C15H18O2	Sesquiterpenoid	
				12	Dehydromyodesmone	C15H18O2	Sesquiterpenoid	
				12	Eremanthin	C15H18O2	Sesquiterpenoid	
				12	Dehydrocostus lactone	C15H18O2	Sesquiterpenoid	
	268.9783333	267.9703333	H+					
		245.9883333	Na+					
		229.8783333	K+	14	D-Xylose-5-phosphate	C5H11O8P	Sugar	
				14	L-Xylulose 1-phosphate	C5H11O8P	Sugar	Pentose and glucuronate interconversions
				14	beta-L-Arabinose 1-phosphate	C5H11O8P	Sugar	Amino acid and nucleotide sugar metabolism
				14	alpha-D-Xylose 1-phosphate	C5H11O8P	Sugar	
				14	D-Arabinose 5-phosphate	C5H11O8P	Sugar	Lipopolysaccharide biosynthesis
				14	L-Ribulose 5-phosphate	C5H11O8P	Sugar	Ascorbate and aldarate metabolism; pentose and glucuronate interconversions

				14	Ribose 1-phosphate	C5H11O8P	Sugar	Pentose phosphate pathway; purine metabolism
				14	D-Xylulose 5-phosphate	C5H11O8P	Sugar	Lots
				14	D-Ribulose 5-phosphate	C5H11O8P	Sugar	Lots
				14	Ribose 5-phosphate	C5H11O8P	Sugar	Lots
	269.0909	268.0829	H+	37	6-Hydroxy-2'-methoxyflavone	C16H12O4	Flavone	
				37	Isoformononetin	C16H12O4	Isoflavone	Isoflavonoid and phenylpropanoid biosynthesis
				37	Tectochrysin	C16H12O4	Flavone	
				4	Saphenic acid	C15H12N2O3	Alkaloid	
				15	2-O-(alpha-D-Mannosyl)-D-glycerate	C9H16O9	Sugar	Fructose and mannose metabolism
				37	Dalbergin	C16H12O4	Neoflavonoid	
				37	Formononetin	C16H12O4	Isoflavone	Isoflavonoid and phenylpropanoid biosynthesis
		246.1009	Na+					
		229.9909	K+	10	Isodehydrocostus lactone	C15H18O2	Sesquiterpenoid	
				10	Linderenol	C15H18O2	Sesquiterpenoid	
				10	Furanodienone	C15H18O2	Sesquiterpenoid	
				10	Dehydromyodesmone	C15H18O2	Sesquiterpenoid	
				10	Eremanthin	C15H18O2	Sesquiterpenoid	
				10	Dehydrocostus lactone	C15H18O2	Sesquiterpenoid	
	268.9797667	267.9717667	H+					
		245.9897667	Na+					
		229.8797667	K+	9	D-Xylose-5-phosphate	C5H11O8P	Sugar	
				9	L-Xylulose 1-phosphate	C5H11O8P	Sugar	Pentose and glucuronate interconversions
				9	beta-L-Arabinose 1-phosphate	C5H11O8P	Sugar	Amino acid and nucleotide sugar metabolism
				9	alpha-D-Xylose 1-phosphate	C5H11O8P	Sugar	
				9	D-Arabinose 5-phosphate	C5H11O8P	Sugar	Lipopolysaccharide biosynthesis
				9	L-Ribulose 5-phosphate	C5H11O8P	Sugar	Ascorbate and aldarate metabolism; pentose and glucuronate interconversions
				9	Ribose 1-phosphate	C5H11O8P	Sugar	Pentose phosphate pathway; purine metabolism
				9	D-Xylulose 5-phosphate	C5H11O8P	Sugar	Lots
				9	D-Ribulose 5-phosphate	C5H11O8P	Sugar	Lots
				9	Ribose 5-phosphate	C5H11O8P	Sugar	Lots
	269.0393667	268.0313667	H+	18	Coumestrol	C15H8O5	Coumestanes	Isoflavonoid and phenylpropanoid biosynthesis
		246.0493667	Na+	9	Pimpinellin	C13H10O5	Furanocoumarin	
				9	Isopimpinellin	C13H10O5	Furanocoumarin	Phenylpropanoid biosynthesis
		229.9393667	K+					
	269.0914333	268.0834333	H+	39	6-Hydroxy-2'-methoxyflavone	C16H12O4	Flavone	
				39	Isoformononetin	C16H12O4	Isoflavone	Isoflavonoid and phenylpropanoid biosynthesis

				39	Tectochrysin	C16H12O4	Flavone	
				2	Saphenic acid	C15H12N2O3	Alkaloid	
				17	2-O-(alpha-D-Mannosyl)-D-glycerate	C9H16O9	Sugar	Fructose and mannose metabolism
				39	Dalbergin	C16H12O4	Neoflavonoid	
				39	Formononetin	C16H12O4	Isoflavone	Isoflavonoid and phenylpropanoid biosynthesis
		246.1014333	Na+					
		229.9914333	K+	8	Isodehydrocostus lactone	C15H18O2	Sesquiterpenoid	
				8	Linderenol	C15H18O2	Sesquiterpenoid	
				8	Furanodienone	C15H18O2	Sesquiterpenoid	
				8	Dehydromyodesmone	C15H18O2	Sesquiterpenoid	
				8	Eremanthin	C15H18O2	Sesquiterpenoid	
				8	Dehydrocostus lactone	C15H18O2	Sesquiterpenoid	
271	270.9674333	269.9594333	H+					
		247.9774333	Na+					
		231.8674333	K+					
	271.0708667	270.0628667	H+	14	S-(Hydroxyphenylacetothiohydroximoyl)-L-cysteine	C11H14N2O4S	Amino acid	Glucosinolate and 2-oxocarboxylic acid biosynthesis and metabolism
				39	Islandicin	C15H10O5	Anthraquinone	
				39	3,6,4'-Trihydroxyflavone	C15H10O5	Flavone	
				39	6-Hydroxydaidzein	C15H10O5	Isoflavone	Isoflavonoid biosynthesis
				39	3',4',7-Trihydroxyisoflavone	C15H10O5	Isoflavone	
				39	Purpurin 1-methyl ether	C15H10O5	Anthraquinone	
				39	2-Hydroxychrysophanol	C15H10O5	Anthraquinone	
				39	Morindone	C15H10O5	Anthraquinone	
				39	Lucidin	C15H10O5	Anthraquinone	
				39	Emodin	C15H10O5	Anthraquinone	
				39	Aloe-emodin	C15H10O5	Anthraquinone	
				39	Norwogonin	C15H10O5	Flavone	
				39	Galangin	C15H10O5	Flavone	Flavonoid biosynthesis
				39	5-Deoxykaempferol	C15H10O5	Flavonol	
				39	Baicalein	C15H10O5	Flavone	
				39	Sulphuretin	C15H10O5	Aurone	
				39	Genistein	C15H10O5	Isoflavone	Isoflavonoid and phenylpropanoid biosynthesis
				39	2'-Hydroxydaidzein	C15H10O5	Isoflavone	Isoflavonoid biosynthesis
				39	Apigenin	C15H10O5	Flavone	Flavonoid, isoflavonoid, flavone, flavonol and phenylpropanoid biosynthesis
				34	D-Lombricine	C6H15N4O6P	Amino acid	Glycine, serine and threonine metabolism
		248.0808667	Na+	7	5-Hydroxyindoleacetylglycine	C12H12N2O4	Amino acid	Tryptophan metabolism
		231.9708667	K+	20	2-Oxo-10-methylthiodecanoic acid	C11H20O3S	Fatty acid	Glucosinolate and 2-oxocarboxylic acid biosynthesis and metabolism
				6	gamma-Glutamyl-GABA	C9H16N2O5	Amino acid	Arginine and proline metabolism
				8	Mexicanin E	C14H16O3	Sesquiterpenoid	

				28	Cryptolepine	C16H12N2	Alkaloid	
				6	N6-Acetyl-LL-2,6-diaminoheptanedioate	C9H16N2O5	Amino acid	Amino acid and lysine biosynthesis
				6	N2-Succinyl-L-ornithine	C9H16N2O5	Amino acid	Arginine and proline metabolism
				6	N-alpha-Boc-L-asparagine	C9H16N2O5	Amino acid	
	270.9696667	269.9616667	H+					
		247.9796667	Na+					
		231.8696667	K+					
	271.0705667	270.0625667	H+	15	S-(Hydroxyphenylacetothiohydroximoyl)-L-cysteine	C11H14N2O4S	Amino acid	Glucosinolate and 2-oxocarboxylic acid biosynthesis and metabolism
				38	Islandicin	C15H10O5	Anthraquinone	
				38	3,6,4'-Trihydroxyflavone	C15H10O5	Flavone	
				38	6-Hydroxydaidzein	C15H10O5	Isoflavone	Isoflavonoid biosynthesis
				38	3',4',7-Trihydroxyisoflavone	C15H10O5	Isoflavone	
				38	Purpurin 1-methyl ether	C15H10O5	Anthraquinone	
				38	2-Hydroxychrysophanol	C15H10O5	Anthraquinone	
				38	Morindone	C15H10O5	Anthraquinone	
				38	Lucidin	C15H10O5	Anthraquinone	
				38	Emodin	C15H10O5	Anthraquinone	
				38	Aloe-emodin	C15H10O5	Anthraquinone	
				38	Norwogonin	C15H10O5	Flavone	
				38	Galangin	C15H10O5	Flavone	Flavonoid biosynthesis
				38	5-Deoxykaempferol	C15H10O5	Flavonol	
				38	Baicalein	C15H10O5	Flavone	
				38	Sulphuretin	C15H10O5	Aurone	
				38	Genistein	C15H10O5	Isoflavone	Isoflavonoid and phenylpropanoid biosynthesis
				38	2'-Hydroxydaidzein	C15H10O5	Isoflavone	Isoflavonoid biosynthesis
				38	Apigenin	C15H10O5	Flavone	Flavonoid, isoflavonoid, flavone, flavonol and phenylpropanoid biosynthesis
				35	D-Lombricine	C6H15N4O6P	Amino acid	Glycine, serine and threonine metabolism
		248.0805667	Na+	6	5-Hydroxyindoleacetylglycine	C12H12N2O4	Amino acid	Tryptophan metabolism
		231.9705667	K+	21	2-Oxo-10-methylthiodecanoic acid	C11H20O3S	Fatty acid	Glucosinolate and 2-oxocarboxylic acid biosynthesis and metabolism
				5	gamma-Glutamyl-GABA	C9H16N2O5	Amino acid	Arginine and proline metabolism
				9	Mexicanin E	C14H16O3	Sesquiterpenoid	
				27	Cryptolepine	C16H12N2	Alkaloid	
				5	N6-Acetyl-LL-2,6-diaminoheptanedioate	C9H16N2O5	Amino acid	Amino acid and lysine biosynthesis
				5	N2-Succinyl-L-ornithine	C9H16N2O5	Amino acid	Arginine and proline metabolism
				5	N-alpha-Boc-L-asparagine	C9H16N2O5	Amino acid	
	270.9674	269.9594	H+					
		247.9774	Na+					
		231.8674	K+					
	271.071	270.063	H+	13	S-(Hydroxyphenylacetothiohydroximoyl)-L-cysteine	C11H14N2O4S	Amino acid	Glucosinolate and 2-oxocarboxylic acid biosynthesis and metabolism

				33	D-Lombricine	C6H15N4O6P	Amino acid	Glycine, serine and threonine metabolism
		248.081	Na+	7	5-Hydroxyindoleacetylglycine	C12H12N2O4	Amino acid	Tryptophan metabolism
		231.971	K+	20	2-Oxo-10-methylthiodecanoic acid	C11H20O3S	Fatty acid	Glucosinolate and 2-oxocarboxylic acid biosynthesis and metabolism
				7	gamma-Glutamyl-GABA	C9H16N2O5	Amino acid	Arginine and proline metabolism
				7	Mexicanin E	C14H16O3	Sesquiterpenoid	
				28	Cryptolepine	C16H12N2	Alkaloid	
				7	N6-Acetyl-LL-2,6-diaminoheptanedioate	C9H16N2O5	Amino acid	Amino acid and lysine biosynthesis
				7	N2-Succinyl-L-ornithine	C9H16N2O5	Amino acid	Arginine and proline metabolism
				7	N-alpha-Boc-L-asparagine	C9H16N2O5	Amino acid	
285	284.9933	283.9853	H+					
		262.0033	Na+					
		245.8933	K+					
	285.0862333	284.0782333	H+	36	Emodin monomethyl ether	C16H12O5	Anthraquinone	
				36	Obtusifolin	C16H12O5	Anthraquinone	
				36	(+)-Maackiain	C16H12O5	Pterocarpan	Isoflavonoid biosynthesis
				36	Glycitein	C16H12O5	Isoflavone	Isoflavonoid biosynthesis
				36	3-Methylgalangin	C16H12O5	Flavonol	
				36	Texasin	C16H12O5	Isoflavone	
				36	Prunetin	C16H12O5	Isoflavone	Isoflavonoid biosynthesis
				36	Melannin	C16H12O5	Neoflavonoid	
				36	(-)-Maackiain	C16H12O5	Pterocarpan	Isoflavonoid biosynthesis
				36	Lucidin omega-methyl ether	C16H12O5	Anthraquinone	
				36	Cypripedin	C16H12O5	Anthraquinone	
				36	Wogonin	C16H12O5	Flavone	
				36	5-Deoxychrysoeriol	C16H12O5	Flavone	
				36	Apigenin 7-methyl ether	C16H12O5	Flavone	
				36	2'-Hydroformononetin	C16H12O5	Isoflavone	Isoflavonoid biosynthesis
				11	Xanthosine	C10H12N4O6	Nucleotide	Purine, caffeine and alkaloid biosynthesis
				36	3'-Hydroxyformononetin	C16H12O5	Isoflavone	Isoflavonoid biosynthesis
				36	Acacetin	C16H12O5	Flavone	Flavone and flavonol biosynthesis
				36	Questin	C16H12O5	Anthraquinone	
				36	Biochanin A	C16H12O5	Isoflavone	Isoflavonoid and phenylpropanoid biosynthesis
		262.0962333	Na+	28	Thiamine aldehyde	C12H15N4OS	Vitamin	Thiamine biosynthesis
		245.9862333	K+	5	2,4-Bis(acetamido)-2,4,6-trideoxy-beta-L-altropyranose	C10H18N2O5	Sugar	Amino acid and nucleotide sugar metabolism
				8	Zedoarol	C15H18O3	Sesquiterpenoid	
				8	Zederone	C15H18O3	Sesquiterpenoid	
				8	Isozaluzanin C	C15H18O3	Sesquiterpenoid	
				8	Zaluzanin C	C15H18O3	Sesquiterpenoid	
				8	Xerantholide	C15H18O3	Sesquiterpenoid	
				8	Xanthatin	C15H18O3	Sesquiterpenoid	
				8	beta-Santonin	C15H18O3	Sesquiterpenoid	

				8	7alpha-Hydroxydehydrocostus lactone	C15H18O3	Sesquiterpenoid	
				8	Leucodin	C15H18O3	Sesquiterpenoid	
				8	Aromaticin	C15H18O3	Sesquiterpenoid	
				8	Ambrosin	C15H18O3	Sesquiterpenoid	
				25	Olivacine	C17H14N2	Indole alkaloid	
				25	Ellipticine	C17H14N2	Indole alkaloid	
				34	L-N2-(2-Carboxyethyl)arginine	C9H18N4O4	Amino acid	Clavulanic acid biosynthesis
				34	D-Octopine	C9H18N4O4	Amino acid	Arginine and proline metabolism
				8	alpha-Santonin	C15H18O3	Sesquiterpenoid	
	284.9075667	283.8995667	H+					
		261.9175667	Na+					
		245.8075667	K+					
	284.984	283.976	H+					
		261.994	Na+					
		245.884	K+					
	285.0876333	284.0796333	H+	16	Xanthosine	C10H12N4O6	Nucleotide	Purine, caffeine and alkaloid biosynthesis
		262.0976333	Na+	33	Thiamine aldehyde	C12H15N4OS	Vitamin	Thiamine biosynthesis
		245.9876333	K+	10	2,4-Bis(acetamido)-2,4,6-trideoxy-beta-L-altropyranose	C10H18N2O5	Sugar	Amino acid and nucleotide sugar metabolism
				3	Zedoarol	C15H18O3	Sesquiterpenoid	
				3	Zederone	C15H18O3	Sesquiterpenoid	
				3	Isozaluzanin C	C15H18O3	Sesquiterpenoid	
				3	Zaluzanin C	C15H18O3	Sesquiterpenoid	
				3	Xerantholide	C15H18O3	Sesquiterpenoid	
				3	Xanthatin	C15H18O3	Sesquiterpenoid	
				3	beta-Santonin	C15H18O3	Sesquiterpenoid	
				3	7alpha-Hydroxydehydrocostus lactone	C15H18O3	Sesquiterpenoid	
				3	Leucodin	C15H18O3	Sesquiterpenoid	
				3	Aromaticin	C15H18O3	Sesquiterpenoid	
				3	Ambrosin	C15H18O3	Sesquiterpenoid	
				30	Olivacine	C17H14N2	Indole alkaloid	
				30	Ellipticine	C17H14N2	Indole alkaloid	
				29	L-N2-(2-Carboxyethyl)arginine	C9H18N4O4	Amino acid	Clavulanic acid biosynthesis
				29	D-Octopine	C9H18N4O4	Amino acid	Arginine and proline metabolism
				3	alpha-Santonin	C15H18O3	Sesquiterpenoid	
	284.9936	283.9856	H+					
		262.0036	Na+					
		245.8936	K+					
	285.0869333	284.0789333	H+	39	Emodin monomethyl ether	C16H12O5	Anthraquinone	
				39	Obtusifolin	C16H12O5	Anthraquinone	
				39	(+)-Maackiain	C16H12O5	Pterocarpan	Isoflavonoid biosynthesis
				39	Glycitein	C16H12O5	Isoflavone	Isoflavonoid biosynthesis
				39	3-Methylgalangin	C16H12O5	Flavonol	
				39	Texasin	C16H12O5	Isoflavone	
				39	Prunetin	C16H12O5	Isoflavone	Isoflavonoid biosynthesis

				39	Melannin	C16H12O5	Neoflavonoid	
				39	(-)-Maackiain	C16H12O5	Pterocarpan	Isoflavonoid biosynthesis
				39	Lucidin omega-methyl ether	C16H12O5	Anthraquinone	
				39	Cypripedin	C16H12O5	Anthraquinone	
				39	Wogonin	C16H12O5	Flavone	
				39	5-Deoxychrysoeriol	C16H12O5	Flavone	
				39	Apigenin 7-methyl ether	C16H12O5	Flavone	
				39	2'-Hydroformononetin	C16H12O5	Isoflavone	Isoflavonoid biosynthesis
				13	Xanthosine	C10H12N4O6	Nucleotide	Purine, caffeine and alkaloid biosynthesis
				39	3'-Hydroxyformononetin	C16H12O5	Isoflavone	Isoflavonoid biosynthesis
				39	Acacetin	C16H12O5	Flavone	Flavone and flavonol biosynthesis
				39	Questin	C16H12O5	Anthraquinone	
				39	Biochanin A	C16H12O5	Isoflavone	Isoflavonoid and phenylpropanoid biosynthesis
		262.0969333	Na+	31	Thiamine aldehyde	C12H15N4OS	Vitamin	Thiamine biosynthesis
		245.9869333	K+	7	2,4-Bis(acetamido)-2,4,6-trideoxy-beta-L-altropyranose	C10H18N2O5	Sugar	Amino acid and nucleotide sugar metabolism
				6	Zedoarol	C15H18O3	Sesquiterpenoid	
				6	Zederone	C15H18O3	Sesquiterpenoid	
				6	Isozaluzanin C	C15H18O3	Sesquiterpenoid	
				6	Zaluzanin C	C15H18O3	Sesquiterpenoid	
				6	Xerantholide	C15H18O3	Sesquiterpenoid	
				6	Xanthatin	C15H18O3	Sesquiterpenoid	
				6	beta-Santonin	C15H18O3	Sesquiterpenoid	
				6	7alpha-Hydroxydehydrocostus lactone	C15H18O3	Sesquiterpenoid	
				6	Leucodin	C15H18O3	Sesquiterpenoid	
				6	Aromaticin	C15H18O3	Sesquiterpenoid	
				6	Ambrosin	C15H18O3	Sesquiterpenoid	
				28	Olivacine	C17H14N2	Indole alkaloid	
				28	Ellipticine	C17H14N2	Indole alkaloid	
				31	L-N2-(2-Carboxyethyl)arginine	C9H18N4O4	Amino acid	Clavulanic acid biosynthesis
				31	D-Octopine	C9H18N4O4	Amino acid	Arginine and proline metabolism
				6	alpha-Santonin	C15H18O3	Sesquiterpenoid	
287	287.0679	286.0599	H+	14	5'-Phosphoribosylglycinamide	C7H15N2O8P	Amino acid	Purine metabolism
		264.0779	Na+	38	Perlolyrine	C16H12N2O2	Indole alkaloid	
		247.9679	K+	0	Prenyl caffeate	C14H16O4	Phenolic acid	
	287.0679667	286.0599667	H+	14	5'-Phosphoribosylglycinamide	C7H15N2O8P	Amino acid	Purine metabolism
		264.0779667	Na+	38	Perlolyrine	C16H12N2O2	Indole alkaloid	
		247.9679667	K+	0	Prenyl caffeate	C14H16O4	Phenolic acid	
	287.0685667	286.0605667	H+	16	5'-Phosphoribosylglycinamide	C7H15N2O8P	Amino acid	Purine metabolism
		264.0785667	Na+	36	Perlolyrine	C16H12N2O2	Indole alkaloid	
		247.9685667	K+	1	Prenyl caffeate	C14H16O4	Phenolic acid	
470.2	470.1068333	469.0988333	H+					
		447.1168333	Na+					

		431.0068333	K+					
	470.2461333	469.2381333	H+					
		447.2561333	Na+					
		431.1461333	K+					
	470.1103333	469.1023333	H+					
		447.1203333	Na+					
		431.0103333	K+					
	470.2463667	469.2383667	H+					
		447.2563667	Na+					
		431.1463667	K+					
	470.1037667	469.0957667	H+					
		447.1137667	Na+					
		431.0037667	K+					
353.2	353.2604	352.2524	H+	23	Montanol	C21H36O4	Diterpenoid	
		330.2704	Na+					
		314.1604	K+					
	353.2595333	352.2515333	H+	25	Montanol	C21H36O4	Diterpenoid	
		330.2695333	Na+					
		314.1595333	K+					
	353.2582333	352.2502333	H+	29	Montanol	C21H36O4	Diterpenoid	
		330.2682333	Na+	37	Docosapentaenoic acid	C22H34O2	Fatty acid	Unsaturated fatty acid biosynthesis
		314.1582333	K+					
523.2	523.1587667	522.1507667	H+	27	Iridin	C24H26O13	Isoflavone	
		500.1687667	Na+					
		484.0587667	K+					
	523.1596	522.1516	H+	28	Iridin	C24H26O13	Isoflavone	
		500.1696	Na+					
		484.0596	K+					
	523.1604333	522.1524333	H+	30	Iridin	C24H26O13	Isoflavone	
				39	Melampodinin	C25H30O12	Sesquiterpenoid	
		500.1704333	Na+					
		484.0604333	K+					
509.2	509.1445667	508.1365667	H+					
		486.1545667	Na+					
		470.0445667	K+	24	Isobutyrylmallotochromene	C26H30O8	Phloroglucinol	
				24	Drummondin A	C26H30O8	Phloroglucinol	
				24	Butyrylmallotochromene	C26H30O8	Phloroglucinol	
				24	Zapoterin	C26H30O8	Triterpenoid	
				24	Limonin	C26H30O8	Triterpenoid	
	509.1449667	508.1369667	H+					
		486.1549667	Na+					
		470.0449667	K+	24	Isobutyrylmallotochromene	C26H30O8	Phloroglucinol	
				24	Drummondin A	C26H30O8	Phloroglucinol	
				24	Butyrylmallotochromene	C26H30O8	Phloroglucinol	

				24	Zapoterin	C26H30O8	Triterpenoid	
				24	Limonin	C26H30O8	Triterpenoid	
	509.1464667	508.1384667	H+					
		486.1564667	Na+					
		470.0464667	K+	21	Isobutyrylmallotochromene	C26H30O8	Phloroglucinol	
				21	Drummondin A	C26H30O8	Phloroglucinol	
				21	Butyrylmallotochromene	C26H30O8	Phloroglucinol	
				21	Zapoterin	C26H30O8	Triterpenoid	
				21	Limonin	C26H30O8	Triterpenoid	
537.2	537.1705333	536.1625333	H+	8	Cellulose	(C6H10O5)n	Trisaccharide	Starch and sucrose metabolism
		514.1805333	Na+	4	Baohuoside I	C27H30O10	Flavone	
				4	Icariside II	C27H30O10	Flavone	
		498.0705333	K+	13	Strictosamide	C26H30N2O8	Indole alkaloid	Alkaloids from shikimate pathway biosynthesis
				5	8-Epiiridodial glucoside tetraacetate	C24H34O11	Iridoid	
				5	Iridodial glucoside tetraacetate	C24H34O11	Iridoid	
	537.1722333	536.1642333	H+	11	Cellulose	(C6H10O5)n	Trisaccharide	Starch and sucrose metabolism
		514.1822333	Na+	1	Baohuoside I	C27H30O10	Flavone	
				1	Icariside II	C27H30O10	Flavone	
		498.0722333	K+	16	Strictosamide	C26H30N2O8	Indole alkaloid	Alkaloids from shikimate pathway biosynthesis
				1	8-Epiiridodial glucoside tetraacetate	C24H34O11	Iridoid	
				1	Iridodial glucoside tetraacetate	C24H34O11	Iridoid	
	537.1740667	536.1660667	H+	14	Cellulose	(C6H10O5)n	Trisaccharide	Starch and sucrose metabolism
		514.1840667	Na+	1	Baohuoside I	C27H30O10	Flavone	
				1	Icariside II	C27H30O10	Flavone	
		498.0740667	K+	19	Strictosamide	C26H30N2O8	Indole alkaloid	Alkaloids from shikimate pathway biosynthesis
				1	8-Epiiridodial glucoside tetraacetate	C24H34O11	Iridoid	
				1	Iridodial glucoside tetraacetate	C24H34O11	Iridoid	
524.2	524.1619333	523.1539333	H+					
		501.1719333	Na+					
		485.0619333	K+					
	524.1633667	523.1553667	H+					
		501.1733667	Na+					
		485.0633667	K+					
	524.1631333	523.1551333	H+					
		501.1731333	Na+					
		485.0631333	K+					
270	269.9776667	268.9696667	H+					
		246.9876667	Na+					
		230.8776667	K+					
	270.0909	269.0829	H+					
		247.1009	Na+	14	Linamarin	C10H17NO6	Cyanogenic glycoside	Cyanamino acid metabolism

		230.9909	K+	6	Leiokinine A	C14H17NO2	Quinoline alkaloid	
	269.9796	268.9716	H+					
		246.9896	Na+					
		230.8796	K+					
	270.0911333	269.0831333	H+					
		247.1011333	Na+	13	Linamarin	C10H17NO6	Cyanogenic glycoside	Cyanamino acid metabolism
		230.9911333	K+	7	Leiokinine A	C14H17NO2	Quinoline alkaloid	
	269.9659	268.9579	H+					
		246.9759	Na+					
		230.8659	K+					
	270.0916333	269.0836333	H+					
		247.1016333	Na+	11	Linamarin	C10H17NO6	Cyanogenic glycoside	Cyanamino acid metabolism
		230.9916333	K+	9	Leiokinine A	C14H17NO2	Quinoline alkaloid	
510.2	510.1509667	509.1429667	H+					
		487.1609667	Na+					
		471.0509667	K+					
	510.1487667	509.1407667	H+					
		487.1587667	Na+					
		471.0487667	K+					
	510.1497	509.1417	H+					
		487.1597	Na+					
		471.0497	K+					
256	255.9517667	254.9437667	H+					
		232.9617667	Na+					
		216.8517667	K+					
	256.0780333	255.0700333	H+	13	Nicotinate D-ribonucleoside	C11H14NO6	Glycoside	Nicotinate and nicotinamide metabolism
				17	Apigeninidin	C15H11O4	3-DA	
		233.0880333	Na+					
		216.9780333	K+	33	N-Acetyl-L-citrulline	C8H15N3O4	Amino acid	Arginine biosynthesis
				17	Securinine	C13H15NO2	Alkaloid	
	255.9896333	254.9816333	H+					
		232.9996333	Na+					
		216.8896333	K+					
	256.0784667	255.0704667	H+	12	Nicotinate D-ribonucleoside	C11H14NO6	Glycoside	Nicotinate and nicotinamide metabolism
				19	Apigeninidin	C15H11O4	3-DA	
		233.0884667	Na+					
		216.9784667	K+	35	N-Acetyl-L-citrulline	C8H15N3O4	Amino acid	Arginine biosynthesis
				19	Securinine	C13H15NO2	Alkaloid	
	255.9911	254.9831	H+					

		233.0011	Na+					
		216.8911	K+					
	256.0789667	255.0709667	H+	10	Nicotinate D-ribonucleoside	C11H14NO6	Glycoside	Nicotinate and nicotinamide metabolism
				21	Apigeninidin	C15H11O4	3-DA	
		233.0889667	Na+					
		216.9789667	K+	37	N-Acetyl-L-citrulline	C8H15N3O4	Amino acid	Arginine biosynthesis
				21	Securinine	C13H15NO2	Alkaloid	
257	256.9683333	255.9603333	H+					
		233.9783333	Na+					
		217.8683333	K+					
	257.0889	256.0809	H+	31	Aloe emodin anthrone	C15H12O4	Anthraquinone	
				31	Pinocembrin chalcone	C15H12O4	Chalcone	Flavonoid biosynthesis
				31	3',5'-Dihydroxyflavanone	C15H12O4	Flavanone	
				31	Hydrangenol	C15H12O4	Stilbenoid	
				31	Pinocembrin	C15H12O4	Flavanone	Flavonoid biosynthesis
				31	Liquiritigenin	C15H12O4	Flavanone	Flavonoid, isoflavonoid and phenylpropanoid biosynthesis
				31	Isoliquiritigenin	C15H12O4	Chalcone	Flavonoid and phenylpropanoid biosynthesis
				31	3,9-Dihydroxypterocarpan	C15H12O4	Pterocarpan	Isoflavonoid biosynthesis
		234.0989	Na+					
		217.9889	K+					
	257.0894	256.0814	H+	33	Aloe emodin anthrone	C15H12O4	Anthraquinone	
				33	Pinocembrin chalcone	C15H12O4	Chalcone	Flavonoid biosynthesis
				33	3',5'-Dihydroxyflavanone	C15H12O4	Flavanone	
				33	Hydrangenol	C15H12O4	Stilbenoid	
				33	Pinocembrin	C15H12O4	Flavanone	Flavonoid biosynthesis
				33	Liquiritigenin	C15H12O4	Flavanone	Flavonoid, isoflavonoid and phenylpropanoid biosynthesis
				33	Isoliquiritigenin	C15H12O4	Chalcone	Flavonoid and phenylpropanoid biosynthesis
				33	3,9-Dihydroxypterocarpan	C15H12O4	Pterocarpan	Isoflavonoid biosynthesis
		234.0994	Na+					
		217.9894	K+					
	256.9652	255.9572	H+					
		233.9752	Na+					
		217.8652	K+					
	257.0367333	256.0287333	H+	30	Purpurin	C14H8O5	Anthraquinone	
				30	Anthragallol	C14H8O5	Anthraquinone	
		234.0467333	Na+					
		217.9367333	K+					
	257.0905667	256.0825667	H+	37	Aloe emodin anthrone	C15H12O4	Anthraquinone	
				37	Pinocembrin chalcone	C15H12O4	Chalcone	Flavonoid biosynthesis
				37	3',5'-Dihydroxyflavanone	C15H12O4	Flavanone	
				37	Hydrangenol	C15H12O4	Stilbenoid	

				37	Pinocembrin	C15H12O4	Flavanone	Flavonoid biosynthesis
				37	Liquiritigenin	C15H12O4	Flavanone	Flavonoid, isoflavonoid and phenylpropanoid biosynthesis
				37	Isoliquiritigenin	C15H12O4	Chalcone	Flavonoid and phenylpropanoid biosynthesis
				37	3,9-Dihydroxypterocarpan	C15H12O4	Pterocarpan	Isoflavonoid biosynthesis
		234.1005667	Na+					
		217.9905667	K+					
273	272.9502333	271.9422333	H+					
		249.9602333	Na+					
		233.8502333	K+					
	272.9965667	271.9885667	H+					
		250.0065667	Na+					
		233.8965667	K+					
	273.0847	272.0767	H+	32	Toralactone	C15H12O5	Napthopyranone	
				32	6,7,4'-Trihydroxyflavanone	C15H12O5	Flavanone	Isoflavonoid biosynthesis
				32	2,7,4'-Trihydroxyisoflavanone	C15H12O5	Isoflavanone	Isoflavonoid biosynthesis
				32	Dihydrogenistein	C15H12O5	Flavanone	
				32	p-Coumaroyltriacetic acid lactone	C15H12O5	Phenolic acid	
				32	Pinobanksin	C15H12O5	Flavanone	Flavonoid biosynthesis
				32	Garbanzol	C15H12O5	Flavanone	Flavonoid biosynthesis
				32	Butin	C15H12O5	Flavanone	Flavonoid biosynthesis
				32	Rubrofusarin	C15H12O5	Napthopyranone	
				32	Butein	C15H12O5	Chalcone	Flavonoid biosynthesis
				32	Naringenin chalcone	C15H12O5	Chalcone	Flavonoid and phenylpropanoid biosynthesis
				32	2'-Hydroxydihydrodaidzein	C15H12O5	Isoflavanone	Isoflavonoid biosynthesis
				32	Licodione	C15H12O5	Chalcone	
				32	(-)-Glycinol	C15H12O5	Pterocarpan	Isoflavonoid biosynthesis
				32	Naringenin	C15H12O5	Flavanone	Flavonoid, isoflavonoid and phenylpropanoid biosynthesis
		250.0947	Na+	29	3-(5'-Methylthio)pentylmalic acid	C10H18O5S	Amino acid	Glucosinolate and 2-oxocarboxylic acid biosynthesis and metabolism
				29	2-(5'-Methylthio)pentylmalic acid	C10H18O5S	Amino acid	Glucosinolate and 2-oxocarboxylic acid biosynthesis and metabolism
				14	Flindersiachromone	C17H14O2	Sesquiterpenoid	
		233.9847	K+	14	Strigolactone ABC-rings	C14H18O3	Phytohormone	Carotenoid biosynthesis
	272.9646333	271.9566333	H+					
		249.9746333	Na+					
		233.8646333	K+					
	273.0853	272.0773	H+	34	Toralactone	C15H12O5	Napthopyranone	
				34	6,7,4'-Trihydroxyflavanone	C15H12O5	Flavanone	Isoflavonoid biosynthesis
				34	2,7,4'-Trihydroxyisoflavanone	C15H12O5	Isoflavanone	Isoflavonoid biosynthesis
				34	Dihydrogenistein	C15H12O5	Flavanone	
				34	p-Coumaroyltriacetic acid lactone	C15H12O5	Phenolic acid	
				34	Pinobanksin	C15H12O5	Flavanone	Flavonoid biosynthesis

				34	Garbanzol	C15H12O5	Flavanone	Flavonoid biosynthesis
				34	Butin	C15H12O5	Flavanone	Flavonoid biosynthesis
				34	Rubrofusarin	C15H12O5	Napthopyranone	
				34	Butein	C15H12O5	Chalcone	Flavonoid biosynthesis
				34	Naringenin chalcone	C15H12O5	Chalcone	Flavonoid and phenylpropanoid biosynthesis
				34	2'-Hydroxydihydrodaidzein	C15H12O5	Isoflavanone	Isoflavonoid biosynthesis
				34	Licodione	C15H12O5	Chalcone	
				34	(-)-Glycinol	C15H12O5	Pterocarpan	Isoflavonoid biosynthesis
				34	Naringenin	C15H12O5	Flavanone	Flavonoid, isoflavonoid and phenylpropanoid biosynthesis
		250.0953	Na+	31	3-(5'-Methylthio)pentylmalic acid	C10H18O5S	Amino acid	Glucosinolate and 2-oxocarboxylic acid biosynthesis and metabolism
				31	2-(5'-Methylthio)pentylmalic acid	C10H18O5S	Amino acid	Glucosinolate and 2-oxocarboxylic acid biosynthesis and metabolism
				12	Flindersiachromone	C17H14O2	Sesquiterpenoid	
		233.9853	K+	12	Strigolactone ABC-rings	C14H18O3	Phytohormone	Carotenoid biosynthesis
	272.9824	271.9744	H+					
		249.9924	Na+					
		233.8824	K+					
	273.0854	272.0774	H+	35	Toralactone	C15H12O5	Napthopyranone	
				35	6,7,4'-Trihydroxyflavanone	C15H12O5	Flavanone	Isoflavonoid biosynthesis
				35	2,7,4'-Trihydroxyisoflavanone	C15H12O5	Isoflavanone	Isoflavonoid biosynthesis
				35	Dihydrogenistein	C15H12O5	Flavanone	
				35	p-Coumaroyltriacetic acid lactone	C15H12O5	Phenolic acid	
				35	Pinobanksin	C15H12O5	Flavanone	Flavonoid biosynthesis
				35	Garbanzol	C15H12O5	Flavanone	Flavonoid biosynthesis
				35	Butin	C15H12O5	Flavanone	Flavonoid biosynthesis
				35	Rubrofusarin	C15H12O5	Napthopyranone	
				35	Butein	C15H12O5	Chalcone	Flavonoid biosynthesis
				35	Naringenin chalcone	C15H12O5	Chalcone	Flavonoid and phenylpropanoid biosynthesis
				35	2'-Hydroxydihydrodaidzein	C15H12O5	Isoflavanone	Isoflavonoid biosynthesis
				35	Licodione	C15H12O5	Chalcone	
				35	(-)-Glycinol	C15H12O5	Pterocarpan	Isoflavonoid biosynthesis
				35	Naringenin	C15H12O5	Flavanone	Flavonoid, isoflavonoid and phenylpropanoid biosynthesis
		250.0954	Na+	31	3-(5'-Methylthio)pentylmalic acid	C10H18O5S	Amino acid	Glucosinolate and 2-oxocarboxylic acid biosynthesis and metabolism
				31	2-(5'-Methylthio)pentylmalic acid	C10H18O5S	Amino acid	Glucosinolate and 2-oxocarboxylic acid biosynthesis and metabolism
				11	Flindersiachromone	C17H14O2	Sesquiterpenoid	
		233.9854	K+	12	Strigolactone ABC-rings	C14H18O3	Phytohormone	Carotenoid biosynthesis
539.2	539.1562	538.1482	H+					
		516.1662	Na+	21	Rottlerin	C30H28O8	Phloroglucinol	
		500.0562	K+					

	539.1569	538.1489	H+					
		516.1669	Na+	19	Rottlerin	C30H28O8	Phloroglucinol	
		500.0569	K+					

Table B3.5 Cracka sorghum polyphenol extract putative identifications from OPLS-DA (ESI [+])

Bin	Detected Mass	Accurate Mass	Adduct	Δppm	Name	Formula	Chemical Group	Pathway
271	270.9687667	269.9607667	H+					
		247.9787667	Na+					
		231.8687667	K+					
	271.0709667	270.0629667	H+	13	S-(Hydroxyphenylacetothiohydroximoyl)-L-cysteine	C11H14N2O4S	Amino acid	Glucosinolate and 2-oxocarboxylic acid biosynthesis and metabolism
				34	D-Lombricine	C6H15N4O6P	Amino acid	Glycine, serine and threonine metabolism
		248.0809667	Na+	7	5-Hydroxyindoleacetylglycine	C12H12N2O4	Amino acid	Tryptophan metabolism
		231.9709667	K+	20	2-Oxo-10-methylthiodecanoic acid	C11H20O3S	Fatty acid	Glucosinolate and 2-oxocarboxylic acid biosynthesis and metabolism
				6	gamma-Glutamyl-GABA	C9H16N2O5	Amino acid	Arginine and proline metabolism
				7	Mexicanin E	C14H16O3	Sesquiterpenoid	
				28	Cryptolepine	C16H12N2	Alkaloid	
				6	N6-Acetyl-LL-2,6-diaminoheptanedioate	C9H16N2O5	Amino acid	Amino acid and lysine biosynthesis
				6	N2-Succinyl-L-ornithine	C9H16N2O5	Amino acid	Arginine and proline metabolism
				6	N-alpha-Boc-L-asparagine	C9H16N2O5	Amino acid	
	270.9688333	269.9608333	H+					
		247.9788333	Na+					
		231.8688333	K+					
	271.0710667	270.0630667	H+	13	S-(Hydroxyphenylacetothiohydroximoyl)-L-cysteine	C11H14N2O4S	Amino acid	Glucosinolate and 2-oxocarboxylic acid biosynthesis and metabolism
				33	D-Lombricine	C6H15N4O6P	Amino acid	Glycine, serine and threonine metabolism
		248.0810667	Na+	7	5-Hydroxyindoleacetylglycine	C12H12N2O4	Amino acid	Tryptophan metabolism
		231.9710667	K+	19	2-Oxo-10-methylthiodecanoic acid	C11H20O3S	Fatty acid	Glucosinolate and 2-oxocarboxylic acid biosynthesis and metabolism
				7	gamma-Glutamyl-GABA	C9H16N2O5	Amino acid	Arginine and proline metabolism
				7	Mexicanin E	C14H16O3	Sesquiterpenoid	
				28	Cryptolepine	C16H12N2	Alkaloid	
				7	N6-Acetyl-LL-2,6-diaminoheptanedioate	C9H16N2O5	Amino acid	Amino acid and lysine biosynthesis
				7	N2-Succinyl-L-ornithine	C9H16N2O5	Amino acid	Arginine and proline metabolism
				7	N-alpha-Boc-L-asparagine	C9H16N2O5	Amino acid	

	270.9652333	269.9572333	H+					
		247.9752333	Na+					
		231.8652333	K+					
	271.0711667	270.0631667	H+	13	S-(Hydroxyphenylacetothiohydroximoyl)-L-cysteine	C11H14N2O4S	Amino acid	Glucosinolate and 2-oxocarboxylic acid biosynthesis and metabolism
				33	D-Lombricine	C6H15N4O6P	Amino acid	Glycine, serine and threonine metabolism
		248.0811667	Na+	8	5-Hydroxyindoleacetylglycine	C12H12N2O4	Amino acid	Tryptophan metabolism
		231.9711667	K+	19	2-Oxo-10-methylthiodecanoic acid	C11H20O3S	Fatty acid	Glucosinolate and 2-oxocarboxylic acid biosynthesis and metabolism
				7	gamma-Glutamyl-GABA	C9H16N2O5	Amino acid	Arginine and proline metabolism
				7	Mexicanin E	C14H16O3	Sesquiterpenoid	
				29	Cryptolepine	C16H12N2	Alkaloid	
				7	N6-Acetyl-LL-2,6-diaminoheptanedioate	C9H16N2O5	Amino acid	Amino acid and lysine biosynthesis
				7	N2-Succinyl-L-ornithine	C9H16N2O5	Amino acid	Arginine and proline metabolism
				7	N-alpha-Boc-L-asparagine	C9H16N2O5	Amino acid	
285	284.9950333	283.9870333	H+					
		262.0050333	Na+	17	(2E)-4-hydroxy-3-methylbut-2-en-1-yl trihydrogen diphosphate	C5H12O8P2	Terpenoid	Terpenoid, terpenoid backbone and steroid biosynthesis
		245.8950333	K+					
	285.0872333	284.0792333	H+	14	Xanthosine	C10H12N4O6	Nucleotide	Purine, caffeine and alkaloid biosynthesis
		262.0972333	Na+	32	Thiamine aldehyde	C12H15N4OS	Vitamin	Thiamine biosynthesis
		245.9872333	K+	8	2,4-Bis(acetamido)-2,4,6-trideoxy-beta-L-altropyranose	C10H18N2O5	Sugar	Amino acid and nucleotide sugar metabolism
				5	Zedoarol	C15H18O3	Sesquiterpenoid	
				5	Zederone	C15H18O3	Sesquiterpenoid	
				5	Isozaluzanin C	C15H18O3	Sesquiterpenoid	
				5	Zaluzanin C	C15H18O3	Sesquiterpenoid	
				5	Xerantholide	C15H18O3	Sesquiterpenoid	
				5	Xanthatin	C15H18O3	Sesquiterpenoid	
				5	beta-Santonin	C15H18O3	Sesquiterpenoid	
				5	7alpha-Hydroxydehydrocostus lactone	C15H18O3	Sesquiterpenoid	
				5	Leucodin	C15H18O3	Sesquiterpenoid	
				5	Aromaticin	C15H18O3	Sesquiterpenoid	
				5	Ambrosin	C15H18O3	Sesquiterpenoid	
				29	Olivacine	C17H14N2	Indole alkaloid	
				29	Ellipticine	C17H14N2	Indole alkaloid	
				30	L-N2-(2-Carboxyethyl)arginine	C9H18N4O4	Amino acid	Clavulanic acid biosynthesis
				30	D-Octopine	C9H18N4O4	Amino acid	Arginine and proline metabolism
				5	alpha-Santonin	C15H18O3	Sesquiterpenoid	
	284.9901	283.9821	H+					
		262.0001	Na+	0	(2E)-4-hydroxy-3-methylbut-2-en-1-yl trihydrogen diphosphate	C5H12O8P2	Terpenoid	Terpenoid, terpenoid backbone and steroid biosynthesis

		245.8901	K+					
	285.0873667	284.0793667	H+	15	Xanthosine	C10H12N4O6	Nucleotide	Purine, caffeine and alkaloid biosynthesis
		262.0973667	Na+	32	Thiamine aldehyde	C12H15N4OS	Vitamin	Thiamine biosynthesis
		245.9873667	K+	9	2,4-Bis(acetamido)-2,4,6-trideoxy-beta-L-altropyranose	C10H18N2O5	Sugar	Amino acid and nucleotide sugar metabolism
				4	Zedoarol	C15H18O3	Sesquiterpenoid	
				4	Zederone	C15H18O3	Sesquiterpenoid	
				4	Isozaluzanin C	C15H18O3	Sesquiterpenoid	
				4	Zaluzanin C	C15H18O3	Sesquiterpenoid	
				4	Xerantholide	C15H18O3	Sesquiterpenoid	
				4	Xanthatin	C15H18O3	Sesquiterpenoid	
				4	beta-Santonin	C15H18O3	Sesquiterpenoid	
				4	7alpha-Hydroxydehydrocostus lactone	C15H18O3	Sesquiterpenoid	
				4	Leucodin	C15H18O3	Sesquiterpenoid	
				4	Aromaticin	C15H18O3	Sesquiterpenoid	
				4	Ambrosin	C15H18O3	Sesquiterpenoid	
				29	Olivacine	C17H14N2	Indole alkaloid	
				29	Ellipticine	C17H14N2	Indole alkaloid	
				30	L-N2-(2-Carboxyethyl)arginine	C9H18N4O4	Amino acid	Clavulanic acid biosynthesis
				30	D-Octopine	C9H18N4O4	Amino acid	Arginine and proline metabolism
				4	alpha-Santonin	C15H18O3	Sesquiterpenoid	
	285.0874333	284.0794333	H+	15	Xanthosine	C10H12N4O6	Nucleotide	Purine, caffeine and alkaloid biosynthesis
		262.0974333	Na+	32	Thiamine aldehyde	C12H15N4OS	Vitamin	Thiamine biosynthesis
		245.9874333	K+	9	2,4-Bis(acetamido)-2,4,6-trideoxy-beta-L-altropyranose	C10H18N2O5	Sugar	Amino acid and nucleotide sugar metabolism
				4	Zedoarol	C15H18O3	Sesquiterpenoid	
				4	Zederone	C15H18O3	Sesquiterpenoid	
				4	Isozaluzanin C	C15H18O3	Sesquiterpenoid	
				4	Zaluzanin C	C15H18O3	Sesquiterpenoid	
				4	Xerantholide	C15H18O3	Sesquiterpenoid	
				4	Xanthatin	C15H18O3	Sesquiterpenoid	
				4	beta-Santonin	C15H18O3	Sesquiterpenoid	
				4	7alpha-Hydroxydehydrocostus lactone	C15H18O3	Sesquiterpenoid	
				4	Leucodin	C15H18O3	Sesquiterpenoid	
				4	Aromaticin	C15H18O3	Sesquiterpenoid	
				4	Ambrosin	C15H18O3	Sesquiterpenoid	
				30	Olivacine	C17H14N2	Indole alkaloid	
				30	Ellipticine	C17H14N2	Indole alkaloid	
				29	L-N2-(2-Carboxyethyl)arginine	C9H18N4O4	Amino acid	Clavulanic acid biosynthesis
				29	D-Octopine	C9H18N4O4	Amino acid	Arginine and proline metabolism
				4	alpha-Santonin	C15H18O3	Sesquiterpenoid	
365.2	365.1196667	364.1116667	H+					

		342.1296667	Na+	38	3-O-alpha-D-Mannopyranosyl-alpha-D-mannopyranose	C12H22O11	Disaccharide	
				38	Turanose	C12H22O11	Disaccharide	
				38	Melibiulose	C12H22O11	Disaccharide	
				38	Maltulose	C12H22O11	Disaccharide	
				38	Kojibiose	C12H22O11	Disaccharide	
				38	2-alpha-D-Glucosyl-D-glucose	C12H22O11	Disaccharide	
				38	Sophorose	C12H22O11	Disaccharide	
				38	Gentiobiose	C12H22O11	Disaccharide	
				38	Melibiose	C12H22O11	Disaccharide	Galactose metabolism
				38	Epimelibiose	C12H22O11	Disaccharide	Galactose metabolism
				38	alpha-D-Glucosyl-(1,3)-D-mannose	C12H22O11	Disaccharide	
				38	Laminaribiose	C12H22O11	Disaccharide	
				38	beta-Lactose	C12H22O11	Disaccharide	
				38	Palatinose	C12H22O11	Disaccharide	
				38	Levanbiose	C12H22O11	Disaccharide	Starch and sucrose metabolism
				38	Inulobiose	C12H22O11	Disaccharide	
				38	Nigerose	C12H22O11	Disaccharide	
				38	1-alpha-D-Galactosyl-myo-inositol	C12H22O11	Disaccharide	Galactose metabolism
				38	Trehalose	C12H22O11	Disaccharide	Starch and sucrose metabolism
				38	Isomaltose	C12H22O11	Disaccharide	Starch and sucrose metabolism
				38	Lactose	C12H22O11	Disaccharide	Galactose metabolism
				38	Maltose	C12H22O11	Disaccharide	Starch and sucrose metabolism
				38	Cellobiose	C12H22O11	Disaccharide	Starch and sucrose metabolism
				38	Sucrose	C12H22O11	Disaccharide	Galactose, starch and sucrose metabolism
				2	Coniferin	C16H22O8	Monolignol	Phenylpropanoid biosynthesis
		326.0196667	K+	12	Licarin A	C20H22O4	Neolignan	
				12	Dehydrodieugenol	C20H22O4	Neolignan	
				12	Uncinatone	C20H22O4	Terpenoid	
				12	Pulverochromenol	C20H22O4	Chromone	
				12	8-(3,3-Dimethylallyl)spatheliachromene	C20H22O4	Chromone	
				17	Caribine	C19H22N2O3	Isoquinoline alkaloid	
	365.1893	364.1813	H+	17	Cinncassiol C2	C20H28O6	Sesquiterpenoid	
				9	11-Methoxy-vinorine	C22H24N2O3	Indole alkaloid	
				17	Pycnolide	C20H28O6	Sesquiterpenoid	
				17	Eriolangin	C20H28O6	Sesquiterpenoid	
				17	Resiniferonol	C20H28O6	Diterpenoid	
				17	Phorbol	C20H28O6	Diterpenoid	
				17	Gibberellin A44 diacid	C20H28O6	Diterpenoid	
		342.1993	Na+					
		326.0893	K+					
	365.1198333	364.1118333	H+					
		342.1298333	Na+	39	3-O-alpha-D-Mannopyranosyl-alpha-D-mannopyranose	C12H22O11	Disaccharide	

				39	Turanose	C12H22O11	Disaccharide	
				39	Melibiulose	C12H22O11	Disaccharide	
				39	Maltulose	C12H22O11	Disaccharide	
				39	Kojibiose	C12H22O11	Disaccharide	
				39	2-alpha-D-Glucosyl-D-glucose	C12H22O11	Disaccharide	
				39	Sophorose	C12H22O11	Disaccharide	
				39	Gentiobiose	C12H22O11	Disaccharide	
				39	Melibiose	C12H22O11	Disaccharide	Galactose metabolism
				39	Epimelibiose	C12H22O11	Disaccharide	Galactose metabolism
				39	alpha-D-Glucosyl-(1,3)-D-mannose	C12H22O11	Disaccharide	
				39	Laminaribiose	C12H22O11	Disaccharide	
				39	beta-Lactose	C12H22O11	Disaccharide	
				39	Palatinose	C12H22O11	Disaccharide	
				39	Levanbiose	C12H22O11	Disaccharide	Starch and sucrose metabolism
				39	Inulobiose	C12H22O11	Disaccharide	
				39	Nigerose	C12H22O11	Disaccharide	
				39	1-alpha-D-Galactosyl-myo-inositol	C12H22O11	Disaccharide	Galactose metabolism
				39	Trehalose	C12H22O11	Disaccharide	Starch and sucrose metabolism
				39	Isomaltose	C12H22O11	Disaccharide	Starch and sucrose metabolism
				39	Lactose	C12H22O11	Disaccharide	Galactose metabolism
				39	Maltose	C12H22O11	Disaccharide	Starch and sucrose metabolism
				39	Cellobiose	C12H22O11	Disaccharide	Starch and sucrose metabolism
				39	Sucrose	C12H22O11	Disaccharide	Galactose, starch and sucrose metabolism
				2	Coniferin	C16H22O8	Monolignol	Phenylpropanoid biosynthesis
		326.0198333	K+	13	Licarin A	C20H22O4	Neolignan	
				13	Dehydrodieugenol	C20H22O4	Neolignan	
				13	Uncinatone	C20H22O4	Terpenoid	
				13	Pulverochromenol	C20H22O4	Chromone	
				13	8-(3,3-Dimethylallyl)spatheliachromene	C20H22O4	Chromone	
				17	Caribine	C19H22N2O3	Isoquinoline alkaloid	
	365.1917667	364.1837667	H+	11	Cinncassiol C2	C20H28O6	Sesquiterpenoid	
				15	11-Methoxy-vinorine	C22H24N2O3	Indole alkaloid	
				11	Pycnolide	C20H28O6	Sesquiterpenoid	
				11	Eriolangin	C20H28O6	Sesquiterpenoid	
				11	Resiniferonol	C20H28O6	Diterpenoid	
				11	Phorbol	C20H28O6	Diterpenoid	
				11	Gibberellin A44 diacid	C20H28O6	Diterpenoid	
		342.2017667	Na+					
		326.0917667	K+					
	365.1198667	364.1118667	H+					
		342.1298667	Na+	39	3-O-alpha-D-Mannopyranosyl-alpha-D-mannopyranose	C12H22O11	Disaccharide	
				39	Turanose	C12H22O11	Disaccharide	
				39	Melibiulose	C12H22O11	Disaccharide	

				39	Maltulose	C12H22O11	Disaccharide	
				39	Kojibiose	C12H22O11	Disaccharide	
				39	2-alpha-D-Glucosyl-D-glucose	C12H22O11	Disaccharide	
				39	Sophorose	C12H22O11	Disaccharide	
				39	Gentiobiose	C12H22O11	Disaccharide	
				39	Melibiose	C12H22O11	Disaccharide	Galactose metabolism
				39	Epimelibiose	C12H22O11	Disaccharide	Galactose metabolism
				39	alpha-D-Glucosyl-(1,3)-D-mannose	C12H22O11	Disaccharide	
				39	Laminaribiose	C12H22O11	Disaccharide	
				39	beta-Lactose	C12H22O11	Disaccharide	
				39	Palatinose	C12H22O11	Disaccharide	
				39	Levanbiose	C12H22O11	Disaccharide	Starch and sucrose metabolism
				39	Inulobiose	C12H22O11	Disaccharide	
				39	Nigerose	C12H22O11	Disaccharide	
				39	1-alpha-D-Galactosyl-myo-inositol	C12H22O11	Disaccharide	Galactose metabolism
				39	Trehalose	C12H22O11	Disaccharide	Starch and sucrose metabolism
				39	Isomaltose	C12H22O11	Disaccharide	Starch and sucrose metabolism
				39	Lactose	C12H22O11	Disaccharide	Galactose metabolism
				39	Maltose	C12H22O11	Disaccharide	Starch and sucrose metabolism
				39	Cellobiose	C12H22O11	Disaccharide	Starch and sucrose metabolism
				39	Sucrose	C12H22O11	Disaccharide	Galactose, starch and sucrose metabolism
				2	Coniferin	C16H22O8	Monolignol	Phenylpropanoid biosynthesis
		326.0198667	K+	13	Licarin A	C20H22O4	Neolignan	
				13	Dehydrodieugenol	C20H22O4	Neolignan	
				13	Uncinatone	C20H22O4	Terpenoid	
				13	Pulverochromenol	C20H22O4	Chromone	
				13	8-(3,3-Dimethylallyl)spatheliachromene	C20H22O4	Chromone	
				17	Caribine	C19H22N2O3	Isoquinoline alkaloid	
	365.1817667	364.1737667	H+	38	Cinncassiol C2	C20H28O6	Sesquiterpenoid	
				11	11-Methoxy-vinorine	C22H24N2O3	Indole alkaloid	
				38	Pycnolide	C20H28O6	Sesquiterpenoid	
				38	Eriolangin	C20H28O6	Sesquiterpenoid	
				38	Resiniferonol	C20H28O6	Diterpenoid	
				38	Phorbol	C20H28O6	Diterpenoid	
				38	Gibberellin A44 diacid	C20H28O6	Diterpenoid	
		342.1917667	Na+					
		326.0817667	K+					
257	256.9540333	255.9460333	H+					
		233.9640333	Na+					
		217.8540333	K+					
	257.039	256.031	H+	21	Purpurin	C14H8O5	Anthraquinone	
				21	Anthragallol	C14H8O5	Anthraquinone	
		234.049	Na+					
		217.939	K+					

	257.0907667	256.0827667	H+	38	Aloe emodin anthrone	C15H12O4	Anthraquinone	
				38	Pinocembrin chalcone	C15H12O4	Chalcone	Flavonoid biosynthesis
				38	3',5'-Dihydroxyflavanone	C15H12O4	Flavanone	
				38	Hydrangenol	C15H12O4	Stilbenoid	
				38	Pinocembrin	C15H12O4	Flavanone	Flavonoid biosynthesis
				38	Liquiritigenin	C15H12O4	Flavanone	Flavonoid, isoflavonoid and phenylpropanoid biosynthesis
				38	Isoliquiritigenin	C15H12O4	Chalcone	Flavonoid and phenylpropanoid biosynthesis
				38	3,9-Dihydroxypterocarpan	C15H12O4	Pterocarpan	Isoflavonoid biosynthesis
		234.1007667	Na+					
		217.9907667	K+					
	257.0376333	256.0296333	H+	26	Purpurin	C14H8O5	Anthraquinone	
				26	Anthragallol	C14H8O5	Anthraquinone	
		234.0476333	Na+					
		217.9376333	K+					
	257.0908667	256.0828667	H+	39	Aloe emodin anthrone	C15H12O4	Anthraquinone	
				39	Pinocembrin chalcone	C15H12O4	Chalcone	Flavonoid biosynthesis
				39	3',5'-Dihydroxyflavanone	C15H12O4	Flavanone	
				39	Hydrangenol	C15H12O4	Stilbenoid	
				39	Pinocembrin	C15H12O4	Flavanone	Flavonoid biosynthesis
				39	Liquiritigenin	C15H12O4	Flavanone	Flavonoid, isoflavonoid and phenylpropanoid biosynthesis
				39	Isoliquiritigenin	C15H12O4	Chalcone	Flavonoid and phenylpropanoid biosynthesis
				39	3,9-Dihydroxypterocarpan	C15H12O4	Pterocarpan	Isoflavonoid biosynthesis
		234.1008667	Na+					
		217.9908667	K+					
	256.9677333	255.9597333	H+					
		233.9777333	Na+					
		217.8677333	K+					
	257.0419333	256.0339333	H+	9	Purpurin	C14H8O5	Anthraquinone	
				9	Anthragallol	C14H8O5	Anthraquinone	
		234.0519333	Na+					
		217.9419333	K+					
	257.091	256.083	H+	39	Aloe emodin anthrone	C15H12O4	Anthraquinone	
				39	Pinocembrin chalcone	C15H12O4	Chalcone	Flavonoid biosynthesis
				39	3',5'-Dihydroxyflavanone	C15H12O4	Flavanone	
				39	Hydrangenol	C15H12O4	Stilbenoid	
				39	Pinocembrin	C15H12O4	Flavanone	Flavonoid biosynthesis
				39	Liquiritigenin	C15H12O4	Flavanone	Flavonoid, isoflavonoid and phenylpropanoid biosynthesis
				39	Isoliquiritigenin	C15H12O4	Chalcone	Flavonoid and phenylpropanoid biosynthesis
				39	3,9-Dihydroxypterocarpan	C15H12O4	Pterocarpan	Isoflavonoid biosynthesis
		234.101	Na+					

		217.991	K+					
555.2	555.1537	554.1457	H+	38	3-O-(6-O-alpha-D-Xylosylphospho-alpha-D-mannopyranosyl)-alpha-D-mannopyranose	C17H31O18P	Trisaccharide	
		532.1637	Na+	11	Flavonol 3-O-D-xylosylgalactoside	C26H28O12	Flavonol	
				11	Flavonol 3-O-D-xylosylglycoside	C26H28O12	Flavonol	
		516.0537	K+	21	Rottlerin	C30H28O8	Phloroglucinol	
				16	Spicatin	C27H32O10	Sesquiterpenoid	
				16	Harrisonin	C27H32O10	Triterpenoid	
	555.1536333	554.1456333	H+	38	3-O-(6-O-alpha-D-Xylosylphospho-alpha-D-mannopyranosyl)-alpha-D-mannopyranose	C17H31O18P	Trisaccharide	
		532.1636333	Na+	11	Flavonol 3-O-D-xylosylgalactoside	C26H28O12	Flavonol	
				11	Flavonol 3-O-D-xylosylglycoside	C26H28O12	Flavonol	
				11	Flavonol 3-O-D-xylosylglucoside	C26H28O12	Flavonol	
		516.0536333	K+	21	Rottlerin	C30H28O8	Phloroglucinol	
				16	Spicatin	C27H32O10	Sesquiterpenoid	
				16	Harrisonin	C27H32O10	Triterpenoid	
	555.1540333	554.1460333	H+	39	3-O-(6-O-alpha-D-Xylosylphospho-alpha-D-mannopyranosyl)-alpha-D-mannopyranose	C17H31O18P	Trisaccharide	
		532.1640333	Na+	12	Flavonol 3-O-D-xylosylgalactoside	C26H28O12	Flavonol	
				12	Flavonol 3-O-D-xylosylglycoside	C26H28O12	Flavonol	
				12	Flavonol 3-O-D-xylosylglucoside	C26H28O12	Flavonol	
		516.0540333	K+	22	Rottlerin	C30H28O8	Phloroglucinol	
				15	Spicatin	C27H32O10	Sesquiterpenoid	
				15	Harrisonin	C27H32O10	Triterpenoid	
255	254.9470667	253.9390667	H+					
		231.9570667	Na+					
		215.8470667	K+					
	255.0754667	254.0674667	H+	16	S-(Phenylacetothiohydroximoyl)-L-cysteine	C11H14N2O3S	Amino acid	Glucosinolate and 2-oxocarboxylic acid biosynthesis and metabolism
		232.0854667	Na+					
		215.9754667	K+	5	gamma-Glutamyl-gamma-aminobutyraldehyde	C9H16N2O4	Amino acid	Arginine and proline metabolism
	254.9829	253.9749	H+					
		231.9929	Na+					
		215.8829	K+					
	255.0759667	254.0679667	H+	14	S-(Phenylacetothiohydroximoyl)-L-cysteine	C11H14N2O3S	Amino acid	Glucosinolate and 2-oxocarboxylic acid biosynthesis and metabolism
				36	L-Arginine phosphate	C6H15N4O5P	Amino acid	Arginine and proline metabolism
		232.0859667	Na+					
		215.9759667	K+	7	gamma-Glutamyl-gamma-aminobutyraldehyde	C9H16N2O4	Amino acid	Arginine and proline metabolism
	254.9448667	253.9368667	H+					
		231.9548667	Na+					

		215.8448667	K+					
	255.0756	254.0676	H+	16	S-(Phenylacetothiohydroximoyl)-L-cysteine	C11H14N2O3S	Amino acid	Glucosinolate and 2-oxocarboxylic acid biosynthesis and metabolism
				37	L-Arginine phosphate	C6H15N4O5P	Amino acid	Arginine and proline metabolism
		232.0856	Na+					
		215.9756	K+	5	gamma-Glutamyl-gamma-aminobutyraldehyde	C9H16N2O4	Amino acid	Arginine and proline metabolism
269	268.9792	267.9712	H+					
		245.9892	Na+					
		229.8792	K+	11	D-Xylose-5-phosphate	C5H11O8P	Sugar	
				11	L-Xylulose 1-phosphate	C5H11O8P	Sugar	Pentose and glucuronate interconversions
				11	beta-L-Arabinose 1-phosphate	C5H11O8P	Sugar	Amino acid and nucleotide sugar metabolism
				11	alpha-D-Xylose 1-phosphate	C5H11O8P	Sugar	
				11	D-Arabinose 5-phosphate	C5H11O8P	Sugar	
				11	L-Ribulose 5-phosphate	C5H11O8P	Sugar	Ascorbate and aldarate metabolism; pentose and glucuronate interconversions
				11	Ribose 1-phosphate	C5H11O8P	Sugar	Pentose phosphate pathway; purine metabolism
				11	D-Xylulose 5-phosphate	C5H11O8P	Sugar	Lots
				11	D-Ribulose 5-phosphate	C5H11O8P	Sugar	Lots
				11	Ribose 5-phosphate	C5H11O8P	Sugar	Lots
	269.0912333	268.0832333	H+	38	6-Hydroxy-2'-methoxyflavone	C16H12O4	Flavone	
				38	Isoformononetin	C16H12O4	Isoflavone	Isoflavonoid and phenylpropanoid biosynthesis
				38	Tectochrysin	C16H12O4	Flavone	
				3	Saphenic acid	C15H12N2O3	Alkaloid	
				16	2-O-(alpha-D-Mannosyl)-D-glycerate	C9H16O9	Sugar	Fructose and mannose metabolism
				38	Dalbergin	C16H12O4	Neoflavonoid	
				38	Formononetin	C16H12O4	Isoflavone	Isoflavonoid and phenylpropanoid biosynthesis
		246.1012333	Na+					
		229.9912333	K+	9	Isodehydrocostus lactone	C15H18O2	Sesquiterpenoid	
				9	Linderenol	C15H18O2	Sesquiterpenoid	
				9	Furanodienone	C15H18O2	Sesquiterpenoid	
				9	Dehydromyodesmone	C15H18O2	Sesquiterpenoid	
				9	Eremanthin	C15H18O2	Sesquiterpenoid	
				9	Dehydrocostus lactone	C15H18O2	Sesquiterpenoid	
	268.9736333	267.9656333	H+					
		245.9836333	Na+					
		229.8736333	K+	32	D-Xylose-5-phosphate	C5H11O8P	Sugar	
				32	L-Xylulose 1-phosphate	C5H11O8P	Sugar	Pentose and glucuronate interconversions
				32	beta-L-Arabinose 1-phosphate	C5H11O8P	Sugar	Amino acid and nucleotide sugar metabolism

				32	alpha-D-Xylose 1-phosphate	C5H11O8P	Sugar	
				32	D-Arabinose 5-phosphate	C5H11O8P	Sugar	
				32	L-Ribulose 5-phosphate	C5H11O8P	Sugar	Ascorbate and aldarate metabolism; pentose and glucuronate interconversions
				32	Ribose 1-phosphate	C5H11O8P	Sugar	Pentose phosphate pathway; purine metabolism
				32	D-Xylulose 5-phosphate	C5H11O8P	Sugar	Lots
				32	D-Ribulose 5-phosphate	C5H11O8P	Sugar	Lots
				32	Ribose 5-phosphate	C5H11O8P	Sugar	Lots
	269.0912667	268.0832667	H+	38	6-Hydroxy-2'-methoxyflavone	C16H12O4	Flavone	
				38	Isoformononetin	C16H12O4	Isoflavone	Isoflavonoid and phenylpropanoid biosynthesis
				38	Tectochrysin	C16H12O4	Flavone	
				2	Saphenic acid	C15H12N2O3	Alkaloid	
				16	2-O-(alpha-D-Mannosyl)-D-glycerate	C9H16O9	Sugar	Fructose and mannose metabolism
				38	Dalbergin	C16H12O4	Neoflavonoid	
				38	Formononetin	C16H12O4	Isoflavone	Isoflavonoid and phenylpropanoid biosynthesis
		246.1012667	Na+					
		229.9912667	K+	9	Isodehydrocostus lactone	C15H18O2	Sesquiterpenoid	
				9	Linderenol	C15H18O2	Sesquiterpenoid	
				9	Furanodienone	C15H18O2	Sesquiterpenoid	
				9	Dehydromyodesmone	C15H18O2	Sesquiterpenoid	
				9	Eremanthin	C15H18O2	Sesquiterpenoid	
				9	Dehydrocostus lactone	C15H18O2	Sesquiterpenoid	
	268.9803333	267.9723333	H+					
		245.9903333	Na+					
		229.8803333	K+	7	D-Xylose-5-phosphate	C5H11O8P	Sugar	
				7	L-Xylulose 1-phosphate	C5H11O8P	Sugar	Pentose and glucuronate interconversions
				7	beta-L-Arabinose 1-phosphate	C5H11O8P	Sugar	Amino acid and nucleotide sugar metabolism
				7	alpha-D-Xylose 1-phosphate	C5H11O8P	Sugar	
				7	D-Arabinose 5-phosphate	C5H11O8P	Sugar	
				7	L-Ribulose 5-phosphate	C5H11O8P	Sugar	Ascorbate and aldarate metabolism; pentose and glucuronate interconversions
				7	Ribose 1-phosphate	C5H11O8P	Sugar	Pentose phosphate pathway; purine metabolism
				7	D-Xylulose 5-phosphate	C5H11O8P	Sugar	Lots
				7	D-Ribulose 5-phosphate	C5H11O8P	Sugar	Lots
				7	Ribose 5-phosphate	C5H11O8P	Sugar	Lots
	269.0913	268.0833	H+	38	6-Hydroxy-2'-methoxyflavone	C16H12O4	Flavone	
				38	Isoformononetin	C16H12O4	Isoflavone	Isoflavonoid and phenylpropanoid biosynthesis
				38	Tectochrysin	C16H12O4	Flavone	

				2	Saphenic acid	C15H12N2O3	Alkaloid	
				17	2-O-(alpha-D-Mannosyl)-D-glycerate	C9H16O9	Sugar	Fructose and mannose metabolism
				38	Dalbergin	C16H12O4	Neoflavonoid	
				38	Formononetin	C16H12O4	Isoflavone	Isoflavonoid and phenylpropanoid biosynthesis
		246.1013	Na+					
		229.9913	K+	9	Isodehydrocostus lactone	C15H18O2	Sesquiterpenoid	
				9	Linderenol	C15H18O2	Sesquiterpenoid	
				9	Furanodienone	C15H18O2	Sesquiterpenoid	
				9	Dehydromyodesmone	C15H18O2	Sesquiterpenoid	
				9	Eremanthin	C15H18O2	Sesquiterpenoid	
				9	Dehydrocostus lactone	C15H18O2	Sesquiterpenoid	
541.2	541.1403667	540.1323667	H+					
		518.1503667	Na+	16	Medicarpin 3-O-glucoside-6'-malonate	C25H26O12	Pterocarpan	Isoflavonoid biosynthesis
		502.0403667	K+					
	541.1403333	540.1323333	H+					
		518.1503333	Na+	16	Medicarpin 3-O-glucoside-6'-malonate	C25H26O12	Pterocarpan	Isoflavonoid biosynthesis
		502.0403333	K+					
	541.1411	540.1331	H+					
		518.1511	Na+	17	Medicarpin 3-O-glucoside-6'-malonate	C25H26O12	Pterocarpan	Isoflavonoid biosynthesis
		502.0411	K+					
309	308.9214667	307.9134667	H+					
		285.9314667	Na+					
		269.8214667	K+					
	309.0199667	308.0119667	H+					
		286.0299667	Na+					
		269.9199667	K+	34	S-(Hydroxyphenylacetothiohydroximoyl)-L-cysteine	C11H14N2O4S	Amino acid	Glucosinolate and 2-oxocarboxcylic acid biosynthesis
				12	Islandicin	C15H10O5	Anthraquinone	
				12	3,6,4'-Trihydroxyflavone	C15H10O5	Flavone	
				12	6-Hydroxydaidzein	C15H10O5	Isoflavone	Isoflavonoid biosynthesis
				12	3',4',7-Trihydroxyisoflavone	C15H10O5	Isoflavone	
				12	Purpurin 1-methyl ether	C15H10O5	Anthraquinone	
				12	2-Hydroxychrysophanol	C15H10O5	Anthraquinone	
				12	Morindone	C15H10O5	Anthraquinone	
				12	Lucidin	C15H10O5	Anthraquinone	
				12	Emodin	C15H10O5	Anthraquinone	
				12	Aloe-emodin	C15H10O5	Anthraquinone	
				12	Norwogonin	C15H10O5	Flavone	
				12	Galangin	C15H10O5	Flavone	Flavonoid biosynthesis
				12	5-Deoxykaempferol	C15H10O5	Flavone	
				12	Baicalein	C15H10O5	Flavone	
				12	Sulphuretin	C15H10O5	Aurone	

				12	Apigenin	C15H10O5	Flavone	Flavonoid, isoflavonoid, flavone, flavonol and phenylpropanoid biosynthesis
				12	2'-Hydroxydaidzein	C15H10O5	Isoflavone	Isoflavonoid biosynthesis
				12	Genistein	C15H10O5	Isoflavone	Isoflavonoid and phenylpropanoid biosynthesis
	309.0889333	308.0809333	H+	25	Allamandin	C15H16O7	Iridoid	
		286.0989333	Na+	17	Gastrodin	C13H18O7	Phenolic acid	
				17	Methylarbutin	C13H18O7	Phenolic acid	
				17	Salicin	C13H18O7	Phenolic acid	Glycolysis and phenylpropanoid biosynthesis
		269.9889333	K+					
	309.0198333	308.0118333	H+					
		286.0298333	Na+					
		269.9198333	K+	34	S-(Hydroxyphenylacetothiohydroximoyl)-L-cysteine	C11H14N2O4S	Amino acid	Glucosinolate and 2-oxocarboxcylic acid biosynthesis
				12	Islandicin	C15H10O5	Anthraquinone	
				12	3,6,4'-Trihydroxyflavone	C15H10O5	Flavone	
				12	6-Hydroxydaidzein	C15H10O5	Isoflavone	Isoflavonoid biosynthesis
				12	3',4',7-Trihydroxyisoflavone	C15H10O5	Isoflavone	
				12	Purpurin 1-methyl ether	C15H10O5	Anthraquinone	
				12	2-Hydroxychrysophanol	C15H10O5	Anthraquinone	
				12	Morindone	C15H10O5	Anthraquinone	
				12	Lucidin	C15H10O5	Anthraquinone	
				12	Emodin	C15H10O5	Anthraquinone	
				12	Aloe-emodin	C15H10O5	Anthraquinone	
				12	Norwogonin	C15H10O5	Flavone	
				12	Galangin	C15H10O5	Flavone	Flavonoid biosynthesis
				12	5-Deoxykaempferol	C15H10O5	Flavone	
				12	Baicalein	C15H10O5	Flavone	
				12	Sulphuretin	C15H10O5	Aurone	
				12	Apigenin	C15H10O5	Flavone	Flavonoid, isoflavonoid, flavone, flavonol and phenylpropanoid biosynthesis
				12	2'-Hydroxydaidzein	C15H10O5	Isoflavone	Isoflavonoid biosynthesis
				12	Genistein	C15H10O5	Isoflavone	Isoflavonoid and phenylpropanoid biosynthesis
	309.0890667	308.0810667	H+	25	Allamandin	C15H16O7	Iridoid	
		286.0990667	Na+	17	Gastrodin	C13H18O7	Phenolic acid	
				17	Methylarbutin	C13H18O7	Phenolic acid	
				17	Salicin	C13H18O7	Phenolic acid	Glycolysis and phenylpropanoid biosynthesis
		269.9890667	K+					
	309.0191667	308.0111667	H+					
		286.0291667	Na+					

		269.9191667	K+	36	S-(Hydroxyphenylacetothiohydroximoyl)-L-cysteine	C11H14N2O4S	Amino acid	Glucosinolate and 2-oxocarboxcylic acid biosynthesis
				10	Islandicin	C15H10O5	Anthraquinone	
				10	3,6,4'-Trihydroxyflavone	C15H10O5	Flavone	
				10	6-Hydroxydaidzein	C15H10O5	Isoflavone	Isoflavonoid biosynthesis
				10	3',4',7-Trihydroxyisoflavone	C15H10O5	Isoflavone	
				10	Purpurin 1-methyl ether	C15H10O5	Anthraquinone	
				10	2-Hydroxychrysophanol	C15H10O5	Anthraquinone	
				10	Morindone	C15H10O5	Anthraquinone	
				10	Lucidin	C15H10O5	Anthraquinone	
				10	Emodin	C15H10O5	Anthraquinone	
				10	Aloe-emodin	C15H10O5	Anthraquinone	
				10	Norwogonin	C15H10O5	Flavone	
				10	Galangin	C15H10O5	Flavone	Flavonoid biosynthesis
				10	5-Deoxykaempferol	C15H10O5	Flavone	
				10	Baicalein	C15H10O5	Flavone	
				10	Sulphuretin	C15H10O5	Aurone	
				10	Apigenin	C15H10O5	Flavone	Flavonoid, isoflavonoid, flavone, flavonol and phenylpropanoid biosynthesis
				10	2'-Hydroxydaidzein	C15H10O5	Isoflavone	Isoflavonoid biosynthesis
				10	Genistein	C15H10O5	Isoflavone	Isoflavonoid and phenylpropanoid biosynthesis
	309.0892667	308.0812667	H+					
		286.0992667	Na+	24	Allamandin	C15H16O7	Iridoid	
				16	Gastrodin	C13H18O7	Phenolic acid	
				16	Methylarbutin	C13H18O7	Phenolic acid	
				16	Salicin	C13H18O7	Phenolic acid	Glycolysis and phenylpropanoid biosynthesis
		269.9892667	K+					
272	271.9188333	270.9108333	H+					
		248.9288333	Na+					
		232.8188333	K+					
	272.0746667	271.0666667	H+					
		249.0846667	Na+	0	S-Acetyldihydrolipoamide-E	C10H18NO2S2	Amino acid	Glycolysis, TCA cycle, pyruvate metabolism
				23	Dubamine	C16H11NO2	Quinoline alkaloid	
		232.9746667	K+	3	N(omega)-Nitro-L-arginine methyl ester	C7H15N5O4	Amino acid	
	271.9113667	270.9033667	H+					
		248.9213667	Na+					
		232.8113667	K+					
	272.0753	271.0673	H+					
		249.0853	Na+	1	S-Acetyldihydrolipoamide-E	C10H18NO2S2	Amino acid	Glycolysis, TCA cycle, pyruvate metabolism

				26	Dubamine	C16H11NO2	Quinoline alkaloid	
		232.9753	K+	0	N(omega)-Nitro-L-arginine methyl ester	C7H15N5O4	Amino acid	
	272.0746	271.0666	H+					
		249.0846	Na+	1	S-Acetyldihydrolipoamide-E	C10H18NO2S2	Amino acid	Glycolysis, TCA cycle, pyruvate metabolism
				23	Dubamine	C16H11NO2	Quinoline alkaloid	
		232.9746	K+	3	N(omega)-Nitro-L-arginine methyl ester	C7H15N5O4	Amino acid	
569.2	569.1672667	568.1592667	H+					
		546.1772667	Na+	7	Flavonol 3-O-rutinoside	C27H30O12	Flavonol	
		530.0672667	K+	39	Strictosidine	C27H34N2O9	Indole alkaloid	Indole and shikimate pathway alkaloid biosynthesis
	569.1668333	568.1588333	H+					
		546.1768333	Na+	6	Flavonol 3-O-rutinoside	C27H30O12	Flavonol	
		530.0668333	K+	39	Strictosidine	C27H34N2O9	Indole alkaloid	Indole and shikimate pathway alkaloid biosynthesis
	569.1664667	568.1584667	H+					
		546.1764667	Na+	6	Flavonol 3-O-rutinoside	C27H30O12	Flavonol	
		530.0664667	K+					
286	286.0898667	285.0818667	H+	7	Buchananine	C12H15NO7	Piperadine alkaloid	
		263.0998667	Na+					
		246.9898667	K+	20	Fagaramide	C14H17NO3	Phenolic amide	
	286.0903333	285.0823333	H+	6	Buchananine	C12H15NO7	Piperadine alkaloid	
		263.1003333	Na+					
		246.9903333	K+	22	Fagaramide	C14H17NO3	Phenolic amide	
	285.9340667	284.9260667	H+					
		262.9440667	Na+					
		246.8340667	K+					
	286.0897	285.0817	H+	8	Buchananine	C12H15NO7	Piperadine alkaloid	
		263.0997	Na+					
		246.9897	K+	19	Fagaramide	C14H17NO3	Phenolic amide	
556.2	556.1571667	555.1491667	H+					
		533.1671667	Na+					
		517.0571667	K+					
	556.1573	555.1493	H+					
		533.1673	Na+					
		517.0573	K+					
	556.1569333	555.1489333	H+					
		533.1669333	Na+					
		517.0569333	K+					
297	296.9434333	295.9354333	H+					
		273.9534333	Na+					
		257.8434333	K+					
	297.0829667	296.0749667	H+					
		274.0929667	Na+	32	5-Deoxyleucopelargonidin	C15H14O5	Flavan-3,4-diol	Flavonoid biosynthesis

				32	5,8-Diethoxypsoralen	C15H14O5	Psolaren	
				32	(-)-Epiafzelechin	C15H14O5	Flavan-3-ol	Flavonoid biosynthesis
				32	Apiforol	C15H14O5	Flavan-4-ol	Flavonoid biosynthesis
				32	Luteoliflavan	C15H14O5	Flavan	
				32	Methysticin	C15H14O5	Pyrone	
				32	Afzelechin	C15H14O5	Flavan-3-ol	Flavonoid biosynthesis
				32	Ptaerochromenol	C15H14O5	Chromone	
				32	beta-Pyrufuran	C15H14O5	Dibenzofuran	
				32	alpha-Pyrufuran	C15H14O5	Dibenzofuran	
				32	Phloretin	C15H14O5	Dihydrochalcone	Flavonoid biosynthesis
		257.9829667	K+	19	Dihydroechinofuran	C16H18O3	Benzoquinone	Ubiquinone and terpenoid biosynthesis
				19	3'-O-Methylbatatasin III	C16H18O3	Stilbenoid	
				19	Heritonin	C16H18O3	Sesquiterpenoid	
	296.9382	295.9302	H+					
		273.9482	Na+					
		257.8382	K+					
	297.0797	296.0717	H+					
		274.0897	Na+	21	5-Deoxyleucopelargonidin	C15H14O5	Flavan-3,4-diol	Flavonoid biosynthesis
				21	5,8-Diethoxypsoralen	C15H14O5	Psolaren	
				21	(-)-Epiafzelechin	C15H14O5	Flavan-3-ol	Flavonoid biosynthesis
				21	Apiforol	C15H14O5	Flavan-4-ol	Flavonoid biosynthesis
				21	Luteoliflavan	C15H14O5	Flavan	
				21	Methysticin	C15H14O5	Pyrone	
				21	Afzelechin	C15H14O5	Flavan-3-ol	Flavonoid biosynthesis
				21	Ptaerochromenol	C15H14O5	Chromone	
				21	beta-Pyrufuran	C15H14O5	Dibenzofuran	
				21	alpha-Pyrufuran	C15H14O5	Dibenzofuran	
				21	Phloretin	C15H14O5	Dihydrochalcone	Flavonoid biosynthesis
		257.9797	K+	30	Dihydroechinofuran	C16H18O3	Benzoquinone	Ubiquinone and terpenoid biosynthesis
				30	3'-O-Methylbatatasin III	C16H18O3	Stilbenoid	
				30	Heritonin	C16H18O3	Sesquiterpenoid	
	297.0834667	296.0754667	H+					
		274.0934667	Na+	34	5-Deoxyleucopelargonidin	C15H14O5	Flavan-3,4-diol	Flavonoid biosynthesis
				34	5,8-Diethoxypsoralen	C15H14O5	Psolaren	
				34	(-)-Epiafzelechin	C15H14O5	Flavan-3-ol	Flavonoid biosynthesis
				34	Apiforol	C15H14O5	Flavan-4-ol	Flavonoid biosynthesis
				34	Luteoliflavan	C15H14O5	Flavan	
				34	Methysticin	C15H14O5	Pyrone	
				34	Afzelechin	C15H14O5	Flavan-3-ol	Flavonoid biosynthesis
				34	Ptaerochromenol	C15H14O5	Chromone	
				34	beta-Pyrufuran	C15H14O5	Dibenzofuran	
				34	alpha-Pyrufuran	C15H14O5	Dibenzofuran	
				34	Phloretin	C15H14O5	Dihydrochalcone	Flavonoid biosynthesis

		257.9834667	K+	17	Dihydroechinofuran	C16H18O3	Benzoquinone	Ubiquinone and terpenoid biosynthesis
				17	3'-O-Methylbatatasin III	C16H18O3	Stilbenoid	
				17	Heritonin	C16H18O3	Sesquiterpenoid	
587.2	587.1727333	586.1647333	H+	5	Phyllanthostatin A	C29H30O13	Lignan	
				5	Amarogentin	C29H30O13	Iridoid	
		564.1827333	Na+	1	Aloinoside B	C27H32O13	Anthraquinone	
				1	Aloinoside A	C27H32O13	Anthraquinone	
				1	Cascaroside C	C27H32O13	Anthraquinone	
				1	Cascaroside D	C27H32O13	Anthraquinone	
				1	Pinocembrin 7-rhamnosylglucoside	C27H32O13	Flavanone	
				1	Naringenin 5,7-dimethyl ether 4'-O-xylosyl-(1->4)-arabinoside	C27H32O13	Flavanone	
				1	Isoliquiritigenin 2'-glucosyl-(1->4)-rhamnoside	C27H32O13	Chalcone	
		548.0727333	K+	34	Flavanone 7-O-[alpha-L-rhamnosyl-(1->2)-beta-D-glucoside]	C27H32O12	Flavanone	
				27	Bruceantin	C28H36O11	Triterpenoid	
	587.1773	586.1693	H+	2	Phyllanthostatin A	C29H30O13	Lignan	
				2	Amarogentin	C29H30O13	Iridoid	
		564.1873	Na+	6	Aloinoside B	C27H32O13	Anthraquinone	
				6	Aloinoside A	C27H32O13	Anthraquinone	
				6	Cascaroside C	C27H32O13	Anthraquinone	
				6	Cascaroside D	C27H32O13	Anthraquinone	
				6	Pinocembrin 7-rhamnosylglucoside	C27H32O13	Flavanone	
				6	Naringenin 5,7-dimethyl ether 4'-O-xylosyl-(1->4)-arabinoside	C27H32O13	Flavanone	
				6	Isoliquiritigenin 2'-glucosyl-(1->4)-rhamnoside	C27H32O13	Chalcone	
		548.0773	K+	19	Bruceantin	C28H36O11	Triterpenoid	
	587.1732667	586.1652667	H+	4	Phyllanthostatin A	C29H30O13	Lignan	
				4	Amarogentin	C29H30O13	Iridoid	
		564.1832667	Na+	0	Aloinoside B	C27H32O13	Anthraquinone	
				0	Aloinoside A	C27H32O13	Anthraquinone	
				0	Cascaroside C	C27H32O13	Anthraquinone	
				0	Cascaroside D	C27H32O13	Anthraquinone	
				0	Pinocembrin 7-rhamnosylglucoside	C27H32O13	Flavanone	
				0	Naringenin 5,7-dimethyl ether 4'-O-xylosyl-(1->4)-arabinoside	C27H32O13	Flavanone	
				0	Isoliquiritigenin 2'-glucosyl-(1->4)-rhamnoside	C27H32O13	Chalcone	
		548.0732667	K+	35	Flavanone 7-O-[alpha-L-rhamnosyl-(1->2)-beta-D-glucoside]	C27H32O12	Flavanone	
				26	Bruceantin	C28H36O11	Triterpenoid	
539.2	539.1553667	538.1473667	H+					
		516.1653667	Na+	22	Rottlerin	C30H28O8	Phloroglucinol	

		500.0553667	K+					
	539.1551333	538.1471333	H+					
		516.1651333	Na+	23	Rottlerin	C30H28O8	Phloroglucinol	
		500.0551333	K+					
	539.1552333	538.1472333	H+					
		516.1652333	Na+	23	Rottlerin	C30H28O8	Phloroglucinol	
		500.0552333	K+					
273	272.9793	271.9713	H+					
		249.9893	Na+					
		233.8793	K+					
	273.0860667	272.0780667	H+	37	Toralactone	C15H12O5	Napthopyranone	
				37	6,7,4'-Trihydroxyflavanone	C15H12O5	Flavanone	Isoflavonoid biosynthesis
				37	2,7,4'-Trihydroxyisoflavanone	C15H12O5	Isoflavanone	Isoflavonoid biosynthesis
				37	Dihydrogenistein	C15H12O5	Flavanone	
				37	p-Coumaroyltriacetic acid lactone	C15H12O5	Phenolic acid	
				37	Pinobanksin	C15H12O5	Flavanone	Flavonoid biosynthesis
				37	Garbanzol	C15H12O5	Flavanone	Flavonoid biosynthesis
				37	Butin	C15H12O5	Flavanone	Flavonoid biosynthesis
				37	Rubrofusarin	C15H12O5	Napthopyranone	
				37	Butein	C15H12O5	Chalcone	Flavonoid biosynthesis
				37	Naringenin chalcone	C15H12O5	Chalcone	Flavonoid and phenylpropanoid biosynthesis
				37	2'-Hydroxydihydrodaidzein	C15H12O5	Isoflavanone	Isoflavonoid biosynthesis
				37	Licodione	C15H12O5	Chalcone	
				37	(-)-Glycinol	C15H12O5	Pterocarpan	Isoflavonoid biosynthesis
				37	Naringenin	C15H12O5	Flavanone	Flavonoid, isoflavonoid and phenylpropanoid biosynthesis
		250.0960667	Na+	34	3-(5'-Methylthio)pentylmalic acid	C10H18O5S	Amino acid	Glucosinolate and 2-oxocarboxylic acid biosynthesis and metabolism
				34	2-(5'-Methylthio)pentylmalic acid	C10H18O5S	Amino acid	Glucosinolate and 2-oxocarboxylic acid biosynthesis and metabolism
		233.9860667	K+	9	Flindersiachromone	C17H14O2	Sesquiterpenoid	
				9	Strigolactone ABC-rings	C14H18O3	Phytohormone	Carotenoid biosynthesis
	273.0859	272.0779	H+	37	Toralactone	C15H12O5	Napthopyranone	
				37	6,7,4'-Trihydroxyflavanone	C15H12O5	Flavanone	Isoflavonoid biosynthesis
				37	2,7,4'-Trihydroxyisoflavanone	C15H12O5	Isoflavanone	Isoflavonoid biosynthesis
				37	Dihydrogenistein	C15H12O5	Flavanone	
				37	p-Coumaroyltriacetic acid lactone	C15H12O5	Phenolic acid	
				37	Pinobanksin	C15H12O5	Flavanone	Flavonoid biosynthesis
				37	Garbanzol	C15H12O5	Flavanone	Flavonoid biosynthesis
				37	Butin	C15H12O5	Flavanone	Flavonoid biosynthesis
				37	Rubrofusarin	C15H12O5	Napthopyranone	
				37	Butein	C15H12O5	Chalcone	Flavonoid biosynthesis
				37	Naringenin chalcone	C15H12O5	Chalcone	Flavonoid and phenylpropanoid biosynthesis
				37	2'-Hydroxydihydrodaidzein	C15H12O5	Isoflavanone	Isoflavonoid biosynthesis

				37	Licodione	C15H12O5	Chalcone	
				37	(-)-Glycinol	C15H12O5	Pterocarpan	Isoflavonoid biosynthesis
				37	Naringenin	C15H12O5	Flavanone	Flavonoid, isoflavonoid and phenylpropanoid biosynthesis
		250.0959	Na+	33	3-(5'-Methylthio)pentylmalic acid	C10H18O5S	Amino acid	Glucosinolate and 2-oxocarboxylic acid biosynthesis and metabolism
				33	2-(5'-Methylthio)pentylmalic acid	C10H18O5S	Amino acid	Glucosinolate and 2-oxocarboxylic acid biosynthesis and metabolism
		233.9859	K+	9	Flindersiachromone	C17H14O2	Sesquiterpenoid	
				9	Strigolactone ABC-rings	C14H18O3	Phytohormone	Carotenoid biosynthesis
	272.9747333	271.9667333	H+					
		249.9847333	Na+					
		233.8747333	K+					
	273.085	272.077	H+	33	Toralactone	C15H12O5	Napthopyranone	
		250.095	Na+	33	6,7,4'-Trihydroxyflavanone	C15H12O5	Flavanone	Isoflavonoid biosynthesis
		233.985	K+	33	2,7,4'-Trihydroxyisoflavanone	C15H12O5	Isoflavanone	Isoflavonoid biosynthesis
				33	Dihydrogenistein	C15H12O5	Flavanone	
				33	p-Coumaroyltriacetic acid lactone	C15H12O5	Phenolic acid	
				33	Pinobanksin	C15H12O5	Flavanone	Flavonoid biosynthesis
				33	Garbanzol	C15H12O5	Flavanone	Flavonoid biosynthesis
				33	Butin	C15H12O5	Flavanone	Flavonoid biosynthesis
				33	Rubrofusarin	C15H12O5	Napthopyranone	
				33	Butein	C15H12O5	Chalcone	Flavonoid biosynthesis
				33	Naringenin chalcone	C15H12O5	Chalcone	Flavonoid and phenylpropanoid biosynthesis
				33	2'-Hydroxydihydrodaidzein	C15H12O5	Isoflavanone	Isoflavonoid biosynthesis
				33	Licodione	C15H12O5	Chalcone	
				33	(-)-Glycinol	C15H12O5	Pterocarpan	Isoflavonoid biosynthesis
				33	Naringenin	C15H12O5	Flavanone	Flavonoid, isoflavonoid and phenylpropanoid biosynthesis
				30	3-(5'-Methylthio)pentylmalic acid	C10H18O5S	Amino acid	Glucosinolate and 2-oxocarboxylic acid biosynthesis and metabolism
				30	2-(5'-Methylthio)pentylmalic acid	C10H18O5S	Amino acid	Glucosinolate and 2-oxocarboxylic acid biosynthesis and metabolism
				13	Flindersiachromone	C17H14O2	Sesquiterpenoid	
				13	Strigolactone ABC-rings	C14H18O3	Phytohormone	Carotenoid biosynthesis

Table B3.6 Liberty sorghum polyphenol extract putative identifications from OPLS-DA (ESI [+])

Bin	Detected Mass	Accurate Mass	Adduct	Δppm	Name	Formula	Chemical Group	Pathway
365.2	365.1208667	364.1128667	H+					
		342.1308667	Na+	0	Coniferin	C16H22O8	Monolignol	Phenylpropanoid biosynthesis
		326.0208667	K+	16	Licarin A	C20H22O4	Neolignan	
				16	Dehydrodieugenol	C20H22O4	Neolignan	

				16	Uncinatone	C20H22O4	Terpenoid	
				16	Pulverochromenol	C20H22O4	Chromone	
				16	8-(3,3-Dimethylallyl)spatheliachromene	C20H22O4	Chromone	
				14	Caribine	C19H22N2O3	Isoquinoline alkaloid	
	365.1837667	364.1757667	H+	33	Cinncassiol C2	C20H28O6	Sesquiterpenoid	
				11	11-Methoxy-vinorine	C22H24N2O3	Indole alkaloid	
				33	Pycnolide	C20H28O6	Sesquiterpenoid	
				33	Eriolangin	C20H28O6	Sesquiterpenoid	
				33	Resiniferonol	C20H28O6	Diterpenoid	
				33	Phorbol	C20H28O6	Diterpenoid	
				33	Gibberellin A44 diacid	C20H28O6	Diterpenoid	
		342.1937667	Na+					
		326.0837667	K+					
	365.2812667	364.2732667	H+					
		342.2912667	Na+					
		326.1812667	K+					
	365.1210333	364.1130333	H+					
		342.1310333	Na+	0	Coniferin	C16H22O8	Monolignol	Phenylpropanoid biosynthesis
		326.0210333	K+	16	Licarin A	C20H22O4	Neolignan	
				16	Dehydrodieugenol	C20H22O4	Neolignan	
				16	Uncinatone	C20H22O4	Terpenoid	
				16	Pulverochromenol	C20H22O4	Chromone	
				16	8-(3,3-Dimethylallyl)spatheliachromene	C20H22O4	Chromone	
				14	Caribine	C19H22N2O3	Isoquinoline alkaloid	
	365.1856667	364.1776667	H+	27	Cinncassiol C2	C20H28O6	Sesquiterpenoid	
				0	11-Methoxy-vinorine	C22H24N2O3	Indole alkaloid	
				27	Pycnolide	C20H28O6	Sesquiterpenoid	
				27	Eriolangin	C20H28O6	Sesquiterpenoid	
				27	Resiniferonol	C20H28O6	Diterpenoid	
				27	Phorbol	C20H28O6	Diterpenoid	
				27	Gibberellin A44 diacid	C20H28O6	Diterpenoid	
		342.1956667	Na+					
		326.0856667	K+					
	365.2816333	364.2736333	H+					
		342.2916333	Na+					
		326.1816333	K+					
	365.1213	364.1133	H+					
		342.1313	Na+	1	Coniferin	C16H22O8	Monolignol	Phenylpropanoid biosynthesis
				17	Licarin A	C20H22O4	Neolignan	
				17	Dehydrodieugenol	C20H22O4	Neolignan	
				17	Uncinatone	C20H22O4	Terpenoid	
				17	Pulverochromenol	C20H22O4	Chromone	
				17	8-(3,3-Dimethylallyl)spatheliachromene	C20H22O4	Chromone	

				13	Caribine	C19H22N2O3	Isoquinoline alkaloid	
		326.0213	K+					
	365.1844667	364.1764667	H+	31	Cinncassiol C2	C20H28O6	Sesquiterpenoid	
				4	11-Methoxy-vinorine	C22H24N2O3	Indole alkaloid	
				31	Pycnolide	C20H28O6	Sesquiterpenoid	
				31	Eriolangin	C20H28O6	Sesquiterpenoid	
				31	Resiniferonol	C20H28O6	Diterpenoid	
				31	Phorbol	C20H28O6	Diterpenoid	
				31	Gibberellin A44 diacid	C20H28O6	Diterpenoid	
		342.1944667	Na+					
		326.0844667	K+					
	365.2842	364.2762	H+					
		342.2942	Na+					
		326.1842	K+					
381	381.0972667	380.0892667	H+	1	Diphyllin	C21H16O7	Lignan	
		358.1072667	Na+	30	Pantetheine 4'-phosphate	C11H23N2O7PS	CoA precursor	Pantothenate and CoA biosynthesis
				39	alpha-Ribazole 5'-phosphate	C14H19N2O7P	Sugar	Riboflavin, porphyrin and chlorophyll metabolism
				7	Gardenin B	C19H18O7	Flavone	
				7	Chryso-obtusin	C19H18O7	Anthraquinone	
		341.9972667	K+	6	Coniferin	C16H22O8	Monolignol	Phenylpropanoid biosynthesis
				33	Phaseollidin hydrate	C20H22O5	Pterocarpan	
	381.0968333	380.0888333	H+	0	Diphyllin	C21H16O7	Lignan	
		358.1068333	Na+	29	Pantetheine 4'-phosphate	C11H23N2O7PS	CoA precursor	Pantothenate and CoA biosynthesis
				38	alpha-Ribazole 5'-phosphate	C14H19N2O7P	Sugar	Riboflavin, porphyrin and chlorophyll metabolism
				6	Gardenin B	C19H18O7	Flavone	
				6	Chryso-obtusin	C19H18O7	Anthraquinone	
		341.9968333	K+	5	Coniferin	C16H22O8	Monolignol	Phenylpropanoid biosynthesis
				34	Phaseollidin hydrate	C20H22O5	Pterocarpan	
	381.0977	380.0897	H+	2	Diphyllin	C21H16O7	Lignan	
		358.1077	Na+	31	Pantetheine 4'-phosphate	C11H23N2O7PS	CoA precursor	Pantothenate and CoA biosynthesis
				8	Gardenin B	C19H18O7	Flavone	
				8	Chryso-obtusin	C19H18O7	Anthraquinone	
		341.9977	K+	8	Coniferin	C16H22O8	Monolignol	Phenylpropanoid biosynthesis
				31	Phaseollidin hydrate	C20H22O5	Pterocarpan	
527.2	527.1817667	526.1737667	H+	11	Inumakilactone A glycoside	C24H30O13	Diterpenoid	
		504.1917667	Na+					
		488.0817667	K+	26	Ichangin	C26H32O9	Triterpenoid	
				26	Limonoate A-ring-lactone	C26H32O9	Triterpenoid	
				26	Limonoate D-ring-lactone	C26H32O9	Triterpenoid	
	527.1824667	526.1744667	H+	12	Inumakilactone A glycoside	C24H30O13	Diterpenoid	
		504.1924667	Na+					
		488.0824667	K+	27	Ichangin	C26H32O9	Triterpenoid	
				27	Limonoate A-ring-lactone	C26H32O9	Triterpenoid	

				27	Limonoate D-ring-lactone	C26H32O9	Triterpenoid	
	527.1817667	526.1737667	H+	11	Inumakilactone A glycoside	C24H30O13	Diterpenoid	
		504.1917667	Na+					
		488.0817667	K+	26	Ichangin	C26H32O9	Triterpenoid	
				26	Limonoate A-ring-lactone	C26H32O9	Triterpenoid	
				26	Limonoate D-ring-lactone	C26H32O9	Triterpenoid	
520.4	520.3627667	519.3547667	H+					
		497.3727667	Na+					
		481.2627667	K+					
	520.3632	519.3552	H+					
		497.3732	Na+					
		481.2632	K+					
	520.3630667	519.3550667	H+					
		497.3730667	Na+					
		481.2630667	K+					
543.2	543.1574	542.1494	H+					
		520.1674	Na+	18	Chryso-obtusin glucoside	C25H28O12	Anthraquinone	
				18	Quercetin 5,7,3',4'-tetramethyl ether 3-galactoside	C25H28O12	Flavonol	
		504.0574	K+					
	543.1575333	542.1495333	H+					
		520.1675333	Na+	18	Chryso-obtusin glucoside	C25H28O12	Anthraquinone	
				18	Quercetin 5,7,3',4'-tetramethyl ether 3-galactoside	C25H28O12	Flavonol	
		504.0575333	K+					
	543.1574	542.1494	H+					
		520.1674	Na+	18	Chryso-obtusin glucoside	C25H28O12	Anthraquinone	
				18	Quercetin 5,7,3',4'-tetramethyl ether 3-galactoside	C25H28O12	Flavonol	
		504.0574	K+					
366.2	366.1261333	365.1181333	H+					
		343.1361333	Na+					
		327.0261333	K+					
	366.1262	365.1182	H+					
		343.1362	Na+					
		327.0262	K+					
	366.1272667	365.1192667	H+					
		343.1372667	Na+					
		327.0272667	K+					
496.4	496.3618333	495.3538333	H+					
		473.3718333	Na+					
		457.2618333	K+					
	496.3619333	495.3539333	H+					
		473.3719333	Na+					
		457.2619333	K+					
	496.3621333	495.3541333	H+					
		473.3721333	Na+					
		457.2621333	K+					
104.2	104.1118333	103.1038333	H+					

		81.12183333	Na+					
		65.01183333	K+					
	104.1506333	103.1426333	H+					
		81.16063333	Na+					
		65.05063333	K+					
	104.1847	103.1767	H+					
		81.1947	Na+					
		65.0847	K+					
	104.2192	103.2112	H+					
		81.2292	Na+					
		65.1192	K+					
	104.2514667	103.2434667	H+					
		81.26146667	Na+					
		65.15146667	K+					
	104.2821333	103.2741333	H+					
		81.29213333	Na+					
		65.18213333	K+					
	104.1113	103.1033	H+					
		81.1213	Na+					
		65.0113	K+					
	104.1508333	103.1428333	H+					
		81.16083333	Na+					
		65.05083333	K+					
	104.2328333	103.2248333	H+					
		81.24283333	Na+					
		65.13283333	K+					
	104.1119	103.1039	H+					
		81.1219	Na+					
		65.0119	K+					
	104.1544667	103.1464667	H+					
		81.16446667	Na+					
		65.05446667	K+					
	104.1988	103.1908	H+					
		81.2088	Na+					
		65.0988	K+					
	104.2922667	103.2842667	H+					
		81.30226667	Na+					
		65.19226667	K+					
527.4	527.3583667	526.3503667	H+					
		504.3683667	Na+					
		488.2583667	K+					
	527.3684667	526.3604667	H+					
		504.3784667	Na+					
		488.2684667	K+					
	527.3542	526.3462	H+					
		504.3642	Na+					

		488.2542	K+					
689.2	689.2437333	688.2357333	H+					
		666.2537333	Na+	3	3,4,7-Trihydroxy-5-methoxy-8-prenylflavan 4-O-(beta-D-xylopyranosyl-(1->6)-beta-D-glucopyranoside)	C32H42O15	Flavan	
		650.1437333	K+	33	Limonin 17-beta-D-glucoside	C32H42O14	Triterpenoid	
				33	Ichangin 4-glucoside	C32H42O14	Triterpenoid	
	689.2425667	688.2345667	H+					
		666.2525667	Na+	1	3,4,7-Trihydroxy-5-methoxy-8-prenylflavan 4-O-(beta-D-xylopyranosyl-(1->6)-beta-D-glucopyranoside)	C32H42O15	Flavan	
		650.1425667	K+	31	Limonin 17-beta-D-glucoside	C32H42O14	Triterpenoid	
				31	Ichangin 4-glucoside	C32H42O14	Triterpenoid	
	689.2427667	688.2347667	H+					
		666.2527667	Na+	1	3,4,7-Trihydroxy-5-methoxy-8-prenylflavan 4-O-(beta-D-xylopyranosyl-(1->6)-beta-D-glucopyranoside)	C32H42O15	Flavan	
		650.1427667	K+	32	Limonin 17-beta-D-glucoside	C32H42O14	Triterpenoid	
				32	Ichangin 4-glucoside	C32H42O14	Triterpenoid	
665.2	665.1990333	664.1910333	H+	12	Pectolinarigenin 7-(4'''-acetylrutinoside)	C31H36O16	Flavone	
				12	Scutellarein 6,4'-dimethyl ether 7-(3'''-acetylrutinoside)	C31H36O16	Flavone	
		642.2090333	Na+	9	Triphyllin B	C29H38O16	Flavan-4-ol	
		626.0990333	K+	22	Pneumatopterin A	C29H38O15	Flavan-4-ol	
				22	Salicifolioside A	C29H38O15	Chalcone	
	665.1984667	664.1904667	H+	13	Pectolinarigenin 7-(4'''-acetylrutinoside)	C31H36O16	Flavone	
				13	Scutellarein 6,4'-dimethyl ether 7-(3'''-acetylrutinoside)	C31H36O16	Flavone	
		642.2084667	Na+	10	Triphyllin B	C29H38O16	Flavan-4-ol	
		626.0984667	K+	21	Pneumatopterin A	C29H38O15	Flavan-4-ol	
				21	Salicifolioside A	C29H38O15	Chalcone	
	665.1989667	664.1909667	H+	12	Pectolinarigenin 7-(4'''-acetylrutinoside)	C31H36O16	Flavone	
				12	Scutellarein 6,4'-dimethyl ether 7-(3'''-acetylrutinoside)	C31H36O16	Flavone	
		642.2089667	Na+	9	Triphyllin B	C29H38O16	Flavan-4-ol	
		626.0989667	K+	22	Pneumatopterin A	C29H38O15	Flavan-4-ol	
				22	Salicifolioside A	C29H38O15	Chalcone	
136	135.9702	134.9622	H+					
		112.9802	Na+					
		96.8702	K+					
	136.0251333	135.0171333	H+					
		113.0351333	Na+					
		96.92513333	K+					
	136.0686	135.0606	H+					
		113.0786	Na+					
		96.9686	K+					

	135.9155667	134.9075667	H+					
		112.9255667	Na+					
		96.81556667	K+					
	135.9655333	134.9575333	H+					
		112.9755333	Na+					
		96.86553333	K+					
	136.0238	135.0158	H+					
		113.0338	Na+					
		96.9238	K+					
	136.0686333	135.0606333	H+					
		113.0786333	Na+					
		96.96863333	K+					
	135.9681667	134.9601667	H+					
		112.9781667	Na+					
		96.86816667	K+					
	136.0257667	135.0177667	H+					
		113.0357667	Na+					
		96.92576667	K+					
	136.0686333	135.0606333	H+					
		113.0786333	Na+					
		96.96863333	K+					
498.2	498.1580333	497.1500333	H+					
		475.1680333	Na+					
		459.0580333	K+					
	498.2807667	497.2727667	H+					
		475.2907667	Na+	16	Alangimarckine	C29H37N3O3	Isoquinoline alkaloid	Isoquinoline alkaloid biosynthesis
				16	Tubulosine	C29H37N3O3	Isoquinoline alkaloid	Isoquinoline alkaloid biosynthesis
		459.1807667	K+					
	498.1535333	497.1455333	H+					
		475.1635333	Na+					
		459.0535333	K+					
	498.2811667	497.2731667	H+					
		475.2911667	Na+	16	Alangimarckine	C29H37N3O3	Isoquinoline alkaloid	Isoquinoline alkaloid biosynthesis
				16	Tubulosine	C29H37N3O3	Isoquinoline alkaloid	Isoquinoline alkaloid biosynthesis
		459.1811667	K+					
	498.1561667	497.1481667	H+					
		475.1661667	Na+					
		459.0561667	K+					
	498.2811	497.2731	H+					
		475.2911	Na+	16	Alangimarckine	C29H37N3O3	Isoquinoline alkaloid	Isoquinoline alkaloid biosynthesis

				16	Tubulosine	C29H37N3O3	Isoquinoline alkaloid	Isoquinoline alkaloid biosynthesis
		459.1811	K+					

Table B3.7 MR-Buster sorghum polyphenol extract putative identifications from OPLS-DA (MALDI [+])

Bin	Detected Mass	Accurate Mass	Adduct	Δppm	Name	Formula	Chemical Group	Pathway
523.2	523.1488667	522.1408667	H+	8	Iridin	C24H26O13	Isoflavone	
		500.1588667	Na+					
		484.0488667	K+					
	523.2558667	522.2478667	H+	4	Trilobolide	C27H38O10	Sesquiterpenoid	
		500.2658667	Na+					
		484.1558667	K+					
	523.1513333	522.1433333	H+	12	Iridin	C24H26O13	Isoflavone	
		500.1613333	Na+					
		484.0513333	K+					
	523.2606333	522.2526333	H+	13	Trilobolide	C27H38O10	Sesquiterpenoid	
		500.2706333	Na+					
		484.1606333	K+					
	523.1518	522.1438	H+	13	Iridin	C24H26O13	Isoflavone	
		500.1618	Na+					
		484.0518	K+					
	523.2627667	522.2547667	H+	17	Trilobolide	C27H38O10	Sesquiterpenoid	
		500.2727667	Na+					
		484.1627667	K+					
509.2	509.1388667	508.1308667	H+					
		486.1488667	Na+					
		470.0388667	K+	36	Limonin	C26H30O8	Triterpenoid	
				36	Zapoterin	C26H30O8	Triterpenoid	
				36	Isobutyrylmallotochromene	C26H30O8	Phloroglucinol	
				36	Butyrylmallotochromene	C26H30O8	Phloroglucinol	
				36	Drummondin A	C26H30O8	Phloroglucinol	
	509.1400333	508.1320333	H+					
		486.1500333	Na+					
		470.0400333	K+	33	Limonin	C26H30O8	Triterpenoid	
				33	Zapoterin	C26H30O8	Triterpenoid	
				33	Isobutyrylmallotochromene	C26H30O8	Phloroglucinol	
				33	Butyrylmallotochromene	C26H30O8	Phloroglucinol	
				33	Drummondin A	C26H30O8	Phloroglucinol	
	509.1410667	508.1330667	H+					
		486.1510667	Na+					
		470.0410667	K+	31	Limonin	C26H30O8	Triterpenoid	
				31	Zapoterin	C26H30O8	Triterpenoid	

				31	Isobutyrylmallotochromene	C26H30O8	Phloroglucinol	
				31	Butyrylmallotochromene	C26H30O8	Phloroglucinol	
				31	Drummondin A	C26H30O8	Phloroglucinol	
	509.2756667	508.2676667	H+					
		486.2856667	Na+					
		470.1756667	K+					
269	268.9089	267.9009	H+					
		245.9189	Na+					
		229.8089	K+					
	269.088	268.08	H+	26	6-Hydroxy-2'-methoxyflavone	C16H12O4	Flavone	
				26	Isoformononetin	C16H12O4	Isoflavone	Isoflavonoid and phenylpropanoid biosynthesis
				15	Saphenic acid	C15H12N2O3	Alkaloid	
				26	Tectochrysin	C16H12O4	Flavone	
				4	2-O-(alpha-D-Mannosyl)-D-glycerate	C9H16O9	Monosaccharide	Fructose and mannose metabolism
				26	Dalbergin	C16H12O4	Neoflavonoid	
				26	Formononetin	C16H12O4	Isoflavone	Isoflavonoid and phenylpropanoid biosynthesis
				0	Inosine	C10H12N4O5	Nucleotide	Purine metabolism
		246.098	Na+	35	(+)-Columbianetin	C14H14O4	Furanocoumarin	Phenylpropanoid biosynthesis
				35	Torachrysone	C14H14O4	Napthol	
				35	(-)-Marmesin	C14H14O4	Furanocoumarin	
				35	Decursinol	C14H14O4	Furanocoumarin	
				35	(-)-Columbianetin	C14H14O4	Furanocoumarin	
		229.988	K+	21	Isodehydrocostus lactone	C15H18O2	Sesquiterpenoid	
				21	Linderenol	C15H18O2	Sesquiterpenoid	
				21	Furanodienone	C15H18O2	Sesquiterpenoid	
				21	Dehydromyodesmone	C15H18O2	Sesquiterpenoid	
				21	Eremanthin	C15H18O2	Sesquiterpenoid	
				21	Dehydrocostus lactone	C15H18O2	Sesquiterpenoid	
	268.9086	267.9006	H+					
		245.9186	Na+					
		229.8086	K+					
	268.9540667	267.9460667	H+					
		245.9640667	Na+					
		229.8540667	K+					
	269.0885667	268.0805667	H+	28	6-Hydroxy-2'-methoxyflavone	C16H12O4	Flavone	
				28	Isoformononetin	C16H12O4	Isoflavone	Isoflavonoid and phenylpropanoid biosynthesis
				13	Saphenic acid	C15H12N2O3	Alkaloid	
				28	Tectochrysin	C16H12O4	Flavone	
				6	2-O-(alpha-D-Mannosyl)-D-glycerate	C9H16O9	Monosaccharide	Fructose and mannose metabolism
				28	Dalbergin	C16H12O4	Neoflavonoid	
				28	Formononetin	C16H12O4	Isoflavone	Isoflavonoid and phenylpropanoid biosynthesis

				1	Inosine	C10H12N4O5	Nucleotide	Purine metabolism
		246.0985667	Na+	37	(+)-Columbianetin	C14H14O4	Furanocoumarin	Phenylpropanoid biosynthesis
				37	Torachrysone	C14H14O4	Napthol	
				37	(-)-Marmesin	C14H14O4	Furanocoumarin	
				37	Decursinol	C14H14O4	Furanocoumarin	
				37	(-)-Columbianetin	C14H14O4	Furanocoumarin	
		229.9885667	K+	19	Isodehydrocostus lactone	C15H18O2	Sesquiterpenoid	
				19	Linderenol	C15H18O2	Sesquiterpenoid	
				19	Furanodienone	C15H18O2	Sesquiterpenoid	
				19	Dehydromyodesmone	C15H18O2	Sesquiterpenoid	
				19	Eremanthin	C15H18O2	Sesquiterpenoid	
				19	Dehydrocostus lactone	C15H18O2	Sesquiterpenoid	
	268.9479333	267.9399333	H+					
		245.9579333	Na+					
		229.8479333	K+					
	269.0028	267.9948	H+					
		246.0128	Na+	28	Isopentenyl diphosphate	C5H12O7P2	Isoprenoid	Terpenoid, steroid and zeatin biosynthesis
				28	Dimethylallyl diphosphate	C5H12O7P2	Isoprenoid	Terpenoid, steroid and zeatin biosynthesis
		229.9028	K+					
	269.0893	268.0813	H+	31	6-Hydroxy-2'-methoxyflavone	C16H12O4	Flavone	
				31	Isoformononetin	C16H12O4	Isoflavone	Isoflavonoid and phenylpropanoid biosynthesis
				10	Saphenic acid	C15H12N2O3	Alkaloid	
				31	Tectochrysin	C16H12O4	Flavone	
				9	2-O-(alpha-D-Mannosyl)-D-glycerate	C9H16O9	Monosaccharide	Fructose and mannose metabolism
				31	Dalbergin	C16H12O4	Neoflavonoid	
				31	Formononetin	C16H12O4	Isoflavone	Isoflavonoid and phenylpropanoid biosynthesis
				4	Inosine	C10H12N4O5	Nucleotide	Purine metabolism
		246.0993	Na+					
		229.9893	K+	16	Isodehydrocostus lactone	C15H18O2	Sesquiterpenoid	
				16	Linderenol	C15H18O2	Sesquiterpenoid	
				16	Furanodienone	C15H18O2	Sesquiterpenoid	
				16	Dehydromyodesmone	C15H18O2	Sesquiterpenoid	
				16	Eremanthin	C15H18O2	Sesquiterpenoid	
				16	Dehydrocostus lactone	C15H18O2	Sesquiterpenoid	
255	254.9698667	253.9618667	H+					
		231.9798667	Na+					
		215.8698667	K+					
	255.0728	254.0648	H+	27	S-(Phenylacetothiohydroximoyl)-L-cysteine	C11H14N2O3S	Amino acid	2-oxocarboxylic acid and glucosinolate biosynthesis
				29	4',6-Dihydroxyflavone	C15H10O4	Flavone	
				29	7,4'-Dihydroxyflavone	C15H10O4	Flavone	Flavonoid and isoflavonoid biosynthesis

				29	Rubiadin	C15H10O4	Anthraquinone	
				29	1,4-Dihydroxy-2-methylanthraquinone	C15H10O4	Anthraquinone	
				29	Digiferrugineol	C15H10O4	Anthraquinone	
				29	Chrysophanol	C15H10O4	Anthraquinone	
				29	Alizarin 2-methyl ether	C15H10O4	Anthraquinone	
				29	Daidzein	C15H10O4	Isoflavone	Isoflavonoid and phenylpropanoid biosynthesis
				29	Anhydroglycinol	C15H10O4	Pterocarpan	Isoflavonoid biosynthesis
				29	Primetin	C15H10O4	Flavone	
				29	Chrysin	C15H10O4	Flavone	Flavonoid biosynthesis
				29	Hispidol	C15H10O4	Aurone	
				32	Glutaurine	C7H14N2O6S	Amino acid	Taurine and hypotaurine metabolism
		232.0828	Na+	39	Altholactone	C13H12O4	Styryllactone	
		215.9728	K+	5	gamma-Glutamyl-gamma-aminobutyraldehyde	C9H16N2O4	Amino acid	Arginine and proline metabolism
	254.9077333	253.8997333	H+					
		231.9177333	Na+					
		215.8077333	K+					
	254.9711667	253.9631667	H+					
		231.9811667	Na+					
		215.8711667	K+					
	255.0734	254.0654	H+	25	S-(Phenylacetothiohydroximoyl)-L-cysteine	C11H14N2O3S	Amino acid	2-oxocarboxylic acid and glucosinolate biosynthesis
				32	4',6-Dihydroxyflavone	C15H10O4	Flavone	
				32	7,4'-Dihydroxyflavone	C15H10O4	Flavone	Flavonoid and isoflavonoid biosynthesis
				32	Rubiadin	C15H10O4	Anthraquinone	
				32	1,4-Dihydroxy-2-methylanthraquinone	C15H10O4	Anthraquinone	
				32	Digiferrugineol	C15H10O4	Anthraquinone	
				32	Chrysophanol	C15H10O4	Anthraquinone	
				32	Alizarin 2-methyl ether	C15H10O4	Anthraquinone	
				32	Daidzein	C15H10O4	Isoflavone	Isoflavonoid and phenylpropanoid biosynthesis
				32	Anhydroglycinol	C15H10O4	Pterocarpan	Isoflavonoid biosynthesis
				32	Primetin	C15H10O4	Flavone	
				32	Chrysin	C15H10O4	Flavone	Flavonoid biosynthesis
				32	Hispidol	C15H10O4	Aurone	
				34	Glutaurine	C7H14N2O6S	Amino acid	Taurine and hypotaurine metabolism
		232.0834	Na+					
		215.9734	K+	2	gamma-Glutamyl-gamma-aminobutyraldehyde	C9H16N2O4	Amino acid	Arginine and proline metabolism
	254.9078333	253.8998333	H+					
		231.9178333	Na+					
		215.8078333	K+					
	254.9702	253.9622	H+					
		231.9802	Na+					

		215.8702	K+					
	255.0736	254.0656	H+	24	S-(Phenylacetothiohydroximoyl)-L-cysteine	C11H14N2O3S	Amino acid	2-oxocarboxylic acid and glucosinolate biosynthesis
				32	4',6-Dihydroxyflavone	C15H10O4	Flavone	
				32	7,4'-Dihydroxyflavone	C15H10O4	Flavone	Flavonoid and isoflavonoid biosynthesis
				32	Rubiadin	C15H10O4	Anthraquinone	
				32	1,4-Dihydroxy-2-methylanthraquinone	C15H10O4	Anthraquinone	
				32	Digiferrugineol	C15H10O4	Anthraquinone	
				32	Chrysophanol	C15H10O4	Anthraquinone	
				32	Alizarin 2-methyl ether	C15H10O4	Anthraquinone	
				32	Daidzein	C15H10O4	Isoflavone	Isoflavonoid and phenylpropanoid biosynthesis
				32	Anhydroglycinol	C15H10O4	Pterocarpan	Isoflavonoid biosynthesis
				32	Primetin	C15H10O4	Flavone	
				32	Chrysin	C15H10O4	Flavone	Flavonoid biosynthesis
				32	Hispidol	C15H10O4	Aurone	
				35	Glutaurine	C7H14N2O6S	Amino acid	Taurine and hypotaurine metabolism
		232.0836	Na+					
		215.9736	K+	2	gamma-Glutamyl-gamma-aminobutyraldehyde	C9H16N2O4	Amino acid	Arginine and proline metabolism
470.2	470.2424	469.2344	H+					
		447.2524	Na+					
		431.1424	K+					
	470.2430667	469.2350667	H+					
		447.2530667	Na+					
		431.1430667	K+					
	470.2432333	469.2352333	H+					
		447.2532333	Na+					
		431.1432333	K+					
524.2	524.1550667	523.1470667	H+					
		501.1650667	Na+					
		485.0550667	K+					
	524.2518	523.2438	H+					
		501.2618	Na+					
		485.1518	K+					
	524.1552	523.1472	H+					
		501.1652	Na+					
		485.0552	K+					
	524.2546	523.2466	H+					
		501.2646	Na+					
		485.1546	K+					
	524.1558667	523.1478667	H+					
		501.1658667	Na+					
		485.0558667	K+					
	524.2581667	523.2501667	H+					

		501.2681667	Na+					
		485.1581667	K+					
510.2	510.1426667	509.1346667	H+					
		487.1526667	Na+					
		471.0426667	K+					
	510.2435	509.2355	H+					
		487.2535	Na+					
		471.1435	K+					
	510.1422667	509.1342667	H+					
		487.1522667	Na+					
		471.0422667	K+					
	510.1428333	509.1348333	H+					
		487.1528333	Na+					
		471.0428333	K+					
	510.2304	509.2224	H+					
		487.2404	Na+					
		471.1304	K+					
287	286.9069667	285.8989667	H+					
		263.9169667	Na+					
		247.8069667	K+					
	287.0694	286.0614	H+	19	5'-Phosphoribosylglycinamide	C7H15N2O8P	Amino acid	Purine metabolism
		264.0794	Na+	33	Perlolyrine	C16H12N2O2	Indole alkaloid	
		247.9694	K+	4	Prenyl caffeate	C14H16O4	Phenolic acid	
	286.9057	285.8977	H+					
		263.9157	Na+					
		247.8057	K+					
	286.9834	285.9754	H+					
		263.9934	Na+					
		247.8834	K+					
	287.07	286.062	H+	21	5'-Phosphoribosylglycinamide	C7H15N2O8P	Amino acid	Purine metabolism
		264.08	Na+	31	Perlolyrine	C16H12N2O2	Indole alkaloid	
		247.97	K+	6	Prenyl caffeate	C14H16O4	Phenolic acid	
	286.9057	285.8977	H+					
		263.9157	Na+					
		247.8057	K+					
	287.0703	286.0623	H+	20	5'-Phosphoribosylglycinamide	C7H15N2O8P	Amino acid	Purine metabolism
		264.0803	Na+	32	Perlolyrine	C16H12N2O2	Indole alkaloid	
		247.9703	K+	7	Prenyl caffeate	C14H16O4	Phenolic acid	
377	377.0229333	376.0149333	H+					
		354.0329333	Na+					
		337.9229333	K+	7	1-(5'-Phosphoribosyl)-5-amino-4-imidazolecarboxamide	C9H15N4O8P	Nucleotide	Amino acid and alkaloid metabolism
	377.0961667	376.0881667	H+					
		354.1061667	Na+	8	Sesamin	C20H18O6	Lignan	
				8	Hinokinin	C20H18O6	Lignan	
				8	Luteone	C20H18O6	Isoflavone	

				8	Licoisoflavone A	C20H18O6	Isoflavone	
				8	Cyclokievitone	C20H18O6	Isoflavanone	
				31	Biflorin	C16H18O9	Chromone	
				31	Scopolin	C16H18O9	Coumarin	Phenylpropanoid biosynthesis
				31	Chlorogenic acid	C16H18O9	Monolignol	Phenylpropanoid, flavonoid and stilbenoid biosynthesis
		337.9961667	K+	9	1-Peroxyferolide	C17H22O7	Sesquiterpenoid	
	376.9166	375.9086	H+					
		353.9266	Na+					
		337.8166	K+					
	377.0223333	376.0143333	H+					
		354.0323333	Na+					
		337.9223333	K+	9	1-(5'-Phosphoribosyl)-5-amino-4-imidazolecarboxamide	C9H15N4O8P	Nucleotide	Amino acid and alkaloid metabolism
	377.0964667	376.0884667	H+					
		354.1064667	Na+	8	Sesamin	C20H18O6	Lignan	
				8	Hinokinin	C20H18O6	Lignan	
				8	Luteone	C20H18O6	Isoflavone	
				8	Licoisoflavone A	C20H18O6	Isoflavone	
				8	Cyclokievitone	C20H18O6	Isoflavanone	
				32	Biflorin	C16H18O9	Chromone	
				32	Scopolin	C16H18O9	Coumarin	Phenylpropanoid biosynthesis
				32	Chlorogenic acid	C16H18O9	Monolignol	Phenylpropanoid, flavonoid and stilbenoid biosynthesis
		337.9964667	K+	8	1-Peroxyferolide	C17H22O7	Sesquiterpenoid	
	376.9089	375.9009	H+					
		353.9189	Na+					
		337.8089	K+					
	377.0216	376.0136	H+					
		354.0316	Na+					
		337.9216	K+	11	1-(5'-Phosphoribosyl)-5-amino-4-imidazolecarboxamide	C9H15N4O8P	Nucleotide	Amino acid and alkaloid metabolism
	377.0973333	376.0893333	H+					
		354.1073333	Na+	5	Sesamin	C20H18O6	Lignan	
				5	Hinokinin	C20H18O6	Lignan	
				5	Luteone	C20H18O6	Isoflavone	
				5	Licoisoflavone A	C20H18O6	Isoflavone	
				5	Cyclokievitone	C20H18O6	Isoflavanone	
				34	Biflorin	C16H18O9	Chromone	
				34	Scopolin	C16H18O9	Coumarin	Phenylpropanoid biosynthesis
				34	Chlorogenic acid	C16H18O9	Monolignol	Phenylpropanoid, flavonoid and stilbenoid biosynthesis
		337.9973333	K+	6	1-Peroxyferolide	C17H22O7	Sesquiterpenoid	
289	288.9154	287.9074	H+					
		265.9254	Na+					
		249.8154	K+					

	289.0989667	288.0909667	H+	27	Shikonin	C16H16O5	Napthoquinone	Ubiquinone and terpenoid biosynthesis
				27	7,2'-Dihydroxy-4'-methoxy-isoflavanol	C16H16O5	Isoflavane	Isoflavonoid biosynthesis
				27	Phloretin 4'-methyl ether	C16H16O5	Dihydrochalcone	
		266.1089667	Na+					
		249.9989667	K+					
	289.1008333	288.0928333	H+	21	Shikonin	C16H16O5	Napthoquinone	Ubiquinone and terpenoid biosynthesis
				21	7,2'-Dihydroxy-4'-methoxy-isoflavanol	C16H16O5	Isoflavane	Isoflavonoid biosynthesis
				21	Phloretin 4'-methyl ether	C16H16O5	Dihydrochalcone	
		266.1108333	Na+					
		250.0008333	K+					
	288.9175	287.9095	H+					
		265.9275	Na+					
		249.8175	K+					
	289.1011667	288.0931667	H+	20	Shikonin	C16H16O5	Napthoquinone	Ubiquinone and terpenoid biosynthesis
				20	7,2'-Dihydroxy-4'-methoxy-isoflavanol	C16H16O5	Isoflavane	Isoflavonoid biosynthesis
				20	Phloretin 4'-methyl ether	C16H16O5	Dihydrochalcone	
		266.1111667	Na+					
		250.0011667	K+					
383.2	383.1071	382.0991	H+	14	Austrobailignan 1	C21H18O7	Lignan	
		360.1171	Na+	7	Goyazensolide	C19H20O7	Sesquiterpenoid	
				7	Elephantopin	C19H20O7	Sesquiterpenoid	
				2	Acalyphin	C14H20N2O9	Cyanogenic glycoside	
				7	2,3-Dihydro-2-(4-hydroxyphenyl)-5,6,7,8-tetramethoxy-4H-1-benzopyran-4-one	C19H20O7	Flavone	
				37	3-Methoxytyramine-betaxanthin	C18H20N2O6	Betalain	Betalain biosynthesis
				7	Vernodalin	C19H20O7	Sesquiterpenoid	
		344.0071	K+	31	Clusianose	C12H24O11	Disaccharide	
				31	6-O-alpha-D-Galactosyl-D-glucitol	C12H24O11	Disaccharide	Galactose metabolism
				8	Iridotrial glucoside	C16H24O8	Iridoid glycoside	
				8	8-Epiiridotrial glucoside	C16H24O8	Iridoid glycoside	
	383.1860333	382.1780333	H+	27	Akuammine	C22H26N2O4	Alkaloid	
				27	Aricine	C22H26N2O4	Indole alkaloid	
				27	Cabucine	C22H26N2O4	Indole alkaloid	
		360.1960333	Na+	8	Cinerin II	C21H28O5	Monoterpenoid	
				21	O-Acetylcypholophine	C20H28N2O4	Alkaloid	
		344.0860333	K+	25	Lochnerinine	C22H26N2O4	Indole alkaloid	Indole alkaloid biosynthesis
	383.2742333	382.2662333	H+					
		360.2842333	Na+					
		344.1742333	K+					
	383.1082	382.1002	H+	11	Austrobailignan 1	C21H18O7	Lignan	
		360.1182	Na+	5	Goyazensolide	C19H20O7	Sesquiterpenoid	
				5	Elephantopin	C19H20O7	Sesquiterpenoid	

				5	Acalyphin	C14H20N2O9	Cyanogenic glycoside	
				5	2,3-Dihydro-2-(4-hydroxyphenyl)-5,6,7,8-tetramethoxy-4H-1-benzopyran-4-one	C19H20O7	Flavone	
				34	3-Methoxytyramine-betaxanthin	C18H20N2O6	Betalain	Betalain biosynthesis
				5	Vernodalin	C19H20O7	Sesquiterpenoid	
		344.0082	K+	34	Clusianose	C12H24O11	Disaccharide	
				34	6-O-alpha-D-Galactosyl-D-glucitol	C12H24O11	Disaccharide	Galactose metabolism
				5	Iridotrial glucoside	C16H24O8	Iridoid glycoside	
				5	8-Epiiridotrial glucoside	C16H24O8	Iridoid glycoside	
	383.1846333	382.1766333	H+	31	Akuammine	C22H26N2O4	Alkaloid	
				31	Aricine	C22H26N2O4	Indole alkaloid	
				31	Cabucine	C22H26N2O4	Indole alkaloid	
		360.1946333	Na+	4	Cinerin II	C21H28O5	Monoterpenoid	
				24	O-Acetylcypholophine	C20H28N2O4	Alkaloid	
		344.0846333	K+	31	Lochnerinine	C22H26N2O4	Indole alkaloid	Indole alkaloid biosynthesis
	383.2565667	382.2485667	H+					
		360.2665667	Na+					
		344.1565667	K+					
	383.1099667	382.1019667	H+	6	Austrobailignan 1	C21H18O7	Lignan	
		360.1199667	Na+	0	Goyazensolide	C19H20O7	Sesquiterpenoid	
				0	Elephantopin	C19H20O7	Sesquiterpenoid	
				10	Acalyphin	C14H20N2O9	Cyanogenic glycoside	
				0	2,3-Dihydro-2-(4-hydroxyphenyl)-5,6,7,8-tetramethoxy-4H-1-benzopyran-4-one	C19H20O7	Flavone	
				29	3-Methoxytyramine-betaxanthin	C18H20N2O6	Betalain	Betalain biosynthesis
				0	Vernodalin	C19H20O7	Sesquiterpenoid	
		344.0099667	K+	39	Clusianose	C12H24O11	Disaccharide	
				39	6-O-alpha-D-Galactosyl-D-glucitol	C12H24O11	Disaccharide	Galactose metabolism
				0	Iridotrial glucoside	C16H24O8	Iridoid glycoside	
				0	8-Epiiridotrial glucoside	C16H24O8	Iridoid glycoside	
	383.1914333	382.1834333	H+	39	Cinncassiol A	C20H30O7	Terpene lactone	
				39	Cinncassiol C3	C20H30O7	Terpene lactone	
				13	Akuammine	C22H26N2O4	Alkaloid	
				13	Aricine	C22H26N2O4	Indole alkaloid	
				13	Cabucine	C22H26N2O4	Indole alkaloid	
		360.2014333	Na+	22	Cinerin II	C21H28O5	Monoterpenoid	
				7	O-Acetylcypholophine	C20H28N2O4	Alkaloid	
		344.0914333	K+	13	Lochnerinine	C22H26N2O4	Indole alkaloid	Indole alkaloid biosynthesis
	383.2613333	382.2533333	H+					
		360.2713333	Na+					
		344.1613333	K+					
536.2	536.1445667	535.1365667	H+	14	Malvidin 3-(6-acetylglucoside)	C25H27O13	Anthocyaninidin	
		513.1545667	Na+					
		497.0445667	K+					

	536.2431	535.2351	H+					
		513.2531	Na+					
		497.1431	K+					
	536.1499333	535.1419333	H+	4	Malvidin 3-(6-acetylglucoside)	C25H27O13	Anthocyaninidin	
		513.1599333	Na+					
		497.0499333	K+					
	536.2438333	535.2358333	H+					
		513.2538333	Na+					
		497.1438333	K+					
	536.1497667	535.1417667	H+	4	Malvidin 3-(6-acetylglucoside)	C25H27O13	Anthocyaninidin	
		513.1597667	Na+					
		497.0497667	K+					
	536.2502667	535.2422667	H+					
		513.2602667	Na+					
		497.1502667	K+					
537.2	537.1599667	536.1519667	H+	0	Dihidroxy-tetramethoxy flavone glucoside	C25H28O13	Flavone	
				11	Cellulose	(C6H10O5)n	Trisaccharide	Starch and sucrose metabolism
		514.1699667	Na+	24	Icariside II	C27H30O10	Flavone	
				24	Baohuoside I	C27H30O10	Flavone	
		498.0599667	K+	6	Strictosamide	C26H30N2O8	Indole alkaloid	Shikimate alkaloids
				24	8-Epiiridodial glucoside tetraacetate	C24H34O11	Iridoid glycoside	
				24	Iridodial glucoside tetraacetate	C24H34O11	Iridoid glycoside	
	537.26	536.252	H+					
		514.27	Na+	13	Cinncassiol D1 glucoside	C26H42O10	Terpene lactone	
				13	Cinncassiol D4 2-glucoside	C26H42O10	Terpene lactone	
		498.16	K+					
	537.1644333	536.1564333	H+	7	Dihidroxy-tetramethoxy flavone glucoside	C25H28O13	Flavone	
				3	Cellulose	(C6H10O5)n	Trisaccharide	Starch and sucrose metabolism
		514.1744333	Na+	16	Icariside II	C27H30O10	Flavone	
				16	Baohuoside I	C27H30O10	Flavone	
		498.0644333	K+	1	Strictosamide	C26H30N2O8	Indole alkaloid	Shikimate alkaloids
				16	8-Epiiridodial glucoside tetraacetate	C24H34O11	Iridoid glycoside	
				16	Iridodial glucoside tetraacetate	C24H34O11	Iridoid glycoside	
	537.1656	536.1576	H+	9	Dihidroxy-tetramethoxy flavone glucoside	C25H28O13	Flavone	
				1	Cellulose	(C6H10O5)n	Trisaccharide	Starch and sucrose metabolism
		514.1756	Na+	13	Icariside II	C27H30O10	Flavone	
				13	Baohuoside I	C27H30O10	Flavone	
		498.0656	K+	4	Strictosamide	C26H30N2O8	Indole alkaloid	Shikimate alkaloids
				14	8-Epiiridodial glucoside tetraacetate	C24H34O11	Iridoid glycoside	
				14	Iridodial glucoside tetraacetate	C24H34O11	Iridoid glycoside	
	537.2574667	536.2494667	H+					
		514.2674667	Na+	17	Cinncassiol D1 glucoside	C26H42O10	Terpene lactone	
				17	Cinncassiol D4 2-glucoside	C26H42O10	Terpene lactone	
		498.1574667	K+					
271	270.9094	269.9014	H+					
		247.9194	Na+					

		231.8094	K+					
	270.9794	269.9714	H+					
		247.9894	Na+					
		231.8794	K+					
	271.0696667	270.0616667	H+	18	S-(Hydroxyphenylacetothiohydroximoyl)-L-cysteine	C11H14N2O4S	Amino acid	2-oxocarboxylic acid and glucosinolate biosynthesis
				35	Islandicin	C15H10O5	Anthraquinone	
				35	3,6,4'-Trihydroxyflavone	C15H10O5	Flavone	
				35	6-Hydroxydaidzein	C15H10O5	Isoflavone	Isoflavonoid biosynthesis
				35	3',4',7-Trihydroxyisoflavone	C15H10O5	Isoflavone	
				35	Purpurin 1-methyl ether	C15H10O5	Anthraquinone	
				35	2-Hydroxychrysophanol	C15H10O5	Anthraquinone	
				35	Morindone	C15H10O5	Anthraquinone	
				35	Lucidin	C15H10O5	Anthraquinone	
				35	Emodin	C15H10O5	Anthraquinone	
				35	Aloe-emodin	C15H10O5	Anthraquinone	
				35	Norwogonin	C15H10O5	Flavone	
				35	Galangin	C15H10O5	Flavone	Flavonoid biosynthesis
				35	5-Deoxykaempferol	C15H10O5	Flavonol	
				35	Baicalein	C15H10O5	Flavone	
				35	Sulphuretin	C15H10O5	Aurone	
				35	Genistein	C15H10O5	Isoflavone	Isoflavonoid and phenylpropanoid biosynthesis
				35	Apigenin	C15H10O5	Flavone	Isoflavonoid, flavonoid, phenylpropanoid, flavone and flavonol biosynthesis
				35	2'-Hydroxydaidzein	C15H10O5	Isoflavone	Isoflavonoid biosynthesis
				38	D-Lombricine	C6H15N4O6P	Amino acid	Glycine, serine and threonine metabolism
		248.0796667	Na+	2	5-Hydroxyindoleacetylglycine	C12H12N2O4	Amino acid	Tryptophan metabolism
		231.9696667	K+	25	2-Oxo-10-methylthiodecanoic acid	C11H20O3S	Fatty acid	2-oxocarboxylic acid and glucosinolate biosynthesis
				2	gamma-Glutamyl-GABA	C9H16N2O5	Amino acid	Arginine and proline metabolism
				12	Mexicanin E	C14H16O3	Seqsquiterpenoid	
				12	Encecalin	C14H16O3	Chromone	
				23	Cryptolepine	C16H12N2	Indole alkaloid	
				2	N6-Acetyl-LL-2,6-diaminoheptanedioate	C9H16N2O5	Amino acid	Lysine and amino acid metabolism
				2	N2-Succinyl-L-ornithine	C9H16N2O5	Amino acid	Arginine and proline metabolism
				2	N-alpha-Boc-L-asparagine	C9H16N2O5	Amino acid	
	270.9101	269.9021	H+					
		247.9201	Na+					
		231.8101	K+					
	270.9777667	269.9697667	H+					
		247.9877667	Na+					
		231.8777667	K+					

	271.0698	270.0618	H+	18	S-(Hydroxyphenylacetothiohydroximoyl)-L-cysteine	C11H14N2O4S	Amino acid	2-oxocarboxylic acid and glucosinolate biosynthesis
				35	Islandicin	C15H10O5	Anthraquinone	
				35	3,6,4'-Trihydroxyflavone	C15H10O5	Flavone	
				35	6-Hydroxydaidzein	C15H10O5	Isoflavone	Isoflavonoid biosynthesis
				35	3',4',7-Trihydroxyisoflavone	C15H10O5	Isoflavone	
				35	Purpurin 1-methyl ether	C15H10O5	Anthraquinone	
				35	2-Hydroxychrysophanol	C15H10O5	Anthraquinone	
				35	Morindone	C15H10O5	Anthraquinone	
				35	Lucidin	C15H10O5	Anthraquinone	
				35	Emodin	C15H10O5	Anthraquinone	
				35	Aloe-emodin	C15H10O5	Anthraquinone	
				35	Norwogonin	C15H10O5	Flavone	
				35	Galangin	C15H10O5	Flavone	Flavonoid biosynthesis
				35	5-Deoxykaempferol	C15H10O5	Flavonol	
				35	Baicalein	C15H10O5	Flavone	
				35	Sulphuretin	C15H10O5	Aurone	
				35	Genistein	C15H10O5	Isoflavone	Isoflavonoid and phenylpropanoid biosynthesis
				35	Apigenin	C15H10O5	Flavone	Isoflavonoid, flavonoid, phenylpropanoid, flavone and flavonol biosynthesis
				35	2'-Hydroxydaidzein	C15H10O5	Isoflavone	Isoflavonoid biosynthesis
				38	D-Lombricine	C6H15N4O6P	Amino acid	Glycine, serine and threonine metabolism
		248.0798	Na+	2	5-Hydroxyindoleacetylglycine	C12H12N2O4	Amino acid	Tryptophan metabolism
		231.9698	K+	24	2-Oxo-10-methylthiodecanoic acid	C11H20O3S	Fatty acid	2-oxocarboxylic acid and glucosinolate biosynthesis
				2	gamma-Glutamyl-GABA	C9H16N2O5	Amino acid	Arginine and proline metabolism
				12	Mexicanin E	C14H16O3	Seqsquiterpenoid	
				12	Encecalin	C14H16O3	Chromone	
				23	Cryptolepine	C16H12N2	Indole alkaloid	
				2	N6-Acetyl-LL-2,6-diaminoheptanedioate	C9H16N2O5	Amino acid	Lysine and amino acid metabolism
				2	N2-Succinyl-L-ornithine	C9H16N2O5	Amino acid	Arginine and proline metabolism
				2	N-alpha-Boc-L-asparagine	C9H16N2O5	Amino acid	
	270.9114333	269.9034333	H+					
		247.9214333	Na+					
		231.8114333	K+					
	271.0698	270.0618	H+	18	S-(Hydroxyphenylacetothiohydroximoyl)-L-cysteine	C11H14N2O4S	Amino acid	2-oxocarboxylic acid and glucosinolate biosynthesis
				35	Islandicin	C15H10O5	Anthraquinone	
				35	3,6,4'-Trihydroxyflavone	C15H10O5	Flavone	
				35	6-Hydroxydaidzein	C15H10O5	Isoflavone	Isoflavonoid biosynthesis

				35	3',4',7-Trihydroxyisoflavone	C15H10O5	Isoflavone	
				35	Purpurin 1-methyl ether	C15H10O5	Anthraquinone	
				35	2-Hydroxychrysophanol	C15H10O5	Anthraquinone	
				35	Morindone	C15H10O5	Anthraquinone	
				35	Lucidin	C15H10O5	Anthraquinone	
				35	Emodin	C15H10O5	Anthraquinone	
				35	Aloe-emodin	C15H10O5	Anthraquinone	
				35	Norwogonin	C15H10O5	Flavone	
				35	Galangin	C15H10O5	Flavone	Flavonoid biosynthesis
				35	5-Deoxykaempferol	C15H10O5	Flavonol	
				35	Baicalein	C15H10O5	Flavone	
				35	Sulphuretin	C15H10O5	Aurone	
				35	Genistein	C15H10O5	Isoflavone	Isoflavonoid and phenylpropanoid biosynthesis
				35	Apigenin	C15H10O5	Flavone	Isoflavonoid, flavonoid, phenylpropanoid, flavone and flavonol biosynthesis
				35	2'-Hydroxydaidzein	C15H10O5	Isoflavone	Isoflavonoid biosynthesis
				38	D-Lombricine	C6H15N4O6P	Amino acid	Glycine, serine and threonine metabolism
		248.0798	Na+	2	5-Hydroxyindoleacetylglycine	C12H12N2O4	Amino acid	Tryptophan metabolism
		231.9698	K+	24	2-Oxo-10-methylthiodecanoic acid	C11H20O3S	Fatty acid	2-oxocarboxylic acid and glucosinolate biosynthesis
				2	gamma-Glutamyl-GABA	C9H16N2O5	Amino acid	Arginine and proline metabolism
				12	Mexicanin E	C14H16O3	Seqsquiterpenoid	
				12	Encecalin	C14H16O3	Chromone	
				23	Cryptolepine	C16H12N2	Indole alkaloid	
				2	N6-Acetyl-LL-2,6-diaminoheptanedioate	C9H16N2O5	Amino acid	Lysine and amino acid metabolism
				2	N2-Succinyl-L-ornithine	C9H16N2O5	Amino acid	Arginine and proline metabolism
				2	N-alpha-Boc-L-asparagine	C9H16N2O5	Amino acid	
285	284.9238	283.9158	H+					
		261.9338	Na+					
		245.8238	K+					
	284.9944333	283.9864333	H+					
		262.0044333	Na+	15	(2E)-4-hydroxy-3-methylbut-2-en-1-yl trihydrogen diphosphate	C5H12O8P2	Terpenoid	Terpenoid, terpenoid backbone and steroid biosynthesis
		245.8944333	K+					
	285.0825667	284.0745667	H+	1	Xanthosine	C10H12N4O6	Nucleotide	Purine, caffeine and alkaloid biosynthesis
				23	Emodin monomethyl ether	C16H12O5	Anthraquinone	
				23	Obtusifolin	C16H12O5	Anthraquinone	
				23	(+)-Maackiain	C16H12O5	Pterocarpan	Isoflavonoid biosynthesis
				23	Glycitein	C16H12O5	Isoflavone	Isoflavonoid biosynthesis
				23	3-Methylgalangin	C16H12O5	Flavonol	
				23	Texasin	C16H12O5	Isoflavone	
				23	Prunetin	C16H12O5	Isoflavone	Isoflavonoid biosynthesis

				23	Melannin	C16H12O5	Neoflavonoid	
				23	(-)-Maackiain	C16H12O5	Pterocarpan	Isoflavonoid biosynthesis
				23	Lucidin omega-methyl ether	C16H12O5	Anthraquinone	
				23	Cypripedin	C16H12O5	Anthraquinone	
				23	Wogonin	C16H12O5	Flavone	
				23	5-Deoxychrysoeriol	C16H12O5	Flavone	
				23	Apigenin 7-methyl ether	C16H12O5	Flavone	
				23	2'-Hydroxyformononetin	C16H12O5	Isoflavone	Isoflavonoid biosynthesis
				23	3'-Hydroxyformononetin	C16H12O5	Isoflavone	Isoflavonoid biosynthesis
				23	Acacetin	C16H12O5	Flavone	Flavone and flavonol biosynthesis
				23	Questin	C16H12O5	Anthraquinone	
				23	Biochanin A	C16H12O5	Isoflavone	Isoflavonoid and phenylpropanoid biosynthesis
		262.0925667	Na+	15	Thiamine aldehyde	C12H15N4OS	Vitamin	Thiamine biosynthesis
		245.9825667	K+	7	2,4-Bis(acetamido)-2,4,6-trideoxy-beta-L-altropyranose	C10H18N2O5	Sugar	Amino acid and nucleotide sugar metabolism
				21	Zedoarol	C15H18O3	Sesquiterpenoid	
				21	Zederone	C15H18O3	Sesquiterpenoid	
				21	Isozaluzanin C	C15H18O3	Sesquiterpenoid	
				21	Zaluzanin C	C15H18O3	Sesquiterpenoid	
				21	Xerantholide	C15H18O3	Sesquiterpenoid	
				21	Xanthatin	C15H18O3	Sesquiterpenoid	
				21	beta-Santonin	C15H18O3	Sesquiterpenoid	
				21	7alpha-Hydroxydehydrocostus lactone	C15H18O3	Sesquiterpenoid	
				21	Leucodin	C15H18O3	Sesquiterpenoid	
				21	Aromaticin	C15H18O3	Sesquiterpenoid	
				21	Ambrosin	C15H18O3	Sesquiterpenoid	
				21	Olivacine	C17H14N2	Indole alkaloid	
				21	Ellipticine	C17H14N2	Indole alkaloid	
				21	alpha-Santonin	C15H18O3	Sesquiterpenoid	
	284.9266	283.9186	H+					
		261.9366	Na+					
		245.8266	K+					
	284.9911333	283.9831333	H+					
		262.0011333	Na+	4	(2E)-4-hydroxy-3-methylbut-2-en-1-yl trihydrogen diphosphate	C5H12O8P2	Terpenoid	Terpenoid, terpenoid backbone and steroid biosynthesis
		245.8911333	K+					
	285.0836667	284.0756667	H+	2	Xanthosine	C10H12N4O6	Nucleotide	Purine, caffeine and alkaloid biosynthesis
				27	Emodin monomethyl ether	C16H12O5	Anthraquinone	
				27	Obtusifolin	C16H12O5	Anthraquinone	
				27	(+)-Maackiain	C16H12O5	Pterocarpan	Isoflavonoid biosynthesis
				27	Glycitein	C16H12O5	Isoflavone	Isoflavonoid biosynthesis
				27	3-Methylgalangin	C16H12O5	Flavonol	
				27	Texasin	C16H12O5	Isoflavone	
				27	Prunetin	C16H12O5	Isoflavone	Isoflavonoid biosynthesis

				27	Melannin	C16H12O5	Neoflavonoid	
				27	(-)-Maackiain	C16H12O5	Pterocarpan	Isoflavonoid biosynthesis
				27	Lucidin omega-methyl ether	C16H12O5	Anthraquinone	
				27	Cypripedin	C16H12O5	Anthraquinone	
				27	Wogonin	C16H12O5	Flavone	
				27	5-Deoxychrysoeriol	C16H12O5	Flavone	
				27	Apigenin 7-methyl ether	C16H12O5	Flavone	
				27	2'-Hydroxyformononetin	C16H12O5	Isoflavone	Isoflavonoid biosynthesis
				27	3'-Hydroxyformononetin	C16H12O5	Isoflavone	Isoflavonoid biosynthesis
				27	Acacetin	C16H12O5	Flavone	Flavone and flavonol biosynthesis
				27	Questin	C16H12O5	Anthraquinone	
				27	Biochanin A	C16H12O5	Isoflavone	Isoflavonoid and phenylpropanoid biosynthesis
		262.0936667	Na+	19	Thiamine aldehyde	C12H15N4OS	Vitamin	Thiamine biosynthesis
		245.9836667	K+	3	2,4-Bis(acetamido)-2,4,6-trideoxy-beta-L-altropyranose	C10H18N2O5	Sugar	Amino acid and nucleotide sugar metabolism
				17	Zedoarol	C15H18O3	Sesquiterpenoid	
				17	Zederone	C15H18O3	Sesquiterpenoid	
				17	Isozaluzanin C	C15H18O3	Sesquiterpenoid	
				17	Zaluzanin C	C15H18O3	Sesquiterpenoid	
				17	Xerantholide	C15H18O3	Sesquiterpenoid	
				17	Xanthatin	C15H18O3	Sesquiterpenoid	
				17	beta-Santonin	C15H18O3	Sesquiterpenoid	
				17	7alpha-Hydroxydehydrocostus lactone	C15H18O3	Sesquiterpenoid	
				17	Leucodin	C15H18O3	Sesquiterpenoid	
				17	Aromaticin	C15H18O3	Sesquiterpenoid	
				17	Ambrosin	C15H18O3	Sesquiterpenoid	
				17	Olivacine	C17H14N2	Indole alkaloid	
				17	Ellipticine	C17H14N2	Indole alkaloid	
				17	alpha-Santonin	C15H18O3	Sesquiterpenoid	
	284.9223333	283.9143333	H+					
		261.9323333	Na+					
		245.8223333	K+					
	284.994	283.986	H+					
		262.004	Na+	14	(2E)-4-hydroxy-3-methylbut-2-en-1-yl trihydrogen diphosphate	C5H12O8P2	Terpenoid	Terpenoid, terpenoid backbone and steroid biosynthesis
		245.894	K+					
	285.0841	284.0761	H+	3	Xanthosine	C10H12N4O6	Nucleotide	Purine, caffeine and alkaloid biosynthesis
				29	Emodin monomethyl ether	C16H12O5	Anthraquinone	
				29	Obtusifolin	C16H12O5	Anthraquinone	
				29	(+)-Maackiain	C16H12O5	Pterocarpan	Isoflavonoid biosynthesis
				29	Glycitein	C16H12O5	Isoflavone	Isoflavonoid biosynthesis
				29	3-Methylgalangin	C16H12O5	Flavonol	
				29	Texasin	C16H12O5	Isoflavone	
				29	Prunetin	C16H12O5	Isoflavone	Isoflavonoid biosynthesis

				29	Melannin	C16H12O5	Neoflavonoid	
				29	(-)-Maackiain	C16H12O5	Pterocarpan	Isoflavonoid biosynthesis
				29	Lucidin omega-methyl ether	C16H12O5	Anthraquinone	
				29	Cypripedin	C16H12O5	Anthraquinone	
				29	Wogonin	C16H12O5	Flavone	
				29	5-Deoxychrysoeriol	C16H12O5	Flavone	
				29	Apigenin 7-methyl ether	C16H12O5	Flavone	
				29	2'-Hydroxyformononetin	C16H12O5	Isoflavone	Isoflavonoid biosynthesis
				29	3'-Hydroxyformononetin	C16H12O5	Isoflavone	Isoflavonoid biosynthesis
				29	Acacetin	C16H12O5	Flavone	Flavone and flavonol biosynthesis
				29	Questin	C16H12O5	Anthraquinone	
				29	Biochanin A	C16H12O5	Isoflavone	Isoflavonoid and phenylpropanoid biosynthesis
		262.0941	Na+	21	Thiamine aldehyde	C12H15N4OS	Vitamin	Thiamine biosynthesis
		245.9841	K+	2	2,4-Bis(acetamido)-2,4,6-trideoxy-beta-L-altropyranose	C10H18N2O5	Sugar	Amino acid and nucleotide sugar metabolism
				16	Zedoarol	C15H18O3	Sesquiterpenoid	
				16	Zederone	C15H18O3	Sesquiterpenoid	
				16	Isozaluzanin C	C15H18O3	Sesquiterpenoid	
				16	Zaluzanin C	C15H18O3	Sesquiterpenoid	
				16	Xerantholide	C15H18O3	Sesquiterpenoid	
				16	Xanthatin	C15H18O3	Sesquiterpenoid	
				16	beta-Santonin	C15H18O3	Sesquiterpenoid	
				16	7alpha-Hydroxydehydrocostus lactone	C15H18O3	Sesquiterpenoid	
				16	Leucodin	C15H18O3	Sesquiterpenoid	
				16	Aromaticin	C15H18O3	Sesquiterpenoid	
				16	Ambrosin	C15H18O3	Sesquiterpenoid	
				16	Olivacine	C17H14N2	Indole alkaloid	
				16	Ellipticine	C17H14N2	Indole alkaloid	
				16	alpha-Santonin	C15H18O3	Sesquiterpenoid	
539.2	539.1433667	538.1353667	H+	7	Isolimocitrol 3-glucoside	C24H26O14	Flavonol	
				7	6-Hydroxymyricetin 6,3',5'-trimethyl ether 3-glucoside	C24H26O14	Flavonol	
				7	Limocitrol 3-glucoside	C24H26O14	Flavonol	
		516.1533667	Na+	16	Luteone 7-glucoside	C26H28O11	Isoflavone	
				16	Epimedoside C	C26H28O11	Flavonoid	
				16	Vitexin 2"-O-(2'"-methylbutyryl)	C26H28O11	Flavone	
				22	Gericudranins A	C29H24O9	Dihydroflavonol	
		500.0433667	K+	22	Baohuoside II	C26H28O10	Flavone	
				22	Ikarisoside A	C26H28O10	Flavonoid	
	539.2409667	538.2329667	H+					
		516.2509667	Na+					
		500.1409667	K+					
	539.1466	538.1386	H+	13	Isolimocitrol 3-glucoside	C24H26O14	Flavonol	
				13	6-Hydroxymyricetin 6,3',5'-trimethyl ether 3-glucoside	C24H26O14	Flavonol	

				13	Limocitrol 3-glucoside	C24H26O14	Flavonol	
		516.1566	Na+	10	Luteone 7-glucoside	C26H28O11	Isoflavone	
				10	Epimedoside C	C26H28O11	Flavonoid	
				10	Vitexin 2"-O-(2'"-methylbutyryl)	C26H28O11	Flavone	
				39	Rottlerin	C30H28O8	Phloroglucinol	
		500.0466	K+	28	Gericudranins A	C29H24O9	Dihydroflavonol	
				28	Baohuoside II	C26H28O10	Flavone	
				28	Ikarisoside A	C26H28O10	Flavonoid	
	539.2466333	538.2386333	H+					
		516.2566333	Na+					
		500.1466333	K+					
	539.1476	538.1396	H+	14	Isolimocitrol 3-glucoside	C24H26O14	Flavonol	
				14	6-Hydroxymyricetin 6,3',5'-trimethyl ether 3-glucoside	C24H26O14	Flavonol	
				14	Limocitrol 3-glucoside	C24H26O14	Flavonol	
		516.1576	Na+	8	Luteone 7-glucoside	C26H28O11	Isoflavone	
				8	Epimedoside C	C26H28O11	Flavonoid	
				8	Vitexin 2"-O-(2'"-methylbutyryl)	C26H28O11	Flavone	
				38	Rottlerin	C30H28O8	Phloroglucinol	
		500.0476	K+	30	Gericudranins A	C29H24O9	Dihydroflavonol	
				30	Baohuoside II	C26H28O10	Flavone	
				30	Ikarisoside A	C26H28O10	Flavonoid	
	539.248	538.24	H+					
		516.258	Na+					
		500.148	K+					
525.2	525.1422	524.1342	H+	34	5,7,2',3',4'-Pentahydroxy-3,6-dimethoxyflavone 7-glucoside	C23H24O14	Flavone	
		502.1522	Na+	0	beta-Fabatriose	C18H30O16	Trisaccharide	
				18	Demethoxyisogemichalcone C	C29H26O8	Chalcone	
		486.0422	K+	0	Haplodimerine	C28H26N2O6	Quinoline alkaloid	
				18	Rutaevin	C26H30O9	Triterpenoid	
				18	2',4',4-Trihydroxy-3'-prenylchalcone 4'-O-glucoside	C26H30O9	Chalcone	
				21	Isogemichalcone B	C29H26O7	Chalcone	
				21	Gemichalcone B	C29H26O7	Chalcone	
	525.2699667	524.2619667	H+					
		502.2799667	Na+					
		486.1699667	K+					
	525.1418333	524.1338333	H+	34	5,7,2',3',4'-Pentahydroxy-3,6-dimethoxyflavone 7-glucoside	C23H24O14	Flavone	
		502.1518333	Na+	1	beta-Fabatriose	C18H30O16	Trisaccharide	
				19	Demethoxyisogemichalcone C	C29H26O8	Chalcone	
		486.0418333	K+	0	Haplodimerine	C28H26N2O6	Quinoline alkaloid	
				19	Rutaevin	C26H30O9	Triterpenoid	

				19	2',4',4-Trihydroxy-3'-prenylchalcone 4'-O-glucoside	C26H30O9	Chalcone	
				20	Isogemichalcone B	C29H26O7	Chalcone	
				20	Gemichalcone B	C29H26O7	Chalcone	
	525.2659	524.2579	H+					
		502.2759	Na+					
		486.1659	K+					
	525.1425667	524.1345667	H+	35	5,7,2',3',4'-Pentahydroxy-3,6-dimethoxyflavone 7-glucoside	C23H24O14	Flavone	
		502.1525667	Na+	0	beta-Fabatriose	C18H30O16	Trisaccharide	
				17	Demethoxyisogemichalcone C	C29H26O8	Chalcone	
		486.0425667	K+	0	Haplodimerine	C28H26N2O6	Quinoline alkaloid	
				18	Rutaevin	C26H30O9	Triterpenoid	
				18	2',4',4-Trihydroxy-3'-prenylchalcone 4'-O-glucoside	C26H30O9	Chalcone	
				22	Isogemichalcone B	C29H26O7	Chalcone	
				22	Gemichalcone B	C29H26O7	Chalcone	
	525.2619	524.2539	H+					
		502.2719	Na+					
		486.1619	K+					
553.2	553.1608	552.1528	H+	10	6-Hydroxymyricetin 3,6,3',5'-tetramethyl ether 7-glucoside	C25H28O14	Flavonol	
				10	1-Hydroxy-3-methoxy-7-primeverosyloxyxanthone	C25H28O14	Flavonol	
				10	5,2',5'-Trihydroxy-3,6,7,4'-tetramethoxyflavone 5'-glucoside	C25H28O14	Flavone	
				10	Gentioside	C25H28O14	Xanthone	
				10	3',5,6-Trihydroxy-3,4',7,8-tetramethoxyflavone 3-glucoside	C25H28O14	Flavone	
				17	Cucumerin A	C29H28O11	Curcuminoid	
				17	Cucumerin B	C29H28O11	Curcuminoid	
		530.1708	Na+	13	Curcumin monoglucoside	C27H30O11	Curcuminoid	Stilbenoid, diarylheptanoid and gingerol biosynthesis
				13	Wushanicariin	C27H30O11	Flavone	
				13	Icariside I	C27H30O11	Flavone	
				13	Isoswertisin 2"-O-(2'"-methylbutyrate)	C27H30O11	Flavone	
				13	8-Prenylquercetin 4'-methyl ether 3-rhamnoside	C27H30O11	Flavonol	
				13	Isoswertisin 3"-O-(2'"-methylbutyrate)	C27H30O11	Flavonol	
		514.0608	K+	24	Icariside II	C27H30O10	Flavone	
	553.1583667	552.1503667	H+	5	6-Hydroxymyricetin 3,6,3',5'-tetramethyl ether 7-glucoside	C25H28O14	Flavonol	
				5	1-Hydroxy-3-methoxy-7-primeverosyloxyxanthone	C25H28O14	Flavonol	
				5	5,2',5'-Trihydroxy-3,6,7,4'-tetramethoxyflavone 5'-glucoside	C25H28O14	Flavone	

				5	Gentioside	C25H28O14	Xanthone	
				5	3',5,6-Trihydroxy-3,4',7,8-tetramethoxyflavone 3-glucoside	C25H28O14	Flavone	
				21	Cucumerin A	C29H28O11	Curcuminoid	
				21	Cucumerin B	C29H28O11	Curcuminoid	
		530.1683667	Na+	17	Curcumin monoglucoside	C27H30O11	Curcuminoid	Stilbenoid, diarylheptanoid and gingerol biosynthesis
				17	Wushanicariin	C27H30O11	Flavone	
				17	Icariside I	C27H30O11	Flavone	
				17	Isoswertisin 2"-O-(2'"-methylbutyrate)	C27H30O11	Flavone	
				17	8-Prenylquercetin 4'-methyl ether 3-rhamnoside	C27H30O11	Flavonol	
				17	Isoswertisin 3"-O-(2'"-methylbutyrate)	C27H30O11	Flavonol	
		514.0583667	K+	20	Icariside II	C27H30O10	Flavone	
	553.1599333	552.1519333	H+	8	6-Hydroxymyricetin 3,6,3',5'-tetramethyl ether 7-glucoside	C25H28O14	Flavonol	
				8	1-Hydroxy-3-methoxy-7-primeverosyloxyxanthone	C25H28O14	Flavonol	
				8	5,2',5'-Trihydroxy-3,6,7,4'-tetramethoxyflavone 5'-glucoside	C25H28O14	Flavone	
				8	Gentioside	C25H28O14	Xanthone	
				8	3',5,6-Trihydroxy-3,4',7,8-tetramethoxyflavone 3-glucoside	C25H28O14	Flavone	
				18	Cucumerin A	C29H28O11	Curcuminoid	
				18	Cucumerin B	C29H28O11	Curcuminoid	
		530.1699333	Na+	14	Curcumin monoglucoside	C27H30O11	Curcuminoid	Stilbenoid, diarylheptanoid and gingerol biosynthesis
				14	Wushanicariin	C27H30O11	Flavone	
				14	Icariside I	C27H30O11	Flavone	
				14	Isoswertisin 2"-O-(2'"-methylbutyrate)	C27H30O11	Flavone	
				14	8-Prenylquercetin 4'-methyl ether 3-rhamnoside	C27H30O11	Flavonol	
				14	Isoswertisin 3"-O-(2'"-methylbutyrate)	C27H30O11	Flavonol	
		514.0599333	K+	23	Icariside II	C27H30O10	Flavone	
541.2	541.1327	540.1247	H+					
		518.1427	Na+	1	Medicarpin 3-O-glucoside-6'-malonate	C25H26O12	Pterocarpan	Isoflavonoid biosynthesis
				1	Scutellarein 6,4'-dimethyl ether 7-(6"-acetylglucoside)	C25H26O12	Flavone	
		502.0327	K+	29	beta-Fabatriose	C18H30O16	Trisaccharide	
				12	Demethoxyisogemichalcone C	C29H26O8	Chalcone	
				26	Limonexic acid	C26H30O10	Terpenoid	
				26	Phellodensin F	C26H30O10	Flavonoid	
	541.2504	540.2424	H+					
		518.2604	Na+	9	ditrans,dicis-Pentaprenyl diphosphate	C25H44O7P2	Isoprenoid	
				9	Geranylfarnesyl diphosphate	C25H44O7P2	Isoprenoid	
		502.1504	K+	38	Kolanone	C33H42O4	Isoprenoid	

	541.1341667	540.1261667	H+					
		518.1441667	Na+	4	Medicarpin 3-O-glucoside-6'-malonate	C25H26O12	Pterocarpan	Isoflavonoid biosynthesis
				4	Scutellarein 6,4'-dimethyl ether 7-(6''-acetylglucoside)	C25H26O12	Flavone	
		502.0341667	K+	32	beta-Fabatriose	C18H30O16	Trisaccharide	
				15	Demethoxyisogemichalcone C	C29H26O8	Chalcone	
				23	Limonexic acid	C26H30O10	Terpenoid	
				23	Phellodensin F	C26H30O10	Flavonoid	
	541.2503	540.2423	H+					
		518.2603	Na+	8	ditrans,dicis-Pentaprenyl diphosphate	C25H44O7P2	Isoprenoid	
				8	Geranylfarnesyl diphosphate	C25H44O7P2	Isoprenoid	
		502.1503	K+	39	Kolanone	C33H42O4	Isoprenoid	
	541.1348667	540.1268667	H+					
		518.1448667	Na+	5	Medicarpin 3-O-glucoside-6'-malonate	C25H26O12	Pterocarpan	Isoflavonoid biosynthesis
				5	Scutellarein 6,4'-dimethyl ether 7-(6''-acetylglucoside)	C25H26O12	Flavone	
		502.0348667	K+	33	beta-Fabatriose	C18H30O16	Trisaccharide	
				16	Demethoxyisogemichalcone C	C29H26O8	Chalcone	
				22	Limonexic acid	C26H30O10	Terpenoid	
				22	Phellodensin F	C26H30O10	Flavonoid	
	541.2507	540.2427	H+					
		518.2607	Na+	9	ditrans,dicis-Pentaprenyl diphosphate	C25H44O7P2	Isoprenoid	
				9	Geranylfarnesyl diphosphate	C25H44O7P2	Isoprenoid	
		502.1507	K+	38	Kolanone	C33H42O4	Isoprenoid	
555.2	555.145	554.137	H+	23	3-O-(6-O-alpha-D-Xylosylphospho-alpha-D-mannopyranosyl)-alpha-D-mannopyranose	C17H31O18P	Trisaccharide	
		532.155	Na+	31	Trichotomine	C30H20N4O6	Alkaloid	
				4	Flavonol 3-O-D-xylosylglycoside	C26H28O12	Flavonol	
				4	Orientin 2''-O-(2'''-methylbutyrate)	C26H28O12	Flavone	
				4	Luteolin 7-[6''-(2-methylbutyryl)glucoside]	C26H28O12	Flavone	
				4	Isoscutellarein 4'-methyl ether 8-(6''-n-butylglucuronide)	C26H28O12	Flavone	
				4	5,7-Dihydroxy-6-C-methylflavone 7-xylosyl-(1->3)-xyloside	C26H28O12	Flavone	
				4	Sesaminol glucoside	C26H28O12	Lignan	
				31	Isogemichalcone C	C30H28O9	Chalcone	
				31	Gemichalcone C	C30H28O9	Chalcone	
				31	4-Hydroxyrottlerin	C30H28O9	Phloroglucinol	
		516.045	K+	6	Rottlerin	C30H28O8	Phloroglucinol	
				31	Spicatin	C27H32O10	Sesquiterpenoid	
				31	Harrisonin	C27H32O10	Triterpenoid	
				4	Cyclocalopin D	C23H32O13	Furopyran	
				6	Gemichalcone A	C30H28O8	Chalcone	
				33	Vitexin 2''-O-(2'''-methylbutyryl)	C26H28O11	Flavone	
				33	Luteone 7-glucoside	C26H28O11	Flavone	

				33	Epimedoside C	C26H28O11	Flavanonol	
	555.2496	554.2416	H+	16	Toonacilin	C31H38O9	Triterpenoid	
		532.2596	Na+	12	Calotropin	C29H40O9	Cardiac glycoside	
		516.1496	K+					
	555.1468667	554.1388667	H+	26	3-O-(6-O-alpha-D-Xylosylphospho-alpha-D-mannopyranosyl)-alpha-D-mannopyranose	C17H31O18P	Trisaccharide	
		532.1568667	Na+	34	Trichotomine	C30H20N4O6	Alkaloid	
				0	Flavonol 3-O-D-xylosylglycoside	C26H28O12	Flavonol	
				0	Orientin 2"-O-(2'"-methylbutyrate)	C26H28O12	Flavone	
				0	Luteolin 7-[6"-(2-methylbutyryl)glucoside]	C26H28O12	Flavone	
				0	Isoscutellarein 4'-methyl ether 8-(6"-n-butylglucuronide)	C26H28O12	Flavone	
				0	5,7-Dihydroxy-6-C-methylflavone 7-xylosyl-(1->3)-xyloside	C26H28O12	Flavone	
				0	Sesaminol glucoside	C26H28O12	Lignan	
				28	Isogemichalcone C	C30H28O9	Chalcone	
				28	Gemichalcone C	C30H28O9	Chalcone	
				28	4-Hydroxyrottlerin	C30H28O9	Phloroglucinol	
		516.0468667	K+	9	Rottlerin	C30H28O8	Phloroglucinol	
				28	Spicatin	C27H32O10	Sesquiterpenoid	
				28	Harrisonin	C27H32O10	Triterpenoid	
				1	Cyclocalopin D	C23H32O13	Furopyran	
				9	Gemichalcone A	C30H28O8	Chalcone	
				37	Vitexin 2"-O-(2'"-methylbutyryl)	C26H28O11	Flavone	
				37	Luteone 7-glucoside	C26H28O11	Flavone	
				37	Epimedoside C	C26H28O11	Flavanonol	
	555.2524667	554.2444667	H+	11	Toonacilin	C31H38O9	Triterpenoid	
		532.2624667	Na+	7	Calotropin	C29H40O9	Cardiac glycoside	
		516.1524667	K+	34	Adynerin	C30H44O7	Cardiac glycoside	
	555.1477	554.1397	H+	28	3-O-(6-O-alpha-D-Xylosylphospho-alpha-D-mannopyranosyl)-alpha-D-mannopyranose	C17H31O18P	Trisaccharide	
		532.1577	Na+	26	Trichotomine	C30H20N4O6	Alkaloid	
				0	Flavonol 3-O-D-xylosylglycoside	C26H28O12	Flavonol	
				0	Orientin 2"-O-(2'"-methylbutyrate)	C26H28O12	Flavone	
				0	Luteolin 7-[6"-(2-methylbutyryl)glucoside]	C26H28O12	Flavone	
				0	Isoscutellarein 4'-methyl ether 8-(6"-n-butylglucuronide)	C26H28O12	Flavone	
				0	5,7-Dihydroxy-6-C-methylflavone 7-xylosyl-(1->3)-xyloside	C26H28O12	Flavone	
				0	Sesaminol glucoside	C26H28O12	Lignan	
				26	Isogemichalcone C	C30H28O9	Chalcone	
				26	Gemichalcone C	C30H28O9	Chalcone	

				26	4-Hydroxyrottlerin	C30H28O9	Phloroglucinol	
		516.0477	K+	22	Rottlerin	C30H28O8	Phloroglucinol	
				27	Spicatin	C27H32O10	Sesquiterpenoid	
				27	Harrisonin	C27H32O10	Triterpenoid	
				0	Cyclocalopin D	C23H32O13	Furopyran	
				11	Gemichalcone A	C30H28O8	Chalcone	
				38	Vitexin 2"-O-(2'"-methylbutyryl)	C26H28O11	Flavone	
				38	Luteone 7-glucoside	C26H28O11	Flavone	
				38	Epimedoside C	C26H28O11	Flavanonol	
	555.2533333	554.2453333	H+	9	Toonacilin	C31H38O9	Triterpenoid	
		532.2633333	Na+	5	Calotropin	C29H40O9	Cardiac glycoside	
		516.1533333	K+	3	Adynerin	C30H44O7	Cardiac glycoside	

Table B3.8 Cracka sorghum polyphenol extract putative identifications from OPLS-DA (MALDI [+])

Bin	Detected Mass	Accurate Mass	Adduct	Δppm	Name	Formula	Chemical Group	Pathway
271	270.9095333	269.9015333	H+					
		247.9195333	Na+					
		231.8095333	K+					
	271.0695333	270.0615333	H+	19	S-(Hydroxyphenylacetothiohydroximoyl)-L-cysteine	C11H14N2O4S	Amino acid	2-oxocarboxylic acid and glucosinolate biosynthesis
				34	Islandicin	C15H10O5	Anthraquinone	
				34	3,6,4'-Trihydroxyflavone	C15H10O5	Flavone	
				34	6-Hydroxydaidzein	C15H10O5	Isoflavone	Isoflavonoid biosynthesis
				34	3',4',7-Trihydroxyisoflavone	C15H10O5	Isoflavone	
				34	Purpurin 1-methyl ether	C15H10O5	Anthraquinone	
				34	2-Hydroxychrysophanol	C15H10O5	Anthraquinone	
				34	Morindone	C15H10O5	Anthraquinone	
				34	Lucidin	C15H10O5	Anthraquinone	
				34	Emodin	C15H10O5	Anthraquinone	
				34	Aloe-emodin	C15H10O5	Anthraquinone	
				34	Norwogonin	C15H10O5	Flavone	
				34	Galangin	C15H10O5	Flavone	Flavonoid biosynthesis
				34	5-Deoxykaempferol	C15H10O5	Flavonol	
				34	Baicalein	C15H10O5	Flavone	
				34	Sulphuretin	C15H10O5	Aurone	
				34	Genistein	C15H10O5	Isoflavone	Isoflavonoid and phenylpropanoid biosynthesis
				34	Apigenin	C15H10O5	Flavone	Isoflavonoid, flavonoid, phenylpropanoid, flavone and flavonol biosynthesis

				34	2'-Hydroxydaidzein	C15H10O5	Isoflavone	Isoflavonoid biosynthesis
				39	D-Lombricine	C6H15N4O6P	Amino acid	Glycine, serine and threonine metabolism
		248.0795333	Na+	2	5-Hydroxyindoleacetylglycine	C12H12N2O4	Amino acid	Tryptophan metabolism
		231.9695333	K+	25	2-Oxo-10-methylthiodecanoic acid	C11H20O3S	Fatty acid	2-oxocarboxylic acid and glucosinolate biosynthesis
				1	gamma-Glutamyl-GABA	C9H16N2O5	Amino acid	Arginine and proline metabolism
				13	Mexicanin E	C14H16O3	Seqsquiterpenoid	
				13	Encecalin	C14H16O3	Chromone	
				23	Cryptolepine	C16H12N2	Indole alkaloid	
				1	N6-Acetyl-LL-2,6-diaminoheptanedioate	C9H16N2O5	Amino acid	Lysine and amino acid metabolism
				1	N2-Succinyl-L-ornithine	C9H16N2O5	Amino acid	Arginine and proline metabolism
				1	N-alpha-Boc-L-asparagine	C9H16N2O5	Amino acid	
	270.9105333	269.9025333	H+					
		247.9205333	Na+					
		231.8105333	K+					
	271.0698667	270.0618667	H+	17	S-(Hydroxyphenylacetothiohydroximoyl)-L-cysteine	C11H14N2O4S	Amino acid	2-oxocarboxylic acid and glucosinolate biosynthesis
				36	Islandicin	C15H10O5	Anthraquinone	
				36	3,6,4'-Trihydroxyflavone	C15H10O5	Flavone	
				36	6-Hydroxydaidzein	C15H10O5	Isoflavone	Isoflavonoid biosynthesis
				36	3',4',7-Trihydroxyisoflavone	C15H10O5	Isoflavone	
				36	Purpurin 1-methyl ether	C15H10O5	Anthraquinone	
				36	2-Hydroxychrysophanol	C15H10O5	Anthraquinone	
				36	Morindone	C15H10O5	Anthraquinone	
				36	Lucidin	C15H10O5	Anthraquinone	
				36	Emodin	C15H10O5	Anthraquinone	
				36	Aloe-emodin	C15H10O5	Anthraquinone	
				36	Norwogonin	C15H10O5	Flavone	
				36	Galangin	C15H10O5	Flavone	Flavonoid biosynthesis
				36	5-Deoxykaempferol	C15H10O5	Flavonol	
				36	Baicalein	C15H10O5	Flavone	
				36	Sulphuretin	C15H10O5	Aurone	
				36	Genistein	C15H10O5	Isoflavone	Isoflavonoid and phenylpropanoid biosynthesis
				36	Apigenin	C15H10O5	Flavone	Isoflavonoid, flavonoid, phenylpropanoid, flavone and flavonol biosynthesis
				36	2'-Hydroxydaidzein	C15H10O5	Isoflavone	Isoflavonoid biosynthesis
				38	D-Lombricine	C6H15N4O6P	Amino acid	Glycine, serine and threonine metabolism
		248.0798667	Na+	3	5-Hydroxyindoleacetylglycine	C12H12N2O4	Amino acid	Tryptophan metabolism

		231.9698667	K+	24	2-Oxo-10-methylthiodecanoic acid	C11H20O3S	Fatty acid	2-oxocarboxylic acid and glucosinolate biosynthesis
				2	gamma-Glutamyl-GABA	C9H16N2O5	Amino acid	Arginine and proline metabolism
				11	Mexicanin E	C14H16O3	Seqsquiterpenoid	
				11	Encecalin	C14H16O3	Chromone	
				24	Cryptolepine	C16H12N2	Indole alkaloid	
				2	N6-Acetyl-LL-2,6-diaminoheptanedioate	C9H16N2O5	Amino acid	Lysine and amino acid metabolism
				2	N2-Succinyl-L-ornithine	C9H16N2O5	Amino acid	Arginine and proline metabolism
				2	N-alpha-Boc-L-asparagine	C9H16N2O5	Amino acid	
	270.9090667	269.9010667	H+					
		247.9190667	Na+					
		231.8090667	K+					
	270.9733667	269.9653667	H+					
		247.9833667	Na+					
		231.8733667	K+					
	271.0700667	270.0620667	H+	17	S-(Hydroxyphenylacetothiohydroximoyl)-L-cysteine	C11H14N2O4S	Amino acid	2-oxocarboxylic acid and glucosinolate biosynthesis
				36	Islandicin	C15H10O5	Anthraquinone	
				36	3,6,4'-Trihydroxyflavone	C15H10O5	Flavone	
				36	6-Hydroxydaidzein	C15H10O5	Isoflavone	Isoflavonoid biosynthesis
				36	3',4',7-Trihydroxyisoflavone	C15H10O5	Isoflavone	
				36	Purpurin 1-methyl ether	C15H10O5	Anthraquinone	
				36	2-Hydroxychrysophanol	C15H10O5	Anthraquinone	
				36	Morindone	C15H10O5	Anthraquinone	
				36	Lucidin	C15H10O5	Anthraquinone	
				36	Emodin	C15H10O5	Anthraquinone	
				36	Aloe-emodin	C15H10O5	Anthraquinone	
				36	Norwogonin	C15H10O5	Flavone	
				36	Galangin	C15H10O5	Flavone	Flavonoid biosynthesis
				36	5-Deoxykaempferol	C15H10O5	Flavonol	
				36	Baicalein	C15H10O5	Flavone	
				36	Sulphuretin	C15H10O5	Aurone	
				36	Genistein	C15H10O5	Isoflavone	Isoflavonoid and phenylpropanoid biosynthesis
				36	Apigenin	C15H10O5	Flavone	Isoflavonoid, flavonoid, phenylpropanoid, flavone and flavonol biosynthesis
				36	2'-Hydroxydaidzein	C15H10O5	Isoflavone	Isoflavonoid biosynthesis
				37	D-Lombricine	C6H15N4O6P	Amino acid	Glycine, serine and threonine metabolism
		248.0800667	Na+	4	5-Hydroxyindoleacetylglycine	C12H12N2O4	Amino acid	Tryptophan metabolism
		231.9700667	K+	23	2-Oxo-10-methylthiodecanoic acid	C11H20O3S	Fatty acid	2-oxocarboxylic acid and glucosinolate biosynthesis

				3	gamma-Glutamyl-GABA	C9H16N2O5	Amino acid	Arginine and proline metabolism
				11	Mexicanin E	C14H16O3	Seqsquiterpenoid	
				11	Encecalin	C14H16O3	Chromone	
				25	Cryptolepine	C16H12N2	Indole alkaloid	
				3	N6-Acetyl-LL-2,6-diaminoheptanedioate	C9H16N2O5	Amino acid	Lysine and amino acid metabolism
				3	N2-Succinyl-L-ornithine	C9H16N2O5	Amino acid	Arginine and proline metabolism
				3	N-alpha-Boc-L-asparagine	C9H16N2O5	Amino acid	
285	284.9301333	283.9221333	H+					
		261.9401333	Na+					
		245.8301333	K+					
	284.9909333	283.9829333	H+					
		262.0009333	Na+	3	(2E)-4-hydroxy-3-methylbut-2-en-1-yl trihydrogen diphosphate	C5H12O8P2	Terpenoid	Terpenoid, terpenoid backbone and steroid biosynthesis
		245.8909333	K+					
	285.0847333	284.0767333	H+	6	Xanthosine	C10H12N4O6	Nucleotide	Purine, caffeine and alkaloid biosynthesis
				31	Emodin monomethyl ether	C16H12O5	Anthraquinone	
				31	Obtusifolin	C16H12O5	Anthraquinone	
				31	(+)-Maackiain	C16H12O5	Pterocarpan	Isoflavonoid biosynthesis
				31	Glycitein	C16H12O5	Isoflavone	Isoflavonoid biosynthesis
				31	3-Methylgalangin	C16H12O5	Flavonol	
				31	Texasin	C16H12O5	Isoflavone	
				31	Prunetin	C16H12O5	Isoflavone	Isoflavonoid biosynthesis
				31	Melannin	C16H12O5	Neoflavonoid	
				31	(-)-Maackiain	C16H12O5	Pterocarpan	Isoflavonoid biosynthesis
				31	Lucidin omega-methyl ether	C16H12O5	Anthraquinone	
				31	Cypripedin	C16H12O5	Anthraquinone	
				31	Wogonin	C16H12O5	Flavone	
				31	5-Deoxychrysoeriol	C16H12O5	Flavone	
				31	Apigenin 7-methyl ether	C16H12O5	Flavone	
				31	2'-Hydroxyformononetin	C16H12O5	Isoflavone	Isoflavonoid biosynthesis
				31	3'-Hydroxyformononetin	C16H12O5	Isoflavone	Isoflavonoid biosynthesis
				31	Acacetin	C16H12O5	Flavone	Flavone and flavonol biosynthesis
				31	Questin	C16H12O5	Anthraquinone	
				31	Biochanin A	C16H12O5	Isoflavone	Isoflavonoid and phenylpropanoid biosynthesis
		262.0947333	Na+	23	Thiamine aldehyde	C12H15N4OS	Vitamin	Thiamine biosynthesis
		245.9847333	K+	0	2,4-Bis(acetamido)-2,4,6-trideoxy-beta-L-altropyranose	C10H18N2O5	Sugar	Amino acid and nucleotide sugar metabolism
				14	Zedoarol	C15H18O3	Sesquiterpenoid	

				14	Zederone	C15H18O3	Sesquiterpenoid	
				14	Isozaluzanin C	C15H18O3	Sesquiterpenoid	
				14	Zaluzanin C	C15H18O3	Sesquiterpenoid	
				14	Xerantholide	C15H18O3	Sesquiterpenoid	
				14	Xanthatin	C15H18O3	Sesquiterpenoid	
				14	beta-Santonin	C15H18O3	Sesquiterpenoid	
				14	7alpha-Hydroxydehydrocostus lactone	C15H18O3	Sesquiterpenoid	
				14	Leucodin	C15H18O3	Sesquiterpenoid	
				14	Aromaticin	C15H18O3	Sesquiterpenoid	
				14	Ambrosin	C15H18O3	Sesquiterpenoid	
				20	Olivacine	C17H14N2	Indole alkaloid	
				20	Ellipticine	C17H14N2	Indole alkaloid	
				14	alpha-Santonin	C15H18O3	Sesquiterpenoid	
				39	Octopine	C9H18N4O4	Amino acid	Arginine and proline metabolism
				39	N2-(2-Carboxyethyl)-L-arginine	C9H18N4O4	Amino acid	Clavulanic acid biosynthesis
	284.9898	283.9818	H+					
		261.9998	Na+	0	(2E)-4-hydroxy-3-methylbut-2-en-1-yl trihydrogen diphosphate	C5H12O8P2	Terpenoid	Terpenoid, terpenoid backbone and steroid biosynthesis
		245.8898	K+					
	285.0851333	284.0771333	H+	7	Xanthosine	C10H12N4O6	Nucleotide	Purine, caffeine and alkaloid biosynthesis
				32	Emodin monomethyl ether	C16H12O5	Anthraquinone	
				32	Obtusifolin	C16H12O5	Anthraquinone	
				32	(+)-Maackiain	C16H12O5	Pterocarpan	Isoflavonoid biosynthesis
				32	Glycitein	C16H12O5	Isoflavone	Isoflavonoid biosynthesis
				32	3-Methylgalangin	C16H12O5	Flavonol	
				32	Texasin	C16H12O5	Isoflavone	
				32	Prunetin	C16H12O5	Isoflavone	Isoflavonoid biosynthesis
				32	Melannin	C16H12O5	Neoflavonoid	
				32	(-)-Maackiain	C16H12O5	Pterocarpan	Isoflavonoid biosynthesis
				32	Lucidin omega-methyl ether	C16H12O5	Anthraquinone	
				32	Cypripedin	C16H12O5	Anthraquinone	
				32	Wogonin	C16H12O5	Flavone	
				32	5-Deoxychrysoeriol	C16H12O5	Flavone	
				32	Apigenin 7-methyl ether	C16H12O5	Flavone	
				32	2'-Hydroxyformononetin	C16H12O5	Isoflavone	Isoflavonoid biosynthesis
				32	3'-Hydroxyformononetin	C16H12O5	Isoflavone	Isoflavonoid biosynthesis
				32	Acacetin	C16H12O5	Flavone	Flavone and flavonol biosynthesis
				32	Questin	C16H12O5	Anthraquinone	
				32	Biochanin A	C16H12O5	Isoflavone	Isoflavonoid and phenylpropanoid biosynthesis
		262.0951333	Na+	24	Thiamine aldehyde	C12H15N4OS	Vitamin	Thiamine biosynthesis

		245.9851333	K+	1	2,4-Bis(acetamido)-2,4,6-trideoxy-beta-L-altropyranose	C10H18N2O5	Sugar	Amino acid and nucleotide sugar metabolism
				12	Zedoarol	C15H18O3	Sesquiterpenoid	
				12	Zederone	C15H18O3	Sesquiterpenoid	
				12	Isozaluzanin C	C15H18O3	Sesquiterpenoid	
				12	Zaluzanin C	C15H18O3	Sesquiterpenoid	
				12	Xerantholide	C15H18O3	Sesquiterpenoid	
				12	Xanthatin	C15H18O3	Sesquiterpenoid	
				12	beta-Santonin	C15H18O3	Sesquiterpenoid	
				12	7alpha-Hydroxydehydrocostus lactone	C15H18O3	Sesquiterpenoid	
				12	Leucodin	C15H18O3	Sesquiterpenoid	
				12	Aromaticin	C15H18O3	Sesquiterpenoid	
				12	Ambrosin	C15H18O3	Sesquiterpenoid	
				22	Olivacine	C17H14N2	Indole alkaloid	
				22	Ellipticine	C17H14N2	Indole alkaloid	
				12	alpha-Santonin	C15H18O3	Sesquiterpenoid	
				37	Octopine	C9H18N4O4	Amino acid	Arginine and proline metabolism
				37	N2-(2-Carboxyethyl)-L-arginine	C9H18N4O4	Amino acid	Clavulanic acid biosynthesis
	284.9129	283.9049	H+					
		261.9229	Na+					
		245.8129	K+					
	284.9907667	283.9827667	H+					
		262.0007667	Na+	2	(2E)-4-hydroxy-3-methylbut-2-en-1-yl trihydrogen diphosphate	C5H12O8P2	Terpenoid	Terpenoid, terpenoid backbone and steroid biosynthesis
		245.8907667	K+					
	285.0852667	284.0772667	H+	8	Xanthosine	C10H12N4O6	Nucleotide	Purine, caffeine and alkaloid biosynthesis
				33	Emodin monomethyl ether	C16H12O5	Anthraquinone	
				33	Obtusifolin	C16H12O5	Anthraquinone	
				33	(+)-Maackiain	C16H12O5	Pterocarpan	Isoflavonoid biosynthesis
				33	Glycitein	C16H12O5	Isoflavone	Isoflavonoid biosynthesis
				33	3-Methylgalangin	C16H12O5	Flavonol	
				33	Texasin	C16H12O5	Isoflavone	
				33	Prunetin	C16H12O5	Isoflavone	Isoflavonoid biosynthesis
				33	Melannin	C16H12O5	Neoflavonoid	
				33	(-)-Maackiain	C16H12O5	Pterocarpan	Isoflavonoid biosynthesis
				33	Lucidin omega-methyl ether	C16H12O5	Anthraquinone	
				33	Cypripedin	C16H12O5	Anthraquinone	
				33	Wogonin	C16H12O5	Flavone	
				33	5-Deoxychrysoeriol	C16H12O5	Flavone	
				33	Apigenin 7-methyl ether	C16H12O5	Flavone	
				33	2'-Hydroxyformononetin	C16H12O5	Isoflavone	Isoflavonoid biosynthesis
				33	3'-Hydroxyformononetin	C16H12O5	Isoflavone	Isoflavonoid biosynthesis

				33	Acacetin	C16H12O5	Flavone	Flavone and flavonol biosynthesis
				33	Questin	C16H12O5	Anthraquinone	
				33	Biochanin A	C16H12O5	Isoflavone	Isoflavonoid and phenylpropanoid biosynthesis
		262.0952667	Na+	25	Thiamine aldehyde	C12H15N4OS	Vitamin	Thiamine biosynthesis
		245.9852667	K+	1	2,4-Bis(acetamido)-2,4,6-trideoxy-beta-L-altropyranose	C10H18N2O5	Sugar	Amino acid and nucleotide sugar metabolism
				12	Zedoarol	C15H18O3	Sesquiterpenoid	
				12	Zederone	C15H18O3	Sesquiterpenoid	
				12	Isozaluzanin C	C15H18O3	Sesquiterpenoid	
				12	Zaluzanin C	C15H18O3	Sesquiterpenoid	
				12	Xerantholide	C15H18O3	Sesquiterpenoid	
				12	Xanthatin	C15H18O3	Sesquiterpenoid	
				12	beta-Santonin	C15H18O3	Sesquiterpenoid	
				12	7alpha-Hydroxydehydrocostus lactone	C15H18O3	Sesquiterpenoid	
				12	Leucodin	C15H18O3	Sesquiterpenoid	
				12	Aromaticin	C15H18O3	Sesquiterpenoid	
				12	Ambrosin	C15H18O3	Sesquiterpenoid	
				22	Olivacine	C17H14N2	Indole alkaloid	
				22	Ellipticine	C17H14N2	Indole alkaloid	
				12	alpha-Santonin	C15H18O3	Sesquiterpenoid	
				37	Octopine	C9H18N4O4	Amino acid	Arginine and proline metabolism
				37	N2-(2-Carboxyethyl)-L-arginine	C9H18N4O4	Amino acid	Clavulanic acid biosynthesis
555.2	555.1489667	554.1409667	H+	30	3-O-(6-O-alpha-D-Xylosylphospho-alpha-D-mannopyranosyl)-alpha-D-mannopyranose	C17H31O18P	Trisaccharide	
		532.1589667	Na+	38	Trichotomine	C30H20N4O6	Alkaloid	
				3	Flavonol 3-O-D-xylosylglycoside	C26H28O12	Flavonol	
				3	Orientin 2"-O-(2"'-methylbutyrate)	C26H28O12	Flavone	
				3	Luteolin 7-[6"-(2-methylbutyryl)glucoside]	C26H28O12	Flavone	
				3	Isoscutellarein 4'-methyl ether 8-(6"-n-butylglucuronide)	C26H28O12	Flavone	
				3	5,7-Dihydroxy-6-C-methylflavone 7-xylosyl-(1->3)-xyloside	C26H28O12	Flavone	
				3	Sesaminol glucoside	C26H28O12	Lignan	
				24	Isogemichalcone C	C30H28O9	Chalcone	
				24	Gemichalcone C	C30H28O9	Chalcone	
				24	4-Hydroxyrottlerin	C30H28O9	Phloroglucinol	
		516.0489667	K+	13	Rottlerin	C30H28O8	Phloroglucinol	
				24	Spicatin	C27H32O10	Sesquiterpenoid	
				24	Harrisonin	C27H32O10	Triterpenoid	
				2	Cyclocalopin D	C23H32O13	Furopyran	
				13	Gemichalcone A	C30H28O8	Chalcone	

	555.1488333	554.1408333	H+	30	3-O-(6-O-alpha-D-Xylosylphospho-alpha-D-mannopyranosyl)-alpha-D-mannopyranose	C17H31O18P	Trisaccharide	
		532.1588333	Na+	38	Trichotomine	C30H20N4O6	Alkaloid	
				2	Flavonol 3-O-D-xylosylglycoside	C26H28O12	Flavonol	
				2	Orientin 2"-O-(2"'-methylbutyrate)	C26H28O12	Flavone	
				2	Luteolin 7-[6"-(2-methylbutyryl)glucoside]	C26H28O12	Flavone	
				2	Isoscutellarein 4'-methyl ether 8-(6"-n-butylglucuronide)	C26H28O12	Flavone	
				2	5,7-Dihydroxy-6-C-methylflavone 7-xylosyl-(1->3)-xyloside	C26H28O12	Flavone	
				2	Sesaminol glucoside	C26H28O12	Lignan	
				24	Isogemichalcone C	C30H28O9	Chalcone	
				24	Gemichalcone C	C30H28O9	Chalcone	
				24	4-Hydroxyrottlerin	C30H28O9	Phloroglucinol	
		516.0488333	K+	13	Rottlerin	C30H28O8	Phloroglucinol	
				24	Spicatin	C27H32O10	Sesquiterpenoid	
				24	Harrisonin	C27H32O10	Triterpenoid	
				2	Cyclocalopin D	C23H32O13	Furopyran	
				13	Gemichalcone A	C30H28O8	Chalcone	
	555.2518667	554.2438667	H+	12	Toonacilin	C31H38O9	Triterpenoid	
		532.2618667	Na+	8	Calotropin	C29H40O9	Cardiac glycoside	
		516.1518667	K+	36	Adynerin	C30H44O7	Cardiac glycoside	
	555.1509	554.1429	H+	33	3-O-(6-O-alpha-D-Xylosylphospho-alpha-D-mannopyranosyl)-alpha-D-mannopyranose	C17H31O18P	Trisaccharide	
		532.1609	Na+	6	Flavonol 3-O-D-xylosylglycoside	C26H28O12	Flavonol	
				6	Orientin 2"-O-(2"'-methylbutyrate)	C26H28O12	Flavone	
				6	Luteolin 7-[6"-(2-methylbutyryl)glucoside]	C26H28O12	Flavone	
				6	Isoscutellarein 4'-methyl ether 8-(6"-n-butylglucuronide)	C26H28O12	Flavone	
				6	5,7-Dihydroxy-6-C-methylflavone 7-xylosyl-(1->3)-xyloside	C26H28O12	Flavone	
				6	Sesaminol glucoside	C26H28O12	Lignan	
				20	Isogemichalcone C	C30H28O9	Chalcone	
				20	Gemichalcone C	C30H28O9	Chalcone	
				20	4-Hydroxyrottlerin	C30H28O9	Phloroglucinol	
		516.0509	K+	16	Rottlerin	C30H28O8	Phloroglucinol	
				21	Spicatin	C27H32O10	Sesquiterpenoid	
				21	Harrisonin	C27H32O10	Triterpenoid	
				6	Cyclocalopin D	C23H32O13	Furopyran	
				16	Gemichalcone A	C30H28O8	Chalcone	
541.2	541.1338333	540.1258333	H+					
		518.1438333	Na+	4	Medicarpin 3-O-glucoside-6'-malonate	C25H26O12	Pterocarpan	Isoflavonoid biosynthesis
				4	Scutellarein 6,4'-dimethyl ether 7-(6"-acetylglucoside)	C25H26O12	Flavone	

		502.0338333	K+	31	beta-Fabatriose	C18H30O16	Trisaccharide	
				14	Demethoxyisogemichalcone C	C29H26O8	Chalcone	
				24	Limonexic acid	C26H30O10	Terpenoid	
				24	Phellodensin F	C26H30O10	Flavonoid	
	541.2579333	540.2499333	H+					
		518.2679333	Na+	23	ditrans,dicis-Pentaprenyl diphosphate	C25H44O7P2	Isoprenoid	
				23	Geranylfarnesyl diphosphate	C25H44O7P2	Isoprenoid	
		502.1579333	K+	25	Kolanone	C33H42O4	Isoprenoid	
	541.1342	540.1262	H+					
		518.1442	Na+	4	Medicarpin 3-O-glucoside-6'-malonate	C25H26O12	Pterocarpan	Isoflavonoid biosynthesis
				4	Scutellarein 6,4'-dimethyl ether 7-(6"-acetylglucoside)	C25H26O12	Flavone	
		502.0342	K+	32	beta-Fabatriose	C18H30O16	Trisaccharide	
				15	Demethoxyisogemichalcone C	C29H26O8	Chalcone	
				23	Limonexic acid	C26H30O10	Terpenoid	
				23	Phellodensin F	C26H30O10	Flavonoid	
	541.2581667	540.2501667	H+					
		518.2681667	Na+	23	ditrans,dicis-Pentaprenyl diphosphate	C25H44O7P2	Isoprenoid	
				23	Geranylfarnesyl diphosphate	C25H44O7P2	Isoprenoid	
		502.1581667	K+	24	Kolanone	C33H42O4	Isoprenoid	
	541.1350333	540.1270333	H+					
		518.1450333	Na+	6	Medicarpin 3-O-glucoside-6'-malonate	C25H26O12	Pterocarpan	Isoflavonoid biosynthesis
				6	Scutellarein 6,4'-dimethyl ether 7-(6"-acetylglucoside)	C25H26O12	Flavone	
		502.0350333	K+	34	beta-Fabatriose	C18H30O16	Trisaccharide	
				16	Demethoxyisogemichalcone C	C29H26O8	Chalcone	
				22	Limonexic acid	C26H30O10	Terpenoid	
				22	Phellodensin F	C26H30O10	Flavonoid	
	541.2531667	540.2451667	H+					
		518.2631667	Na+	14	ditrans,dicis-Pentaprenyl diphosphate	C25H44O7P2	Isoprenoid	
				14	Geranylfarnesyl diphosphate	C25H44O7P2	Isoprenoid	
		502.1531667	K+	33	Kolanone	C33H42O4	Isoprenoid	
569.2	569.1616333	568.1536333	H+	6	Viscutin 2	C29H28O12	Flavone	
				20	5,7,3',5'-Tetrahydroxy-3,6,8,4'-tetramethoxyflavone 3'-glucoside	C25H28O15	Flavone	
		546.1716333	Na+	34	Guibourtinidol-(4alpha->6)-catechin	C30H26O10	Proanthocyanidin	
				2	Flavonol 3-O-rutinoside	C27H30O12	Flavonol	
				2	Daidzein 4',7-dirhamnoside; 4-{7-[(6-Deoxy-?-L-mannopyranosyl)oxy]-4-oxo-4H-chromen-3-yl}phenyl 6-deoxy-?-L-mannopyranoside	C27H30O12	Isoflavanone	
				34	Asticolorin C	C30H26O10	Proanthocyanidin	
		530.0616333	K+	34	Curcumin monoglucoside	C27H30O11	Curcuminoid	Stilbenoid, diarylheptanoid and gingerol biosynthesis
				7	Eriosemaone C	C31H30O8	Flavonoid	

				34	8-Prenylquercetin 4'-methyl ether 3-rhamnoside		Flavone	
				34	Isoswertisin 2"-O-(2"'-methylbutyrate)		Flavone	
				34	Isoswertisin 3"-O-(2"'-methylbutyrate)		Flavone	
				34	Icariside I		Flavone	
				34	Baohuoside-1		Flavone	
				34	Wushanicariin		Flavone	
	569.1621667	568.1541667	H+	5	Viscutin 2	C29H28O12	Flavone	
				21	5,7,3',5'-Tetrahydroxy-3,6,8,4'-tetramethoxyflavone 3'-glucoside	C25H28O15	Flavone	
		546.1721667	Na+	35	Guibourtinidol-(4alpha->6)-catechin	C30H26O10	Proanthocyanidin	
				1	Flavonol 3-O-rutinoside	C27H30O12	Flavonol	
				1	Daidzein 4',7-dirhamnoside; 4-{7-[(6-Deoxy-?-L-mannopyranosyl)oxy]-4-oxo-4H-chromen-3-yl}phenyl 6-deoxy-?-L-mannopyranoside	C27H30O12	Isoflavanone	
				32	Asticolorin C	C30H26O10	Proanthocyanidin	
		530.0621667	K+	35	Curcumin monoglucoside	C27H30O11	Curcuminoid	Stilbenoid, diarylheptanoid and gingerol biosynthesis
				8	Eriosemaone C	C31H30O8	Flavonoid	
				35	8-Prenylquercetin 4'-methyl ether 3-rhamnoside		Flavone	
				35	Isoswertisin 2"-O-(2"'-methylbutyrate)		Flavone	
				35	Isoswertisin 3"-O-(2"'-methylbutyrate)		Flavone	
				35	Icariside I		Flavone	
				35	Baohuoside-1		Flavone	
				35	Wushanicariin		Flavone	
	569.1629	568.1549	H+	4	Viscutin 2	C29H28O12	Flavone	
				22	5,7,3',5'-Tetrahydroxy-3,6,8,4'-tetramethoxyflavone 3'-glucoside	C25H28O15	Flavone	
		546.1729	Na+	37	Guibourtinidol-(4alpha->6)-catechin	C30H26O10	Proanthocyanidin	
				0	Flavonol 3-O-rutinoside	C27H30O12	Flavonol	
				0	Daidzein 4',7-dirhamnoside; 4-{7-[(6-Deoxy-?-L-mannopyranosyl)oxy]-4-oxo-4H-chromen-3-yl}phenyl 6-deoxy-?-L-mannopyranoside	C27H30O12	Isoflavanone	
				31	Asticolorin C	C30H26O10	Proanthocyanidin	
		530.0629	K+	36	Curcumin monoglucoside	C27H30O11	Curcuminoid	Stilbenoid, diarylheptanoid and gingerol biosynthesis
				9	Eriosemaone C	C31H30O8	Flavonoid	
				36	8-Prenylquercetin 4'-methyl ether 3-rhamnoside		Flavonol	
				36	Isoswertisin 2"-O-(2"'-methylbutyrate)		Flavone	
				36	Isoswertisin 3"-O-(2"'-methylbutyrate)		Flavone	
				36	Icariside I		Flavone	
				36	Baohuoside-1		Flavone	
				36	Wushanicariin		Flavone	

309	308.9121333	307.9041333	H+					
		285.9221333	Na+					
		269.8121333	K+					
	309.0879	308.0799	H+	29	Allamandin	C15H16O7	Iridoid	
		286.0979	Na+	21	Gastrodin	C13H18O7	Phenolic acid	
				21	Methylarbutin	C13H18O7	Phenolic acid	
				21	Salicin	C13H18O7	Phenolic acid	Glycolysis and phenylpropanoid biosynthesis
		269.9879	K+	2	cis/trans-trismethoxy Resveratrol	C17H18O3	Stilbenoid	
	308.9036333	307.8956333	H+					
		285.9136333	Na+					
		269.8036333	K+					
	309.0882333	308.0802333	H+	27	Allamandin	C15H16O7	Iridoid	
		286.0982333	Na+	20	Gastrodin	C13H18O7	Phenolic acid	
				20	Methylarbutin	C13H18O7	Phenolic acid	
				20	Salicin	C13H18O7	Phenolic acid	Glycolysis and phenylpropanoid biosynthesis
		269.9882333	K+	1	cis/trans-trismethoxy Resveratrol	C17H18O3	Stilbenoid	
	309.0871333	308.0791333	H+	31	Allamandin	C15H16O7	Iridoid	
		286.0971333	Na+	23	Gastrodin	C13H18O7	Phenolic acid	
				23	Methylarbutin	C13H18O7	Phenolic acid	
				23	Salicin	C13H18O7	Phenolic acid	Glycolysis and phenylpropanoid biosynthesis
		269.9871333	K+	5	cis/trans-trismethoxy Resveratrol	C17H18O3	Stilbenoid	
323	323.0976333	322.0896333	H+					
		300.1076333	Na+	26	Isophellopterin	C17H16O5	Furanocoumarin	
				26	Astrapterocarpan	C17H16O5	Pterocarpan	
				26	Phellopterin	C17H16O5	Furanocoumarin	
				26	(-)-Variabilin	C17H16O5	Pterocarpan	
				26	(-)-Sparticarpin	C17H16O5	Pterocarpan	
				26	4-Hydroxyhomopterocarpin	C17H16O5	Pterocarpan	
				26	Coelogin	C17H16O5	Stilbenoid	
				26	Farrerol	C17H16O5	Flavonol	
				38	Salidroside	C14H20O7	Phenolic glycoside	Tyrosine metabolism
		283.9976333	K+	20	3,4,4'-Trihydroxy-alpha,alpha'-diethylstilbene	C18H20O3	Stilbenoid	
	323.0974	322.0894	H+					
		300.1074	Na+	26	Isophellopterin	C17H16O5	Furanocoumarin	
				26	Astrapterocarpan	C17H16O5	Pterocarpan	
				26	Phellopterin	C17H16O5	Furanocoumarin	
				26	(-)-Variabilin	C17H16O5	Pterocarpan	
				26	(-)-Sparticarpin	C17H16O5	Pterocarpan	
				26	4-Hydroxyhomopterocarpin	C17H16O5	Pterocarpan	

				26	Coelogin	C17H16O5	Stilbenoid	
				26	Farrerol	C17H16O5	Flavonol	
				39	Salidroside	C14H20O7	Phenolic glycoside	Tyrosine metabolism
		283.9974	K+	21	3,4,4'-Trihydroxy-alpha,alpha'-diethylstilbene	C18H20O3	Stilbenoid	
	322.9448333	321.9368333	H+					
		299.9548333	Na+					
		283.8448333	K+					
	323.0996333	322.0916333	H+					
		300.1096333	Na+	32	Isophellopterin	C17H16O5	Furanocoumarin	
				32	Astrapterocarpan	C17H16O5	Pterocarpan	
				32	Phellopterin	C17H16O5	Furanocoumarin	
				32	(-)-Variabilin	C17H16O5	Pterocarpan	
				32	(-)-Sparticarpin	C17H16O5	Pterocarpan	
				32	4-Hydroxyhomopterocarpin	C17H16O5	Pterocarpan	
				32	Coelogin	C17H16O5	Stilbenoid	
				32	Farrerol	C17H16O5	Flavonol	
				32	Salidroside	C14H20O7	Phenolic glycoside	Tyrosine metabolism
		283.9996333	K+	14	3,4,4'-Trihydroxy-alpha,alpha'-diethylstilbene	C18H20O3	Stilbenoid	
556.2	556.1505667	555.1425667	H+					
		533.1605667	Na+					
		517.0505667	K+					
	556.2565333	555.2485333	H+					
		533.2665333	Na+					
		517.1565333	K+					
	556.1504	555.1424	H+					
		533.1604	Na+					
		517.0504	K+					
	556.2526333	555.2446333	H+					
		533.2626333	Na+					
		517.1526333	K+					
	556.1526667	555.1446667	H+					
		533.1626667	Na+					
		517.0526667	K+					
542.2	542.1365333	541.1285333	H+					
		519.1465333	Na+					
		503.0365333	K+	10	Gravacridonediol glucoside	C25H29NO10	Alkaloid	
				21	beta-D-Galactopyranosyl-(1->4)-2-amino-2-deoxy-beta-D-glucopyranosyl-(1->6)-D-mannose	C18H33NO15	Trisaccharide	
	542.1387	541.1307	H+					
		519.1487	Na+					
		503.0387	K+	6	Gravacridonediol glucoside	C25H29NO10	Alkaloid	

				17	beta-D-Galactopyranosyl-(1->4)-2-amino-2-deoxy-beta-D-glucopyranosyl-(1->6)-D-mannose	C18H33NO15	Trisaccharide	
	542.2605	541.2525	H+					
		519.2705	Na+					
		503.1605	K+					
	542.1386333	541.1306333	H+					
		519.1486333	Na+					
		503.0386333	K+	6	Gravacridonediol glucoside	C25H29NO10	Alkaloid	
				17	beta-D-Galactopyranosyl-(1->4)-2-amino-2-deoxy-beta-D-glucopyranosyl-(1->6)-D-mannose	C18H33NO15	Trisaccharide	
	542.2514	541.2434	H+					
		519.2614	Na+					
		503.1514	K+					
447.4	447.3515333	446.3435333	H+					
		424.3615333	Na+					
		408.2515333	K+	28	Dehydrosqualene	C30H48	Isoprenoid	
	447.3477667	446.3397667	H+					
		424.3577667	Na+					
		408.2477667	K+	20	Dehydrosqualene	C30H48	Isoprenoid	
	447.3247667	446.3167667	H+					
		424.3347667	Na+					
		408.2247667	K+	31	Dehydrosqualene	C30H48	Isoprenoid	
403	403.0841	402.0761	H+	23	(R)-4'-Phosphopantothenoyl-L-cysteine	C12H23N2O9PS	Amino acid	Pantotheate and CoA biosynthesis
		380.0941	Na+	13	Diphyllin	C21H16O7	Lignan	
		363.9841	K+					
	403.0835	402.0755	H+	24	(R)-4'-Phosphopantothenoyl-L-cysteine	C12H23N2O9PS	Amino acid	Pantotheate and CoA biosynthesis
		380.0935	Na+	11	Diphyllin	C21H16O7	Lignan	
		363.9835	K+					
	402.9239333	401.9159333	H+					
		379.9339333	Na+					
		363.8239333	K+					
	403.0833333	402.0753333	H+	25	(R)-4'-Phosphopantothenoyl-L-cysteine	C12H23N2O9PS	Amino acid	Pantotheate and CoA biosynthesis
		380.0933333	Na+	11	Diphyllin	C21H16O7	Lignan	
		363.9833333	K+					
307	306.9943	305.9863	H+					
		284.0043	Na+					
		267.8943	K+	19	Coumestrol	C15H8O5	Isoflavonoid	Isoflavonoid and phenylpropanoid biosynthesis
	307.0957667	306.0877667	H+					
		284.1057667	Na+	5	Caffeic acid phenethyl ester	C17H16O4	Phenolic acid	

				5	Isobatatasin I	C17H16O4	Stilbenoid	
				5	Batatasin I	C17H16O4	Stilbenoid	
		267.9957667	K+					
	306.9198333	305.9118333	H+					
		283.9298333	Na+					
		267.8198333	K+					
	306.9991667	305.9911667	H+					
		284.0091667	Na+					
		267.8991667	K+	3	Coumestrol	C15H8O5	Isoflavonoid	Isoflavonoid and phenylpropanoid biosynthesis
	307.0988	306.0908	H+					
		284.1088	Na+	15	Caffeic acid phenethyl ester	C17H16O4	Phenolic acid	
				15	Isobatatasin I	C17H16O4	Stilbenoid	
				15	Batatasin I	C17H16O4	Stilbenoid	
		267.9988	K+					
	306.9183	305.9103	H+					
		283.9283	Na+					
		267.8183	K+					
	306.9968	305.9888	H+					
		284.0068	Na+	11	Coumestrol	C15H8O5	Isoflavonoid	Isoflavonoid and phenylpropanoid biosynthesis
		267.8968	K+					
	307.0996667	306.0916667	H+					
		284.1096667	Na+	18	Caffeic acid phenethyl ester	C17H16O4	Phenolic acid	
				18	Isobatatasin I	C17H16O4	Stilbenoid	
				18	Batatasin I	C17H16O4	Stilbenoid	
		267.9996667	K+					
539.2	539.1436667	538.1356667	H+					
		516.1536667	Na+	7	Isolimocitrol 3-glucoside	C24H26O14	Flavonol	
				7	6-Hydroxymyricetin 6,3',5'-trimethyl ether 3-glucoside	C24H26O14	Flavonol	
				7	Limocitrol 3-glucoside	C24H26O14	Flavonol	
				16	Luteone 7-glucoside	C26H28O11	Isoflavone	
				16	Epimedoside C	C26H28O11	Flavonoid	
				16	Vitexin 2"-O-(2'"-methylbutyryl)	C26H28O11	Flavone	
				23	Gericudranins A	C29H24O9	Dihydroflavonol	
		500.0436667	K+	22	Baohuoside II	C26H28O10	Flavone	
				22	Ikarisoside A	C26H28O10	Flavonoid	
	539.2441333	538.2361333	H+					
		516.2541333	Na+					
		500.1441333	K+					
	539.1428	538.1348	H+					
		516.1528	Na+	7	Isolimocitrol 3-glucoside	C24H26O14	Flavonol	

				7	6-Hydroxymyricetin 6,3',5'-trimethyl ether 3-glucoside	C24H26O14	Flavonol	
				7	Limocitrol 3-glucoside	C24H26O14	Flavonol	
				17	Luteone 7-glucoside	C26H28O11	Isoflavone	
				17	Epimedoside C	C26H28O11	Flavonoid	
				17	Vitexin 2"-O-(2'"-methylbutyryl)	C26H28O11	Flavone	
				21	Gericudranins A	C29H24O9	Dihydroflavonol	
		500.0428	K+	21	Baohuoside II	C26H28O10	Flavone	
				21	Ikarisoside A	C26H28O10	Flavonoid	
	539.2461	538.2381	H+					
		516.2561	Na+					
		500.1461	K+					
	539.1448	538.1368	H+					
		516.1548	Na+	9	Isolimocitrol 3-glucoside	C24H26O14	Flavonol	
				9	6-Hydroxymyricetin 6,3',5'-trimethyl ether 3-glucoside	C24H26O14	Flavonol	
				9	Limocitrol 3-glucoside	C24H26O14	Flavonol	
				14	Luteone 7-glucoside	C26H28O11	Isoflavone	
				14	Epimedoside C	C26H28O11	Flavonoid	
				14	Vitexin 2"-O-(2'"-methylbutyryl)	C26H28O11	Flavone	
				25	Gericudranins A	C29H24O9	Dihydroflavonol	
		500.0448	K+	24	Baohuoside II	C26H28O10	Flavone	
				24	Ikarisoside A	C26H28O10	Flavonoid	
	539.2481	538.2401	H+					
		516.2581	Na+					
		500.1481	K+					
553.2	553.1558667	552.1478667	H+	1	6-Hydroxymyricetin 3,6,3',5'-tetramethyl ether 7-glucoside	C25H28O14	Flavonol	
				1	1-Hydroxy-3-methoxy-7-primeverosyloxyxanthone	C25H28O14	Flavonol	
				1	5,2',5'-Trihydroxy-3,6,7,4'-tetramethoxyflavone 5'-glucoside	C25H28O14	Flavone	
				1	Gentioside	C25H28O14	Xanthone	
				1	3',5,6-Trihydroxy-3,4',7,8-tetramethoxyflavone 3-glucoside	C25H28O14	Flavone	
				26	Cucumerin A	C29H28O11	Curcuminoid	
				26	Cucumerin B	C29H28O11	Curcuminoid	
		530.1658667	Na+	21	Curcumin monoglucoside	C27H30O11	Curcuminoid	Stilbenoid, diarylheptanoid and gingerol biosynthesis
				21	Wushanicariin	C27H30O11	Flavone	
				21	Icariside I	C27H30O11	Flavone	
				21	Isoswertisin 2"-O-(2'"-methylbutyrate)	C27H30O11	Flavone	
				21	8-Prenylquercetin 4'-methyl ether 3-rhamnoside	C27H30O11	Flavonol	
				21	Isoswertisin 3"-O-(2'"-methylbutyrate)	C27H30O11	Flavonol	
		514.0558667	K+	15	Icariside II	C27H30O10	Flavone	

	553.1560667	552.1480667	H+	1	6-Hydroxymyricetin 3,6,3',5'-tetramethyl ether 7-glucoside	C25H28O14	Flavonol	
				1	1-Hydroxy-3-methoxy-7-primeverosyloxyxanthone	C25H28O14	Flavonol	
				1	5,2',5'-Trihydroxy-3,6,7,4'-tetramethoxyflavone 5'-glucoside	C25H28O14	Flavone	
				1	Gentioside	C25H28O14	Xanthone	
				1	3',5,6-Trihydroxy-3,4',7,8-tetramethoxyflavone 3-glucoside	C25H28O14	Flavone	
				25	Cucumerin A	C29H28O11	Curcuminoid	
				25	Cucumerin B	C29H28O11	Curcuminoid	
		530.1660667	Na+	21	Curcumin monoglucoside	C27H30O11	Curcuminoid	Stilbenoid, diarylheptanoid and gingerol biosynthesis
				21	Wushanicariin	C27H30O11	Flavone	
				21	Icariside I	C27H30O11	Flavone	
				21	Isoswertisin 2"-O-(2'"-methylbutyrate)	C27H30O11	Flavone	
				21	8-Prenylquercetin 4'-methyl ether 3-rhamnoside	C27H30O11	Flavonol	
				21	Isoswertisin 3"-O-(2'"-methylbutyrate)	C27H30O11	Flavonol	
		514.0560667	K+	16	Icariside II	C27H30O10	Flavone	
	553.1567	552.1487	H+	2	6-Hydroxymyricetin 3,6,3',5'-tetramethyl ether 7-glucoside	C25H28O14	Flavonol	
				2	1-Hydroxy-3-methoxy-7-primeverosyloxyxanthone	C25H28O14	Flavonol	
				2	5,2',5'-Trihydroxy-3,6,7,4'-tetramethoxyflavone 5'-glucoside	C25H28O14	Flavone	
				2	Gentioside	C25H28O14	Xanthone	
				2	3',5,6-Trihydroxy-3,4',7,8-tetramethoxyflavone 3-glucoside	C25H28O14	Flavone	
				24	Cucumerin A	C29H28O11	Curcuminoid	
				24	Cucumerin B	C29H28O11	Curcuminoid	
		530.1667	Na+	20	Curcumin monoglucoside	C27H30O11	Curcuminoid	Stilbenoid, diarylheptanoid and gingerol biosynthesis
				20	Wushanicariin	C27H30O11	Flavone	
				20	Icariside I	C27H30O11	Flavone	
				20	Isoswertisin 2"-O-(2'"-methylbutyrate)	C27H30O11	Flavone	
				20	8-Prenylquercetin 4'-methyl ether 3-rhamnoside	C27H30O11	Flavonol	
				20	Isoswertisin 3"-O-(2'"-methylbutyrate)	C27H30O11	Flavonol	
		514.0567	K+	17	Icariside II	C27H30O10	Flavone	
525.2	525.1394	524.1314	H+	29	5,7,2',3',4'-Pentahydroxy-3,6-dimethoxyflavone 7-glucoside	C23H24O14	Flavone	
		502.1494	Na+	6	beta-Fabatriose	C18H30O16	Trisaccharide	
				23	Demethoxyisogemichalcone C	C29H26O8	Chalcone	
		486.0394	K+	5	Haplodimerine	C28H26N2O6	Quinoline alkaloid	
				24	Rutaevin	C26H30O9	Triterpenoid	

				24	2',4',4-Trihydroxy-3'-prenylchalcone 4'-O-glucoside	C26H30O9	Chalcone	
				15	Isogemichalcone B	C29H26O7	Chalcone	
				15	Gemichalcone B	C29H26O7	Chalcone	
	525.2643667	524.2563667	H+					
		502.2743667	Na+					
		486.1643667	K+					
	525.1407667	524.1327667	H+	32	5,7,2',3',4'-Pentahydroxy-3,6-dimethoxyflavone 7-glucoside	C23H24O14	Flavone	
		502.1507667	Na+	3	beta-Fabatriose	C18H30O16	Trisaccharide	
				21	Demethoxyisogemichalcone C	C29H26O8	Chalcone	
		486.0407667	K+	2	Haplodimerine	C28H26N2O6	Quinoline alkaloid	
				21	Rutaevin	C26H30O9	Triterpenoid	
				21	2',4',4-Trihydroxy-3'-prenylchalcone 4'-O-glucoside	C26H30O9	Chalcone	
				18	Isogemichalcone B	C29H26O7	Chalcone	
				18	Gemichalcone B	C29H26O7	Chalcone	
	525.2713	524.2633	H+					
		502.2813	Na+					
		486.1713	K+					
	525.1416	524.1336	H+	33	5,7,2',3',4'-Pentahydroxy-3,6-dimethoxyflavone 7-glucoside	C23H24O14	Flavone	
		502.1516	Na+	1	beta-Fabatriose	C18H30O16	Trisaccharide	
				19	Demethoxyisogemichalcone C	C29H26O8	Chalcone	
		486.0416	K+	1	Haplodimerine	C28H26N2O6	Quinoline alkaloid	
				20	Rutaevin	C26H30O9	Triterpenoid	
				20	2',4',4-Trihydroxy-3'-prenylchalcone 4'-O-glucoside	C26H30O9	Chalcone	
				20	Isogemichalcone B	C29H26O7	Chalcone	
				20	Gemichalcone B	C29H26O7	Chalcone	
	525.2644667	524.2564667	H+					
		502.2744667	Na+					
		486.1644667	K+					
540.2	540.1400667	539.1320667	H+					
		517.1500667	Na+	30	Vitisin B	C25H25O12	Pyranoanthocyanidin	
		501.0400667	K+					
	540.2396	539.2316	H+					
		517.2496	Na+					
		501.1396	K+					
	540.1402333	539.1322333	H+					
		517.1502333	Na+	30	Vitisin B	C25H25O12	Pyranoanthocyanidin	
		501.0402333	K+					
	540.2496667	539.2416667	H+					
		517.2596667	Na+					
		501.1496667	K+					
	540.1414667	539.1334667	H+					

		517.1514667	Na+	32	Vitisin B	C25H25O12	Pyranoanthocyanidin	
		501.0414667	K+					
	540.2498667	539.2418667	H+					
		517.2598667	Na+					
		501.1498667	K+					

Table B3.9 Liberty sorghum polyphenol extract putative identifications from OPLS-DA (MALDI [+])

Bin	Detected Mass	Accurate Mass	Adduct	Δppm	Name	Formula	Chemical Group	Pathway
335.2	335.1148	334.1068	H+	6	Byakangelicin	C17H18O7	Furanocoumarin	
		312.1248	Na+	13	p-Coumaryl alcohol 4-O-glucoside	C15H20O7	Monolignol	Phenylpropanoid biosynthesis
				31	m-(beta-Acetyl-alpha-ethyl-p-hydroxyphenethyl)benzoic acid	C19H20O4	Stilbenoid	
				31	4'-Prenyloxyresveratrol	C19H20O4	Stilbenoid	
				31	Montanin A	C19H20O4	Diterpenoid	
		296.0148	K+	31	4-Prenylresveratrol	C19H20O3	Stilbenoid	
	335.2412667	334.2332667	H+					
		312.2512667	Na+					
		296.1412667	K+	19	17-Methyl-6Z-octadecenoic acid	C19H36O2	Fatty acid	
	335.1149333	334.1069333	H+	7	Byakangelicin	C17H18O7	Furanocoumarin	
		312.1249333	Na+	14	p-Coumaryl alcohol 4-O-glucoside	C15H20O7	Monolignol	Phenylpropanoid biosynthesis
				31	m-(beta-Acetyl-alpha-ethyl-p-hydroxyphenethyl)benzoic acid	C19H20O4	Stilbenoid	
				31	4'-Prenyloxyresveratrol	C19H20O4	Stilbenoid	
				31	Montanin A	C19H20O4	Diterpenoid	
		296.0149333	K+	31	4-Prenylresveratrol	C19H20O3	Stilbenoid	
	335.1954333	334.1874333	H+					
		312.2054333	Na+					
		296.0954333	K+	8	18-Oxooleate	C18H32O3	Fatty acid	Cutin, suberine and wax biosynthesis
				8	(12R,13S)-(9Z)-12,13-Epoxyoctadecenoic acid	C18H32O3	Fatty acid	Linoleic acid metabolism
				8	(9R,10S)-(12Z)-9,10-Epoxyoctadecenoic acid	C18H32O3	Fatty acid	Linoleic acid metabolism
				8	(9S)-Hydroxyoctadecadienoic acid	C18H32O3	Fatty acid	Linoleic acid metabolism
				8	(13S)-Hydroxyoctadecadienoic acid	C18H32O3	Fatty acid	Linoleic acid metabolism
				8	Vernolic acid	C18H32O3	Fatty acid	
				8	Laetisaric acid	C18H32O3	Fatty acid	
	335.2567667	334.2487667	H+					
		312.2667667	Na+					

		296.1567667	K+					
	335.1153	334.1073	H+	8	Byakangelicin	C17H18O7	Furanocoumarin	
		312.1253	Na+	15	p-Coumaryl alcohol 4-O-glucoside	C15H20O7	Monolignol	Phenylpropanoid biosynthesis
				30	m-(beta-Acetyl-alpha-ethyl-p-hydroxyphenethyl)benzoic acid	C19H20O4	Stilbenoid	
				30	Montanin A	C19H20O4	Diterpenoid	
				30	4'-Prenyloxyresveratrol	C19H20O4	Stilbenoid	
		296.0153	K+	32	4-Prenylresveratrol	C19H20O3	Stilbenoid	
	335.1979333	334.1899333	H+					
		312.2079333	Na+					
		296.0979333	K+	1	18-Oxooleate	C18H32O3	Fatty acid	Cutin, suberine and wax biosynthesis
				1	(12R,13S)-(9Z)-12,13-Epoxyoctadecenoic acid	C18H32O3	Fatty acid	Linoleic acid metabolism
				1	(9R,10S)-(12Z)-9,10-Epoxyoctadecenoic acid	C18H32O3	Fatty acid	Linoleic acid metabolism
				1	(9S)-Hydroxyoctadecadienoic acid	C18H32O3	Fatty acid	Linoleic acid metabolism
				1	(13S)-Hydroxyoctadecadienoic acid	C18H32O3	Fatty acid	Linoleic acid metabolism
				1	Vernolic acid	C18H32O3	Fatty acid	
				1	Laetisaric acid	C18H32O3	Fatty acid	
	335.2523667	334.2443667	H+					
		312.2623667	Na+					
		296.1523667	K+					
279.2	279.0982667	278.0902667	H+	32	Tuliposide A	C11H18O8	Monosaccharide	
				25	Thiamine acetic acid	C12H15N4O2S	Nucleotide	Thiamine metabolism
		256.1082667	Na+	3	Pterostilbene	C16H16O3	Stilbenoid	Stilbenoid, diarylheptanoid and gingerol biosynthesis
				3	Orchinol	C16H16O3	Stilbenoid	
				3	Loroglossol	C16H16O3	Stilbenoid	
				3	7,4'-Dihydroxy-8-methylflavan	C16H16O3	Flavan	
				3	7-Hydroxy-4'-methoxyflavan	C16H16O3	Flavan	
				3	Xenognosin A	C16H16O3	Cinnamylphenol	
		239.9982667	K+					
	279.2382	278.2302	H+	22	(9Z,11E,13E)-Octadecatrienoic acid	C18H30O2	Fatty acid	
				22	(9Z)-Octadec-9-en-12-ynoate	C18H30O2	Fatty acid	Linoleic acid metabolism
				22	alpha-Linolenic acid	C18H30O2	Fatty acid	Plant hormone, alpha-linolenic acid metabolism
				22	gamma-Linolenic acid	C18H30O2	Fatty acid	Linoleic acid metabolism
				31	Palmitic acid	C18H30O2	Fatty acid	Cutin, suberine and wax biosynthesis
				22	Punicic acid	C18H30O2	Fatty acid	
		256.2482	Na+					
		240.1382	K+					

	279.2392667	278.2312667	H+	26	(9Z,11E,13E)-Octadecatrienoic acid	C18H30O2	Fatty acid	
				26	(9Z)-Octadec-9-en-12-ynoate	C18H30O2	Fatty acid	Linoleic acid metabolism
				26	alpha-Linolenic acid	C18H30O2	Fatty acid	Plant hormone, alpha-linolenic acid metabolism
				26	gamma-Linolenic acid	C18H30O2	Fatty acid	Linoleic acid metabolism
				35	Palmitic acid	C18H30O2	Fatty acid	Cutin, suberine and wax biosynthesis
				26	Punicic acid	C18H30O2	Fatty acid	
		256.2492667	Na+					
		240.1392667	K+					
	279.103	278.095	H+	15	Tuliposide A	C11H18O8	Monosaccharide	
		256.113	Na+	13	Pterostilbene	C16H16O3	Stilbenoid	Stilbenoid, diarylheptanoid and gingerol biosynthesis
				13	Orchinol	C16H16O3	Stilbenoid	
				13	Loroglossol	C16H16O3	Stilbenoid	
				13	7,4'-Dihydroxy-8-methylflavan	C16H16O3	Flavan	
				13	7-Hydroxy-4'-methoxyflavan	C16H16O3	Flavan	
				13	Xenognosin A	C16H16O3	Cinnamylphenol	
		240.003	K+					
	279.2384333	278.2304333	H+	23	(9Z,11E,13E)-Octadecatrienoic acid	C18H30O2	Fatty acid	
				23	(9Z)-Octadec-9-en-12-ynoate	C18H30O2	Fatty acid	Linoleic acid metabolism
				23	alpha-Linolenic acid	C18H30O2	Fatty acid	Plant hormone, alpha-linolenic acid metabolism
				23	gamma-Linolenic acid	C18H30O2	Fatty acid	Linoleic acid metabolism
				32	Palmitic acid	C18H30O2	Fatty acid	Cutin, suberine and wax biosynthesis
				23	Punicic acid	C18H30O2	Fatty acid	
		256.2484333	Na+					
		240.1384333	K+					
277.2	277.2259667	276.2179667	H+	35	Stearidonic acid	C18H28O2	Fatty acid	Alpha-linolenic acid metabolism
		254.2359667	Na+					
		238.1259667	K+					
	277.1283667	276.1203667	H+	39	Saccharopine	C11H20N2O6	Amino acid	Lysine biosynthesis
		254.1383667	Na+	9	Elymoclavine	C16H18N2O	Indole alkaloid	
		238.0283667	K+					
	277.2254333	276.2174333	H+	33	Stearidonic acid	C18H28O2	Fatty acid	Alpha-linolenic acid metabolism
		254.2354333	Na+					
		238.1254333	K+					
	277.2256	276.2176	H+	33	Stearidonic acid	C18H28O2	Fatty acid	Alpha-linolenic acid metabolism
		254.2356	Na+					
		238.1256	K+					
293.2	293.1388333	292.1308333	H+					
		270.1488333	Na+					
		254.0388333	K+	29	4-(1-Ethyl-2-phenylbutyl)phenol	C18H22O	Stilbenoid	

	293.2251333	292.2171333	H+					
		270.2351333	Na+					
		254.1251333	K+					
	293.1388	292.1308	H+					
		270.1488	Na+					
		254.0388	K+	29	4-(1-Ethyl-2-phenylbutyl)phenol	C18H22O	Stilbenoid	
	293.2229333	292.2149333	H+					
		270.2329333	Na+					
		254.1229333	K+					
	293.2736	292.2656	H+					
		270.2836	Na+					
		254.1736	K+					
	293.1368	292.1288	H+					
		270.1468	Na+					
		254.0368	K+	22	4-(1-Ethyl-2-phenylbutyl)phenol	C18H22O	Stilbenoid	
	293.2257667	292.2177667	H+					
		270.2357667	Na+					
		254.1257667	K+					
489.4	489.3468	488.3388	H+	21	Asiatic acid	C30H48O5	Triterpenoid	
				21	Euscaphic acid	C30H48O5	Triterpenoid	
				21	Cimigenol	C30H48O5	Triterpenoid	
		466.3568	Na+	26	Vitamin K1 epoxide	C31H46O3	Vitamin K	Ubiquinone and terpenoid biosynthesis
				16	6alpha-Hydroxy-castasterone	C28H50O5	Sterol	Brassinosteroid biosynthesis
				26	6-Deoxocastasterone	C28H50O5	Sterol	Brassinosteroid biosynthesis
		450.2468	K+					
	489.3497667	488.3417667	H+	15	Asiatic acid	C30H48O5	Triterpenoid	
				15	Euscaphic acid	C30H48O5	Triterpenoid	
				15	Cimigenol	C30H48O5	Triterpenoid	
		466.3597667	Na+	32	Vitamin K1 epoxide	C31H46O3	Vitamin K	Ubiquinone and terpenoid biosynthesis
				10	6alpha-Hydroxy-castasterone	C28H50O5	Sterol	Brassinosteroid biosynthesis
				32	6-Deoxocastasterone	C28H50O5	Sterol	Brassinosteroid biosynthesis
		450.2497667	K+					
	489.3530667	488.3450667	H+	8	Asiatic acid	C30H48O5	Triterpenoid	
				8	Euscaphic acid	C30H48O5	Triterpenoid	
				8	Cimigenol	C30H48O5	Triterpenoid	
		466.3630667	Na+	39	Vitamin K1 epoxide	C31H46O3	Vitamin K	Ubiquinone and terpenoid biosynthesis
				4	6alpha-Hydroxy-castasterone	C28H50O5	Sterol	Brassinosteroid biosynthesis
				38	6-Deoxocastasterone	C28H50O5	Sterol	Brassinosteroid biosynthesis
		450.2530667	K+					
291.2	291.1196	290.1116	H+	10	5-O-Methylvisamminol	C16H18O5	Chromone	
				3	N-Succinyl-LL-2,6-diaminopimelate	C11H18N2O7	Amino acid	Lysine biosynthesis

				35	N-(L-Arginino)succinate	C10H18N4O6	Amino acid	Arginine, alanine, aspartate and glutamate metabolism
		268.1296	Na+					
		252.0196	K+					
	291.1964	290.1884	H+	35	4'-Hydroxyropivacaine	C17H26N2O2	Amino acid	
				35	3'-Hydroxyropivacaine	C17H26N2O2	Amino acid	
		268.2064	Na+					
		252.0964	K+					
	291.2539333	290.2459333	H+					
		268.2639333	Na+					
		252.1539333	K+					
	291.1201333	290.1121333	H+	8	5-O-Methylvisamminol	C16H18O5	Chromone	
				5	N-Succinyl-LL-2,6-diaminopimelate	C11H18N2O7	Amino acid	Lysine biosynthesis
				33	N-(L-Arginino)succinate	C10H18N4O6	Amino acid	Arginine, alanine, aspartate and glutamate metabolism
		268.1301333	Na+					
		252.0201333	K+					
	291.1966	290.1886	H+	34	4'-Hydroxyropivacaine	C17H26N2O2	Amino acid	
				34	3'-Hydroxyropivacaine	C17H26N2O2	Amino acid	
		268.2066	Na+					
		252.0966	K+					
	291.2547	290.2467	H+					
		268.2647	Na+					
		252.1547	K+					
	291.1206667	290.1126667	H+	6	5-O-Methylvisamminol	C16H18O5	Chromone	
				6	N-Succinyl-LL-2,6-diaminopimelate	C11H18N2O7	Amino acid	Lysine biosynthesis
				31	N-(L-Arginino)succinate	C10H18N4O6	Amino acid	Arginine, alanine, aspartate and glutamate metabolism
		268.1306667	Na+					
		252.0206667	K+					
	291.2008667	290.1928667	H+	20	4'-Hydroxyropivacaine	C17H26N2O2	Amino acid	
				20	3'-Hydroxyropivacaine	C17H26N2O2	Amino acid	
		268.2108667	Na+					
		252.1008667	K+					
	291.2548667	290.2468667	H+					
		268.2648667	Na+					
		252.1548667	K+					
487.4	487.3346333	486.3266333	H+	14	Glabric acid	C30H46O5	Triterpenoid	
				14	Alisol C	C30H46O5	Triterpenoid	
				14	Quillaic acid	C30H46O5	Triterpenoid	
		464.3446333	Na+	9	7-Oxatyphasterol	C28H48O5	Sterol	Brassinosteroid biosynthesis
				9	7-Oxateasterone	C28H48O5	Sterol	Brassinosteroid biosynthesis
				9	Castasterone	C28H48O5	Sterol	Brassinosteroid biosynthesis
		448.2346333	K+	33	Typhasterol	C28H48O4	Sterol	Brassinosteroid biosynthesis

				33	Teasterone	C28H48O4	Sterol	Brassinosteroid biosynthesis
	487.3356	486.3276	H+	12	Glabric acid	C30H46O5	Triterpenoid	
				12	Alisol C	C30H46O5	Triterpenoid	
				12	Quillaic acid	C30H46O5	Triterpenoid	
		464.3456	Na+	7	7-Oxatyphasterol	C28H48O5	Sterol	Brassinosteroid biosynthesis
				7	7-Oxateasterone	C28H48O5	Sterol	Brassinosteroid biosynthesis
				7	Castasterone	C28H48O5	Sterol	Brassinosteroid biosynthesis
		448.2356	K+	35	Typhasterol	C28H48O4	Sterol	Brassinosteroid biosynthesis
				35	Teasterone	C28H48O4	Sterol	Brassinosteroid biosynthesis
	487.4730333	486.4650333	H+					
		464.4830333	Na+					
		448.3730333	K+					
	487.3406667	486.3326667	H+	2	Glabric acid	C30H46O5	Triterpenoid	
				2	Alisol C	C30H46O5	Triterpenoid	
				2	Quillaic acid	C30H46O5	Triterpenoid	
		464.3506667	Na+	2	7-Oxatyphasterol	C28H48O5	Sterol	Brassinosteroid biosynthesis
				2	7-Oxateasterone	C28H48O5	Sterol	Brassinosteroid biosynthesis
				2	Castasterone	C28H48O5	Sterol	Brassinosteroid biosynthesis
		448.2406667	K+					
289.2	289.1043	288.0963	H+	9	Shikonin	C16H16O5	Napthoquinone	Ubiquinone and other terpenoid-quinone biosynthesis
				9	7,2'-Dihydroxy-4'-methoxy-isoflavanol	C16H16O5	Isoflavane	Isoflavonoid biosynthesis
				9	Phloretin 4'-methyl ether	C16H16O5	Dihydrochalcone	
		266.1143	Na+					
		250.0043	K+					
	289.1873	288.1793	H+					
		266.1973	Na+	34	Juvabione	C16H26O3	Sesquiterpenoid	
		250.0873	K+					
	289.2393333	288.2313333	H+	6	10,16-Dihydroxyhexadecanoic acid	C16H32O4	Fatty acid	Cutin, suberine and wax biosynthesis
		266.2493333	Na+					
		250.1393333	K+					
	289.1026667	288.0946667	H+	15	Shikonin	C16H16O5	Napthoquinone	Ubiquinone and other terpenoid-quinone biosynthesis
				15	7,2'-Dihydroxy-4'-methoxy-isoflavanol	C16H16O5	Isoflavane	Isoflavonoid biosynthesis
				15	Phloretin 4'-methyl ether	C16H16O5	Dihydrochalcone	
		266.1126667	Na+					
		250.0026667	K+					
	289.1870667	288.1790667	H+					
		266.1970667	Na+	33	Juvabione	C16H26O3	Sesquiterpenoid	
		250.0870667	K+					
	289.2401667	288.2321667	H+	9	10,16-Dihydroxyhexadecanoic acid	C16H32O4	Fatty acid	Cutin, suberine and wax biosynthesis
		266.2501667	Na+					

		250.1401667	K+					
	289.1059667	288.0979667	H+	3	Shikonin	C16H16O5	Napthoquinone	Ubiquinone and other terpenoid-quinone biosynthesis
				3	7,2'-Dihydroxy-4'-methoxy-isoflavanol	C16H16O5	Isoflavane	Isoflavonoid biosynthesis
				3	Phloretin 4'-methyl ether	C16H16O5	Dihydrochalcone	
		266.1159667	Na+					
		250.0059667	K+					
	289.1881667	288.1801667	H+					
		266.1981667	Na+	37	Juvabione	C16H26O3	Sesquiterpenoid	
		250.0881667	K+					
	289.2401333	288.2321333	H+	9	10,16-Dihydroxyhexadecanoic acid	C16H32O4	Fatty acid	Cutin, suberine and wax biosynthesis
		266.2501333	Na+					
		250.1401333	K+					
275.2	275.2085	274.2005	H+	11	Sauroxine	C17H26N2O	Terpenoid	
				11	alpha-Obscurine	C17H26N2O		
		252.2185	Na+	37	Hydnocarpic acid	C16H28O2	Fatty acid	
		236.1085	K+					
	275.2094333	274.2014333	H+	8	Sauroxine	C17H26N2O	Terpenoid	
				8	alpha-Obscurine	C17H26N2O	Terpenoid	
		252.2194333	Na+					
		236.1094333	K+					
	275.2091333	274.2011333	H+	9	Sauroxine	C17H26N2O	Terpenoid	
				9	alpha-Obscurine	C17H26N2O	Terpenoid	
		252.2191333	Na+	39	Hydnocarpic acid	C16H28O2	Fatty acid	
		236.1091333	K+					
292.2	292.1190333	291.1110333	H+					
		269.1290333	Na+					
		253.0190333	K+					
	292.2339667	291.2259667	H+					
		269.2439667	Na+					
		253.1339667	K+					
	292.1188667	291.1108667	H+					
		269.1288667	Na+					
		253.0188667	K+					
	292.233	291.225	H+					
		269.243	Na+					
		253.133	K+					
	292.1237667	291.1157667	H+					
		269.1337667	Na+					
		253.0237667	K+					
	292.2356333	291.2276333	H+					
		269.2456333	Na+					
		253.1356333	K+					
337.2	337.1268	336.1188	H+					

		314.1368	Na+					
		298.0268	K+	20	Glepidotin C	C19H22O3	Stilbenoid	
				20	Ostruthin	C19H22O3	Coumarin	
	337.2127333	336.2047333	H+					
		314.2227333	Na+					
		298.1127333	K+	3	18-Hydroxyoleate	C18H34O3	Fatty acid	Cutin, suberine and wax biosynthesis
				3	cis-9,10-Epoxystearic acid	C18H34O3	Fatty acid	Cutin, suberine and wax biosynthesis
				3	Ricinoleic acid	C18H34O3	Fatty acid	
	337.2728	336.2648	H+					
		314.2828	Na+					
		298.1728	K+					
	337.1283	336.1203	H+					
		314.1383	Na+	37	Heliettin	C19H22O4	Furanocoumarin	
		298.0283	K+	24	Glepidotin C	C19H22O3	Stilbenoid	
				24	Ostruthin	C19H22O3	Coumarin	
	337.2132333	336.2052333	H+					
		314.2232333	Na+					
		298.1132333	K+	2	18-Hydroxyoleate	C18H34O3	Fatty acid	Cutin, suberine and wax biosynthesis
				2	cis-9,10-Epoxystearic acid	C18H34O3	Fatty acid	Cutin, suberine and wax biosynthesis
				2	Ricinoleic acid	C18H34O3	Fatty acid	
	337.2717	336.2637	H+					
		314.2817	Na+					
		298.1717	K+					
	337.1289667	336.1209667	H+					
		314.1389667	Na+	35	Heliettin	C19H22O4	Furanocoumarin	
		298.0289667	K+	26	Glepidotin C	C19H22O3	Stilbenoid	
				26	Ostruthin	C19H22O3	Coumarin	
	337.2160667	336.2080667	H+					
		314.2260667	Na+					
		298.1160667	K+	6	18-Hydroxyoleate	C18H34O3	Fatty acid	Cutin, suberine and wax biosynthesis
				6	cis-9,10-Epoxystearic acid	C18H34O3	Fatty acid	Cutin, suberine and wax biosynthesis
				6	Ricinoleic acid	C18H34O3	Fatty acid	
	337.2750667	336.2670667	H+					
		314.2850667	Na+					
		298.1750667	K+					
486.4	486.3244	485.3164	H+					
		463.3344	Na+					
		447.2244	K+					
	486.3983333	485.3903333	H+					
		463.4083333	Na+					

		447.2983333	K+					
	486.3141	485.3061	H+					
		463.3241	Na+					
		447.2141	K+					
	486.3979333	485.3899333	H+					
		463.4079333	Na+					
		447.2979333	K+					
	486.3164333	485.3084333	H+					
		463.3264333	Na+					
		447.2164333	K+					
	486.3946333	485.3866333	H+					
		463.4046333	Na+					
		447.2946333	K+					
377	377.0251333	376.0171333	H+					
		354.0351333	Na+					
		337.9251333	K+	2	1-(5'-Phosphoribosyl)-5-amino-4-imidazolecarboxamide	C9H15N4O8P	Nucleotide	Amino acid and alkaloid metabolism
	377.0918333	376.0838333	H+					
		354.1018333	Na+	20	Sesamin	C20H18O6	Lignan	
				20	Hinokinin	C20H18O6	Lignan	
				20	Luteone	C20H18O6	Isoflavone	
				20	Licoisoflavone A	C20H18O6	Isoflavone	
				20	Cyclokievitone	C20H18O6	Isoflavanone	
				19	Biflorin	C16H18O9	Chromone	
				19	Scopolin	C16H18O9	Coumarin	Phenylpropanoid biosynthesis
				19	Chlorogenic acid	C16H18O9	Monolignol	Phenylpropanoid, flavonoid and stilbenoid biosynthesis
		337.9918333	K+	20	1-Peroxyferolide	C17H22O7	Sesquiterpenoid	
				35	Demethoxycurcumin	C20H18O5	Stilbenoid	Stilbenoid, diarylheptanoid and gingerol biosynthesis
				35	Glyceollin III	C20H18O5	Pterocarpan	Isoflavonoid biosynthesis
				35	8-(1,1-Dimethylallyl)galangin	C20H18O5	Flavonol	
				35	6-(3,3-Dimethylallyl)galangin	C20H18O5	Flavonol	
				35	Wighteone	C20H18O5	Isoflavone	
				35	(-)-Glyceollin II	C20H18O5	Pterocarpan	Isoflavonoid biosynthesis
				35	2-Isoprenylemodin	C20H18O5	Anthraquinone	
				35	8-Prenylgalangin	C20H18O5	Flavonol	
				35	(-)-Glyceollin I	C20H18O5	Pterocarpan	Isoflavonoid biosynthesis
	377.0253667	376.0173667	H+					
		354.0353667	Na+					
		337.9253667	K+	1	1-(5'-Phosphoribosyl)-5-amino-4-imidazolecarboxamide	C9H15N4O8P	Nucleotide	Amino acid and alkaloid metabolism
	377.0922	376.0842	H+					
		354.1022	Na+	19	Sesamin	C20H18O6	Lignan	
				19	Hinokinin	C20H18O6	Lignan	
				19	Luteone	C20H18O6	Isoflavone	

				19	Licoisoflavone A	C20H18O6	Isoflavone	
				19	Cyclokievitone	C20H18O6	Isoflavanone	
				20	Biflorin	C16H18O9	Chromone	
				20	Scopolin	C16H18O9	Coumarin	Phenylpropanoid biosynthesis
				20	Chlorogenic acid	C16H18O9	Monolignol	Phenylpropanoid, flavonoid and stilbenoid biosynthesis
		337.9922	K+	19	1-Peroxyferolide	C17H22O7	Sesquiterpenoid	
				36	Demethoxycurcumin	C20H18O5	Stilbenoid	Stilbenoid, diarylheptanoid and gingerol biosynthesis
				36	Glyceollin III	C20H18O5	Pterocarpan	Isoflavonoid biosynthesis
				36	8-(1,1-Dimethylallyl)galangin	C20H18O5	Flavonol	
				36	6-(3,3-Dimethylallyl)galangin	C20H18O5	Flavonol	
				36	Wighteone	C20H18O5	Isoflavone	
				36	(-)-Glyceollin II	C20H18O5	Pterocarpan	Isoflavonoid biosynthesis
				36	2-Isoprenylemodin	C20H18O5	Anthraquinone	
				36	8-Prenylgalangin	C20H18O5	Flavonol	
				36	(-)-Glyceollin I	C20H18O5	Pterocarpan	Isoflavonoid biosynthesis
	376.9361667	375.9281667	H+					
		353.9461667	Na+					
		337.8361667	K+					
	377.0264	376.0184	H+					
		354.0364	Na+					
		337.9264	K+	1	1-(5'-Phosphoribosyl)-5-amino-4-imidazolecarboxamide	C9H15N4O8P	Nucleotide	Amino acid and alkaloid metabolism
	377.0932667	376.0852667	H+					
		354.1032667	Na+	16	Sesamin	C20H18O6	Lignan	
				16	Hinokinin	C20H18O6	Lignan	
				16	Luteone	C20H18O6	Isoflavone	
				16	Licoisoflavone A	C20H18O6	Isoflavone	
				16	Cyclokievitone	C20H18O6	Isoflavanone	
				23	Biflorin	C16H18O9	Chromone	
				23	Scopolin	C16H18O9	Coumarin	Phenylpropanoid biosynthesis
				23	Chlorogenic acid	C16H18O9	Monolignol	Phenylpropanoid, flavonoid and stilbenoid biosynthesis
		337.9932667	K+	17	1-Peroxyferolide	C17H22O7	Sesquiterpenoid	
				38	Demethoxycurcumin	C20H18O5	Stilbenoid	Stilbenoid, diarylheptanoid and gingerol biosynthesis
				38	Glyceollin III	C20H18O5	Pterocarpan	Isoflavonoid biosynthesis
				38	8-(1,1-Dimethylallyl)galangin	C20H18O5	Flavonol	
				38	6-(3,3-Dimethylallyl)galangin	C20H18O5	Flavonol	
				38	Wighteone	C20H18O5	Isoflavone	
				38	(-)-Glyceollin II	C20H18O5	Pterocarpan	Isoflavonoid biosynthesis
				38	2-Isoprenylemodin	C20H18O5	Anthraquinone	
				38	8-Prenylgalangin	C20H18O5	Flavonol	
				38	(-)-Glyceollin I	C20H18O5	Pterocarpan	Isoflavonoid biosynthesis

Appendix B

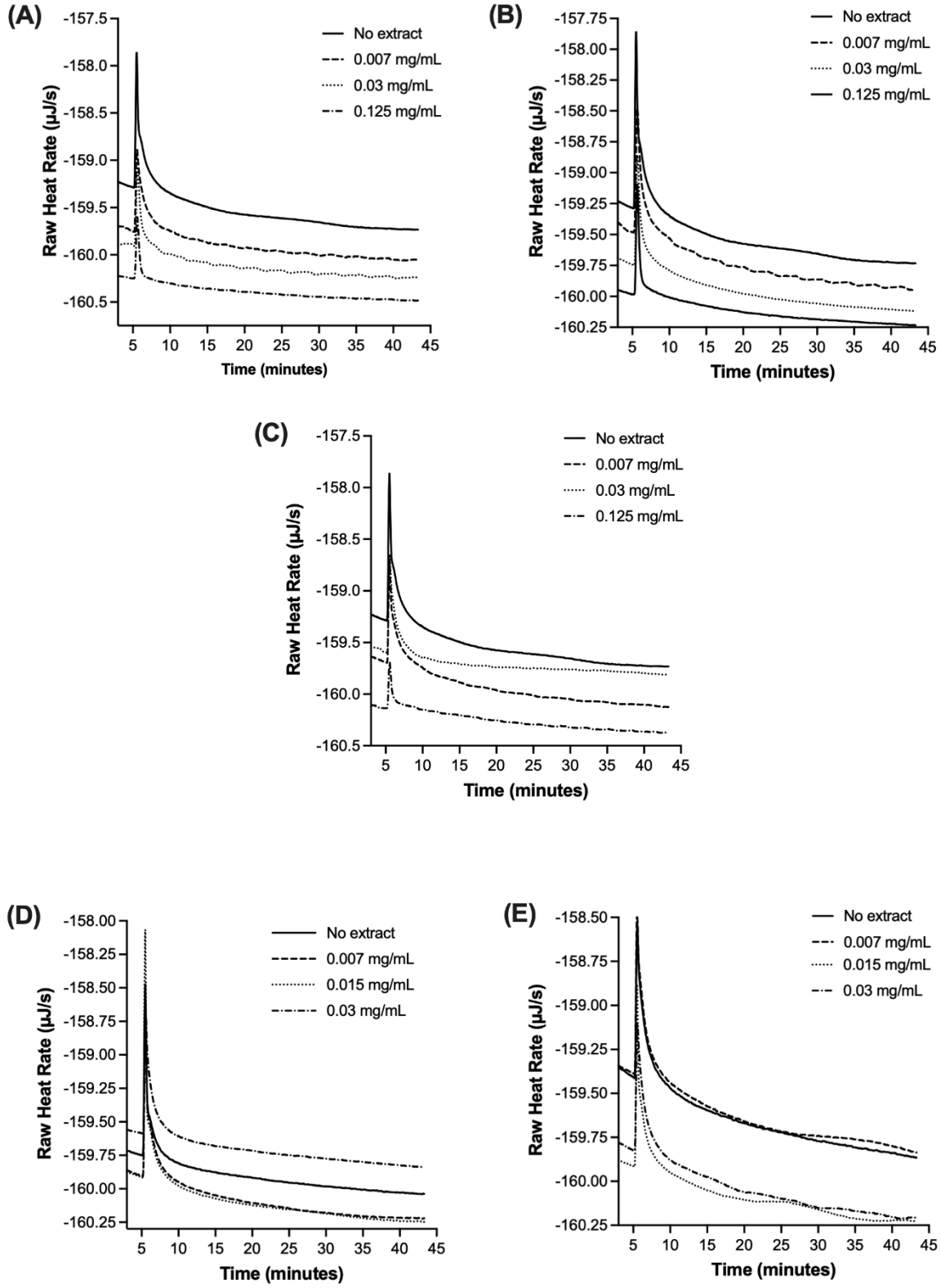

Figure B.1 ITC enzyme blanks
The raw heat rate (µJ/s) was recorded as 5% ethanol was titrated into a mixture of phytase enzyme and (A) Liberty sorghum polyphenol extract, (B) MR-Buster sorghum polyphenol extract, (C) Cracka sorghum polyphenol extract, (D) grape seed tannin extract and (E) quebracho tannin extract.

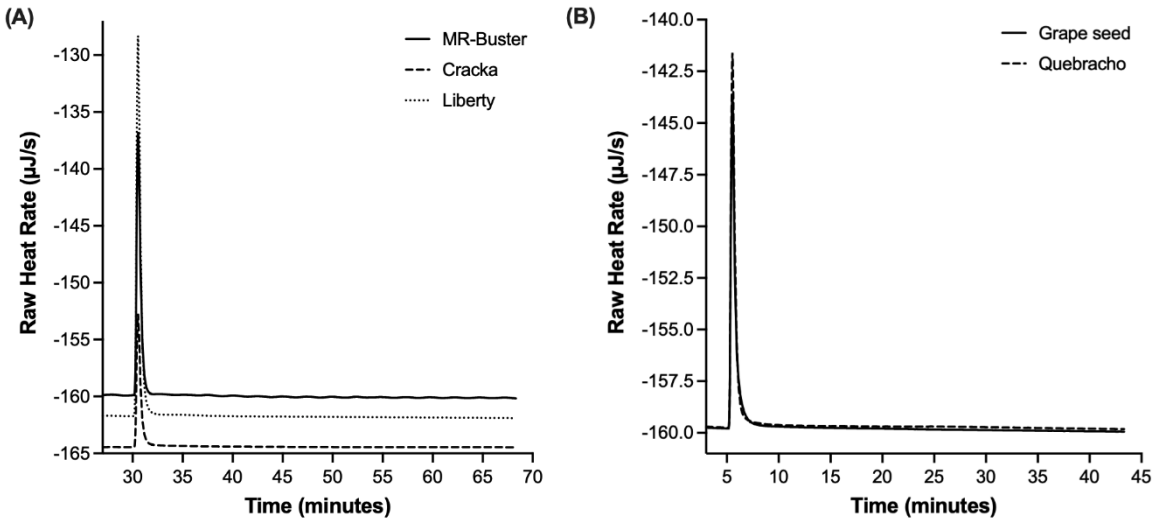

Figure B.2 ITC heat of dilution thermogram
The raw heat rate (µJ/s) was recorded as 20 mM phytic acid was titrated into 0.125 mg/mL sorghum acetone polyphenol extracts and grape seed and quebracho tannin extracts.

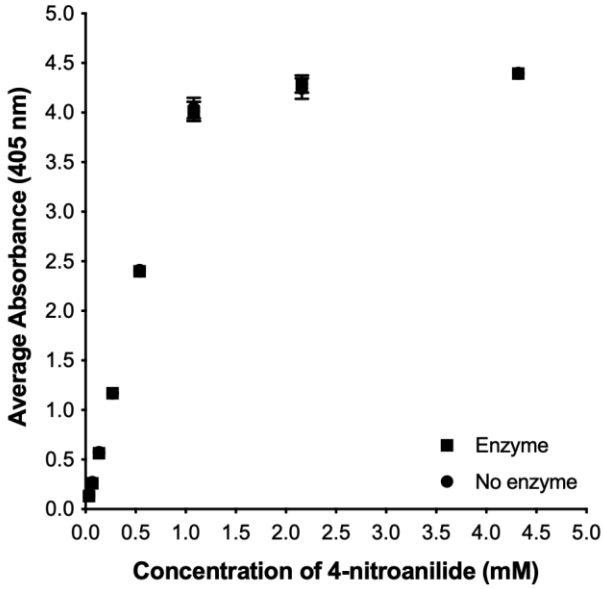

Figure B.3 Determination of detection limit for protease assay
The maximum detection limit of 4-nitroaniline, following the protease assay protocol, was determined to be approximately 1 mM both with and without the protease included. Error bars represent ± 1 SD; n = 15.

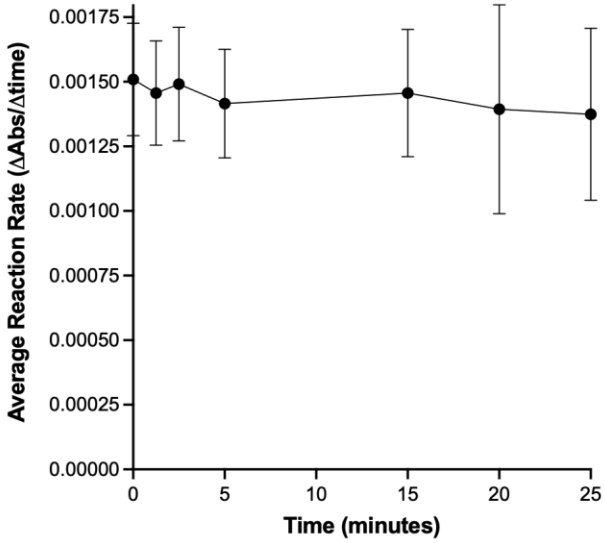

Figure B.4 Ethanol and incubation on activity
The protease enzyme was incubated with 5% ethanol at varying incubation times to determine the effect of the solvent on enzyme activity. One-way ANOVA with multiple comparisons (GraphPad Prism) was used to determine significance between time points. There were no significant differences between the times points. Error bars represent ± 1 SD; n = 15.

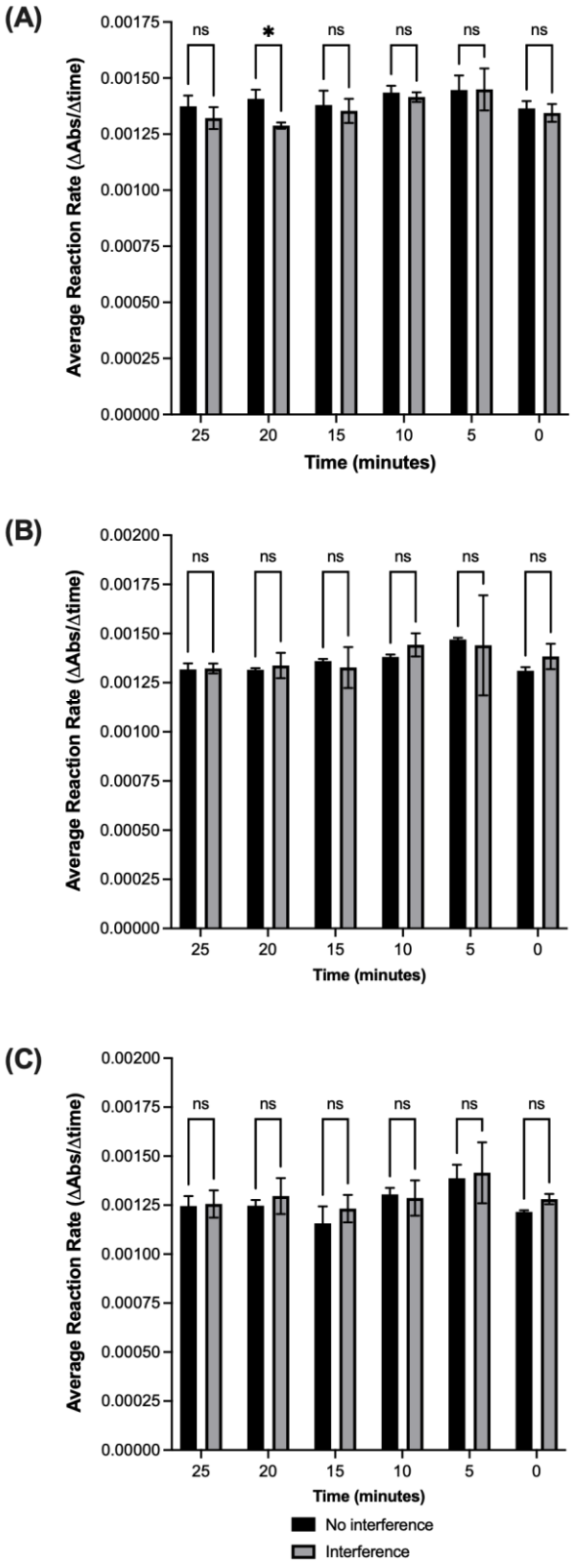

Figure B.5 Sorghum polyphenol extracts and substrate interaction
Sorghum acetone polyphenol extracts were incubated with the substrate, SAPNA, instead of the protease to determine if inhibition was occurring via substrate interference; (A) MR-Buster, (B) Cracka and (C) Liberty. Two-way ANOVA with multiple comparisons (GraphPad Prism) was used to determine significance between time points. ns – no significance, * - $P < 0.05$. Error bars represent ± 1 SD; n = 3.

Appendix C

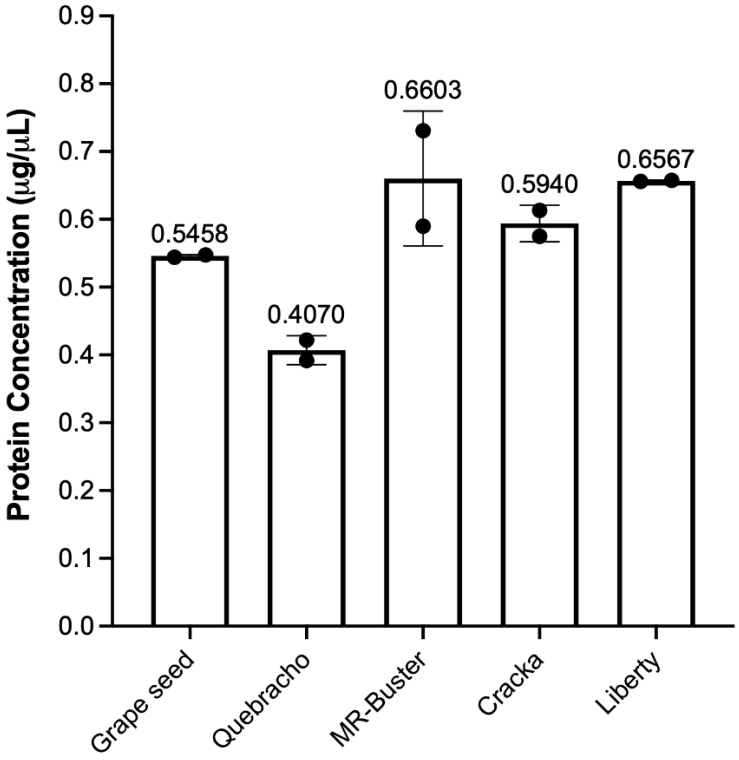

Figure C.1 Protein content of tannin and sorghum polyphenol extracts
Protein content was determined in 200 uL of 10 mg/mL polyphenol and tannin extracts from sorghum (MR-Buster, Cracka, Liberty), grape seed and quebracho. Error bars represent ± 1 SD; n = 2.

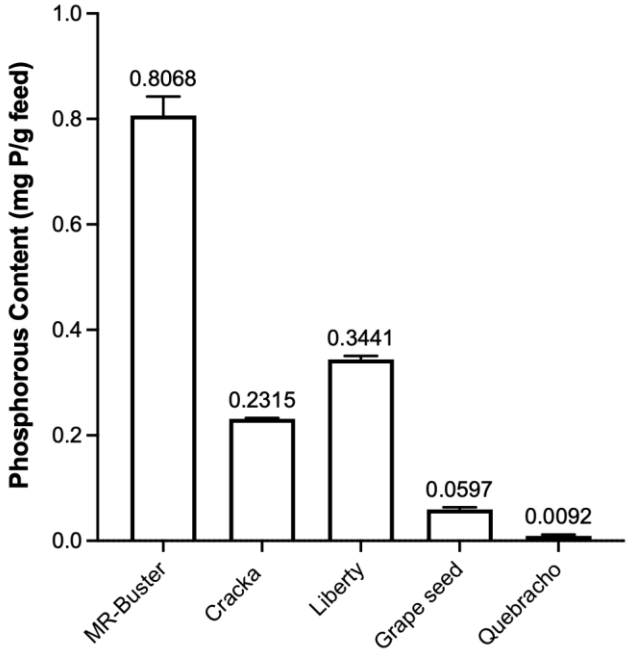

Figure C.2 Total phosphorous of sorghum polyphenol and tannin extracts
Total phosphorous was determined, using the malachite assay, in extracts from sorghum (MR-Buster, Cracka, Liberty), grape seed and quebracho. Error bars represent ± 1 SD; n = 2.

Table C.1 Temperature and pH measurements during simulated digestion*

Sample	Temperature (°C)	Crop pH	Gastric pH	Intestinal pH
Control	40.0	4.6	3.0	7.0
Grape seed	38.9	4.57	3.07	6.78
Quebracho	39.3	4.59	3.02	6.96
MR-Buster	39.3	4.66	3.16	6.92
Cracka	39.2	4.65	3.12	6.93
Liberty	38.9	4.65	3.16	6.85

***Endogenous enzymes were included in these trials while exogenous feed enzymes were not

Initially, experiments were conducted to determine the effects of the tannin and sorghum polyphenol extracts on digesta pH during the crop, gastric and intestinal phases of simulated digestion. Tannin and sorghum polyphenol extracts were added at 10 and 20 mg, respectively, and pH readings were taken at each phase of digestion. The presence of the tannin and sorghum polyphenol extracts altered the pH of each phase of simulated digestion. With the exception of grape seed extract during the intestinal phase, the two tannin extracts affected the three phases of digestion minimally. The decrease in pH during the intestinal phase with grape seed extract indicated the presence of acidic compounds, most likely those with multiple hydroxyl groups prevalent in large condensed tannins. These types of polyphenols were previously identified in this extract (see **Section 3.4.4**). The sorghum polyphenol extracts also lowered the pH during the intestinal phase but altered the pH of the gastric phase more substantially than both tannin extracts.

Appendix D

Hodges, H., Cowieson, A., Falconer, R., Cameron, D., (2020). Chemical profile and effects of modern Australian sorghum polyphenolic-rich extracts on feed phytase and protease activity. *Proceedings of the Australian Poultry Science Symposium* [online]. 31, 76-79. Available from: doi: https://az659834.vo.msecnd.net/eventsairaueprod/production-usyd-public/8f563f4140d24984879bd01be567dfc2.

CHEMICAL PROFILE AND EFFECTS OF MODERN AUSTRALIAN SORGHUM POLYPHENOLIC-RICH EXTRACTS ON FEED PHYTASE AND PROTEASE ACTIVITY

HAYDEN HODGES[1], AARON COWIESON[2], ROBERT FALCONER[3] and DUNCAN CAMERON[4]

Summary

While the beneficial roles of feed enzymes for poultry are well-established both in increasing nutrient bioavailability and reducing the impact of anti-nutritional factors (ANFs), their possible interactions with polyphenols are unknown. The purpose of the current work was to investigate the chemical composition of polyphenol-rich extracts from Australian sorghum (Liberty, Cracka, Buster) and tentatively identify compounds in a complex mixture. These extracts were then tested as inhibitors of two poultry feed enzymes, phytase and serine protease. Effects were measured through the novel use and interpretation of isothermal titration calorimetry (ITC) and a colourimetric, kinetic assay.

I. INTRODUCTION

While the inclusion of feed enzymes is routine in poultry fed sorghum-based diets, the effects of these enzymes is often muted or substandard, especially with phytase (Selle et al., 2018). The exact mechanism for this underperformance is not known, however, it is most likely caused by one or all of three key endogenous grain components: kafirin, phytate and phenolic compounds. Phenolic compounds, routinely identified in sorghum, are known to be antinutritional, especially with regard to animal nutrition (Velickovic and Stanic-Vucinic, 2018). This antinutritional effect comes through precipitation of macromolecules thus limiting digestibility, interactions with the complex grain matrix and interference with digestive enzymes. Higher molecular weight compounds such as condensed and hydrolyzable tannins are thought to be one of the culprits of these effects (Bravo, 1998).

Feed manufacturers must take these potential interactions into account when preparing grain and formulating feed mixtures to include exogenous enzymes. Modern Australian varieties have been bred to reduce tannin content and are, for the most part, considered to be tannin-free (Selle et al., 2018). While ‘tannins’ in the traditional sense may be significantly reduced in modern varieties, ‘non-tannin’ phenolics are very much still present and have the potential to produce anti-nutritional effects (Liu et al., 2015). These phenolics along with

[1] Department of Chemical and Biological Engineering, University of Sheffield; hehodges1@sheffield.ac.uk
[2] DSM Nutritional Products; aaron.cowieson@dsm.com
[3] School of Chemical Engineering and Advanced Materials, University of Adelaide; robert.falconer@adelaide.edu.au
[4] Department of Plant and Animal Sciences, University of Sheffield; d.cameron@sheffield.ac.uk

kafirin and phytate may be interacting in complex ways that might reduce the effectiveness of feed enzymes, overall digestibility and energy utilisation. Therefore, a thorough analysis of the complex matrix and its components can lead to better understanding of the grain's role in animal feed and ways to increase its performance and profitability.

II. METHOD

MR-Buster (Buster), Cracka and Liberty sorghum were provided by DSM Nutritional Products and harvested in 2017 in Queensland. Phytase and serine protease feed enzymes were also provided by DSM. Sorghum grain was defatted and extracted for polyphenols using 70% aqueous acetone following Harbertson et al. (2014). The Folin-Ciocalteu (F-C) method, following Ainsworth and Gillespie (2007), was used to determine the total phenolic content (TPC) of the polyphenol-rich extract. Commercial extracts were kindly provided by Silvateam (Italy). FT-IR analysis was performed using a diamond ATR crystal between the wavenumbers 4000 and 400 cm^{-1}. Mass spectrometry was performed on a Waters Synapt G2-Si MALDI-ToF and ESI-ToF mass spectrometer. The effect of sorghum polyphenol-rich extracts on phytase activity was determined through ITC. ITC analysis was conducted using a TA Analysis NanoITC (TA Instruments, New Castle, DE). The injection syringe contained 20 mM phytate and was titrated into a mixture of sorghum polyphenol-rich extract and phytase over two injections, two and five μL, at 30°C, pH 5.0 ± 0.2 and 285 rpm stirring speed. The sample cell contained phytase, 4.075 FYT/mL, alone or with a range of sorghum polyphenol-rich extracts. The effect of sorghum polyphenol-rich extracts on serine protease activity was determined by colourimetric enzyme activity assay using a small, synthetic substrate.

III. RESULTS

Twenty grams of defatted sorghum were extracted with 70% aqueous acetone and freeze-dried. Table 1 shows the extracts quantified as grams of polyphenol extract per kilogram of grain (g/kg) and as TPC in milligrams gallic acid equivalent per gram of extract (mg GAE/g). Liberty was found to have a significantly ($P < 0.001$) lower TPC than both red sorghums, Buster and Cracka.

Table 1 - Quantification of sorghum polyphenol-rich extracts

	Buster	Cracka	Liberty
Color	Red	Red	White
Amount of extract (g/kg)	4.02 ± 1.05 (n = 3)	4.75 ± 0.84 (n = 6)	3.52 ± 1.00 (n = 6)
TPC (mg GAE/g)	8.69 ± 2.99 (n = 24)	7.99 ± 1.33 (n = 21)	3.53 ± 0.79 (n = 27)

Values are ± 1 standard deviation

FT-IR analysis indicated the spectra for sorghum extracts matched closely to each other and shared similar features to two commercial extracts, quebracho and grape seed, known to contain tannins (Figure 1). Analysis by MALDI-ToF-MS allowed for the clear separation between red and white sorghum through principal components analysis (PCA) (Figure 2). ESI-MS^2 provided tentative identifications of compounds present in the extracts to find primarily fatty acids, polyphenols and lignin-like compounds, including caffeoyl, feruloyl and coumaroyl glycerol esters.

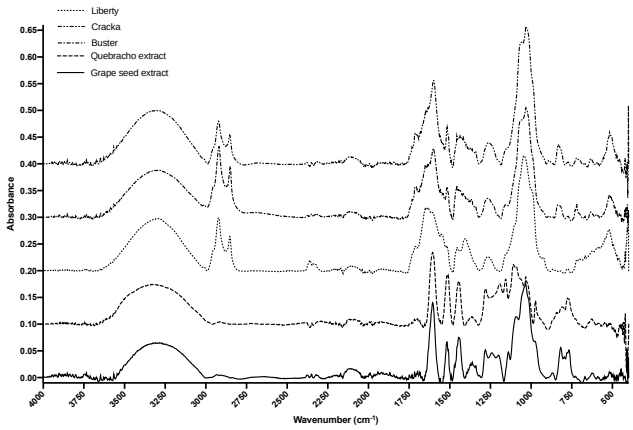

Figure 1 – FT-IR spectra of sorghum polyphenol-rich extracts and commercial extracts

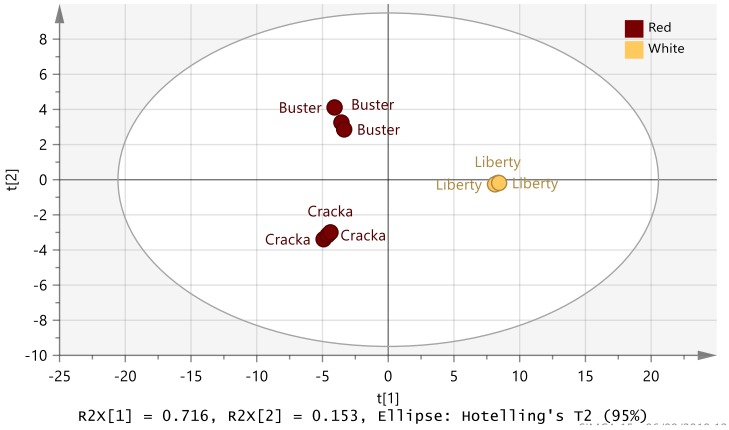

Figure 2 – PCA plot from MALDI-ToF-MS of sorghum polyphenol-rich extracts

The presence of sorghum polyphenol-rich extracts inhibited phytase activity up to 100% in the ITC *in vitro* model (Figure 3) whereas serine protease inhibition was limited to 20-30% (Figure 4). Liberty and Cracka inhibited phytase the most. Inhibition of the serine protease was found to be mixed non-competitive.

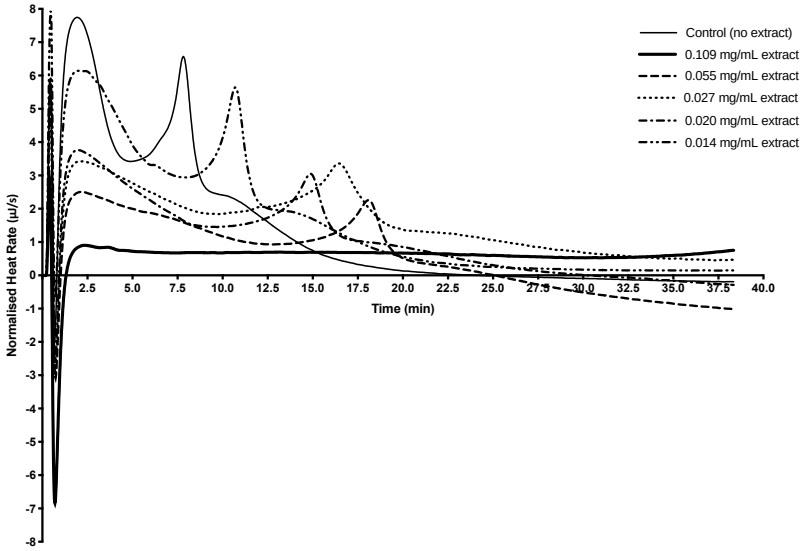

Figure 3 – ITC monitoring of phytase inhibition by Liberty extract

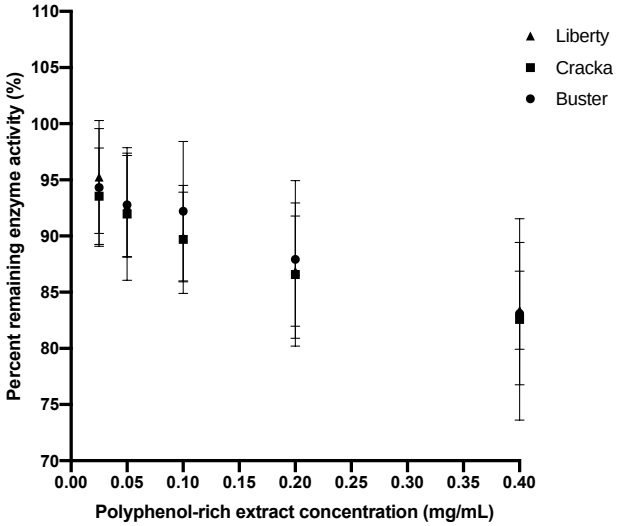

Figure 4 – Percent inhibition of serine protease activity by sorghum extracts

IV. DISCUSSION

Polyphenol-rich extracts prepared from three Australian sorghums (Liberty, Buster and Cracka) were found to contain low to intermediate levels of phenolics and tentatively identified lignin-like derivatives, often associated with cross-linking polysaccharides in the cell wall matrix (Hatfield et al., 2017). Taylor (2005) has suggested these types of phenolics may hinder normal digestion. Further analysis of the polyphenol-rich extract including LC-MS is still needed to isolate specific compounds of interest. Phytase proved much more susceptible to inhibition than the serine protease and was inhibited most by Liberty and Cracka. This inhibition may explain the muted responses often seen in sorghum diets dosed with phytase (Selle et al., 2018). It is possible that in *in vivo* conditions phenolic compounds in sorghum may only partially inhibit phytase activity which could contribute to variance in digestible phosphorus yield, especially when low phytase inclusion concentrations are used. In addition to direct enzyme inhibition, phenolics may interact with phytate *in vivo* either directly or indirectly through phytate-starch/kafirin complexes. Phenolics and phytate have been found to positively correlate, most likely due to their proximity in the aleurone layer (Selle et al., 2018). Effects under more commercial conditions still need to be investigated and whether these *in vitro* responses can be replicated *in vivo* is uncertain. Serine protease, on the other hand, was least inhibited by Liberty and most by Buster. Inhibition values of the serine protease approached 30% indicating that even at high levels of polyphenol inclusion the enzyme remained robust and maintained sufficient activity.

ACKNOLWLEDGEMENTS: We would like to thank Dr Heather Walker in the biOMICS Facility in the Faculty of Science at the University of Sheffield for her assistance with mass spectrometry methodology and analysis.

REFERENCES

Ainsworth, EA & Gillespie, KM (2007) *Nature Protocols* **2**: 875-877.
Bravo, L (1998) *Nutrition Reviews* **56**: 317-333.
Harbertson, JF, Kilmister, RL, Kelm, MA & Downey, MO (2014) *Food Chemistry* **160**: 16-21.

Hatfield, RD, Rancour, DM & Marita, JM (2017) *Frontiers in Plant Science* **7**: 1-15.
Liu, SY, Fox, G, Khoddami, A, Neilson, KA, Truong, HH, Moss, AF & Selle, PH (2015) *Agriculture* **5**: 1224-1251.
Selle, PH, Moss, AF, Truong, HH, Khoddami, A, Cadogan, DJ, Godwin, ID & Liu, SY (2018) *Animal Nutrition* **4**: 17-30.
Taylor, JRN (2005) *Proceedings of the Australian Poultry Science Symposium* **17**: 9-16.
Velickovic, TJC & Stanic-Vucinic, DJ (2018) *Comprehensive Reviews in Food Science and Food Safety* **17**: 82-103.

Kempapidis, T.*, Bradshaw, N.J.*, **Hodges, H.E.***, Cowieson, A.J., Cameron, D.D., Falconer, R.J., (2020). Phytase Catalysis of Dephosphorylation Studied using Isothermal Titration Calorimetry and Electrospray Ionization Time-of-Flight Mass Spectroscopy. *Analytical Biochemistry* [online]. **606**, 113859. Available from: doi: 10.1016/j.ab.2020.113859. (*denotes equal authorship)

Phytase Catalysis of Dephosphorylation Studied using Isothermal Titration Calorimetry and Electrospray Ionization Time-of-Flight Mass Spectroscopy

Theofilos Kempapidis[a,1], Niall J. Bradshaw[a,1], Hayden E. Hodges[a,1], Aaron J. Cowieson[b], Duncan D. Cameron[c], Robert J. Falconer[d,*]

[a] Department of Chemical and Biological Engineering, University of Sheffield, Sheffield S1 3JD, United Kingdom

[b] DSM Nutritional Products, 4303 Kaiseraugst, Switzerland

[c] Department of Animal and Plant Science, University of Sheffield, Sheffield S1 3JD, United Kingdom

[d] Department of Chemical Engineering and Advanced Materials, University of Adelaide, Adelaide, SA 5005, Australia

* Corresponding author. Telephone +61 8 8313 5446, Email robert.falconer@adelaide.edu.au

[1] Contributed equally to this work

Abstract

Phytases are important commercial enzymes that catalyze the dephosphorylation of *myo*-inositol hexakisphosphate (phytate) to its lower inositol phosphate (IP) esters, IP6 to IP1. Digestion of phytate by *Citrobacter braakii* 6-phytase deviates significantly from monophasic Michaelis-Menten kinetics. Analysis of phytate digestion using isothermal titration calorimetry (ITC) using the single injection method produced a thermogram with two peaks consistent with two periods of high enzyme activity. Continuous-flow electrospray ionization time-of-flight mass spectroscopy (ESI-ToF-MS) was able to show that the first two cleavage steps were rapid and concurrent but the third cleavage step from IP4 to IP3 was slow. The third (IP4 to IP3), fourth (IP3 to IP2) and fifth (IP2 to IP1) cleavages were

effectively sequential due to the preferred association of the more phosphorylated species with the phytase catalytic site. This created a bottleneck during the cleavage of IP4 to IP3 until the point at which IP4 was exhausted and was followed by the rapid cleavage of IP3 to IP2, which was observed as the second peak in the ITC thermogram. This work illustrates the importance of an orthogonal approach when studying non-specific or complex enzyme catalyzed reactions.

Keywords

Phytate, *myo*-inositol hexakisphosphate, *myo*-inositol, phosphohydrolase, ITC, enzyme kinetics

Abbreviations

IP, inositol phosphate esters; ITC, isothermal titration calorimetry; ESI, electrospray ionization; ESI-ToF-MS, electrospray ionization time-of-flight mass spectroscopy; FTU, unit of phytase activity; PTFE, polytetrafluoroethylene; ΔH, change in enthalpy; K_a, association constant; k, rate constant.

1. Introduction

The introduction of ultra-sensitive microcalorimetry instrumentation in the 1990s enabled a range of molecular interactions and reactions to be studied where there is a small but measurable change in enthalpy [1]. Isothermal titration calorimetry (ITC) has become an increasingly widely used technique for studying molecular interactions [2] and has a major advantage over the alternative analytical techniques whereby the analytes don't need to be tethered to a surface or chemically altered for the analysis to work (which is required for surface plasmon resonance and fluorescence resonance transfer methods). ITC is also a powerful tool for studying enzyme kinetics [3]. There is no need for use of colorimetric substrates which are often unavailable or limit the experimentation that can be conducted. ITC is potentially more flexible than traditional enzyme assays using colorimetric substrates as it can be used to study digestion of unmodified and complex substrates and can be used under turbid conditions where spectroscopy is impractical. The interpretation of ITC thermograms for enzymatic catalysis of single step reactions is simple and well recorded in the literature [4-5]. The change in enthalpy is constant for each reaction event so the rate of energy required to maintain a constant temperature is proportional to the reaction rate. Michaelis-Menten kinetics applies, so the mathematics is well established.

There are enzymes that are imprecise in the reactions they catalyze and for which the reaction kinetics are complex. The endoproteases cleave multiple peptide bonds along a polypeptide backbone, where some cleavage sites are preferred and are cleaved quickly, and others that are less favorable are cleaved more slowly. The resulting ITC thermograms of proteases cleaving peptide bonds on protein substrates are unlikely to follow simple Michaelis-Menten kinetics. Enzymes like the laccases and lipases are often able to catalyze reactions with a

diverse range of substrates which can complicate the reaction kinetics when more than one substrate is present. ITC provides an analytical approach that can be applied to study complex enzymatic reactions providing real-time data on the generation or adsorption of the heat of the catalytic process.

In this study, the digestion of phytate (*myo*-inositol hexakisphosphate) by a *Citrobacter braakii* phytase was studied using two continuous data collection techniques, ITC and continuous-flow electrospray ionization time-of-flight mass spectrometry (ESI-ToF-MS). The enzyme catalysis consists of the five sequential dephosphorylation reactions and required an orthogonal approach to understand the action of this physiologically and commercially important enzyme.

2. Materials and methods

2.1 Chemical and enzymes

Phytic acid sodium salt hydrate (extracted from rice bran), ethanol and acetone were purchased from Sigma-Aldrich (Gillingham, U.K). ESI-ToF-MS analysis confirmed the sodium phytate was predominantly *myo*-inositol hexakisphosphate with traces of *myo*-inositol pentakisphosphate (Supplementary Figure 1, the peak identification shown in Supplementary Table 1). The phytase (RONOZYME®HiPhos; the enzyme originating from *Citrobacter braakii*) was supplied by DSM Animal Nutrition & Health (Kaiseraugst, Switzerland).

2.2 ITC monitoring of phytase-phytate reaction

Calorimetric analysis was conducted using a Nano ITC (TA Instruments, New Castle, DE) set at 30℃ and 285 rpm stirring speed. Phytate and phytase solutions were degassed prior to the start of the experiment. Phytate was prepared to a concentration of 20 mM in ultra-high purity water while phytase was prepared to 32.6 FTU mL^{-1} in 5% ethanol. Note, one unit of enzyme activity (FTU) is equal to the amount of enzyme that releases 1 μmol of inorganic phosphate from phytate per minute at 5 mM phytate, pH 5.5 and 37°C [6]. The injection syringe contained 20 mM phytate was which titrated into the phytase solution with a 2 μL injection followed by three 5 μL injections. Initial and final baselines were recorded for 300 seconds before and after each injection. The first injection of 2 μL was monitored for 1800 seconds while the three 5 μL injections were monitored for 2000 seconds each. The first injection of 2 μL was used to prime the needle and was discarded from further analysis. The heat of injection for the phytate addition to the solution in the ITC cell and an example of an injection into a 32.6 FTU mL^{-1} phytase solution is shown in Supplementary Figure 2.

2.3 Continuous-flow electrospray ionization time-of-flight mass spectroscopy

ESI-ToF-MS analysis was performed on a SYNAPT G2-Si mass spectrometer (Waters, USA) with an electrospray ionization (ESI) source. Phytate was prepared to a concentration of 20 mM in ultra-high purity water, and phytase was prepared to 2.038 FTU mL^{-1} in ultra-

high purity water. MS analysis was performed in negative ion mode over a mass range of 50-800 Da and was tuned to the singly charged phytate ion (*m/z* 658.8 [M-H]-). For all analyses, source temperature was set to 350°C with a capillary voltage of -2.4 kV. Cone gas (nitrogen) flow rate was 10 L H^{-1}, with desolvation gas flow rate at 700 L H^{-1}

An individual spectrum was produced for phytate alone prior to the analysis of the phytate-phytase reaction (Supplementary Figure 1). A solution of 20 mM phytic acid sodium salt hydrate was introduced into the ESI source as a continuous flow using the internal injection system. Specifically, phytate solution was added to a 25 mL polytetrafluoroethylene (PTFE) vessel and drawn into a 250 µL syringe, then injected into the ESI source at a flow rate of 10 µL min^{-1}. The spectrum was acquired as an average of 174 scans with a scan time of 1 second.

For the phytate-phytase reaction, the system was first purged with 2.038 FTU mL^{-1} phytase solution introduced into the ESI source as a continuous flow (as described above) for a period of 20 minutes with a flow rate of 10 µL min^{-1}. The internal syringe was then emptied and the PTFE vessel replaced with a second 25 mL PTFE vessel (the reaction vessel). The reaction vessel contained 15 mL of 2.038 FTU mL^{-1} phytase to which 0.25 mL of 20 mM phytate solution was added by pipette to give a final concentration of 0.328 mM. The reaction vessel was then manually agitated for 5 seconds and the internal syringe was refilled to a volume of 250 µL and injected into the ESI source at a flow rate of 10 µL min^{-1}. Spectra were acquired over a 22 minute period comprising a total of 1288 scans with a scan time of 1 second. For each of the reaction products (IP6-IP1) total spectral counts for each product ion and their concurrent sodium adduct(s) were summed in each spectrum. The data was then smoothed by combining sets of 10 consecutive spectra and presenting a mean counts value for each reaction product. Note, the acronym for *myo*-inositol hexakisphosphate is IP6, *myo*-inositol pentakisphosphate is IP5, *myo*-inositol tetrakisphosphate is IP4, down to *myo*-inositol monophosphate which is IP1.

3. Results and discussion

3.1 ITC monitoring of phytate digestion

The ITC study of phytate digestion by a *Citrobacter braakii* phytase used an injection of the sodium phytate into the solution containing phytase in the sample cell. The heat of injection from phytate injected into the sample cell containing no phytase is shown in Supplementary Figure 2. A 2 µL injection was used to prime the needle and was followed by three 5 µL injections (Figure 1). The resulting thermogram contained an initial spike associated with the heat of dilution of the phytate solution in the sample cell (this was also observed in the control injection of phytate into a sample cell containing solution without phytase). This was followed by a rise in heat generated by the phytate digestion which peaked around 2 minutes then steadily declined. The unusual feature was a second peak of heat generated around 20 minutes after the injection. The heat generated then plateaued around 25 minutes then declined. The reaction ceased between 40 and 50 minutes after the injection. This phytase thermogram is quite unlike a thermogram generated by an enzyme that catalyzes a single

reaction, which start at maximum reaction rate (limited by the enzyme activity) followed by a declining reaction rate obeying Michaelis–Menten kinetics as the substrate was used up [5].

The three repeat injections of phytate into the phytase are very similar (Figure 1 insert) suggesting the build-up of phosphate within the sample cell has minimal inhibition of the activity of phytase.

The interpretation of a thermogram with two peaks of heat presents a challenge. It is unlikely that the change in enthalpy (ΔH) for the hydrolysis of each different phosphate ester bond is radically different enough to produce the large second peak in the thermogram. The association constant (K_a) of the phytase active site and the different phytate degradation products is likely to differ but ITC alone cannot resolve what is happening during phytate digestion at the molecular level.

3.2 Continuous-flow ESI-ToF-MS analysis of phytate digestion

To complement the ITC analysis, an analytical system was designed in which the molecular composition of the reaction between 2.068 FTU mL^{-1} phytase and 0.328 mM phytate was monitored in real time using ESI-ToF-MS. From the resulting data set, total spectral counts of each identified reaction product and their respective Na^+ adduct(s) were summed for each scan. The ESI-mass spectrum of 20 mM sodium phytate hydrate is shown in Supplementary Figure 1 with peak identification in Supplementary Table 1. For the enzyme reaction, the data from sets of 10 consecutive scans were then averaged and presented over time. The relative amounts of the different inositol species measured by ESI-ToF-MS is shown in Supplementary Figure 3. Signal to noise ratio was low immediately after injection of the reaction solution, so data is presented from 1 minute to 22 minutes. In Figure 2, the x-axis was adjusted by multiplying the time by 1.8 to match the ITC data shown in Figure 1.

The continuous-flow ESI-ToF-MS analysis of phytate dephosphorylation showed that from 1 minute, IP6 levels declined rapidly to near-zero at approximately 3 minutes (Supplementary Figure 3). Concurrently, IP5 counts fall at a similar rate to near-zero by approximately 5 minutes. IP4 levels at the 1 minute mark are close to that of IP5 and increase rapidly to peak at 4 minutes, after which levels fall, at a slower rate than that of IP6 and IP5, reaching near-zero at just after 10 minutes. Accompanying this fall is a gradual increase in IP3 between 2-6 minutes, which accumulates to a plateau between 6-10 minutes. At 10 minutes when IP4 is no longer present, IP3 levels rapidly fall over 3 minutes accompanied by a sharp increase in IP2. Between 12 and 20 minutes, IP2 is the predominant inositol phosphate in the reaction solution, gradually falling with an accompanied increase in IP1. The spectral count data for IP2 and IP1 is characterized by a lower signal to noise ratio than for the more highly phosphorylated inositol phosphates, a factor that may be attributed to the instrument having been tuned to the *m/z* value for singly charged IP6 (*m/z* 658.75), although both IP1 and IP2 are observed in the reaction solution at the end of the 22 minute analysis period.

Rapid dephosphorylation of IP6 and IP5 is accompanied by an accumulation of IP4 within the first 5 minutes of the reaction, which indicates that the affinity of phytase for the IP6 and IP5 as substrates is greater than that for IP4. Moreover, we also observed a decline in the rate

of IP4 degradation relative to the degradation rates for IP6, IP5 and IP3 (see Supplementary Figure 3 and 4). These observations of the dynamics of phytate degradation are supported by results obtained from an alternative methodology using high-performance ion chromatography (HPIC) to measure reaction composition at various time points during phytate dephosphorylation by the same phytase enzyme, revealing similar temporal patterns of IP6, IP5 and IP4 concentrations [7]. IP3 accumulated gradually as IP4 was dephosphorylated, reaching a plateau, between 6-10 minutes as the predominant inositol phosphate. The rate of degradation of IP3 to IP2 was greater than that of IP4-IP3, commencing only when almost all IP4 had become dephosphorylated and there was no longer competition from IP4 for the active site of the enzyme. Once IP3 levels have fallen to near-zero, the reaction rate slows greatly, with IP2 levels gradually falling from an initial spike at 12 minutes during IP3 dephosphorylation. Only during the final 2 minutes of the analysis do IP1 levels overtake IP2 as the predominant inositol phosphate in solution, and no evidence was present of fully dephosphorylated *myo*-inositol (IP0) in the spectra.

The pathways for phytate digestion have previously been studied using HPIC where the reaction is quenched and analyzed at time points during the reaction pathway [8-9]. Recently there has been increased focus on achieving more direct detection of the inositol phosphates by linking the separating power of chromatography with the specificity achieved by mass spectrometry. Anion exchange chromatography with tandem mass spectrometry has been employed for the separation and simultaneous determination of the inositol phosphates [10]. The authors developed and validated a method utilizing both HPIC and ESI tandem mass spectrometry, previously considered a challenge due to the incompatibility of ESI with the high salt levels of typical eluents, and achieved limits of detection of 0.25 pmol for all analytes. Another approach used reversed-phase high performance liquid chromatography with positive mode ESI tandem mass spectrometry detection to separate and identify the products of the reaction between phytate and an *Aspergillus niger* phytase [11].

3.3 Kinetics of C. braakii phytase digestion of phytate

To understand phytase catalysis fully the reaction itself should be considered. Breaking of the bond between the inositol ring and the phosphate by a histidine phosphatase (including *Citrobacter braakii* phytase) is a two-step process [12-13]. The histidine in the phytase active site firstly effects a nucleophilic attack on the phosphorous atom in the scissile phosphate forming a phospho-histidine intermediate. This is followed by hydrolysis of the phospho-histidine intermediate. The binding of phytate to phytase has been studied using the closely related phytase from *Escherichia coli* [14]. The scissile phosphate is guided to its position in the catalytic site by Arg 16 and Arg 30 in the conserved RHGXRXP sequence at the active site, along with conserved Arg 92, His 303 and Asp 304. The electron pair on His 17 undergoes nucleophilic attack on the scissile phosphate forming a covalently linked phospho-histidine intermediate releasing the remainder of the phytate from the binding site. The phospho-histidine intermediate is then hydrolyzed to release the phosphate from the histidine [14]. The order that the phosphate residues are cleaved from the phytase molecule is

dependent on the specific phytase and tends to follow a preferred order, with a minority of the phytate digestion following secondary pathways [8-9].

The first step in phytate degradation is the association of the IP6 molecule with the catalytic site on the phytase enzyme with association constant ($K_{a6.1}$). This association is dominated by electrostatic attraction between the strongly positive active site and the multiple negative charges carried by the phytate. The first step of the cleavage reaction is the formation of the phospho-histidine intermediate and release of the *myo*-inositol pentakisphosphate (IP5) back into the solution. The hydrolysis of the phospho-histidine intermediate leaves the phosphate molecule free to disassociate from the phytase active site with an association constant ($K_{a6.2}$). The formation of the phospho-histidine intermediate and its subsequent hydrolysis would have a combined rate constant (k_6). This is repeated for each subsequent degradation step as shown in Figure 3. As the association of phytate and its degradation products with the phytate binding site is dominated by electrostatic attraction, and the negative charge on the degradation products is reduced as the phosphates are removed, this also reduces the association constants of the degradation products.

$$K_{a6} > K_{a5.1} > K_{a4.1} > K_{a3.1} > K_{a2.1}$$

At times during the reaction there are multiple phytate degradation products in solution. At 5 minutes there is a mixture of IP5, IP4 and IP3, all competing for binding to the catalytic site, with IP5 favored over IP4 and IP3 binding the least favored, resulting in accumulation of IP3. The cleavage of IP3 is rapid compared to the cleavage of IP4 ($k_3 > k_4$) as seen in Figure 2. The result was a rise in the degradation of IP3 to IP2 with a resulting spike in the heat generated as seen in Figure 1 around 20 minutes after injection. Degradation of IP2 to IP1 was slower than IP3 to IP2 and can be observed as the plateauing of the reaction after the second peak. Weak association of IP1 with the active site of the enzyme and the resultant lack of phosphate displacement may explain the persistence of IP1 at the end of the reaction and absence of detectable IP0. The rate of decline of the different inositol phosphate species measured by ESI-ToF-MS is consistent with the rate of IP6 dephosphorylation to IP5 being faster than IP5 to IP4, and that IP4 conversion to IP3 is relatively slow and that IP3 conversion to IP2 is relatively fast, as shown in Supplementary Figure 4. The ESI-ToF-MS data is less informative on IP2 conversion to IP1 but interpretation of the ITC data is uncomplicated for the later stages of this series of phytase catalyzed dephosphorylation reactions.

3.4 Interpreting ITC data for complex enzyme catalyzed reactions

The specificity of enzymes is highly variable. Some enzymes are able to catalyze one specific reaction but others can catalyze a diverse range of reactions. The study of non-specific enzymes is simple if a single substrate is used in the experiment and it can be expected to observe Michaelis-Menten kinetics. The difficulty arises when non-specific enzymes are used to catalyze reactions in complex mixtures of substrates, which is common an occurrence when studying natural systems, such as digestion in animals or degradation of lignin.

The digestive enzymes include examples that are involved in breaking down homopolymers (polymers made up with one identical component) like starch and heteropolymers (polymers made up of multiple components) like proteins. ITC has been used to study homopolymers; cellulase [15-18], chitinase [19], human saliva α-amylase [20], porcine pancreatic α-amylase [21], and pullulanase [22]. Under ideal conditions digestion of homopolymers can be described using Michaelis-Menten kinetics as each cleavage step will have an identical change in enthalpy. Deviation from Michaelis-Menten kinetics occurs with digestion of homopolymers due to phenomenon such as branching, which occurs in polymers like starch or crystallization which occurs with cellulose. Polymers like xylan, which is in theory is a homopolymer, but when isolated from a natural source like birch xylan is not perfectly uniform, differ in molecular mass, side chain distribution, and acetylation, can be expected to deviate from Michaelis-Menten kinetics [23].

Enzymes like the exopeptidases catalyze the breaking of peptide bonds irrespective of the amino acid composition of the polypeptide. Endoproteases like trypsin, chymotrypsin and pepsin also break peptide bonds but have preferred amino acid sequences at which they can catalyze the reaction. A single injection assay using ITC to study trypsin catalysis of the hydrolysis of casein predictably deviates from Michaelis-Menten kinetics [24] as it does not comply with the assumption behind the mathematics that it is a single reaction.

Other enzymes that catalyze reactions that are non-specific comprise a diverse group including the lipases, laccases, phytases and versatile peroxidases. ITC studies on porcine pancreatic lipase [25] and laccase [26] use a simple substrate, simplifying kinetics but missing the preference that the enzymes would have for one substrate over another that would happen in the mixed compositions that occur naturally. Possibly the most ambitious ITC study was of a particularly non-specific enzyme, versatile peroxidase, which can catalyze a range of oxidation and cleavage reactions. This study used mixed substrates, including humic acid, fulvic acid as well as effluent from a pulp and paper plant, and fouled membrane solids extracted from a ground water treatment membrane and provides a useful example of the use of ITC to study the kinetics of the digestion of complex substrates by a non-specific enzyme [27].

The commonly used assay for phytase activity is a colorimetric assay that measures the phosphate released by the action of the phytase on the phytate [6]. As shown in this paper, the difference in the enzymatic rates for the different dephosphorylation reactions means the simple measurement of enzyme activity based on phosphate release will have a systematic error associated with it. The interest in commercial phytase and its digestion of phytate is due to its inclusion in animal feed where it reduces the anti-nutritional properties of phytate naturally occurring in the grain component of pig and poultry feed [28-29]. Phytate can bind to proteins electrostatically cross-linking the proteins to form aggregates [301-31] and has the potential to interfere with both digestive enzymes and protein substrates. It has been shown that greater phosphorylation of the inositol phosphate species imparts greater anti-nutritional potential [32-33]. This is likely as the binding of phytate to proteins (food substrates and digestive enzymes) is predominantly electrostatic, and the negative charge of IP6 is greater than IP5, and so on. It is likely that the anti-nutritional potential of the low phosphorylated

inositol phosphate species (IP3, IP2 and IP1) is inconsequential within an animal's digestive tract. If an experiment is interested in reducing the anti-nutritional potential of phytate it should focus the early phase of the reaction sequence. The use of ITC to study the rates of phytate digestion needs to take into consideration the aim of the research. The ITC thermogram data shows power (μJ/s) against time, the total area under the curve represents the total heat generated by the sequence of reactions is Q_{total}, and the area under the curve is the heat generated by a specific time (t) is Q. If the experimentation aims to study the decline in the highly phosphorylated inositol phosphate species, a suitable cut-off point in the reaction sequence could be in the first half of the sequence, i.e. $Q/Q_{total} = 0.4$, and the rate could be measured as inverse of the time to reach 40% of the Q_{total} ($Rate = 1/t_{40\%}$). This would avoid distortion of the rate estimation caused by the "irrelevant" conversion of IP4 to IP3 while capturing the important early stages of the reaction sequence. If the experimentation is interested in the release of phosphate from phytate then a cut-off point in later phases of the reaction sequence, i.e. $Q/Q_{total} = 0.9$, would be more suitable, and the rate could be measured as inverse of the time to reach 90% of the Q_{total} ($Rate = 1/t_{90\%}$). This would include the relevant conversion of IP4 to IP3 as well as most of the later stages of the reaction sequence.

Finally, it is relevant that the data presented above represents a closed *in vitro* system. Under *in vivo* conditions the sequential dephosphorylation of phytate to free phosphate and *myo*-inositol is achieved by the concerted effort of both exogenous microbial phytase and endogenous phosphatases from the intestinal mucosa and the resident microbiome. Appreciable concentrations of endogenous phosphatase in the intestine of avian species has been previously reported [34] and this may influence the reaction sequence and subsequent composition of lower esters in the digestive milieu. Indeed, it has recently been demonstrated *in vivo* that this exogenous phytase generates substantial increases in the concentration of free *myo*-inositol in the plasma of pigs and poultry [35-36] which suggests complementarity of exogenous and endogenous phytases and phosphatases *in praxis*.

4. Conclusion

Analysis of the digestion of *myo*-inositol hexakisphosphate (phytate) by *Citrobacter braakii* phytase using the single injection method with ITC demonstrates the reaction deviates significantly from Michaelis-Menten kinetics. The second peak in heat generated proved to be due to a bottleneck at the cleavage of IP4 to IP3 which is relatively slow, as the association between the phytase catalytic site and IP4 was preferred to its association with IP3, causing an accumulation of IP3. When IP4 was finally used up the rapid cleavage of IP3 to IP2 caused the second peak in heat generated in the thermogram. The use of ITC alone is useful for demonstrating when enzyme catalysis is not a simple single reaction but requires further investigation to understand the complexity of the reaction. An orthogonal approach using a second analytical method such as continuous-flow electrospray ionization time-of-flight mass spectroscopy is required to understand what is happening on the molecular level.

Acknowledgements

This work was supported by two postgraduate studentships provided by DSM Nutritional Products, 4303 Kaiseraugst, Switzerland and one provided by the Grantham Centre for Sustainable Futures, University of Sheffield. Invaluable technical advice was provided by Dr Heather Walker in the Mass Spectroscopy Centre, The University of Sheffield.

References

[1] E. Freire, O.L. Mayorga, M. Straume, Isothermal titration calorimetry, Anal. Chem. 62 (1990) 950A–959A. https://doi.org/10.1021/ac00217a002.

[2] R.J. Falconer, Applications of isothermal titration calorimetry - the research and technical developments from 2011-2015, J. Mol. Recognit. 29 (2016) 504–515. https://doi.org/ 10.1002/jmr.2550.

[3] M.J. Todd, J. Gomez, Enzyme kinetics determined using calorimetry: A general assay for enzyme activity? Anal. Biochem. 296 (2001) 179-187. https://doi.org/ 10.1006/abio.2001.5218.

[4] M.L. Bianconi, Calorimetry of enzyme-catalyzed reactions, Biophys. Chem. 126 (2007) 59–64. https://doi.org/ 10.1016/j.bpc.2006.05.017.

[5] S.N. Olsen, Applications of isothermal titration calorimetry to measure enzyme kinetics and activity in complex solutions, Thermochim. Acta 448 (2006) 12-18. https://doi.org/ 10.1016/j.tca.2006.06.019.

[6] AOAC Official Method 2000.12 Phytase activity in feed: colorimetric enzymatic method. Official Methods of Analysis of AOAC International. 17th Edn. Arlington, VA.

[7] K. Pontoppidan, V. Glitsoe, P. Guggenbuhl, A.P. Quintana, C.S. Nunes, D. Petersen, A.S. Sandberg, In vitro and in vivo degradation of myo-inositol hexakisphosphate by a phytase from *Citrobacter braakii*, Arch. Anim. Nutr. 66 (2012) 431-444. https://doi.org/ 10.1080/1745039X.2012.735082.

[8] A. Ariza, O.V. Moroz, E.V. Blagova, J.P. Turkenburg, J. Waterman, S.M. Roberts, J. Vind, C. Sjoholm, S.F. Lassen, L. De Maria, V. Glitsoe, L.K. Skov, K.S. Wilson, Degradation of phytate by the 6-phytase from *Hafnia alvei*: A combined structural and solution study, PLoS ONE 8 (2013) e65062. https://doi.org/ 10.1371/journal.pone.0065062.

[9] M. Sun, J. Alikhani, A. Massourdieh, R. Greiner, D.P. Jaisi, Phytate degradation by different phosphohydrolase enzymes: Contrasting kinetics, decay rates, pathways, and isotope effects, Soil Sci. Soc. Am. J. 81 (2017) 61-75. https://doi.org/ 10.2136/sssaj2016.07.0219.

[10] X. Liu, P.W. Villalta, S.J. Sturla, Simultaneous detection of inositol phosphates in complex biological matrices: quantitative ion-exchange chromatography/tandem mass

spectrometry, Rapid Commun. Mass Sp. 23 (2009) 705–712. https://doi.org/ 10.1002/rcm.3923.

[11] P. Vats, B. Bhushan, A.K. Chakarborti, U.C. Banerjee, Separation and identification of enzymatically prepared dephosphorylated products of myo-inositolhexakisphosphate using LC-MS, J. Sep. Sci. 31, (2008) 3829–3833. https://doi.org/10.1002/jssc.200800372.

[12] J.B. Vincent, M.W. Crowder, B.A. Averill, Hydrolysis of phosphate monoesters: a biological problem with multiple chemical solutions, Trends Biochem. Sci. 17 (1992) 105–110. https://doi.org/ 10.1016/0968-0004(92)90246-6.

[13] R.L. Van Etten, Human prostatic acid phosphatase: A histidine phosphatase, Ann. N. Y. Acad. Sci. 390 (1992) 27–51. https://doi.org/ 10.1111/j.1749-6632.1982.tb40302.x.

[14] D. Lim, S. Golovan, C.W. Forsberg, Z. Jia, Crystal structures of *Escherichia coli* phytase and its complex with phytate, Nat. Struct. Mol. Biol. 7 (2000) 108-113. https://doi.org/ 10.1038/72371.

[15] N. Karim, S. Kidokoro, Precise and continuous observation of cellulase-catalyzed hydrolysis of cello-oligosaccharides using isothermal titration calorimetry, Thermochim. Acta 412 (2004) 91-96. https://doi.org/ 10.1016/j.tca.2003.09.001.

[16] N. Karim, H. Okada, S. Kidokoro, Calorimetric evaluation of the activity and the mechanism of cellulases for the hydrolysis of cello-oligosaccharides accompanied by the mutarotation reaction of the hydrolyzed products, Thermochim. Acta 431 (2005) 9-20. https://doi.org/ 10.1016/j.tca.2005.01.025.

[17] L. Murphy, M.J. Baumann, K. Borch, M. Sweeney, P. Westh, An enzymatic signal amplification system for calorimetric studies of cellobiohydrolases, Anal. Biochem. 404 (2010) 140-148. https://doi.org/ 10.1016/j.ab.2010.04.020.

[18] Y. Yu, S. Qi, X. Zhang, W. Qi, H. Zhang, The kinetics of cellulase in reverse micelles using an isothermal titration microcalorimetry technique, Colloid Surface A 586 (2020) 124314. https://doi.org/ 10.1016/j.colsurfa.2019.124314.

[19] I.-M. Krokeide, V.G.H. Eijsink, M. Sørlie, Enzyme assay for chitinase catalyzed hydrolysis of tetra-N-acetylchitotetraose by isothermal titration calorimetry, Thermochim. Acta 454 (2007) 144-146. https://doi.org/ 10.1016/j.tca.2007.01.002.

[20] G. Lehoczki, K. Szabó, I. Takács, L. Kandra, G. Gyémánt, Simple ITC method for activity and inhibition studies on human salivary alpha-amylase, J. Enzyme Inhib. Med. Chem. 31 (2016) 1648-1653. https://doi.org/ 10.3109/14756366.2016.1161619.

[21] J.A.H. Kaeswurm, B. Claasen, M.P. Fischer, M. Buchweitz, Interaction of Structurally Diverse Phenolic Compounds with Porcine Pancreatic alpha-Amylase, J Agric. Food Chem. 67 (2019) 11108-11118. https://doi.org/ 10.1021/acs.jafc.9b04798.

[22] G. Ali, V. Dulong, S.N. Gasmi., C. Rihouey, L. Picton, D. Le Cerf, Covalent immobilization of pullulanase on alginate and study of its hydrolysis of pullulan, Biotechnol. Prog. 31 (2015) 883-889. https://doi.org/ 10.1002/btpr.2093.

[23] M.J. Baumann, L. Murphy, N. Lei, K.B.R.M. Krogh, K. Borch, P. Westh, Advantages of isothermal titration calorimetry for xylanase kinetics in comparison to chemical-reducing-end assays, Anal. Biochem. 410 (2011) 19-26. https://doi.org/10.1016/j.ab.2010.11.001.

[24] K. Maximova, J. Trylska, Kinetics of trypsin-catalyzed hydrolysis determined by isothermal titration calorimetry, Anal. Biochem. 486 (2015) 24-34. https://doi.org/10.1016/j.ab.2015.06.027.

[25] Y. Zhang, X.-A. Luo, L.-J. Zhu, Z. Wang, M.-Q. Jai, Z.-X Chen, Catalytic behavior of pancreatic lipase in crowded medium for hydrolysis of medium-chain and long-chain lipid: An isothermal titration calorimetry study, Thermochim. Acta 672 (2019) 70-78. https://doi.org/ 10.1016/j.tca.2018.12.015.

[26] N. Volkova, V. Ibrahim, R. Hatti-Kaul, Laccase catalysed oxidation of syringic acid: Calorimetric determination of kinetic parameters, Enzyme Microb. Technol. 50 (2012) 233-237. https://doi.org/ 10.1016/j.enzmictec.2012.01.005.

[27] K.S. Siddiqui, H. Ertan, T. Charlton, A. Poljak, A.K. Daud Khaled, X. Yang, G. Marshall, R. Cavicchioli, Versatile peroxidase degradation of humic substances: Use of isothermal titration calorimetry to assess kinetics, and applications to industrial wastes, J. Biotechnol. 178 (2014) 1-11. https://doi.org/ 10.1016/j.jbiotec.2014.03.002.

[28] P.H. Selle, V. Ravindran, Microbial phytase in poultry nutrition, Anim. Feed Sci. Tech. 135 (2007) 1–41. https://doi.org/ 10.1016/j.anifeedsci.2006.06.010.

[29] P.H. Selle, V. Ravindran, Phytate-degrading enzymes in pig nutrition, Livest. Sci. 113 (2008) 99–122. https://doi.org/ 10.1016/j.livsci.2007.05.014.

[30] J.W. Bye, N.P. Cowieson, A.J. Cowieson, P.H. Selle, R.J. Falconer, Dual effects of sodium phytate on the structural stability and solubility of proteins, J. Agric. Food Chem. 61 (2012) 290-295. https://doi.org/ 10.1021/jf303926v.

[31] S.J. Darby, L. Platts, A.J. Cowieson, R.J. Falconer, An isothermal titration calorimetry study of phytate binding to lysozyme, J. Therm. Anal. Calorim. 127 (2017) 1201–1208. https://doi.org/ 10.1007/s10973-016-5487-6.

[32] A. Yu, A. Cowieson, C. Gilbert, P. Plumstead, S. Dalsgaard, Interactions of phytate and *myo*-inositol phosphate esters (IP1-5) including IP5 isomers with dietary protein and iron and inhibition of pepsin, J. Anim. Sci. 90 (2012) 1824-1832. https://doi.org/10.2527/jas2011-3866.

[33] A.J. Cowieson, V. Ravindran, Effect of phytic acid and microbial phytase on the flow and amino acid composition of endogenous protein at the terminal ileum of growing broiler chickens, Brit. J. Nutr. 98 (2007) 745-752. https://doi.org/10.1017/S0007114507750894.

[34] D.D. Maenz, H.L. Classen, Phytase activity in the small intestinal brush border membrane of the chicken, Poult. Sci. (1998) 557-563. https://doi.org/10.1093/ps/77.4.557.

[35] A.J. Cowieson, F.F. Roos, J.-P. Ruckebusch, J.W. Wilson, P. Guggenbuhl, H. Lu, K.M. Ajuwon, O. Adeola, Time-series responses of swine plasma metabolites to ingestion of diets containing *myo*-inositol or phytase, Brit. J. Nutr. 118 (2017) 897-905. https://doi.org/ 10.1017/S0007114517003026.

[36] A.J. Cowieson, R. Aureli, P. Guggenbuhl, F. Fru-Nji, Possible involvement of *myo*-inositol in the physiological response of broilers to high doses of microbial phytase, Anim. Prod. Sci. 55 (2013) 710-719. https://doi.org/ 10.1071/AN14044.

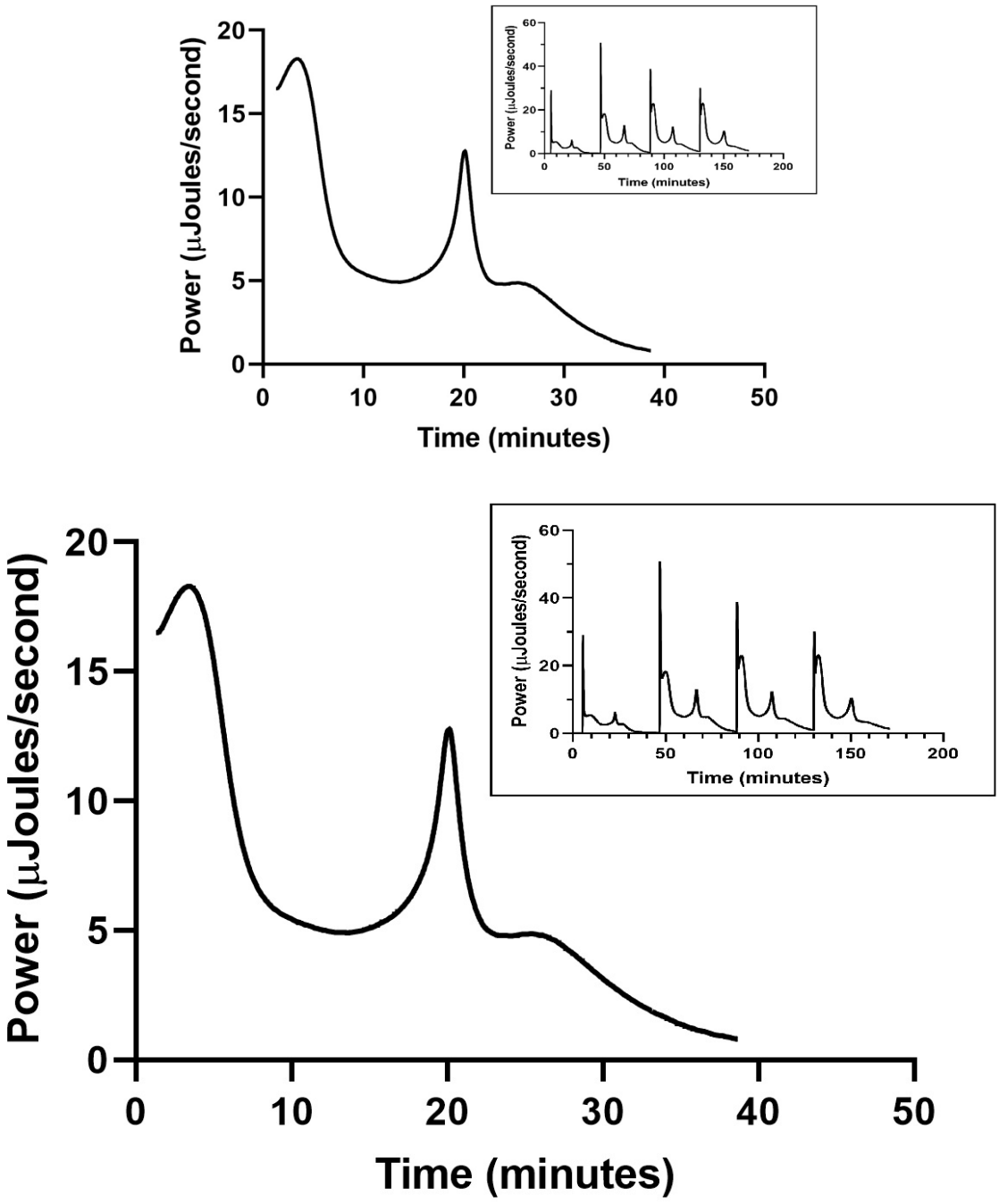

Figure 1. The enzymatic degradation of phytate by a *Citrobacter braakii* phytase followed by ITC. The inset shows the 2 μL injection followed by three 5 μL injections of 20 mM phytate into 32.6 FTU mL^{-1} phytase solution.

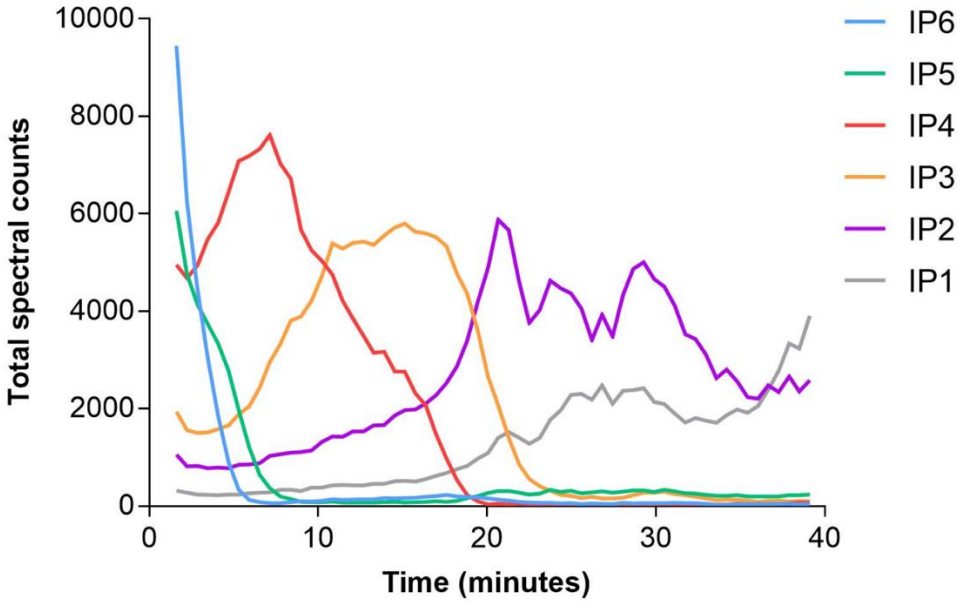

Figure 2. Enzymatic dephosphorylation of 0.328 mM sodium phytate by a *C. braakii* phytase. 0.25 mL of 20mM phytate was added to 15 mL 2.038 FTU mL^{-1} phytase and the reaction measured by continuous flow electrospray ionization time of flight mass spectrometry (ESI-ToF-MS). Note: The x-axis was adjusted to match the ITC data by multiplying time by 1.8.

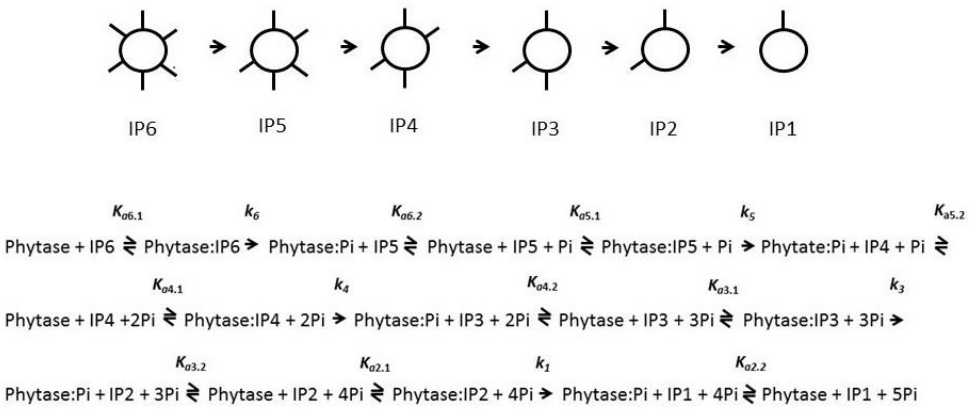

Figure 3. The sequence of association, cleavage and disassociation reactions that constitute phytase degradation of a phytate (*myo*-inositol hexakisphosphate) down to *myo*-inositol phosphate plus five phosphate molecules by *Citrobacter braakii* phytase. The association and rate constants are shown for each step.

Hodges, H.E., Walker, H.J., Cowieson, A.J., Falconer, R.J., Cameron, D.D., (2021). Latent Anti-nutrients and Unintentional Breeding Consequences in Australian *Sorghum bicolor* Varieties. *Frontiers in Plant Science* [online]. **12**(625260), 1-12. Available from: doi:10.3389/fpls.2021.625260.

Latent Anti-Nutrients and Unintentional Breeding Consequences in Australian *Sorghum bicolor* Varieties

Hayden E. Hodges[1*], Heather J. Walker[2], Aaron J. Cowieson[3], Robert J. Falconer[4§], Duncan D. Cameron[5§]

[1] Department of Chemical & Biological Engineering, University of Sheffield, Sheffield, S10 2TN, England

[2] biOMICS Facility, Faculty of Science, University of Sheffield, Sheffield, S10 2TN

[3] DSM Nutritional Products, 4303 Kaiseraugst, Switzerland

[4] Department of Chemical Engineering and Advanced Materials, University of Adelaide, SA 5005, Australia

[5] Department of Animal and Plant Science, University of Sheffield, Sheffield, S10 2TN, England

[§] Denotes equal authorship

*** Correspondence:**
Hayden E. Hodges
hehodges1@sheffield.ac.uk

Keywords: *Sorghum bicolor*[1], metabolomics[2], FT-IR[3], mass spectrometry[4], anti-nutrients[5], polyphenols[6], animal feed[7]

Number of words: 4659**; Number of figures/tables:** Seven

Abstract

Modern feed quality sorghum grain has been bred to reduce anti-nutrients, most conspicuously condensed tannins, but its inclusion in the diets of monogastric animals can still result in variable performance that is only partially understood. Sorghum grain contains several negative intrinsic factors, including non-tannin phenolics and polyphenols, phytate, and kafirin protein, which may be responsible for these muted feed performances. To better understand the non-tannin phenolic and polyphenolic metabolites that may have negative effects on nutritional parameters, the chemical composition of sorghum grain polyphenol extracts from three commercial varieties (MR-Buster, Cracka, Liberty) was determined through the use of an under-studied, alternative analytical approach involving Fourier-transform infrared (FT-IR) spectroscopy and direct ionization mass spectrometry. Supervised analyses and interrogation of the data contributing to variation resulted in the identification of a variety of metabolites including established polyphenols, lignin-like anti-nutrients, and complex sugars, as well as high levels of fatty acids which could contribute to nutritional variation and underperformance in monogastrics. FT-IR and mass spectrometry could both

discriminate among the different sorghum varieties indicating that FT-IR, rather than more sophisticated mass spectrometric methods, could be incorporated into quality control applications.

Introduction

Intensification of the global meat industry has stimulated innovation in the animal feed sector. Advances in feed technology strive towards intensification through a reduction in feed conversion ratio (FCR), greater energy and nutrient utilization, improved animal welfare and environmental sustainability, reduction in endogenous grain anti-nutrients, and optimization of costs (Makkar and Ankers, 2014). Using poultry production as a specific example, the yield of chicken meat (with Australia as a model market) has exponentially increased from the 1970s until today where it has begun to level off (**Figure S1**). This increase in production is mirrored by a similar decrease and leveling off of FCR (increased efficiency). This gain of efficiency is due to several global innovations, including directed poultry and feed grain breeding, implementation of new feed additives, and use of higher quality grains and supplements in dietary formulations (Mottet and Tempio, 2017). Supplementation of monogastric feed with exogenous enzymes has become routine to support measures of performance, as well as to mitigate the effects of anti-nutrients, most commonly phytate, non-digestible starches and proteins, and polyphenolic compounds (Cowieson et al., 2006). Polyphenols are well-established anti-nutrients and antifeedants, particularly to monogastrics, and routinely cause reduced feed intake and weight gain, increased FCR (reduced efficiency), and enzyme inhibition (Bravo, 1998; Cadogan and Finn, 2010; Pasquali et al., 2016; Alu'datt et al., 2017).

While phenolic and polyphenolic compounds are found in all feed grains, sorghum, *Sorghum bicolor* (L.), is well-established as having markedly high levels of these secondary metabolites, including condensed tannins (Glennie et al., 1981; Awika and Rooney, 2004). Sorghum is the fifth-most important cereal crop grown in the world and has many diverse applications, including alcoholic beverages, biofuel, human food products, and animal feed. Approximately 59 million tons of sorghum was produced in 2018 with half of the production in Africa and a third in the Americas (Food and Agriculture Organization of the United Nations, 2020). As sorghum has high levels of phenolic and polyphenolic compounds, it has developed a split nature as these metabolites have proven positive effects in human diets. The polyphenols found in sorghum are well-established antioxidants that can reduce oxidative stress and the diseases that arise from imbalances in reactive oxygen species (Awika and Rooney, 2004; Stefoska-Needham et al., 2015).

The higher concentrations of polyphenols, up to 10% of the grain's mass, have played a key role in sorghum being stigmatized as having lower nutritional quality when incorporated into monogastric animal feed (Jambunathan and Mertz, 1973; Armstrong et al., 1974; Bravo, 1998; Selle et al., 2017). Previous studies on sorghum have identified a diverse range of phenolics, from small ferulic and caffeic acids to large condensed tannins with high degrees of polymerization (Stafford, 1965; Gupta and Haslam, 1978; Kang et al., 2016). High-tannin sorghum varieties are not commonly used in monogastric animal feed as deleterious nutritional effects have been observed in animals fed these particular grains (Nyachoti et al., 1996). These negative effects have encouraged sorghum breeders to preferentially select low-tannin varieties for use in monogastric animal feed. Sorghum grains low in tannin content, such as most red and white varieties in use today, have also been reported as having

higher levels of digestible protein (Youssef, 1998). White sorghum grain, most commonly the Liberty variety in Australia, has been found to better support weight gain, FCR, and growth performance in pigs and chickens than its red colored counterparts. This may be due to the absence of large polyphenols, such as condensed tannins (Cadogan and Finn, 2010; Liu et al., 2010).

Currently, there is discussion about whether modern varieties, important to the animal feed industry, contain relevant/detectable levels of condensed tannins (Perez-Maldonado and Rodrigues, 2009; Liu et al., 2015). This debate seeks to move the conversation from condensed tannins to smaller phenolic and polyphenolic compounds which may contribute subtle differences in varietal performance, even in sorghum grains designated 'tannin-free.' In their study of six 'tannin-free' sorghum diets, Truong et al. (2016) found no difference in broiler chicken performance with regard to FCR and weight gain but did find differences in nutrient utilization between white and red grains. Negative correlations were found between phenolic acids, flavonols, kafirin protein (sorghum's major storage protein) and measures of digestibility. Even the beneficial impacts of certain feed additive enzymes have been reported to be muted when formulated into sorghum diets. This has been observed primarily with phytase, with regard to the enzyme's extra-phosphoric effects on protein and amino acid digestibility, (Liu et al., 2014; Truong et al., 2014; Selle et al., 2017). As the grains used in these studies were 'tannin-free,' compounds other than traditional condensed tannins may have caused the anti-nutritional effects observed.

The majority of sorghum phenolic analyses have used liquid chromatography – mass spectrometry (LC-MS) with identifications achieved through use of standards, retention time comparison, and MS^n fragmentation (Kang et al., 2016; Rao et al., 2018; Tugizimana et al., 2019; Jiang et al., 2020; Zhou et. al, 2020). The use and comparison of less intensive methodological approaches, including direct ionization and infrared spectroscopy, has been little studied in sorghum, especially with regard to characterizing metabolic variation between grain varieties important to the animal feed industry. Currently, there exists no comparative framework for the assessment of orthogonal methods of analysis for polyphenolic extracts, particularly crude extracts, from feed-relevant sorghum grains. In this paper, we present an alternative analytical framework for characterizing phenolic anti-nutrients in crude polyphenol extracts from three Australian sorghum varieties (MR-Buster, Cracka, Liberty). Using a series of analytical techniques from simple spectroscopy to more complicated mass spectrometric methods, untargeted and targeted metabolomics methodologies were applied to the data to determine both bulk and subtle differences in metabolite profiles.

Materials and Methods

Materials

The sorghum varieties, MR-Buster, Cracka, and Liberty, were provided by DSM Nutritional Products (Kaiseraugst, Switzerland) and harvested in February 2017 from Central Darling Downs, Queensland, Australia. Solvents used were of high-performance liquid chromatography (HPLC) grade.

Preparation of sorghum polyphenol extracts

Sorghum grain was extracted for polyphenols following Harbertson et al. (2014) with modifications. Approximately 20 g of each variety were soaked overnight in ultra-high

purity (UHP) water. The soaked grain was ground in a mortar and pestle, rinsed with UHP water six times, and allowed to dry overnight at room temperature. The dried bran was defatted for four hours with 200 mL of *n*-hexane in a Soxhlet extractor. The defatted bran was allowed to dry overnight at room temperature prior to being extracted twice with 200 mL 70% (v/v) aq. acetone for 30 minutes on an orbital mixer (170 rpm). The acetone extract was filtered through glass filter paper, solvent removed in a rotary evaporator, lyophilized, and stored under nitrogen gas at -80°C. Three separate extracts were prepared per sorghum variety.

Fourier transform – infrared spectroscopy (FT-IR)

FT-IR analysis was performed on an IRAffinity-1S spectrometer (Shimadzu) using a diamond attenuated total reflectance (ATR) crystal (Specac Quest) in the wavenumber region between 4000 and 400 cm^{-1} with a resolution of 4 cm^{-1} using Happ-Genzel Apodization. At each position 40 scans were averaged. The spectra were baseline corrected with IR Solutions software (Shimadzu). Three separate extracts from each variety were each analyzed in triplicate and replicates were averaged. The spectra obtained from the sorghum polyphenol extracts were then analyzed for polyphenol and tannin structural features based on published spectra (Laghi et al., 2010; Falcão and Araújo, 2013; Falcão and Araújo, 2014; Ricci et al., 2016).

Mass spectrometry (MS)

Electrospray ionization (ESI) (negative [-] and positive modes [+]) and matrix-assisted laser desorption/ionization (MALDI) (+) were performed on a Waters Synapt G2-Si ToF mass spectrometer (Waters Corporation, USA). MassLynx data system (Waters Corporation, USA) provided instrument control, data acquisition, and data processing. For all three analyses, sorghum polyphenol extracts were prepared to a concentration of 0.1 mg/mL in 50% (v/v) aq. methanol. Sorghum polyphenol extracts were prepared, run, and analysed in triplicate and three different extracts per variety were analyzed. For ESI, capillary voltage was 2.2 kV, source temperature 100°C, and desolvation temperature was 280°C. Solutions were injected at a flow rate of 5 μL min^{-1}. ESI – tandem MS (MS^2) was performed on specific ions produced by ESI-MS in the negative mode. For MALDI sample preparation, the matrix chemical alpha-cyano-4-hydroxycinnamic acid (CHCA) (5 mg/mL in methanol with 0.1% formic acid [v/v]) was mixed with the prepared extracts in a 1:1 ratio. From this mixture, 1 μL was spotted onto a steel MALDI plate for analysis. All spectra were measured from 50 – 1500 Da for each analysis type.

Data Processing and Statistical Analysis

Raw spectra data from each mass spectrometric analysis was processed following a stepwise method based on Overy et al. (2005) and Austen et al. (2019). Briefly, the raw mass spectrometry data were centroided and converted into text files using an in-house Visual Basic macro. The triplicate runs of each sample were combined to determine the average mass-to-charge ratio (*m/z*) of each compound ion to make-up the metabolite profile for each sample. The masses determined, along with their respective percent total ion count (TIC), were based on equations defined by Overy et al. (2005). For ease of analysis, masses were grouped together into 'mass bins' based on groupings of 0.2 amu.

Principal component analysis (PCA) and orthogonal partial least squares discriminant analysis (OPLS-DA) were performed on the spectra obtained from FT-IR and the mass bins

identified from the MS spectra using SIMCA (Sartorius Stedim Biotech, Sweden). PCA allows for the unsupervised, or untargeted, analysis of the metabolite profiles in the extracts which enables the separation of extracts based on metabolite variations among them. PCA provided the initial overview of the data to determine relationships between extract types and to highlight whether further investigation with more targeted analyses was needed. A covariance matrix was utilized over a correlation matrix as the data sets for each PCA were single-source and of the same data type (relative abundance units for FT-IR and percent total ion count for mass spectrometry) and normalized using Pareto scaling prior to analysis. OPLS-DA is a supervised, or targeted, analysis which allows for pairwise comparisons to be made between two different extract types. This analysis maximizes variation between samples and produces quantitative loadings plots which highlight components of the spectra responsible for causing variation, i.e. wavenumbers (cm^{-1}) from the FT-IR spectra and mass bins from the MS spectra. OPLS-DA was performed between MR-Buster and Cracka, MR-Buster and Liberty, and Cracka and Liberty.

For MS spectra, the top 10 mass bins causing variation for each extract in each pairing, as well as the 10 most abundant peaks, were interrogated further for putative identifications. Compound identification was conducted using online databases, including METLIN (Scripps Research Institute; La Jolla, CA, USA; https://metlin.scripps.edu) and Kyoto Encyclopedia of Genes and Genomes (KEGG) (Kanehisa Laboratories; Kyoto, Japan; https://www.kegg.jp) (Kaneshisa and Goto, 2000). In the negative mode, compounds were identified having an ion adduct of -H (-1.008 Da) while in positive mode ion adducts included +H (+1.008 Da), +Na (+22.99 Da) and +K (+39.10 Da). Following identifications, the KEGG IDs for all possible identifications in each mass bin were analyzed using MetaboAnalyst through the pathway analysis function with *Arabidopsis thaliana* as the pathway library, hypergeometric test as the over representation analysis, and relative-betweeness centrality for the pathway topology analysis (Chong et al., 2019).

The guidelines for compound identification were made following the guidance of the Chemical Analysis Working Group and the Metabolomics Standards Initiative (Sumner et al., 2007). These guidelines allow for four levels of identification of metabolites: 1) identified compound with two independent orthogonal data compared with an authentic sample; 2) putatively annotated compound relying on literature or database comparison; 3) putatively characterized compound classes; and 4) unknown compounds. The data obtained from FT-IR analysis is classified as a level 3 identification as established structural features of compound classes can be clearly identified. The identifications through mass spectrometry are classified as a level 2 identification and were accepted if below an *m/z* margin of error of 40 ppm or less.

Statistical differences in total ion counts of certain compounds were determined through one-way analysis of variance (one-way ANOVA) with Tukey post-hoc comparisons using GraphPad Prism 8 (GraphPad Software, Inc.; San Diego, CA, USA). Chicken yield data in **Figure S1** was plotted as individual values and an asymmetric sigmoidal 5 PL nonlinear model was fitted to the data using GraphPad Prism 8. The same was done to the FCR values collected from the literature, except the same nonlinear model was fitted to average values for each year rather than individual values.

Results

Qualitative analysis of sorghum polyphenol FT-IR spectra

FT-IR spectroscopy was performed on the sorghum polyphenol extracts. The full spectra of the sorghum extracts matched closely to one another (**Figure 1a**). Cracka and MR-Buster spectra were essentially identical, while the Liberty extract spectrum displayed slight variations in peak location, size, and intensity. All extracts showed the presence of a hydroxyl (O – H) functional group marked by the presence of a strong, broad peak centered around 3300 – 3200 cm^{-1}. The sorghum extracts displayed a weak, single peak/shoulder at approximately 3010 cm^{-1} indicative of an aromatic C – H functional group. The sharp, strong peaks present in the spectra from 2957 – 2848 cm^{-1} are representative of an aliphatic C – H functional group. Within the fingerprint region (1800 – 450 cm^{-1}), ten bands/peaks common to published tannin and polyphenol FT-IR spectra were highlighted in the spectra of the sorghum polyphenol extracts (**Figure 1b**). All sorghum extracts matched three of these highlighted wavenumber regions (1736 – 1704 cm^{-1}, 1044 – 1030 cm^{-1}, and 780 – 758 cm^{-1}). The two red sorghum extracts, MR-Buster and Cracka, matched closely with another three regions (1615 – 1600 cm^{-1}, 1522 – 1507 cm^{-1}, and 1162 – 1148 cm^{-1}). The four regions of the spectra not closely matched with any sorghum extract were 1453 – 1446 cm^{-1}, 1288 – 1282 cm^{-1}, 1085 cm^{-1}, and 967 cm^{-1}.

Multivariate analysis (PCA, OPLS-DA) of sorghum polyphenol extract FT-IR spectra

Multivariate analytical methods were applied to the FT-IR spectra using unsupervised PCA to determine if there was variation among extract types (**Figure 2a,b**). MR-Buster and Cracka extracts were clearly differentiated from Liberty extract in each of the analyses. The first two principal components of the sorghum polyphenol extracts explained 84.8% of the variation for the full spectra and 90% for the fingerprint region (1800 – 450 cm^{-1}). Supervised multivariate analysis was then conducted, using OPLS-DA, on the fingerprint regions of the FT-IR spectra to determine specific wavenumbers (cm^{-1}) responsible for variation between extract types (**Table 1**, **Figure S4**). OPLS-DA highlighted regions of the spectra most responsible for variations between pairwise comparisons of the sorghum extracts. Red sorghum (MR-Buster, Cracka) extracts were most varied in the regions corresponding to aromatic C – H (800s cm^{-1}) and aromatic C = C bonds (1600 cm^{-1}), while white grain (Liberty) extract was most different in the aromatic C – H region (1000 – 900 cm^{-1}) and C – O bonding (1030s cm^{-1}).

Unsupervised analysis (PCA) of sorghum polyphenol metabolite profiles from mass spectrometry

Mass spectrometry was performed using ESI (+, -) and MALDI (+) (**Figure S5**). Unsupervised analyses, using PCA, of the spectra allowed for the clear separation of red sorghum (MR-Buster, Cracka) and white sorghum (Liberty) extracts (**Figure 3a-c**). The first two principal components for ESI (-), ESI (+), and MALDI (+) explained 58.4%, 71.6%, and 56.2% of variation among sorghum extracts. These results indicated enough separation and variation between extract types to justify further supervised analyses to quantitatively determine specific mass bins, and thus metabolites, responsible for the variation in the extracts.

Supervised analysis (OPLS-DA) of sorghum polyphenol extract metabolite profiles from mass spectrometry

Supervised analysis of the sorghum polyphenol extract spectra was performed using OPLS-DA and pairwise comparisons were made between extract types. Data was binned to 0.2 amu chunks to minimize the amount of data handling and corresponding loadings plots were used

to select mass bins (top 10) causing variation between extract pairings (**Figure 4**, **Table 2**, **Tables S1,2**, **Figures S6-S8**). The identified mass bins from ESI (-) were then interrogated and identified using metabolite databases, including METLIN and KEGG (**Table S3**). ESI-MS^2 (-) was performed on select ions and found to match METLIN spectra and/or previous MS^2 studies on sorghum polyphenol extracts (Kang et al., 2016) (**Table S4)**

The mass bins responsible for variation of the red sorghum extract MR-Buster from Cracka and Liberty included small sugars, flavones, flavanones, flavonols (and their glycosylated counterparts), unsaturated fatty acids, and several large un-resolved polyphenolic polymers. These putative identifications include commonly detected sorghum polyphenols like apigenin, naringenin, luteolin, and eriodictyol. Both MR-Buster and Cracka were found to have large peaks at the higher end of the spectrum, most notably at *m/z* 689, 851, 1107, and 1269 (**Figure S9**). Smaller peaks were found to surround these and were found to be separated by 16 Da (loss of hydroxyl group), while the larger separations included 162 (loss of sugar), and 272/255 Da (possible loss of flavonoid). These peaks are notably absent from Liberty extract. Cracka sorghum extract was found to have several overlapping mass bins to MR-Buster but with less diversity of metabolites as most mass bin identifications were of routinely identified sorghum polyphenols, including apigenin and naringenin. White Liberty sorghum extract presented little similarity to both red varieties as its mass bins contributing to variation included disaccharides, tricarboxylic acids, fatty acids, and lignans. Interestingly, the most abundant mass bins across the three sorghum extracts were essentially identical. The putative identifications made indicated the presence of phenylpropanoid glycerides, flavone/flavanones, disaccharides, and most predominately fatty acids, including oleic acid, linoleic acid, and oleic/linoleic acid-related compounds. These identified compounds, as well as the 10 most abundant from each extract, were then mapped to specific biosynthetic pathways using MetaboAnalyst Pathway Analysis (**Figure 5**).

4 Discussion

While modern monogastric animal feed has been formulated for optimum nutrient utilization and digestive efficiency, performance gains still remain, especially in feeds composed of sorghum grain. With poultry production as a model, increases in efficiency with sorghum as a feed grain, as measured by FCR, have begun to level out (**Figure S1**). While efforts to reduce anti-nutrient content in sorghum, most notably tannin and polyphenol concentrations, have been successful, gaps in efficiency and efficacy of feed additives remain, possibly due to unintended consequences in feed quality sorghum breeding. An understudied alternative analytical approach was thus used to identify anti-nutrients that may be causing varied performance in sorghum feed and to determine the suitability of different analytical techniques for assessing metabolic variation among sorghum grain extracts.

In this study, all three sorghum extracts, especially the Liberty variety, were found to have high ion counts for mass bins putatively identified as fatty acids, including oleic acid, linoleic acid, vernolic acid, ricinoleic acid, and trihydroxyoctadecenoic acid, which could result in nutritional variation in monogastric diets composed primarily of sorghum. With oleic acid as a starting point, vernolic acid is formed through an epoxidation reaction, ricinoleic acid through hydroxylation, linoleic acid through desaturation, and trihydroxyoctadecenoic acid through the hydroxylation of linoleic acid (Mazur et al., 1999; Cao and Zhang, 2013). The identifications made through mass spectrometry echo the strong, sharp FT-IR peaks between 3000 – 2900 cm^{-1} which correlate with C – H bonding found extensively in fatty acids (Shapaval et al., 2014). MR-Buster has been previously found to contain linoleic and oleic acids as the most dominant fatty acids, making up 80% of unsaturated fatty acid content

(Mehmood et al., 2008). White varieties are similarly dominated by oleic and linoleic acids but at slightly higher proportions (Afify et al., 2012). Broiler chickens fed diets high in oleic acid were found to have a higher FCR, as well as reduced muscle and carcass weights (Toomer et al., 2003). Similar long chain fatty acids have also been shown to inhibit enzyme activity which could result in muted responses of exogenous feed enzymes (Kido et al., 1984). The high levels of fatty acids detected in the current study indicate the potential of implementing an exogenous lipase or emulsifier, as high levels of these compounds could be detrimental to growth and performance parameters.

Sorghum breeding efforts may have triggered metabolic alterations by favoring fatty acid synthesis over polyphenols, particularly condensed tannins. This hypothesis is supported by current work on sorghum grain and its management. Xie et al. (2019) studied sorghum varieties and preference by birds for feeding. They found that varieties avoided by birds had higher anthocyanin and tannin precursors (flavan-3-ols) than those that they preferred to eat. This correlated with the presence or absence of the *Tannin1* gene, previously found in sorghum to be involved in the regulation of polyphenols and tannins (Wu et al., 2012). In addition to determining the difference in polyphenols, the bird-preferred sorghum was found to have increased volatiles associated with fatty acids, as well as higher concentrations of fatty acids, including linolenic acid. Xie et al. (2019) concluded that the modulation of the *Tannin1* gene affects *SbGL2* which is involved in transcription of fatty acids.

In addition to the fatty acids and common polyphenols detected, the red sorghum varieties were found to have peaks with high ion masses and ion count, *m/z* 689, 851, 1107, and 1269, not clearly identifiable as traditional sorghum tannins. Similar peak masses have been previously identified in sorghum extracts as either pyrano-compounds or glucosylated heteropolyflavans. In sorghum leaf sheath, Khalil et al. (2010) describes the structural determination of a novel pyrano-3-deoxyanthocyanidin, pyrano-apigenindin (*m/z* 371.091 [+]). Red and black sorghums were found to have unique flavanone structures including pyrano-naringenin-catechin (*m/z* 689), pyrano-naringenin-catechin-glucoside (*m/z* 851), pyrano-eriodictyol-catechin-glucoside (*m/z* 867), and pyrano-naringenin-pyrano-eriodictyol-catechin (*m/z* 1107) (Yang, 2013; Rao et al., 2018). Glucosylated heteropolyflavans, described by Gujer et al. (1986) and Krueger et al. (2003), are composed of unique polymerizations of eriodictyol/naringenin and luteolinidin/apigeninidin with varying degrees of glycosylation. The masses of these compounds were predicted with the equation 288 + 272*a* +256*b* +162*c* + cation with 288 representing the mass of an eriodictyol base unit, 272 referring to a proluteolinidin unit, 256 to a proapigeninidin unit, 162 to additional sugar units, and the letters referring to possible degrees of polymerizations. The MS^2 spectra support these identifications as the primary fragment masses detected correspond to losses of 256, 272 and 162. Purification of these unknowns is needed along with structural evidence that could be gained using NMR techniques.

In the current study, spectra obtained from ESI (+, -) were clearer than those produced using MALDI (+) with a greater number of clearly identifiable peaks, most likely due to the lack of need for a matrix compound with ESI. ESI (+,-) analyses were also successful in detecting routinely identified polyphenol compounds in sorghum, including apigenin, naringenin, and phenylpropanoid glycerides (Kang et al., 2016). Sorghum grain extracts have been sparingly analyzed using MALDI (Krueger et al., 2003; Qi et al., 2018; Jiang et al., 2020; Reeves et al., 2020). Unsupervised analysis of the ESI and MALDI spectra allowed for the clear separation between red and white varieties and in some cases among all three extracts. Identifications allowed for pathways of interest to be highlighted, as well as comparisons of percent relative

abundances of selected masses. These metabolomic methods are most likely critical when first releasing a new variety of grain to the market. Recently, Zhou et al. (2020) compared three sorghum varieties (black, red, white) to study metabolic variation based on color. PCA revealed a separation of grains based on grain color, and compound identification found that darker grains contained more flavonoids than lighter colored grains, similar to what was determined in the current work. Typically, the color of the grain gives some indication of the polyphenols present with darker and highly colored grains containing higher concentrations and often larger, more complex polyphenols (Rhodes et al., 2014).

FT-IR has been previously shown to be successful in both distinguishing bulk differences among general metabolite profiles (Johnson et al., 2003) as well as nuancing more subtle variations, e.g. tannin extracts separated based on tannin chemistry (Grasel et al., 2016a). In the current study, FT-IR analysis revealed there were structural similarities, with regard to polyphenols and tannins, among the sorghum polyphenol extracts. The subtle differences in sorghum extract peak structures and maxima suggest the presence of competing compounds indicative of a complex plant extract. As reviewed by Ricci et al. (2015), the spectra matched the general profile of extracts containing phenolic, polyphenolic, and tannin compounds, including characteristic O – H hydroxyl groups, aromatic C – H bonds, aromatic C = C bonds, and C – O groups. A similar approach in evaluating the presence/absence of specific metabolite structures was taken by Cameron et al. (2006) in their investigation into alteration to lignin and suberin content in grasses, legumes, and forbs subject to attack by a root hemiparasitic plant.

Comparable values for the O – H maxima have previously been reported in sorghum flour (Manuhara et al., 2017). The strong bands around 3000 cm^{-1}, indicating aliphatic C – H structures, have been detected in similar extract types, including sorghum, and possibly indicate the presence of sugars and/or fatty acids (She et al., 2010; Shapaval et al., 2014; Manuhara et al., 2017). In their natural state, polyphenols are most likely to be conjugated to sugars (Bravo, 1998). Polyphenol and tannin extracts typically contain peaks corresponding to C = O groups (1700s cm^{-1}), especially those containing hydrolyzable tannins (Grasel et al., 2016b; Reeves et al., 2020). This region can also indicate the presence of amide functional groups, most commonly found in proteins. Duodu et al. (2001) studied protein structure in highly digestible sorghum and maize mutants and identified bands between 1670 – 1620 cm^{-1} as amide I and from 1550 – 1500 cm^{-1} as amide II. The subtle differences between red and white sorghum grains in these regions may indicate important differences in protein content and structure with possible nutritional implications. Selle et al. (2020) studied amino acids and kafirin protein in several sorghum varieties, including a Buster variety and Liberty. With regard to crude protein and kafirin content, Liberty had 80.9 and 41.4 g/kg, while Buster reported 99.2 and 44.6 g/kg, respectively (Selle et al., 2020). The higher proportion of kafirin protein found in Liberty may be causing the spectral differences observed in the current study.

The region from 1630 – 1400 cm^{-1} is strongly diagnostic for the presence of polyphenols as it indicates aromatic C = C bonding found in the aromatic rings of phenolic compounds. The peaks identified between 1400 – 1000 cm^{-1} are also characteristic of C – OH as well as C – O – C bonding (Ricci et al., 2015). The differences in the sorghum extract spectra in these regions indicate that the white variety (Liberty) likely has reduced polyphenol content compared to the red varieties (MR-Buster, Cracka), a common finding in sorghum polyphenol studies, which can correlate with nutritional variations observed in feeding (Truong et al., 2016). FT-IR is a useful, simple method of analysis that could be used in on-

line agricultural settings, as opposed to full scale laboratories. Although this study analyzed more laboratory intensive freeze-dried extracts, FT-IR can easily be applied to simple liquid extracts taken on-site.

This study of an alternate analytical framework for polyphenol characterization highlighted the need for complementary methods to fully understand the complexity of sorghum polyphenol extracts. FT-IR spectroscopy provided general chemical profiles which highlighted functional groups and classes of compounds specific to polyphenol and tannin structural chemistry. Multivariate analysis of the FT-IR spectra demonstrated that the technique was robust enough to separate different extract types and to explain greater variance in the data than any MS method. Both ESI analyses produced similar plots to that of FT-IR, albeit with slightly better grouping of the sorghum extracts. ESI also provided a clearer metabolite profile than MALDI. These results indicated that, with regard to untargeted analysis, FT-IR and ESI provide essentially the same end-product allowing for similar conclusions to be drawn on bulk differences in the spectra. Based on these results, compatibility, and pricing, FT-IR may be the most effective tool for determining the applicability of certain grains to feed formulations, particularly with regard to polyphenol content. This application could be especially important in varietal selection for grain breeding and feed applications. Markers for chosen nutritional parameters, such as protein structure and anti-nutrient content, could be selected for and used as a screening tool prior to more intensive analytical methodologies should they be needed. However, mass spectrometric studies of metabolites present in these grains should be used to guide the interpretation of FT-IR spectra in the field to further highlight subtle differences in the grains that may result in monogastric feed performance variation.

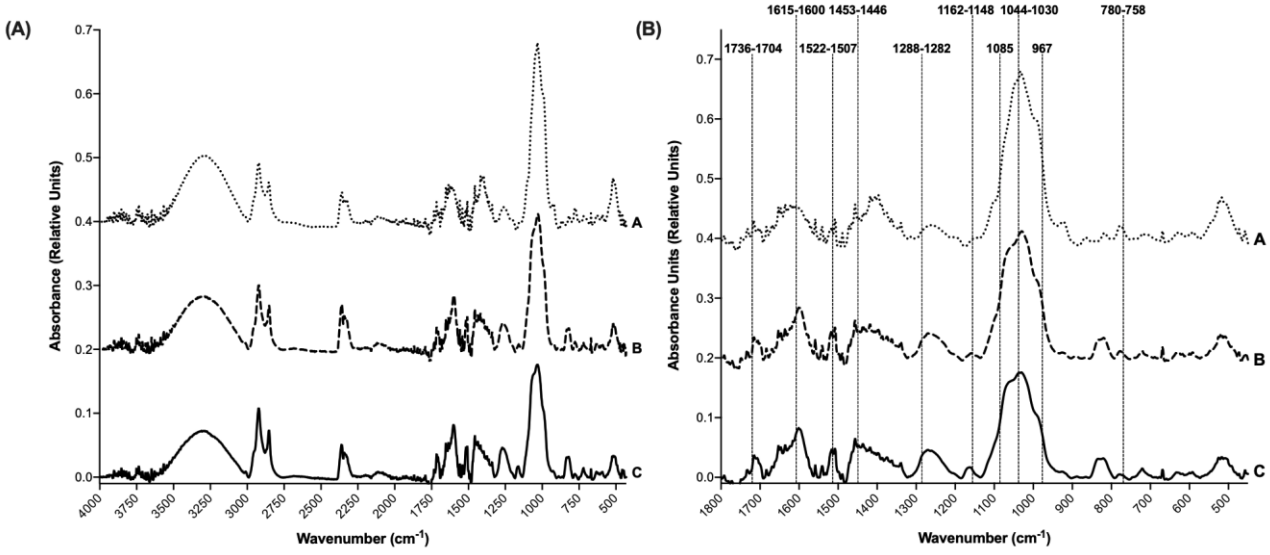

Figure 1. FT-IR spectra of sorghum polyphenol extracts

FT-IR spectra were obtained from (A) 4000 – 400 cm^{-1} and (B) the fingerprint region from 1800 – 450 cm^{-1}. Three replicate spectra were averaged for each extract type. A – Liberty, B – Cracka, C – MR-Buster. For more detail see **Figures S1 and S2**.

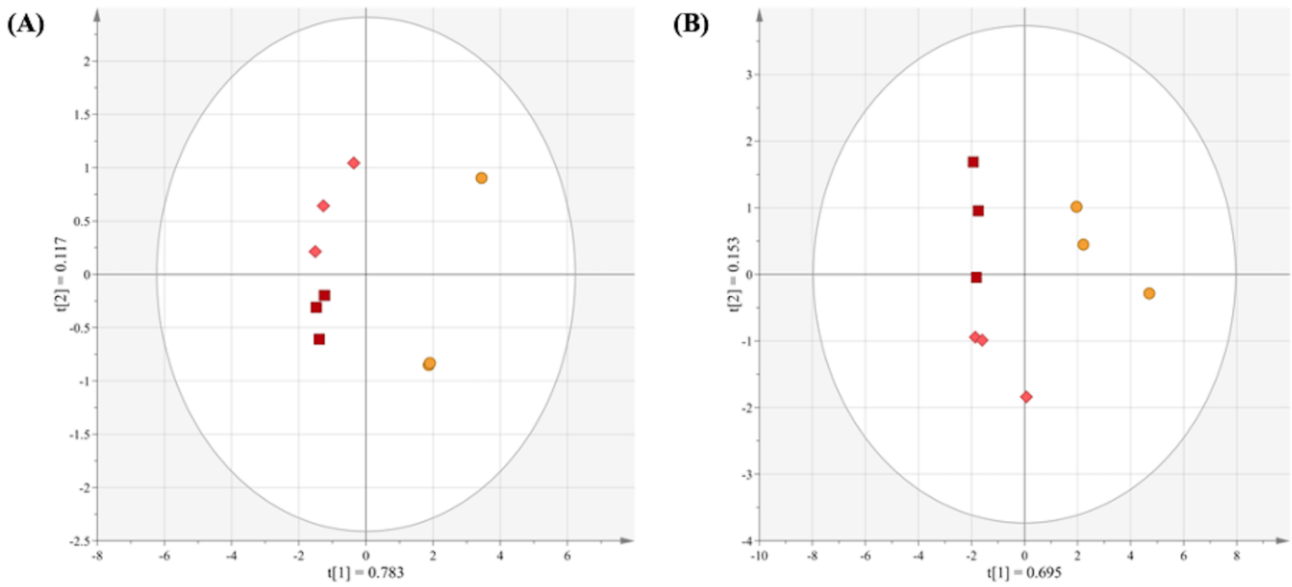

Figure 2. PCA scores plots for FT-IR spectra from sorghum polyphenol extracts

PCA was performed on the full spectra (A: 4000 – 400 cm^{-1}) and fingerprint region (B: 1800 – 450 cm^{-1}) to determine relationships and variance between red and white sorghum polyphenol extracts. The ellipse represents a 95% confidence interval. t[1] and t[2] represent principal components 1 and 2, respectively. MR-Buster (☐) is dark red, Cracka (◇) is light red, and Liberty (◯) is yellow.

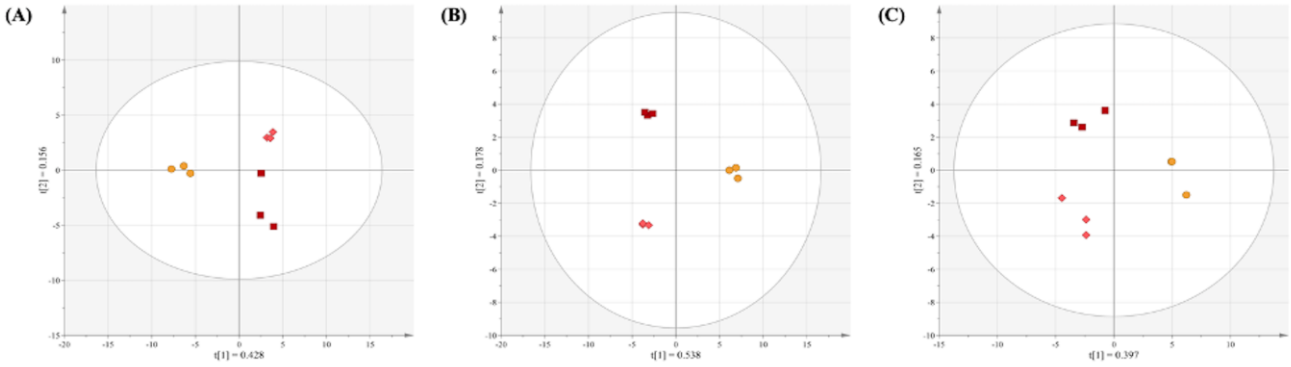

Figure 3. PCA scores plots of mass spectrometric analyses of polyphenol extracts

Unsupervised analyses on data collected using (A) ESI (-), (B) ESI (+), and (C) MALDI (+) to determine relationships between red and white sorghum polyphenol extracts. The ellipse represents a 95% confidence interval. t[1] and t[2] represent principal components 1 and 2, respectively. MR-Buster (☐) is dark red, Cracka (◇) is light red, and Liberty (◯) is yellow.

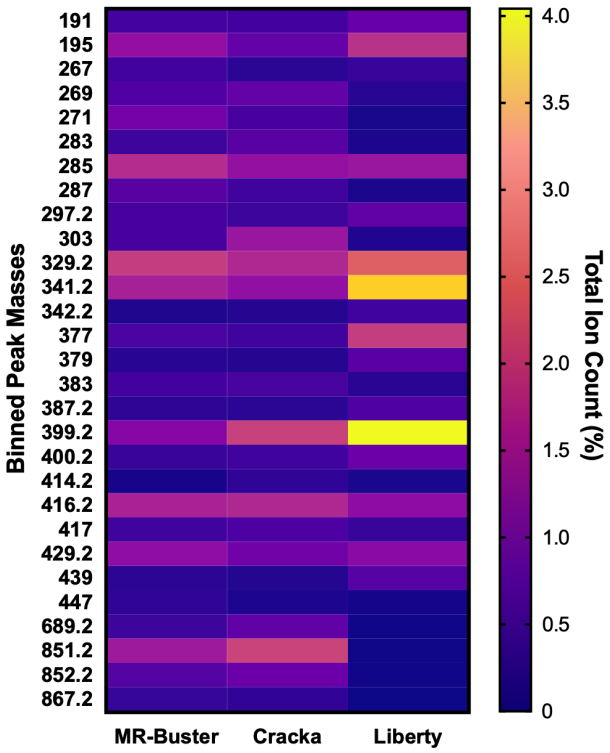

Figure 4. Heat map of percent total ion counts for compounds identified from OPLS-DA

OPLS-DA (ESI [-]) indicated mass bins (*m/z*) most responsible for variation between pairwise comparisons of extracts. The mean relative abundance (total % ion count) and standard deviation were formatted into a heat map, n = 3 for each mass bin (*m/z*).

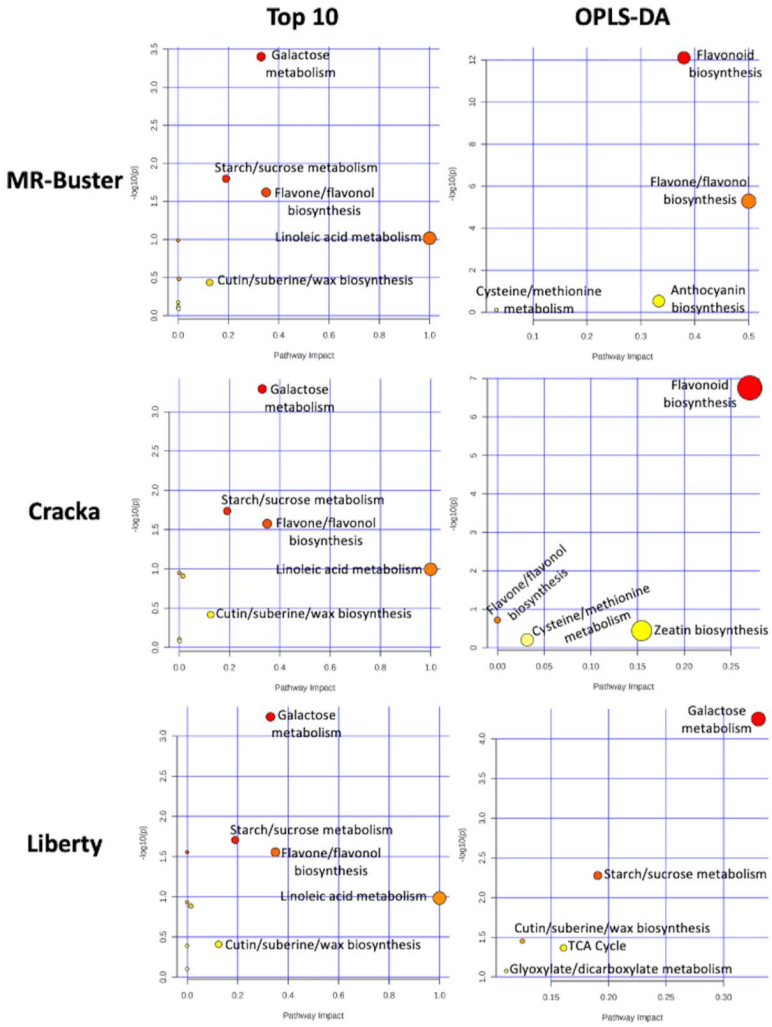

Figure 5. Pathway analysis of identified compounds from ESI (-)

Mass bins (*m/z*) representing the 10 most abundant ions and those highlighted as causing variance between sorghum extracts were identified and mapped to biosynthetic pathways using MetaboAnalyst Pathway Analyst. This analysis identified the most relevant biosynthetic pathways associated with the compounds identified. The pathways were then ranked based on their impact with a value closer to one (red) as being more impactful than a value closer to zero (yellow). The y-axis, -log(10)p, is a measure of statistical significance.

Table 1. FT-IR wavenumbers (cm^{-1}) identified from OPLS-DA loadings plots

	MR-Buster (Red)	Cracka (Red)	Liberty (White)
MR-Buster (Red)	N/A	1167 – 1173 1462 1641 – 1643 1657 – 1161	831 – 837 1593 – 1603
Cracka (Red)	1055 – 1074	N/A	829 – 837 1595 – 1601

Liberty (White)	988 – 997 1030 – 1034 1045	984 – 997 1034 1045	N/A

Table 2. Binned peak masses identified from ESI (-) OPLS-DA loadings plots

	MR-Buster (Red)	**Cracka (Red)**	**Liberty (White)**
MR-Buster (Red)	N/A	271 429.2 285 195 383 287 267 329.2 447 468.2	851.2 271 852.2 287 269 689.2 303 285 867.2 417
Cracka (Red)	399.2 416.2 303 851.2 383.2 689.2 283 852.2 414.2 269	N/A	851.2 303 852.2 689.2 269 283 417 271 383.2 416.2
Liberty (White)	399.2 341.2 377 400.2 379 329.2 387.2 439 191 342.2	341.2 399.2 377 329.2 379 439 400.2 191 297.2 387.2	N/A

Conflict of Interest

The authors declare that the research was conducted in the absence of any commercial or financial relationships that could be construed as a potential conflict of interest.

Author Contributions

All authors contributed to the conception and design of the study. HEH collected the data. HEH, RJF, and DDC analyzed the data. HEH wrote the manuscript. All authors contributed to manuscript revision, reading, and approval of the submitted version.

Funding

This work was supported by a postgraduate studentship provided by DSM Nutritional Products (4303 Kaiseraugst, Switzerland) as well as funding provided by University of Sheffield Faculty of Engineering (Chemical and Biological Engineering).

Acknowledgments

We would like to thank Theofilos Kempapidis for his assistance in using the FT-IR and Nichola Austen for her assistance in using SIMCA for multivariate analysis.

Part of this manuscript was previously published as conference proceedings and given as a talk for the Australian Poultry Science Symposium 2020 and is cited as: Hodges, H., Cowieson, A., Falconer, R., Cameron, D. (2020). Chemical profile and effects of modern Australian sorghum polyphenolic-rich extracts on feed phytase and protease activity. Proc. Aust. Poult. Sci. Symp. 31, 76-79.

References

Afify, A.E.-M.M.R., El-Beltagi, H.S., El-Salam, S.M.A., Omran, A.A. (2012). Oil and Fatty Acid Contents of White Sorghum Varieties under Soaking, Cooking, Germination and Fermentation Processing for Improving Cereal Quality. Not. Bot. Horti. Agrobo. 40, 86-92. doi.org/10.15835/nbha4017585.

Alu'datt, M.H., Rababah, T., Alhamad, M.N., Al-Rabadi, G.J., Tranchant, C.C., Almajwal, A., Kubow, S., Alli, I. (2018). Occurrence, types, properties and interactions of phenolic compounds with other food constituents in oil-bearing plants. Crit. Rev. Food Sci. Nutr. 58, 3209-3218. doi.org/10.1080/10408398.2017.1391169.

Armstrong, W.D., Featherston, W.R., Rogler, J.C. (1974). Effects of Bird Resistant Sorghum Grain and Various Commercial Tannins on Chick Performance. Poult. Sci. 53, 2137-2142. doi.org/10.3382/ps.0532137.

Austen, N., Walker, H.J., Lake, J.A., Phoenix, G.K., Cameron, D.D. (2019). The Regulation of Plant Secondary Metabolism in Response to Abiotic Stress: Interactions Between Heat Shock and Elevated CO_2. Front. Plant Sci. 10, 1463. doi.org/10.3389/fpls.2019.01463.

Awika, J.M., Rooney, L.W. (2004). Sorghum phytochemicals and their potential impact on human health. Phytochem. 65, 1199-1221. doi.org/10.1016/j.phytochem.2004.04.001.

Banda-Nyirenda, D.B.C, Vohra, P. (1990). Nutritional Improvement of Tannin-Containing Sorghums (Sorghum bicolor) by Sodium Bicarbonate. Cereal Chem. 67, 533-537.

Black, J.L., Hughes, R.J., Nielsen, S.G., Tredrea, A.M., MacAlpine, R., van Barneveld, R.J. (2005). The energy value of cereal grains, particularly wheat and sorghum, for poultry. Proc. Aust. Poult. Sci. Symp. 17, 21-29.

Bravo, L. (1998). Polyphenols: Chemistry, Dietary Sources, Metabolism, and Nutritional Significance. Nutr. Rev. 56, 317-333. doi/org/10.1111/j.1753-4887.1998.tb01670.x.

Cadogan, D., Finn, A. (2010). Influence of increasing protease supplementation on two different types of sorghum. Co-operative Research Centre for an Internationally Competitive Pork Industry. Willaston, South Australia.

Cameron, D.D., Coats, A.M., Seel, W.E. (2006). Differential Resistance among Host and Non-host Species Underlies the Variable Success of the Hemi-parasitic Plant *Rhinanthus minor*. Ann. Bot. 98, 1289-1299. doi.org/10.1093/aob/mcl218.

Cao, Y., Zhang, X. (2013). Production of long-chain hydroxy fatty acids by microbial conversion. Appl. Micobiol. Biotechnol. 97, 3323-3331. doi.org/10.1007/s00253-013-4815-z.

Chong, J., Wishart, D.S., Xia, J. (2019). Using MetaboAnalyst 4.0 for Comprehensive and Integrative Metabolomics Data Analysis. Curr. Protoc. Bioinf. 68, e86. doi.org/10.1002/cpbi.86.

Cowieson, A.J., Hruby, M., Pierson, E.E.M. (2006). Evolving enzyme technology: impact on commercial poultry nutrition. Nutr. Res. Rev. 19, 90-103. doi.org/10.1079/NRR2006121.

Duodu, K.G., Tang, H., Grant, A., Wellner, N., Belton, P.S., Taylor, J.R.N. (2001). FTIR and Solid State ^{13}C NMR Spectroscopy of Proteins of Wet Cooked and Popped Sorghum and Maize. J. Cereal Sci. 33, 261-269. doi.org/10.1006/jcrs.2000.0352.

Falcão, L., Araújo, M.E.M. (2013). Tannins characterization in historic leathers by complementary analytical techniques ATR-FTIR, UV-Vis and chemical tests. J. Cul. Her. 14, 499-508. doi.org/10.1016/j.culher.2012.11.003

Falcão, L., Araújo, M.E.M. (2014). Application of ATR–FTIR spectroscopy to the analysis of tannins in historic leathers: The case study of the upholstery from the 19th century Portuguese Royal Train. Vib. Spectrosc. 74, 98-103. doi.org/10.1016/j.vibspec.2014.08.001.

Food and Agricultural Organization of the United Nations (2020). FAOSTAT Food and agriculture data. http://www.fao.org/faostat/en/#home (accessed July 20, 2020).

Glennie, C.W., Kaluza, W.Z., van Niekerk, P.J. (1981). High-Performance Liquid Chromatography of Procyanidins in Developing Sorghum Grain. J. Agric. Food Chem. 29, 965-968. doi.org/10.1021/jf00107a020.

Grasel, F.S., Ferrão, M.F., Wolf, C.R. (2016a). Development of methodology for identification the nature of the polyphenolic extracts by FTIR associated with multivariate analysis. Spectrochim. Acta, Part A. 153, 94-101. doi.org/10.1016/j.saa.2015.08.020.

Grasel, F.S., Ferrão, M.F., Wolf, C.R. (2016b). Ultraviolet spectroscopy and chemometrics for the identification of vegetable tannins. Ind. Crops Prod. 91, 279-285. doi.org/10.1016/j.indcrop.2016.07.022.

Gujer, R., Magnolato, D., Self, R. (1986). Glucosylated flavonoids and other phenolic compounds from sorghum. Phytochem. 25, 1431-1436. doi.org/10.1016/S0031-9422(00)81304-7.

Gupta, R.K., Haslam, E. (1978). Plant Proanthocyanidins. Part 5. Sorghum Polyphenols. J. Chem. Soc., Perkin Trans. 1, 892-896. doi.org/10.1039.P19780000892.

Harbertson, J.F., Kilmister, R.L., Kelm, M.A., Downey, M.O. (2014). Impact of condensed tannin size as individual and mixed polymers on bovine serum albumin precipitation. Food Chem. 160, 16-21. doi.org/10.1016/j.foodchem.2014.03.026.

Hulan, H.W., Proudfoot, F.G. (1982). Nutritive value of sorghum grain for broiler chickens. Can. J. Anim. Sci. 62, 869-875.

Jacob, J.P., Mitaru, B.N., Mbugua, P.N., Blair, R. (1996). The effect of substituting Kenyan Serena sorghum for maize in broiler starter diets with different dietary crude protein and methionine levels. Anim. Feed Sci. Technol. 61, 27-39. doi.org/10.1016/0377-8401(96)00955-8.

Jambunathan, R., Mertz, E.T. (1973). Relationships between Tannin Levels, Rat Growth, and Distribution of Proteins in Sorghum. J. Agric. Food Chem. 21, 692-696. doi.org/10.1021/jf60188a027.

Jiang, Y., Zhang, H., Qi, X., Wu, G., (2020). Structural characterization and antioxidant activity of 2 condensed tannins fractionated from sorghum grain. J. Cereal Chem. 92, 102918. doi.org/ 10.1016/j.jcs.2020.102918.

Johnson, H.E., Broadhurst, D., Goodacre, R., Smith, A.R. (2003). Metabolic fingerprinting of salt-stressed tomatoes. Phytochem. 62, 919-928. doi.org/10.1016/S0031-9422(02)00722-7.

Kaneshisa, M., Goto, S. (2000). KEGG: Kyoto encyclopedia of genes and genomes. Nucleic Acids Res. 28, 27-30. doi.org/10.1093/nar/28.1.27.

Kang, J., Price, W.E., Ashton, J., Tapsell, L.C., Johnson, S. (2016). Identification and characterization of phenolic compounds in hydromethanolic extracts of sorghum wholegrains by LC-ESI-MS^n. Food Chem. 211, 215-226. doi.org/10.1016/j.foodchem.2016.05.052.

Khalil, A., Baltenweck-Guyot, R., Ocampo-Torres, R., Albrecht, P. (2010). A novel symmetrical pyrano-3-deoxyanthocyanidin from a *Sorghum* species. Phytochem. Lett. 3, 93-95. doi.org/10.1016/j.phytol.2010.02.003.

Kido, H., Fukusen, N., Katunuma, N. (1984). Inhibition of Chymase Activity by Long Chain Fatty Acids. Arch. Biochem. Biophys. 230, 610-614.

Krueger, C.G., Vestling, M.M., Reed, J.D. (2003). Matrix-Assisted Laser Desorption/Ionization Time-of-Flight Mass Spectrometry of Heteropolyflavan-3-ols and Glucosylated Heteropolyflavans in Sorghum [*Sorghum bicolor* (L.) Moench]. J. Agric. Food Chem. 51, 538-543. doi.org/10.1021/jf020746b.

Laghi, L., Parpinello, G.P., Del Rio, D., Calani, L., Mattioli, A.U., Versari, A. (2010). Fingerprint of enological tannins by multiple techniques approach. Food Chem. 121, 783-788. doi.org/10.1016/j.foodchem.2010.01.002.

Liu, S., Truong, H., Selle, P. (2010). Sorghum TechNote PRF 3-14A: Red versus white sorghums Part I Is white sorghum really better then red? Feed Grain Partnership TechNote.

http://www.feedgrainpartnership.com.au/items/897/Sorghum%20TechNote%20PRF%203-14A.pdf (accessed 29 July 2020).

Liu, S. Y., Cadogan, D. J., Péron, A., Truong, H. H., Selle, P. H. (2014). Effects of phytase supplementation on growth performance, nutrient utilization and digestive dynamics of starch and protein in broiler chickens offered maize-, sorghum- and wheat-based diets. Anim. Feed Sci. Technol. 197, 164-175. doi.org/10.1016/j.anifeedsci.2014.08.005.

Liu, S.Y., Fox, G., Khoddami, A., Neilson, K.A., Truong, H.H., Moss, A.F., Selle, P.H., (2015). Grain Sorghum: A Conundrum for Chicken-Meat Production. Agric. 5:4, 1224-1251. doi: 10.3390/agriculture5041224.

Liu, S.Y., Truong, H.H., Khoddami, A., Moss, A.F., Thomson, P.C., Roberts, T.H., Selle, P.H. (2016). Comparative performance of broiler chickens offered ten equivalent diets based on three grain sorghum varieties as determined by response surface mixture design. Anim. Feed Sci. Technol. 218, 70-83. doi.org/10.1016/j.anifeedsci.2016.05.008.

Mabelebele, M., Gous, R.M., O'Neill, H.M., Iji, P.A. (2017). The effect of age of introducing whole sorghum grain on performance of broiler chickens. J. Anim. Feed Sci. 29, 151-157. doi.org/10.22358/jafs/124045/2020.

Makkar, H.P.S., Ankers, P. (2014). Towards sustainable animal diets: A suvery-based study. Anim. Feed Sci. Technol. 198, 309-322. doi.org/10.1016/j.anifeedsci.2014.09.018.

Manuhara, G.J., Amanto, B.S., Astuti, T.A. (2017). Effect of drying temperatures on physical characteristics of sorghum flour modified with lactic acid. Int. Conf. Food Sci. Eng. 193, 1-6. doi.org/10.1088/1757-899X/193/1/012024.

Manyelo, T.G., Ng'ambi, J.W., Norris, D., Mabelebele, M. (2019). Substitution of Zea mays by Sorghum bicolor on Performance and Gut Histo-Morphology of Ross 308 Broiler Chickens Aged 1–42 d. J. Appl. Poult. Res. 28, 647-657. doi.org/10.3382/japr/pfz015.

Mazur, B., Krebbers, E., Tingey, S. (1999). Gene Discovery and Product Development for Grain Quality Traits. Sci. 285, 372-375. doi.org/10.1126/science.285.5426.372.

Mehmood, S., Orhan, I., Ahsan, Z., Aslan, S., Gulfraz, M. (2008). Fatty acid compostion of seed oil of different *Sorghum bicolor* varieties. Food Chem. 109, 855-859. doi.org/10.1016/j.foodchem.2008.01.014.

Moss, A.F., Khoddami, A., Chrystal, P.V., Sorbara, J.-O.B., Cowieson, A.J., Selle, P.H., Liu, S.Y. (2020). Starch digestibility and energy utilisation of maize- and wheat- based diets is superior to sorghum-based diets in broiler chickens offered diets supplemented with phytase and xylanase. Anim. Feed Sci. Technol. 264, 114475. doi.org/10.1016/j.anifeedsci.2020.114475.

Mottet, A., Tempio, G. (2017). Global poultry production: current state and future outlook and challenges. World's Poult. Sci. J. 73, 245-256. doi.org/10.1017/S0043933917000071.

Nyachoti, C.M., Atkinson, J.L., Leeson, S. (1996). Response of broiler chicks fed a high-tannin sorghum diet. J. Appl. Poult. Res. 5, 239-245. doi.org/10.1093/japr/5.3.239.

Overy, S.A., Walker, H.J., Malone, S., Howard, T.P., Baxter, C.J., Sweetlove, L.J., Hill, S.A., Quick, W.P. (2005). Application of metabolite profiling to the identification of traits in a population of tomato introgression lines. J. Exp. Bot. 56, 287-296. doi.org/10.1093/jxb/eri070.

Pasquali, G.A.M., Fascina, V.B., Silva, A.L., Aoyagi, M.M., Muro, E.M., Serpa, P.G., Berto, D.A., Saldanha, E.S.P.B., Sartori, J.R. (2016). Maize replacement with sorghum and a combination of protease, xylanase, and phytase on performance, nutrient utilization, litter moisture, and digestive organ size in broiler chicken. Can. J. Anim. Sci. 97, 328-337. doi.org/10.1139/CJAS-2016-0133.

Perez-Maldonado, R.A., Rodrigues, H.D. (2009). Nutritional Characteristics of Sorghums from Queensland and New South Wales for Chicken Meat Production. Rural Industries Research and Development Corporation, Barton, ACT.

Puntigam, R., Brugger, D., Slama, J., Inhuber, V., Boden, B., Krammer, V., Schedle, K., Wetscherek-Seipelt, G., Wetscherek, W. (2020). The effects of a partial or total replacement of ground corn with ground and whole-grain low-tannin sorghum (Sorghum bicolor (L.) Moench) on zootechnical performance, carcass traits and apparent ileal amino acid digestibility of broiler chickens. Livestock Sci. 241, 104187. doi.org/10.1016/j.livsci.2020.104187.

Qi, Y., Zhang, H., Wu, G., Zhang, H., Gu, L., Wang, L., Qian, H., Qi, X. (2018). Mitigation effects of proanthocyanidins with different structures on acrylamide formation in chemical and fried potato crisp models. Food Chem. 250, 98-104. doi.org/10.1016/j.foodchem.2018.01.012.

Rao, S., Santhakumar, A.B., Chinkwo, K.A., Wu, G., Johnson, S.K., Blanchard, C.L. (2018). Characterization of phenolic compounds and antioxidant activity in sorghum grains. J. Cereal Sci. 84, 103-111. doi.org/10.1016/j.jcs.2018.07.013.

Reeves, S.G., Somogyi, A., Zeller, W.E., Ramelot, T.A., Wrighton, K.C., Hagerman, A.E. (2020). Proanthocyanidin Structural Details Revealed by Ultrahigh Resolution FT-ICR MALDI-Mass Spectrometry, $^{1}H–^{13}C$ HSQC NMR, and Thiolysis-HPLC–DAD. J. Agric. Food Chem. 68, 14038-14048. doi.org/10.1021/acs.jafc.0c04877.

Rhodes, D.H., Hoffman Jr., L., Rooney, W.L., Ramu, P., Morris, G.P., Kresovich, S. (2014). Genome-Wide Association Study of Grain Polyphenol Concentrations in Global Sorghum [*Sorghum bicolor* (L.) Moench] Germplasm. J. Agric Food Chem. 62, 10916-10927. doi.org/10.1021/jf503651t.

Ricci, A., Olejar, K.J., Parpinello, G.P., Kilmartin, P.A., Versari, A. (2015). Application of Fourier Transform Infrared (FTIR) Spectroscopy in the Characterization of Tannins. Appl. Spectrosc. Revs. 50, 407-442. doi.org/10.1080/05704928.2014.1000461.

Ricci, A., Lagel, M.-C., Parpinello, G.P., Pizzi, A., Kilmartin, P.A., Versari, A. (2016). Spectroscopy analysis of phenolic and sugar patterns in a food grade chestnut tannin. Food Chem. 203, 425-429. doi.org/10.1016/j.foodchem.2016.02.105.

Rodgers, N.J., Choct, M., Hetland, H., Sundby, F., Svihus, B. (2012). Extent and method of grinding of sorghum prior to inclusion in complete pelleted broiler chicken diets affects

broiler gut development and performance. Anim. Feed Sci. Technol. 171, 60-67. doi.org/10.1016/j.anifeedsci.2011.09.020.

Scripps Center for Metabolomics. (2019). Metlin: Metabolite Search. https://metlin.scripps.edu/index.php [Accessed: 15th October 2019].

Selle, P.H., Cadogan, D.J., Li, X., Bryden, W.L. (2010). Implications of sorghum in broiler chicken nutrition. Anim. Feed Sci. Technol. 156, 57-74. doi.org/10.1016/j.anifeedsci.2010.01.004.

Selle, P.H., Moss, A.F., Truong, H.H., Khoddami, A., Cadogan, D.J., Godwin, I.D., Liu, S.Y. (2017). Outlook: Sorghum as a feed grain for Australian chicken-meat production. Anim. Nutr. 4, 17-30. doi.org/10.1016/j.aninu.2017.08.007.

Selle, P.H., McInerney, B.V., McQuade, L.R., Khoddami, A., Chrystal, P.V., Hughes, R.J., Liu, S.Y. (2020). Composition and characterisation of kafirin, the dominant protein fraction in grain sorghum. Anim. Prod. Sci. 60, 1163-1172. doi.org/ 10.1071/AN19393.

Shapaval, V., Afseth, N.K., Vogt, G., Kohler, A. (2014). Fourier transform infrared spectroscopy for the prediction of fatty acid profiles in *Mucor* fungi grown in media with different carbon sources. Microb. Cell Fact. 13:86. doi.org/10.1186/1475-2859-13-86.

She, D., Xu, F., Geng, Z., Sun, R., Jones, G.L., Baird, M.S. (2010). Physiochemical characterization of extracted lignin from sweet sorghum stem. Ind. Crops Prod. 32, 21-28. doi.org/10.1016/j.indcrop.2010.02.008.

Stafford, H. (1965). Flavonoids and Related Phenolic Compounds Produced in the First Internode of Sorghum vulgare Pers. in Darkness and in Light. Plant Physiol. 40, 130-138. doi.org/10.1104/pp.40.1.130.

Stefoska-Needham, A., Beck, E.J., Johnson, S.K., Tapsell, L.C. (2015). Sorghum: An Underutilized Cereal Whole Grain with the Potential to Assist in the Prevention of Chronic Disease. Food Rev. Int. 31. 401-437. doi.org/10.1080/87559129.2015.1022832.

Sumner, L.W., Amberg, A., Barrett, D., Beale, M.H., Beger, R., Daykin, C.A., Fan, T.W.-M., Fiehn, O., Goodacre, R., Griffin, J.L., Hankemeier, T., Hardy, N., Harnly, J., Higashi, R., Kopka, J., Lane, A.N., Lindon, J.C., Marriott, P., Nicholls, A.W., Reily, M.D., Thaden, J.J., Viant, M.R. (2007). Proposed minimum reporting standards for chemical analysis Chemical Analysis Working Group (CAWG) Metabolomics Standards Initiative (MSI). Metabolomics. 3:3, 211-221. doi: 10.1007/s11306-007-0082-2.Proposed.

Toomer, O.T., Livingston, M., Wall, B., Sanders, E., Vu, T., Malheiros, R.D., Livingston, K.A., Carvalho, L.V., Ferket, P.R., Dean, L.L. (2003). Feeding high-oleic peanuts to meat-type broiler chickens enhances the fatty acid profile of the meat produced. Poult. Sci. 99, 2236-2245. doi.org/10.1016/j.psj.2019.11.015.

Truong, H. H., Yu, S., Peron, A., Cadogan, D. J., Khoddami, A., Roberts, T. H., Liu, S. Y., Selle, P. H. (2014). Phytase supplementation of maize-, sorghum- and wheat-based broiler diets with identified starch pasting properties influences phytate (IP6) and sodium jejunal and ileal digestibility. Anim. Feed Sci. Technol. 198, 248-256. doi.org/10.1016/j.anifeedsci.2014.10.007.

Truong, H.H., Neilson, K.A., McInerney, B.V., Khoddami, A., Robert, T.H., Cadogan, D.J., Liu, S.Y., Selle, P.H. (2016). Comparative performance of broiler chickens offered nutritionally equivalent diets based on six diverse, 'tannin- free' sorghum varieties with quantified concentrations of phenolic compounds, kafirin, and phytate. Anim. Prod. Sci. 57, 828-838. doi.org/10.1071/AN16073.

Tugizimana, F., Djami-Tchatchou, A.T., Steenkamp, P.A., Piater, L.A., Dubery, I.A. (2019). Metabolomic Analysis of Defense-Related Reprogramming in *Sorghum bicolor* in Response to *Colletotrichum sublineolum* Infection Reveals a Functional Metabolic Web of Phenylpropanoid and Flavonoid Pathways. Front. Plant Sci. 9:1840. doi.org/ 10.3389/fpls.2018.01840.

Wu, Y., Li, X., Xiang, W., Zhu, C., Lin, Z., Wu, Y., Li, J., Pandravada, S., Ridder, D.D., Bai, G., Wang, M.L., Trick, H.N., Bean, S.R., Tuinstra, M.R., Tesso, T.T., Yu, J. (2012). Presence of tannins in sorghum grains is conditioned by different natural alleles of *Tannin1*. Proc. Natl. Acad. Sci. 109, 10281-10286. doi.org/10.1073/pnas.1201700109.

Xie, P., Shi, J., Tang, S., Chen, C., Khan, A., Zhang, F., Xiong, Y., Li, C., He, W., Wang, G., Lei, F., Wu, Y., Xie, Q. (2019). Control of Bird Feeding Behavior by *Tannin1* through Modulating the Biosynthesis of Polyphenols and Fatty Acid-Derived Volatiles in Sorghum. Mol. Plant. 12, 1315-1324. doi.org/10.1016/j.molp.2019.08.004.

Yang, L. (2013). Estrogenic properties of sorghum phenolics: possible role in colon cancer prevention. [dissertation]. [College Station (TX)]: Texas A&M University.

Youssef, A.M. (1998). Extractability, fractionation and nutritional value of low and high tannin sorghum proteins. Food Chem. 63, 325-329. doi.org/10.1016/S0308-8146(98)00028-4.

Zhou, Y., Wang, Z., Li, Y., Li, Z., Liu, H., Zhou, W. (2020). Metabolite Profiling of Sorghum Seeds of Different Colors from Different Sweet Sorghum Cultivars Using a Widely Targeted Metabolomics Approach. Int. J. Genomics. 2020:6247429. doi.org/10.1155/2020/6247429.

Supplementary Material

The Supplementary Material for this article can be found in the attached PDF file and Excel spreadsheet.